The University of Sheffield
Department of Civil and Structural Engineering

The Behaviour of Steel Fin Plate Connections in Fire

By
Marwan Sarraj

Supervisors:

Professor Ian Burgess

Dr Buick Davison

Thesis submitted in partial fulfillment of the requirements for the degree of
Doctor of Philosophy

July 2007

Abstract

Steel joints have always been considered as important parts of any structural steel building because they provide the strong links between the principal structural members. The properties and behaviour of joints in both steel and composite structures have been widely studied for some time. The focus has recently been on improving the design of structural frames by taking advantage of realistic connection moment-rotation response. This has necessitated the development of an effective and practicable methodology to describe steel connection behaviour, despite its inherent complexity. Although, the evaluation of steel connections' performance at ambient temperature has been a continuous research topic, the investigation of steel connections at elevated temperatures has only recently been tackled by researchers. However, the determination of the behaviour, available strength and stiffness of moment connections in fire conditions has been a dominant theme in these research works. Moreover, over a number of years the Component Method has been developed to describe the moment-rotation characteristics of end-plate connections, and the method is now included in Eurocode 3. To date, most of the research conducted on steel connections using the component method has focused on relatively stiff and strong connections - flush end-plates and extended end-plates. The modelling of more flexible ("pinned") connections using the Component Method has not received much attention, since the benefits arising from consideration of their behaviour in overall frame response are usually modest. However, in fire conditions connections are subject to complex force combinations of moment and tying forces, as well as vertical shear forces, and the real behaviour, even of nominally pinned connections, can have a significant effect on the overall response of the frame. To date very little information on the behaviour and the resistance of simple shear connections in fire conditions has been generated. Fin plate shear connections, which are economic to fabricate and easy to use in erection, are among these shear connections which are assumed to act as pins in normal service conditions.

In this research, the behaviour and robustness of simple fin plate beam-to-column connections has been investigated, under the conditions of catenary tension from highly deflected beams which occurs in fire. In addition, detailed investigations have been made on applying the component method approach to this connection at both ambient and elevated temperatures.

ABAQUS software has been selected to create a very detailed 3D finite element model. This is a complex model accounting for material nonlinearity, large deformation and contact behaviour. The connection model has been analysed through the elastic and plastic ranges up to failure. Bolt shear and bending, plate and web bearing have been observed as failure modes. A comparison between available experimental data at ambient and elevated temperatures and FEA results shows that the model has a high level of accuracy. However, by implementing the FE model the opportunity was then available to explore the connection tying resistance and the application of the Component Method to the fin plate connection. An intensive investigation has been conducted to develop a representation of this connection type via a simplified component model, enabling prediction of the connection response at both ambient and elevated temperatures. The three main components of a fin-plate connection have been identified as plate bearing, bolt shearing and web-to-plate friction. These components have been described in detail at ambient and elevated temperatures via intensive parametric FE analyses, leading to a simplified component model of a fin plate connection. This model has been evaluated against FE models of complete fin plate joints. Eventually, a fin plate connection spring model is proposed and successfully evaluated for tying, rotation, and shear actions. The Component Model presented in this research offers an opportunity to explore complicated behaviour of fin plate shear joints, and can be incorporated into frame analysis in fire conditions.

Table of Contents

List of Figures

List of Tables

Notations

The following symbols are used in this thesis:

A	Nominal area of the bolt shank	[mm^2]
A_s	The tensile stress area of the bolt	[mm^2]
b_f	The width of a beam flange of an I or H section	[mm]
*C*a	Specific heat of carbon steel	[J/kg K]
d_h	Nominal diameter of the bolt hole	[mm]
d_b	Nominal diameter of the bolt shank	[mm]
d_s	Diameter of the bolt stressed area (A_s)	[mm]
E	Modulus of elasticity (Young's modulus)	[N/mm^2]
e_1	End distance	[mm]
e_2	Edge distance	[mm]
e_3	Beam edge to first bolt row distance	[mm]
e_t	Beam top flange, or top edge, to the top first bolt row distance	[mm]
e_b	Beam bottom flange edge to the bottom bolt row distance	[mm]
F	Applied load	[kN]
F_v	Shear force	[kN]
F_t	Tensile force	[kN]
$F_{v,Rd}$	Design shear resistance of a bolt	[kN]
$F_{t,Rd}$	Design tension resistance of a bolt	[kN]
$F_{b.Rd}$	Design bearing resistance	[kN]
f_y	Yield strength	[N/mm^2]
f_u	Ultimate tensile strength of a steel element	[N/mm^2]
$f_{u,b}$	Nominal ultimate stress of the bolt material	[N/mm^2]
$f_{y,b}$	Nominal yield stress of the bolt material	[N/mm^2]
G	Shear modulus of elasticity	[N/mm^2]
k	stiffness	N/mm
L_p	Length of fin plate	[mm]
n	Number of bolts rows	
P	Pitch between bolt row	[mm]
P_{bs}	Bearing strength of the plate	[N/mm^2]

S	Length of weld	[mm]
t_f	Thickness of the beam flange of an I or H section	[mm]
t_w	Thickness of the beam web of an I or H section	[mm]
t_P	The thickness of a fin plate	[mm]

Greek Letters

ϕ	The angle of rotation	[Rad.]
α_s	Thermal expansion coefficients of steel	[m/m°C]
θ	Temperature	[°C]
μ	Friction coefficient	
ν_s	Poisson's ratio	
Ω	Temperature dependent curve fit parameter	
ψ	Temperature dependent curve fit parameter	
Φ	Temperature dependent curve fit parameter	

ACKNOWLEDGEMENTS

First and foremost, I wish to give all the praise to Almighty God for giving me the strength and time to complete this research.

I am grateful to my supervisor Professor Ian Burgess for his encouragement, wisdom guidance and helpful advices, comments and suggestions. Professor Burgess introduced me to the research environment, supported me and believed in me throughout my postgraduate studies at the University of Sheffield.

I would like to express my sincere gratitude to Dr. Buick Davison for his extensive assistance, support, helpful advices and time that he devoted throughout this research. His encouragement has been significant.

I am deeply indebted to my parents, brother and sisters for their tremendous encouragement and support. I am grateful also to my wife, Marwa, and to my daughter Lana who have provided me with the inspiration.

My special gratitude also goes to all my friends for their warm friendship, support and for being there when I needed them.

I would like to express my thanks towards the sponsors of this project, the Engineering and Physical Sciences Research Council (EPSRC). Last but not least, I would also like to thank all the University staff, and, in particular, the staff in the Department of Civil and Structural Engineering.

DECLARATION

Except where specific reference has been made to the work of others, this thesis is the result of my own work. No part of it has been submitted to any university for a degree, diploma, or other qualification.

Marwan Sarraj

Chapter 1

Introduction and Thesis outline

1.1. Introduction & Overview

According to statistics there were about 4,416,000 fire incidents in the UK from 1986 to 1995, resulting in approximately 8,500 deaths, 145,000 injuries and financial losses of £7,500 million [1.1]. The collapse of the Twin Towers on September 11th 2001 caused almost 2,830 lives loss beside the great financial losses; making it the worst structural disaster in the world [1.2] in which strongly believed that the devastating effects of, simultaneous, multiple floor fires was major cause of the total collapse. However, although it is impossible to completely remove the risk of fire in a building, many ways already exist, and others are yet to be discovered, for minimising the numbers and damaging effects caused by fire.

Fire safety design has become an important aspect of any building design. Zhongcheng [1.3] has reported that the research on fire safety design started almost 80 years ago, according to his reference (Ingberg 1928) [1.4]. Today the concept of fire safety design has been improved significantly and become more rational. Recently, some real fire tests were conducted on full-scale eight storey unprotected composite steel framed building in the UK at Cardington [1.5 - 1.7] to evaluate the overall structural behaviour in fire. These tests demonstrated that appropriately designed building for fire safety can resist severe fires without collapse even if some of the main members are unprotected [1.5].

The following paragraphs are intended to give the reader a brief background of the key issues influencing the behaviour of a steel structural building in a fire. Then a more focused account of the objectives and the methodology of this research will be presented, followed by the thesis outline.

1.2. Natural Fire Behaviour

In order to understand the structural behaviour in a fire and provide active protection measures to avoid, primarily, any human loss and minimise properties damages, it is essential to have sufficient knowledge about the fire development phenomenon in a compartment. In general, fire is initiated by the combination of three main components; ignition, fuel, and oxygen, known as the fire triangle. Depending on the conditions in the compartment (opening size, fuel amount …. and so on), the accumulation of heat may ignite other existing flammable material, allowing for a fire to develop fully and spread rapidly. The typical development of a compartment fire can be divided into three phases: pre-flashover (known as the growth period), post-flashover (fully developed fire or burning period), and the decay period [1.8]. The temperature history during a fire is illustrated by the red time-temperature curve in **Figure 1.1** for a fire development inside a typical room, assuming no fire suppression by sprinklers or fire-fighters.

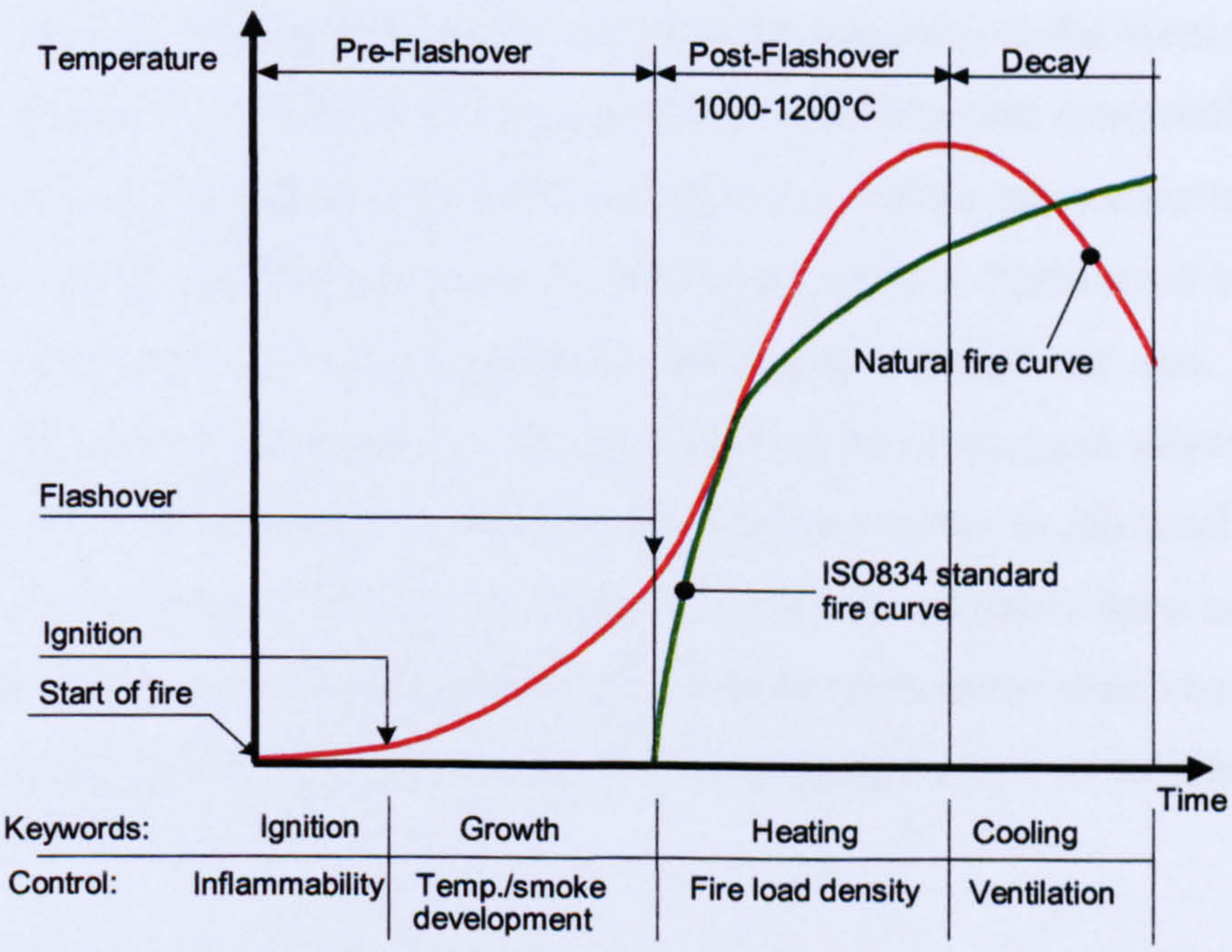

Figure 1.1 Natural fire phases compared with ISO834 standard fire curve [1.9]

a- Pre-flashover period

The pre-flashover stage starts with the ignition period (**Figure 1.1**), which is the start of flaming combustion. Any combustion is restricted to small areas of the compartment. Therefore, only localized rises in temperature occur which may still be considerable. The overall or average rise in temperature within the bounded fire

compartment will be very small and indeed at this stage there may be no obvious signs of a fire. In this stage the chance of escape is relatively high and the risk to life is very low. Additionally, if the fire is put out, the damage to the structure is relatively low. Active measures, such as fire detection devices, fire extinguishers and sprinklers, have an essential role in fighting the fire at this stage.

The growth period (**Figure 1.1**) is not a significant influence on the structure but it is important for evacuation of the occupants and for the fire-fighters to overcome the fire before get to the flashover point. In the growth period, most fires spread slowly at first on combustible surfaces, then more rapidly as the fire grows, providing radiant feedback from flames and hot gases to other fuel items. It should be noted that the rate of burning in the growth period is generally controlled by the nature of the burning fuel surfaces, and in many cases it is human intervention which causes flashover by for example opening a door or window and thereby suddenly increasing the air supply. If the upper layer temperatures reaches about 600°C, the burning rate increases rapidly, leading to flashover which is the transition to the burning period or the transition from a localized fire to combustion of all exposed combustible surfaces in a room and the fire spreads to all the available fuel within one compartment. There are certain pre-conditions necessary for flashover to occur. There must be sufficient fuel and ventilation for a growing fire to develop to a significant size. The ceiling must be able to trap hot gases, and the geometry of the room must allow the radiant heat flux from the hot layer to reach critical ignition levels at the level of the fuel items. However, once a fire hits the flashover point fire-fighters have no control in putting the fire out in the region where the fire initiated, rather their concern should focus on stopping the fire from spreading to the adjacent floors or buildings until the fire dies out [1.8, 1.9].

b- Post-flashover period

This stage is the burning period, where the temperatures and radiant heat flow within the compartment are so great that all exposed surfaces are burning and the rate of heat release within the compartment reaches a peak usually governed by the available ventilation. In compartment fires, maximum temperatures of over 1000°C are possible. The rate of temperature rise continues until the rate of generated

volatiles from the fuel bed begins to fall below the rate of fuel consumption, or when there is insufficient heat available to generate such volatiles.

It is during the post-flashover or burning period that structural elements are exposed to the worst effects of the fire, which impacts on structural elements and compartment boundaries and collapse or loss of integrity is expected. Once the rate of temperature rise reaches a peak, the fire continues into its decay phase [1.9].

c- Decay period

If the fire is left to burn, finally the fuel burns out and temperatures drop in the decay period. In this stage, the rate of burning again becomes a function of the combustible material itself rather than the ventilation. The temperature in the compartment starts to decrease as the rate of fuel combustion decreases. It should be noted that owing to thermal inertia, the temperature in the structural elements will continue to increase for a short while in the decay period, so there will be a time delay before the structure starts to cool [1.9].

1.3. Standard Fire and Fire Test

In 1928, Ingberg introduced the fire load concept [1.10] which is defined as the weight of wood with a heat content equivalent to that of the combustible material per unit floor area of a building or a fire compartment [1.11]. Natural fire in a compartment is a complex phenomenon which varies according to its surrounding conditions. For testing purposes it is convenient to have a standard time-temperature carve for a fire to allow comparison of different structural member performance in a standard heating environment for regulation purposes (but note this does not represent what happens in a real building fire). Therefore, a standard fire gas time-temperature, the green curve shown in **Figure 1.1**, has been adopted internationally and is given in the International Standard ISO 834 [1.12] and also in the BS 476: Part 20 [1.13]. This standard fire is described in the following relationship:

$$T - T_0 = 20 + 345 \log_{10}(8t + 1) \qquad \textbf{(1.1)}$$

T : is the furnace temperature in °C at time t,

T_0 : is initial furnace temperature in °C at time t,

t : is time in minutes,

The distinction between a natural fire curve and the standard time-temperature relationship is that the growth and decay phases are neglected in the standard fire curve. In addition, the ISO standard fire was based on an assumption that the fire severity is independent of the fire load, which is an oversimplification assumption [1.10]. In reality, the severity of a fire depends on several issues, such as the ventilation, fire duration, burning rate, compartment size, thermal properties of walls, ceiling and floor material, and mass of non-combustible material [1.13, 1.14].

Internationally, the fire resistance assessment and design of a structural member is still based on the standard fire test. The fire resistance of an element is defined in BS 4422: Part 1 [1.15] as the ability of a structural element in a building to withstand the effects of fire for a specified period of time without the loss of its fire-separating or load-bearing functions. This period is obtained when the structural member reaches its defined failure criteria. According to BS 476: Part 20 [1.13], failure is considered for a beam element when either a maximum deflection of $L / 20$, or a rate of deflection [mm/min] $L^2/9000d$ (where L is the beam span and d is the beam depth) is exceeded. However, this deflection rate shall not be applied before a deflection of $L/30$ is exceeded. Whereas, in the case of column specimens, the failure is considered to have occurred when the applied load can no longer be supported.

A large number of fire tests on isolated elements [1.16, - 1.18] have been conducted and there is agreement that the behaviour of an element in a real building is significantly different from that in standard furnace testing. These differences are associated with the thermal restraint and thermal interaction between different construction materials, or composite action. Standard fire tests also illustrate their limitation by raising a number of issues; the effect of the member cross-sectional size, span (which is controlled by the furnace size), restraint and structural configuration cannot economically be investigated in full. In addition, the cost of standard tests is found to be extremely high. However, furnace testing using the standard fire curve is a traditional means of assessing the structural elements in a fire, since routine testing of a full-scale structure in a real fire is impractical and extremely costly. An eight-storey composite steel-frame building, designed for the Building Research Establishment (BRE), was tested in six real fires at the Cardington Large Building Test facility [1.5 - 1.7]. Following this test programme, further research is continuing to

investigate whole-frame and structure behaviour under real fires, in order to develop design guidance and design tools which will account for the overall behaviour of the structure in fire conditions, requiring less applied protection and possibly greater use of active fire safety measures.

1.4. Steel Properties at Elevated Temperature

Steel is used in construction of buildings because of its principal advantages of light weight, high strength, and good ductility. Steel mechanical properties are described mainly by the stress-strain relationship. This relationship for a standard specimen under tension stresses and at ambient temperature is well-established and illustrated in (**Figure 1.2**).

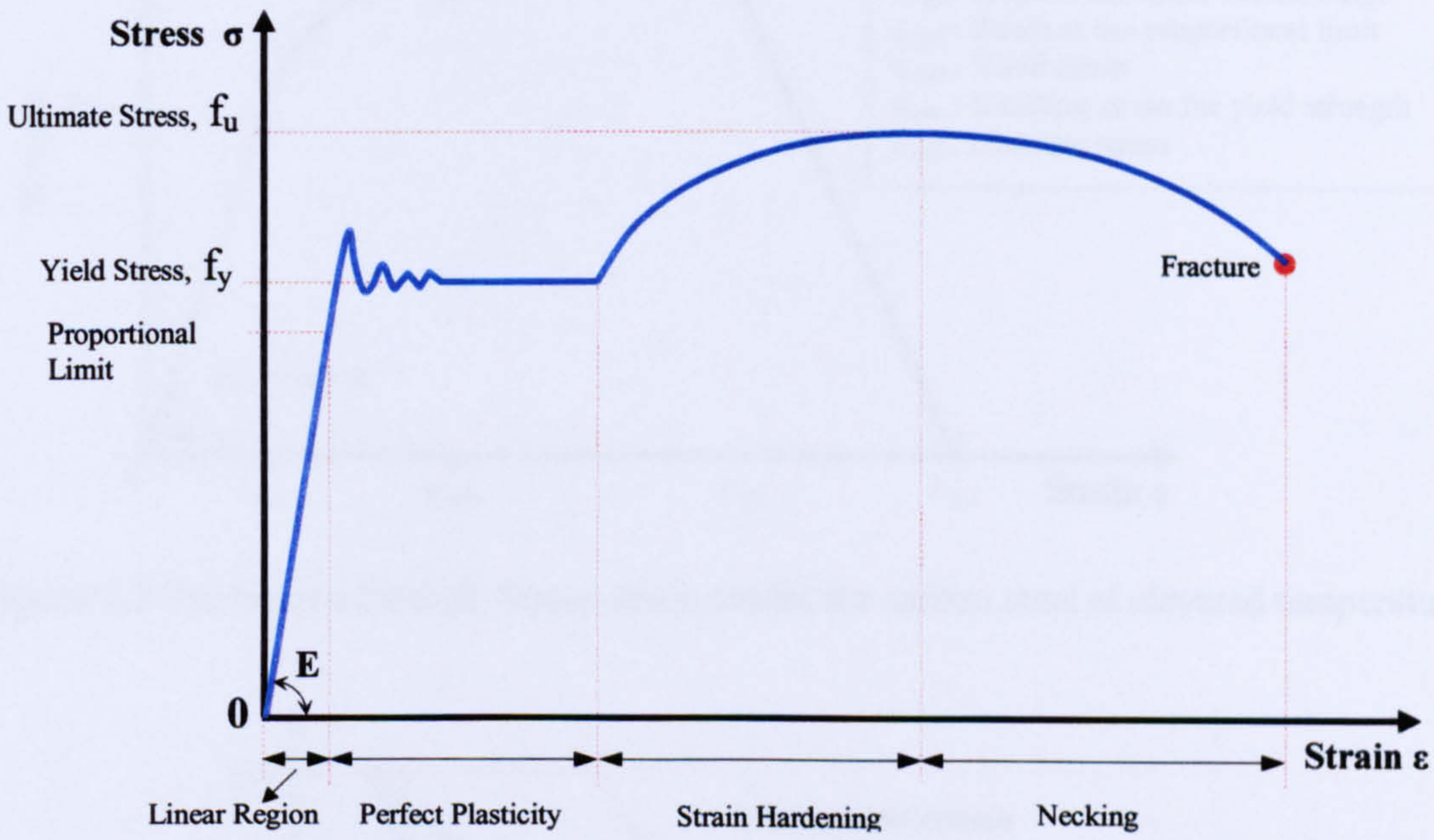

Figure 1.2 Stress-strain relationship for carbon steel at ambient temperatures

However, unprotected steel members have the disadvantage that steel performs relatively poorly if exposed to a fire compared with other construction materials. Due to its high thermal conductivity, it suffers a progressive loss of strength and stiffness when exposed to a fire. This phenomenon may cause possible excessive deformation in structural elements and lead to failure, depending on the applied loads, the support conditions and the fire severity. The increase in steel temperature depends on the severity of the fire, the area of steel exposed to the fire and the amount of applied fire protection. Although the melting point of steel is about 1500°C, only 23% of the

ambient-temperature strength remains at 700°C, whereas, at 800°C strength this reduces to 11%, and at 900°C to just 6% [1.9].

EC3: Part 1.2 [1.19] describes the stress-strain curve for carbon steel at elevated temperature (**Figure 1.3**). Reduction factors (**Figure 1.4**) based on test results are introduced for yield strength, proportional limit and the Young's modulus, in order to describe the stress-strain relationships at elevated temperatures (**Figure 1.5**). For temperatures below 400°C (**Figure 1.5**), strain-hardening may also be considered provided local or overall buckling does not occur, according to annex A of EC3: Part 1.2 [1.19].

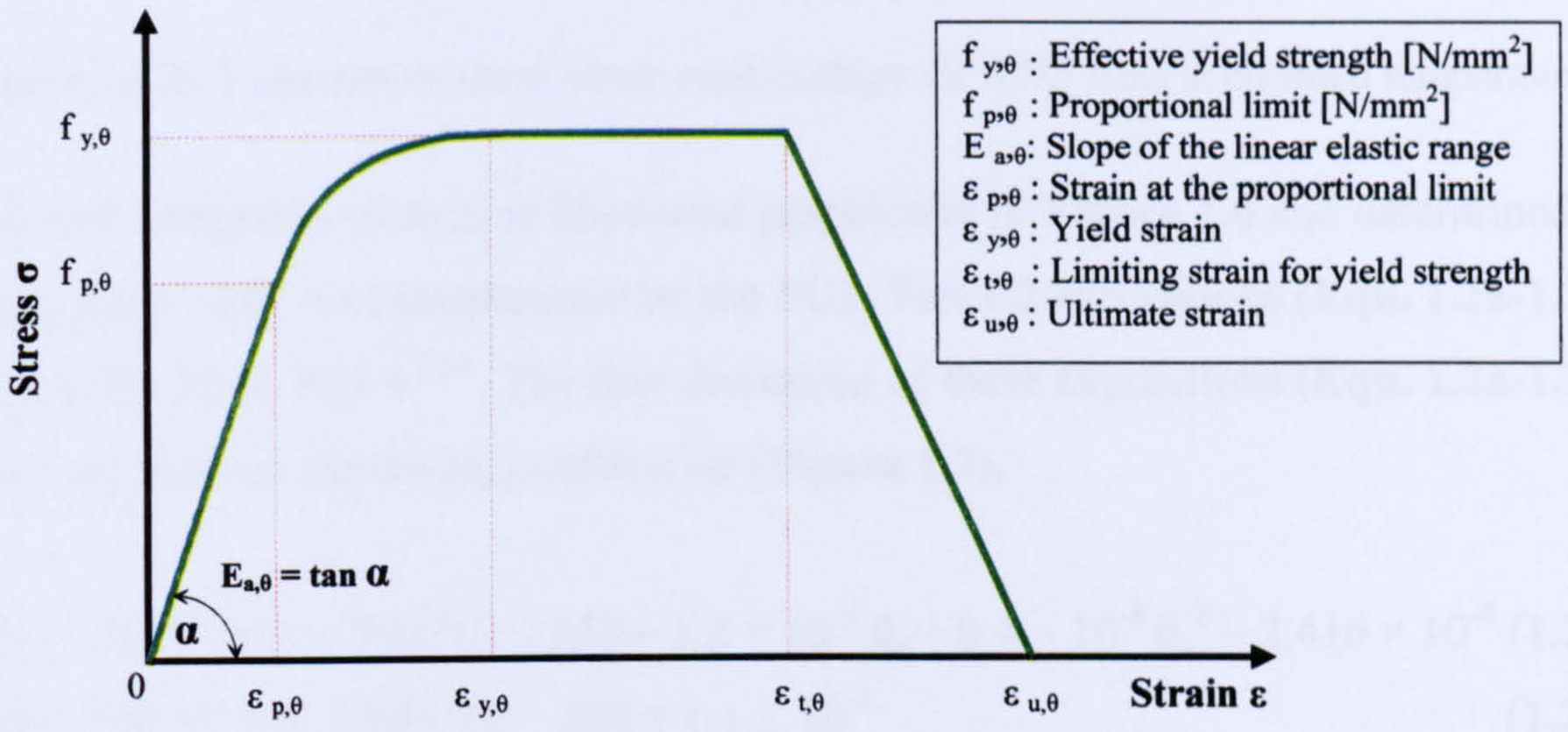

Figure 1.3 Tri-linear-elliptical Stress-strain model for carbon steel at elevated temperatures

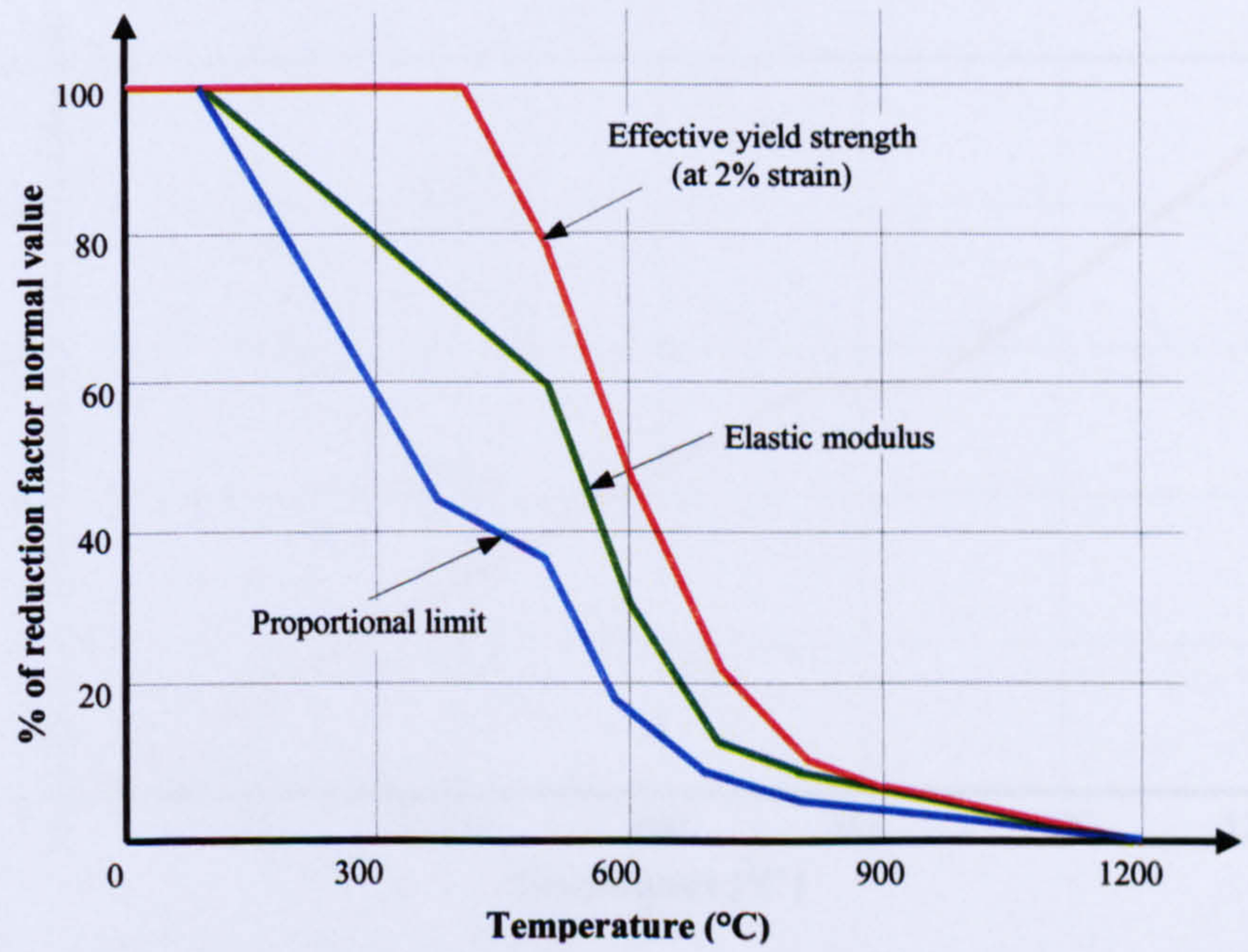

Figure 1.4 Reduction factors for stress-strain curve of carbon steel at elevated temperatures

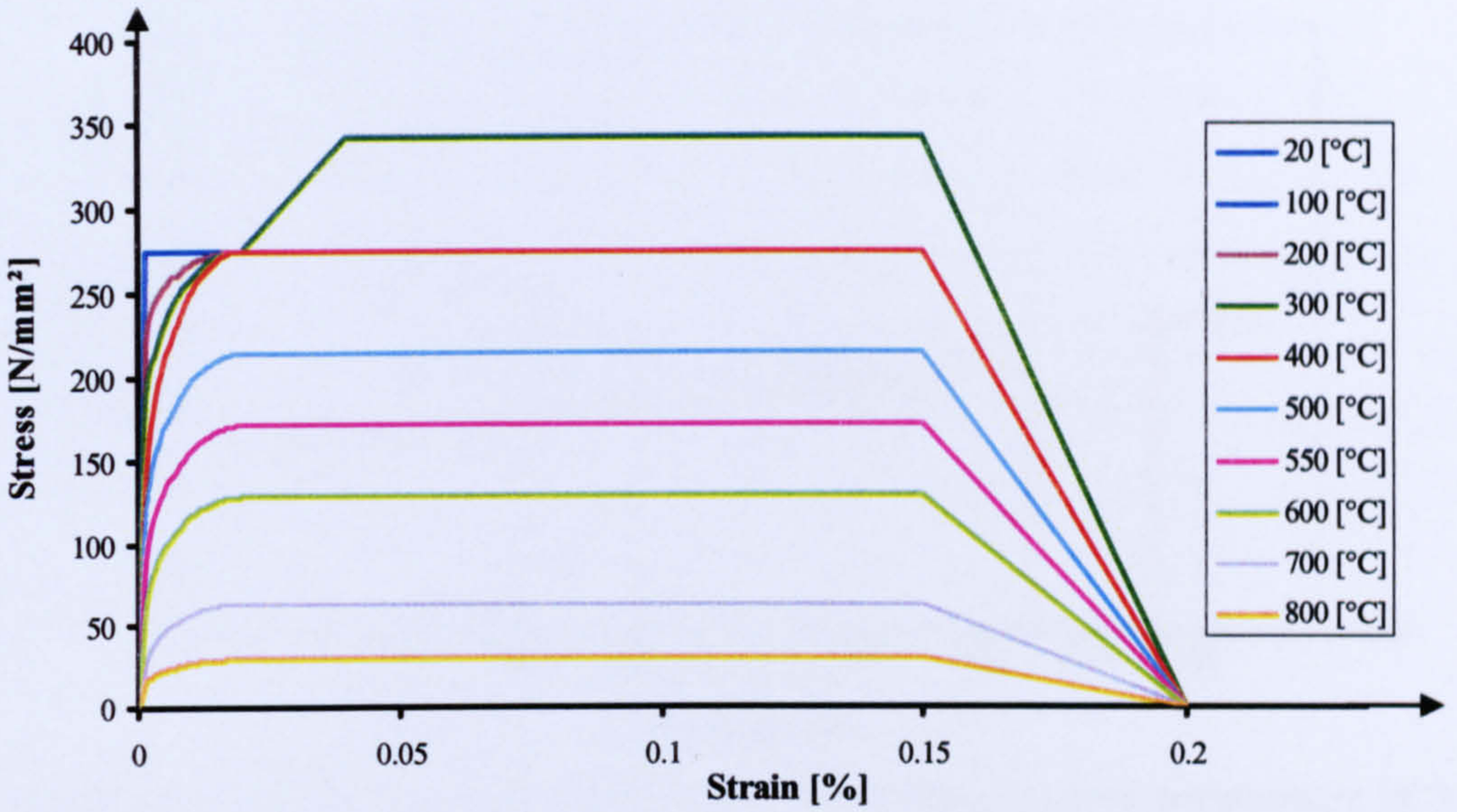

Figure 1.5 EC3 alternative stress-strain relationships for S275 steel at elevated temperatures

Thermal elongation of steel is illustrated graphically in **Figure 1.6** and determined in conjunction with steel temperature by the EC3: Part 1.2 expressions (**Equ. 1.2a-1.2c**) and by BS 5950: Part 8 [1.20]. The first derivative of these expressions (**Equ. 1.2a-1.2c**) gives the thermal expansion coefficients (**Figure 1.7**).

- For $20\ °C \leq \theta_a < 750\ °C$ $\quad \Delta l/l = 1.2 \times 10^{-5}\ \theta_a + 0.4 \times 10^{-8}\ \theta_a^2 - 2.416 \times 10^{-4}$ **(1.2a)**
- For $750\ °C \leq \theta_a \leq 860\ °C$ $\quad \Delta l/l = 1.1 \times 10^{-2}$ **(1.2b)**
- For $860\ °C < \theta_a \leq 1200\ °C$ $\quad \Delta l/l = 2 \times 10^{-5}\ \theta_a - 6.2 \times 10^{-3}$ **(1.2c)**

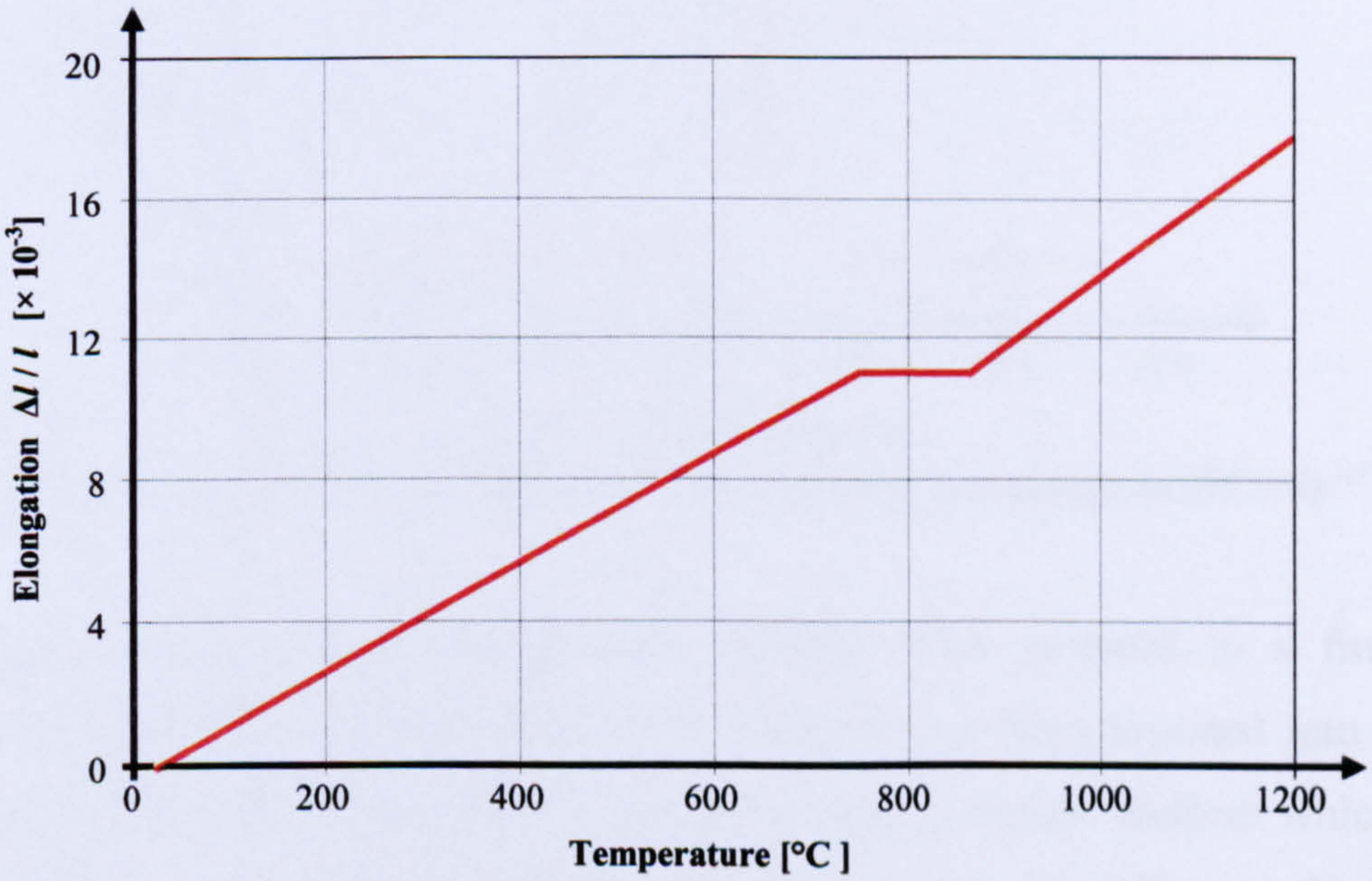

Figure 1.6 Thermal elongation of carbon steel as a function of the temperature [1.9]

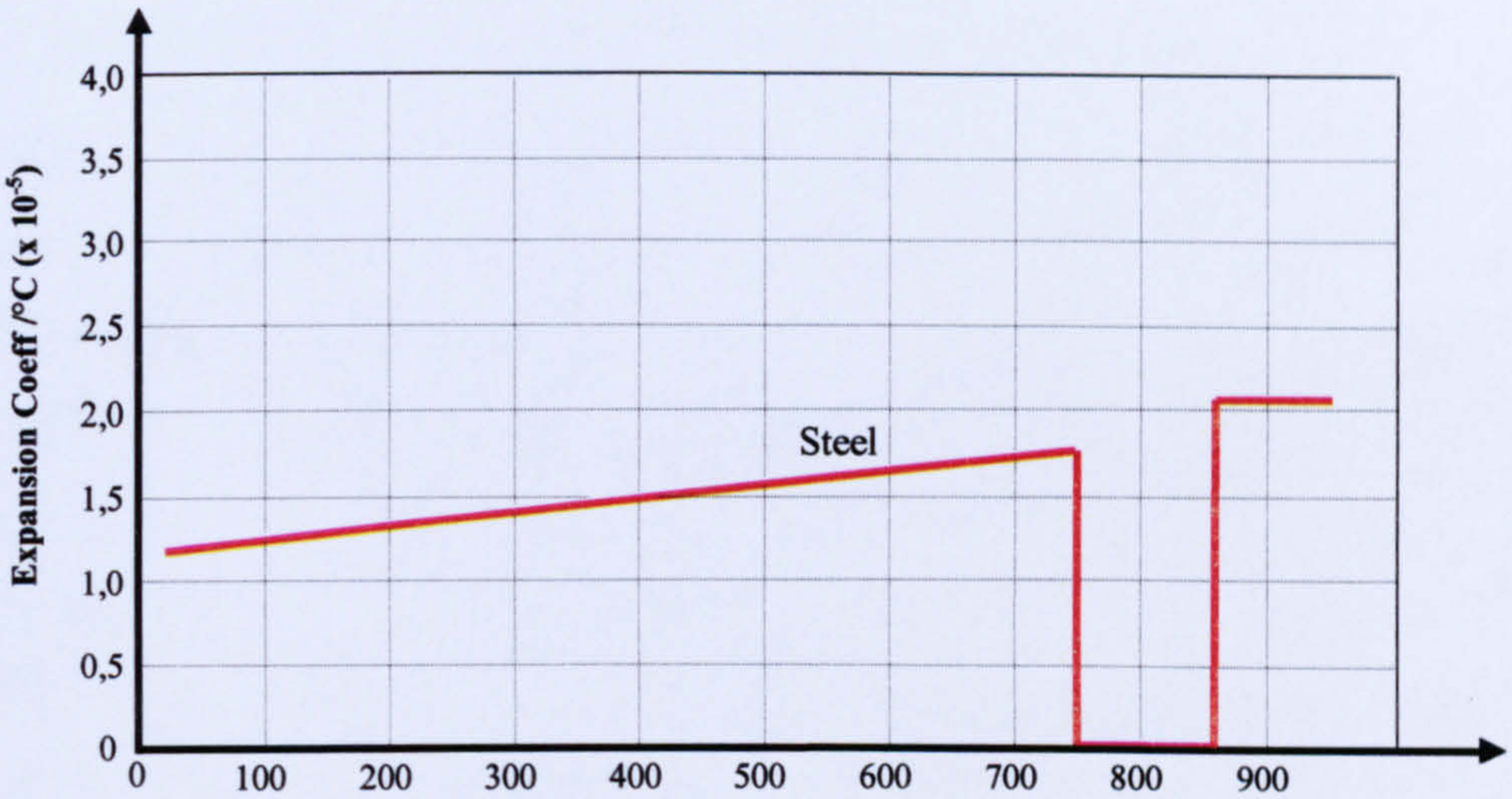

Figure 1.7 Thermal expansion coefficients of steel variation with temperature EC3/4 [1.9]

Specific heat capacity is the measure of the heat energy required to raise the temperature of one kg of steel by one degree Kelvin [1.8] (A Kelvin is a unit increment of thermodynamic temperature and is equal to an increment of one degree Celsius). The variation of specific heat (**Figure 1.8**) with steel temperature is defined in EC3: Part 1.2.

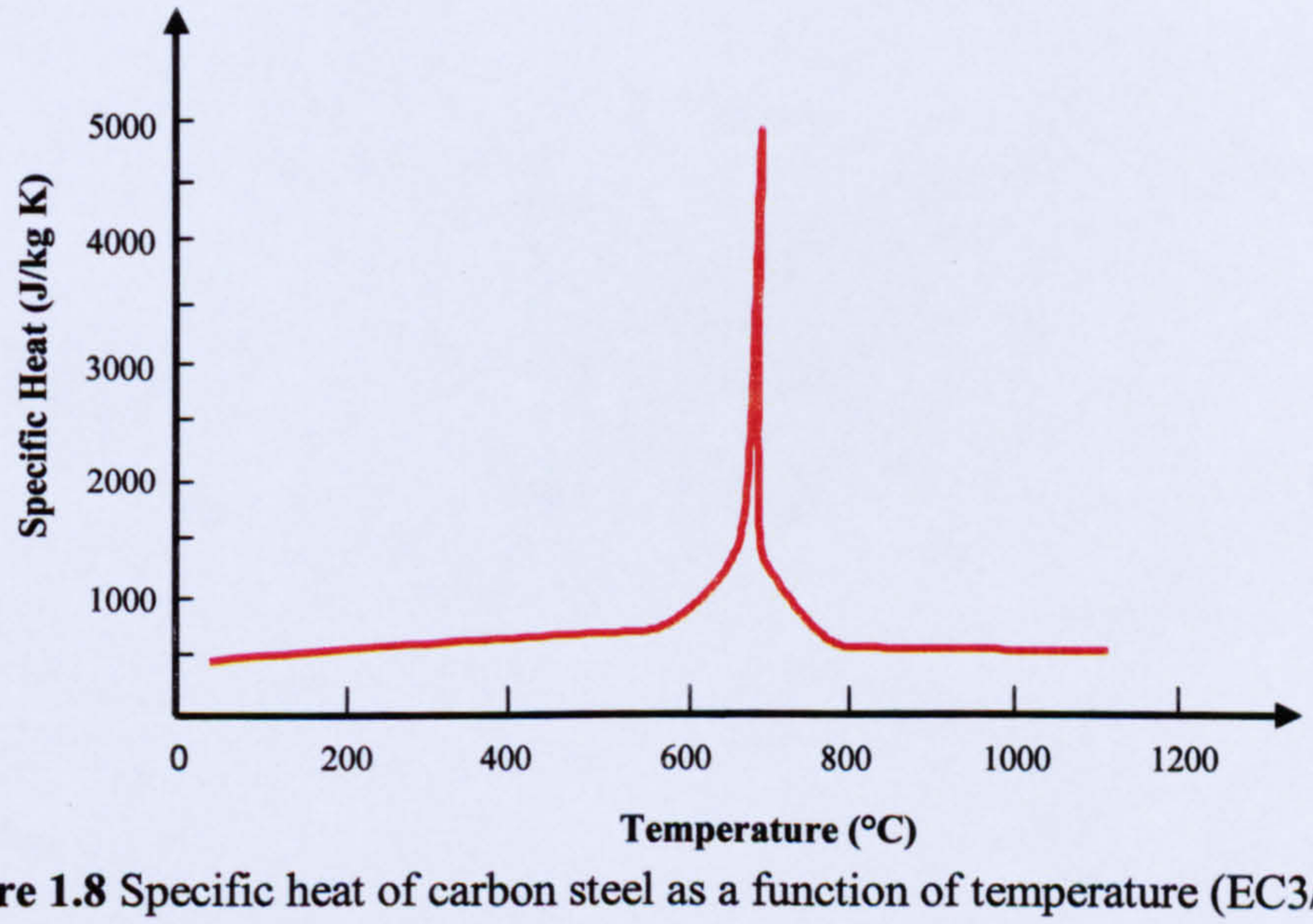

Figure 1.8 Specific heat of carbon steel as a function of temperature (EC3/4) [1.9]

Steel's progressive loss of strength and stiffness when exposed to a fire was recognised quite early, and therefore much research has been invested into either providing better protection materials or developing a design method which can minimise the use of protective material and, eventually, the overall cost of building construction.

1.5. Beam Behaviour and Catenary Action

As stated above, steel members tend to lose strength and stiffness at high temperature. In addition, all beams in steel structures, including beams designed as simply supported, experience a certain degree of axial and rotational restraints at their ends. Beam internal forces are strongly related to the degree of end restraint and beam temperature. End restraints generate axial force and moment within the supported member at elevated temperature. At the initial stage of a fire (100°C - 400°C), a steel beam starts to experience compressive internal forces due to the restraint to thermal expansion and it starts to bow towards the fire. When the beam temperature gets to 400°C, at which point steel begins to lose its strength. the beam internal force begins to turn from compression into tensile force, and then the connections begin to support the steel beam by resisting pull-in forces as well as vertical shears. Thus, at the advanced stage of a fire, a steel beam hangs as a suspension cable from the cooler end connections. Such a phenomenon is called "Catenary Action" (**Figure 1.9**).

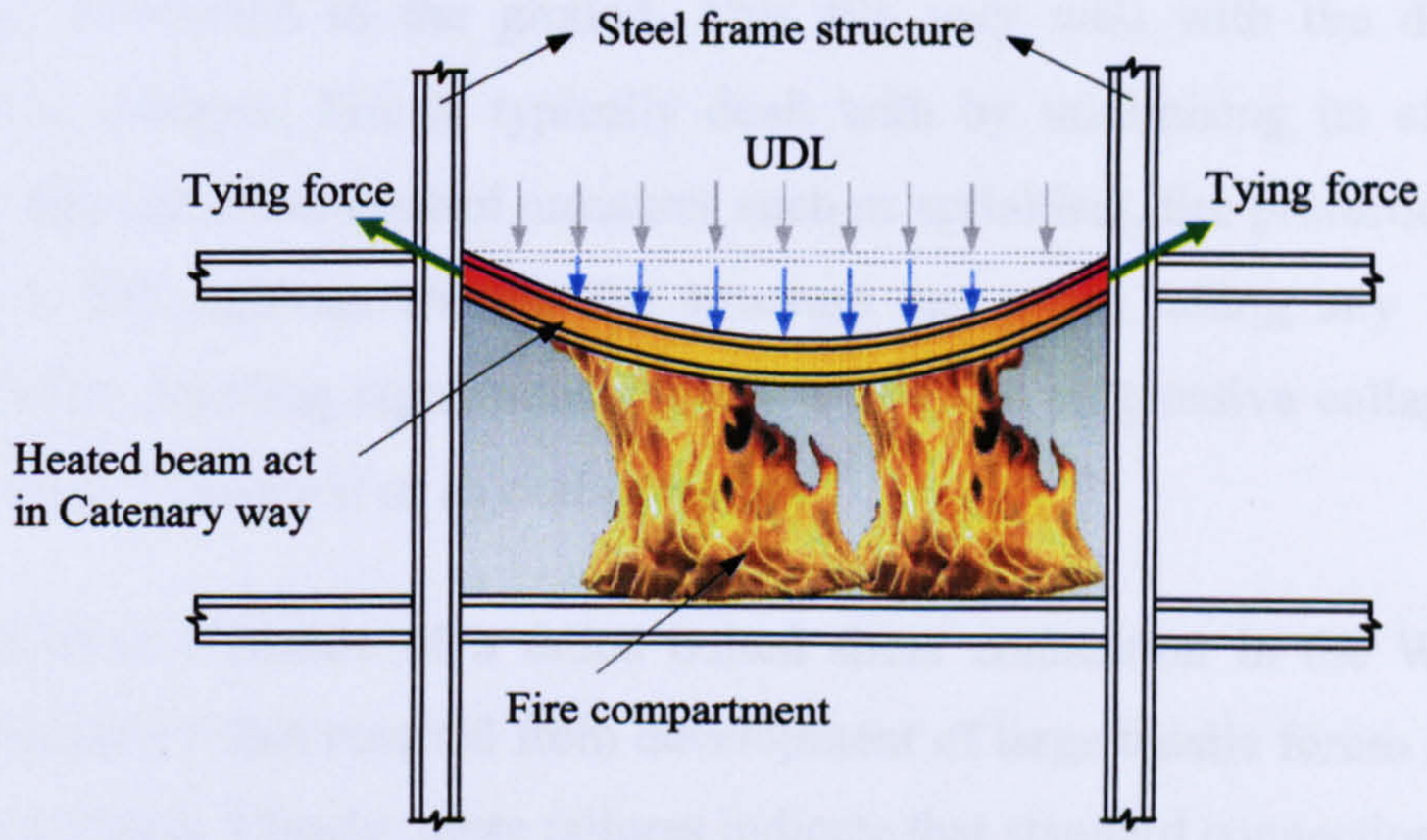

Figure 1.9 Steel beam under fire acting as a suspension cable in catenary way

Consequently, providing the end connections' resistance still exists, the tensile horizontal axial force grows progressively, as the beam mid-span deflection grows. Furthermore, beam end connections are required to resist an additional moment, resulting from rotation due to excessive mid-span deflections. This leads to reductions in the beam mid-span moment. In essence, the behaviour of the beam is affected by the connections' ductility and stiffness. In this manner, catenary action

helps the beam by reducing the mid-span moment and it hangs from the cooler connections which need to sustain the tensile axial force of the beam and prevent the collapse. Therefore, Catenary Action works to improve the survival time of steel beams in fire, provided that the beam end connections still function [1.21].

1.6. Fire-Induced Progressive collapse

Progressive collapse is the collapse of a building due to a failure of a single vertical load carrying element, or a small number, which are disproportionate to the complete building failure. Obviously, element failure could occur as a result of any of several extreme loading events on buildings, including strong earthquakes, blast, vehicle impact, fire, or similar incidents. In the Twin Towers disaster, the local damage from the aircraft impacts was enhanced by high-temperature effects due to an intense fire within the building [1.22]. The structure near the impact zone lost its ability to support the load above it as a result of the combination of impact damage and fire damage. Therefore the structure above the impact zone collapsed, and the weight and the impact of the collapsing upper part of the towers caused a sequence of failure extending downward to the ground. This fits very well with the definition of progressive collapse. Fire is typically dealt with by minimising its effect on the structure through event-control measures such as sprinklers, fire protection materials and active fire fighting, so that the structure can avoid taking any fire effects. Consequently, building regulations attempt to prevent progressive collapse induced by the heat of a fire itself or any other means.

Figure 1.10 is a picture of a failed bolted shear connection in the World Trade Centre Building 5 that resulted from development of large tensile forces in the beam due to fire effects. Clearly, these failures indicate that standard connection types used in steel framing may not be capable of allowing the structure to develop the large inelastic rotations and tensile strains necessary to resist progressive collapse through large deformation behaviour. However, the Cardington fire tests [1.5] illustrate that a standard steel building can be designed and constructed to provide sufficient ductility (deformation capacity) and toughness to withstand large fires. Although it should be noted that even though the building withstood the fire some connections, like the fin plate beam-to-beam steel connection, failed via bolt shearing in Cardington test No.7.

Figure 1.10 Internal collapsed area in WTC 5 with close up of shear connection failure at tree column [1.2].

The two main design approaches adopted to eliminate progressive collapse are either to ensure that tying force requirements [1.23] are met, or to bridge the load over damaged members. The performance of connections is crucial for achieving both approaches. Therefore, "the performance of the connections in steel structures is important for the building's overall stability and often determines whether a collapse is localized or leads to progressive collapse. Thus, the issue of connection performance under fire exposure is critical to understanding building performance and should be a subject of further research" (quotation from the FEMA report [1.2] on the WTC disaster).

1.7. Connection Behaviour and Structural Integrity

Beam-to-column joints in structural steel buildings transfer the floor and beam loads to the columns, and provide the link between the principal structural elements for the overall structural stability. By this means, the forces transmitted through the joints can be axial and shear forces, bending and torsional moments. The effect of torsion on individual members can be neglected in plane frames, as a result of the lateral restraint provided by composite action with floor slabs. Nevertheless, the magnitudes of the other three actions transferred by the connections to the supporting columns depend on the connection type and the surrounding conditions. In the case of steel frame structures with moment-resistant connections, such as bolted end plates, the bending moments are predominant compared to axial and shear force. In contrast, the

use of shear connections, such as fin plates, would make the shear force dominant compared to axial force and bending moment. Also these actions are greatly influenced by unusual circumstances such as an earthquake or a severe fire. An expected severe fire incident would subject the structure to a complex load combination; the axial forces are most likely to be serious, and sometimes dominant. As illustrated above, the large mid-span deformations are induced in beam elements during the stage of a fire when unprotected steel beams lose strength. In the case of simple shear joints, the end joints are forced to provide two unusual kinds of reaction, against tensile catenary action, and against the induced rotations or end moments. Theses end moments provided by the joints reduce the mid-span moments in the beams, by this means improving the load-carrying capability and fire resistance of a nominally simply supported beam, as long as the ductility of the connections is preserved.

Therefore, due to the fact that connections are the only parts of the structure which make the whole assembly of structural members interact and work with each other, the performance of the structural members under high temperatures is greatly influenced by the connections' reliability (inductility and strength), whether these members are exposed or unexposed to the fire. In other words, significant ductility of the connection is required so that, under fire conditions, a reliable deformation of the floor's beams can be achieved prior to failure, such that it is not forestalled by 'brittle type' failure. Accordingly, the design of beam-to-column connections should allow for certain ductility and high tensile forces. Basically, the greater the connection's ductility and capacity to accommodate the induced force, the greater is the beam's survival time in a fire. The question is "how much ductility the connection can take, or should accommodate, to avoid failure or total collapse in a fully-developed fire and how can be this ductility achieved?"

The answers to these questions depend on several factors and issues, such as the type of joint, joint geometry, material properties of its parts, material properties of the supported beams, the profile of temperature across the floor and so on. Research is still underway in different parts of the world in order to address these issues, for better understanding of steel connection behaviour.

1.8. Scope of Research

Structural steel joints, mainly bolted and welded, are a crucial part of any structural steel building. Understanding the connections' actual response and analysing their complex behaviour has been approached frequently in different ways and by different methods, starting from experimental tests and moving on to numerical Finite Element Analyses (FEA). The intensive use of these two typical methods in investigating connection behaviour has led to the development of a simpler approach, the so-called "Component Method", by which connection behaviour and capacity can be described and predicted.

Several research investigations have conducted to explore the behaviour and the tolerance of steel connections at elevated temperature. Nevertheless, this research has been focused mainly on rigid or semi-rigid connections. In contrast, very limited information has been revealed about simple shear connections in fire conditions. This finding will be observed clearly in the subsequent literature review in chapter 2. For this reason the current research has given priority to the investigation of fin plate shear connections in fire conditions.

This research aims to describe generally the behaviour of the bolt bearing and bolt single shear phenomenon in steel shear joints, along with the behaviour of fin plate shear connections. Additionally, exploring the connection tying capacity is an important objective, since the theme of structural robustness and progressive collapse has become the main worry of the structural community in recent years. However, connection mechanical spring models, using the Component Method approach, also warrant attention, because of the great time saving offered in the global structural analysis. Such a method can describe the load-displacement and the moment-rotation response for any given connection, whatever the geometric detail, material properties or temperature of the joint parts. Consequently, the two main connection properties, strength and stiffness, will be recognizable. Development of a connection component model for steel fin plate connections was adopted as a further objective of the current study. For this purpose, the components of a bolt in single shear, a plate in bearing and friction were investigated and described in detail, as they are the three main model components for a fin plate shear connection.

Research conducted on steel joints involves parametric investigation. Such investigations require an active and flexible tool that can fulfil this demand with respect to the time and cost. Laboratory experiments, though reliable, have practical limitations and a well-prepared finite element model (FEM) forms an alternative tool. Therefore, the current research relies on the ABAQUS finite element code for conducting this research, in conjunction with existing test data, for the purpose of the FEM evaluation.

The research presented here has focused on investigating the behaviour of fin plate shear connections in fire conditions. The creation of a reliable FE model to complement existing test results was a primary aim at the starting point of the research. This FE model would form the main source of information, and would be of great benefit by allowing a wider-ranging parametric study to be conducted than would be possible in a laboratory environment. Additionally, the FE analysis results would enable a reliable simplified component model to be developed and validated. Such a simplified model would be in demand for design/analysis software, with a great saving in terms of computing time. Eventually, the FE model and the component model will be used to gain insight into important issues such as the connection tying force capacity of a fin plate at ambient and elevated temperatures, plate bearing, and bolt shearing behaviour.

1.9. Thesis Outline

This thesis is divided into eight chapters. The following is a brief outline of the major topics covered in each chapter:

• **Chapter 1** has give a general introduction about the research background and the thesis scope and outline.

• **Chapter 2** Contains an extensive literature review that gives a general introduction to steel connections, then focuses on describing research which pertains to fin plate shear connections. Research on steel connection in fire conditions is highlighted. A progression of knowledge and research will be presented, from some of the earliest research to the most recent research. Focus is particularly placed upon connections subjected to combined static and fire loading.

• **Chapter 3** presents and describes in detail the development of an accurate finite element model (FEM), using ABAQUS of fin plate connections and shear connections in general. Great importance was given to the evaluation of this model, since it is subsequently used as a tool for further analyses in this research.

• **Chapter 4** contains intensive ambient-temperature investigations on single shear, represented by a steel lap joint to simplify description of single shear. In addition, this chapter explores the tying force capacity of fin plate shear connections.

• **Chapter 5** describes the modification made to the FEM so that it can be used in the investigation of fin plate connections and large deflection behaviour of the supported steel beams at elevated temperatures. Intensive evaluations of this model were conducted against existing test data and well-known analytical models. A particular emphasis is put on the behaviour of axially restrained steel beams in catenary action.

• **Chapter 6** presents an investigation of the application of component method approach to fin plate shear connections at ambient and elevated temperatures. Parametric studies on major connection parameters are conducted using the finite element model. The essential components of shear connections (bolt shear, plate bearing, and friction) are described. Finally, a mechanical spring model of fin plate shear connections is proposed and validated.

• **Chapter 7** presents studies of application of the component model at elevated temperature, and evaluations against FEM. These studies have contributed to better understanding of connection behaviour and resistance at elevated temperature.

• **Chapter 8** gives a review of the work carried out in this thesis. In addition, a summary of the main conclusions from this research are stated. Finally, the necessity for future related research is discussed.

• **Appendix A:** Includes all the FE models associated with convergence testing.

• **Appendix B:** Includes all the FE models associated with the fin plate connection tying resistance investigations at ambient temperature.

• **Appendix C:** Includes all the FE models tying resistance investigations at elevated temperature.

1.10. References

[1.1] IMechE (The Institute of Mechanical Engineers) (1997), "Management of Fire and Explosion", IMechE Conference Transactions.

[1.2] FEMA (Federal Emergency Management Agency) (2002), "World Trade Center Building Performance Study: Data Collection, Preliminary Observations, and Recommendations", Greenhorne & O'Mara, Inc.

[1.3] Zhongcheng Ma, "Fire safety design of composite slim floor structures", PhD. Thesis, Department of Civil and Structural Engineering, Helsinki University of Technology, 7th of December, 2000.

[1.4] Ingberg, S.H., "Tests of the Severity of Building Fires," *Quarterly of the National Fire Protection Association*, Vol. **22**, No. 1, July (1928) pp 43-68.

[1.5] Newman, G. M., Robinson, J. T., Bailey, C. G., "Fire Safety Design: A New Approach to Multi-storey Steel Framed Buildings SCI Publication 288", The Steel Construction Institute, (2000).

[1.6] Bailey, C. G., Newman, G. M., Simms, W. I., "Design of steel framed buildings without applied fire protection", The Steel Construction Institute P186, (1999).

[1.7] Lennon, T., "Cardington fire tests: survey of damage to the eight storey building", Building Research Establishment, Paper no. 127/97, Watford, (1997) p 56.

[1.8] Andrew, H. B., "Structural Design for Fire Safety", England, (2001).

[1.9] SSEDTA, Lecture 11a: Introduction to Structural Fire Engineering, (2001).

[1.10] Uddin, T. A. and Culver, C. G., "Effects of Elevated Temperature on Structural Members" *Journal of the Structural Division*, Vol. **101**, No. 7, (1975) pp 1531-1549.

[1.11] Saab, H.A., "Nonlinear finite element analysis of steel frames in fire", PhD. Thesis, University of Sheffield, 1990.

[1.12] ISO834:"Fire Resistance Tests, Elements of Building Construction", (1975).

[1.13] BS 476. "Fire Tests on Building Material and Structure, Part 20: Methods of Determination of the Fire Resistance of Load-bearing Elements of Construction". London: British Standard Institution (BSI); (1987).

[1.14] Lie, T. T., and Stanzak, W. W., "Structural steel and fire more realistic analysis" *Engineering Journal*, AISC, (1976), Second quarter.

[1.15] BS 4422. "Glossary of Terms Associated with Fire, Part 1: General Terms and Phenomena of Fire". London: British Standard Institution (BSI); (1979).

[1.16] Ellingwood, B., and Lin, T. D., "Flexure and shear behaviour of concrete beams during fires" *Journal of the Structural Engineering*, ASCE, **117** (2), (1991) pp 440–458.

[1.17] Wainman, D.E. and Martin, D.M., "Preliminary Assessment of the Data Arising from a Standard Fire Resistance Test Performed on a Slim Floor Beam at the Warrington Fire Research Centre on 14th February, 1996" Technical Note, SL/HED/TN/S2440/4/96/D, British Steel Swinden Technology Centre, March 1996.

[1.18] Ali, F., O'Connor, D. J., Simms, W. I., Randall, M., Shepherd, P. G. and Burgess, I. W., "The Effect of Axial Restraint on the Fire Resistance of Steel Columns", Second World Conference on Constructional Steel Design, San Sebastian, *J. Construct. Steel Research*, **46:1-3**, Paper No. 71 (1998).

[1.19] European Committee for Standardization (CEN), "Eurocode 3: Design of Steel Structures, Part 1.2: General rules - Structural fire design", EN 1993-1-2, British Standard Institution, London, (2005).

[1.20] BS 5950: "Structural Use of Steelwork in Building, Part 8: Code of Practice for Fire Resistance Design", British Standard Institution (BSI), London (1990).

[1.21] Allam, A.M., Burgess, I.W. and Plank, R.J., "Performance-Based Simplified Model for a Steel Beam at Large Deflection in Fire", Proc. 4th International Conference on Performance-Based Codes and Fire Safety Design Methods, Melbourne, Australia, (2002).

[1.22] Bazant, Z.P., and Zhou, Y., "Why did the World Trade Centre collapse? - Simple analysis", *Journal of Mechanics*, ASCE Vol. **128**, Issue 1, (2002) pp 2-6.

[1.23] BS 5950: "Structural Use of Steelwork in Building, Part 1: Code of Practice for Design - Rolled and Welded Sections", British Standard Institution (BSI), London (2000).

Chapter 2

Literature Review

2.1. Introduction to Steel Connections

Steel connections are an important part of any steel building. They provide the strong links between the other principal structural components, and contribute to overall building stability. Early steel connections were fabricated using rivets, but these have seldom been used since the 1950's. Today steel connections are fabricated mainly using bolts or welding. The behaviour of the connection region of a structural frame is complex because of the wide range of parameters involved. Based on that, much research conducted in the past, and research still underway has attempted to improve understanding of steel connection behaviour and design methods. According to Morris [2.1], the research on the behaviour of steel beam-to-column connections started as early as 1917, when Wilson and Moore [2.2] conducted tests on riveted connections. Since then numerous investigations into the behaviour of beam-to-column connections have been reported during the past eighty years [2.3-2.5]. However, there are many different types of steel connections, of varied configuration and flexibility, and the following paragraphs will briefly review the most commonly used steel connections.

2.2. Steel Connection Types and Configuration

Classic structural analysis has always distinguished between two types of Steel connections that are either pin connections (non-moment resistant) or moment connections (with full-moment resistance). This theoretical assumption has been questioned by experimental investigations on various steel connection types [2.3-2.5] which have demonstrated that all connections, even those which are considered as pinned, have some capacity to resist end beam moments.

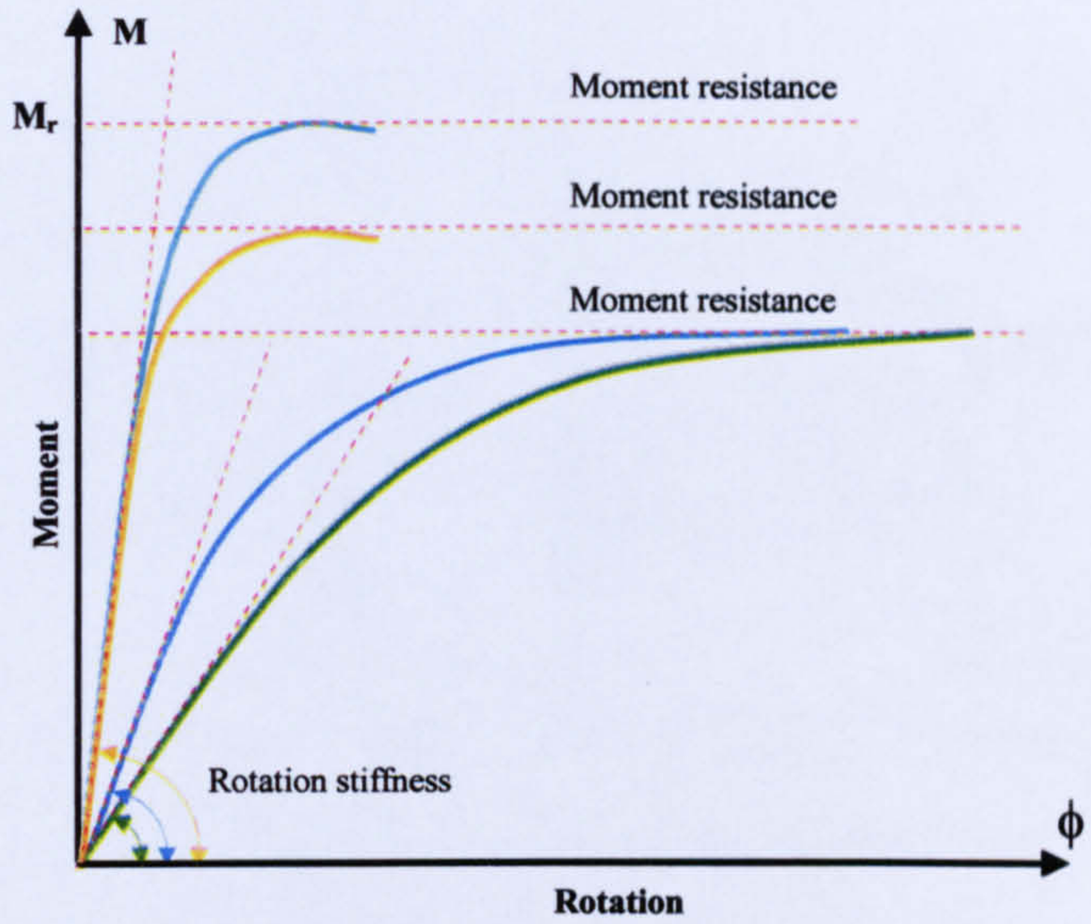

Figure 2.1 Connections varied moment-rotation characteristics

Many factors influence connection behaviour. For instance, there might be two connections having the same moment resistance but having two different rotational stiffnesses. Also, there might be two connections having the same stiffness but with two different moment resistances (**Figure 2.1**). First, consider various connection types according to classic classifications (pinned or moment connections).

2.2.1. Moment connections

- **Extended end-plate connections**

Extended end-plate connections are classified into two types: with an end plate extended on the tension side only, as shown in (**Figure 2.2–a**), or on both the tension and compression sides.

- **T-Stub connections**

A T-stub connection is a fabrication of two T sections bolted to both the column and the beam flange as shown in **Figure (2.2-b)**.

- **Flush end-plate connections**

A flush end-plate connection (**Figure 2.2–c**) is an end-plate welded to the beam end along both the flanges and web in the fabricator's shop, and bolted to the column flange in the field.

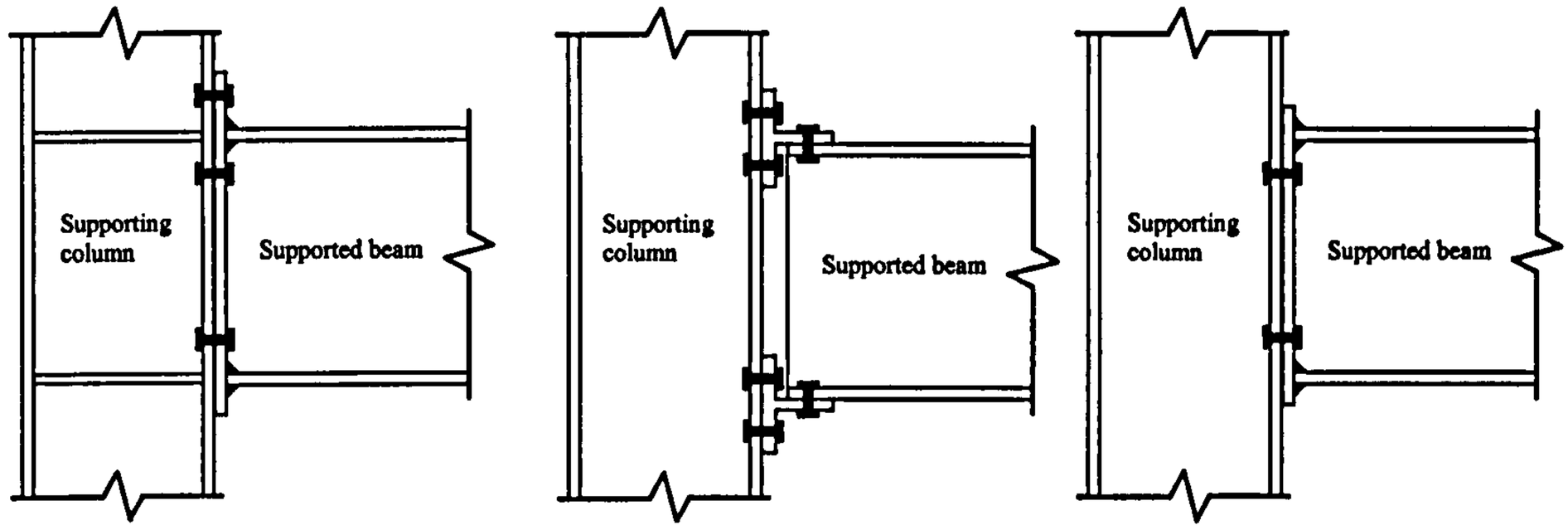

a- Extended end-plate connection **b-** T-Stubs connection **c-**Flush end-plate connection

Figure 2.2 Moment connections

2.2.2. Simple connections (Pin connections)

- **Header plate steel connection**

A header-plate connection consists of an end-pate, whose length is less than the depth of the beam, welded to the beam web and bolted to the column, as shown in **Figure 2.3**. Accordingly, a header-plate connection is used mainly to transfer the reaction of the beam to the column.

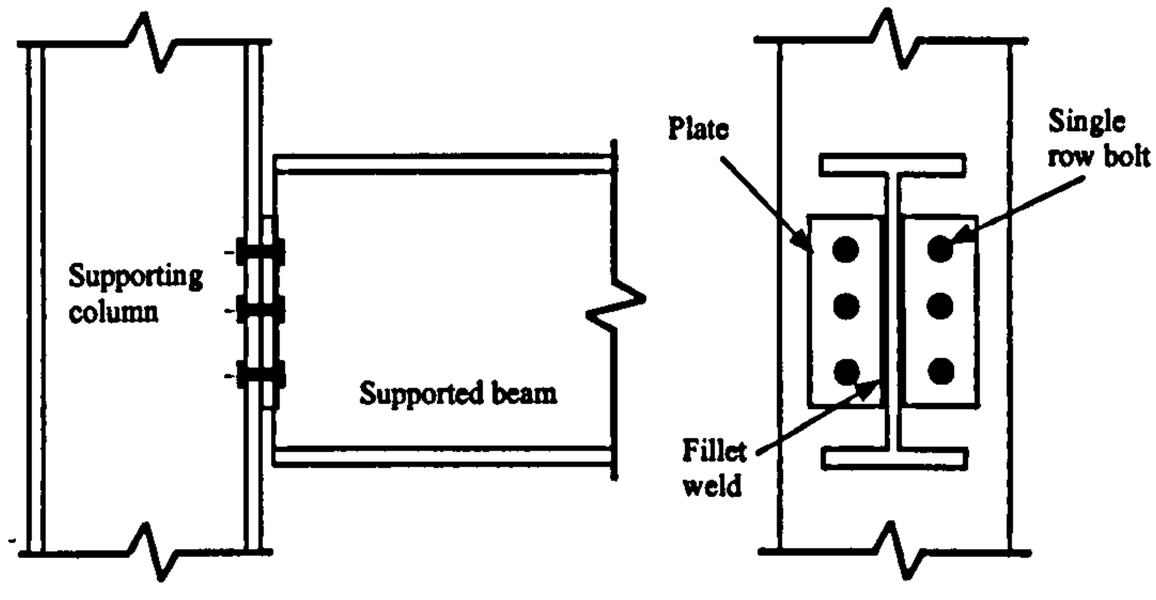

Figure 2.3 Header plate steel connection

- **Top- and seat-angle connection**

A typical top- and seat-angle connection is shown in **Figure 2.4**. The top-angle is used to provide lateral support to the compression flange of the beam and the seat-angle is to transfer only the vertical reaction of the beam to the column.

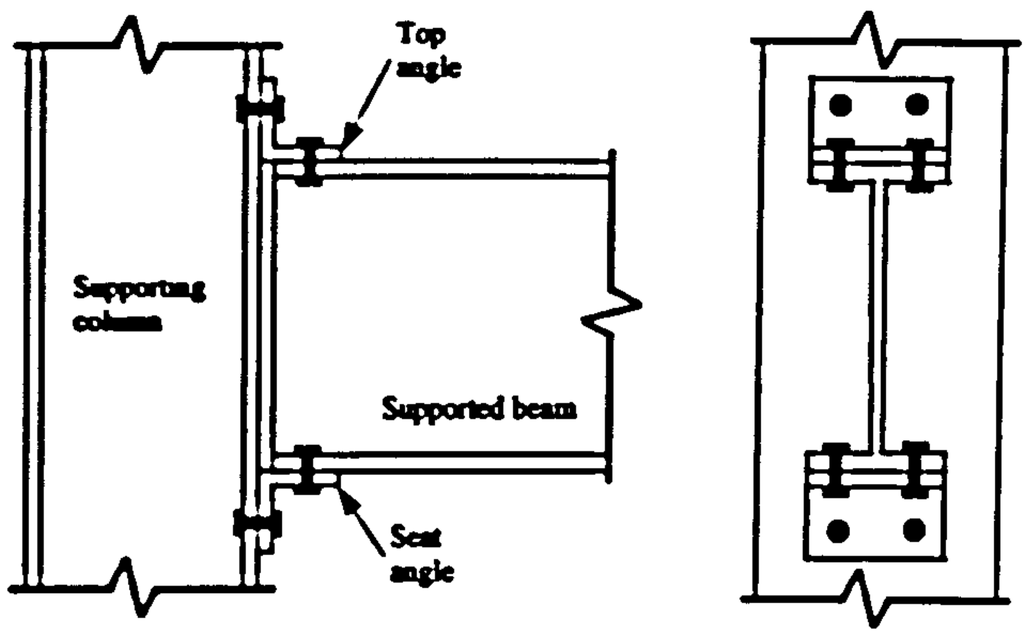

Figure 2.4 Top- and Seat-Angle Connections

- **Double web angle steel connection**

A double web-angle connection consists of two angles bolted to both the column and the beam web, as shown in **Figure 2.5.**

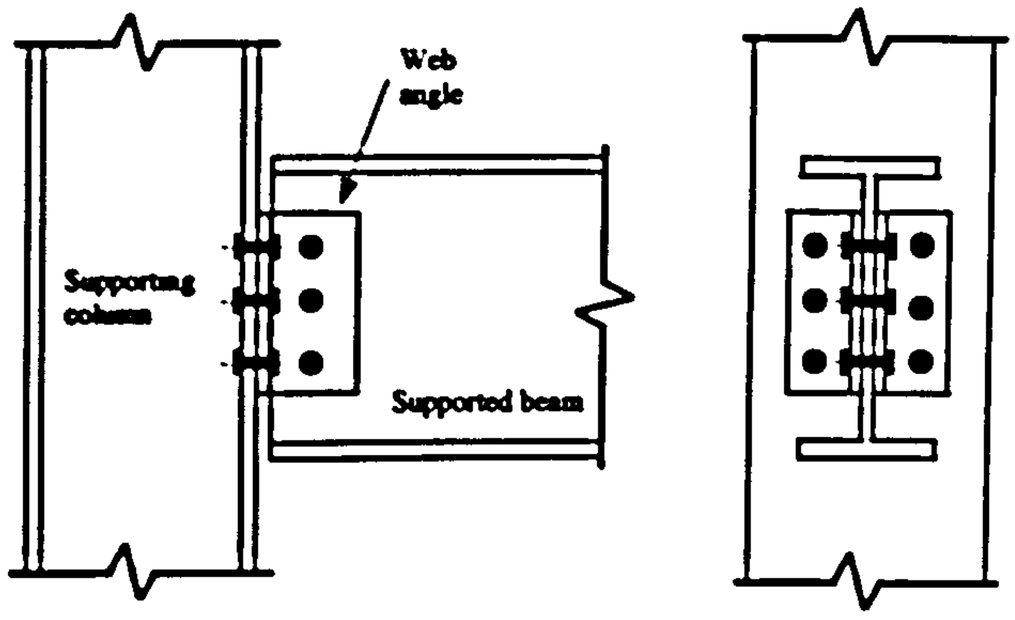

Figure 2.5 Double web angle steel connection

- **Top- and seat-angle with double web-angle connections**

This type of connection is a combination of a top- and seat-angle connection and a double web-angle connection (**Figure 2.6**). Double web-angles are used to improve the connection restraint characteristics of top- and seat-angle connections, and for shear transfer.

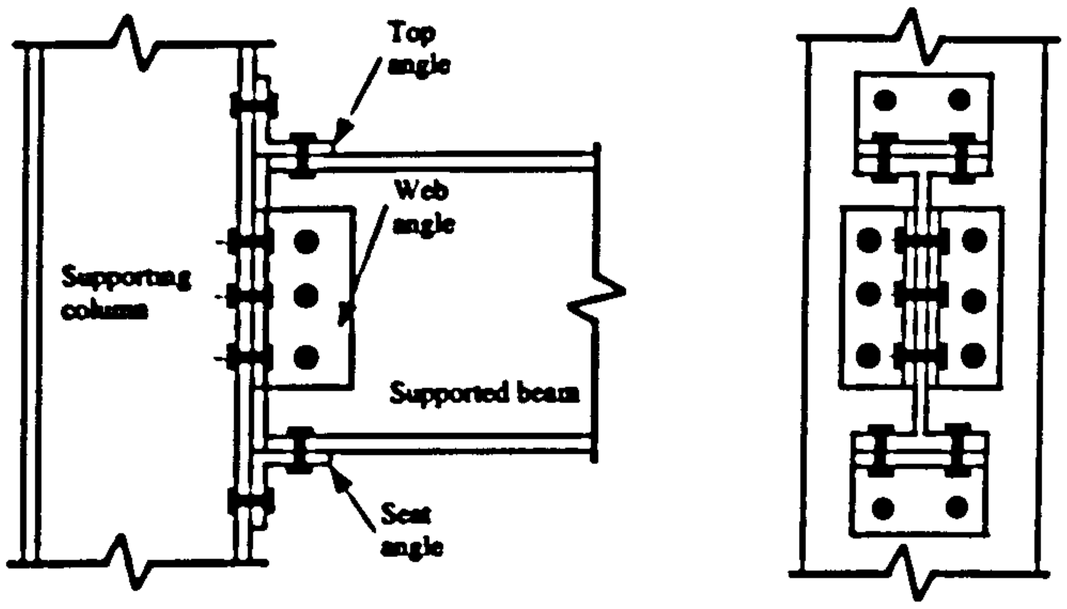

Figure 2.6 Top- and Seat-Angle with Double Web-Angle Connections

- **Single web angle steel connection**

A single web-angle connection consists of one angle bolted to both the column and the beam web, as shown in Figure 2.7.

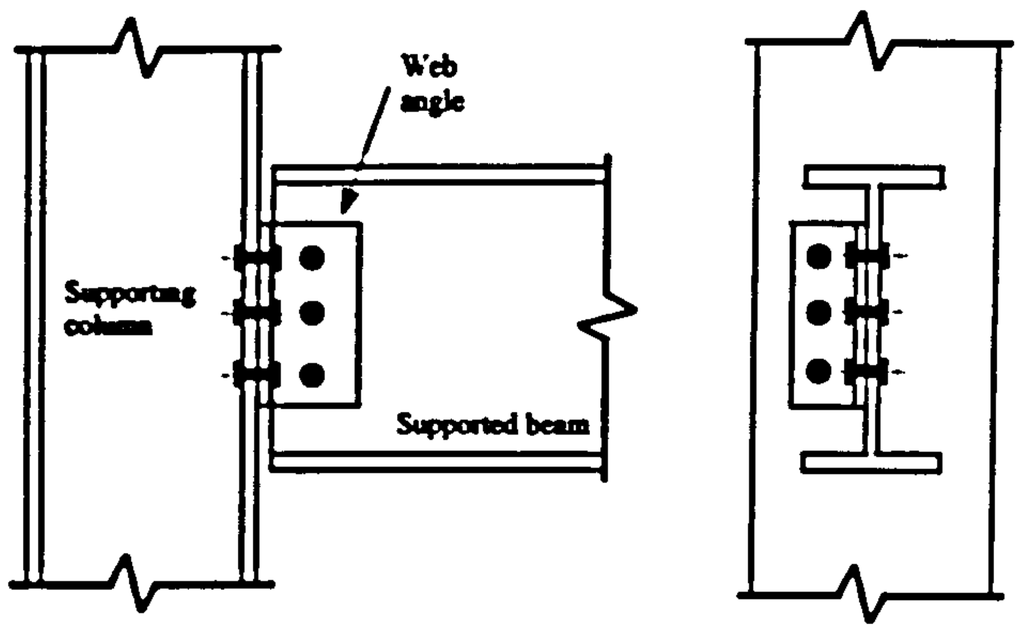

Figure 2.7 Single web angle steel connection

- **Fin plate steel connection**

A fin plate connection consists of a single plate welded to the column flange or web in the workshop and bolted to the beam web, either with a single row of bolts or with a double row (Figure 2.8a-b). This connection type requires less material to fabricate than a single web-angle connection. More detail regarding this connection type will be given in 2.5.

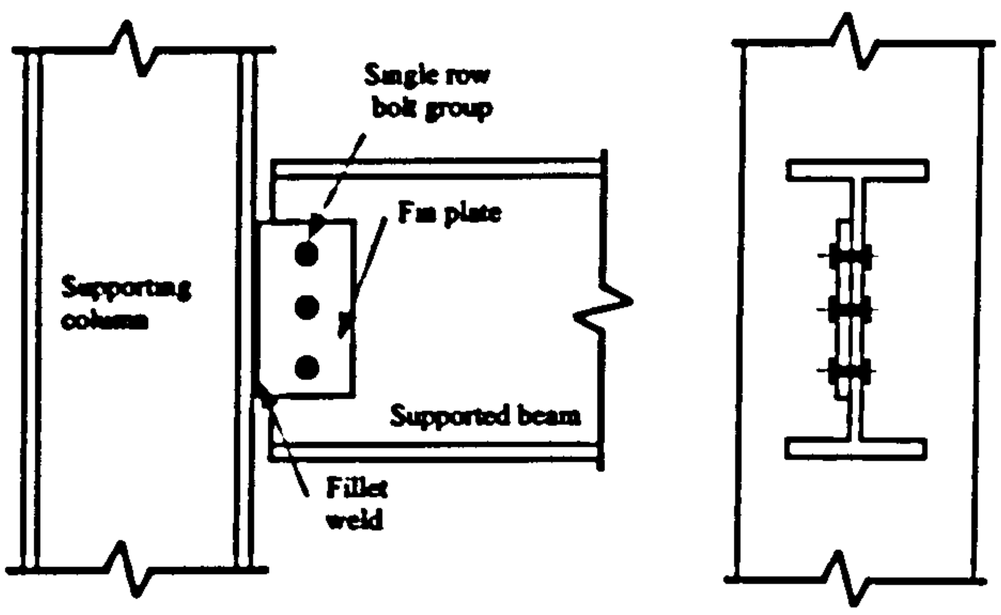

Figure 2.8-a Fin plate steel connection with single bolt row

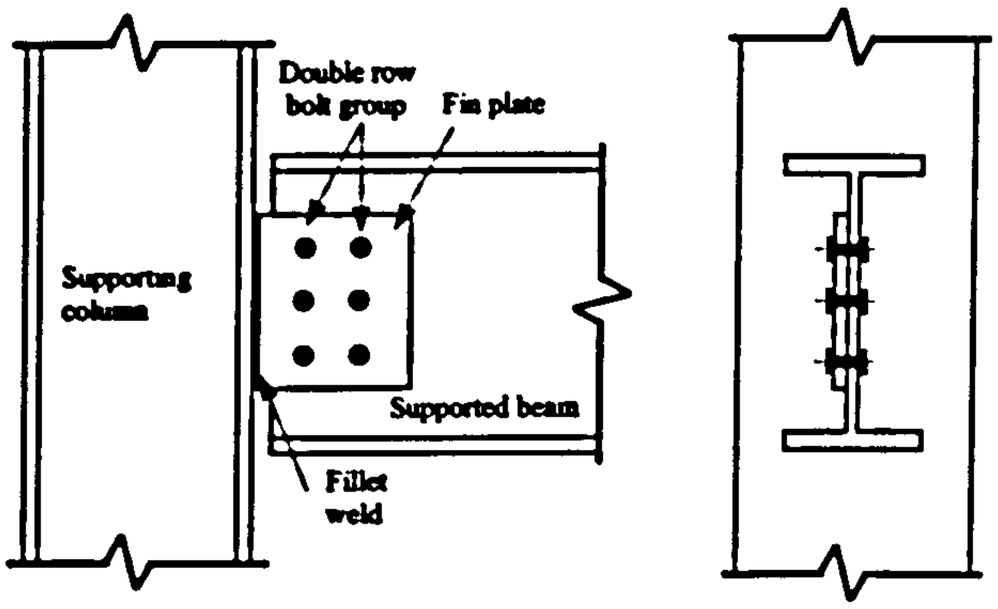

Figure 2.8-b Fin plate steel connection with double bolt row

2.3. Connection Behaviour and Rigidity Classifications

A beam-to-column connection is usually subject to axial force, shear force, bending moment, and torsion (although the effect of torsion can be excluded for an in-plane study). In normal loading conditions the effects of axial forces are usually small compared to that of shear and bending moment. The flexural behaviour of a connection is described by the relationship between the moment transmitted by the connection **M**, (e.g. from beam to column), and the relative rotation of the two members joined by the connection ϕ, **(Figure 2.9).**

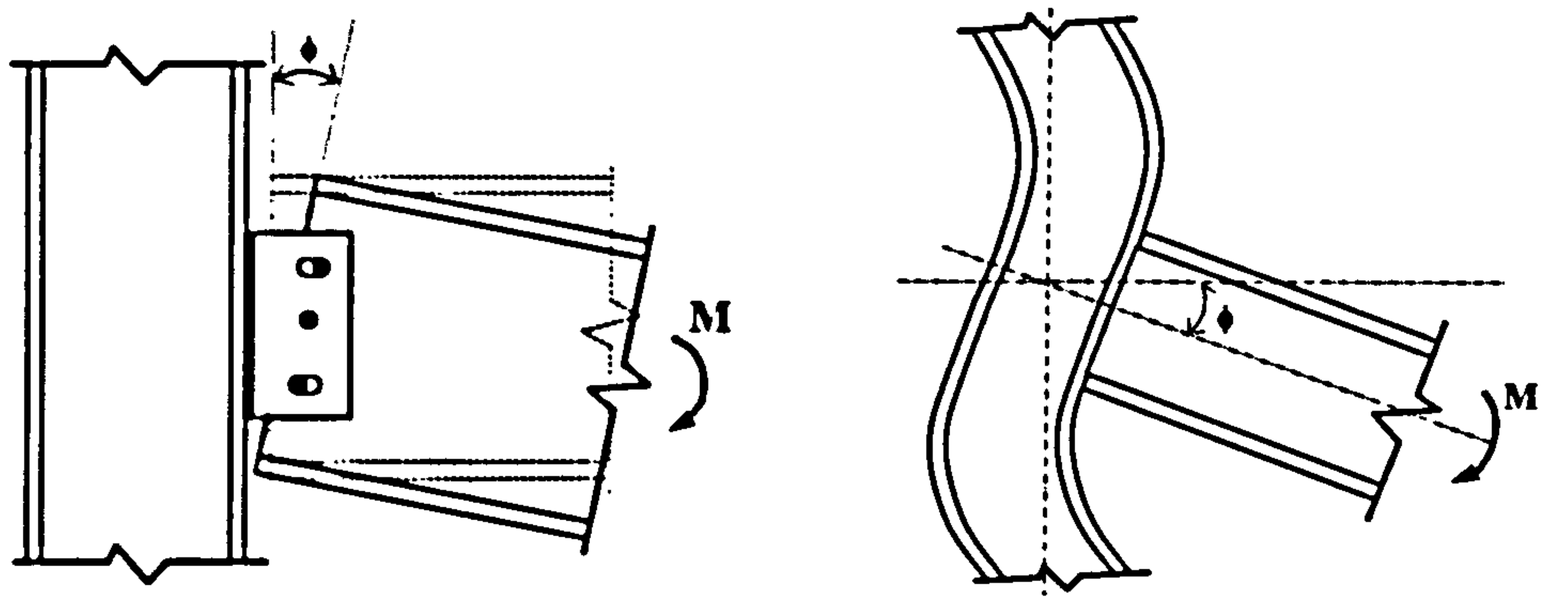

Figure 2.9 Rotational deformation of a connection.

The moment-rotation relationship (M-ϕ) is useful to distinguish between the different types of connection behaviour and flexibility. Therefore, attention is focused on the moment-rotation characteristic, as this is the most important influence on the response of either individual members or complete frames. The nonlinear nature of this characteristic is identified, and methods of representing moment-rotation curves for subsequent use in analytical procedures are discussed.

The moment-rotation behaviour of a variety of commonly used connections is shown in **Figure 2.10.** The horizontal (rotation) axis represents the idealised pinned connection where zero moment is developed for all values of rotation. The vertical (moment) axis represents the idealised fully rigid connection where no joint rotation occurs for all values of moment development. These are two extreme cases, and in practice all types of connections exhibit nonlinear moment-rotation behaviour that falls between the two extreme cases of ideally pinned and fully rigid connections.

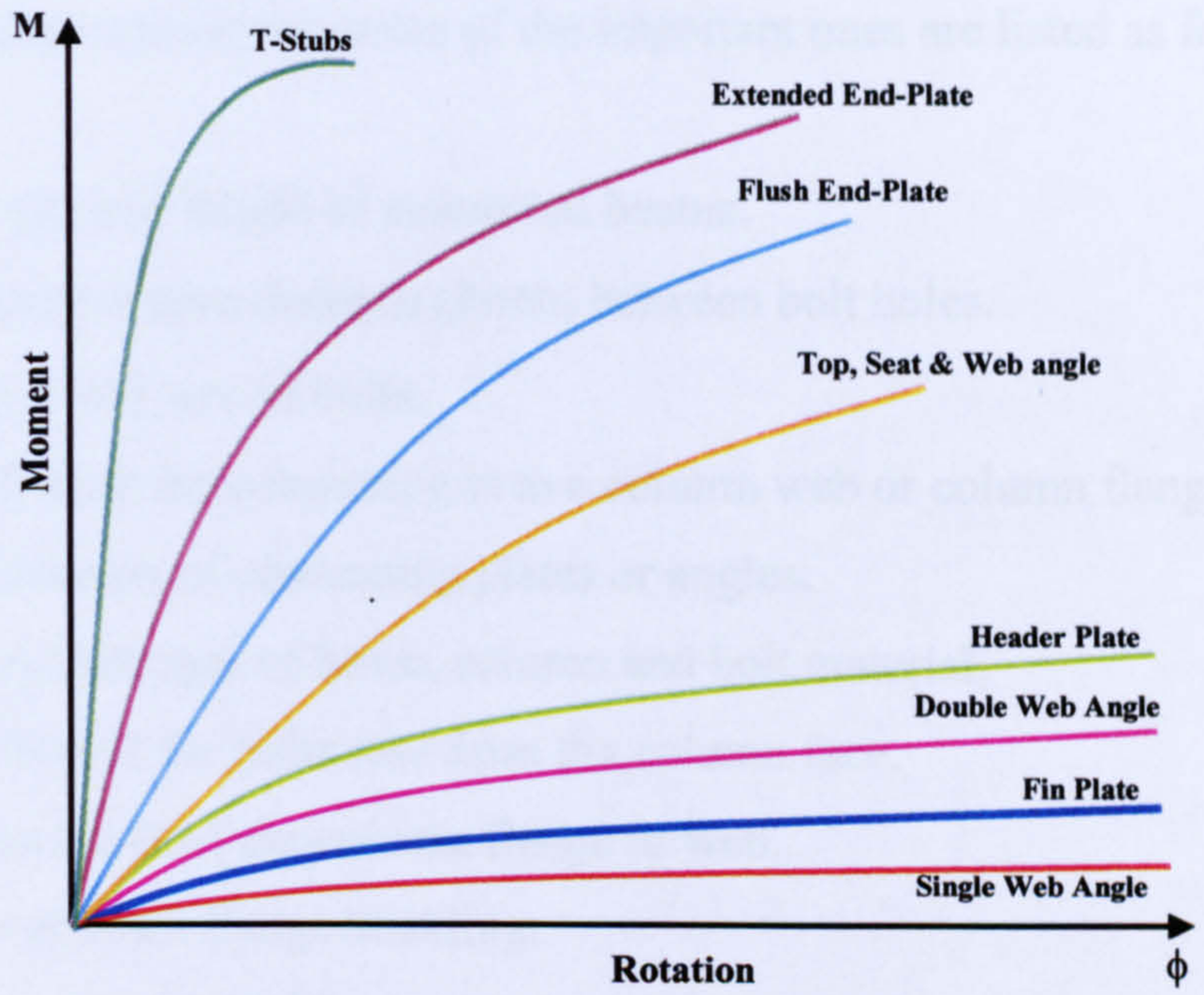

Figure 2.10 Connections typical moment-rotation curves [2.5]

The curves in **Figure 2.10** (from red to the green) represent semi-rigid connections of differing degrees of rigidity. The red curve would represent the moment-rotation relationship produced by a flexible connection, such as a single web angle or fin plate connection. The green curve would represent a much more rigid connection, such as a T-stub or fully welded arrangement. The orange curve represents a connection of intermediate rigidity such as a top and seat angle with double web angle connection. The slope of the moment-rotation curve is a measure of the rigidity or stiffness of the connection at any particular value of rotation. From this fact it can be seen that the rigidity of the different connections decreases as the rotation increases, and it confirms graphically that the connection represented by the green curve is more rigid than those represented by other curves.

However, experimental investigations of actual joint behaviour conducted at various times during past years have clearly demonstrated that most connections normally regarded as "simple or pinned" connections do possess some rotational stiffness, while connections which are regarded as nominally "rigid" often display some degree of flexibility.

In general there are many factors that influence the rigidities of the various types of beam-to-column connection; some of the important ones are listed as follows [2.1, 2.5]:

(a) Depth and length of connected beams.

(b) Centre-centre distance (Pitch) between bolt holes.

(c) Type and size of bolts.

(d) Whether the connection is to a column web or column flange.

(e) Thickness of connecting plates or angles.

(f) Yield strength of beam, column and bolt material.

(g) Offset of the bolts row from the column face.

(h) Thickness of the column flange or web.

(i) Local beam flange buckling.

(j) Column web yield.

(k) Beam and column contact during deformation.

2.4. Shear Connections

Almost all simple connections (**Figures 2.2-2.7**) may be considered as shear connections, which are used in steel structural buildings to transfer primarily the vertical reaction of a simply supported structural element to its supporting members. The term "shear connection" describes those which transfer the load between the connection components via sheared bolts. A lap joint, with a single bolt, is a good example to understand the behaviour of shear connections. This joint is a combination of two plates and one bolt fastening them through an over-sized hole (**Figure 2.11-a**).

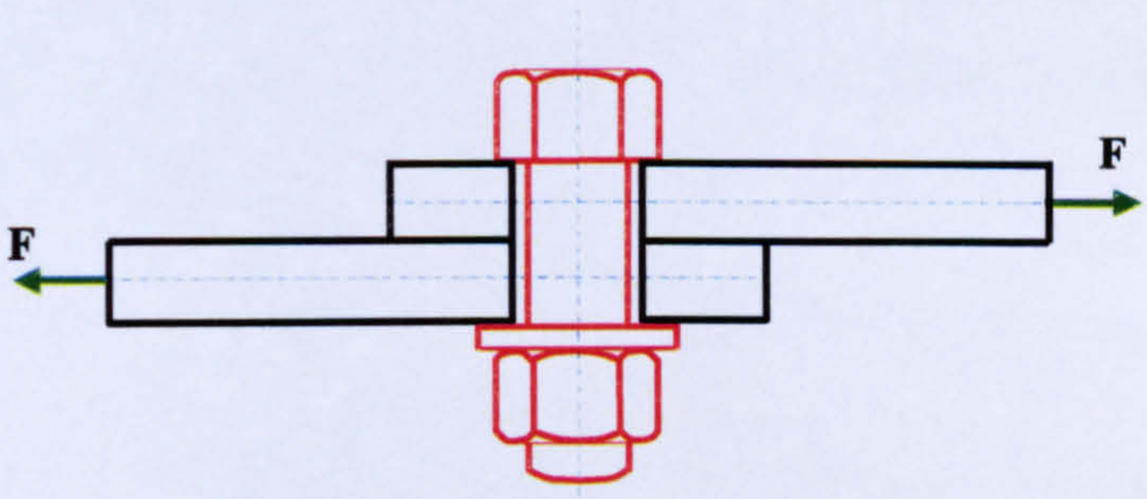

Figure 2.11-a Typical Lap joint with a single bolt

As the far edges of the plates pull apart the two plates start to slide over each other. When the applied load overcomes the plate interface friction the plates slip, setting the bolt into single shear, and the bolt shank surface bears onto the hole's circumference (**Figure 2.11-b**). Due to the load eccentricity in these joints, out-of-plane bending occurs, and secondary bending stresses are developed, causing net section yielding. As the load increases, the bolt tends to rotate and the plates bend in order to align the lines of action of the force on each side of the joint, and the bolt will be partly in tension and partly in shear. Furthermore, the bolt head and nut will dig into the plate at the net section. Because of the plate bending, and the resulted bolt/nut digging into the plate, a reduction in the net section capacity and ultimate bearing capacity will occur. The net section capacity is likely to drop below that given by simple theory to 0.9 × net section area × material tensile strength, and the ultimate bearing stress can reduce to 1.75 × plate ultimate tensile stress [2.6]. Further increase of the external load could lead to shear failure across the bolt shank; however, failure in other modes (plate bearing or net section) might occur before the load **F** reaches this level, and the critical joint component under such loading conditions is not usually the bolt but the plate material.

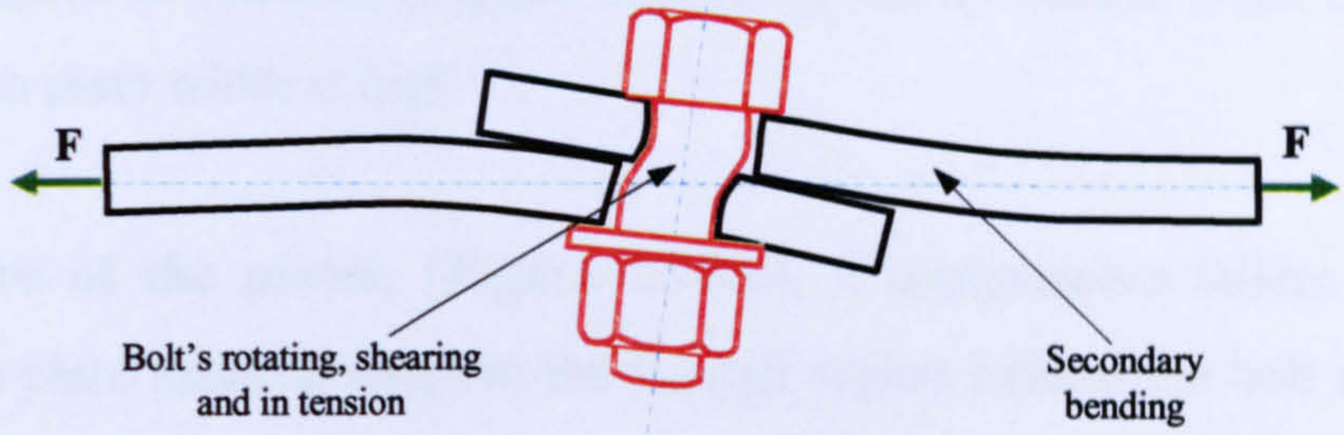

Figure 2.11-b Typical Deformation of Lap joint with a single bolt subjected to single shear

Static tension experiments on single lap joints with restraint against out-of-plane bending show a load versus deformation behaviour that is basically similar to the behaviour observed for symmetric double lap joints (**Figure 2.12**), and the ultimate strength of single shear lap joint is equal to one-half the double shear resistance provided by a double lap joint [2.7].

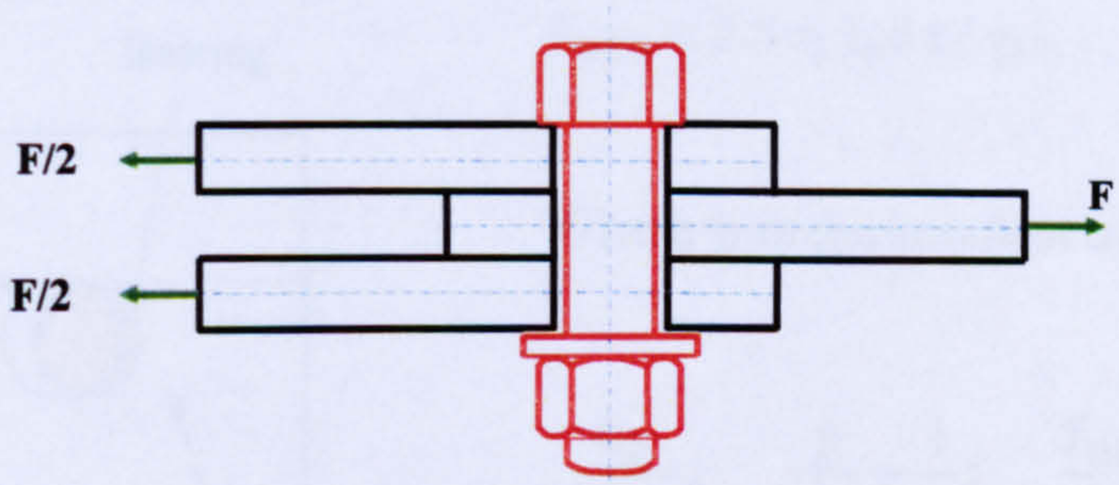

Figure 2.12 Typical symmetric double lap joint subjected to double shear

The possible failure modes of single lap joints are more complex and difficult to predict than those in double lap joints, because of the bending effects associated with the fact that the load path through the joint is not a straight line (**Figure 2.11-b**). There are four possible ways for a single bolted lap joint to fail. Net-section rupture, bearing, shear-out and bolt shear failure are the basic failure modes of a bolted shear joint, as shown in **Figure 2.13**

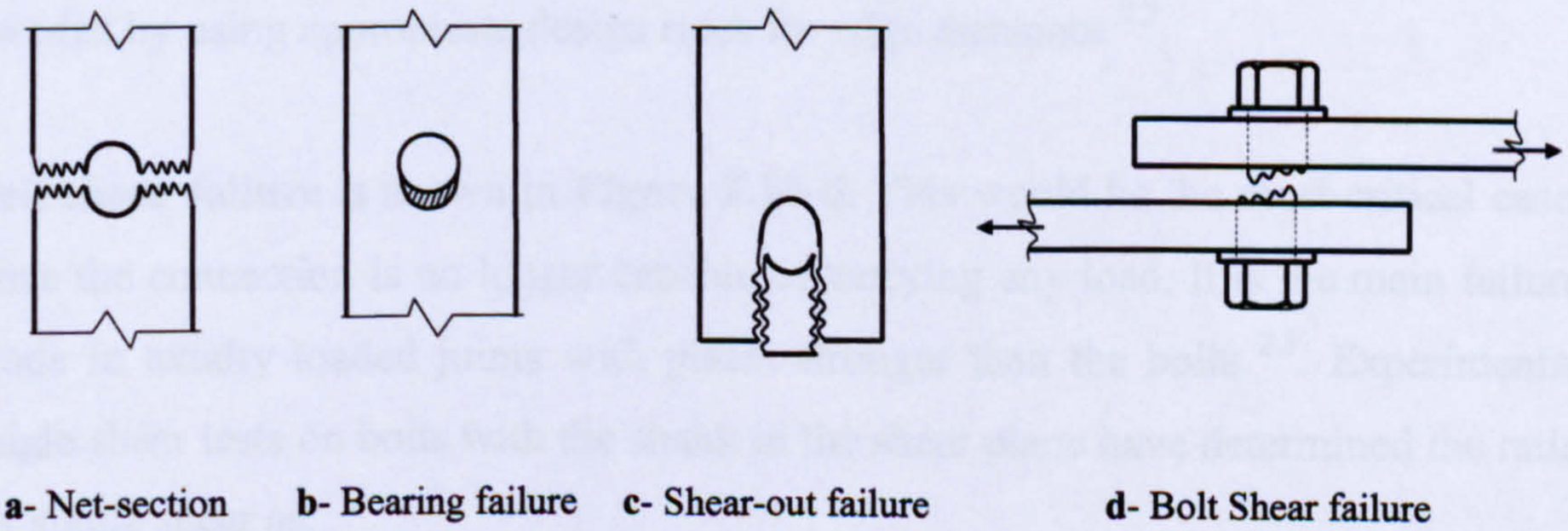

a- Net-section **b**- Bearing failure **c**- Shear-out failure **d**- Bolt Shear failure

Figure 2.13 Failure modes for single shear lap joints.

Net-section failure in tension, (Figure 2.13-a), primarily occurs when the ratio of hole diameter to plate width is high [2.7].

Bearing failure of the plates, (Figure 2.13-b), a compressive failure involving yielding of the plate material close to the contact region behind the bolt at the hole edge, occurs when the ratio of hole diameter to plate width is low. Bearing failure is, like any compressive failure in a steel plate, associated with delaminating and ply-buckling, which means that the bearing strength is strongly affected by the lateral constraint of the material surrounding the loaded hole. This mode of failure is not as critical as others, because the connection does not generally lose any load-carrying capacity [2.8]. The design bearing resistance of a bolt is given by [2.9]:

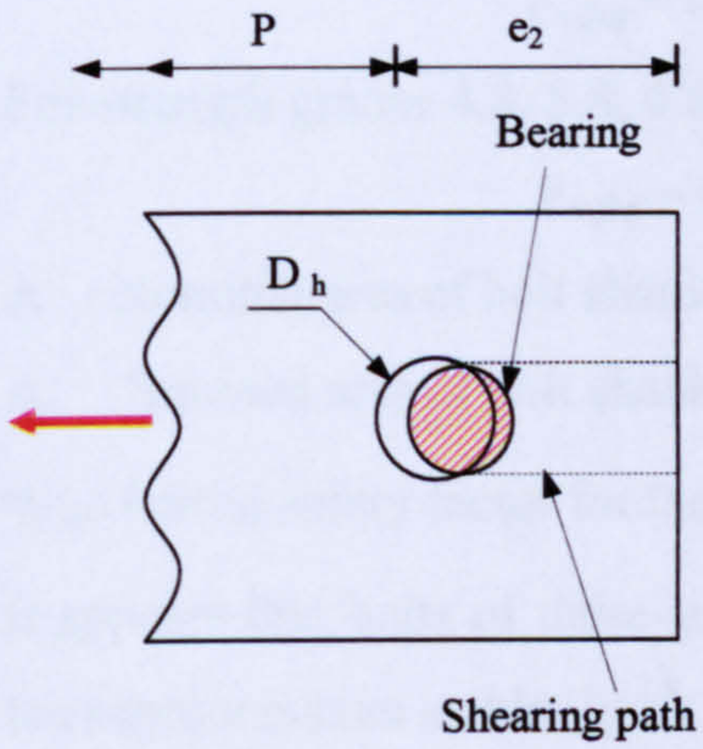

$$F_{b.Rd} = 2.5\,\eta\, f_u\, d\, t / \gamma_{Mb} \qquad \textbf{(2.1)}$$

Where η is the smallest of:

$$\frac{e_2}{3D_h};\quad \frac{p}{3d}-\frac{1}{4};\quad \frac{f_{ub}}{f_u}\quad \text{or}\quad 1.0$$

Figure 2.14 Bolt bearing & shearing path

Shear-out failure (tearing off failure), illustrated in **Figure 2.13-c,** is caused by shear stresses acting through the plate shearing-path **(Figure 2.14)** in the principal load direction. This failure mode occurs mainly in joints where the distance between the hole edge and the edge of the plate is short. The shear-out failure mode can be avoided by using appropriate design rules for edge distances [2.7].

Bolt shear failure is shown in **Figure 2.13-d**. This would be the most critical case, since the connection is no longer capable of carrying any load. It is the main failure mode in axially loaded joints with plates stronger than the bolts [2.8]. Experimental single shear tests on bolts with the shank in the shear plane have determined the ratio for single shear as:

$$\frac{\text{Ultimate shear strength}}{\text{Ultimate tensile strength}} = 0.8 \qquad \textbf{(2.2)}$$

This ratio is likely to be 0.63 for bolts with threads in the shear plane [2.6]. The effective shear strength of bolts in joints is reduced by out-of-plane bending. The ultimate strength of longer lap joints with no restraints against bending should not be as greatly affected by the effects of bending as a shorter lap joint because increasing the length of the joint, and the number of bolts, reduces the bending and hence the reduction of shear resistance [2.8].

The design shear resistance of a bolt ($F_{v.Rd}$) per shear plane in normal conditions, is:

(a) For the shear plane passing through the threaded portion of the bolt [2.9]:

For strength grades 4.6, 5.6 and 8.8

$$F_{v,Rd} = 0.6\, f_{ub}\, A_s / \gamma_{Mb} \qquad \textbf{(2.3)}$$

For strength grades 4.8, 5.8, 6.8 and 10.9

$$F_{v,Rd} = 0.5\, f_{ub}\, A_s / \gamma_{Mb} \qquad \textbf{(2.4)}$$

A : Nominal area of bolt shank [mm^2]

A_s : Stressed area of bolt shank [mm^2]

γ_{Mb}: Partial safety factor for the bolt $\gamma_{Mb}=1.25$

It appears that bolts of these grades (4.8, 5.8, 6.8 and 10.9) are less ductile and that the rupture occurs suddenly [2.9]:

(b) For the shear plane passing through the unthreaded portion of the bolt:

$$F_{v,Rd} = 0.6\, f_{ub}\, A / \gamma_{Mb} \qquad \textbf{(2.5)}$$

The coefficients 0.5 and 0.6 are the result of a statistical evaluation based on a very large number of test results [2.9]:

2.5. Fin Plate Steel Shear Connections

2.5.1. Introduction

A fin plate connection is one of the most common types of shear connection, and is sometimes referred to as a "web side plate" or a "shear tab". In general, fin plate connections comprise a length of predrilled single plate, which is fillet welded to the supporting member in the workshop. The supporting member is normally a flange or web of a column or web of a beam (**Figure 2.15**). During erection, a predrilled supported beam web is bolted to the single plate on site. Once the crane hook lifts the beam to its approximate level it may quickly be brought into its final position by insertion of a single bolt at each end which is enough to secure the beam sufficiently, allowing the crane hook to be released.

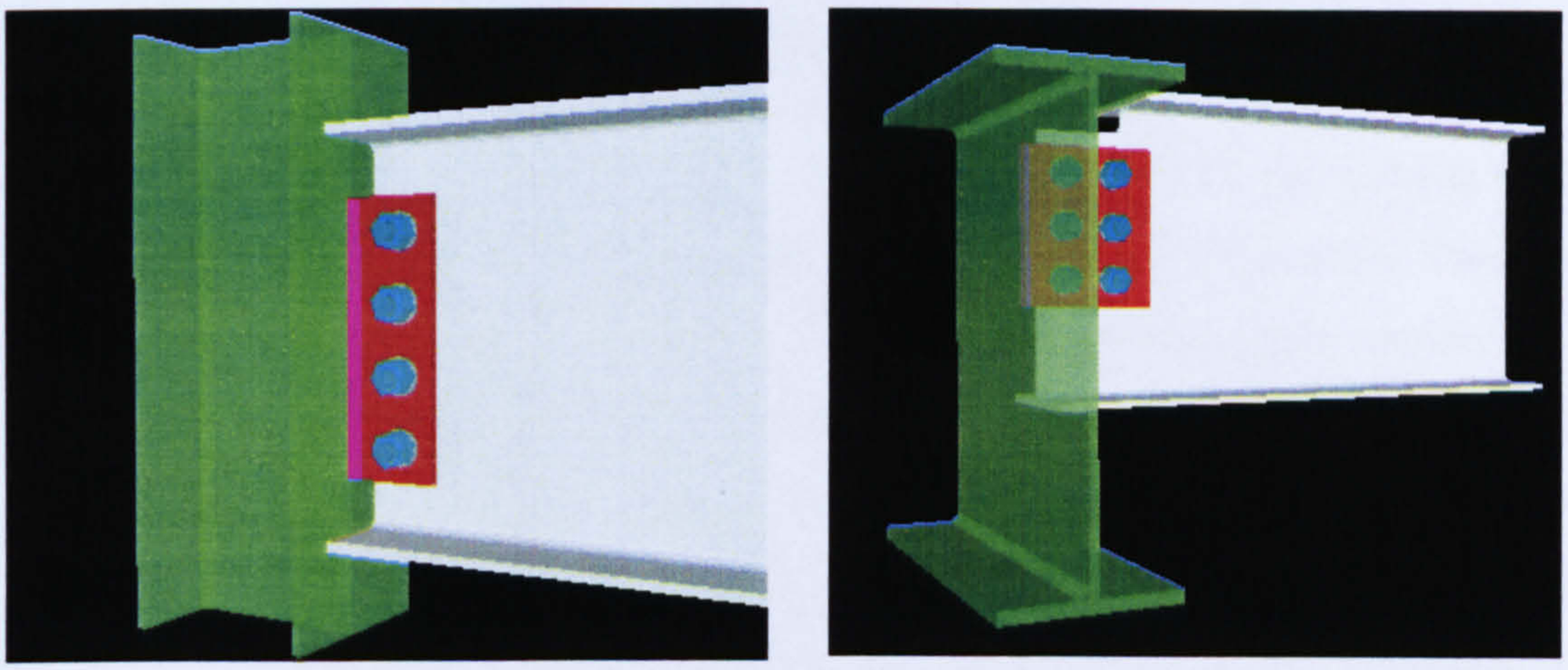

(a) - Beam-to-Column fin plate steel connection **(b)** - Beam-to-Beam fin plate steel connection

Figure 2.15 Fin plate connections [2.10]

The popularity of this connection type is largely due to its simplicity in installation and its economical fabrication. The use of such joints does not require holes to be drilled in the column, and can lead to increased construction speed and resulting economies. The fin plate connection is one of the connections recommended for use by the Steel Construction Institute and the British Constructional Steelwork Association in their joint publication *Joint in Simple Construction Vol.1 Design Methods* [2.11]

2.5.2. Background to fin plate and behaviour

Initially, fin plate connections were used in North America and Australia, and have gained popularity in the UK [2.12]. Fin plate connections are usually considered as simple shear connections. Historically, shear joints have been designed for strength and stiffness with no regard to rotational capacity. This means that fin plate connections are modelled as pins and are assumed to transfer only shear load to the supporting structure elements. Even so, in most cases these types of connections can transfer significant end moments to the beam and supporting member [2.13, 2.14]. Usually, a clearance of 10-20 mm between the end of the supported beam and the supporting column or beam is used to give the end of the supported beam freedom to rotate with ease before the bottom flange hits the supporting member. Fin plate connections derive their ductility and rotation capacity from the bolt deformation in shear, the out-of-plane bending of plate or beam web, and the hole distortion in bearing of the weakest components, which are either the steel plate or beam web [2.14]. As a fin plate connection has one edge of the plate fully welded to the column flange, its deformation capacity is smaller than that for a single angle connection. Therefore, fin plate connections are slightly stiffer than the bolted single-angle connection [2.1]. However, fin plate shear connections should be strong enough to be able to transfer the shear force, and it should be sufficiently flexible and ductile to allow the end of a simply supported beam to rotate with ease and accommodate the rotation demand of the beam. Fin plate connections have six possible failure modes as summarised in **Figure 2.16**.

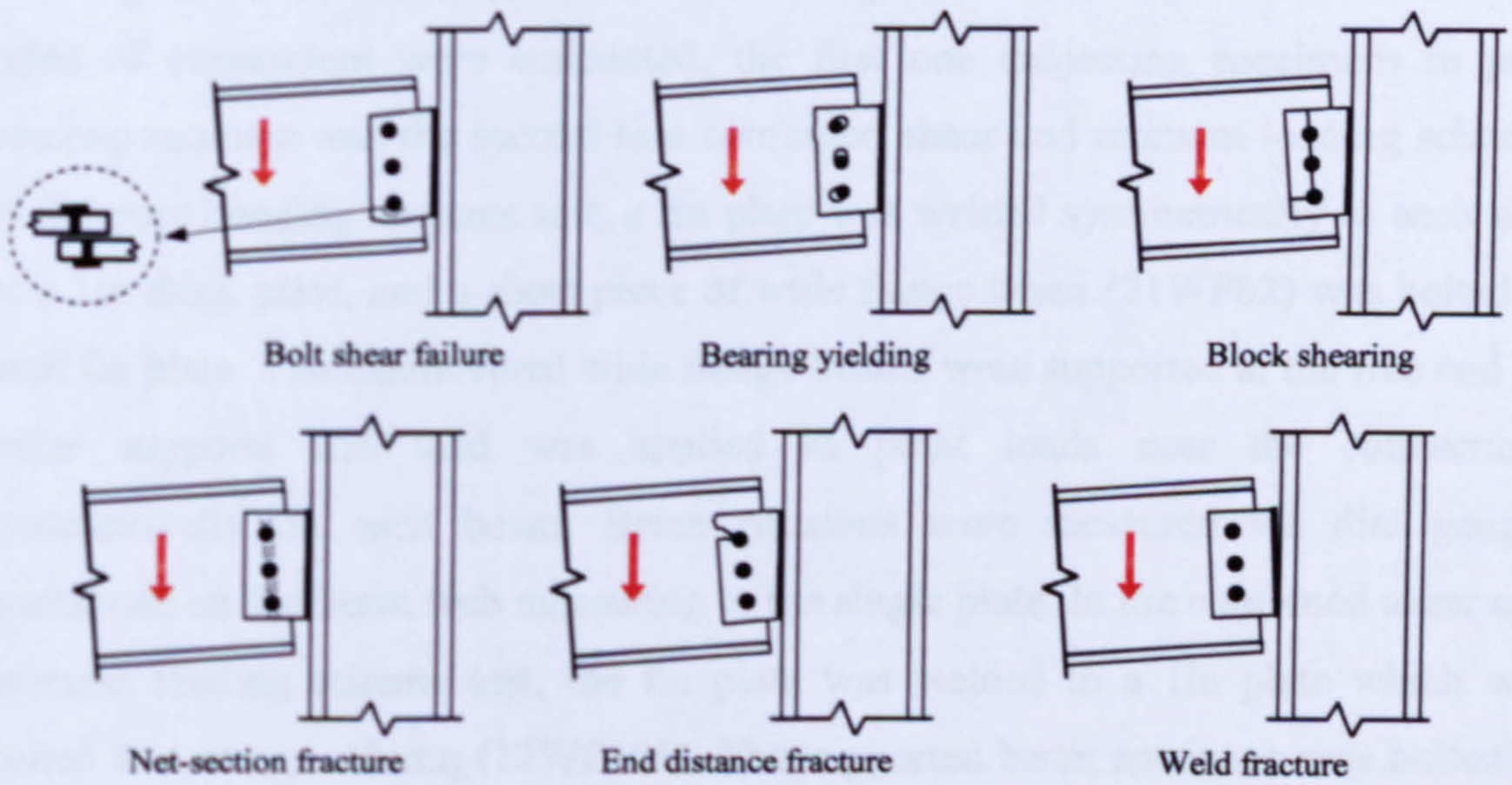

Figure 2.16 Modes of failure for fin plate connections

2.6. Literature Review

The literature review for this research has been divided into two parts. Firstly, experimental work and research investigations on fin plate beam-to-column connections will be described. Secondly, research on steel connections under fire conditions will be summarised.

2.6.1. Experiment investigation and analysis of fin plate connections

Investigations on fin plate shear connections have been limited and because the two main characteristics of simple shear connections are strength and ductility, most of these investigations have focused on either the strength or the moment-rotation relationship under shear loading. The main research investigations on fin plate shear connections have taken place in Canada, USA, Australia, and the UK.

2.6.1.1. Research and documented work in Canada and the USA

Several experimental tests have been conducted to predict the behaviour of the beam-to-column fin plate steel connections during the past forty years. In 1968 Lipson [2.13] carried out a series of tests on fin plate connections at the University of British Columbia in Canada. The fin plates tested were ¼in thick with 1¼in edge distances and were manufactured from A36 steel (S275, UK equivalent). Each fin plate was welded on its two sides to the supporting member via ¼in fillet welds. Two to six ¾ in diameter A325 (8.8 bolt, UK equivalent) high strength bolts were used to assemble the fin plate connections, and these were all tightened to a torque of 356ft-lbs. Two types of experiment were conducted, the first one subjecting specimens to pure bending moment and the second to a combined shear and moment loading scheme. In the pure bending moment test, a fin plate was welded symmetrically to each side of a 1in thick plate, and a short piece of wide flange beam (21WF62) was bolted to each fin plate. The cantilevered wide flange beams were supported at the free end by roller supports and load was applied as point loads near the connections symmetrically on each beam. Beam rotations were measured via dial gauges positioned on the beam web measuring to the single plate. In the combined shear and moment loading scheme test, the fin plate was welded to a 1in plate which was bolted to a heavy column (12WF106). The supported beam specimen was bolted to the fin plate at one end and was supported by the test frame at the free end. The

support for the free end of the test specimen was such that rotation could be introduced to the beam. In this test, load was applied as a point load near the test connection in an incremental manner after a rotation at the supported end was assigned and fixed throughout the test. The following results were observed. With an increased number of bolts, the moment continued to increase but at a decreased rate, and the constant moment region decreased. Shear-deflection curves showed some non-linearity at comparatively small displacements. Also, the centre of rotation was found to be near the centroid of the bolt group. Failure of the single plate specimens occurred under load, either by cracking in the tension edge of the plate or cracking of the weld. The bolts did not fail in shear, however significant bolt hole deformation was observed. From the results obtained, a design procedure was formulated based upon satisfying rotation capacity, load carrying capacity and end fixity. Moment-rotation curves and shear-deflection curves for the connection were presented for between two and six bolts, and demonstrated that the fin plate connection can develop a significant end moment in the beam and supporting member. The amount of moment is generally dependent upon the number, size and configuration of bolts, the thickness of the plate or beam web, the beam span-to-beam depth ratio, and the loading (whether uniform or concentrated).

In the USA, intensive research work on fin plate connections was conducted by Richard, *et. al.*[2.14 - 2.16] with the aims of devising a method for predicting the moment-rotation capacity in the fin plate connections and verifying a design procedure. In the first test series a total of seven tests were conducted [2.14] with two, three, five, and seven bolts. Tests were assembled using short beam lengths equal to the depth of the bolts, which were A325 high strength bolts with the commonly used ¾ in diameter. Moment-rotation curves for these tests were plotted and compared with a non-dimensional expression introduced to represent this relationship with the aid of nonlinear finite element analysis. The researchers concluded that adding more bolts caused the outer bolts to reach maximum capacity at an even lower beam load, because the bottom beam flange hits the column flange at a later stage of beam end rotation which the mater leads to bigger moment with greater lever arm applied on the outer bolt.

In the second test series [2.14] five more full scale beam tests were conducted with three-, five-, and seven-bolt fin plate connections, using A325 high strength bolts of ¾ in and ⅞ in diameter. The test setup illustrated in **Figure 2.17,** consisted of an A36 steel fin plate welded to the face of a column flange. The tested beam was supported at one end by the fin plate connection and a roller support at the opposite end. Load was applied as a concentrated point load at the mid-span of the beam.

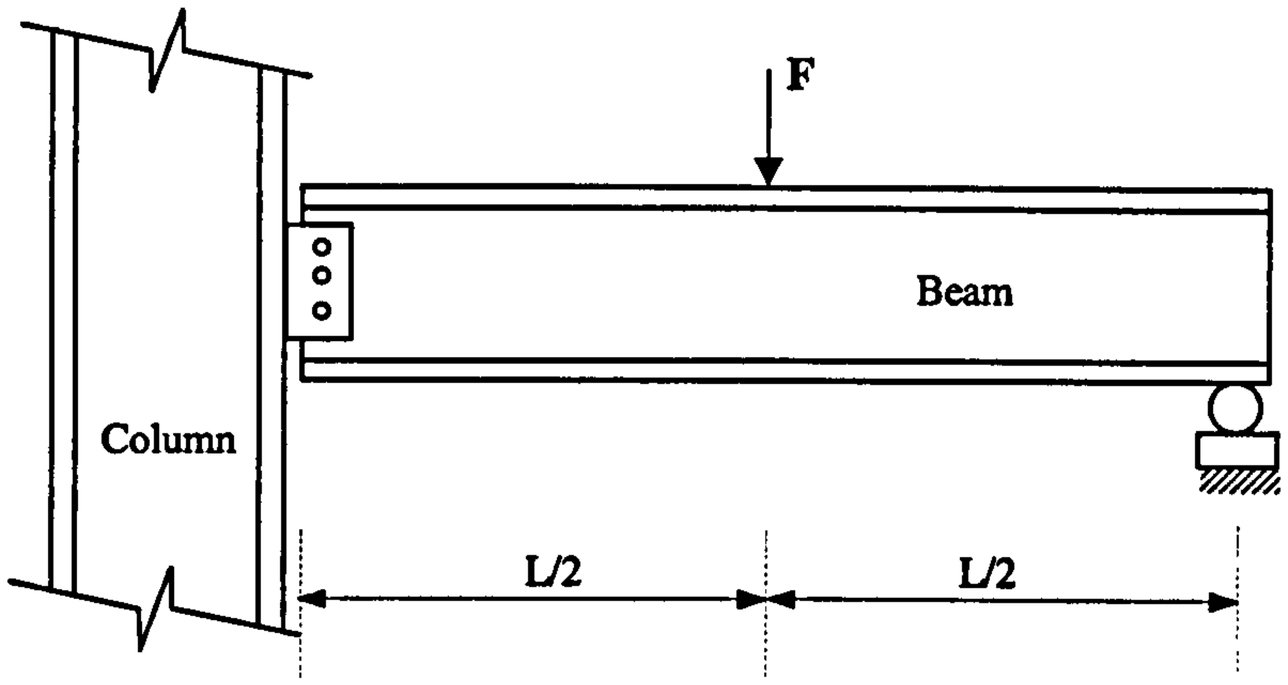

Figure 2.17 Richard *et al.* (1980) fin plate shear connection test setup

The aim of these test series was to establish the relationship of the effective load eccentricity as a function of the applied concentrated load. For the tested W24 x 55 beam with seven bolts, Richard quotes a connection moment as high as 37 % of the elastic fixed end moment value. An equation linking the eccentricity, the distance between the bolt line and the point of inflection in the beam, was presented. Design curves and design guides were introduced, attempting to ensure the connection ductility and rotation capacity. These design procedures are used only for connections assembled via high strength bolts (A325 and A490) in which bolt groups are symmetric about the major axis of the tested beam with stiff support, and A36 non-composite steel beams are used.

Following Richard *et al.* [2.14 - 2.16], Young and Disque (1981) [2.17] further discussed Richard's design procedure with design examples and tabular design aids which could significantly reduce the computation time required for the design of such connections.

Astaneh *et al.* [2.18 - 2.20] continued the investigation of steel fin plate connection behaviour in a research project from the late 80's to early 90's; this was summarised

in a journal article by Astaneh, Liu and McMullin (2002) [2.20]. The main objectives of the research were to determine the rotation capacity, develop design procedures for fin plate connections subjected to realistic shear load and rotation deformation conditions, and evaluate the effects of different geometric and material parameters. Astaneh *et al.* conducted a series of fifteen tests on fin plate connections. Five specimens were parts of beam-to-column connections using standard bolt holes, four specimens were beam-to-column connections using short slotted holes and six were parts of beam-to-beam connections using standard holes. Only the first series of five tests will be reviewed here. These tests investigated, in two stages, various beam-to-column fin plate connection configurations with standard bolt holes. The same test set up and loading procedure was used throughout the experimental investigations. The test unit (**Figure 2.18**) consisted of a beam (approximately 1524 mm in length) and a short column (approximately 914 mm in height). The column was connected to a reaction block. A fin plate was attached via a weld applied to each side of the plate to the column is outer flange. A cantilevered beam was connected to one side of the fin plate using bolts of various strengths. The beam utilized stiffeners under the load to prevent web buckling and used lateral support at the end of the beam to prevent out of plane movement. The load was applied on the beam's top flange via a 'Shear Actuator' placed near the support to provide shear, and a 'Rotation Actuator' placed near the end of the beam to provide moment and rotation. The program simulated loading of beam cross sections from W16 to W33 with spans of 10ft, 30ft, and 50ft lengths, until the ultimate moment capacity at the mid-span of the beam was reached.

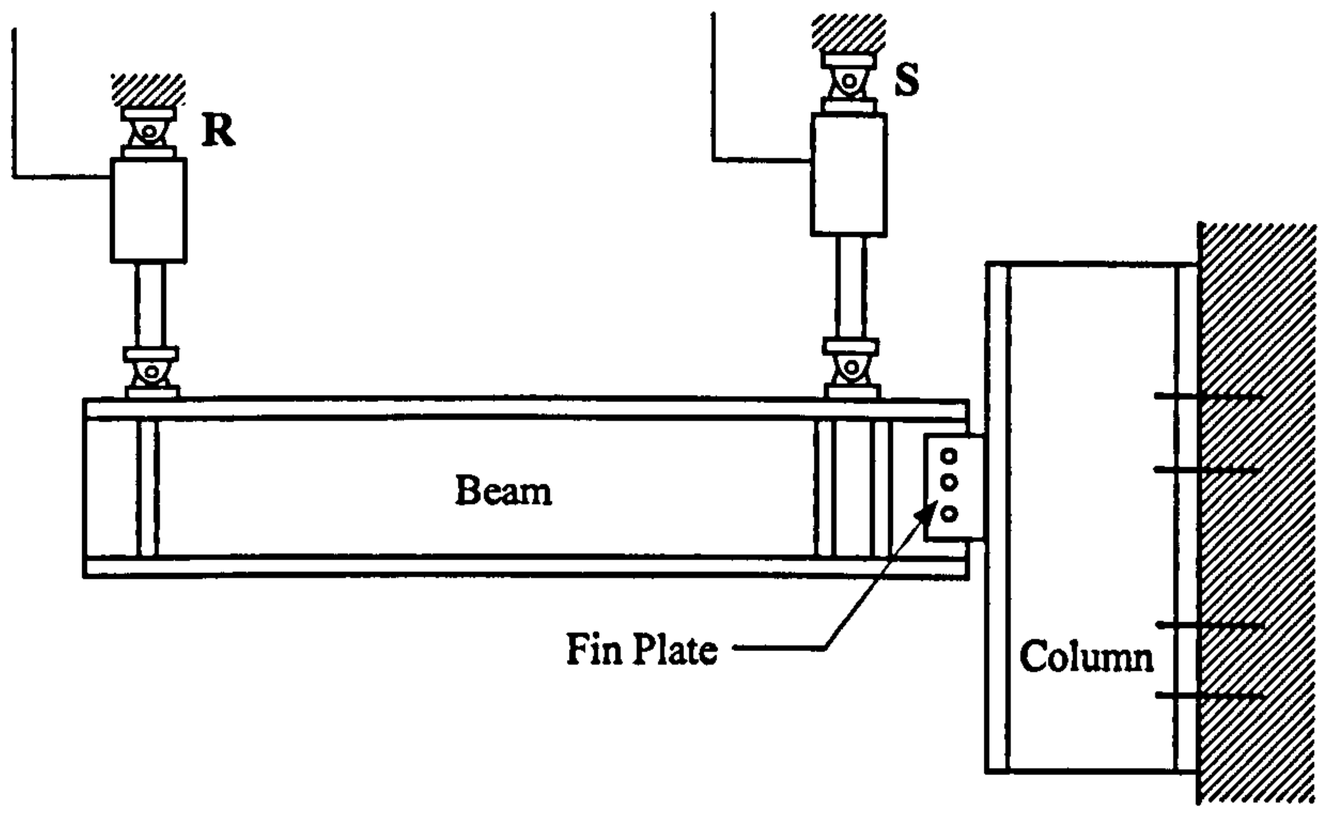

Figure 2.18 Astaneh *et al.* fin plate shear connection test setup

Astaneh *et al.* [2.18 – 2.20] firstly conducted three full-scale fin plate connection tests in which three-, five-, and seven-bolt connections were tested with A325 strength bolts and standard holes. All bolts were fully tightened to approximately 70 % of the proof load using the turn-of-the-nut method. Tested beams and fin plates were fabricated using A36 steel. All test specimens failed in sudden shear rupture of the bolts which suffered significant plastic deformation prior to rupture. The welds did not show any signs of yielding apart from in the 3-bolt specimen, in which minor yielding was evident in the top and bottom of the weld lines prior to bolt rupture. Rotations of 0.03, 0.054, and 0.056 radians were achieved for the seven-bolt, five-bolt, and three-bolt connections respectively at the point of maximum shear. Examination of the bolt holes indicated that almost equal plastic bearing deformations had taken place in both the fin plate and the beam web but in opposite directions.

In the next stage, the two remaining tests of the fin plate connection experiment series were assembled using three and five ¾ in A490 bolts and were tested in the same test set up. The fin plates were manufactured from A36 steel whereas the tested beams were Grade 50 steel. In these two tests, edge distances of 1⅛ in instead of the 1½ in used in the previous three tests. In addition, the weld size was reduced from ¼ in to $^{7}/_{32}$ in for this series of tests. The failure modes for these two tests included bolt fracture in the five-bolt test, and weld and bolt fracture in the three-bolt test. Examination of bolts after failure showed less plastic deformation compared to the previous five- and three-bolt tests using A325 strength bolts. Rotations ranged from 0.053 to 0.061 radians for five-bolt tests and three-bolt tests respectively at the point of maximum shear.

Based on the experiments, it was concluded that yielding of the fin plate caused a reduction of rotational stiffness and released end moment to the mid-span of the beam. The researchers reported that ductility of the plate is essential in accommodating beam end rotation. Accordingly, they recommended that the single plate be made from lower yield stress steel. Rotational ductility was found to decrease with an increase in the number of bolts. Maximum moment was found to occur at approximately 80% of the largest achieved rotation, not occurring at the maximum sustained shear force. Shear force was found to be dominant, but in

combination with the development of bending moments the capacity of the connection was significantly reduced.

Six potential failure modes of fin plate connections were established: yielding of the gross area of the plate, bearing of the plate and beam web bolt holes, fracture of the edge distance of bolts, shear fracture of the net area of the plate, fracture of bolts and fracture of welds. Consistent with the aim of providing a rational design procedure, the above failure modes were divided into two categories: ductile failure modes (Modes 1 and 2) involving yielding of steel and brittle failure modes (Modes 3 to 6) involving fracture of steel. For each failure mode, a design formula was suggested. The design procedures were developed to ensure that the ductile failure mode will occur first, followed by the more brittle ones. These recommended design procedures were adopted by The American Institute of Steel Construction (AISC) in the AISC-ASD manual (AISC 1989).

2.6.1.2. Research and documented work in Australia

Pham and Mansell (1982) [2.21] state that investigation of the behaviour of fin plate connections started in Australia in 1975 with the work of McCormick and Lay [2.22], who demonstrated that plastic hinges could be formed in the fin plate at the stiff support line. Their work forms the basis for fin plate connection design in Australia. Three years later, the AISC (Australian Institute of Steel Construction) published Standardised Structural Connections (Hogan and Firkins 1978), [2.23, 2.24] in which five fully standardised flexible connections were proposed, four of them treated as simple shear connections. With regard to fin plate connections, a distinction was made between the flexible supports (beam-to-beam connection) and fixed or stiff supports (beam-to-column connection). The design model presented by Hogan and Thomas in 1978 [2.24] attempts to establish the maximum allowable moment in a fin plate and considers it as a limiting design criterion.

Since the publication of the second edition of AISC Standardised Connections Manual [2.23, 2.24], the Australian Welding Research Association has sponsored a series of fin plate connection tests. Pham [2.21] conducted five tests on standardized fin plate connections with the principal aim of providing a better understanding of the connection up to the collapse level and finding the allowable loads. The tested

connections were connected to stiff supports using M20, 8.8 bolts in two bolt lines only, with 140mm spacing between the two lines. The main reason for the second line of bolts was to ensure that the allowable strength of the bolt group was greater than that of the fin plate and enhance the moment capacity of the bolt group. The key findings were as follows:

- Considerable rotation of the beam occurred before the plate started to rotate together with the beam web.
- The failure of all fin plate connections was due to yielding and tearing of the plate under combined moment and shear, consistent with the aim of making the plate the weakest component in the design model.
- Extensive deformations were found in the plate on the first line of bolt holes (nearest the column), indicating that they were carrying most of the shear load and that there was little load redistribution between the two bolt lines.
- No sign of deformation or damage appeared in the bolt or in the weld.

As a result of these tests, revisions to the design of fin plate connections were made (Hogan and Firkins 1983) [2.25]. The main modifications to the previous standardised fin plate connection design were, (i) dropping the distinction between fixed and flexible supports (ii) the spacing between the bolt lines was reduced to 70mm from 140mm.

Pham (1985) [2.26], at the CSIRO Division of Building Research, Melbourne, conducted a total of nine tests (**Figure 2.19**) to assess the efficiency of the previous revisions and to investigate further the behaviour of fin plate connections connected to a column flange (stiff support) under the following conditions:

- The use of the 70 mm gauge for the double lines of bolts.
- The use of a single line of bolts.
- The use of 6 mm fillet welds rather than the standard 8 mm fillet welds.

Beam sections 360UB45 and 460UB67 were used in conjunction with Grades 8.8 (A325 strength) and 4.6 (A307 strength) connection bolts. Pham utilized the same

test setup and measurement system as in his 1982 research [2.21]. This test setup consisted of a cantilevered beam attached to the face of the column flange via a fin plate shear connection (rigid support condition). Lateral bracing was provided to the tested beam at regular intervals to prevent out-of-plane buckling. The cantilevered beam is free end was supported via a load cell. A point load was placed at a distance 1.5 times the beam depth from the weld line.

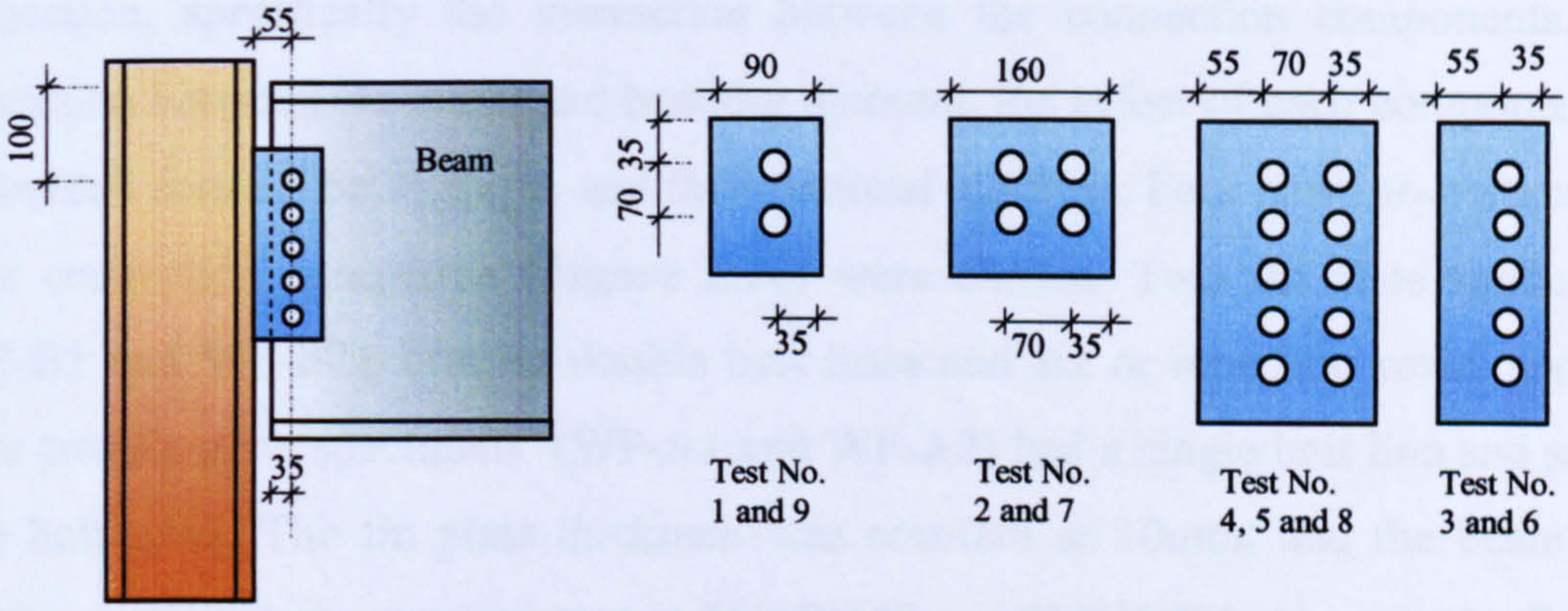

Figure 2.19 Geometric details of Pham *et. al.* tests specimens

Test behaviour indicated a variation in failure modes according to the connection configurations. For example, among connections with a single line of bolts, one failed via ductile failure of the weld, while the other three tests, in which only one test utilized lower-strength bolts, failed via shear failure of the bolts. Weld size in the latter three tests was not the critical component of the connection, although not conforming to the standardized recommended using of 8mm. For connections with a double line of bolts, connection failures were varied, with either ductile failure of the weld (when 6 mm was used), shear failure of the bolts, shear deformation of the plate, or tearing of the fin plate. The researchers concluded that the most accurate method of assessing the allowable load capacity and predicting fin plate connection behaviour is by a 'Simple' model which assumes that the bolt group withstands the entire shear load, but checking the fin plate and the weld for the shear and moment resulting from the eccentricity of the bolt group. Also, researchers recognized that bolt shear brittle failure at the ultimate load is possible for a fin plate connection with a fixed support. Fin plate connections were more ductile in the previous Standard (1978) [2.23, 2.24] because in this the plate was designed to be the weakest component.

Another series of tests supported by the Australian Welding Research Association was conducted on fin plate connections by Patrick *et. al.* [2.27]. The main aim was to validate the capability of the design model and the details specified for fin plate connections against the largest member sizes in the Connection Manual [2.28, 2.29], and to ensure whether the connection had acceptable behaviour at serviceability loads and adequate ductility up to the required strength of the attached beam. However, these tests were also run to improve understanding of the behaviour of this type of connection, specifically the interaction between the connection components, the interaction between the shear and bending moment, the effect of each component on the overall connection strength, and the rotational stiffness. Four beam-to-column fin plate connection specimens (**Figure 2.20**) were chosen. Two fin plate specimens (WP-B1 and WP-B2), utilised double bolt lines and six or nine bolt rows, and the other two fin plate specimens (WP-A1 and WP-A2) had a single bolt line and six or nine bolt rows. The fin plate thickness was constant at 10mm, and the beam and column section sizes were constant at 760UB147 and 310UC283 respectively. For all connection specimens, bolts of Grade 8.8 20 mm in diameter were used in 22mm diameter over-sized holes.

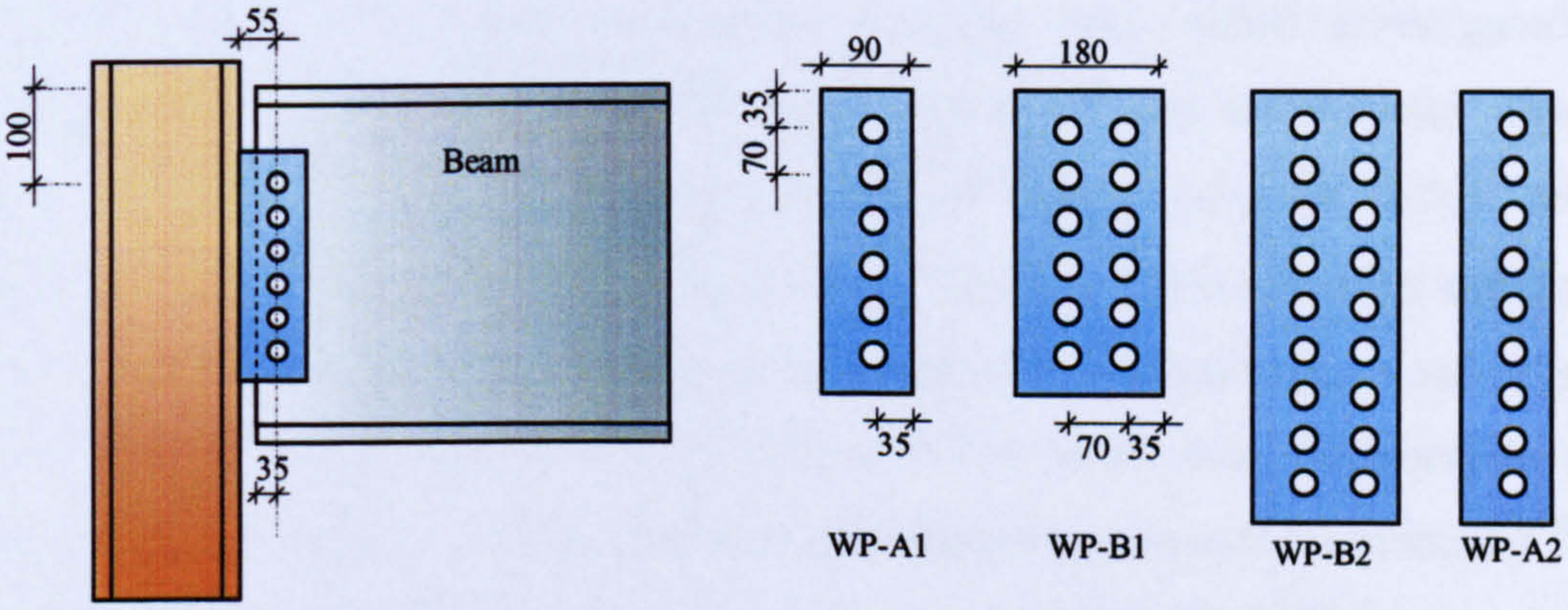

Figure 2.20 Geometric details of Patrick *et. al.* tests specimens

The test setup was designed to simulate uniformly loaded simply supported beam. A hydraulic jack close to the connection was used to apply the required shear force. With the other end of the supported beam on a pin support capable of moving downward so as to apply adequate rotation at the connection, representing the rotation due to the bending of a uniformly loaded simply supported beam. Two specimens (WP-A1 and WP-A2) failed by sudden shear failure of all bolts. The fin

plates were affected very little by local deformation of the bolt holes due to bolt bearing, and no damage to the welds was observed. Connection specimens WP-B1 and WP-B2 failed by sudden shear fracture of the fin plate at the net section, between the weld and the first bolt line, but there was no tearing-out failure. The inner bolt holes were distorted severely due to excessive shear deformation of the plate, not due to bolt bearing. Local damage in the form of a small crack was observed at the top of each weld line.

It was concluded that the level of rotation at failure was significantly affected by the shear load applied to the connection. In addition, there was an interaction between the shear force and the bending moment, particularly noticeable at higher shear loads, where the bending moment was found to decrease as the shear force was increased. Connection strength was found to be a function of weld strength, the strength of the bolt group, the yield strength of the fin plate, and the ultimate strength of the fin plate. The Australian Institute of Steel Construction model was found to be adequate, providing sufficient factors of safety for fin plate connections when used with the largest member sizes included in the manual.

Aggarwal (1988) [2.30] conducted a series of eight tests which investigated the moment-rotation characteristics of fin plate beam-to-column connections. The test setup consisted of 800mm length cantilevered beams of 200UB25.4 section connected to a test column (200UC46.2) via a fin plate with double rows and double lines of bolts. The fin plate was welded to the face of the column flange and offset to the column flange by one half the thickness of the beam web. Connections were designed in accordance with the Australian standardized connections manual [2.28, 2.29]. The nominal yield stress of the steel was 250 N/mm^2. Three bolt diameters, 16mm, 20mm, or 24mm, of AS-1252 strength bolts (which are approximately equivalent to 8.8 strength bolts) were used in combination with 10 mm, 12 mm, or 16mm fin plates respectively. The bolts used in testing were fully pre-tensioned. A single hydraulic jack was used to apply an upward load at the free end of the tested beam. 10mm stiffeners were welded between the flanges and to the web above the hydraulic jack, and similarly to the column opposite the fin plate connection. The first two specimens utilized the above setup, while the other six tests utilized a seat

angle to reduce the affects of slippage. The seat angle was shop-welded to the beam and connected to the test column flange with two M20 bolts. Seven specimens were loaded gradually with increasing static loads. The remaining specimen was subjected to a pulsating loading over 1500 cycles. The two specimens without seat angles were initially loaded to 30kN and the other specimens (with seat angles) were loaded up to 40kN. Test specimens were assumed to have failed when large displacements or slippage occurred, resulting in difficulties in recording any further observations on account of large beam rotations.

From this series of tests, moment-rotation curves for fin plate connections with and without seat angles were obtained. Curves indicated nonlinearity in moment-rotation behaviour over the complete range of loading. Rotation was usually caused by slip and elongation of the bolt holes in the beam web and/or fin plate. In specimens without seat angles, it was observed that the load needed for slippage to occur was directly proportional to the bolt diameter, so for larger-diameter bolts slippage occurred at higher loads. Visible investigation after the test showed that there was almost no deformation in the column or fin plate. The only visible deformation occurred in the two bolt holes nearest the tension flange (bottom flange) of the beam. As both the major and minor axes of the column were unrestrained, this resulted in significant out-of-plane rotations at the joints. Also it was found that joint stiffness increased considerably with the combination of a large bolt diameter and a thick fin plate.

2.6.1.3. Research and documented work in the UK.

Prior to the development of the UK's own design method for steel fin plate connections, an intensive literature survey was conducted to calibrate current design processes [2.12]. The AISC (Australian Institute of Steel Connection) design method [2.28, 2.29] was found to be the best; therefore it was adopted in the UK as a starting point and the SCI and BCSA published a draft steel joint design method (1988) [2.31]. The main difference between this publication and the Australian one was that the British design model requirement is that the bolt diameter / plate thickness ratio should ensure that bolt bearing failure mode occurs before bolt shear failure, as the latter mode is brittle.

After the publication of the draft steel joint design method (1988) [2.31], it was decided that further research was needed to confirm the adequacy of the Australian design procedures when applied to British design regulations. Therefore, SCI and BCSA supported a series of tests on fin plate connections conducted by Moore and Owens (1992) [2.12]. The test setup was chosen as an inverted H frame (**Figure 2.21**) to reproduce the actual connection arrangement in a multi-storey building. The tested beams were connected at both ends. The beam length was 20 times the chosen depth. A total of eleven tests were conducted. Two sizes of beam and column were used; six tests used 356x127x33UB connected to 203x203x46UC while the other five tests used 610x229x101UB connected to 305x305x97UC.

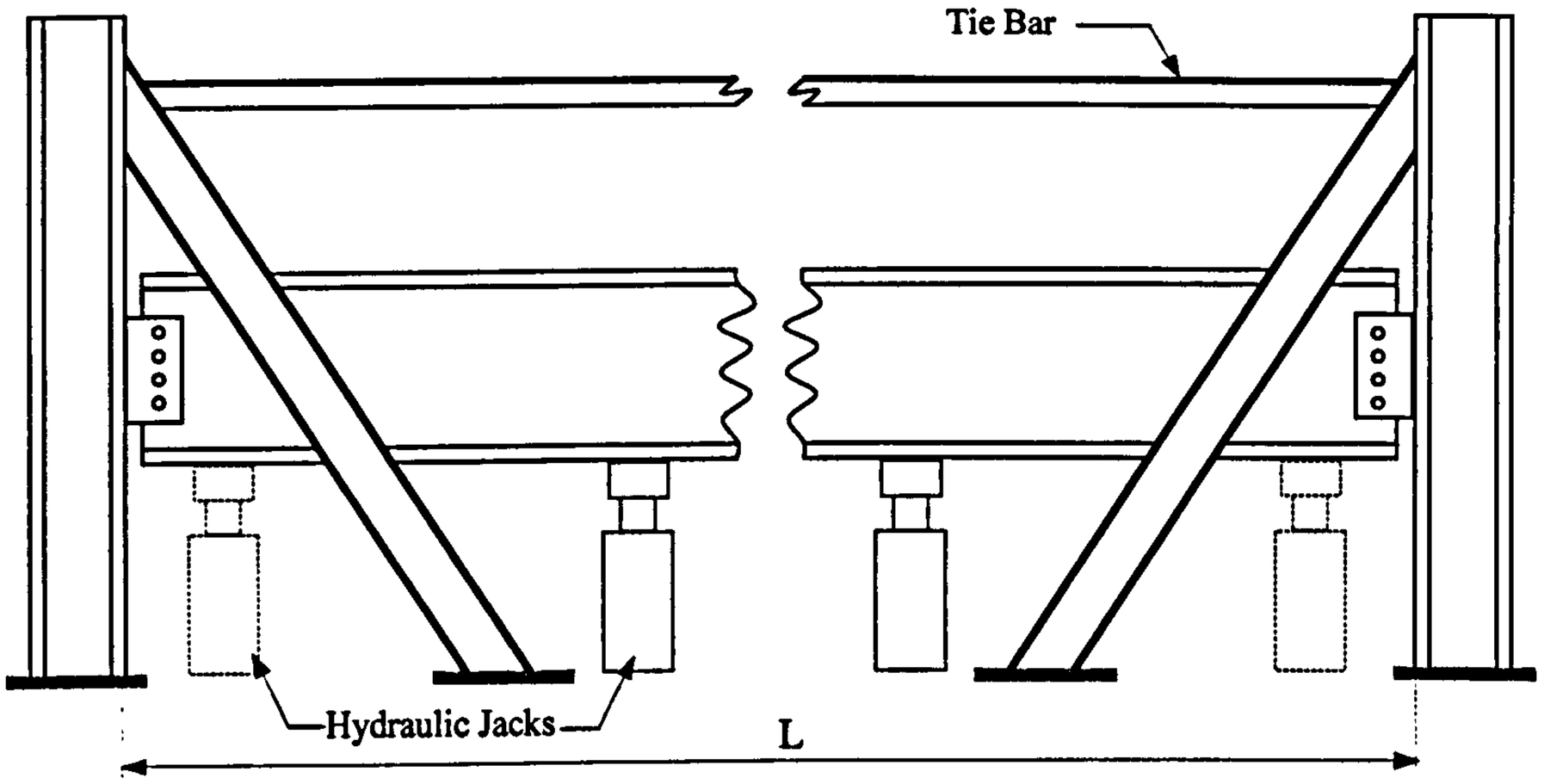

Figure 2.21 Moore and Owens test setup

The depth and length of the fin plate were varied. In most tests, a fin plate was welded to the face of the column, offset from the centre-line by one-half the beam web thickness. The stiffness of the support was varied by carrying out a small number of tests with the connection framing into the column web to investigate the additional flexibility provided by minor axis bending of the column. Punched holes were used in conjunction with Grade 8.8 M20 bolts. Columns were 1500mm in height and were allowed to rotate at either column end via 50mm diameter captive roller bearings. However, the columns were restrained against longitudinal movement via tie bars. The test was designed to apply shear combined with rotation at the end of the beam which introduced a moment into the connection. This test setting allowed the connection rotation capacity to be investigated, establishing

whether the connection was flexible. Each specimen was loaded by two 1000kN hydraulic jacks positioned between the floor and the beam immediately below the centreline of the tested beam and symmetrically about the beam mid-span. The compression flange was restrained at intervals to prevent out-of-plane buckling. Instrumentation measured the applied load, bending moments in the beam, the moment-rotation response of the connection, and the deflected shape. All specimens were tested in two phases. The elastic phase was designed to model a fin plate connection at the end of a uniformly loaded beam. Hydraulic jacks were located nearer the mid-span for this phase and the load was applied in equal increments to a level approximately equal to the service load (unfactored dead and imposed load). The test specimens were then loaded to failure using the hydraulic jacks located nearer the connection to ensure failure.

It was found that the elastically tested specimens resisted some moment by bearing deformations of the fin plate and beam web. The test rotations for specimens with fin plates welded to the column web were found to be significantly greater than the test rotations of similar connections with fin plates welded to the column flange. Typically, the weld and the bolt line experienced a combination of shear and moment.

In tests loaded to failure, short fin plate connections were found to fail more frequently by bearing failure of either the fin plate or the beam web, while long fin plates were found to fail by plate lateral-torsional buckling and / or local beam web buckling. There was no sign of weld yielding after any test. Although the connection bolts did not fracture, plastic deformation was found in the connection bolts, and in one test specimen the design shear capacity of the bolt group exceeded 61%. In addition the bolt holes in both the beam web and fin plate exhibited permanent bearing deformations.

Moore and Owens proved that the adopted design method [2.31] was adequate and conservatively provides safety factors of 1.57 to 3.57, but they did not recommend it for beams deeper than 610 mm without further analysis. Also they observed that "the small number of tests limited the parameters that can be varied and it was not

possible to test for all the modes of failure of the connection, nor was it possible to verify all aspects of the design procedure". However, as a result of the observed behaviour observations and the results of the test programme, a few amendments to the design method [2.31] were introduced in the proposed British design method:

- Long fin plate connections were found to have a tendency to twist and be subject to lateral-torsional buckling. Accordingly, an additional check for lateral-torsional buckling resistance was introduced.
- The use of long fin plates with unrestrained beams was banned as there was an obvious risk of unfavourable interaction between fin plate lateral-torsional buckling and lateral-torsional buckling of the beam.

In the 'Joints in Steel Construction: Simple Joints' design manual which was published in 2002 [2.32], the British design method for fin plate shear connections was finally presented as series of simple checks of an individual component on the load path:

- Compliance with the necessary detailing requirements.
- Bolt group capacity under shear and moment.
- Net section capacity of beam web.
- Net section capacity of fin plate.
- Lateral-torsional buckling capacity of long fin plate.
- Capacity of attachment weld.
- Local capacity checks of web of supporting element.
- Structural integrity check (for beam to column connection only).

The British design of fin plate connections achieves ductile behaviour through bolt bearing or shear and bending of the fin plate. The types of fin plate connections included in the design method are: beam-to-beam web, beam-to-column flange or beam-to-column web, and beam-to-hollow steel tube (rectangular or circular).

and moment capacity, and proposing design procedures). Similar test setups were used in later test programmes in which one beam end was connected to the fin plate and the other was supported on roller supports. In addition, shear force was applied in combination with rotation or moment. To understand the connection behaviour, experimental investigations have been conducted based on parameters such as plate thickness, plate width, pitch distance, gauge distance, edge and end distance, bolt type and bolt diameter, depth and length of the connected beam, and material properties of the connection components (plate, bolt and beam). However, the small number of test series performed has limited the range of variation of parameters. In addition it was not possible to test for all the modes of failure of the connection.

In the test series conducted by Lipson *et al.* [2.13], Richard [2.4] and Pham [2.21] an edge distance yielding, bolt hole bearing failure and weld yielding were observed. The common thing between these tests was the use of small fin plate thickness and beam web thickness combination (6-10 mm) compared to the bolt diameter (M20), in addition to the use of 6 mm welds. Later experiments conducted by Astaneh *et al.* [2.18 - 2.20], Pham [2.26] and Patrick *et. al.* [2.27] experienced failure by sudden bolt shear fracture. That most likely related to the use of more bolts number (5-9) than in the previous test series and the use of a large beam section along with 10 mm plate thickness. Similarly, Moore and Owens (1992) [2.12] used a beam size of (610x229x101UB) with a web thickness greater than the constant fin plate thickness (10 mm). A permanent bolt deformation in all deep fin plate specimens was observed. However, weld failure was a regular failure mode in the early test programs [2.10, 2.11-2.13] due to the use of 6mm welds. In contrast, in the other tests [(2.18 - 2.20), 2.21, (2.26, 2.27, 2.30)] where 8mm welds were used, weld failure was rare.

Most researchers were concerned with finding the moment-rotation or shear-rotation relationships with the shear force eccentricity or beam mid span deflection. The resulting design procedures checked each connection component on the load path for likely failure modes. The limited number of test series, did not allow testing for all failure modes. For example, although the UK design procedures have a design check on fin plate connection tying capacity, none of the conducted tests have directly measured fin plate connection tying force capacity.

2.6.2. Review of the steel connection research in fire conditions

Structural fire engineering research started to explore structural member capacity at elevated temperatures by testing each member in isolation, regardless of its actual support condition [2.33, 2.35]. Spyrou [2.36] reported that the first experimental fire tests on connections were conducted at CTICM [2.37] in 1976. Six different types of connection were tested, ranging from "flexible" to "rigid" under both the ISO 834 fire curve and linear increase in temperature. The initial objective of the tests was to establish the performance of high-strength bolts at elevated temperatures, so there was no intention to investigate the overall behaviour of steel connections. The results demonstrated that bolts and the other connection components could suffer significant deformation in fire. However, the Cardington fire tests on a full-scale steel building [2.38] identified significant discrepancies between the individual member behaviour and behaviour in a real structure under fire conditions. Full-scale fire tests also suggested that connections which were considered as pinned at ambient temperature may provide considerable amounts of both stiffness and strength at elevated temperatures thus enhancing the survival time of the structure. This has demonstrated the significance of member end connections in fire conditions. Consequently, experimental fire research has shifted toward testing the structural member in a sub-frame setting, along with its real connection [2.39 - 2.46]. Despite the fact that fire testing of steel connections has highlighted the potentially beneficial behaviour of steel connections at elevated temperature, these have been insufficiently addressed yet in the design codes [2.47, 2.48]. This is mainly due to the lack of experimental data, which partly relates to the high cost limitation of furnace testing. Structural fire research has taken a further step by utilising finite element modeling for research development. FEM overcomes fire testing limitations and allows for a wide range of parametric connection investigations. Using the available test data for validation, research has been conducted to simulate the connection behaviour via FE modelling [2.49 - 2.54] at elevated temperature.

Liu (1996) [2.49, 2.50] developed a three-dimensional finite element mathematical model, FEAST, to simulate the response of steel structures with connections at elevated temperature. The entire connection (column, beam, and end-plate) was modelled via eight-noded shell elements. Also, nonlinear material properties as well as non-uniform thermal expansion were considered. Further developments were introduced

in the model to simulate the behaviour of steel-concrete composite extended end plate connections at elevated temperatures [2.51, 2.52]. The composite connection consisted of the main beam and the column, in addition to a reinforced concrete slab supported by cold-formed profiled steel sheeting which is connected to the top flange of the main beam by shear studs. The connection temperature-rotation characteristic was investigated at a range of applied bending moments. The mathematical model was compared with a series of fire tests carried out by Building Steel [2.39]. The main finding was that the rotational stiffness of an extended end-plate is dependent upon the plate thickness, beam depth, end plate width, and bolt diameter.

El-Houssieny, *et. al.* (1998) [2.53], conducted analytical evaluations of extended end-plate connections with the main objective to develop simple expressions which could predict the behaviour of different connection components at elevated temperatures. For this purpose a three-dimensional finite element model was created to simulate the extended end-plate connection behaviour at ambient and at elevated temperatures. Beam, shell, and solid elements were used in the model and assigned to each connection component, depending on its features. The end-plate and column flange were modelled by solid elements, whereas the beam and stiffener were modelled using shell elements. Each bolt was assembled using beam elements (**Figure 2.22**). An extensive parametric study was carried out to study the influence of using different connection parameters on the connection behaviour at ambient and elevated temperatures. Equations were proposed to predict the connection stiffness, stresses and bolt forces.

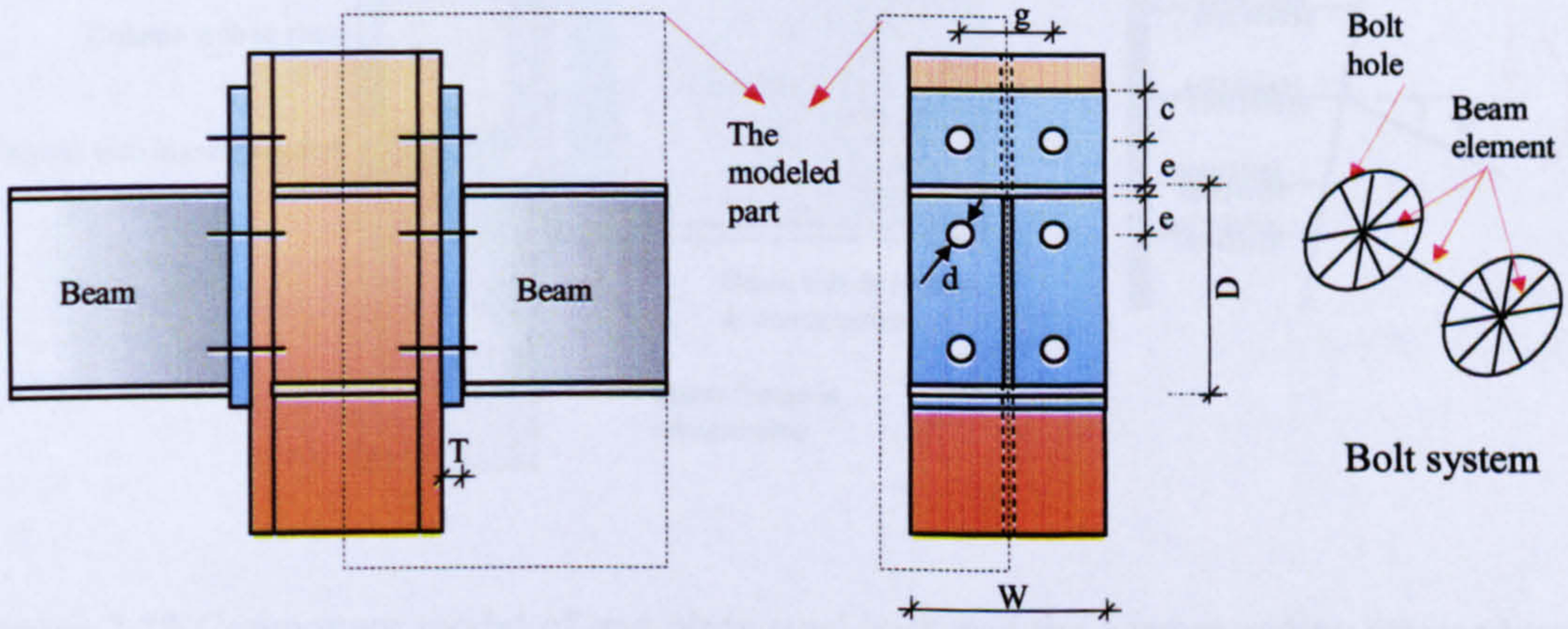

Figure 2.22 Details of the El-Houssieny, *et. al.* connection parameters

FE modelling of steel connections at high temperatures was conducted by Al-Jabri [2.54], who created a three-dimensional finite element model for flush end-plate bare-steel connections using ABAQUS. All the connection components were modelled via three-dimensional brick elements. Nonlinear temperature-dependent material properties were considered. In addition, contact elements between the interacting connection components were introduced. Moment-rotation-temperature relationships and failure modes were shown to be in good agreement with experimental results.

FEM has provided the opportunity for a wider range of parametric investigations to be undertaken, and eliminates some of the limitations associated with experimental studies. Although the finite element technique has some advantages over fire testing, it can be time-consuming in terms of computing calculations for elevated-temperature analyses. The development of the Component Method has introduced a better solution method for connection analyses. In this method the connection behaviour (load-deflection or moment-rotation) can be predicted in less computation time and with satisfactory accuracy compared to FEM. The basic idea of the Component Method (**Figure 2.23**) is to consider any connection as an assembly of non-linear springs, each one representing an individual connection component with its own characteristic of strength and stiffness which degrade as temperature rises. More explanations regarding the Component Method will be given in Chapter 6.

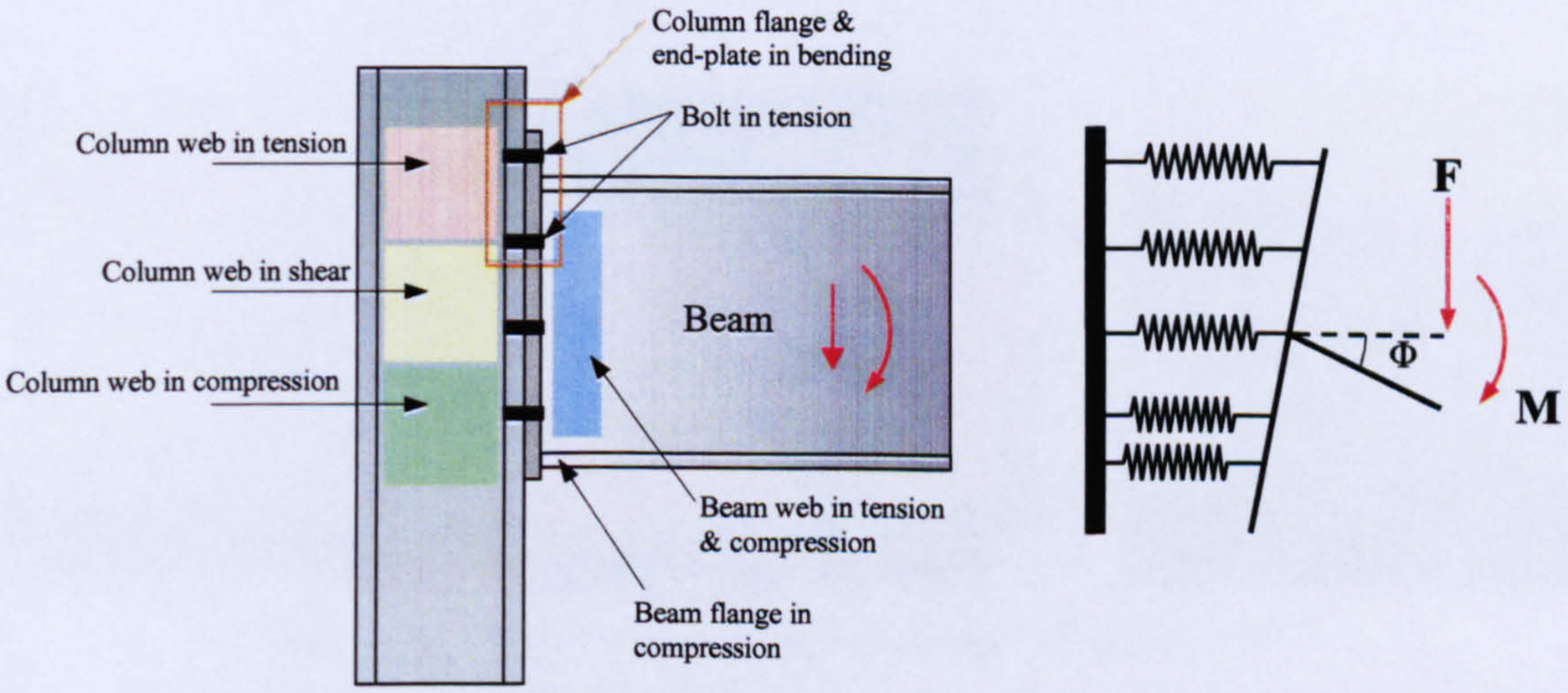

Figure 2.23 Component model of end-plate steel joint and the corresponding stressed zones

The implementation of the Component Method in modelling steel connections at elevated temperature goes back initially to Leston-Jones's research [2.55], in which he developed a component model for bare-steel and composite flush end-plates. The comparison of the component model for bare-steel flush end-plate joints against experimental data showed close agreement. However, the composite flush end-plate component model was not good at including the rate of degradation at elevated temperature. Similarly, da Silva, et al. [2.56] have recently proposed a component model for the bare-steel composite flush end-plate connection, and has shown good agreement with experimental results. Al-Jabri, et al. [2.57, 2.58] used the same approach but to model bare-steel composite flexible end-plate connections. The comparison with test data demonstrates good agreement, especially in the elastic stage. The model has predicted well the rate of stiffness and capacity degradation when compared to experimental measurements.

Spyrou, [2.36], conducted experimental furnace testing of T-stubs to investigate the tension [2.59] and compression zones [2.60] of steel beam-to-column end-plate connections in fire conditions. Based on this, a simplified analytical model, using the Component Method approach, has been developed and validated against test data. The proposed spring model has been shown to be reliable for this common type of joint. It has also produced moment-rotation curves which correlate well with the results of previous furnace testing on complete end-plate connections.

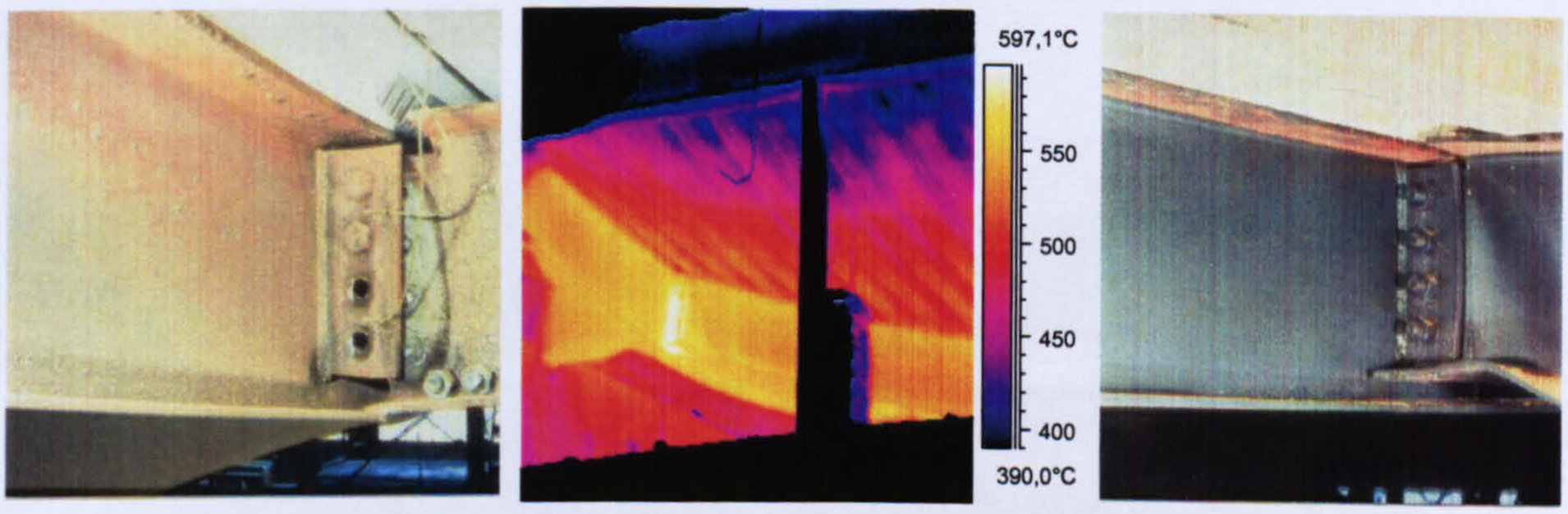

Figure 2.24 Fin plate connection following Cardington test [2.61]

With regard to steel fin plate connections, these were tested for the first time in a real fire as the beam-to-beam connections in the Cardington fire tests [2.61] (**Figure 2.24**). After the tests, investigation has shown that many of the bolts in the fin plate

connections had sheared on one side of the primary beam, due to thermal contraction of the beam during cooling. No signs of weld or edge-distance rupture failure could be seen. The thermal contraction generated very high tensile forces, which were relieved once the bolts sheared in the fin plate connection from the side of the secondary beam.

In 2005 the author had an invitation to witness a fire test conducted by Wald and Ticha on a steel fin plate connection at the Czech Technical University (**Figure 2.25**). A three-bolt fin plate connection, 6×60×125mm, was assembled using fully threaded Grade 8.8 high strength bolts of 12mm diameter. The beam was an IPE160 cross section 3m long, and the loads were applied by two hydraulic jacks (60 kN each) 250mm from the beam ends. The fin plates and beam were both of Grade S235. The furnace gas temperature was controlled to follow the Cardington [2.62] fire test No. 7 for the heating and cooling stages and reach a temperature as high as 1200°C.

Following the test investigation, it could be observed that the fin plate weld showed no sign of failure or fracture, whereas most of the bolts were sheared completely in the direction of the beam mid-span (**Figure 2.25**). Some of the bolts were embedded into the web or fin plate holes, a sign of high-level tying force applied to the bolts. The bolt holes of beam web were distorted a maximum of only 3 mm. Also the beam web suffered diagonal local buckling between the beam edge and the web stiffener at both beam ends.

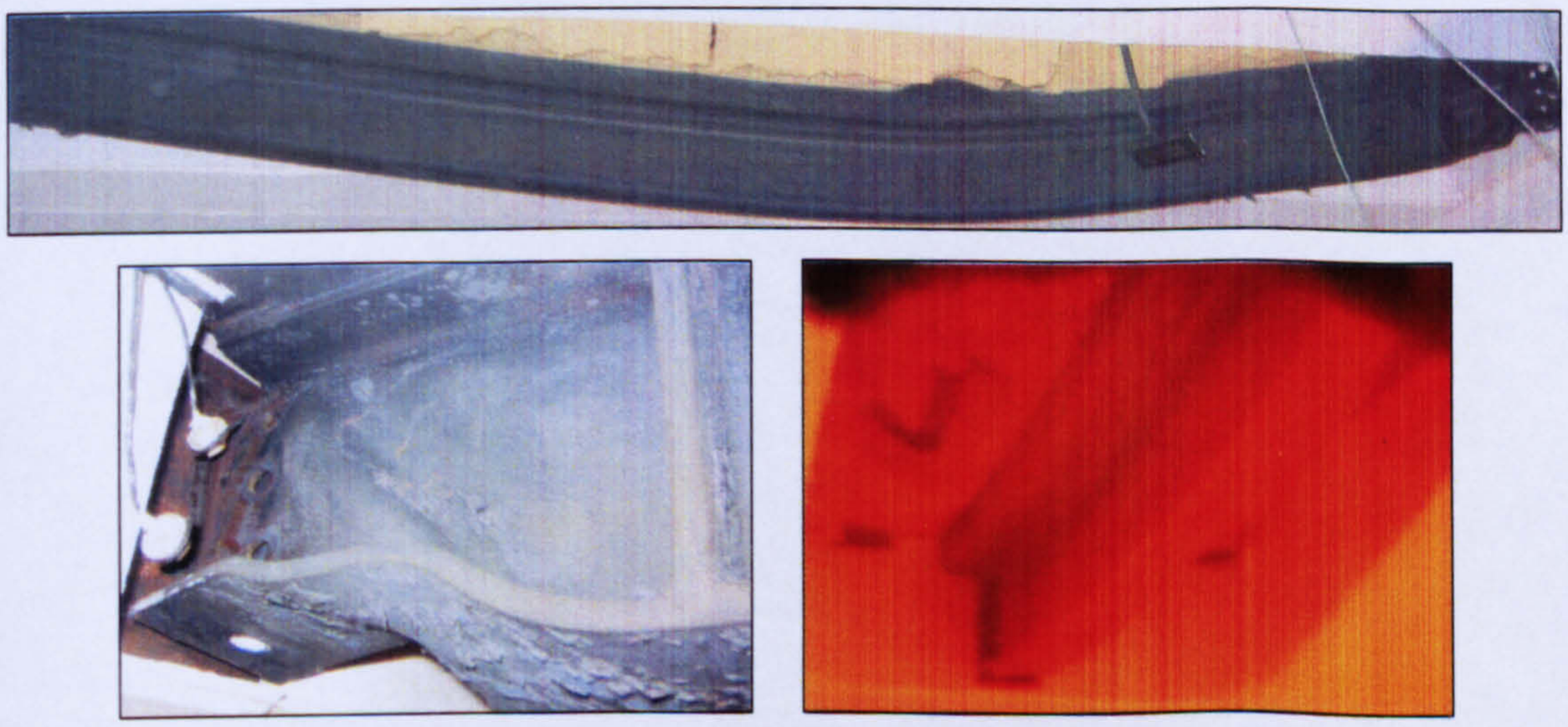

Figure 2.25: Wald and Ticha fin plate connection test

2.7. Conclusions and Discussion on the Literature Review

An assessment of previous research conducted on steel connections in fire conditions shows a limited number of investigations into the behaviour of fin plate shear connections at elevated temperature. Such investigations should highlight the connection strength and stiffness at elevated temperature. Most of the previous research on fin plate connections was at ambient temperature and the main focus was either on the moment-shear or moment-rotation behaviour. To date there is no research on fin plate connections subjected to combined shear, moment, and axial tensile loads, which is the case in any severe fire. Consequently, there is a lack of research on the use of shear connections in fire conditions, as well as at normal temperature under extreme loads. The low levels of available research on fin plate shear connections, together with their economic popularity, has necessitated this research.

2.8. References

[2.1] Glenn, A., Morris G. A. and Packer, J. A., "Beam-to-Column connection in steel frames", *Canadian Journal of Civil Engineering*, Vol. **14**, (1987) pp 68-76.

[2.2] Wilson, W. M., and Moor, H. F., "Test to determine the rigidity of riveted joint in steel structures", Engineering Experimental Station, University of Illinois, Urbana, IL, Bulletin 104, (1917).

[2.3] Nethercot, D. A., "Steel Beam-to-column Connections A Review of Test Data and its Applicability to the Evaluation of Joint Behaviour in the Performance of Steel Frames", CIRIA Project Study, (1985).

[2.4] Li, T.Q., Choo, B. S. and Nethercot, D.A., "Connection Element Method for the Analysis of Semi-rigid Frames", *J. Construct. Steel Research*, Vol. **32**, (1995) pp 143-171.

[2.5] Jones, S.W., Kirby, P.A. and Nethercot, D.A., "The Analysis of Frames with Semi-Rigid Connections- A State-of-the-Art Report", *J. Construct. Steel Research*, Vol. **3**, No. 2, (1983) pp 1-13.

[2.6] Owens, G. W. and Cheal, B. D., "Structural Steelwork Connections", 1stEd, (1989).

[2.7] Geoffrey, L., Kulak, J.W., Fisher, J.H. and Struik, A. "Guide to Design Criteria for Bolted and Riveted Joints", Second Edition, pp.173, (2001), AISC, Suite 3100, Chicago, IL 60601

[2.8] www.kuleuven.be/bwk/materials/Teaching/

[2.9] European Committee for Standardization (CEN). "Eurocode 3: Design of Steel Structures, Part 1.8: Design of joints", EN 1993-1-8, British Standard Institution, London, (2005).

[2.10] www.steel-connections.com

[2.11] BCSA, The British Constructional Steelwork Association, "Joints in Simple Construction – Volume 1: Design Methods (Second Edition)", The Steel Construction Institute (1991).

[2.12] Moore, D.B. and Owens, G.W. "Verification of design methods for fin plate connections", *The Structural Engineer*, Vol. **70**, No.3/4, February (1992).

[2.13] Lipson, S. L., "Single-Angle and single-plate Beam Framing Connections", Proceedings, Canadian Structural Engineering Conference, Toronto, Ontario, Canada, February (1968) pp 141-162.

[2.14] Richard, R. M., Gillett, P. E., Kriegh, J. D. and Lewis, B. A., "The Analysis and Design of Single Plate Framing Connections", *Engineering Journal*, AISC, Vol. **17**, No.2, (1980) Second Quarter.

[2.15] Richard, R. M., Kriegh, J. D. and Hormby, D. E., "Design Single Plate Framing Connections with A307 Bolts", *Engineering journal*, AISC, (1982) pp 209–213, Fourth quarter.

[2.16] Hormby, D. E., Richard, R. M. and Kriegh, J. D., "Single-Plate Framing Connections with Grade-50 Steel and Composite Construction", *Engineering journal*, AISC, Vol. **21**, No. 3, (1984) pp 125-138.

[2.17] Young, N.W. and Disque, R.O. "Design Aids for Single Plate Framing Connections", *Engineering journal*, AISC, Vol. **18**, No.4, (1981), Fourth quarter.

[2.18] Astaneh, A., Call, S. M. and McMullin, K. M., "Design of single plate shear connections", *Engineering journal*, AISC, Vol. **26**, No.1, (1989).

[2.19] Astaneh, A., McMullin, K. M. and Call, S. M., "Behaviour and Design of Steel Single Plate Shear Connections", *Journal of Structural Engineering*, Vol. **119**, No. 8, (1993) pp 2421-2440.

[2.20] Astaneh, A., Liu, J. and McMullin, K. M., "Behaviour and Design of Single Plate Shear Connections", *J. Construct. Steel Research*, Vol. **58**, (2002) pp 1121–1141.

[2.21] Pham, L. and Mansell, D. S., "Testing of Standardized Connection" Australian Welding Research Vol.11, December, (1982).

[2.22] McCormick, M.M. and Lay, M.G., "Steel Structures – part 4, Connections", BHP Melbourne Research Laboratory Report MRL 39/2, Final draft dated 25, 2, (1975).

[2.23] Hogan, T.J. and Firkins, A. "Standardized Structural Connection Manual - Part A: Detail and Design Capacities", Australian Institute of Steel Connection, March (1978).

[2.24] Hogan, T.J. and Thomas, I.R. "Standardized Structural Connection Manual - Part B: Deign Models", Australian Institute of Steel Connection, March (1978).

[2.25] Hogan, T.J. and Firkins, A. "Standardized Structural Connections Manual – Five years on", Metal Structures Conference, Brisbane Australian Institute of Steel Connection, March (1983).

[2.26] Pham, L. "Strength of Web Side Plate Connection with Revised Standardized web Side Plate", Third conference of Steel Developments, Melbourne, Australia, May (1985).

[2.27] Patrick, M., Thomas, I.R. and Bennetts, I.D. "Testing of Web Side Plate Connections", Structure Conference, Auckrick, New Zealand, Aug. (1986).

[2.28] Hogan, T.J. and Firkins, A. "Standardized Structural Connections Manual - Part A: Detail and Design Capacities", Australian Institute of Steel Connection, March. (1981).

[2.29] Hogan, T.J. and Thomas, I.R. "Standardized Structural Connection Manual - Part B: Deign Models", Australian Institute of Steel Connection, March (1981).

[2.30] Aggarwal, A.K. "Behaviour of Web-Side Plate Beam-Column Connections", 10th Australian conference on the mechanics of structures and materials, University of Adelaide, Australia, (1986).

[2.31] Malik, A. (ed): "Detailed design rules for structural connections. Draft rules for simple connections in braced multi-storey frames", SCI/BCSA, (1988).

[2.32] BCSA, "The British Constructional Steelwork Association LTD., Joints in Steel Construction: Simple Connections", The Steel Construction Institute (2002).

[2.33] British Steel Corporation, *Compendium of UK standard fire test data on unprotected structural steel.* Contract report for Department of Environment, (1987).

[2.34] ISO834:"Fire Resistance Tests, Elements of Building Construction", (1975).

[2.35] Shepherd, P.G. "The Performance in Fire of Restrained Columns in Steel-Framed Construction", PhD. Thesis, University of Sheffield, 1999.

[2.36] Spyrou, S. "Development of Components Based Model of Steel Beam-to-Column Joint at Elevated Temperatures", PhD. Thesis, Department of Civil and Structural Engineering, University of Sheffield, 2002.

[2.37] Kruppa, J. "Resistance on feu des assemblage par boulous", Center Technique Industrial de la Construction Metallique, St. Remy Chevzuese, France, 1976, CTTICM Report, Document No. 1103-1, English translation available entitled "Fire Resistance of Joint with High Strength Bolts".

[2.38] SCI, Structural Fire Engineering: Investigation of Broadgate Phase 8 Fire. Steel Construction Institute, UK, (1991).

[2.39] British Steel, "The Performance of Beam/Column/Beam Connections in the BS5950: part 8 Fire Test", British Steel (Swinden labs), Report T/RS/1380/33/82D and T/RS/1380/34/82D. Rotherham, (1982).

[2.40] Lawson, R. M., "Behaviour of steel beam-to-column connections in fire" *The Structural Engineer*, Vol. **68**, No.14, (1990) pp 263-271.

[2.41] Lennon, T. and Leston-Jones, L. C., "Elevated Temperature Composite Connection Moment Rotation Tests", Building Research Establishment, (1995).

[2.42] Leston-Jones, L. C., "The Influence of Semi-Rigid Connections on the Performance of Steel Framed Structures in Fire", PhD. Thesis, Department of Civil and Structural Engineering, University of Sheffield, 1997.

[2.43] Leston-Jones, L. C., Lennon, T., Plank, R. J. and Burgess, I. W., "Elevated Temperature Moment-Rotation Tests on Steelwork Connections", *Proc. Instn. Civ. Engrs. Structs. & Bldgs*, **122**, (1997) pp 410-419.

[2.44] Al-Jabri, K. S., Lennon, T., Burgess, I. W. and Plank, R. J., "Behaviour of Steel and Composite Beam-column Connections in Fire", *J. Construct. Steel Research*. Vol. **46** (1-3), (1998) pp 308-309.

[2.45] Al-Jabri, K. S., "Behaviour of Steel and Composite Beam-column Connections in Fire", PhD. Thesis, Department of Civil and Structural Engineering, University of Sheffield, 1999.

[2.46] Al-Jabri, K. S., Burgess, I. W., Lennon, T. and Plank, R. J., "Moment–rotation–temperature curves for semi-rigid joints", *J. Construct. Steel Research*, Vol. **61**, (2005) pp 281–303.

[2.47] BS 5950: "Structural Use of Steelwork in Building, Part 8: Code of Practice for Fire Resistance Design", British Standard Institution (BSI), London (1995).

[2.48] European Committee for Standardization (CEN), "Eurocode 3: Design of Steel Structures, Part 1.2: General rules - Structural fire design", EN 1993-1-2, British Standard Institution, London, (2005).

[2.49] Liu, T. C. H., "Finite Element Modelling of Behaviours of Steel Beams and Connections in Fire", *J. Construct. Steel Research*, Vol. **36**, (3), (1996) pp181-199.

[2.50] Liu, T. C. H., "Effect of Connection Flexibility on Fire Resistance of Steel Beams", *J. Construct. Steel Research*, Vol. **45**, No.1, (1998) pp 99-118.

[2.51] Liu, T. C. H., "Three-Dimensional Modelling of Steel/Concrete Composite Connection Behaviour in Fire", *J. Construct. Steel Research*, Vol. **46**, (1-3), (1998) pp 319-320.

[2.52] Liu, T. C. H., "Moment – Rotation – Temperature Characteristics of Steel / Composite Connections", *Journal of Structure Engineering*, Vol. **125**, No.10, (1999) pp1188-1197.

[2.53] El-Housseiny, O. M., Abdel Salam, S., Attia, G. A. M. and Saad, A. M., "Behaviour of Extended End Plate Connections at High Temperature", *J. Construct. Steel Research*, Vol. **46**, (1-3), (1998) p 299.

[2.54] Al-Jabri, K. S., Seibi, A. and Karrech, A., "Modelling of unstiffened flush end-plate bolted connections in fire", *J. Construct. Steel Research*, [in press], (2005).

[2.55] Leston-Jones, L. C., "The Influence of Semi-Rigid Connections on the Performance of Steel Framed Structures in Fire", PhD. Thesis, Department of Civil and Structural Engineering, University of Sheffield, 1997.

[2.56] da Silva, L. S., Santiago, A. and Real, V. P., "A component model for the behaviour of steel joints at elevated temperatures", *J. Construct. Steel Research*, Vol. **57**, (2001) pp 1169–1195.

[2.57] Al-Jabria. K. S., "Component-based model of the behaviour of flexible end-plate connections at elevated temperatures", *Composite Structures*; Vol. **66**, (2004) pp 215–221.

[2.58] Al-Jabri, K. S., Burgess, I. W., Lennon, T. and Plank, R. J., "Spring-stiffness model for flexible end-plate bare-steel joints in fire", *J. Construct. Steel Research*, Vol. **61**, No.5, (2005) pp1672–1691.

[2.59] Spyrou, S., Davison, J. B., Burgess, I. W. and Plank, R. J., "Experimental and analytical investigation of the 'tension zone' components within a steel joint at elevated temperatures", *J. Construct. Steel Research*, Vol. **60**, (2004) pp. 867-896.

[2.60] Spyrou, S., Davison, J. B., Burgess, I. W. and Plank, R. J., "Experimental and analytical investigation of the 'compression zone' components within a steel joint at elevated temperatures", *J. Construct. Steel Research*, Vol. **60**, (2004) pp 841–865.

[2.61] Newman, G. M., Robinson, J. T., Bailey, C. G., "Fire Safe Design: A New Approach to Multi-storey Steel Framed Buildings SCI Publication 288", The Steel Construction Institute, p. 49, (2000).

[2.62] Wald, F., Simoes da Silva, L., Moore, D., and Santiago, A. Lennon T, Chaldna M, Santiago M, et al., "Experimental behaviour of a steel joints under natural fire", *Fire Safety Journal*, Vol. **41**, (2006) pp 509-22.

Chapter 3

Finite Element Model at Ambient Temperature

3.1. Introduction

The behaviour of steel connections is nonlinear because the interaction between the connection components includes elastic-plastic deformation, slip, contact, and separation phenomena [3.1]. Furthermore, the determination of the local stress distribution in a bolted connection is in general a three dimensional problem. The three-dimensional stress condition is due to bending effects and to clamping of the bolt. There are three kinds of bending effects: primary bending, secondary bending and bolt bending. Primary bending is caused by an external bending moment acting on the connection, whereas secondary bending is caused by the eccentricity between the forces applied to the bolts in a single shear connection for example. Bolt bending occurs almost in every connection with a shear-loaded bolt [3.2].

Experimental investigations conducted on steel fin plate connections [3.3 – 3.16] provide some understanding regarding the behaviour and the failure mechanism of this connection type. However, these investigations include limitations either in the connection configurations or in the number of tests carried out. As testing is expensive and time consuming, the development of a rigorous finite element model, well validated against experimental data, would form a useful alternative to overcome any experimental limitations. Such a model would be a powerful tool, expanding the understanding of the connection behaviour and helping to extend research beyond the scope of experimental programmes by investigating diverse connection parameters.

This chapter describes in detail the development of a comprehensive three-dimensional finite element model for efficiently predicting the behaviour of fin plate steel connections. Evaluations of this model have been presented by comparison of

the FE calculation results with some experimental data on the basis of load-deflection or moment-rotation curves.

3.2. Overview

Finite element techniques were initially applied to modelling beam-to-column connection behaviour almost thirty years ago [3.17]. Since then, there have been many comprehensive researches on the simulation of moment connections, such as extended end-plate or flush end-plate in 2D and 3D modelling [3.18, 319]. In contrast, relatively little has been reported on the three-dimensional modelling analyses of simple shear connections [(3.21–3.26, 3.29, 3.31)], whether in double or single shear. In general, researchers conducted analyses on flush end-plate or extended end-plate connections simply considering the load to be transferred axially through the bolts. FE simulations are more complicated and expensive in terms of computational time when bolted connections are also subjected to shear load, simply because of the arrangement of additional contact surfaces on the cylindrical surfaces of bolt shanks and bolt holes.

Bursi and Jaspart [3.20] developed a 3D nonlinear finite element model using the ABAQUS code for steel end-plate connections. Throughout this work some issues regarding the connection FE modelling were discussed, (e.g. element type, mesh pattern, material model, friction coefficient in the contact procedure, and bolt pre-tension). The study demonstrated the suitability of the C3D8I incompatible mode brick elements for modelling steel connections. In addition, a friction coefficient, μ, of 0.25 between the contact surfaces was more realistic than other friction coefficient values to match the experimental result.

Swanson *et al* [3.21] described and evaluated the FE simulations of T-stub connections accounting for the bolts in shear as well as in tension. The connection **(Figure 3.1)** consisted of a T-stub section which was attached to a column flange through tension bolts. Shear bolts were used to connect the beam flange to the T-stub. Half of the connection assembly was modelled by means of quadratic, solid elements and only monotonic loading was applied. The authors highlighted the difficulties encountered in the simulation by reporting that a typical full run on a Pentium II - 450 MHz PC

took around 36 hours. Additionally convergence problems, caused by rigid body motions, had to be overcome by assuming artificial boundary conditions along the edge of the T-stub flanges which were in initial contact with the column flange (only for the duration of the first analysis step which was bolt pre-tensioning). The monotonic loading was applied in a second analysis step by imposing displacements to the beam flange section and the shear bolts.

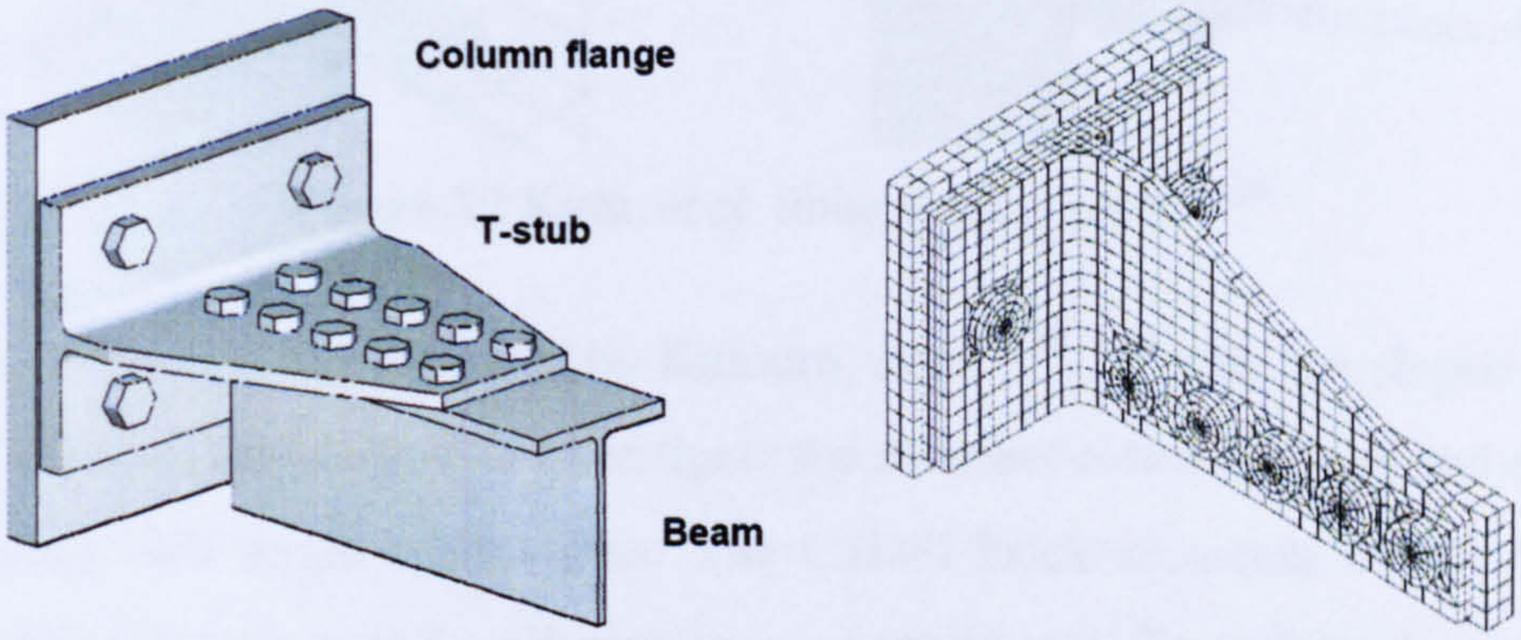

Figure 3.1 Swanson *et al.* finite element model [3.21]

Yang *et al.* [3.22, 3.23] considered a double web angle connection in wich the angles were bolted to the column flanges and welded to the beam web. The bolts and angle were modelled using 3D finite elements, and wedge elements were used to model the weld region. Contact was included between the bolt head and angle with an unusually high friction coefficient of 0.6. The contact between the bolt shank and hole was ignored.

Kishi, *et al.*[3.24] performed non-linear finite element analyses (**Figure 3.2**) to investigate the moment-rotation of top and seat-angles with double web angle connections using ABAQUS Standard. A 3D finite element model was created by means of C3D8I brick elements. A surface-to-surface contact approach with small-sliding option and 0.1 friction coefficient was chosen to represent the interactions between the various connection components. Bolt pre-tension was introduced throughout the analyses. A parametric study was conducted to investigate varying connection parameters such as material properties and bolt pretension. The FE model was well correlated with experimental data, confirming that a well prepared FE connection model can satisfactorily predict the force, deformation and failure mechanism.

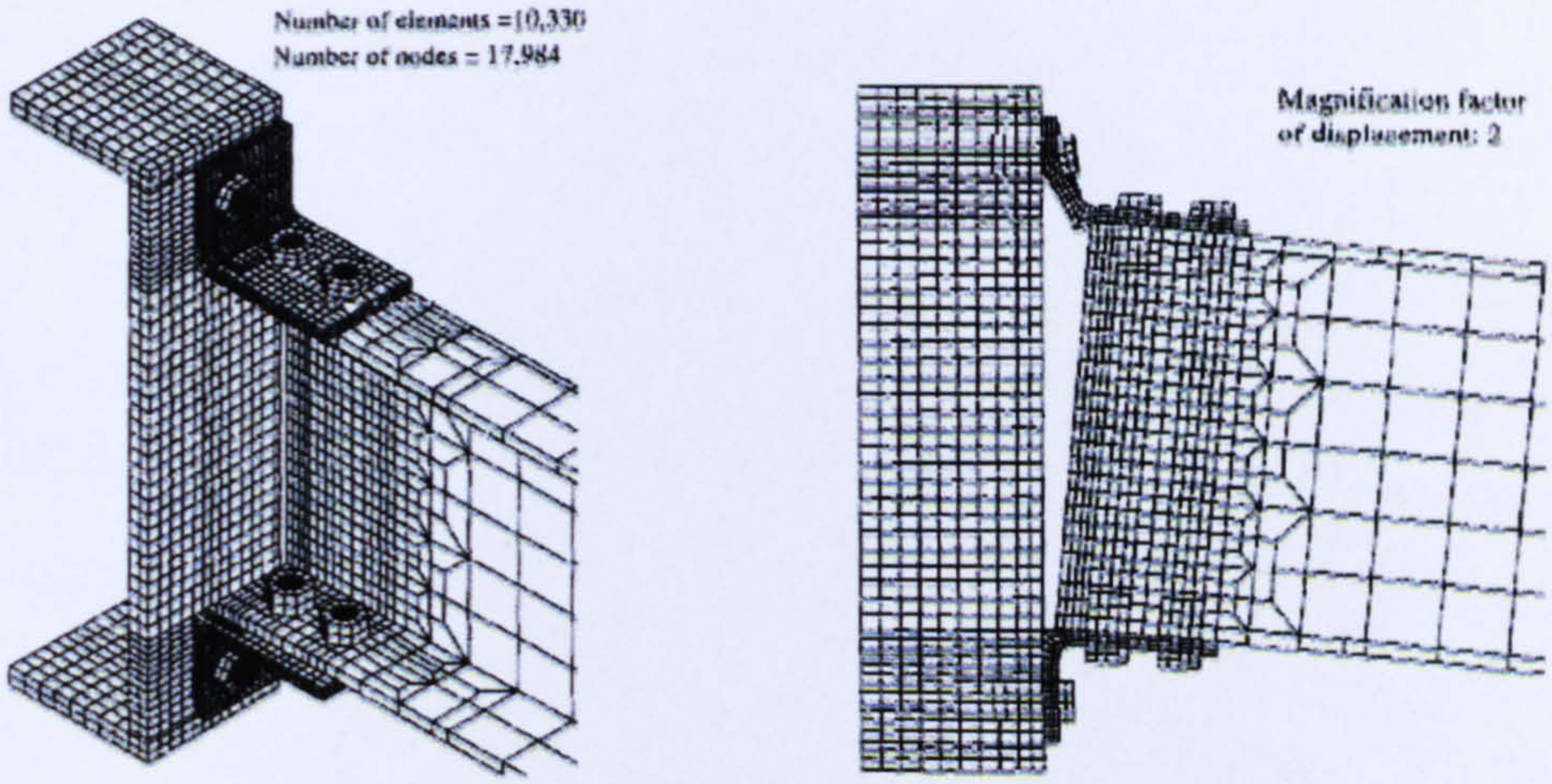

Figure 3.2 Kishi, *et al.* finite element model [3.24]

A similar approach was followed by Komuro, *et al.* [3.25, 3.26] who developed 3D finite element models (**Figure 3.3**) to investigate the moment-rotation of top and seat-angle with double web angle connections. The C3D8I brick elements in the ABAQUS element library were used for all connection components. To accurately simulate the connection behaviour, a contact surface algorithm was considered explicitly and a small-sliding contact option was applied between every pair of adjacent connection components. A friction coefficient of 0.1 was assigned between the probable interacting surfaces.

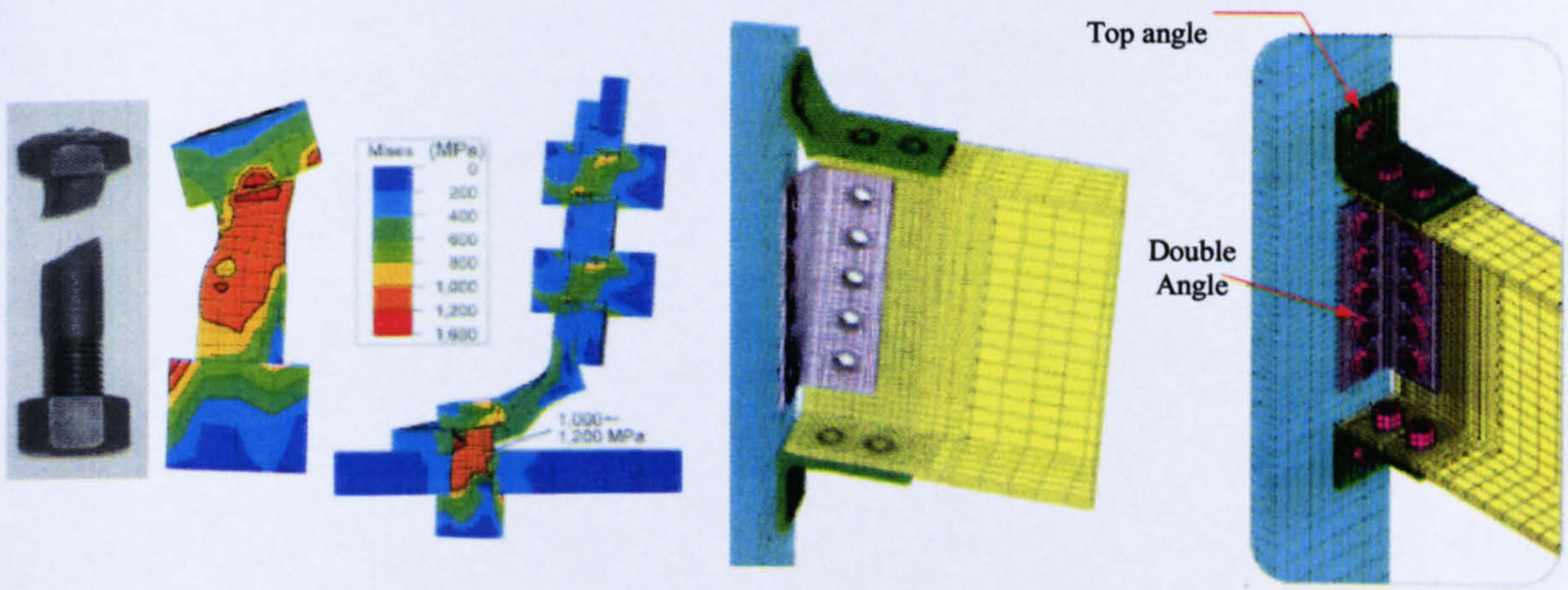

Figure 3.3 Komuro, *et al.* finite element model [3.25]

Material properties were modelled using multi-linear representations with strain hardening for each connection component. Good agreement was found between the experimental data and FE model. Shear stresses of the web bolts were observed in

the model; nevertheless there was no discussion on their effect on the ultimate connection strength under moment loading.

Chung, *et al.*[3.27, 3.28] have established a finite element model with 3D solid elements to investigate the bearing failure of bolted cold-formed steel connections under shear. They emphasised the importance of parameters such as the stress–strain curves, contact stiffness and friction coefficient between element interfaces, and clamping forces in bolt shanks, to accurately predict the load-deformation characteristics of bolted connections. Furthermore, a parametric study on bolted connections with different configurations was performed to provide bearing resistances for practical design. However, in this model the bolt and its washer were assumed to be linear elastic throughout the analysis. In addition, the bolt was fixed in space at its embedded end (**Figure 3.4**). Consequently, in this model only bearing failure, shear-out failure, and net-section failure could be investigated (**Figure 3.4**). The single shear of the high strength bolt (12mm) does not exist in practice, as the plate thicknesses investigated were small (1.5 - 1.6mm) compared to the bolt diameter and material.

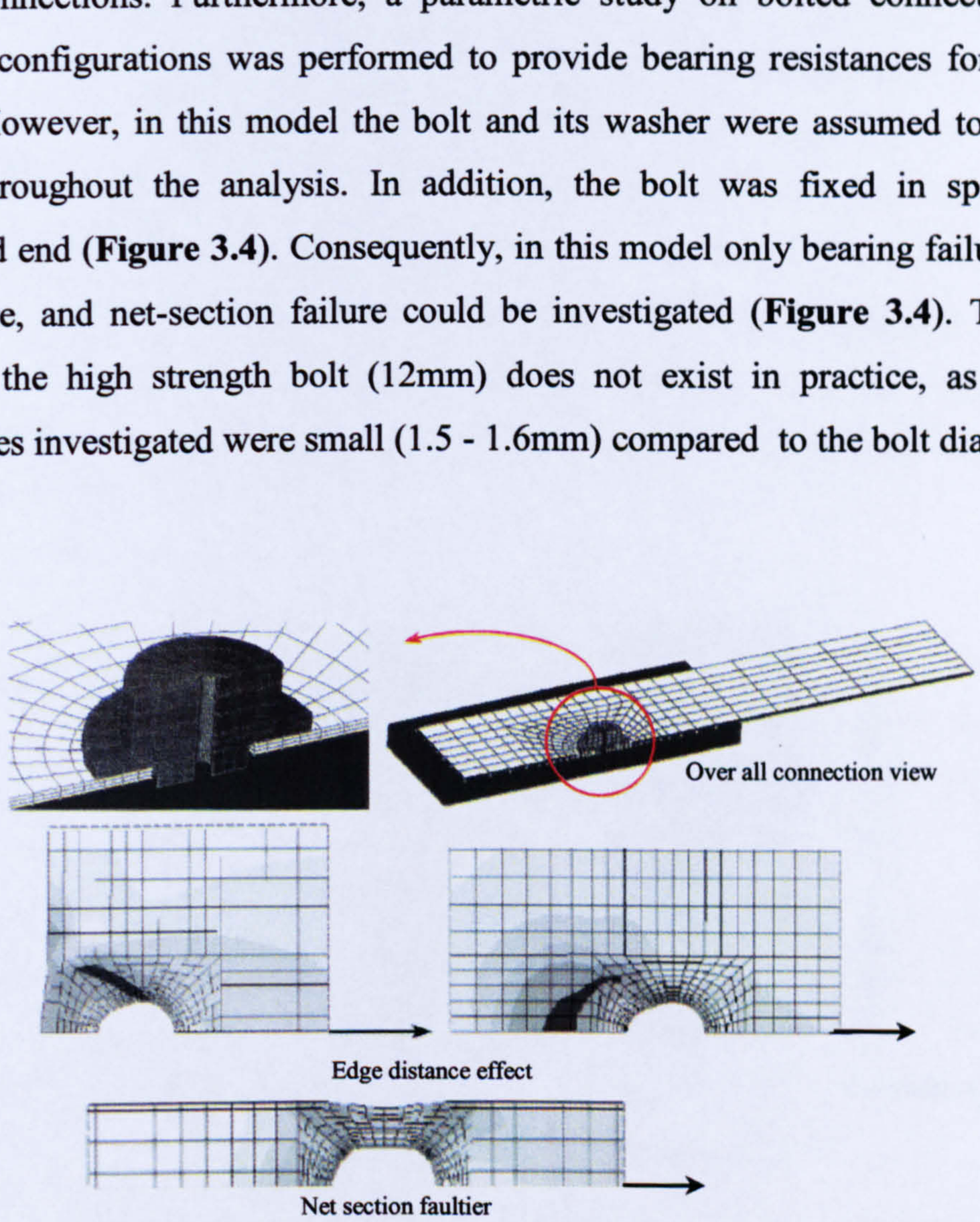

Figure 3.4 Chung *et al.* finite element model [3.27, 3.28]

Citipitioglu *et al.* [3.29] studied the effect of bolt pre-tension and friction coefficient between connection components on moment-rotation response of the top- and seat-angle with double web angles type of connections by means of FE analysis. A nonlinear 3D FE model was developed in which all the connection parts were

modelled via C3D8I brick elements. The column flange was modelled as a rigid plate, assuming that it is a sufficiently rigid part, rather than modelling the whole column section. A surface-to-surface contact scheme was utilized between every interacted connection part and recognized explicitly. A friction coefficient of 0.25-0.255 was found to capture realistically the experimental response.

Barth *et al.* [3.30] investigated single and double angles forming tension members with bolted end connections. The finite element analysis of the angle section was carried out using eight-node brick elements C3D8I in the ABAQUS element library. In the finite element model (**Figure 3.5**), the connecting bolts were assumed to be rigid and a surface-to-surface contact approach was used. A tri-linear type of stress-strain curve was assigned to represent the material nonlinear effects. Load was induced by displacement control throughout the analysis. The finite element methodology presented in this work was capable of predicting the failure capacities, and also of tracing the entire load versus deflection path. However, it is clear from the model description that the bolt stresses were ignored in this study, as bolts were chosen to be infinitely rigid.

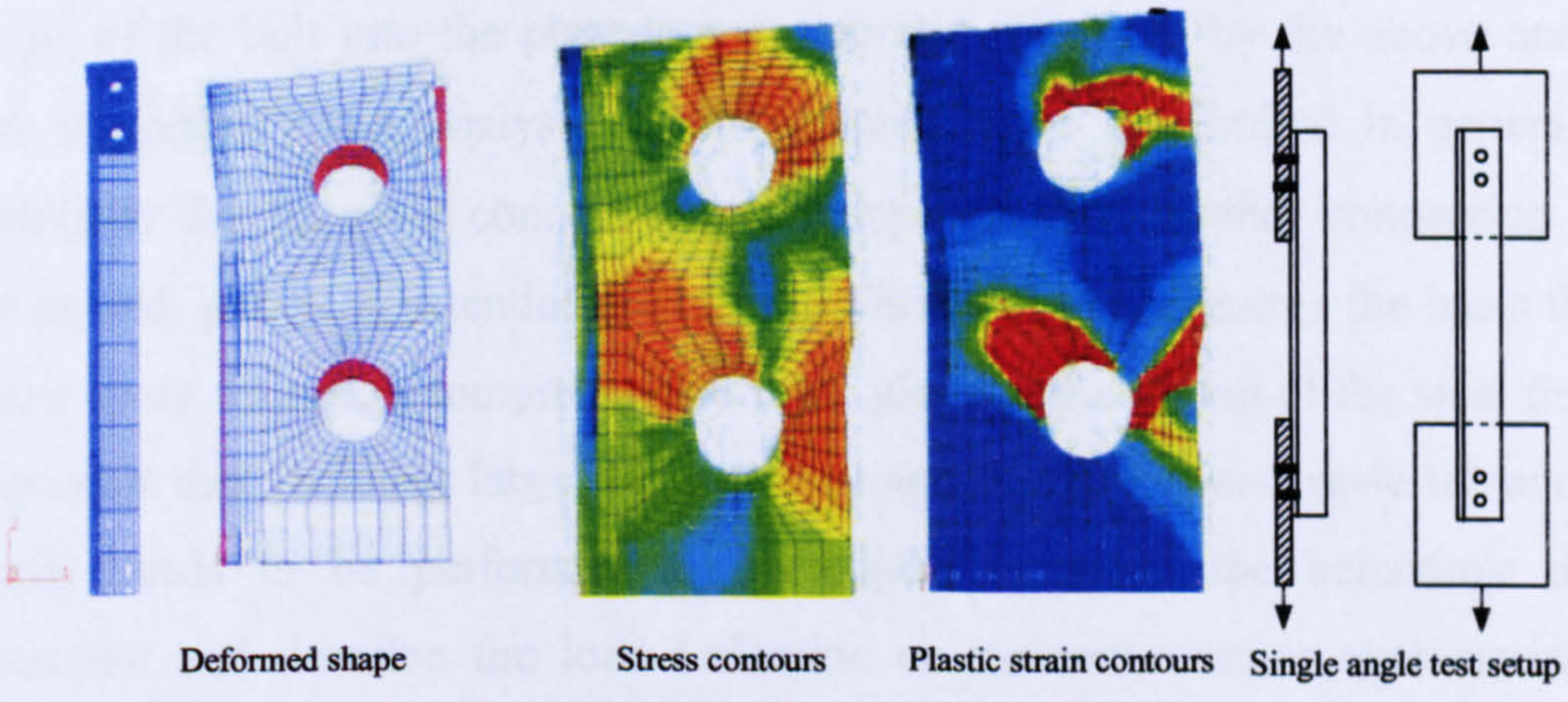

Figure 3.5 Barth *et al* finite element model [3.30]

S.-H. Ju, *et al.* [3.31], studied steel butt-bolted joints via 3D elasto-plastic finite element models using eight-noded isotropic solid elements with incompatible mode (**Figure 3.6**). The contact scheme was node-to-surface contact elements according to the author's developed FE code. The static analyses accounted for the bolt clearance, washer, bolt head, pre-tension, friction (μ = 0.2 for steel connectors) and a deformable bolt. However, it was concluded that the bolt failure is slightly dependent

on the plate thickness, which controls the amount of the bending effect. Moreover, "to calculate the ultimate load for the bolt shear failure of the connection with appropriate bolt spacing and end distance, it is valid to neglect the plate deformation and the bolt bending effects, which are major assumptions in the AISC specification for the bolted-joint problem" [3.31].

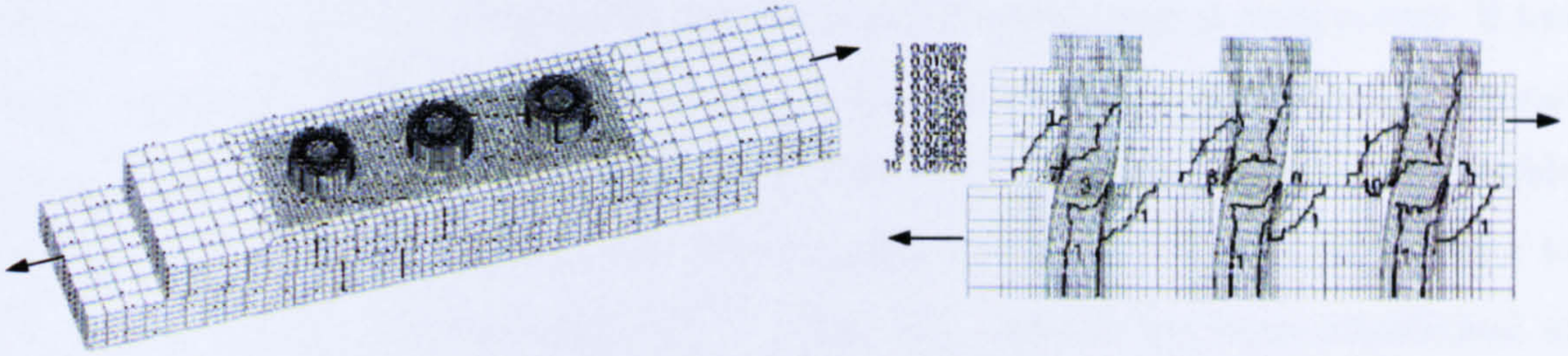

Figure 3.6 S.-H. Ju *et al* finite element model [3.31]

Most of the above analyses model steel connections in 3D fashion via solid brick elements. Furthermore, surface-to-surface contact element arrangements a predominantly used to represent the interactions between the connection components. Nevertheless, the investigation of the bolt in single shear seems almost missing from the field of finite element simulation of steel joints. Additionally, bearing of the bolt into the plate is not accurately captured by the above analyses. More importantly, FE analyses of shear connections are limited in general, and specifically for fin plate connections as compared with another connection types, such as end- plates or extended end-plates. This observation forms the basis for this current study. Hence, a comprehensive finite element modelling of the steel fin plate connection that includes large deformation, and geometric and material nonlinear effects, needs to be performed to investigate in detail the behaviour of this connection and describe the load-deflection or moment-rotation characteristics at ambient and elevated temperatures.

3.3. Description of The Connection Model

A representative three-dimensional refined FE model of a fin plate connection was developed in order to analyse and understand the behaviour of such a connection at ambient and elevated temperatures. The starting point for this model was a simple plate with a bolt bearing against a hole (**Figure 3.7-a**). This model was then

developed to form a single lap joint (**Figure 3.7-b**). Ultimately, the entire fin plate connection (**Figure 3.7-c**) was assembled and modelled using a series of lap joints in which the plates represent the fin plate and the beam web.

However, the three main parts of the steel fin plate connection (beam, fin plate and bolts) were modeled using the C3D8I eight-node continuum hexahedral brick element. This element is first-order with a total of 8 nodes, one at each corner. It has only displacement degrees of freedom, three for each node, but has no rotational degrees of freedom. This element has been enhanced by adding internal incompatible deformation modes to the standard displacement modes of the element in order to improve its bending behaviour [3.32, 3.33]. Thus, this element has been established as capable of representing large deformation, bending-dominated, geometric and material nonlinearity problems.

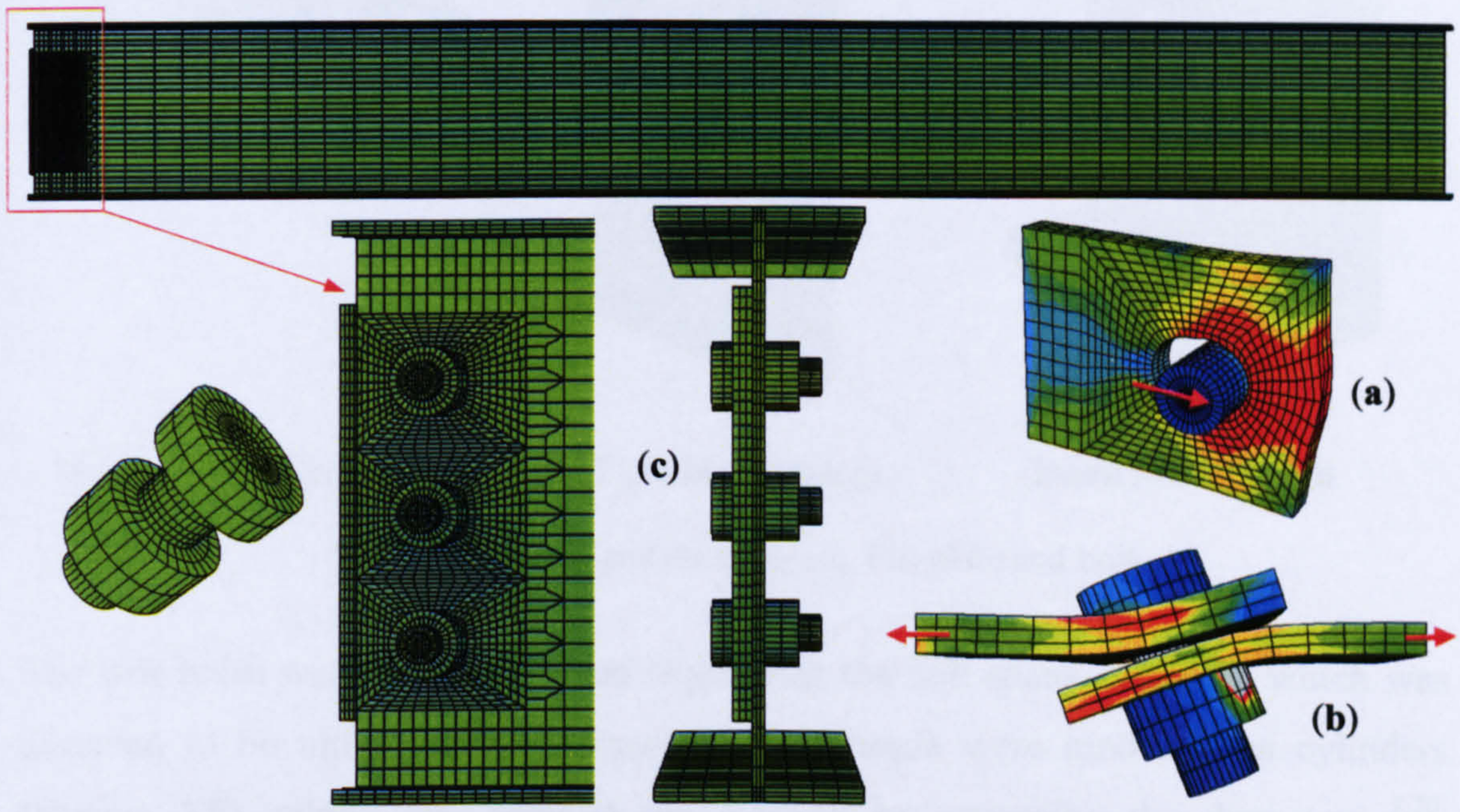

Figure 3.7 FE model development

(**a**) Single bolt in bearing (**b**) Lap splice (**c**) Fin plate and beam model

The C3D8I incompatible mode brick element has been recommended for bending and contact problems. Bursi and Jaspart [3.20] compared the performance of this

continuum element with other brick element formulations and have shown it to give better results than other solid brick elements, especially for bending-dominated problems with relatively small thickness. However, to accurately capture the stress behaviour in the region around the bolt holes where likely failures would probably initiate, an intensive mapped meshing is made in the vicinity of the holes and for the bolts as shown in **Figures 3.7, 3.8**. Just half of the beam was modelled, as symmetry boundary conditions were applied at its free end. Sometimes, an even shorter length of beam was considered, simply for the purpose of parametric study and to reduce the analysis time.

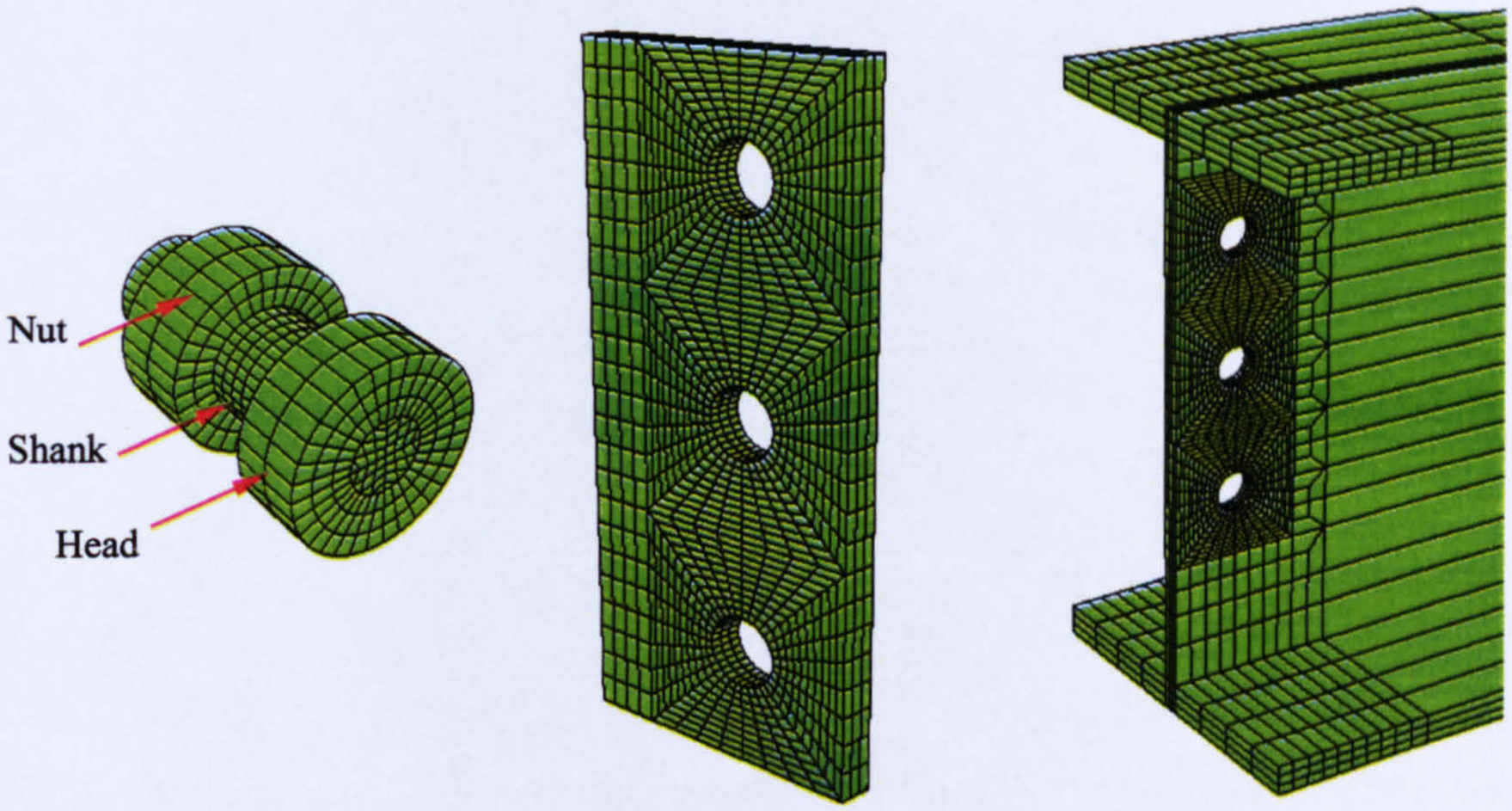

Mesh pattern of bolt model Fin Plate Mesh pattern Beam Mesh pattern

Figure 3.8 Mesh pattern of Beam, Fin plate and bolt

The bolt holes were modelled 2mm larger than the bolt shank diameter, which was assumed to be unthreaded. The hexagon bolt heads were modelled as cylinders **(Figure 3.8)**, taking into account the washers by averaging the diameters [3.20]. However, to reduce the number of contact planes and the complexity of the model, the bolt nut forms an integral component with the bolt shank rather than as an individual part. The flange of the column was modelled as a rigid surface, assuming that it is a sufficiently rigid plate connected to the fin plate. The weld was considered as a fixed boundary condition along the edge of the fin plate.

3.3.1. Contact element modeling

Numerical modelling of any bolted joint requires a realistic representation of the contact interaction between the various joint components. Surface-to-surface contact with a small-sliding option, rather than the finite-sliding, was used for all the contact surfaces to fully transfer the load from the beam web to the fin plate and eventually, to the supporting member. For this option, ABAQUS assumes that a slave node, which comes into contact with a master surface, slides along a line formed by the two adjacent nodes on that surface. This is computationally more efficient than finite-sliding option, which allows the slave nodes to slide over the actual master surface. In general, the contact formulation used in ABAQUS involves a master-slave type algorithm. With this kind of contact approach one surface defines the "master" surface and the other surface defines the "slave" surface. Once the contact formulation recognizes the surfaces that are in contact, interpenetrate or slip, a kinematic constraint is imposed on the slave surface nodes that do not penetrate the master surface. The contacting surfaces do not have to be matched in their meshes; but, the best accuracy is achieved when the meshes are initially matching [3.32 3.33]. Intentionally, all the contact surfaces in the FE model of the fin plate connection were intended to be matching in their meshes. However, it is of great importance to carefully assign the slave and master surfaces. The crucial rule for choosing the master surface is that master surfaces should belong to the body of the stronger material, or bodies of a finer mesh. The contact areas in the fin plate connection are the bolt shank-to-bolt holes, bolt head-to-fin plate, bolt nut-to-beam web and fin plate-to-beam web surface (**Figure 3.9**).

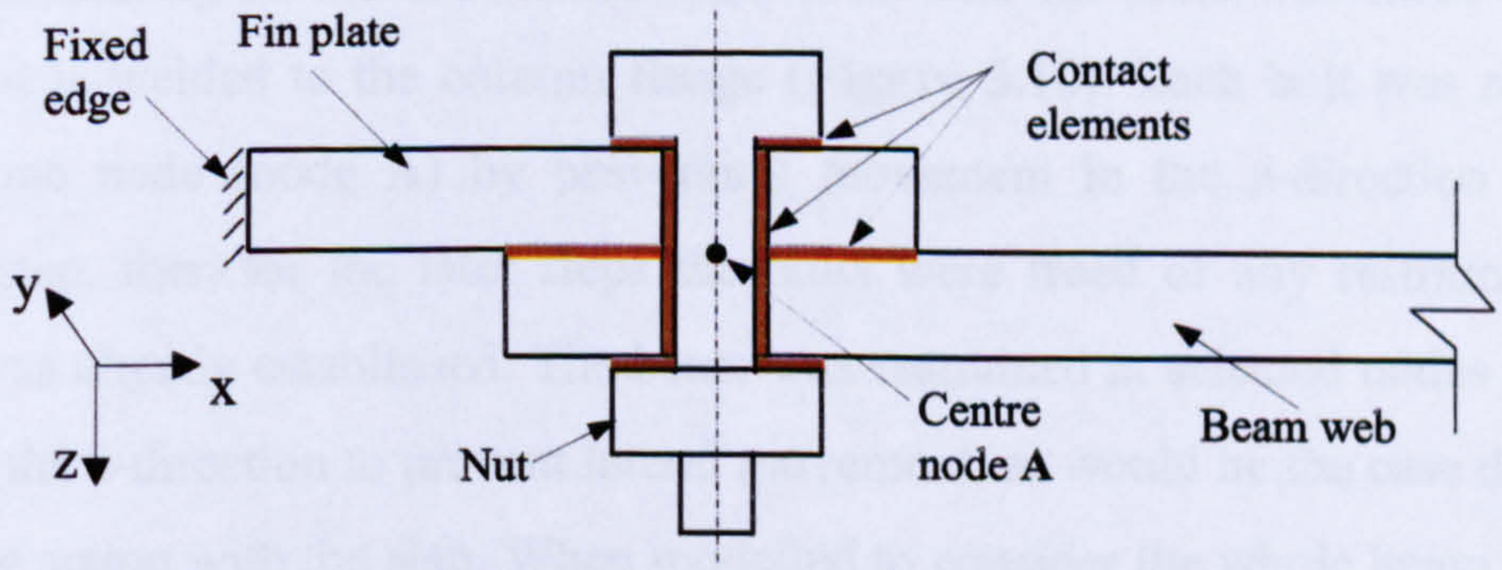

Figure 3.9 Contact elements distribution (Plan section on a fin plate connection)

The contact surfaces of the bolt shank, bolt head, and bolt nut were always chosen to be master surfaces, as they are of stronger material. In addition, the surface of the fin plate in contact with the beam web was also a master surface. All the other contact surfaces mentioned (hole surfaces, beam web surface and fin plate surface at the nut side) were considered to be slave surfaces. Pre-tension was not applied to the bolts during the analysis. A friction coefficient μ of 0.25 was adopted for all the contact surfaces interacting with the bolt. A friction coefficient of $\mu = 0.1$ was assigned for the contacted surfaces between the fin plate and the beam web because no pre-tension was applied on the bolts, in addition to the fact that the bolt clamping effect reduced and spread over a wider area away from the bolt region.

Simulating the contact interaction between the parts of a shear joint using ABAQUS/Standard is difficult to achieve, but is of satisfactory accuracy when established. Difficulties arise because of special arrangements needed to bring the connection parts into initial contact. Firstly, the mesh should be fine enough for each element's node on the master surface to face a corresponding node on the slave surface elements. Secondly, the load should be applied extremely slowly until contact is established. Lastly, the boundary conditions need to be assigned to achieve sensible behaviour at the connection, and to avoid any singularity problems that may arise (see also 3.34).

3.3.2. Boundary conditions

In any case of connection simulation, and especially in shear connections, the boundary conditions are quite crucial and have a significant influence in achieving realistic modelling of the connection behaviour. The fin plate was fixed along its edge, as it is welded to the column flange (**Figure 3.10**). Each bolt was restrained only at one node (node **A**) by preventing movement in the z-direction for first analysis step, then for the later steps the bolts were freed of any restraints as the contact was already established. The beam was restrained at selected nodes along its flange in the z-direction to prevent lateral movement, as would be the case due to the composite action with the slab. When modelled to consider the whole beam length, a symmetric boundary condition was applied at the nodes of the beam mid-span section, as just half of the beam was modelled.

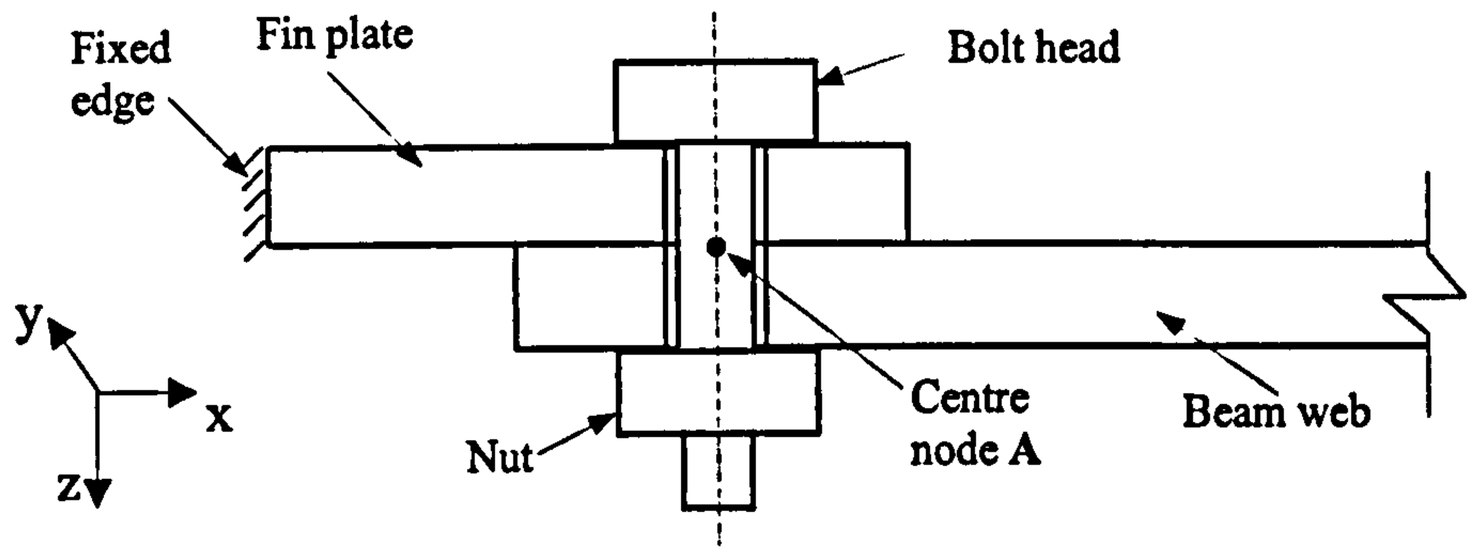

Figure 3.10 Boundary condition (Plan section on a fin plate connection)

3.3.3. Material properties and failure criteria

The material properties for the various components of the connection model were determined from the engineering stress-strain relationship using a multi-linear elastic-plastic constitutive model. Young's modulus (E) of 205 kN/mm^2 and Poisson's ratio (ν) of 0.3 were adopted. Two types of material were considered; S275 or S355 steel for the fin plate and beam material. All bolts were high strength 8.8 bolts throughout the analysis. The yield stress and ultimate strength are assumed based on the nominal steel properties of S275, S355 and 8.8 high strength bolts. The effective material properties of the connection parts are summarised in **Table 3.1,** and the stress-strain relationship curves are shown in **Figures (3.11, 3.12)**. The self-weight of the structure may be significant; therefore, it is included in the analysis by including the steel density of 7850 kg/m^3 in the material description.

Table 3.1 Material properties

Material Type	**S275**	**S355**	**8.8 Bolt**
Yield stress [N/mm^2]	275	355	640
Ultimate strength [N/mm^2]	445	550	800

Since ABAQUS conducts in large-deformation analyses and in order to consider the deformed area, a realistic definition of nonlinear uniaxial material response requires the use of the true stress (σ_{true}) versus the strain ($\varepsilon_{pl,\,true}$) relationship [3.34] This must be determined from the engineering stress-logarithmic strain relationship using the equation.

$$\sigma_{true} = \sigma(1+\varepsilon) \qquad (3.1)$$

σ_{true} : is the true stress

σ : is the elastic (engineering) yield stress

ε : is the effective current value of strain

$$\varepsilon_{pl,true} = \ln(1+\varepsilon) - \frac{\sigma_{true}}{E} \qquad (3.2)$$

$\varepsilon_{pl,true}$: is the true plastic strain

To express model failure, the EC3 [3.35] failure criterion was adopted in which the necking stage of the stress-strain curve starts at 15% strain and drops to 20% strain. For bearing failure, longitudinal displacement of bolt hole of 0.5 of the bolt diameter was adopted.

$$\text{Bearing failure} = 0.5 \times d_b \qquad (3.3)$$

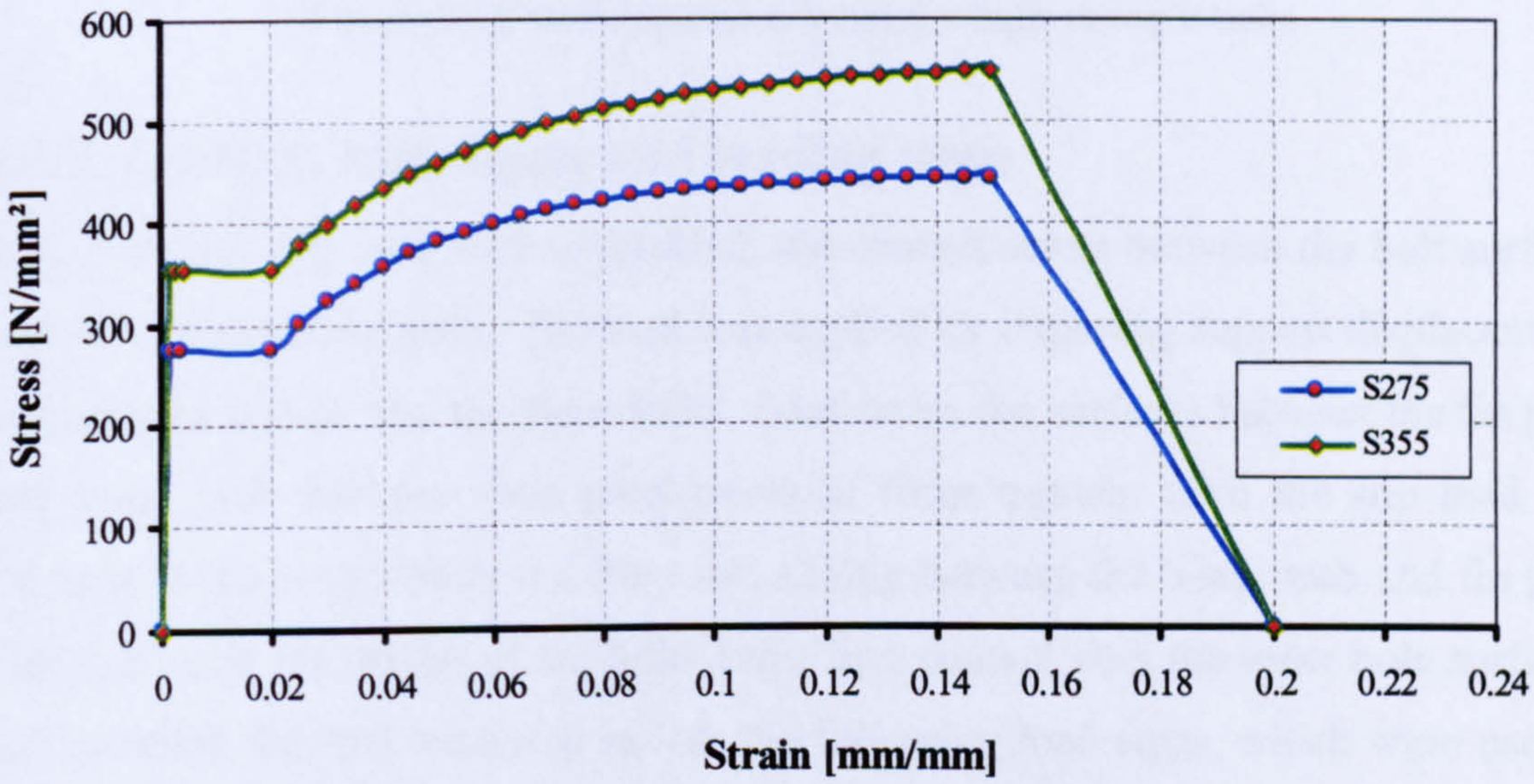

Figure 3.11 Engineering Stress-Strain curves for S275 and S355 steel

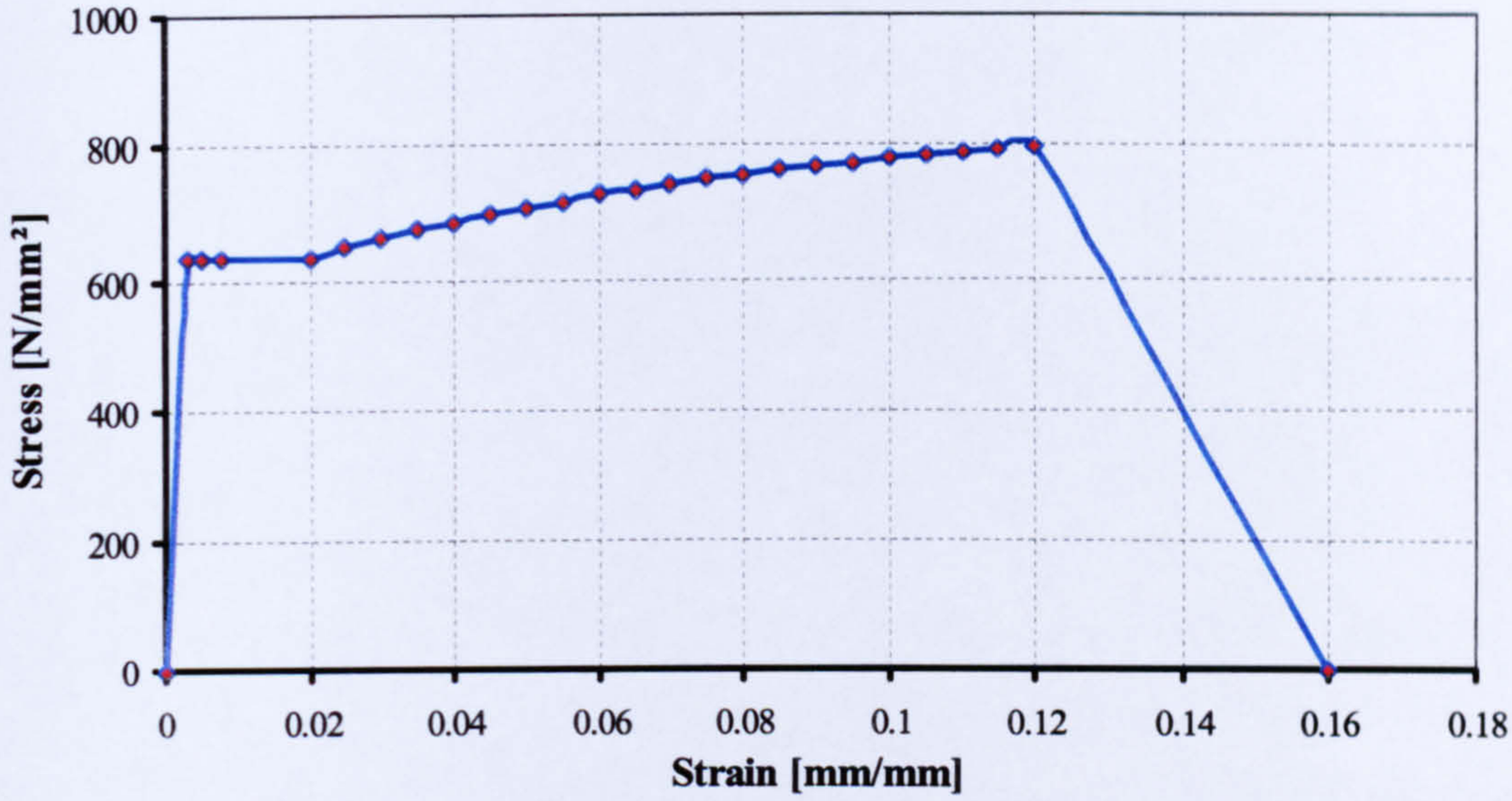

Figure 3.12 Stress-strain curve of 8.8 high strength bolts

3.3.4. Analysis techniques and loading steps

The first load step was used to establish the contact status between the bolt surfaces and other connection parts. The load was applied by imposing support displacements to the beam section and the shear bolts. Friction on the surfaces between the fin plate and beam web was the main mechanism of force transfer until the slip load was reached. After overcoming the slip load, sliding between the beam web and fin plate occurred until the shanks of the bolts came into contact with the inner hole surfaces. At this stage the first load step ended; the following load steps, which were used to apply the desired load to the beam section, commenced.

The load within a nonlinear analysis should be introduced as displacement-controlled, otherwise the negative inclination in some parts of a stress-strain curve cannot be simulated. In addition, it was found that displacement control resulted in easier solution convergence; therefore the load was applied by displacement of a boundary. However, the movement must be imposed extremely slowly, which can cause a considerable demand in computing time but results in increased accuracy.

Determining the initial value for the load increment is very important when performing a nonlinear simulation. This value has a large influence on the final

results and also makes a difference to the simulation running time. The correct choice of initial value provides good results with low computational effort.

3.4. FE Model Convergence Study

The finite element method is a computerised method as it based on matrices analysis. The main principle of the FE method is to divide the analysed body into small section called elements. Each element has its own stiffness matrix according to its material properties. The whole global stiffness matrix of the body [K] is assembled from the individual element stiffness matrices. The main FE method equation, ({F} = [K] {d}), uses the external body forces to solve the global stiffness matrix for the body's deflections. The time needed to solve this matrix is dependent on the number of elements which form the body, and the analysis type (linear or non-linear). The more elements used the greater will be the calculation time needed to solve the finite element equations and the higher will be the accuracy of the solution. Until a certain stage the number of elements make almost no different to the accuracy of results. Consequently, the model which has the minimum number of elements consistent with enough accuracy is needed to minimise the calculation time. Hence, it is necessary to find a model which has enough elements for sufficient accuracy through conducting the convergence test on the finite element model to ensure that a fine enough mesh has been used. This can be done by creating several models with different mesh sizes and comparing the resulting deflections and stresses. It is not sufficient to examine the displacement convergence only, because usually the stresses converge more slowly than the displacement.

Ten finite element models of bolts bearing onto plate holes with different mesh patterns were created (**Appendix A**) to study the influence of the mesh density on the accuracy of calculating deflections and stresses. For each model, the same chosen positions (**Figure 3.13**) were examined, and the deflections and stresses were plotted against the number of mesh elements (**Figures 3.14, 3.15**). Observing the results gives a clear indication that the deflections and stresses started to converge adequately in model number six (approximately 1500 elements). Therefore, the mesh pattern for this model was used throughout the finite element analyses in the current work.

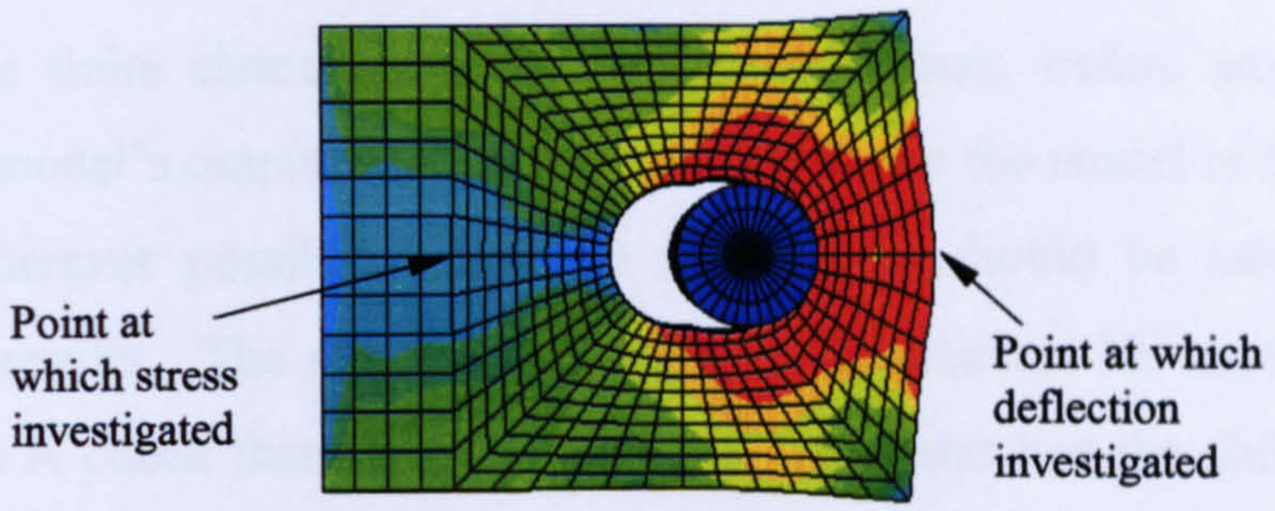

Figure (3.13) Mesh density of model No. 6

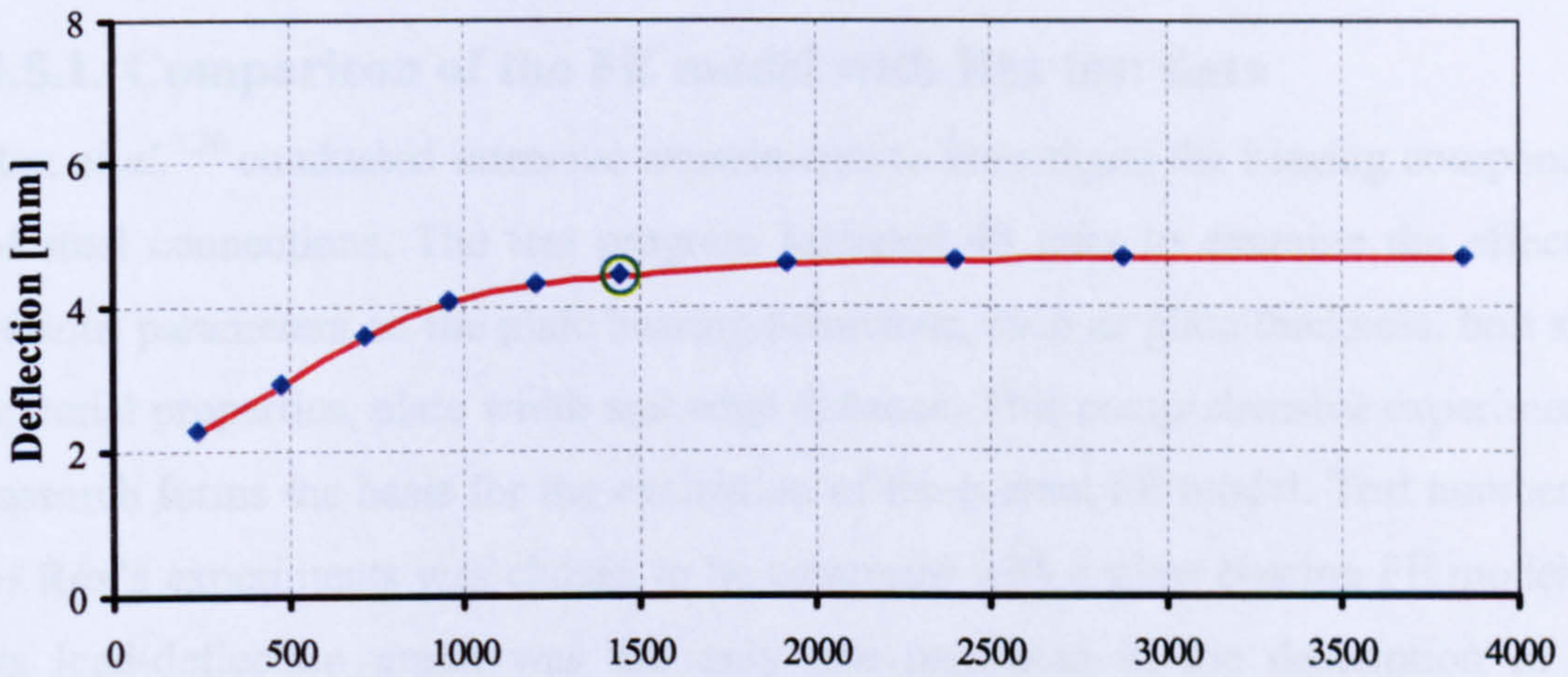

Figure (3.14) Convergence test based on deflection

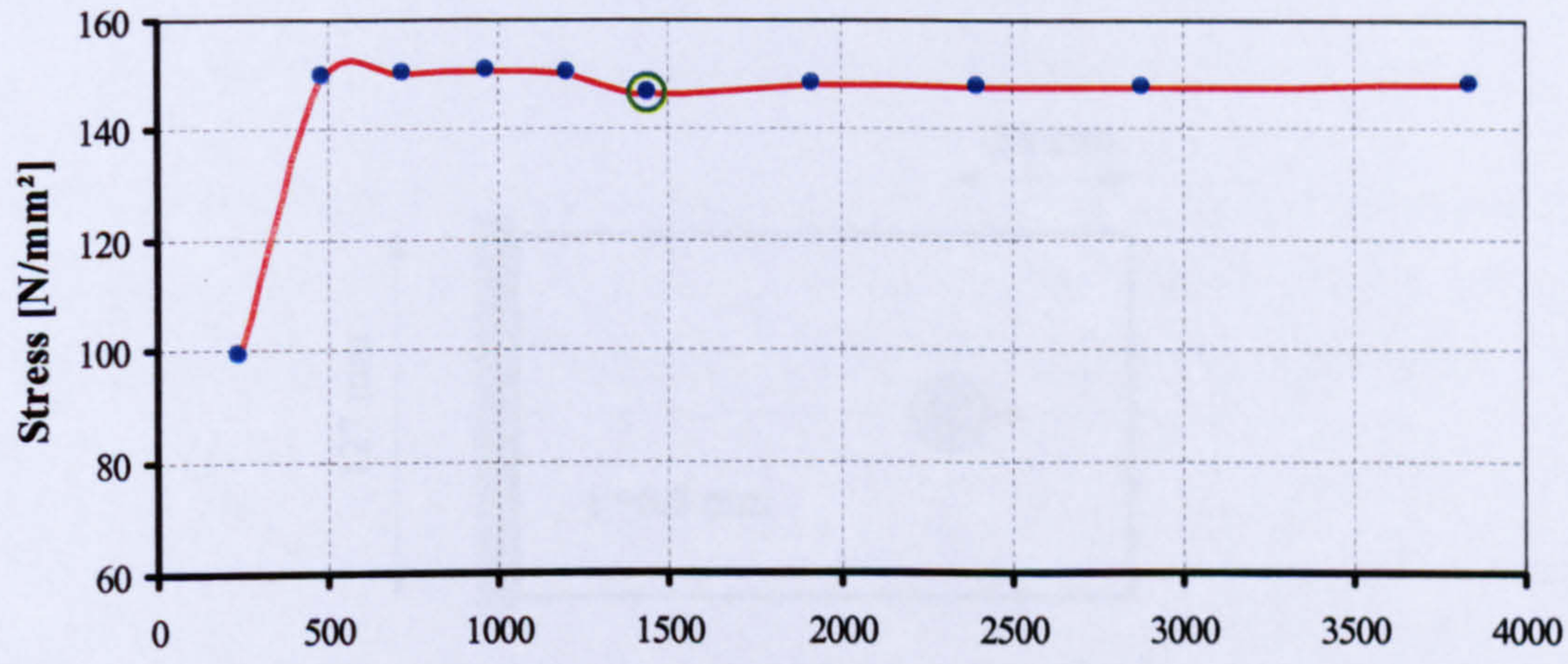

Figure (3.15) Convergence Test based on stress in x direction

3.5. Evaluating the Finite Element Model to Test Data

Evaluating the finite element model is an essential task, before any trust can be placed in the model's output, or it can be decided to use the model in further studies. Therefore, wherever possible, numerical simulations should be validated against experimental results. The evaluation process for the current FE models comprised four stages; i) A check that the specified contact element had the ability to transfer the load; ii) evaluation of the model against a bolt bearing test (pull through); iii) Evaluation of the model against tensile lap joint tests; iv) comparison of the model with steel fin plate connection moment-rotation test data.

3.5.1. Comparison of the FE model with Rex test data

Rex *et al.*[3.36] conducted intensive experiments to investigate the bearing components of steel connections. The test program included 48 tests to examine the effect of various parameters on the plate bearing behaviour, such as plate thickness, bolt size, material properties, plate width and edge distance. This comprehensive experimental research forms the basis for the evaluation of the current FE model. Test number 41 of Rex's experiments was chosen to be compared with a plate bearing FE model, as its load-deflection graph was the only one presented in the description of the experiments. This test specimen (**Figure 3.16**) is a singe plate of 127 mm width, 6.5 mm thickness and 38 mm edge distance. A 25mm high-strength bolt goes through the plate hole. The plate material had a Young's modulus of 205 kN/mm^2, 307 N/mm^2 yield stress and 452 N/mm^2 ultimate strength (**Figure 3.17**).

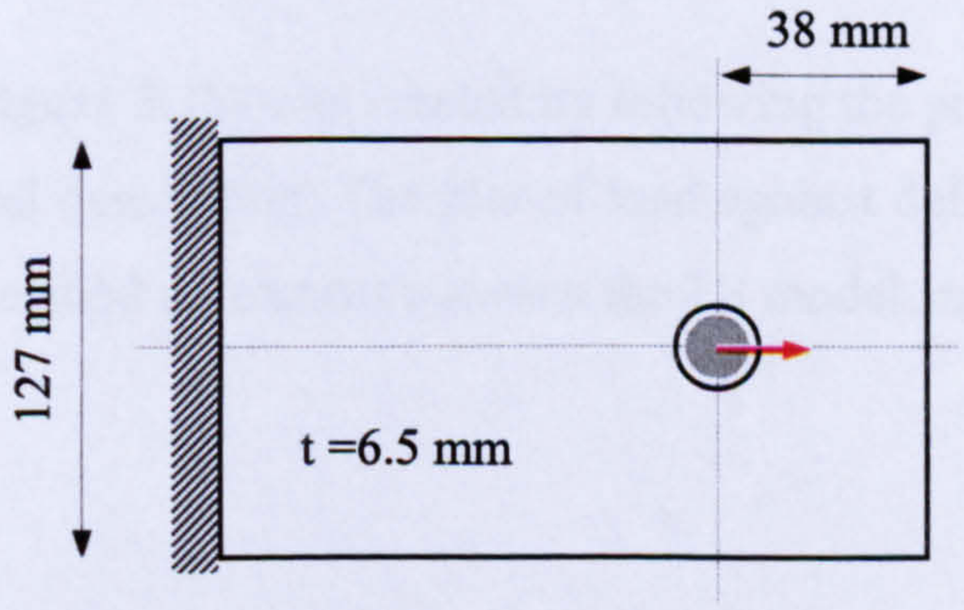

Figure 3.16 Geometrical details of Rex bearing test (No.41)

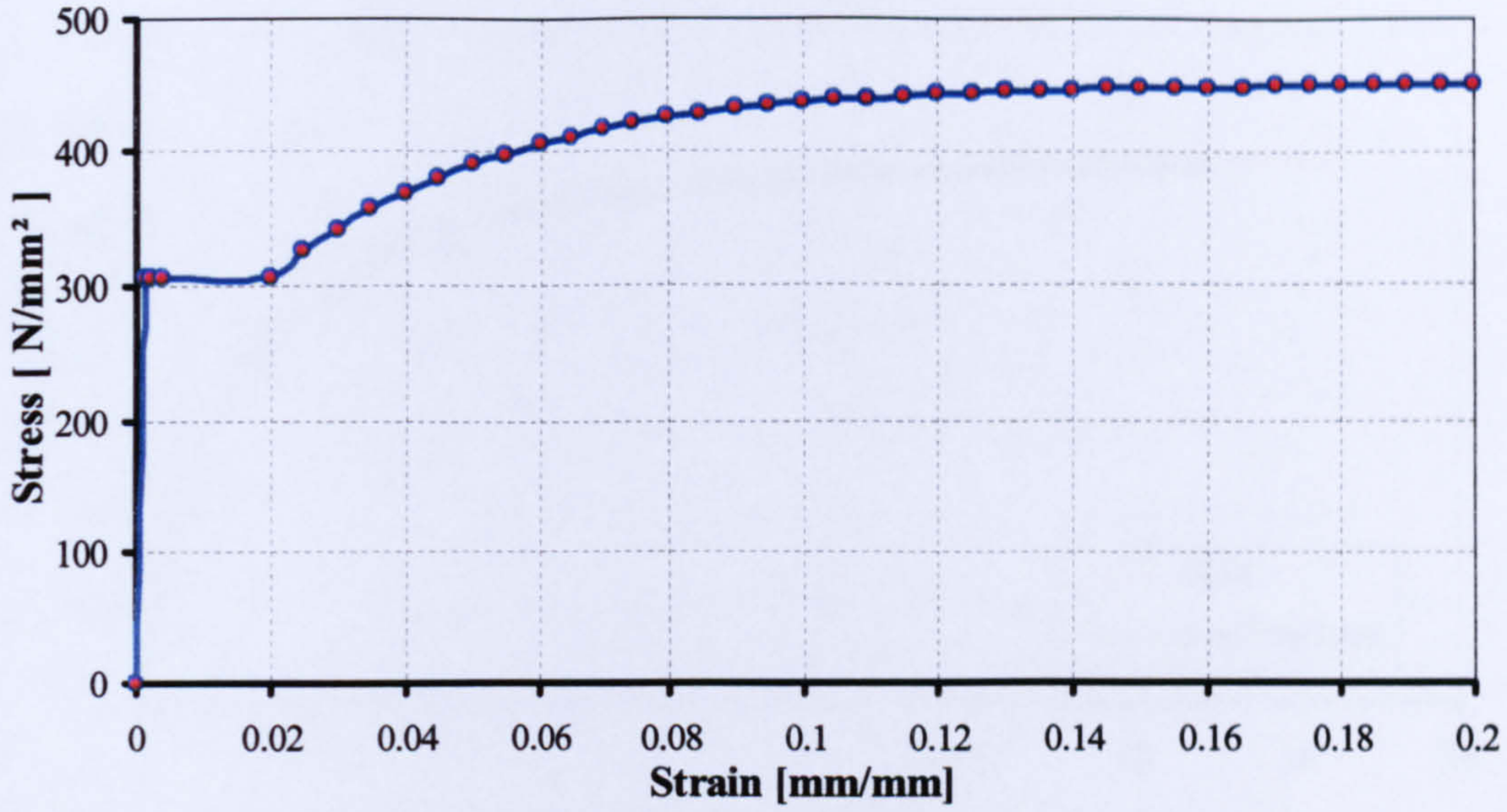

Figure 3.17 Stress-strain curve for the plate material (test No.41)

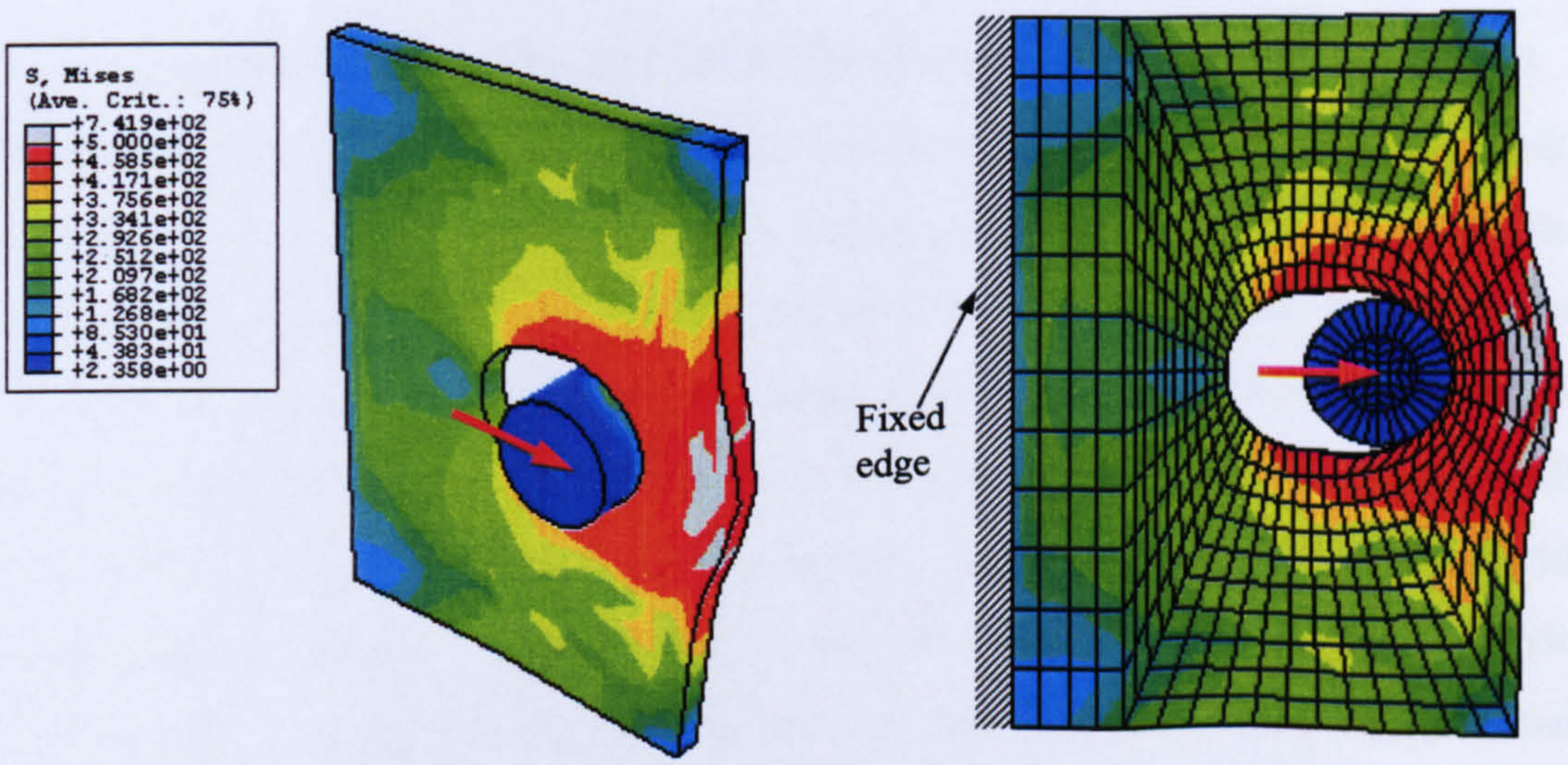

Figure 3.18 Von Mises stresses for FE model of Rex bearing test No.41

The FE model (**Figure 3.18**) was created by following the procedure presented in the previous FE model description. The plot of load against deflection shown in **Figure 3.19** illustrates the good agreement between the FE model and the test results.

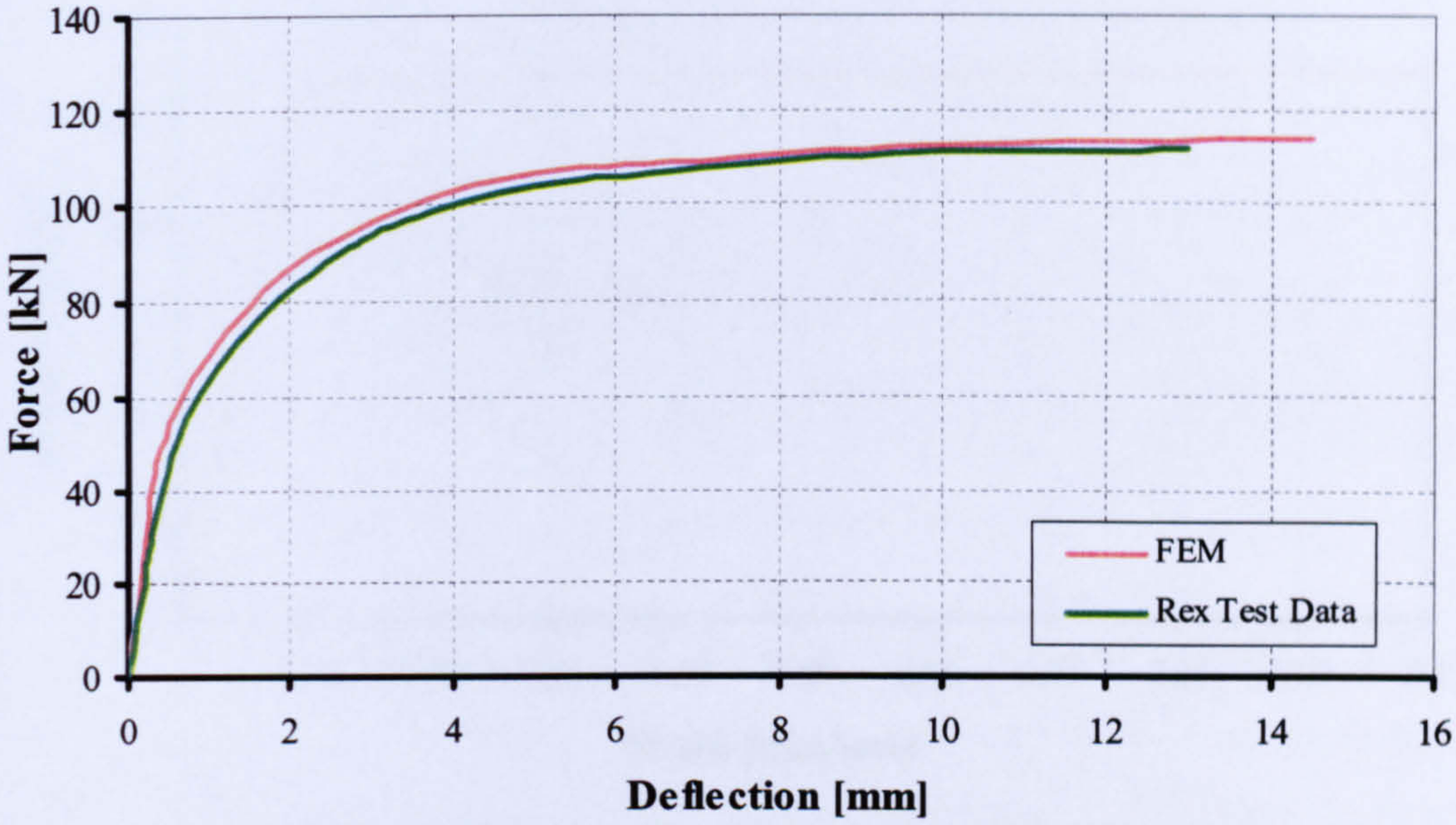

Figure 3.19 Comparison between the FE model and Rex's test data

3.5.2. Comparison of the model with simple Aluminium lap joints

The FE model, as mentioned above, was developed from a single plate and bolt in bearing within a simple lap shear joint. A test of a shear joint was needed to evaluate the fin plate connection modelling. Therefore, it was decided to assemble a lap joint specimen in the laboratory. Aluminium strips were found suitable for such a purpose, especially as aluminium has a non-linear stress-strain curve similar to that of steel at elevated temperature. The test was performed by means of a Hounsfield Tensometer (**Figure 3.20**) which was up-dated to record the load-displacement behaviour electronically via connection to a computer. A material tensile test was conducted (**Figure 3.21**) to describe the material stress-strain curve (**Figure 3.22**).

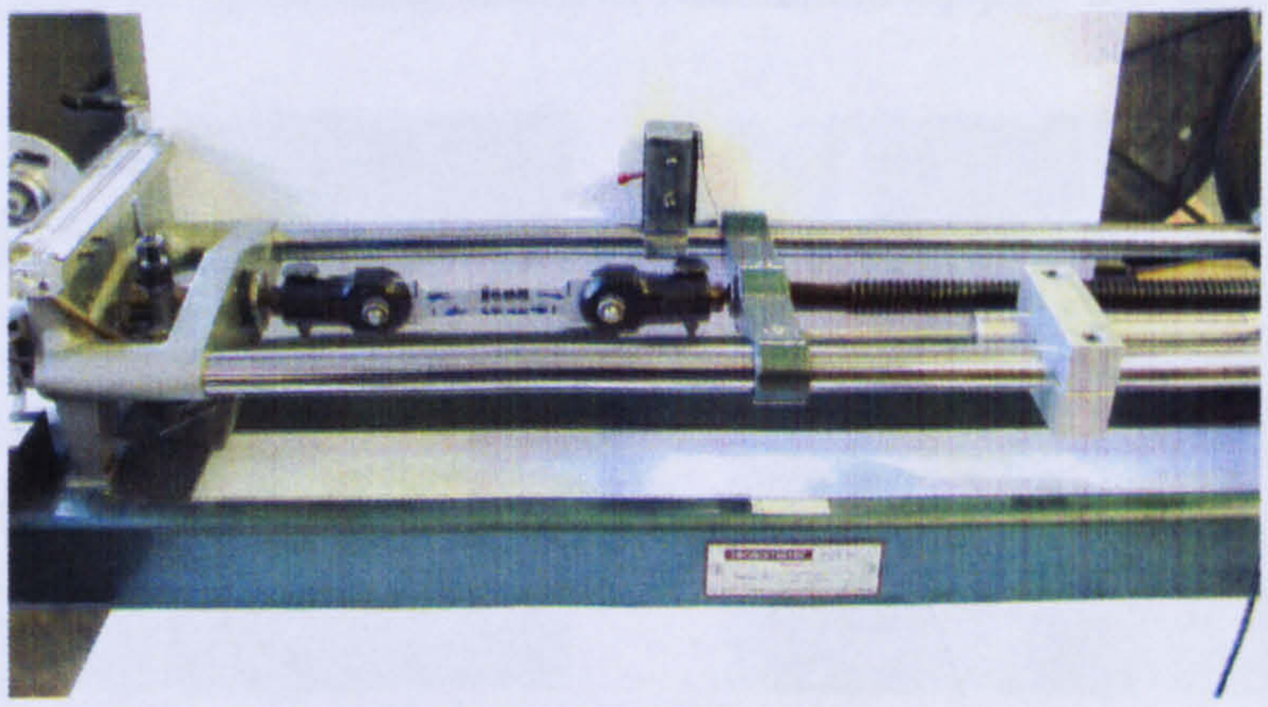

Figure 3.20 Aluminium tensile test

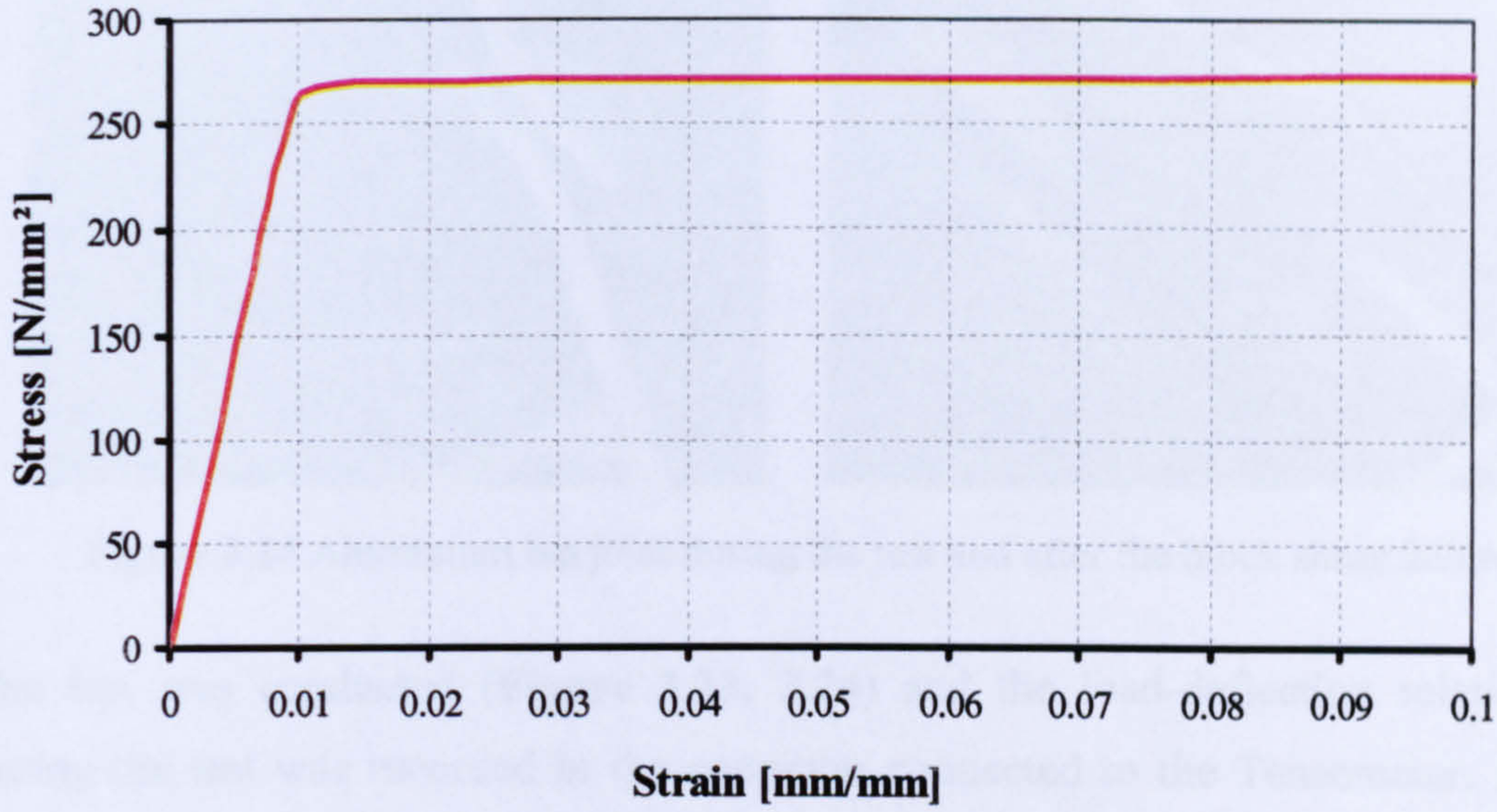

Figure 3.21 Stress-strain curve for Aluminium specimen

The Aluminium lap joint specimen was assembled from two 3.01 mm thickness plates, and a 6.0 mm diameter high-strength bolt was installed in a 7.0 mm over-sized hole as shown below in **Figure 3.22**.

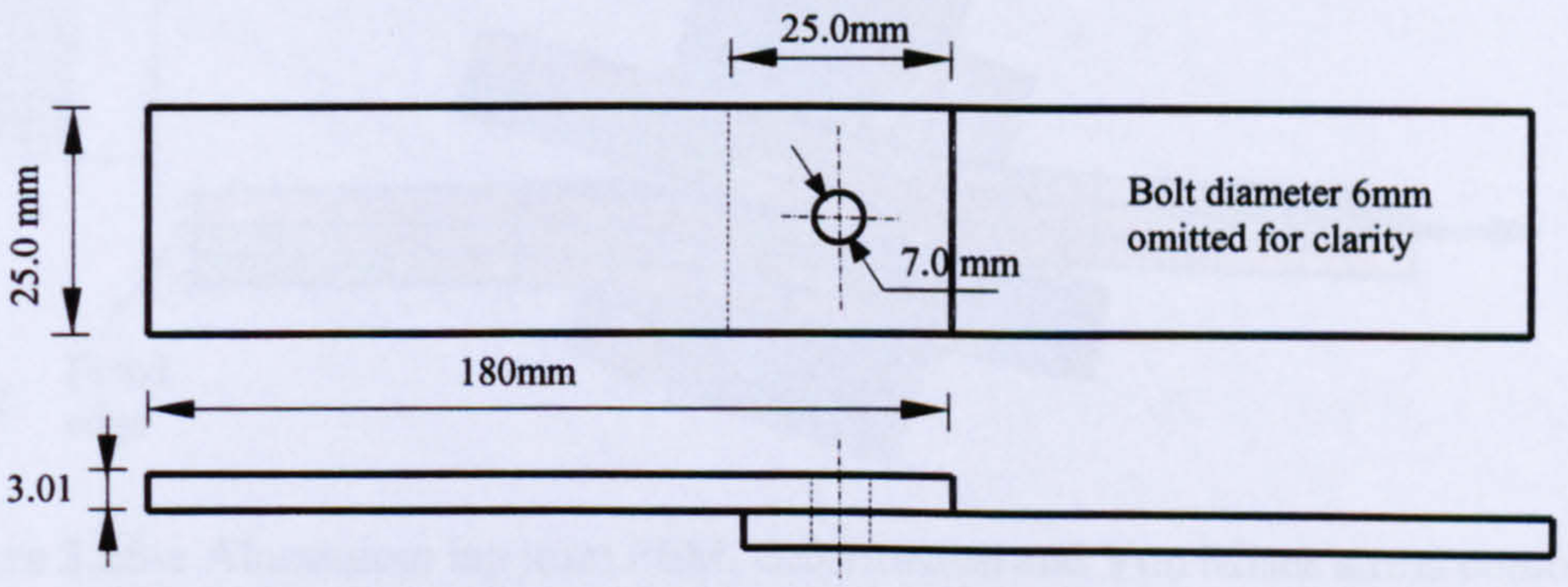

Figure 3.22 Geometrical details of Aluminium lap joint test specimen

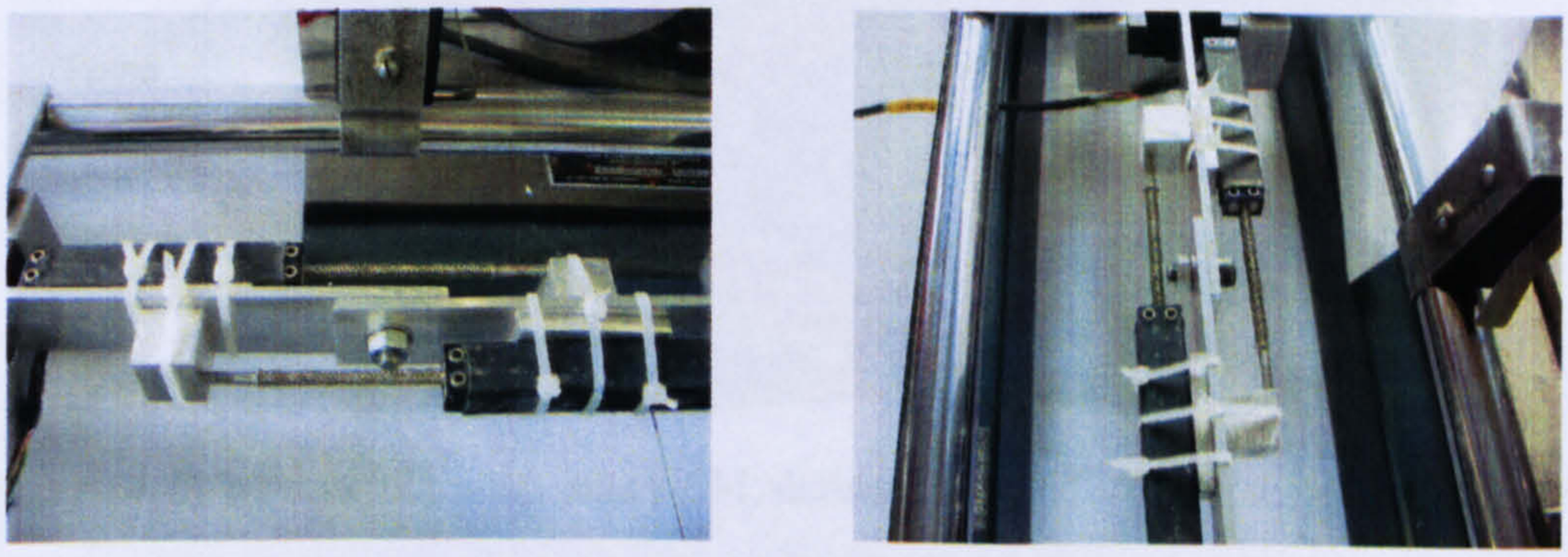

Figure 3.23 General view of test setup for Aluminium lap joint

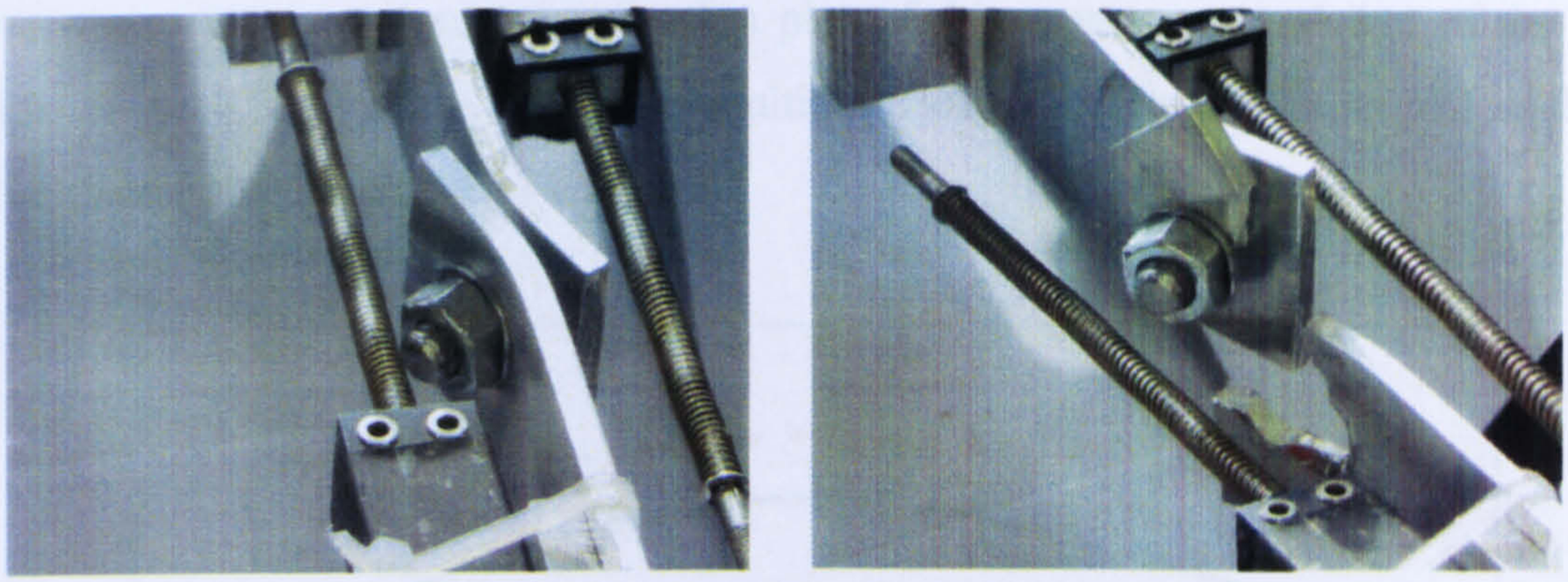

Figure 3.24 Aluminium lap joint during the test and after the block shear failure

The test was conducted (**Figure 3.23, 3.24**) and the load-deflection relationship during the test was recorded in the computer connected to the Tensometer. An FE model was created for this joint configuration and material properties (**Figure 3.21**). A similar deformation and failure mode was observed in the analysis (**Figure 3.25-a, 3.25-b**).

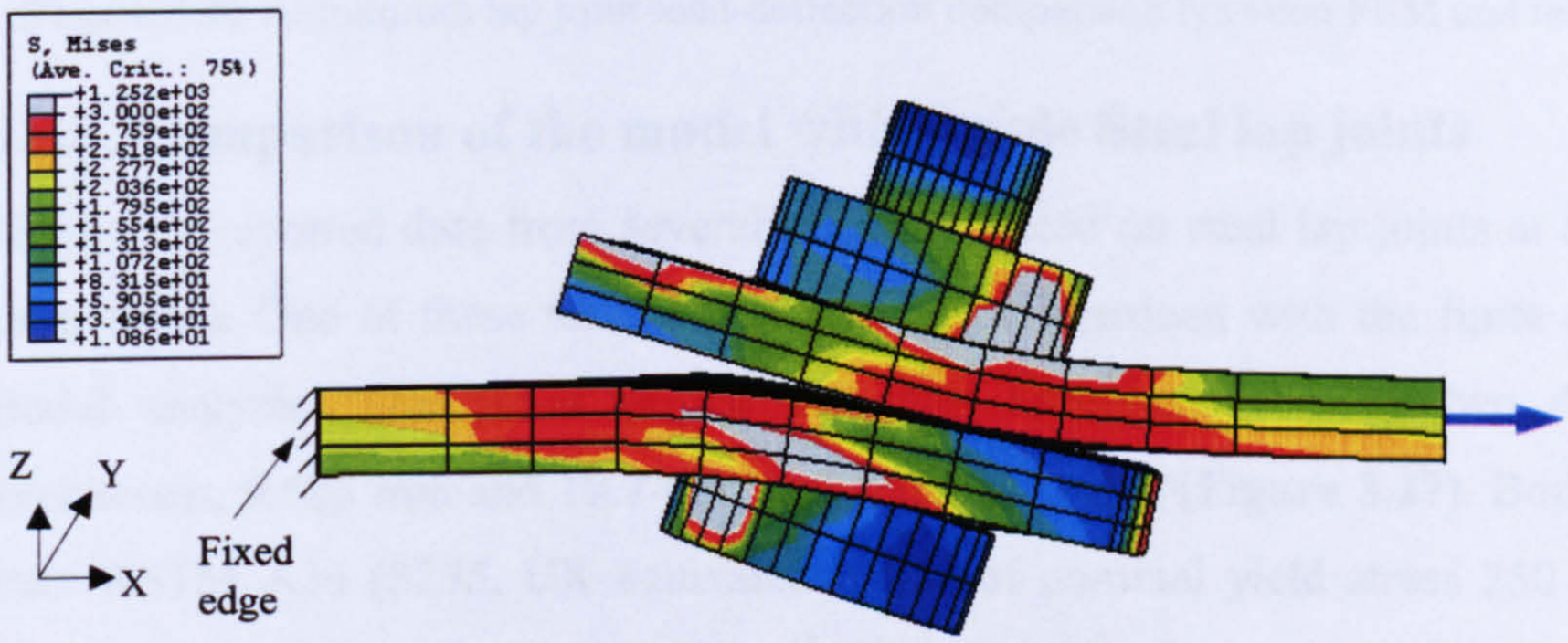

Figure 3.25-a Aluminium lap joint FEM, deformation and Von Mises stress contours

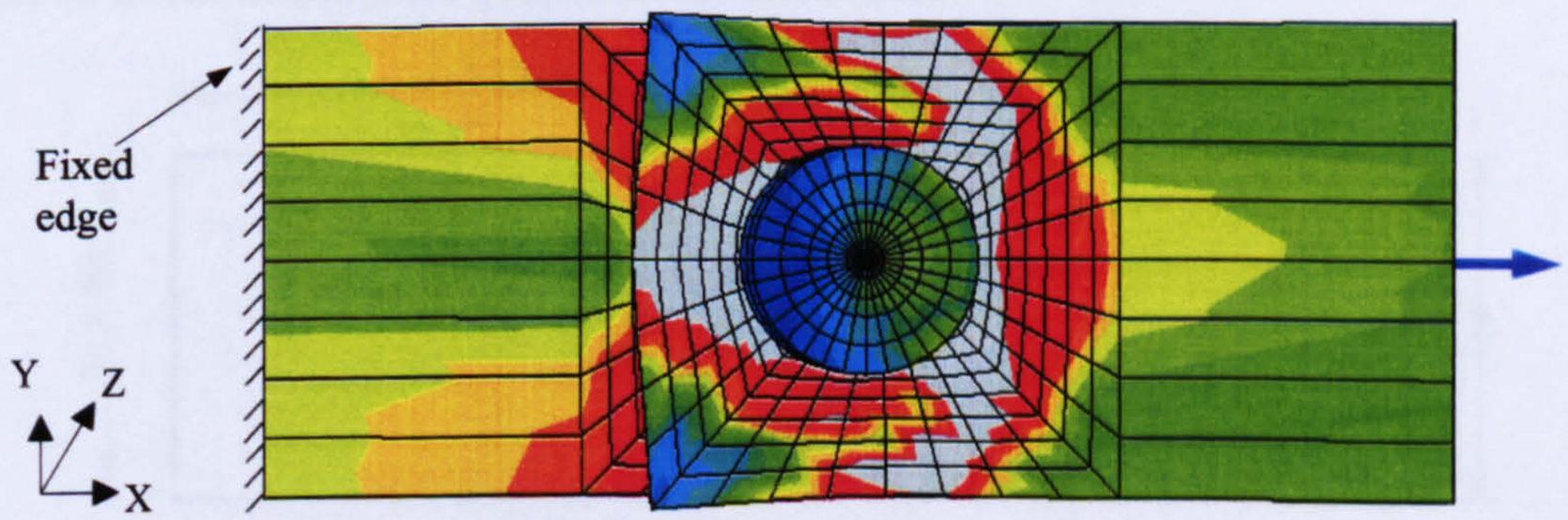

Figure 3.25-b Aluminium lap joint FEM, deformation and Von Mises stress contours

Comparison between the load-deflection plot of the experiment and that of the FE model (**Figure 3.26**) shows a maximum ultimate load capacity difference of less than 8 % between the test and the FE model.

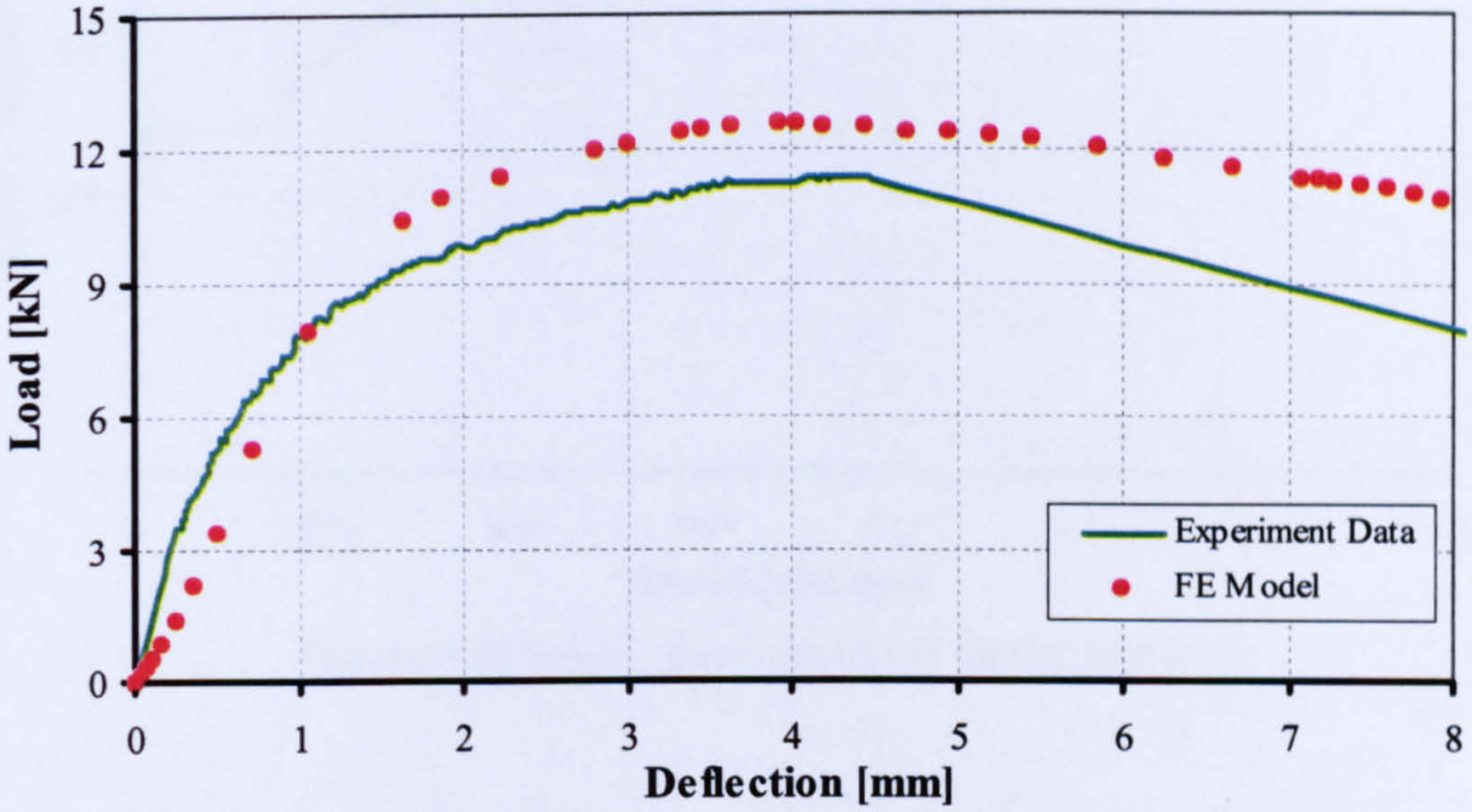

Figure 3.26 Aluminium lap joint load-deflection comparison between FEM and test data

3.5.3. Comparison of the model with simple Steel lap joints

Richard [3.5] reported data from several tests conducted on steel lap joints at ambient temperature. One of these tests was chosen for comparison with the finite element model analyses. The plates in the lap joint specimen were of two different thicknesses, 9.525 mm and 12.7 mm (3/8 inch, 1/2 inch) (**Figure 3.27**). Both plates were ASTM A36 (S275, UK equivalent) steel of nominal yield stress 250 N/mm^2 and nominal ultimate stress 400 N/mm^2 (**Figure 3.28**). The bolt was ASTM A325 (8.8 bolt, UK equivalent) (**Figure 3.29**) of 19mm (3/8 inch) diameter, installed in over-sized holes of 20.6mm (13/16 inch) diameter.

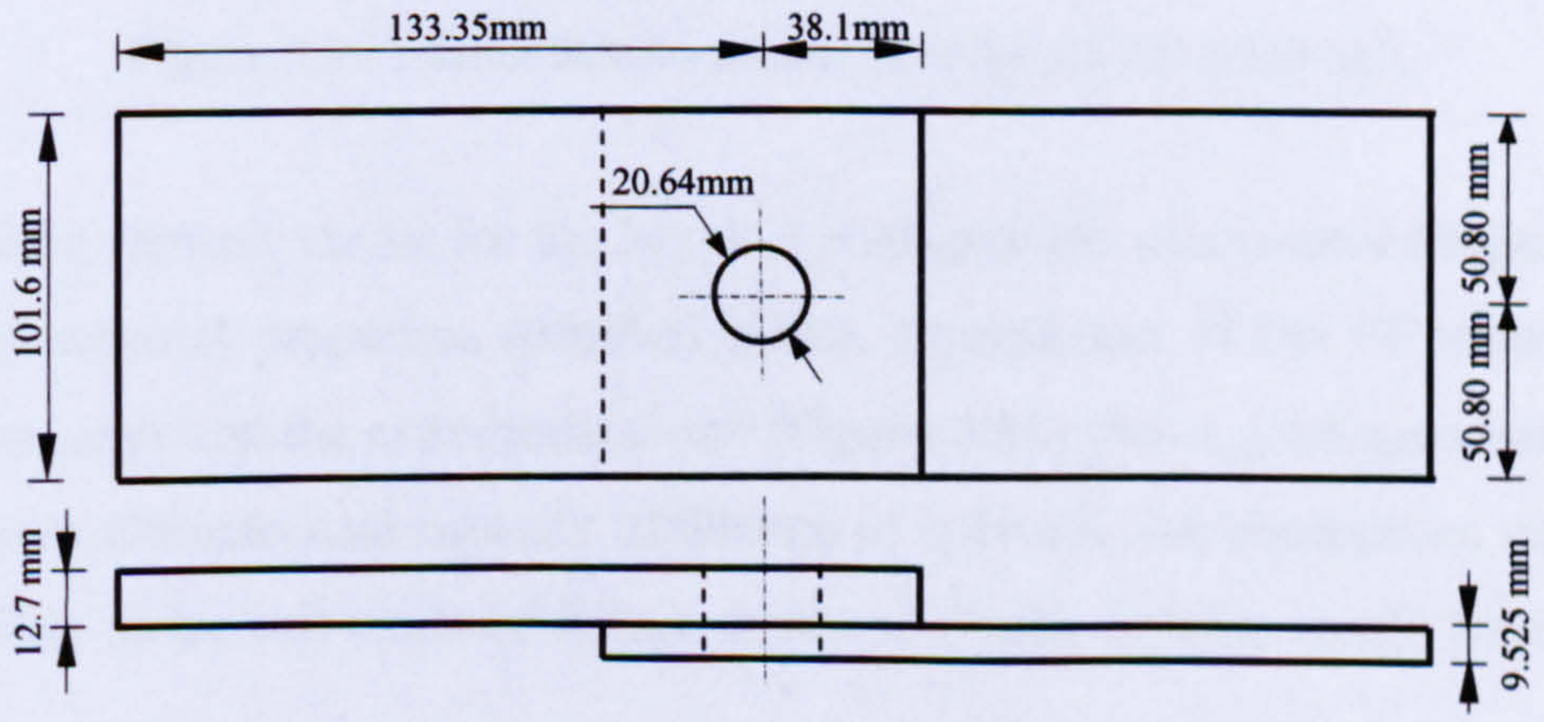

Figure 3.27 Geometrical details of Steel lap joint for test specimen

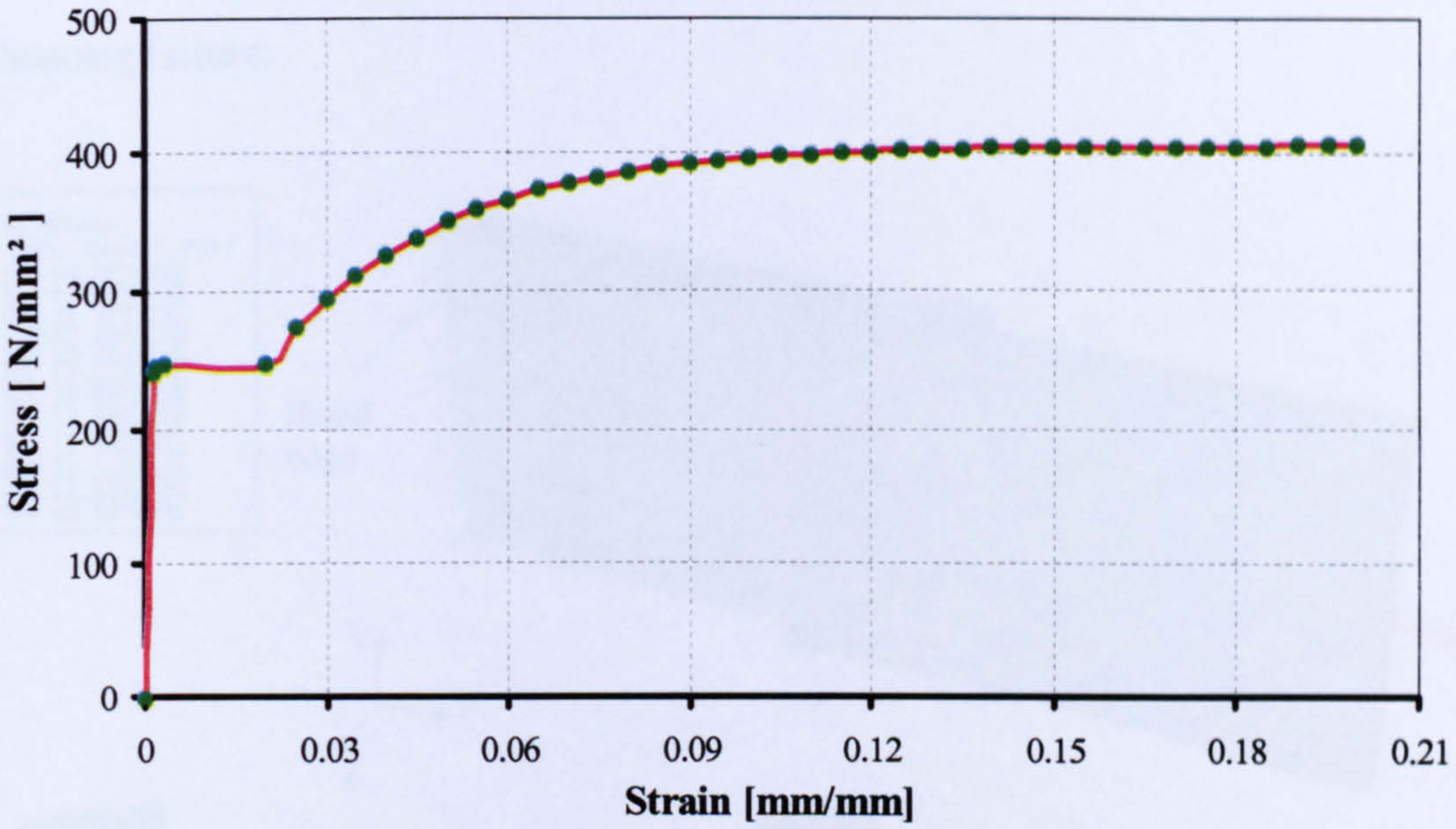

Figure 3.28 Stress - Strain curve for ASTM A36 steel

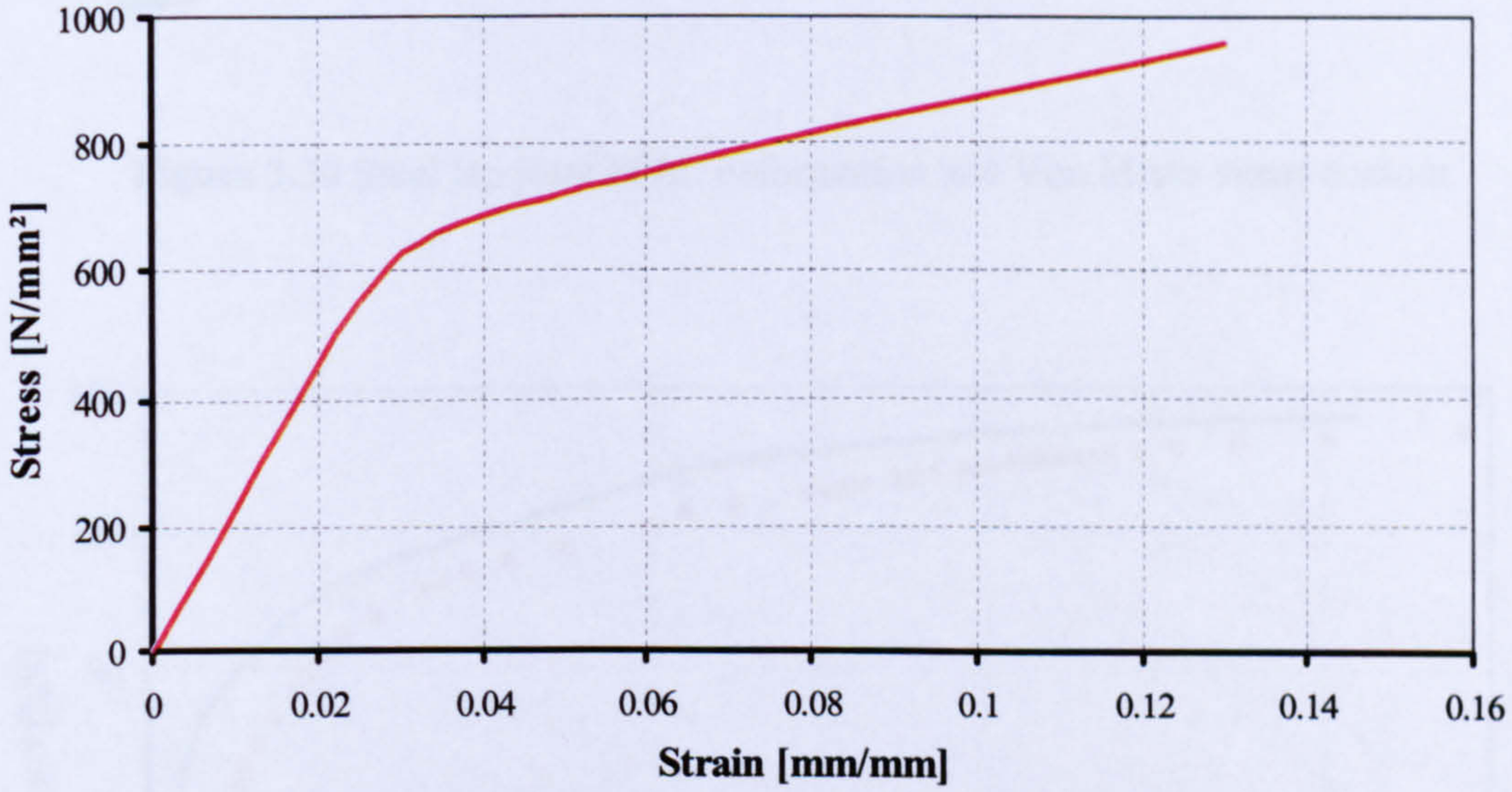

Figure 3.29 Tensile Stress - Strain curve for ASTM A325 bolt

A 3-D finite element model for the lap joint configuration was created (**Figure 3.30**) using the material properties specified above. Comparison of the FE model load-deflection curve and the experimental one (**Figure 3.31**) shows good agreement, with a maximum ultimate load capacity difference of only 6%. An observation of the FE deformation shape and mode of failure shows similarity to what would be expected

in a lap joint tensile test; that is, bolt rotation due to the load eccentricity, and bolt shearing failure.

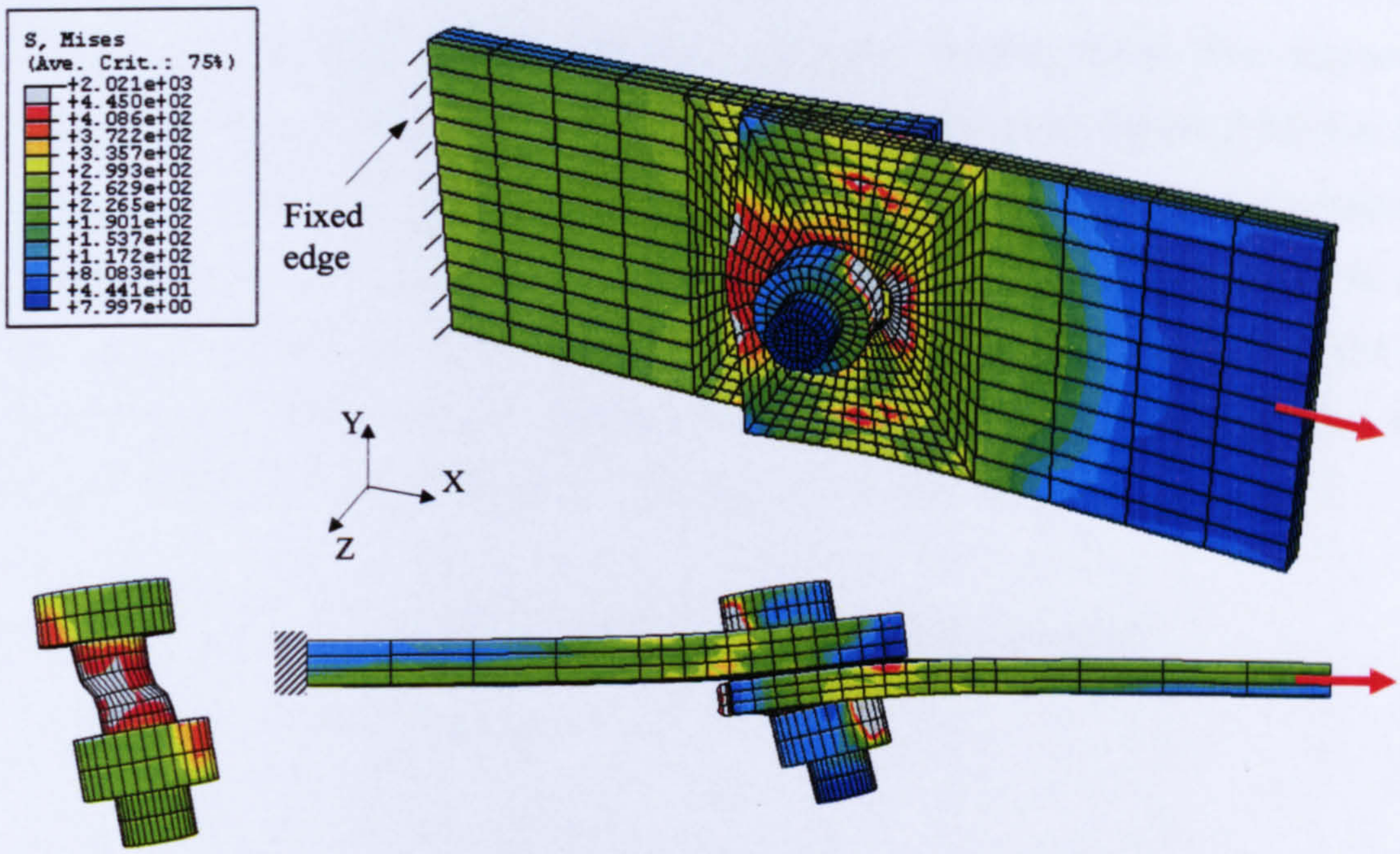

Figure 3.30 Steel lap joint FEM, deformation and Von Mises stress contour

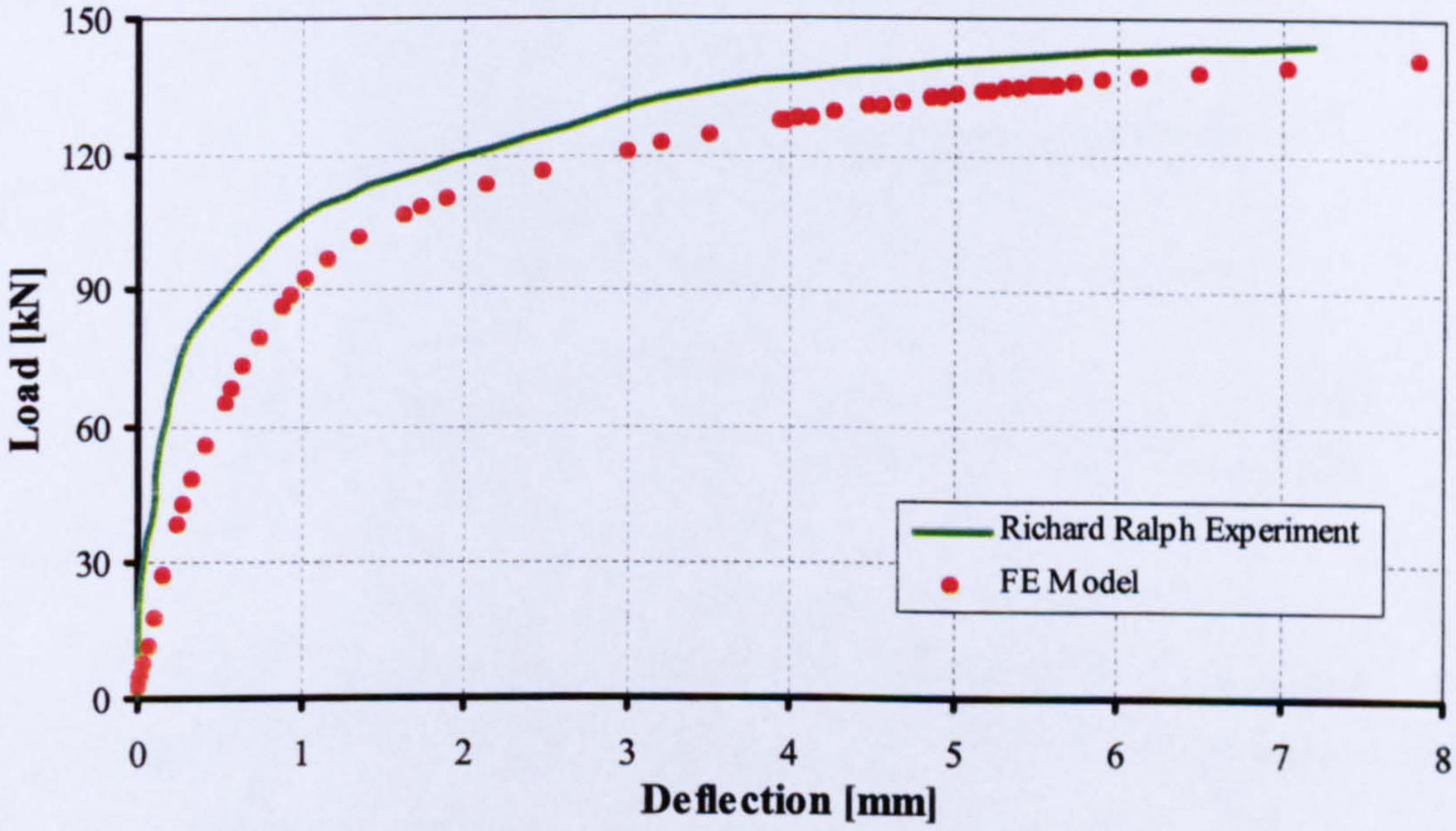

Figure 3.31 Load-deflection comparison between FEM and test data of steel lap joint

3.5.4. Evaluation of the fin plate connection model against moment-rotation test

Richard [3.5] also investigated the moment-rotation characteristics of steel fin plate connections. Full scale experiments were conducted on two-, three-, five- and seven-bolted connections. The three-bolted fin plate connection test **(Figure 3.32)** has been chosen to evaluate the capability of the finite element model to predict the moment-rotation behaviour. This test was carried out on a W18×35 beam connected to a fin plate of 9.5mm (3/8 inch) thickness. Both the beam and fin plate were of ASTM A36 steel **(Figure 3.28)**. The bolts were ASTM A325 **(Figure 3.29)**, of 19mm (3/4 inch) diameter inserted into 20.6 mm (13/16 inch) over-sized holes.

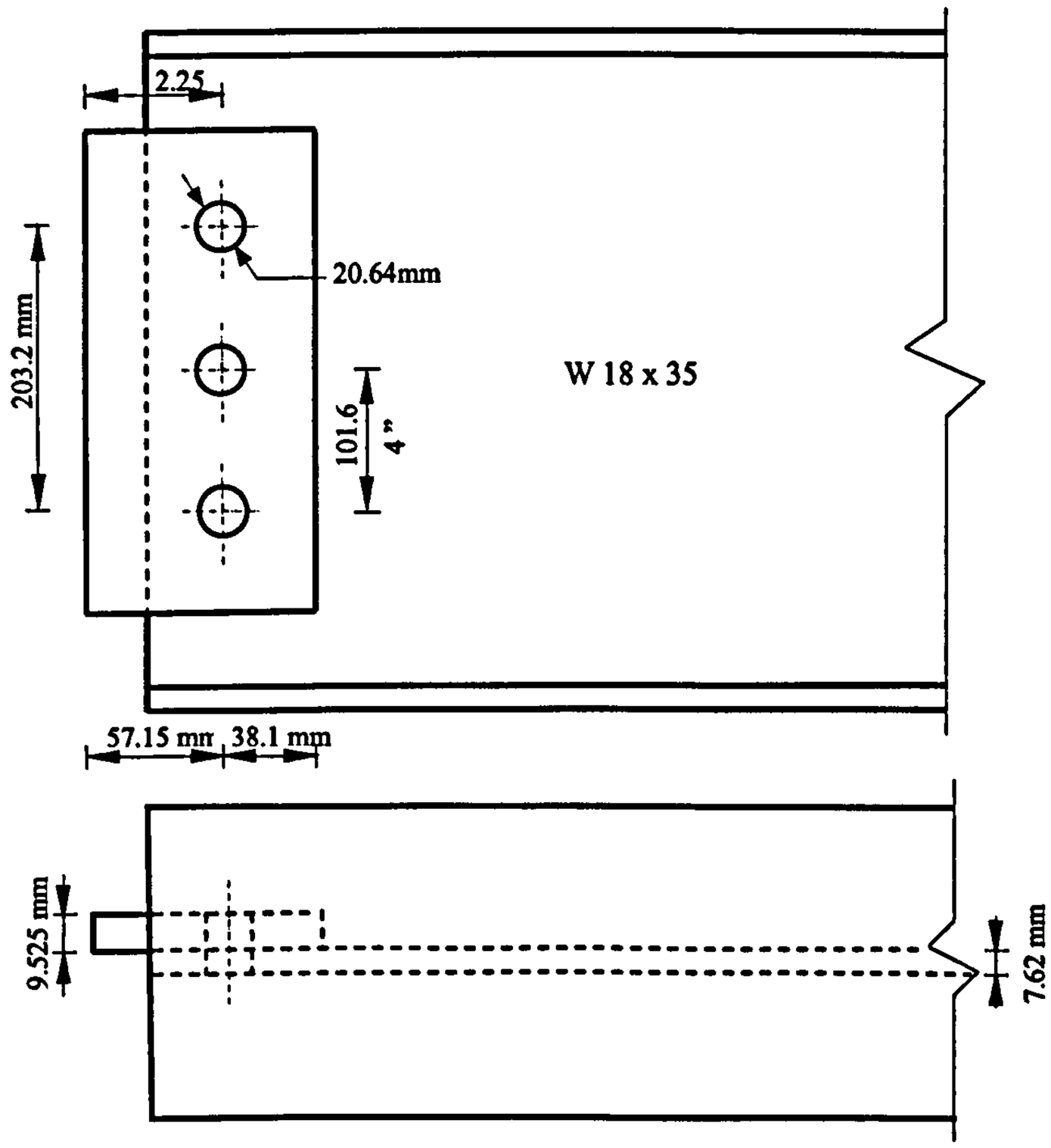

Figure 3.32 Geometrical details of fin plate connection test specimen

(Note: dimensions are shown in mm but the original test data was shown in Imperial units)

The final deformation and von Mises stress contours are shown in **Figure 3.33.** It is clear from the analysis that the middle bolt acts as the centre of rotation, whereas the top hole undergoes a high deflection as the top bolt bears toward the outer edge of the web. In contrast, the bottom bolt has to bear in the opposite direction, where the

web material is not limited by the close proximity of an edge. Consequently, the bottom bolt deforms more than the top bolt and suffers high shearing stresses. **Figure 3.34** shows the moment-rotation response for the FE model together with the experimental moment-rotation curve. In general, the FE model agrees well with the experimental data of Richard's test with reasonable accuracy.

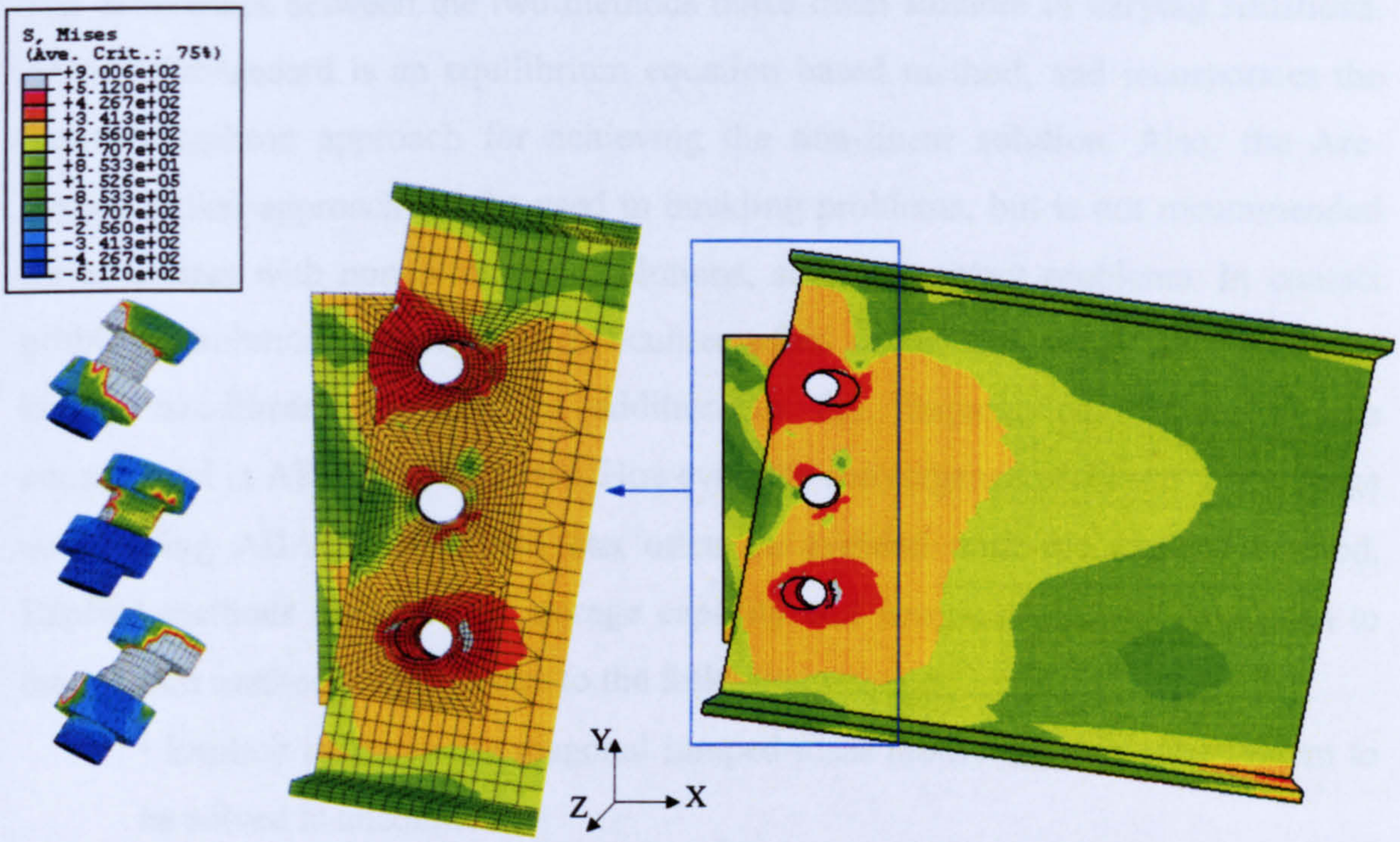

Figure 3.33 FE model of fin plate connection, deformation and von Mises stress contours

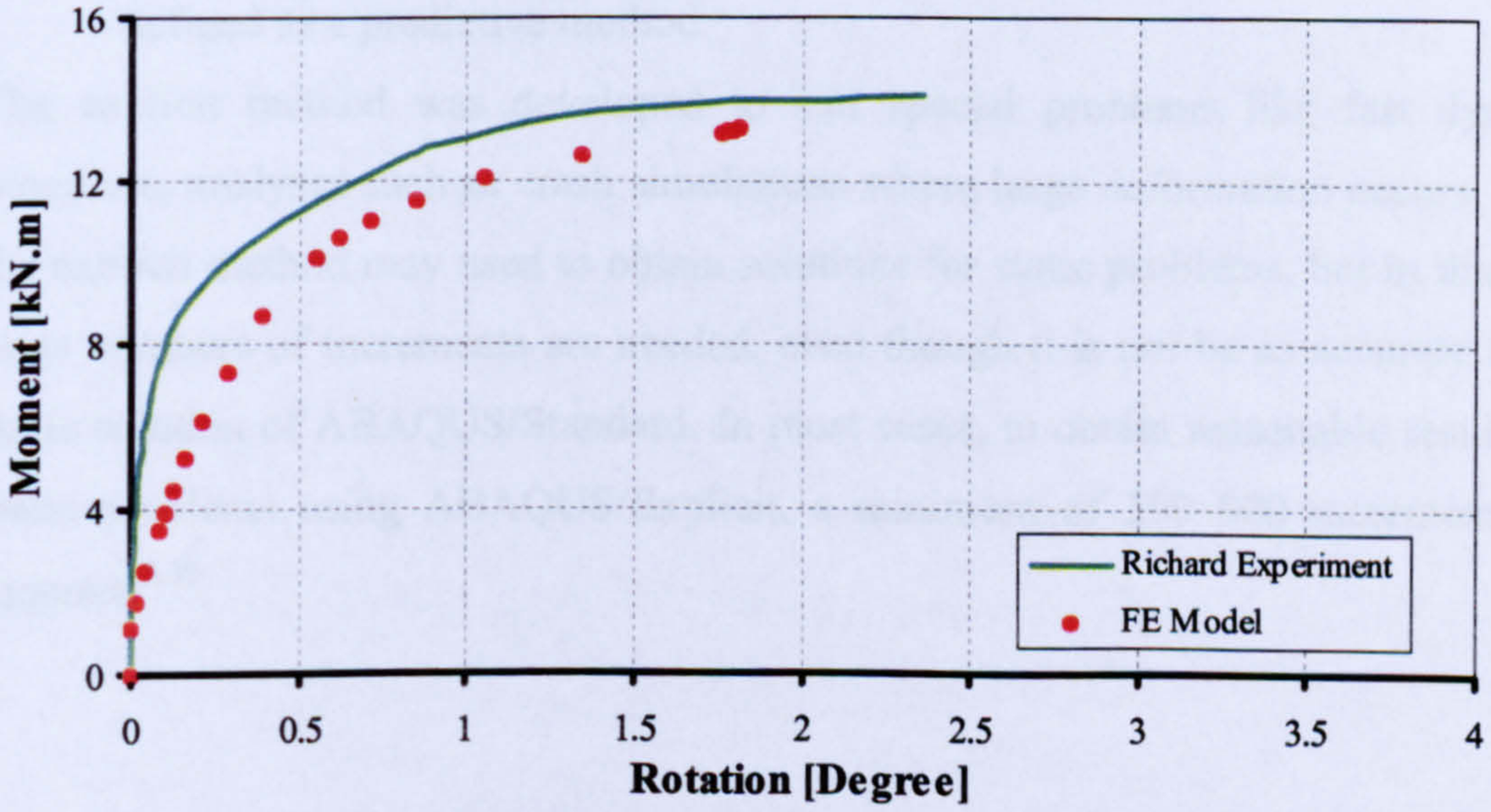

Figure 3.34 Moment–Rotation comparison of FEM and test data for fin plate connection

3.6. Modelling Strategy and Discussions

Modelling steel connections can be achieved using either ABAQUS/Standard (Implicit) or ABAQUS/Explicit. It may be easier to conduct the FE connection modelling via ABAQUS/Explicit, but the difference between the Standard and the Explicit modelling should be highlighted and then the choice based on its suitability. The differences between the two methods make them suitable in varying situations. ABAQUS/Standard is an equilibrium equation based method, and incorporates the Newton-Raphson approach for achieving the non-linear solution. Also, the Arc-Length (Riks) approach can be used in buckling problems, but is not recommended for structures with non-continuous solutions, such as contact problems. In contact problems, solution convergence difficulties often occur, and these are considered highly non-linear problems, in addition to the frequent equilibrium checks encountered in ABAQUS/Standard. However, the convergence problems that emerge when using ABAQUS/Standard can often be avoided with the explicit method. Explicit methods demand less storage capacity and computer-time as compared to the implicit method, which is due to the following reasons:

- Explicit methods use diagonal lumped-mass matrices, so that the system to be solved is uncoupled.
- No equilibrium iterative convergence process (like Newton-Raphson) are needed, so that it is a non-equilibrium equation based method, which may be defined as a predictive method.

The explicit method was developed to suit special problems like fast dynamic processes, analyses such as crash simulations where large deformation occurs. Also, the explicit method may used to obtain solutions for static problems, but in this case large numbers of increments are needed, even though it is not be as accurate as the static solution of ABAQUS/Standard. In most cases, to obtain reasonable results for static problems using ABAQUS/Explicit, a minimum of 300 000 increments are required [3.30].

3.7. Conclusions

The three-dimensional finite element models presented have simulated the shearing and bearing behaviour of simple shear connections. The models incorporate non-linear material properties for all the connection components, geometric non-linearity and contact interaction and use the ABAQUS/Standard code. In most cases, contact elements were crucial for modelling the steel connection performance, and thus it was a big challenge to create the fin plate connection model. However, the contact interactions between the connection components were introduced and achieved successfully. The contact interaction was established carefully between the beam web and the fin plate, as was bearing contact between the bolt shank and the bolt holes.

Several conclusions can be drawn based on the results of the finite element analyses.

- A full 3D solid model incorporating contact and non-linear material properties can be used to accurately model steel fin plate shear connections behaviour using ABAQUS/Standard software.
- It can be seen that C3D8I elements perform well, both in the elastic and inelastic regions, and have the ability to simulate large deformations.
- The proposed finite element models may be used as benchmarks to verify the accuracy of similar shear connection models, incorporating contact elements along with geometric and material non-linearity.
- Parametric studies of factors that influence the strength and stiffness of steel joints are difficult to control in any laboratory testing, because of the dimensional and physical variability among joints and test arrangements. Experimental parametric studies are also expensive and time-consuming. The reasonable accuracy of the FE model for reproducing the experimental behaviour of steel joints makes it a useful model for both analytical and parametric studies. Although validation against experimental test data is needed a numerical simulation, carefully created and validated against test data, enables cost-efficient parametric investigation that may lead to improvements in joint configuration and joint performance.

3.8. References

[3.1] Tschemmernegg, F. and Humer, C., "The design of structural steel frames under consideration of the nonlinear behaviour of joints", *J. Construct. Steel Research*, Vol. **11**, (1988) pp 73-103.

[3.2] Ireman, T. "Design of composite structures containing bolt holes and open holes", Ph.D. Thesis submitted to the Department of Aeronautics, Royal Institute of Technology, Sweden, 1999.

[3.3] Lipson, S. L. "Single-angle and single-plate beam framing connections", Proceedings, Canadian Structural Engineering Conference, Toronto, Ontario, Canada, February (1968) pp 141-162.

[3.4] Richard, R. M., Gillett, P. E., Kriegh, J. D., and Lewis, B. A. "The analysis and design of single plate framing connections", *Engineering Journal*, AISC, Vol. **17**, No.2, Second Quarter, (1980).

[3.5] Richard, R. M., Kriegh, J. D., and Hormby, D. E. "Design single plate framing connections with a 307 bolts", *Engineering journal*, AISC, pp 209–213, Fourth quarter, (1982).

[3.6] Hormby, D. E., Richard, R. M., and Kriegh, J. D. "Single-Plate framing connections with grade-50 steel and composite construction", *Engineering journal*, AISC, Vol. **21**, No. 3, (1984) pp 125-138.

[3.7] Astaneh, A., Call, S. M., and McMullin, K. M. "Design of single plate shear connections", *Engineering journal*, AISC, Vol. **26**, No.1, (1989).

[3.8] Astaneh, A., McMullin, K. M., and Call, S. M. "Behaviour and design of steel single plate shear connections", *Journal of Structural Engineering*, Vol. **119**, No. 8, (1993) pp 2421-2440.

[3.9] Astaneh, A., Liu, J. and McMullin, K. M. "Behaviour and design of single plate shear connections", *J. Construct. Steel Research*, Vol. **58**, (2002) pp 1121–1141.

[3.10] Pham, L. and Mansell, D. S. "Testing of standardized connection", Australian Welding Research Vol.**11**, December (1982).

[3.11] Pham, L. "Strength of web side plate connection with revised standardized web side plate", Third conference of Steel Developments, Melbourne, Australia, May (1985).

[3.12] Patrick, M., Thomas, I. R., and Bennetts, I. D. "Testing of web side plate connections", Structure Conference, Auckrick, New Zealand, Aug. (1986).

[3.13] Aggarwal, A. K. "Behaviour of web-side plate beam-column connections", 10th Australian conference on the mechanics of structures and materials, University of Adelaide, Australia, (1986).

[3.14] Moore, D. B., and Owens, G. W. "Verification of design methods for fin plate connections", *The Structural Engineer*, Vol. **70**, No.3/4, February (1992).

[3.15] Creech, D.D. "Behaviour of single plate shear connections with rigid and flexible supports", MSc. Thesis submitted to the Department of Civil, Construction and Environmental Engineering in North Carolina State University. (2005).

[3.16] Yura, J. A., Birkemoe, P. C., and Ricles, J. M. "Beam web shear connections: An experimental study", *Journal of the Structural Division*, ASCE, Vol. **108**, No. ST2, (1982) pp 311-325.

[3.17] Bose., S. K., McNeice, G. M., and Sherboume, A. N., "Column web in steel beam-to-column connections part I-Formulation and verification", *Computers and Structures*, Vol. **2**, (1972) pp 253-279.

[3.18] Maggia, Y. I., Gonçalvesa, R. M., Leonb, R. T., and Ribeiroc, L. F. L. "Parametric analysis of steel bolted end plate connections using finite element modeling," *J. Construct. Steel Research*, Vol. **61,** (2005) pp 689-708.

[3.19] Bursi, O. S., and Jaspart, J. P., "Benchmarks for Finite Element Modeling of Bolted Steel Connections", *J. Construct. Steel Research*, Vol. **43** (1), (1997) pp 17-42.

[3.20] Bursi., O. S., and Jaspart J. P., "Basic issues in the finite element simulation of extended end plate connections", *Computers and Structures*, Vol. **69**, (1998) pp 361-382.

[3.21] Swanson, J. A., Kokan, D. S., and Leon, R. T., "Advanced finite element modeling of bolted T-stub connection components", *J. Construct. Steel Research*, Vol. **58**, (2002) pp 1015–1031.

[3.22] Yang, J. G., Murray, T. M., and Plaut, R. H., "Three-dimensional finite element analysis of double angle connections under tension and shear", *J. Construct. Steel Research*, Vol. **54**, (2000) pp 227–44.

[3.23] Hong, K., Yang, J. G., and Lee, S. K., "Moment-rotation behaviour of double angle connections subjected to shear load", *Engineering Structures*, Vol. **24** (1), (2000) pp 125-32.

[3.24] Kishi, N., Ahmed, A., Yabuk, N., and Chen, W. F., "Nonlinear finite element analysis of top- and seat-angle with double web-angle connections", *Structural Engineering and Mechanics*, Vol. **12**, No. 2, (2001) pp 201-214.

[3.25] Ahmed, A., Kishi, N., Matsuoka, K. G., and Komuro, M. "Nonlinear analysis on prying of top- and seat-angle connections", *Journal of Applied Mechanics*, Vol. **4**, No. 8, (2001) pp 227-236.

[3.26] Komuro, M., Kishi, N., and Chen, W.F. "Elasto-plastic FE analysis on moment-rotation relations of top- and seat-angle connections", ECCS / AISC Workshop, Amsterdam, Netherlands, June 3-5 (2004).

[3.27] Chung, K. F., and Ip, K. H., "Finite element investigation on the structural behaviour of cold-formed steel bolted connections", *Engineering Structures*, Vol. **23** (9), (2001) pp 1115–25.

[3.28] Chung, K. F. and Ip, K. H., "Finite element modeling of bolted connections between cold formed steel strips and hot rolled steel plates under static shear loading", *Engineering Structures* Vol. **22** (9), (2001) pp1271–1284.

[3.29] Citipitioglu, A. M., Haj-Ali, R. M., and White, D. W., "Refined 3D finite element modeling of partially restrained connections including slip", *J. Construct. Steel Research*, Vol. **58**, (2002) pp 995–1013.

[3.30] Barth, K. E., Orbison, J. G., and Nukala, R. "Behaviour of steel tension members subjected to uniaxial loading", *J. Construct. Steel Research* Vol. **58**, (2002) pp 1103–1120.

[3.31] S.-H. Ju, C.-Y. Fan and Wu, G. H., "Three-dimensional finite elements of steel bolted connections", *Engineering Structures* Vol. **26**, (2004) pp 403-413.

[3.32] ABAQUS, *Theory Manual*, version 6.3, Hibbit, Karlsson and Sorenson, Inc., Providence, RI, (2001).

[3.33] ABAQUS/Standard, *User's Manual I-III*, version 6.3 Hibbit, Karlsson and Sorenson, Inc, (2001).

[3.34] Dowling, P. J., Knowles, P. and Owens, G. W., "Structural steel design" The Steel Construction Institute (1988).

[3.35] European Committee for Standardization (CEN), "Eurocode 3: Design of Steel Structures, Part 1.2: General rules - Structural fire design", EN 1993-1-2, British Standard Institution, London, (2005).

[3.36] Rex, C. O., and Easterling, S. W. "Behaviour and modeling of a bolt bearing on a single plate", *Journal of Structural Engineering,* ASCE, Vol. **129**, No. 6, (2003) pp. 792-800.

Chapter 4

Tying Forces at Ambient Temperature

4.1. Introduction

Since the Ronan Point disaster [4.1] in 1968 the term 'Progressive collapse' has been used widely in the international structural engineering community to describe an incremental type of failure. Progressive collapse describes the local failure of a principal load carrying member, a column for example, which leads to complete or partial collapse of a structure (**Figure 4.1**). Such a collapse occurs when the load supported by the failed member can not be redistributed to other structural members and the structure or part of it, collapses in a progressive manner. Such a complete collapse is clearly very dangerous, especially in multi-storey buildings which accommodate a large number of occupants. Therefore, progressive collapse should be avoided under all possible circumstances, or at least the building should survive for a period sufficient to evacuate all occupants and those in the immediate surrounding area.

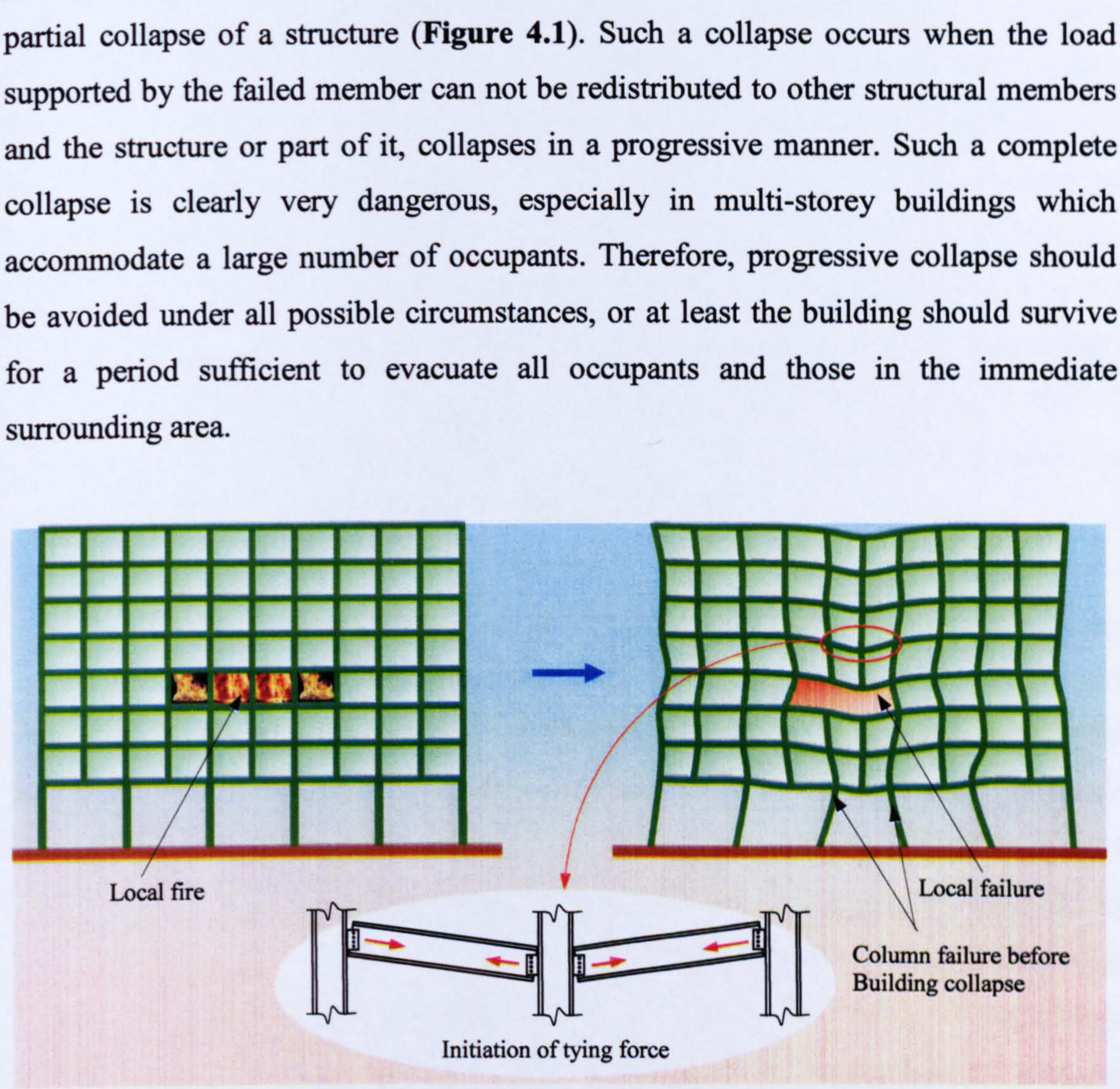

Figure 4.1 Possible scenario for progressive collapse

Certainly, any building should be designed in such a way that the failure of some structural members does not effectively destabilize the structure of the overall building. In response to the collapse of Ronan Point, the Building Regulations (HMSO,1976) [4.2] were changed in the United Kingdom to require that five-storey buildings and higher should not suffer a failure disproportionate to an initial local failure due to an accidental load such as a gas explosion [4.2]. The objective of this requirement was addressed by two main recommended approaches. The first one is by tying the building together horizontally and vertically to increase its structural continuity and create a structure with a high degree of robustness. The other approach to avoid progressive collapse is by designing the structure to bridge over the collapsed members. In this manner, if part of the structure is removed by an accidental action, the remaining members that are still well connected can develop an alternative load path which transfers the load of the collapsed members to stiffer members [4.2]. Accordingly, the Code of practice BS5950: Part 1, in Clause 2.4.5, requires that in steel buildings of over four storey, all connections should be designed to resist a factored tying force of not less than 75 kN at floor levels, or 40 kN at roof level, in order to avoid disproportionate collapse. This requirement was amended in the latest UK Building Regulations [4.3], published on 2004, to include all buildings, irrespective of the number of storeys. Also the new requirement in the latest BS5950: Part-1 [4.4] is that each connection should maintain a tying force equal to its connection vertical reaction, but not less than 75 kN in any case.

The question that may rise here is, "Do fin plate shear connections have sufficient capacity to resist tying forces?" Also, "Can they be used with confidence for tying purposes?" As stated in the literature review, no research has yet examined fin plate connection tying capacity. In addition, all the previous conducted test connection configurations, material properties and test settings were altered from one test to another rather than focussing directly with more detail on exploring the reality of the main failure modes of fin plate connections. However, the main types of failure mode identified in fin plate shear connections are plate bearing and bolt shear failure. Therefore in this chapter a parametric study into these two failure types is conducted to investigate these phenomena and to distinguish when each failure mode would predominate the other. In addition, this chapter will explore whether it is possible to

study the tying capacity of fin plate connections by simplify considering a single lap joint with similar configurations and material properties. Demonstrating this fact would have a major beneficial effect on the way that fin plate connections can be modeled and studied via the FE method. Using a single bolt row lap joint is minimises the analysis time and permits a have more focused study on the lap joint which may then be applied to the whole fin plate connection assembly. Also, this simplification will make application of the component method easier. This chapter will also investigate comprehensively the tying force resistance of fin plate connections.

4.2. Plate Bearing Parametric study

Plate bearing is a shear joint failure mode in which a high strength bolt bears into the circumference of a plate hole. As a result of this the bolt hole suffers considerable elongation, usually 3-10 mm, prior to any edge-distance fracture taking place, depending on the plate material properties. Therefore, this kind of failure mode has always been considered as a ductile failure. If a high strength bolt is used, the most important factors that influence plate bearing are the plate material properties, the edge distance and the plate thickness. Most codes of practice around the world recommend a minimum value of edge distance between $2d_b$ and $3d_b$ for bearing stresses to fully develop [4.4 - 4.7]. It has been established in earlier research that the plate bearing strength is linearly proportional to the plate thickness [4.8] and to the material's ultimate stress [4.9].

The FE model created **(Figure 3.7-a)** and validated in the previous chapter, **(3.5.1)** was used to investigate the bearing phenomenon behaviour. For this purpose the FE model was adjusted to have large plate width ($5d_b$) and edge distances sufficient **(Figure 4.2, 4.3)** to eliminate the net section failure mode. The plate material was assumed to be of S275 (205 kN/mm^2 Young's modulus, yield stress 275 N/mm^2 and ultimate stress 445 N/mm^2). A constant edge distance of $2d_b$ was used. Also a constant bolt diameter of 20 mm and 8.8 high strength bolt material were assumed throughout the analyses. Variable plate thicknesses ranged from 4 to16 mm; each one was investigated individually.

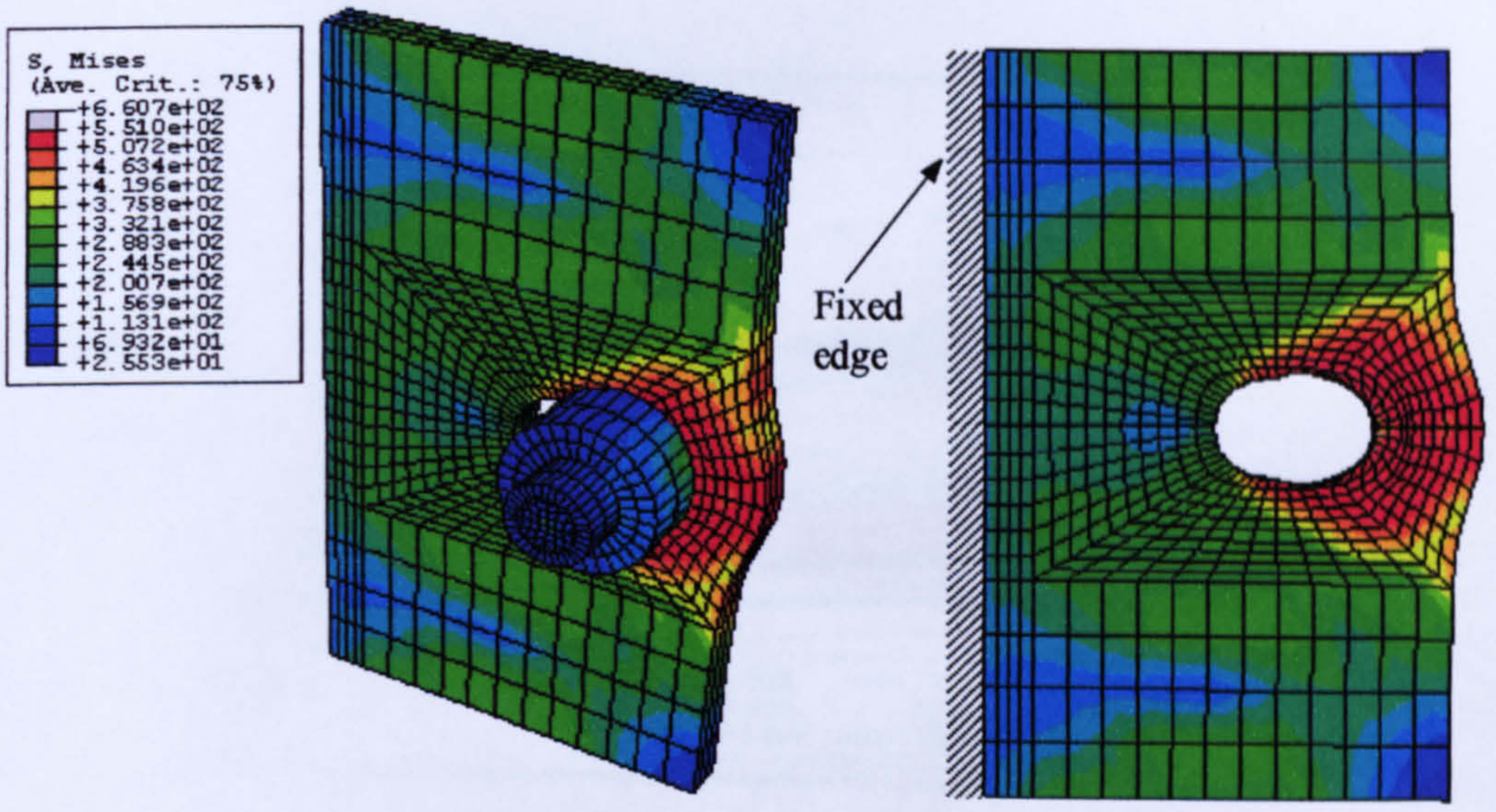

Figure 4.2 Von Mises stress contour of FE model for bolt bearing into plate thickness

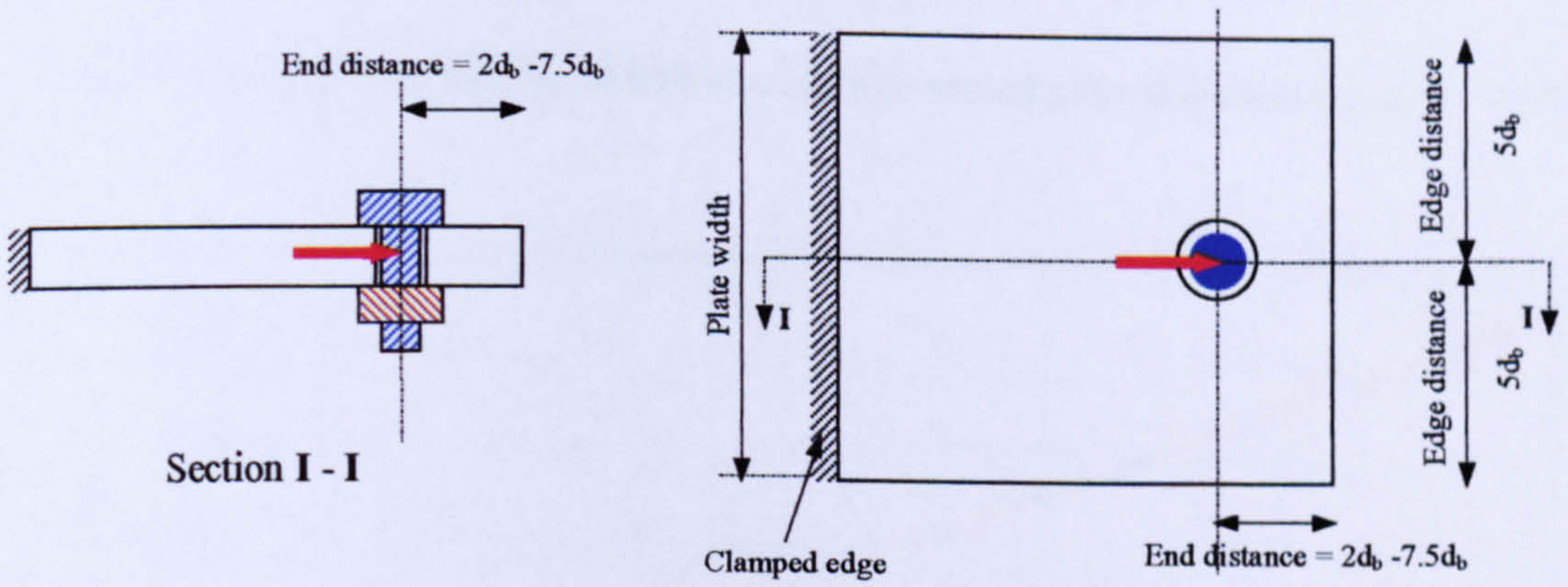

Figure 4.3 Geometrical detail of the plate studied under bolt bearing

According to the model configuration, edge distance rupture is the only possible failure mode. The deformed shape and the Von Mises stress contour of the FE model (**Figure 4.2**) shows the bolt hole plastic elongation and the inevitable edge distance rupture. The axial reaction force against bolt movement is plotted in the same graph (**Figure 4.4**) for various plate thicknesses. **Figure 4.5** represents the relationship between the plate thickness and the ultimate plate bearing capacity. These two plots demonstrate the increase in the plate bearing capacity to be proportional to the plate thickness.

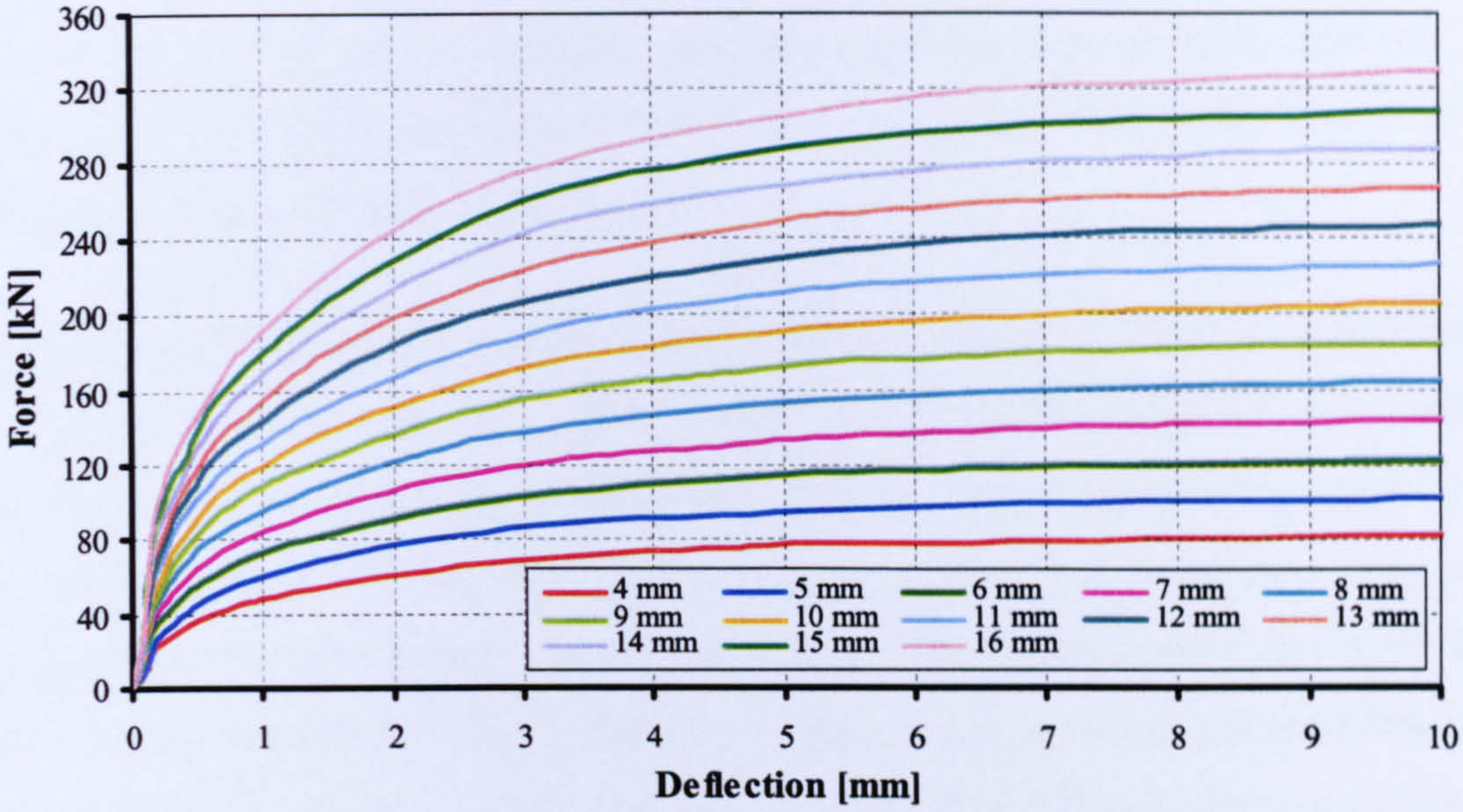

Figure 4.4 Force-deflections of bolt bearing into varied plate thickness range 4 – 16 mm

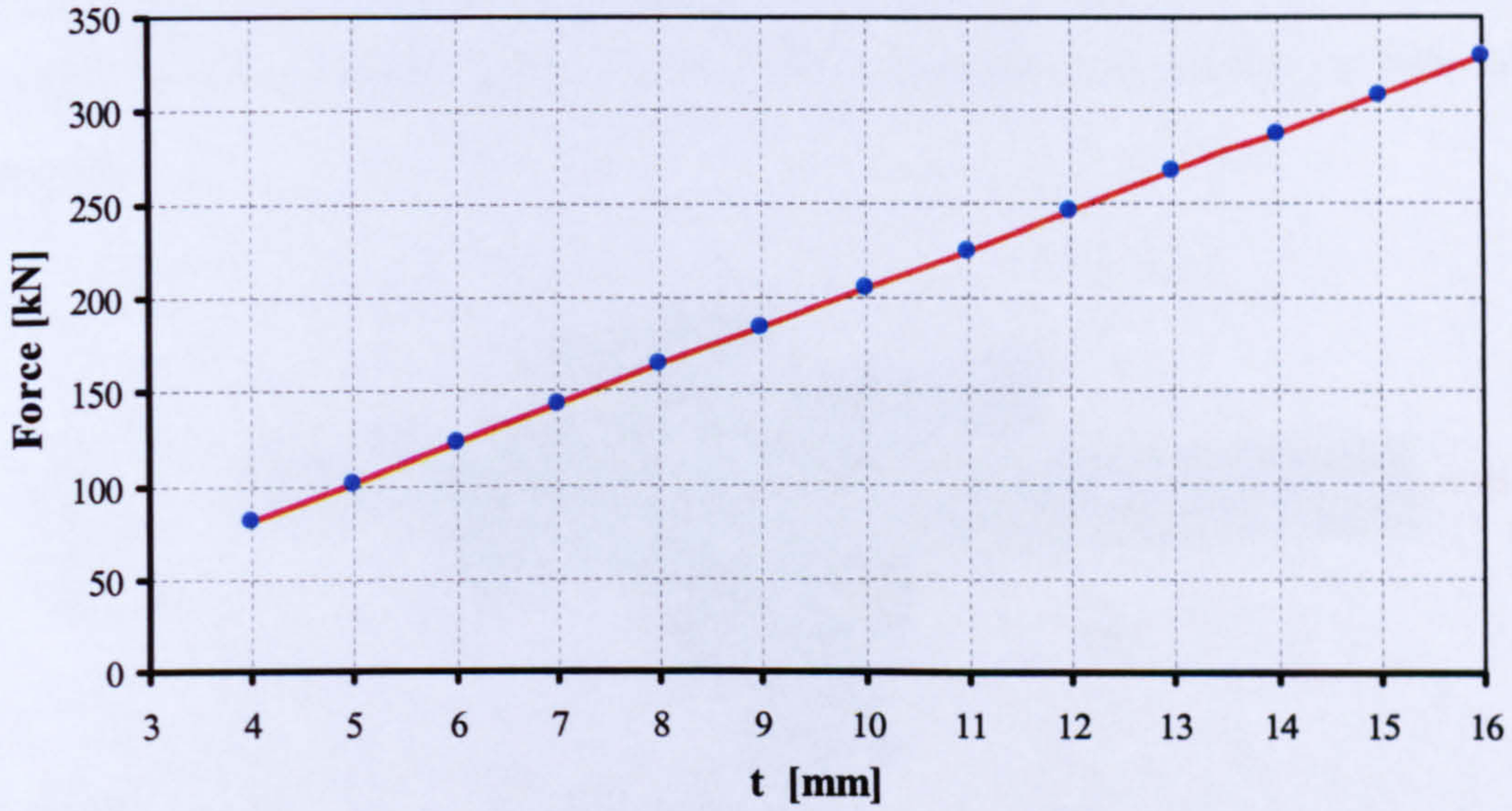

Figure 4.5 Plate ultimate bearing capacity for plate thickness ranging from 4 – 16 mm

4.3. Lap Joint Parametric Study

The lap joint FE model developed (**Figure 3.7-b**) and validated in Chapter 3 (**3.6.2, 3.6.3**) was used to investigate the effects of geometry on failure type. Both connected plates are assumed to be made of S275 steel that has 205 kN/mm^2 Young's modulus, yield stress 275 N/mm^2 and ultimate strength 445 N/mm^2. The model (**Figure 4.6**) was created to have a large plate width ($5d_b$), like that in **Figure 4.3,** in order to eliminate the net section failure mode. The thickness of the fixed plate (t_1) was kept

constant at 10 mm (according to the Green Book recommendations) [4.7] as was the bolt, which was 20 mm in diameter and of Grade 8.8 high strength material. In contrast, the other connected plate thickness (t_2) was chosen to be varied from 5 to 16 mm, making it the only geometric variable.

The deformed shapes and von Mises stress contours (**Figure 4.6**) were investigated for a series of twelve lap joint FE models. The plots of load against unrestrained plate deflection are presented (**Figure 4.7**) for this series of twelve lap joints. It is clear from **Figure 4.7** that the ultimate capacity of a lap joint was improved considerably by the increase of plate thickness. This improvement becomes less visible as the thickness of the unrestrained plate (t_2) approaches the thickness (10 mm) of the fixed plate (t_1). Above this thickness the ultimate load capacity increased only slightly. An intensive investigation into the Von Mises stress contour of the lap joints (**Figure 4.6-a**) and their cross sections through the bolt x-z plan (**Figure 4.6-b**), shows that, with a plate thickness (t_1) of 8 mm and upward, there is a clear indication of bolt shearing failure, before either end-distance yielding or bolt-hole elongation.

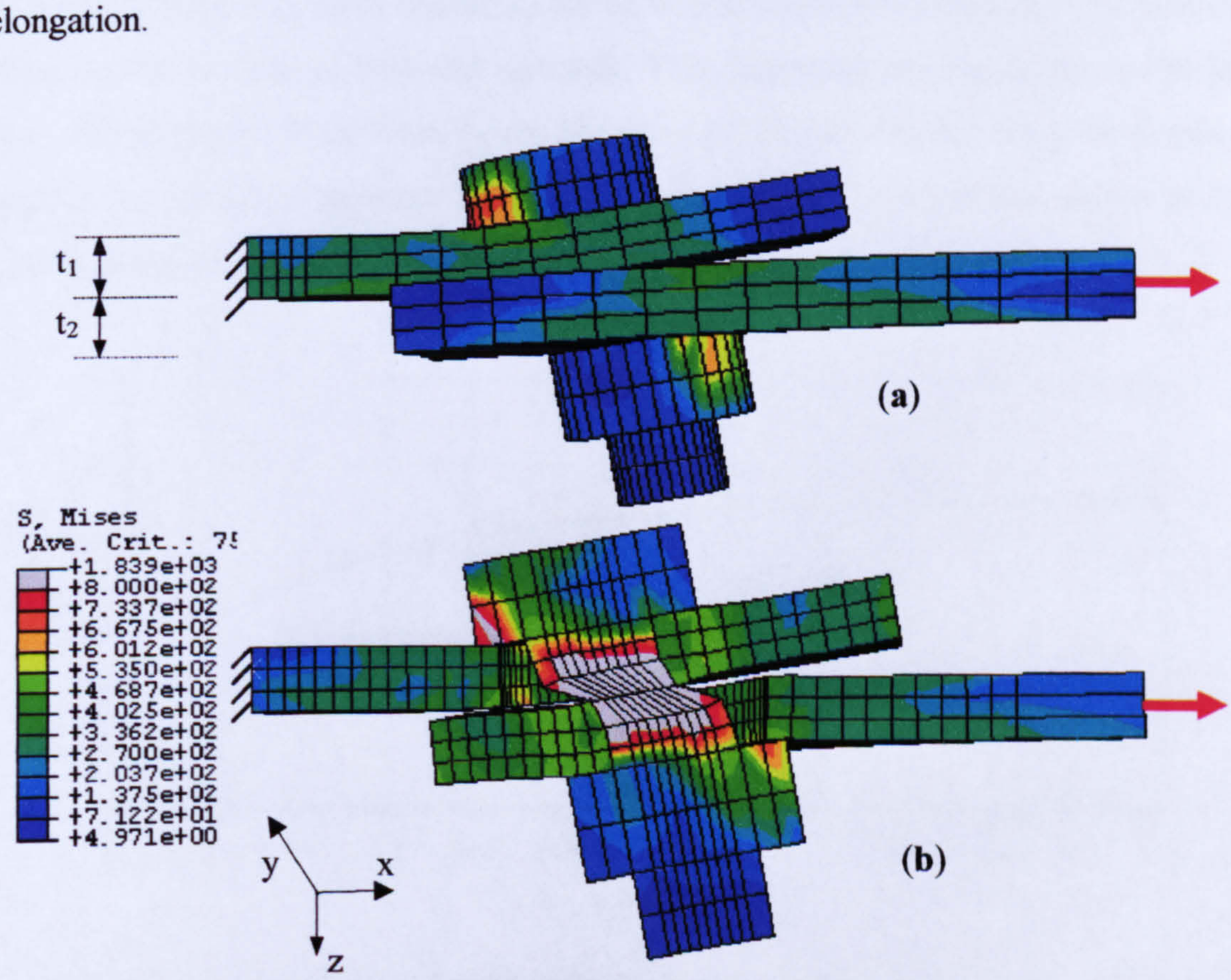

Figure 4.6 FE model of lap joint assembled from two 10 mm thickness plates and M20 8.8 bolt

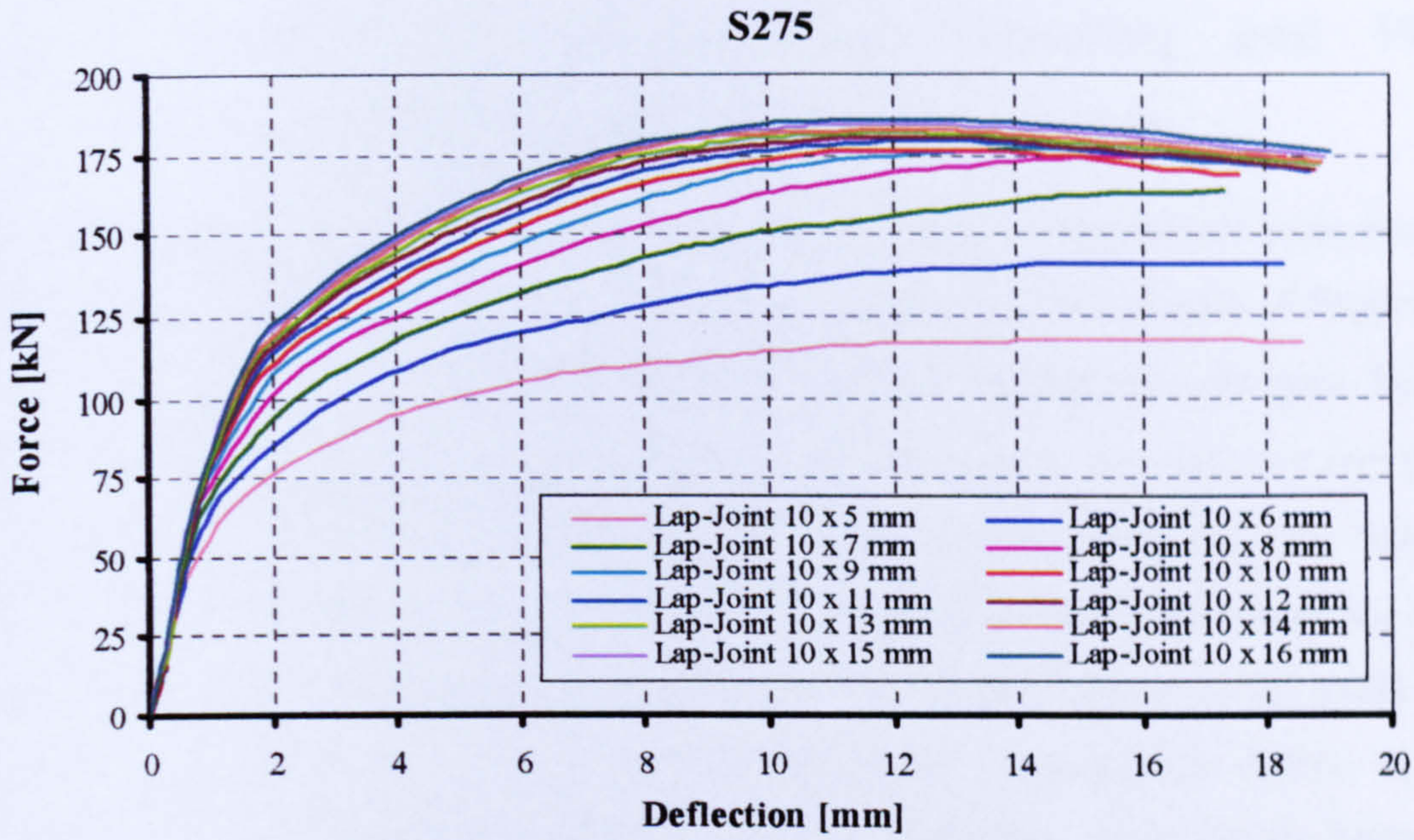

Figure 4.7 Force-deflection behaviour of lap joints with 10 mm fixed plate thickness and the other plate of thickness ranging from 5 – 16 mm using M20 8.8 bolt

This phenomenon is explained more clearly in **Figure 4.8**, which shows the ultimate lap joint capacity plotted against the ratio of the connected plates' thickness as (t_2/t_1). This relationship begins to converges for an unrestrained plate thickness of 8 mm (or plate thickness ratio of 0.8) and upwards. This illustrates the regularity of the lap joint failure mode. In contrast, below the plate thickness of 8 mm the joint shows a regular proportionate increase in the carrying capacity similar to that shown in the plate bearing investigation (**Figure 4.5**).

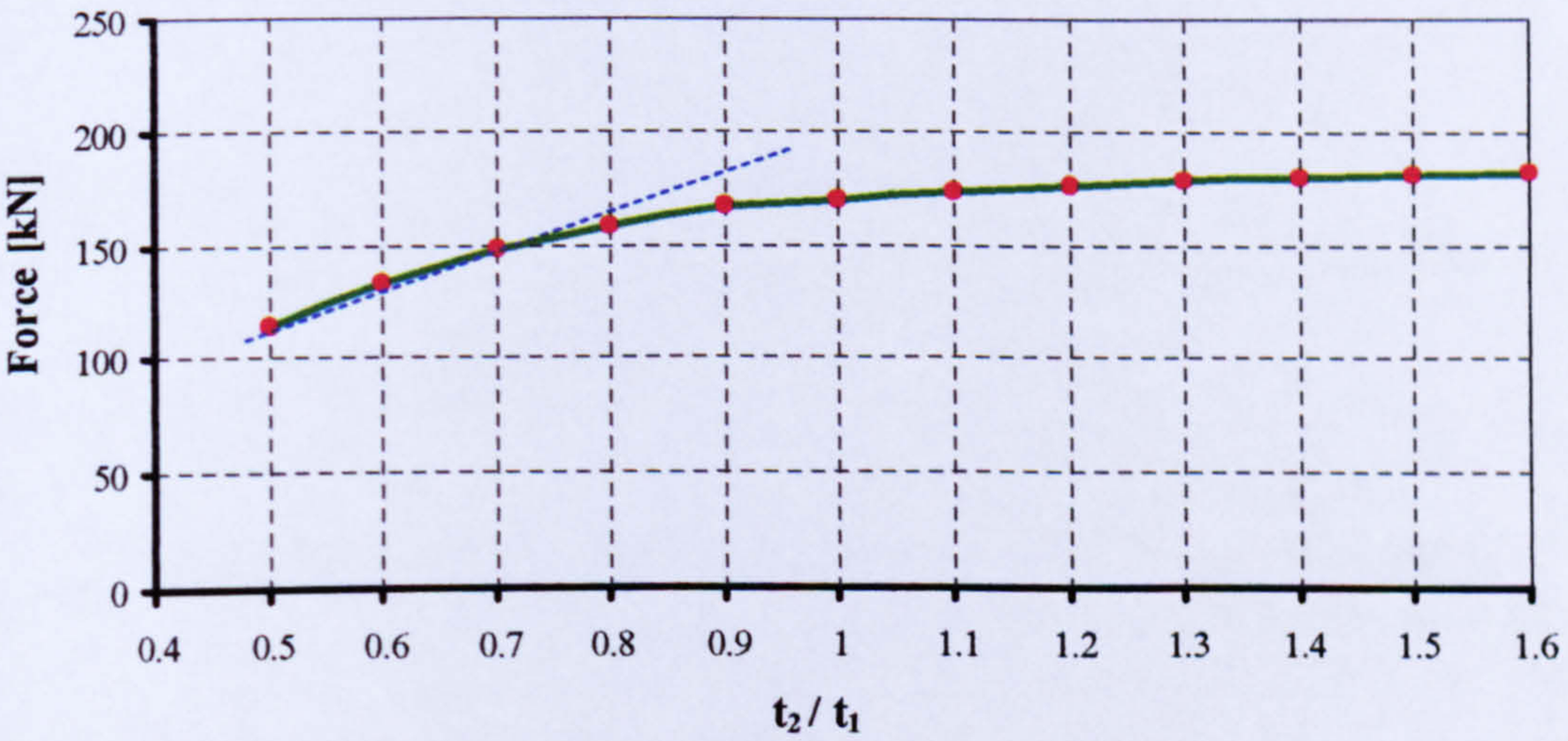

Figure 4.8 Lap joint ultimate capacity against the ratio of the connected plate thicknesses

4.4. Distinguishing Between Bolt Shearing and Plate Bearing Failure Modes in Steel Lap Joint

Provided that the width, or edge distances, of the connected plates are large enough, net section failure in a shear joint may disregarded. The two graphs of **Figure 4.5** and **Figure 4.8** are combined into one plot to distinguish between the plate bearing failure and bolt shearing failure. In this plot (**Figure 4.9**) the vertical axis represents the ultimate load capacity whereas the horizontal axis represents the ratio between the unrestrained plate thickness (t_2) and the constant fixed plate thickness (t_1) of 10 mm (**Figure 4.10**). The green line represents the failure history of lap joints with varied plate thicknesses. This line starts with ductile bearing plate failure, as it is parallel to the single plate failure in bearing (the red line), followed by bolt shear failure when it forms an almost straight horizontal line above 8 mm thickness. Additionally, observation of the stress contours for the lap joints with a free plate thickness (t_2) of 8 mm and upward confirms bolt shear failure. Therefore, the 8 mm plate thickness (t_2) forms the turning point between a plate bearing failure and a bolt shearing failure in this type of lap joint, assembled of two S275 plates and Grade 8.8 high strength bolts. The bolt diameter also has it is own effect in this phenomenon, as its radius is then equal to the connected plate thickness and shear failure becomes dominant.

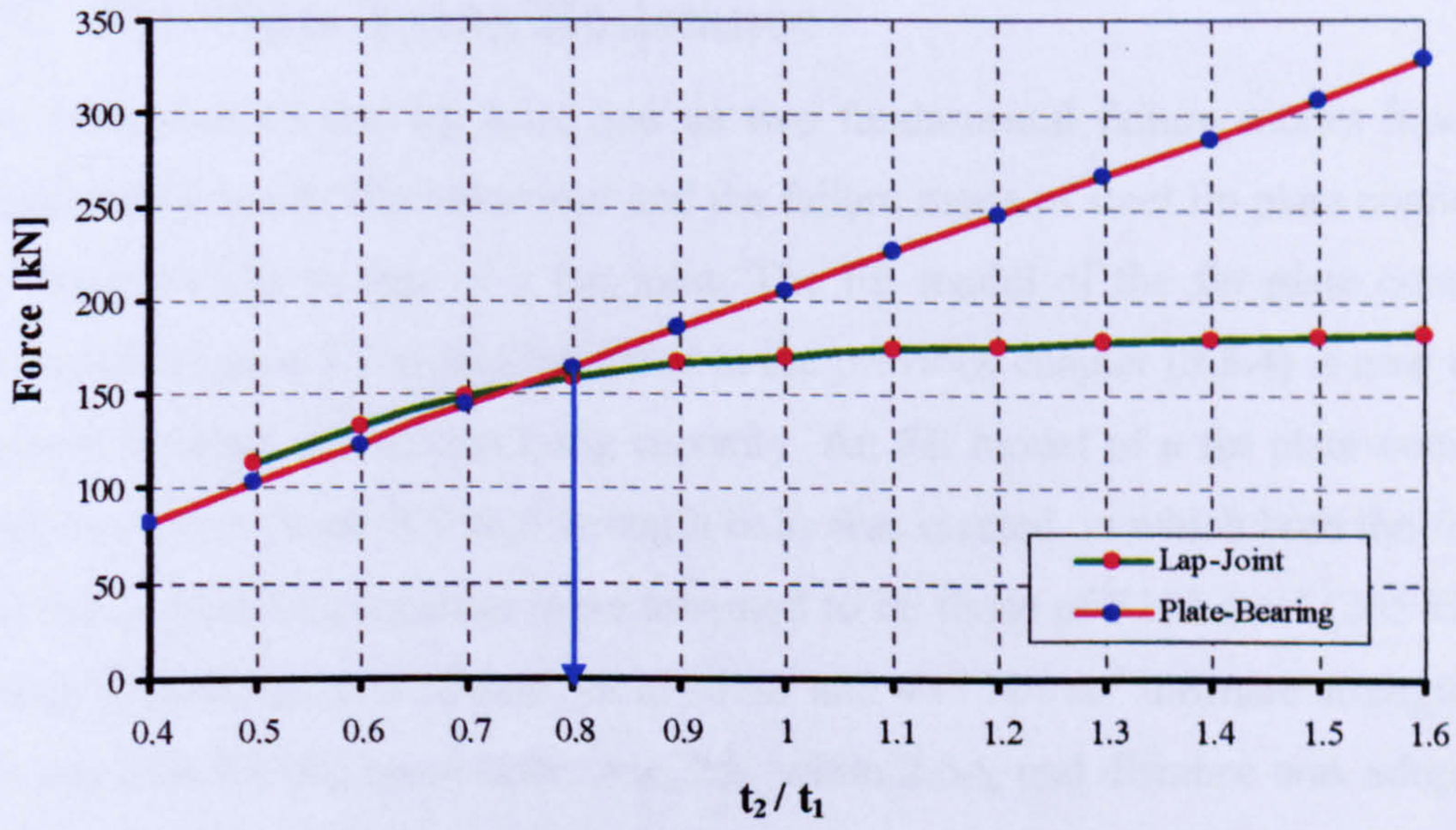

Figure 4.9 Comparisons between plate bearing failure and lap Joint failure

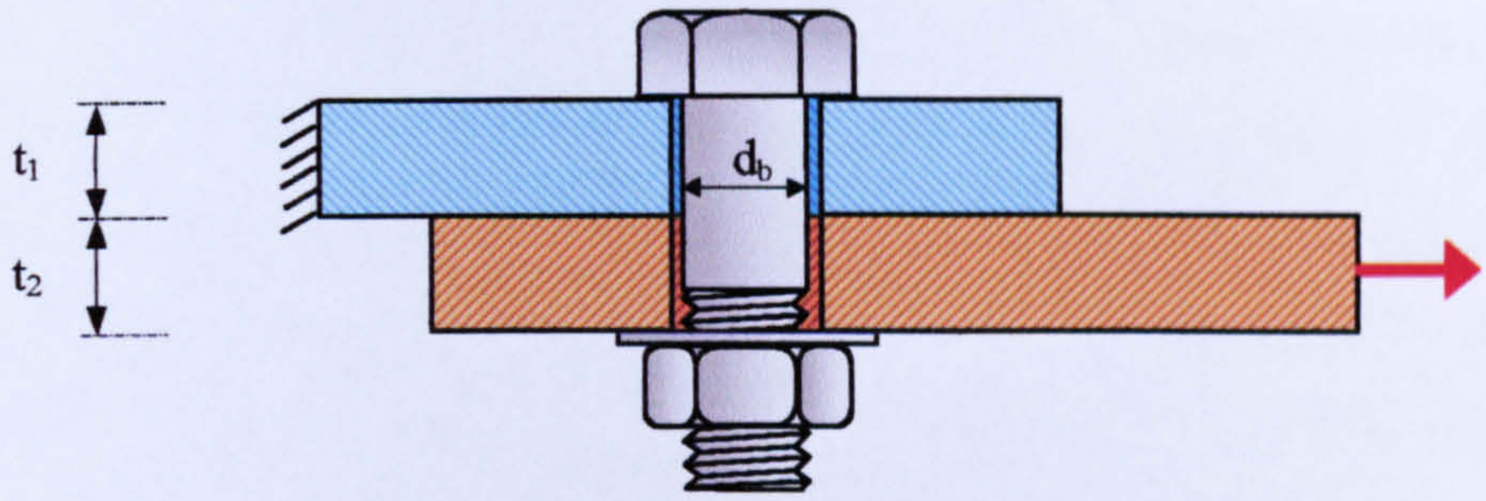

Figure 4.10 Bolt geometrical properties (including washer)

Following these observations, it is possible to predict the two crucial failure modes of this steel lap joint, plate bearing and bolt single shear failure, through the following geometric combination:

$$\text{Plate bearing failure mode} \begin{cases} t_1 \geq 0.5 d_b \\ \text{and} \\ t_2 \leq 0.4 d_b \end{cases} \quad \text{or} \quad \begin{cases} t_1 \leq 0.4 d_b \\ \text{and} \\ t_2 \geq 0.5 d_b \end{cases}$$

$$\text{Bolt shear failure mode} \begin{cases} t_1 \geq 0.4 d_b \\ \text{and} \\ t_2 \geq 0.4 d_b \end{cases}$$

4.5. Fin Plate Tying Resistance

The behaviour of this lap joint and its two fundamental failure modes have been illustrated in detail. The behaviour and the failure mode of steel fin plate connections are fairly similar to that of a lap joint. The FE model of the fin plate connection presented (**Figure 3.7-c**) and validated in the previous chapter (**3.5.4**) is now used to explore fin plate connection tying capacity. An FE model of a fin plate connection using two M20 Grade 8.8 high strength bolts was created, in which both the fin plate and beam material properties were assumed to be those of S275 steel (205 kN/mm^2 Young's modulus, 275 N/mm^2 yield stress and 445 N/mm^2 ultimate strength). The end distance for the beam holes was $2d_b$, while $2.5d_b$ end distance was adopted for the fin plate holes. Only a short beam length was considered in the FE model which has been divided into four regions in addition to the top and bottom flanges (**Figure 4.11**). The influence of these parts on the connection's tying capacity was

investigated. Firstly an FE model of a complete beam section was considered, and displacement boundary conditions were applied horizontally to its free edge (**Figure 4.12**). The next step of this investigation was removing the top and bottom flange to study their effect on the tying capacity (**Figure 4.13**). Similarly, combinations of 2-3 (**Figure 4.14**), 1-2 (**Figure 4.15**) and 1-2-4 (**Figure 4.16**) were modelled and lastly region 2 (**Figure 4.17**) was considered individually. The tying force was studied against beam horizontal movement and this is plotted in **Figure 4.18** for each studied combination.

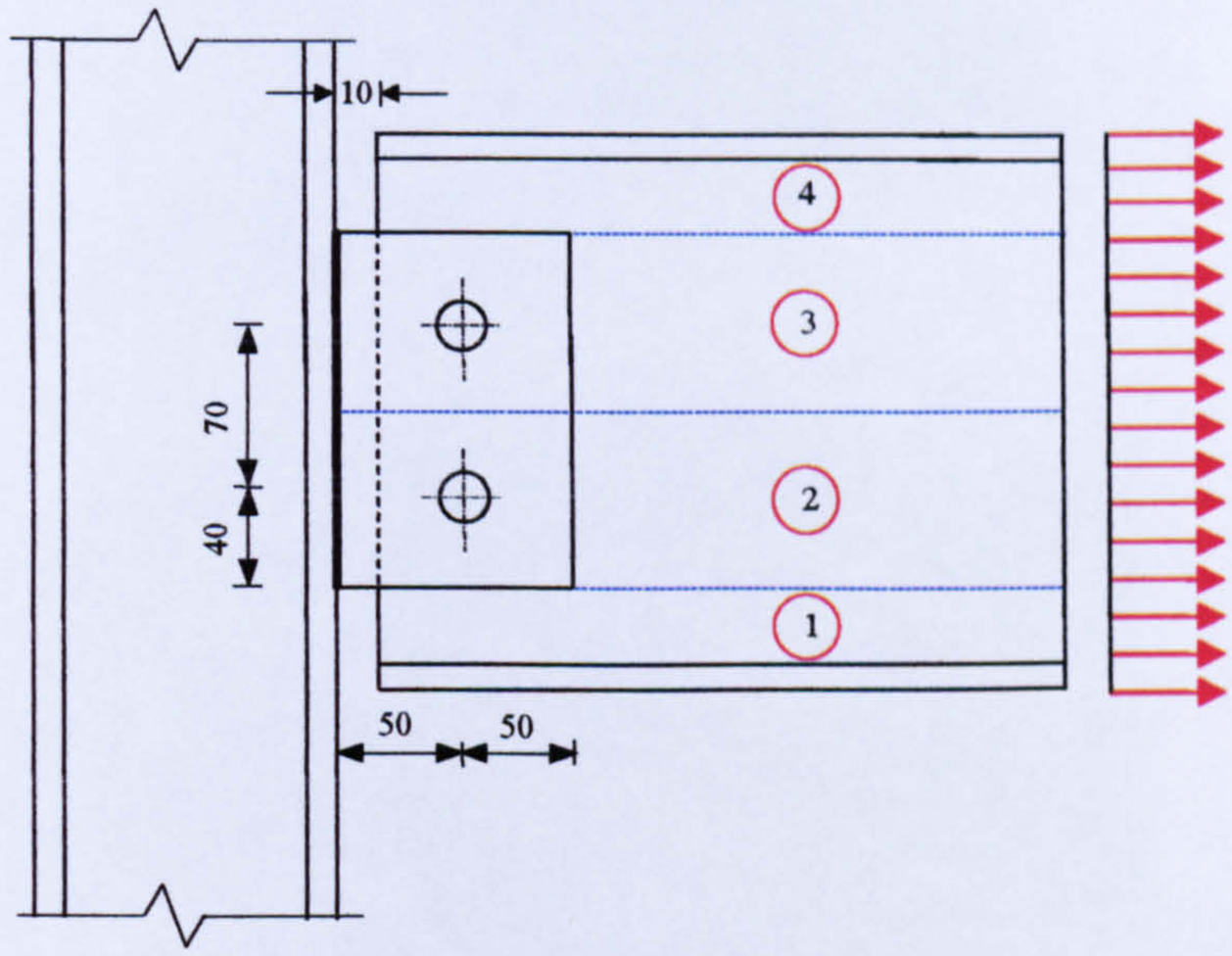

Figure 4.11 Geometrical details of 2-bolt fin plate connection (Note: dimension are shown in mm)

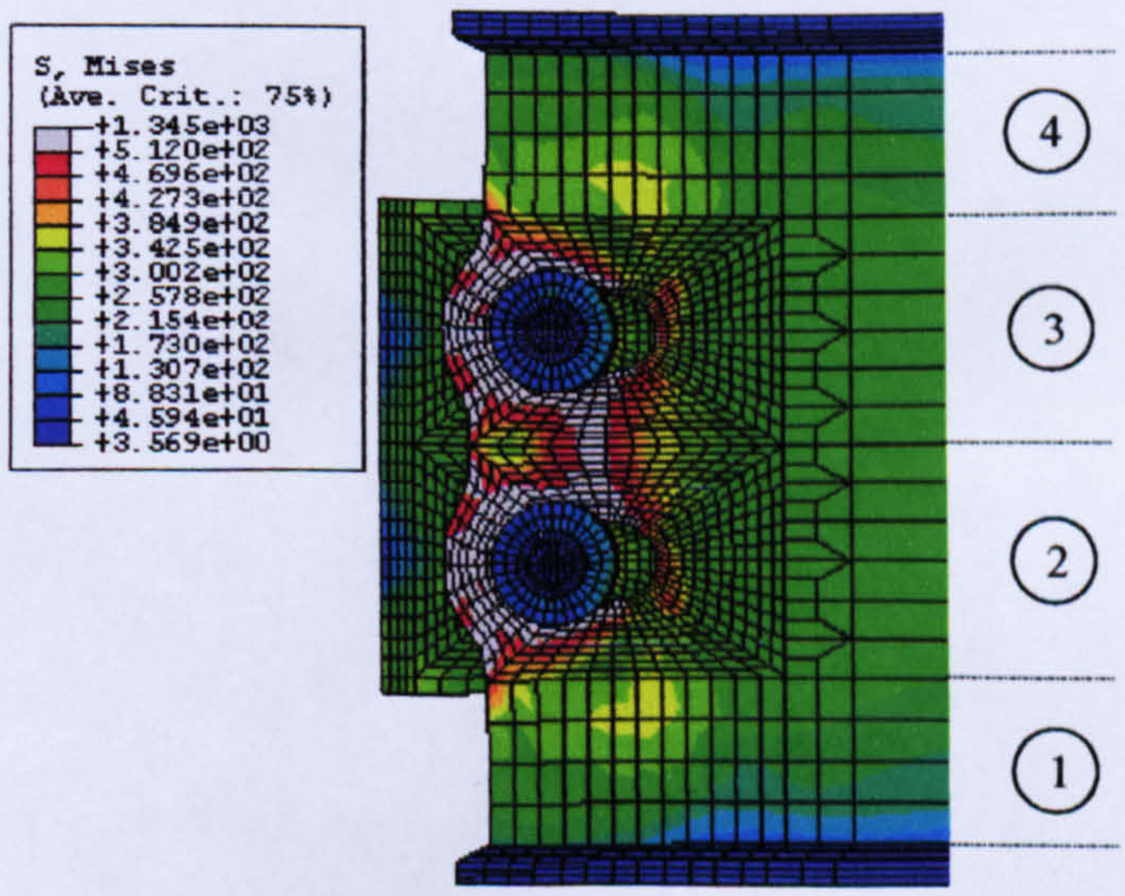

Figure 4.12 FEM of 2-bolt fin plate connection

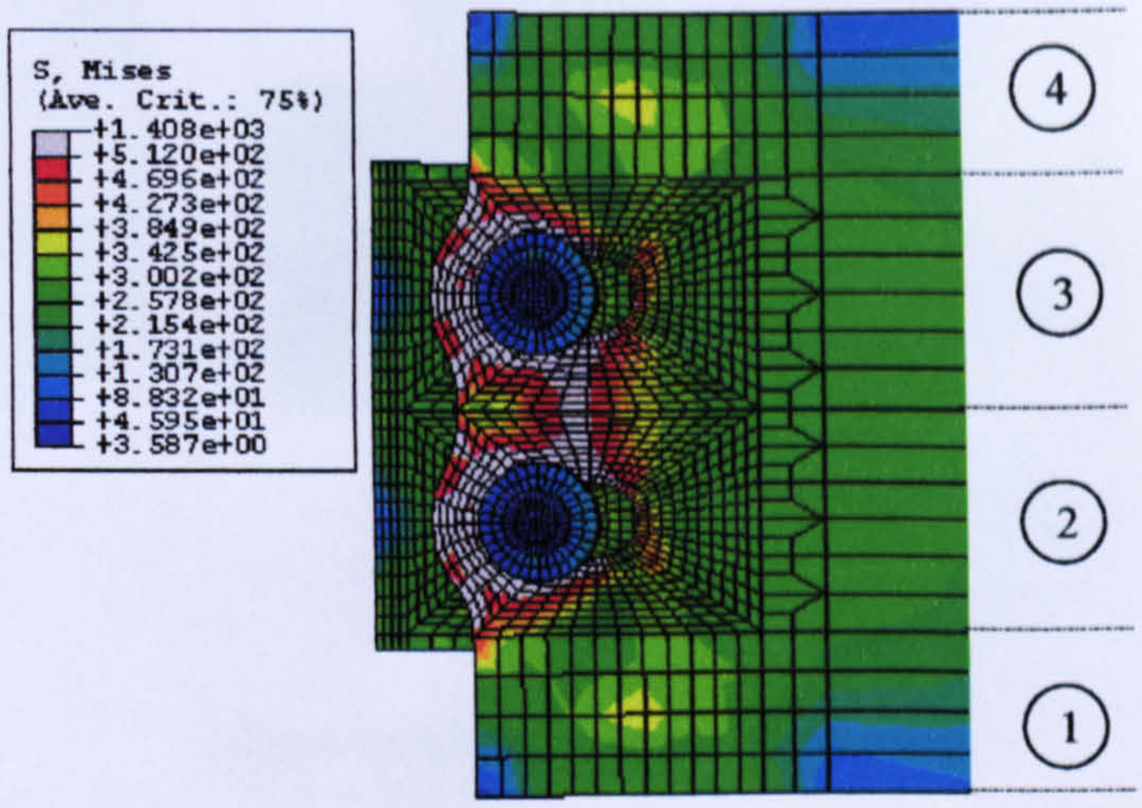

Figure 4.13 FEM of 2-bolt fin plate connection with beam flanges excluded

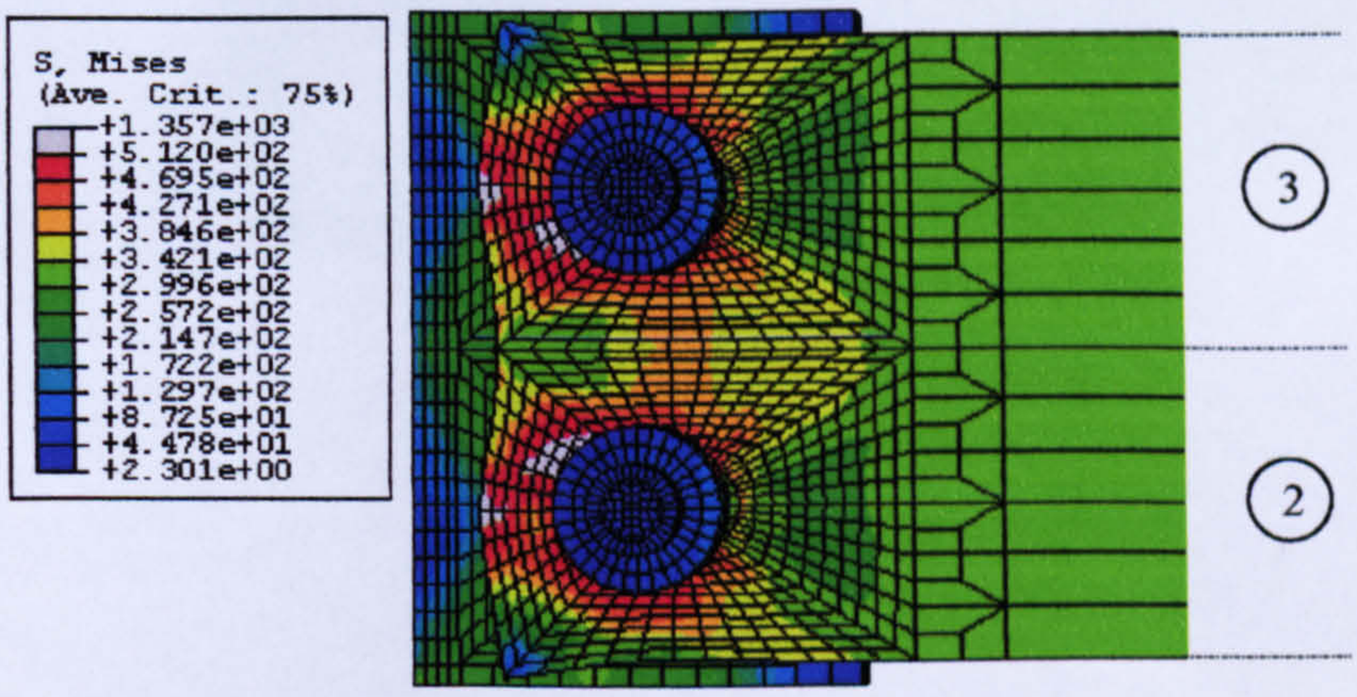

Figure 4.14 FEM of 2-bolt fin plate connection using only regions 2 and 3

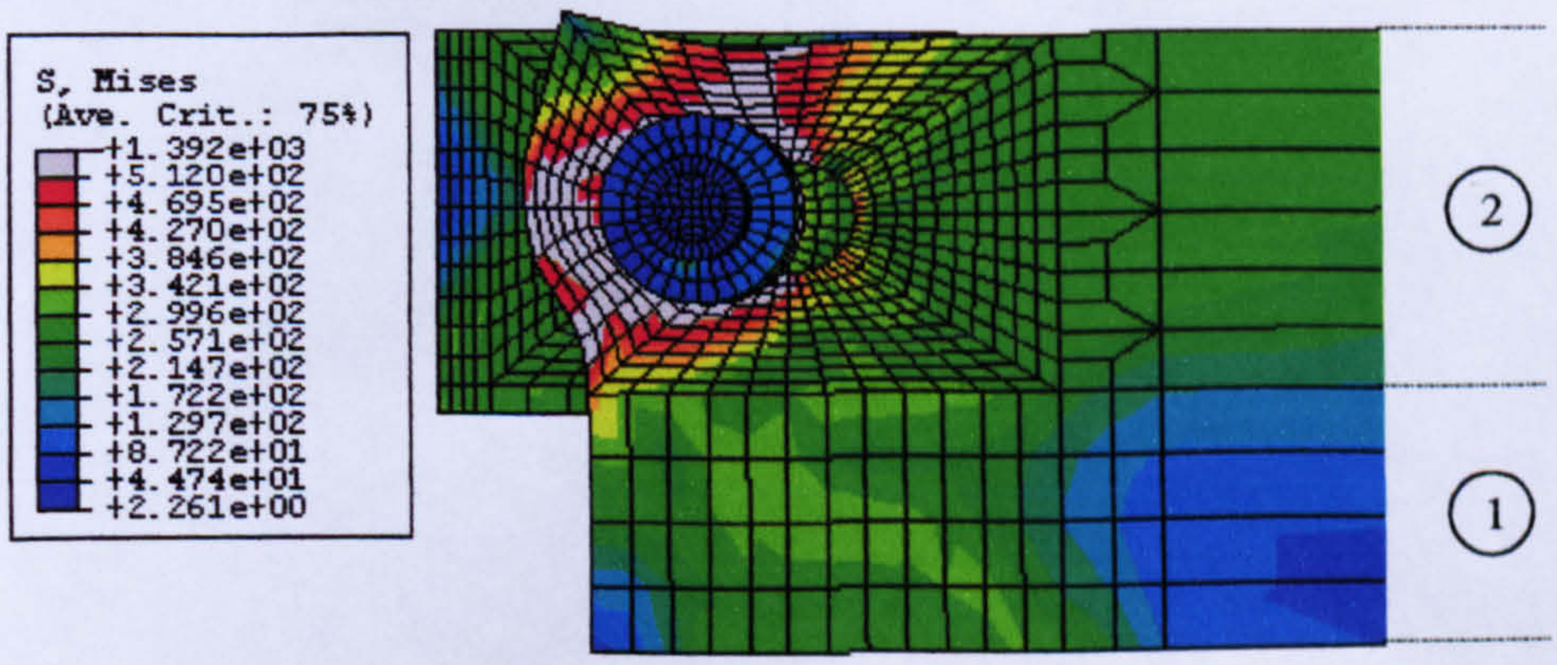

Figure 4.15 FEM of regions 1 and 2

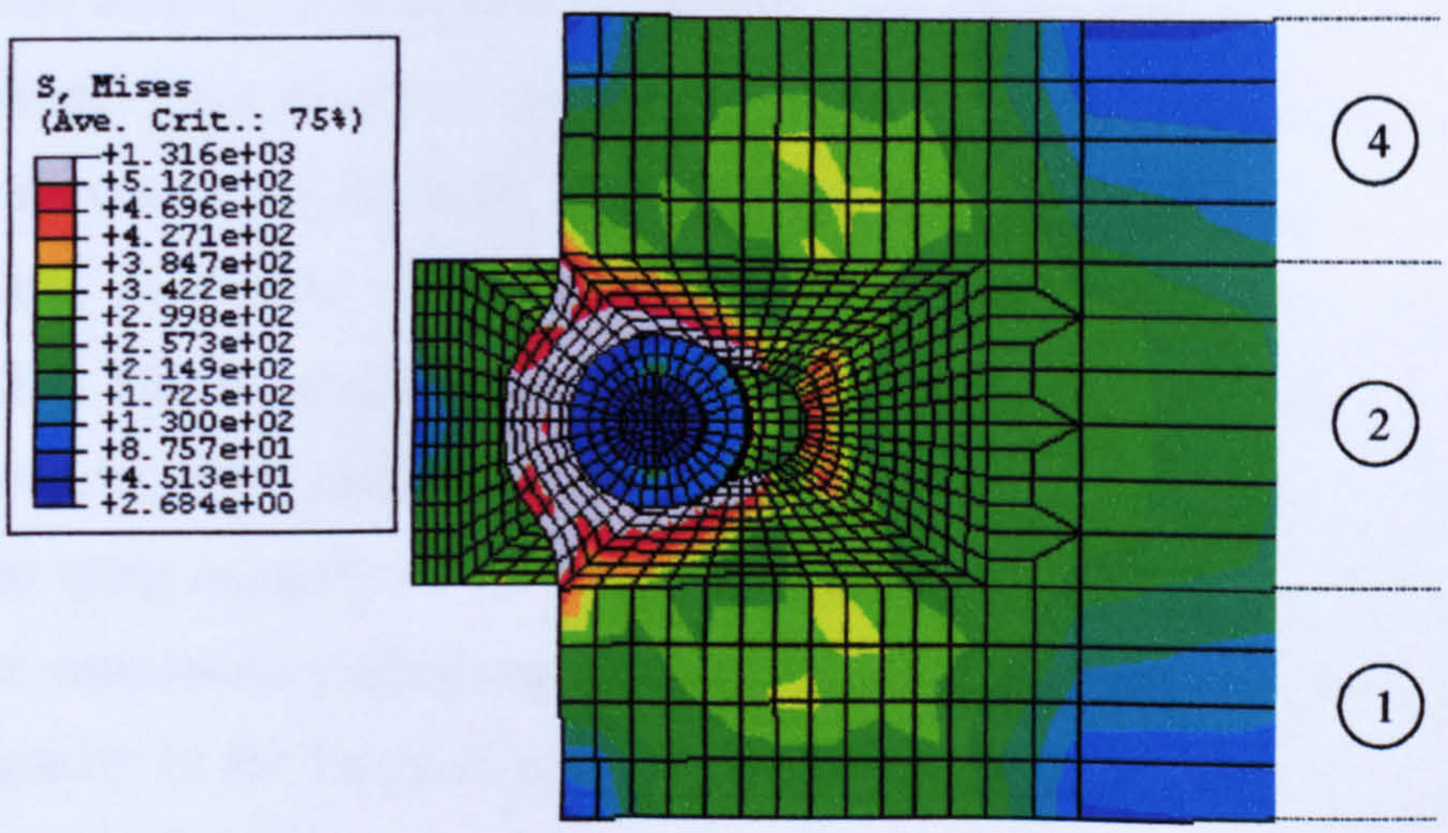

Figure 4.16 FEM of regions 1, 2 and 4

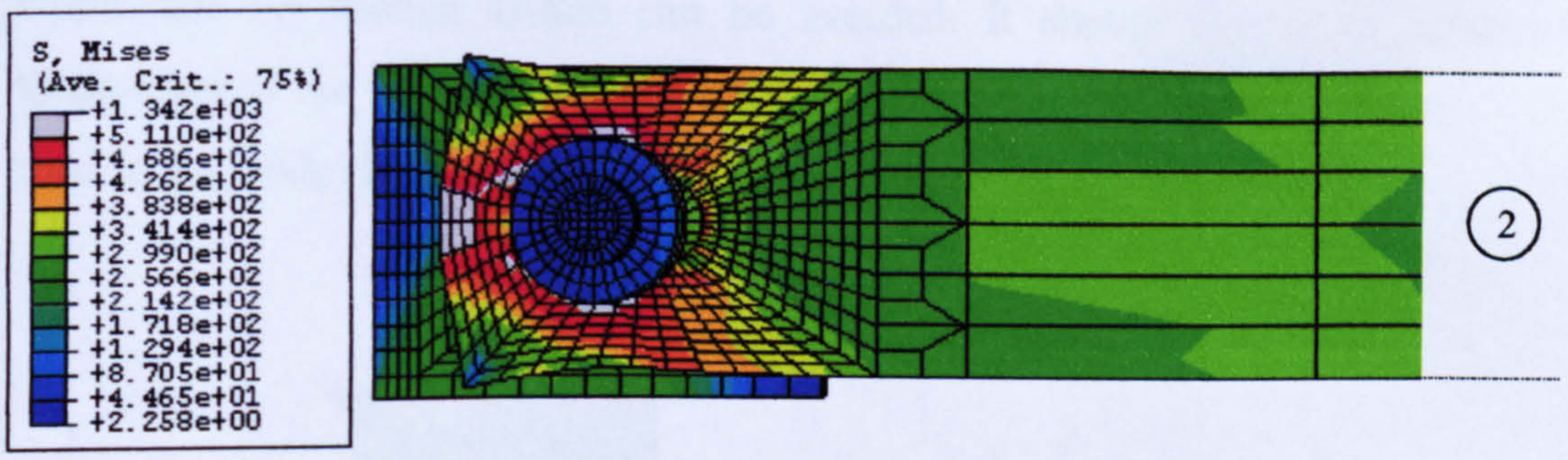

Figure 4.17 FEM of region 2

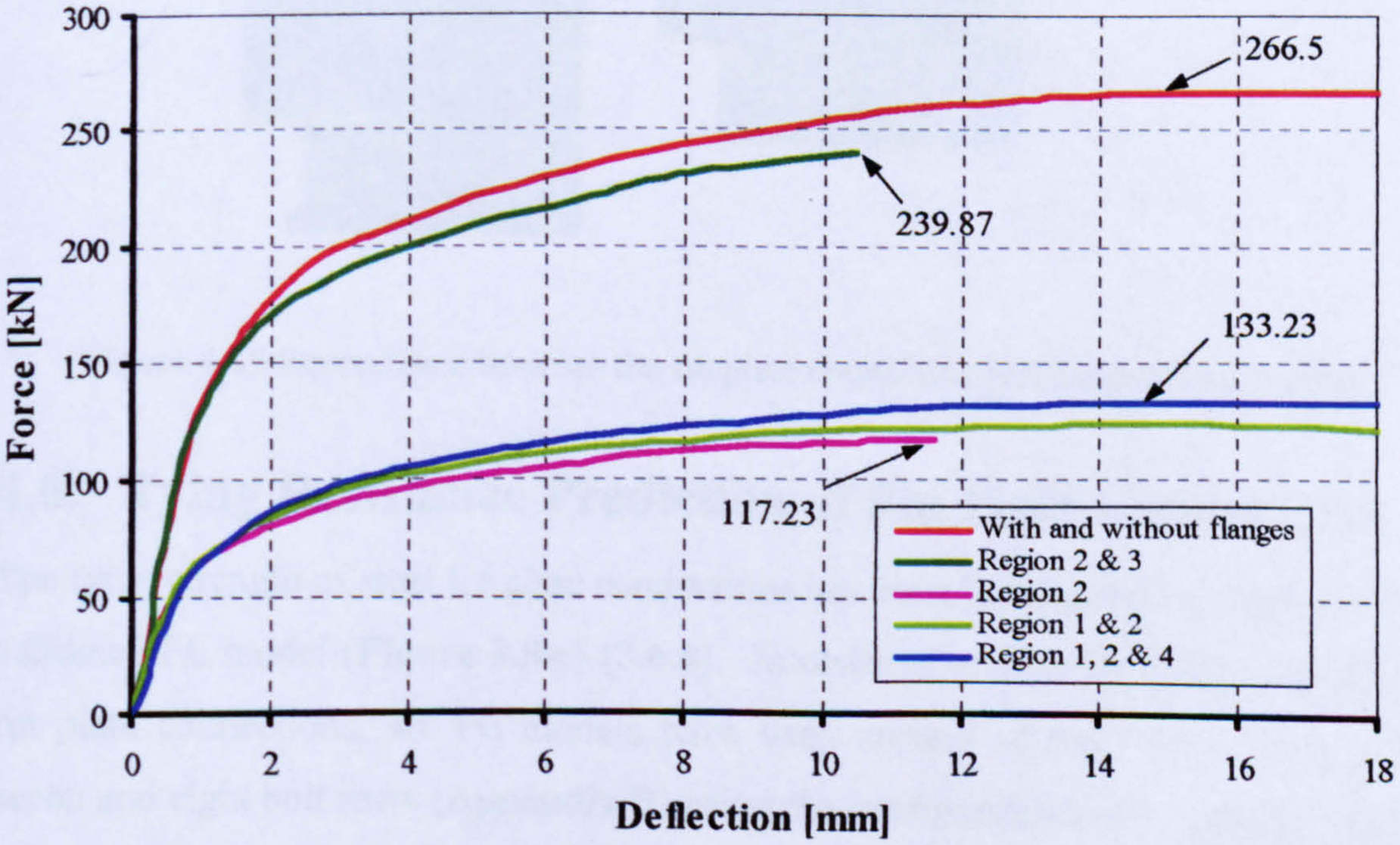

Figure 4.18 Force-deflections for various region combinations for 2-bolt fin plate connection

Out of this detailed investigation some important observation can be highlighted. The beam flanges have no effect on the connection tying force capacity as is clear from the red curves in **Figure 4.18**. Region 2 has a tying capacity of 117 kN (**Figures 4.17, 4.18**), well below the 1-2-4 combination is tying capacity of 133 kN (**Figures 4.16, 4.18**). This is related to the difference in the net section between the two cases (**Figures 4.16, 4.17**) and the corresponding edge distance necking (**Figure 4.17**). Also, the tying capacity of the 1-2-4 combination (133 kN) represents half of the complete connection's tying capacity of 266 kN. It can be concluded that the tying force capacity of the fin plate connection can be represented by the tensile capacity of a single bolt lap joint multiplied by the number of bolt lines (in this case two) that form the fin plate connection. However, this lap joint should have sufficient plate width that net section failure can be avoided. It should also have equal plate thicknesses of the fin plate and the beam web, as well as a similar bolt type to those used in the study (**Figure 4.19**).

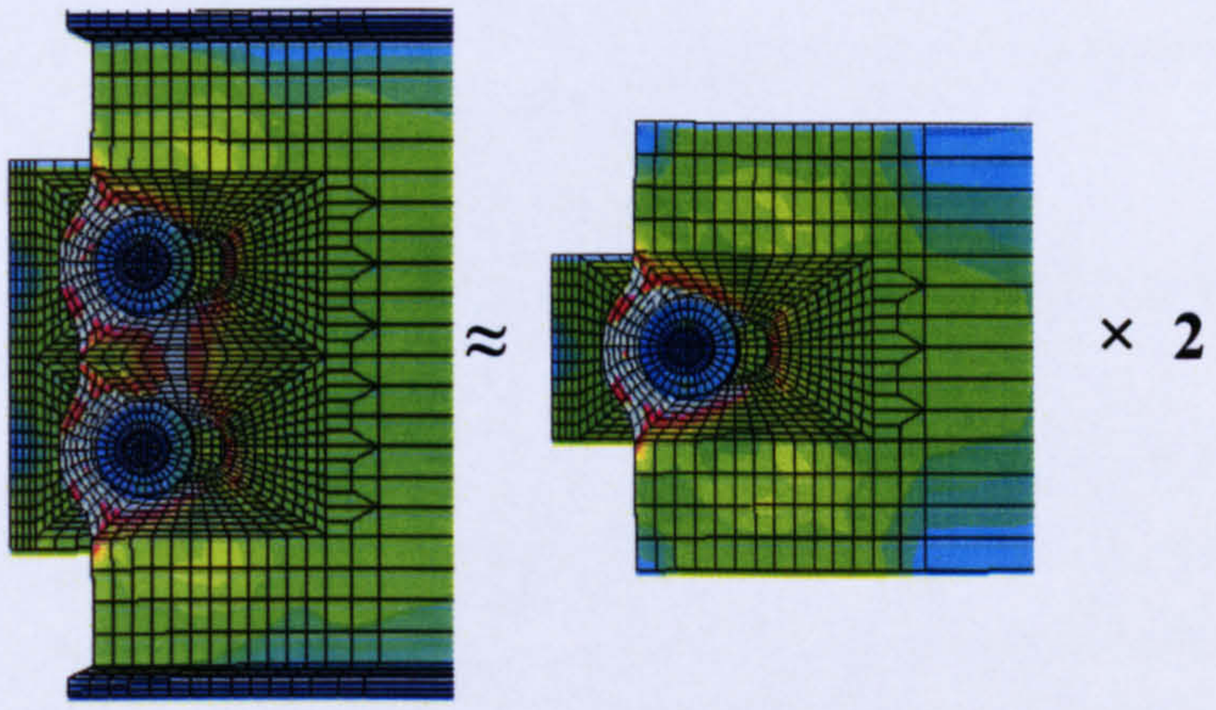

Figure 4.19 Equivalence between the fin plate connection and single-bolt lap joint

4.6. Tying Resistance Prediction of Fin Plate Connections

The tying strength of steel fin plate connections has been highlighted by means of the validated FE model (**Figure 3.8-c**) (**3.6.4**). In order to predict the tying strength of fin plate connections, six FE models have been created of two, three, four, five, seven and eight bolt rows (**Appendix B**) using the configurations shown in **Table 4.1** and studied under horizontal tying force. The tying force against beam horizontal deflection has been plotted for each connection FE model (**Figure 4.20**).

Table 4.1 Fin plate connection FE models geometrical configurations

Model No.	Beam section	No. of bolts	t_w [mm]	t_p [mm]
TY-1	UB 305×102×25	2	5.8	10
TY-2	UB 305×102×25	3	5.8	10
TY-3	UB 406×178×74	4	9.5	10
TY-4	UB 533×210×122	5	12.7	10
TY-5	UB 610×229×125	7	11.9	10
TY-6	UB 686×254×170	8	14.5	10

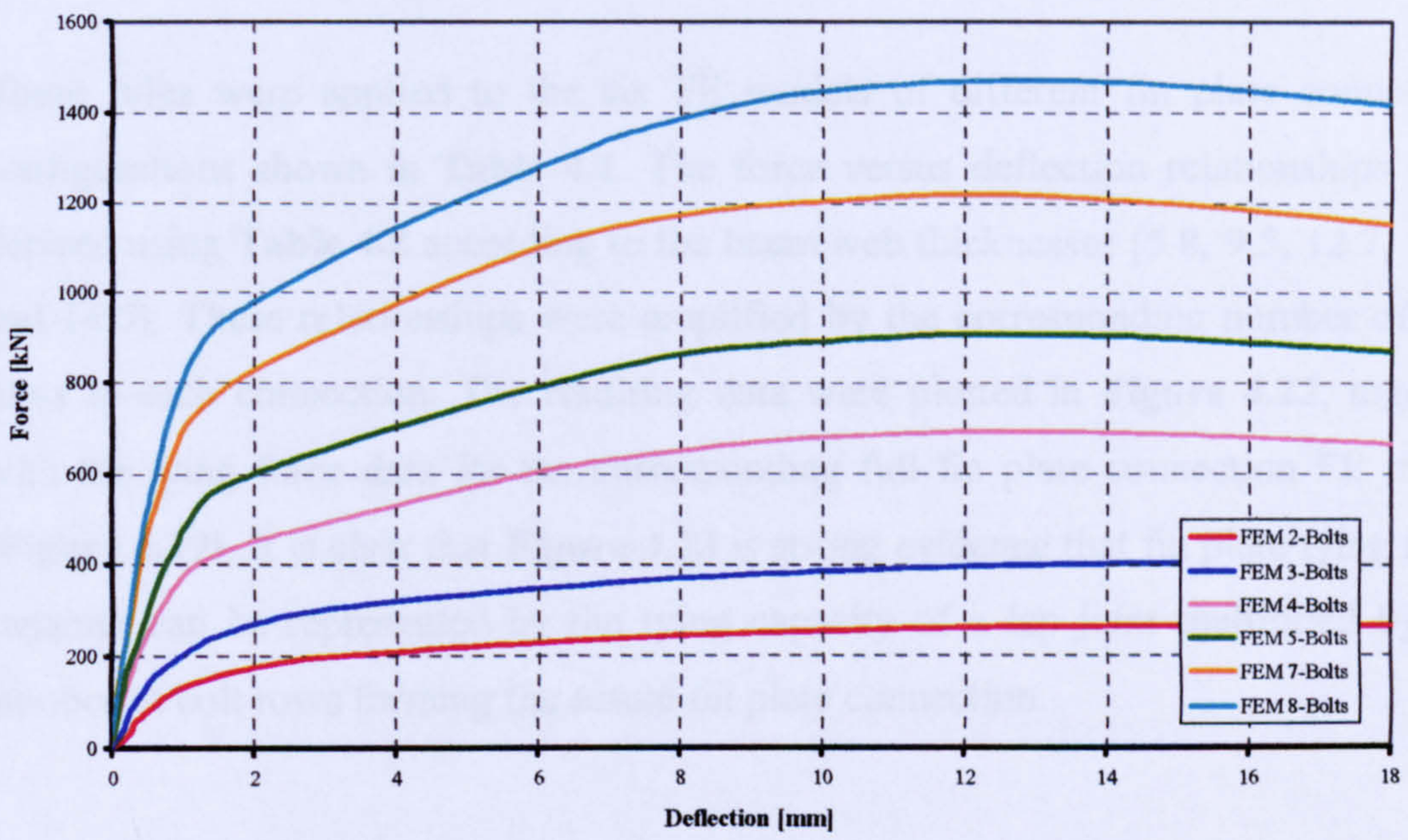

Figure 4.20 Tying force-deflection with variation of bolt numbers in fin plate connections

These relationships are some how related to the beam web thickness, as this is the main variable apart from the bolt numbers. However, it has been demonstrated previously that the tying force capacity of a fin plate connection can be predicted by using the tensile capacity of a wide single-bolt lap joint amplified by the number of bolt rows. Therefore, to extend this finding in predicting the tying resistance of fin plate connections, twelve FE models of single-bolt lap joints, similar to that shown in **Figure 4.16,** were studied. These models represent just one strip of the complete fin plate connection model with different beam web thicknesses. Two types of steel (S275 and S355) were considered for the beam and fin plate material. The beam web thickness was varied from 5mm to 16mm. The fin plate thickness was held constant at 10 mm, as was the diameter of the Grade 8.8 high-strength bolts which was 20 mm. The relationship between tying force free plate longitudinal deflection was plotted for each lap joint FE model (**Figure 4.21, 4.22**) and tabulated in **Table 4.2**

and **Table 4.3**. In order to predict the horizontal tying force capacity for any fin plate connection two steps should be followed:

i) The force should be interpolated depending on the free plate thickness (beam web thickness) using **Table 4.2** or **Table 4.3**.
ii) The load can then be multiplied by the number of bolt rows in the connection.

These rules were applied to the six FE models of different fin plate connection configurations shown in **Table 4.1**. The force versus deflection relationships were derived using **Table 4.2** according to the beam web thicknesses (5.8, 9.5, 12.7, 11.9, and 14.5). These relationships were amplified by the corresponding number of bolt rows in each connection. The resulting data were plotted in **Figure 4.23**, together with the tying force data for the corresponding full fin plate connection FE model (**Figure 4.19**). It is clear that **Figure 4.23** is strong evidence that fin plate tying force capacity can be represented by the tying capacity of a lap joint multiplied by the number of bolt rows forming the actual fin plate connection.

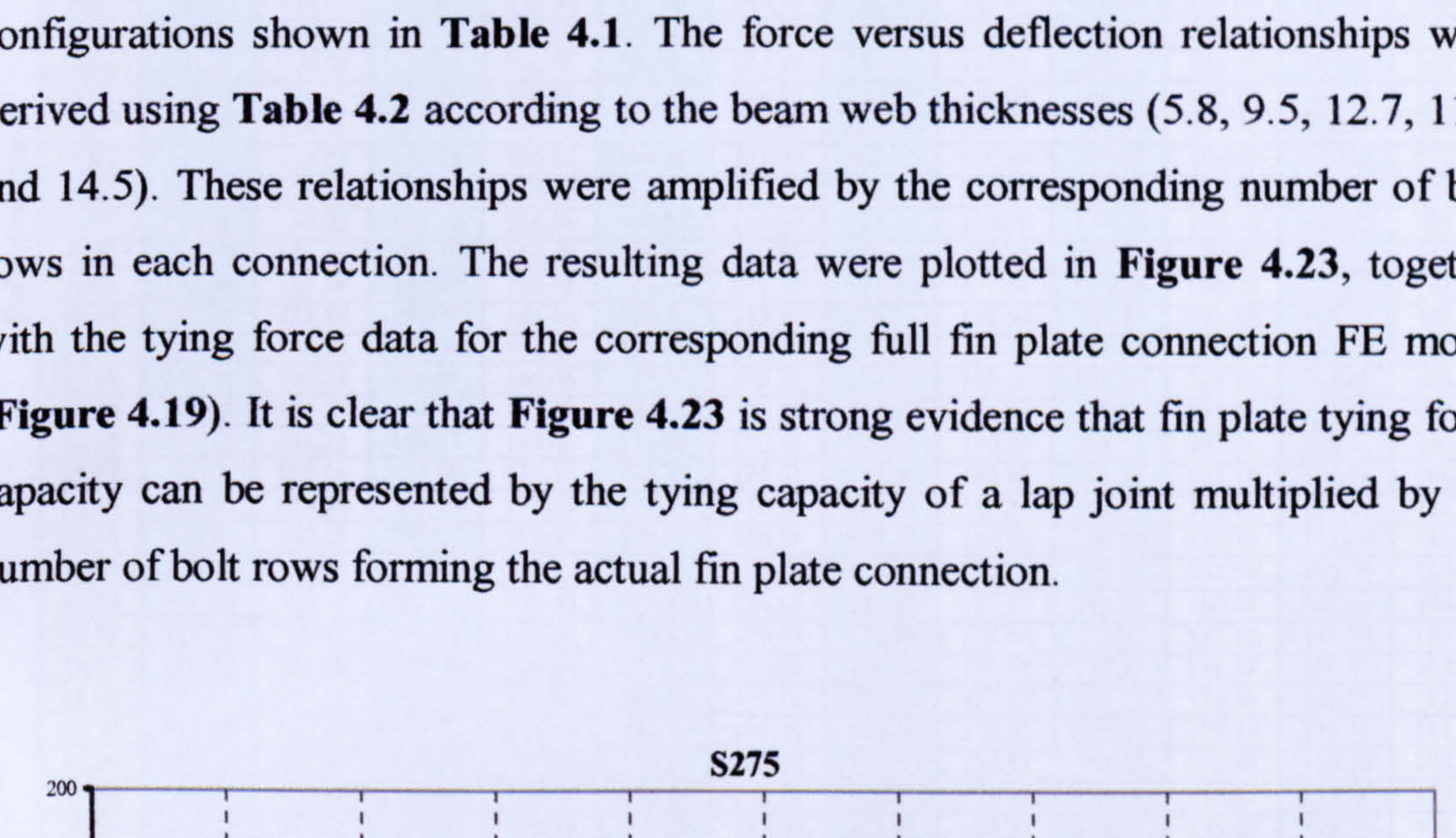

Figure 4.21 Lap joint load capacity in S275 steel

Table 4.2 Tying Resistance of S275 Steel Fin Plate Connections

10 mm Fin Plate, Varied Web Thickness and M20 8.8 Bolt

Deflection [mm] \ Beam Web Thickness [mm]	5	6	7	8	9	10	11	12	13	14	15	16
0.00	0.00	0.00	0.00	0.00	0.00	0.00	0.00	0.00	0.00	0.00	0.00	0.00
0.21	19.38	17.55	17.89	20.59	20.66	20.27	17.97	17.28	18.44	20.02	20.53	20.89
0.50	37.90	39.32	42.74	47.21	47.71	48.31	46.35	45.32	45.55	48.31	48.20	47.31
0.75	47.74	54.43	59.10	63.71	64.62	65.64	65.62	65.67	66.38	67.78	68.22	68.51
0.95	57.15	64.22	69.41	73.76	76.65	78.43	78.56	79.88	80.83	83.17	83.85	83.98
1.32	68.22	76.70	84.49	89.51	93.99	97.25	99.61	102.32	103.09	106.31	106.74	108.83
1.86	75.88	85.86	93.21	100.50	106.67	111.02	114.68	116.20	117.32	119.92	120.40	121.88
2.32	81.58	92.46	101.50	108.78	114.56	118.43	121.27	123.70	125.45	127.60	128.34	129.95
2.92	86.72	98.74	108.22	115.87	120.53	124.36	127.80	130.41	132.83	135.05	135.85	137.56
3.50	91.21	103.81	112.97	120.42	125.77	130.18	133.65	136.64	139.22	141.60	142.37	143.57
4.00	94.78	108.10	117.72	124.98	130.56	135.09	138.87	141.97	144.83	147.19	147.88	149.34
4.50	97.84	112.40	121.73	129.37	135.23	140.00	143.71	147.12	150.09	152.24	152.87	154.56
5.00	100.10	115.57	125.49	133.34	139.65	144.73	148.33	151.77	154.57	156.93	158.08	159.38
5.50	102.20	118.03	128.96	137.30	143.67	148.79	152.37	155.84	159.05	161.12	162.21	163.81
6.00	104.49	120.24	132.18	140.93	147.43	152.73	156.41	159.91	162.71	165.29	166.57	167.76
6.50	106.54	122.42	135.10	144.33	151.11	156.60	160.57	163.97	166.17	168.30	169.62	171.21
7.00	108.59	124.65	137.67	147.73	154.62	159.88	164.04	167.46	169.64	171.31	173.82	174.21
7.50	109.43	126.88	140.18	150.63	158.12	163.09	167.21	170.89	172.84	174.32	176.03	177.76
8.00	110.26	128.68	142.65	153.42	161.11	166.17	170.05	172.93	175.20	176.79	178.51	179.27
8.50	111.25	130.22	145.12	156.06	164.08	168.03	172.31	174.78	176.74	178.50	179.76	180.79
9.00	111.99	131.62	147.30	158.40	166.52	169.89	173.93	176.15	178.18	179.70	181.13	182.43
9.50	112.99	132.59	149.05	160.73	168.63	171.75	175.54	177.51	179.29	180.90	183.10	183.38
10.00	113.98	133.59	150.76	163.06	170.52	173.61	176.75	178.54	180.33	181.64	183.10	184.42
10.50	114.76	134.93	152.08	164.93	171.75	174.70	177.36	179.28	181.05	182.38	184.04	185.26
11.00	115.33	136.28	153.41	166.44	172.97	175.56	177.98	180.03	181.64	183.12	184.45	185.73
11.50	115.90	137.27	154.74	167.94	174.19	176.22	178.59	180.44	181.75	183.31	184.62	186.04
12.00	116.23	138.23	156.07	169.45	174.94	176.45	179.21	180.63	181.86	183.26	184.71	186.05
12.50	116.56	138.96	157.40	170.55	175.39	176.51	179.36	180.48	181.75	183.14	184.55	186.03
13.00	116.78	139.44	158.72	171.64	175.84	176.56	179.36	180.23	181.35	182.71	184.14	185.65
13.50	116.96	140.23	159.77	172.40	176.29	176.23	178.88	179.69	180.86	182.19	183.70	185.12
14.00	117.21	140.46	160.82	173.12	176.74	175.73	178.41	179.07	180.16	181.50	183.06	184.59
14.50	117.30	140.67	161.79	173.62	177.11	174.85	177.81	178.35	179.47	180.81	182.40	184.01
15.00	117.30	140.92	162.58	174.12	176.73	174.03	176.99	177.54	178.72	180.12	181.74	183.34
15.50	117.31	141.08	163.06	174.56	176.32	173.05	176.18	176.73	177.93	179.37	180.97	182.67
16.00	117.31	141.24	163.51	174.80	175.56	171.88	175.36	175.87	177.11	178.58	180.20	181.91
16.50	117.28	141.40	163.83	174.88	174.76	170.81	174.49	175.00	176.26	177.79	179.41	181.12
17.00	117.25	141.39	164.13	174.82	173.86	169.80	173.54	174.13	175.42	176.94	178.59	180.32
17.50	117.13	141.34	164.14	174.70	172.97	168.78	172.59	173.21	174.50	175.97	177.76	179.49
18.00	117.02	141.26	164.13	174.51	172.03	167.50	171.65	172.23	173.56	175.06	176.85	178.64

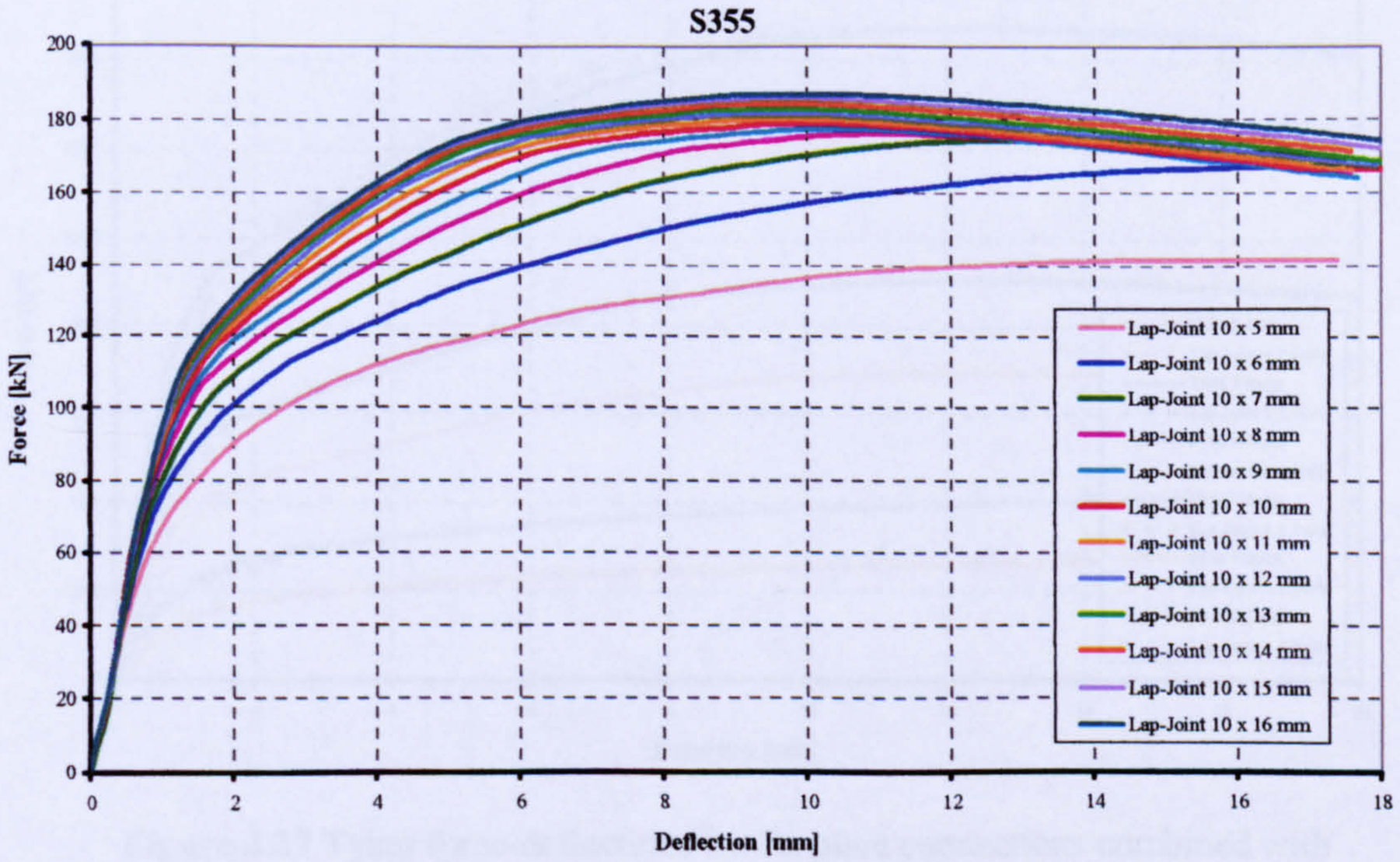

Figure 4.22 Lap joint load capacity in S355 steel

Table 4.3 Tying Resistance of S355 Steel Fin Plate Connections

10 mm Fin Plate, Varied Web Thickness and M20 8.8 Bolt

Deflection [mm] \ Beam Web Thickness [mm]	5	6	7	8	9	10	11	12	13	14	15	16
0.00	0.00	0.00	0.00	0.00	0.00	0.00	0.00	0.00	0.00	0.00	0.00	0.00
0.21	20.54	21.46	18.79	21.32	21.07	20.82	21.30	21.28	20.81	21.65	21.53	22.32
0.50	42.03	45.18	47.28	51.56	52.92	52.47	50.92	50.67	50.88	50.64	50.56	50.58
0.75	56.81	63.26	67.02	71.32	72.91	74.14	75.47	73.10	75.61	74.60	74.79	74.70
0.95	67.09	75.82	79.89	84.82	87.32	88.87	90.45	90.81	92.55	93.51	92.42	94.48
1.32	80.11	90.56	97.63	104.01	106.68	110.12	111.84	111.91	114.49	116.36	117.75	118.05
1.86	89.90	100.75	108.37	113.98	118.09	121.15	122.99	124.46	126.19	127.85	129.09	130.40
2.32	97.33	108.54	116.12	121.65	126.04	129.69	132.21	134.45	136.58	137.71	138.94	140.16
2.92	103.28	114.65	122.28	128.44	133.02	137.16	140.20	142.99	145.26	145.97	147.68	148.81
3.50	108.08	119.64	128.02	134.68	139.94	144.34	148.07	150.60	152.62	153.95	155.46	156.11
4.00	111.79	124.12	133.41	140.53	146.03	150.23	154.46	157.12	159.10	159.84	162.06	162.49
4.50	115.17	128.60	138.23	146.04	151.96	156.13	160.05	163.02	164.65	165.72	167.71	168.17
5.00	117.73	132.83	142.68	150.90	156.83	161.32	165.04	167.20	169.27	171.12	172.00	173.27
5.50	120.30	136.28	147.09	155.32	161.40	165.45	169.30	170.84	173.38	174.82	175.29	176.37
6.00	122.99	139.31	150.91	159.26	164.96	169.57	172.03	174.39	175.52	177.20	178.15	179.41
6.50	125.59	142.21	154.29	162.90	168.51	171.95	174.51	176.32	177.65	179.11	179.71	181.02
7.00	127.64	144.89	157.68	165.55	171.08	173.72	175.86	177.63	179.04	180.32	181.27	182.60
7.50	129.27	147.55	160.63	168.19	172.74	175.48	177.22	178.93	180.14	181.30	182.59	183.77
8.00	130.73	150.18	163.04	170.83	174.41	176.62	178.23	179.78	181.01	182.26	183.89	184.88
8.50	132.20	152.37	165.44	172.32	175.24	177.40	179.01	180.59	182.07	183.22	184.51	185.81
9.00	133.72	154.10	167.22	173.46	176.07	178.01	179.70	181.05	182.50	183.81	185.24	186.59
9.50	135.25	155.74	168.60	174.47	176.82	178.72	179.95	181.29	182.62	183.98	185.40	186.78
10.00	136.39	157.28	169.98	175.47	177.29	178.85	179.82	181.16	182.60	184.00	185.37	186.77
10.50	137.51	158.82	171.36	175.90	177.33	178.66	179.48	180.83	182.27	183.68	185.11	186.68
11.00	138.28	160.06	172.56	176.06	177.26	178.16	179.00	180.31	181.72	183.22	184.78	186.42
11.50	139.06	161.27	173.33	175.96	176.78	177.67	178.38	179.74	181.10	182.75	184.20	185.91
12.00	139.58	162.49	174.04	175.58	176.20	176.84	177.72	178.98	180.46	182.03	183.52	185.32
12.50	140.11	163.61	174.34	174.88	175.28	175.95	176.98	178.21	179.61	181.31	182.84	184.63
13.00	140.59	164.40	174.43	174.18	174.30	175.06	176.00	177.35	178.75	180.40	182.04	183.89
13.50	140.99	165.03	174.34	173.48	173.34	174.15	175.05	176.44	177.89	179.50	181.21	183.12
14.00	141.29	165.65	174.03	172.64	172.38	173.22	174.12	175.52	176.99	178.64	180.36	182.27
14.50	141.39	166.15	173.56	171.80	171.42	172.11	173.17	174.59	176.06	177.79	179.51	181.46
15.00	141.49	166.65	173.01	170.82	170.38	171.11	172.19	173.59	175.08	176.81	178.60	180.57
15.50	141.50	167.14	172.33	169.81	169.20	170.11	171.04	172.57	174.04	175.81	177.62	179.59
16.00	141.49	167.03	171.44	168.68	168.21	168.96	169.94	171.41	173.09	174.80	176.61	178.54
16.50	141.47	167.22	170.63	167.48	167.06	167.82	168.87	170.28	172.02	173.71	175.64	177.47
17.00	141.44	167.35	169.62	166.43	165.67	166.65	167.61	169.15	170.86	172.55	174.49	176.54
17.50	141.44	167.33	168.59	165.28	164.71	165.42	166.50	168.03	169.64	171.52	173.33	175.36
18.00	141.43	167.32	167.61	164.82	163.50	164.02	165.58	167.06	168.53	170.32	171.97	174.21

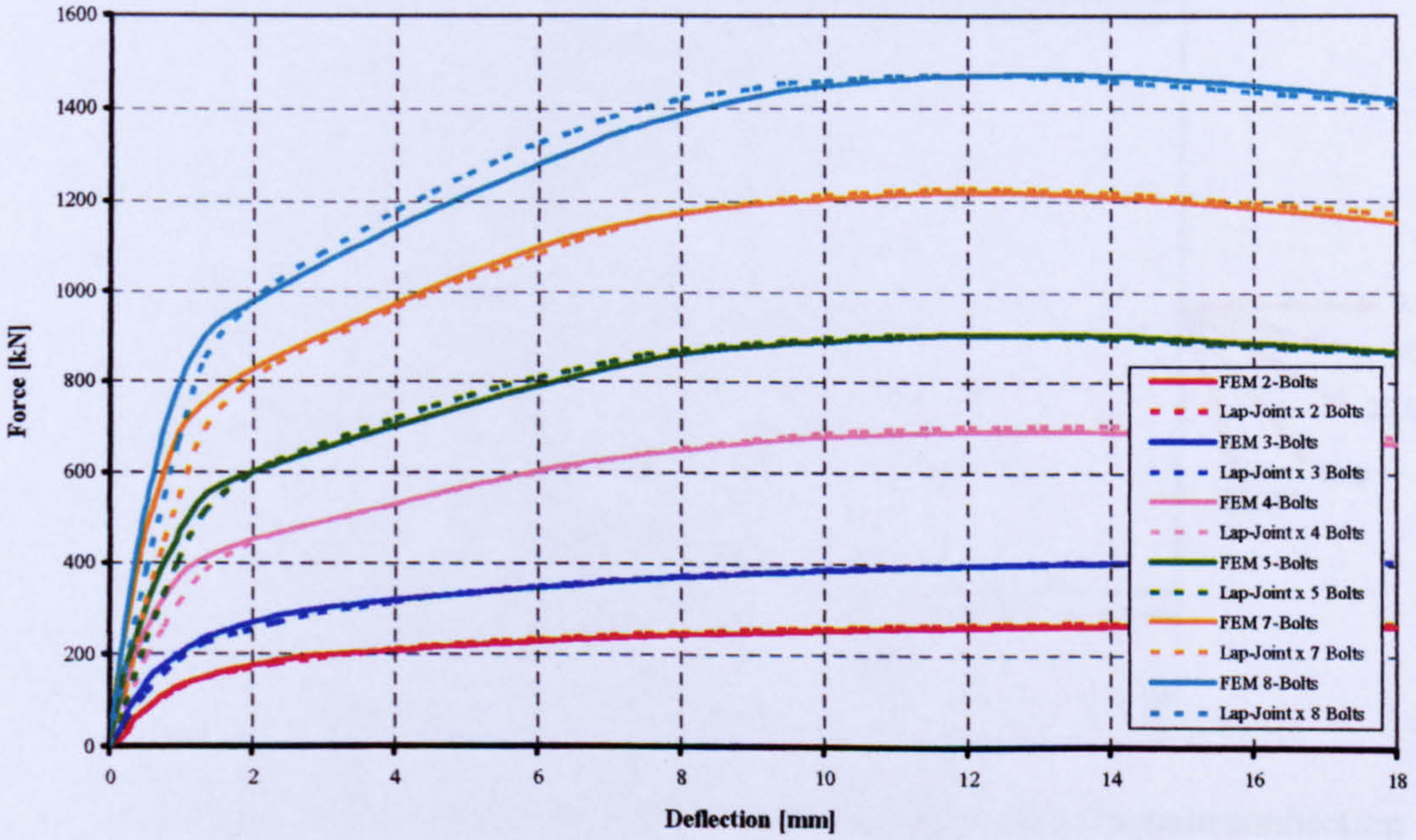

Figure 4.23 Tying force-deflections for fin plate connections combined with corresponding lap joint response amplified by the bolt number

corresponding lap joint response amplified by the bolt number

4.7. Inclined Tying Force

Horizontal tying forces have been investigated fully, but it is rare in real structural behaviour that horizontal forces are applied. Most often tying forces are applied at an angle, as a result of either large mid-span deflections or the loss of a supporting member between two beams (**Figure 4.1**). Therefore, it is necessary to investigate the influence of the force angle on tying force capacity. For this purpose, the FE model TY-2 (**Table-1**) of the 3-bolt fin plate connection with a 480 mm length beam was analysed under different inclinations of tying force applied at the free beam end (**Figure 4.24, 4.25**).

The resultant force was plotted against the resultant deflection of the beam web (**Figure 4.26**). The main finding is that the angle of the tying force does not have a strong influence on the connection is tying force capacity. When a completely vertical movement is applied to the beam, such that the whole beam end moves downward, the horizontal tying capacity was equal to the vertical reaction capacity (**Figure 4.27**).

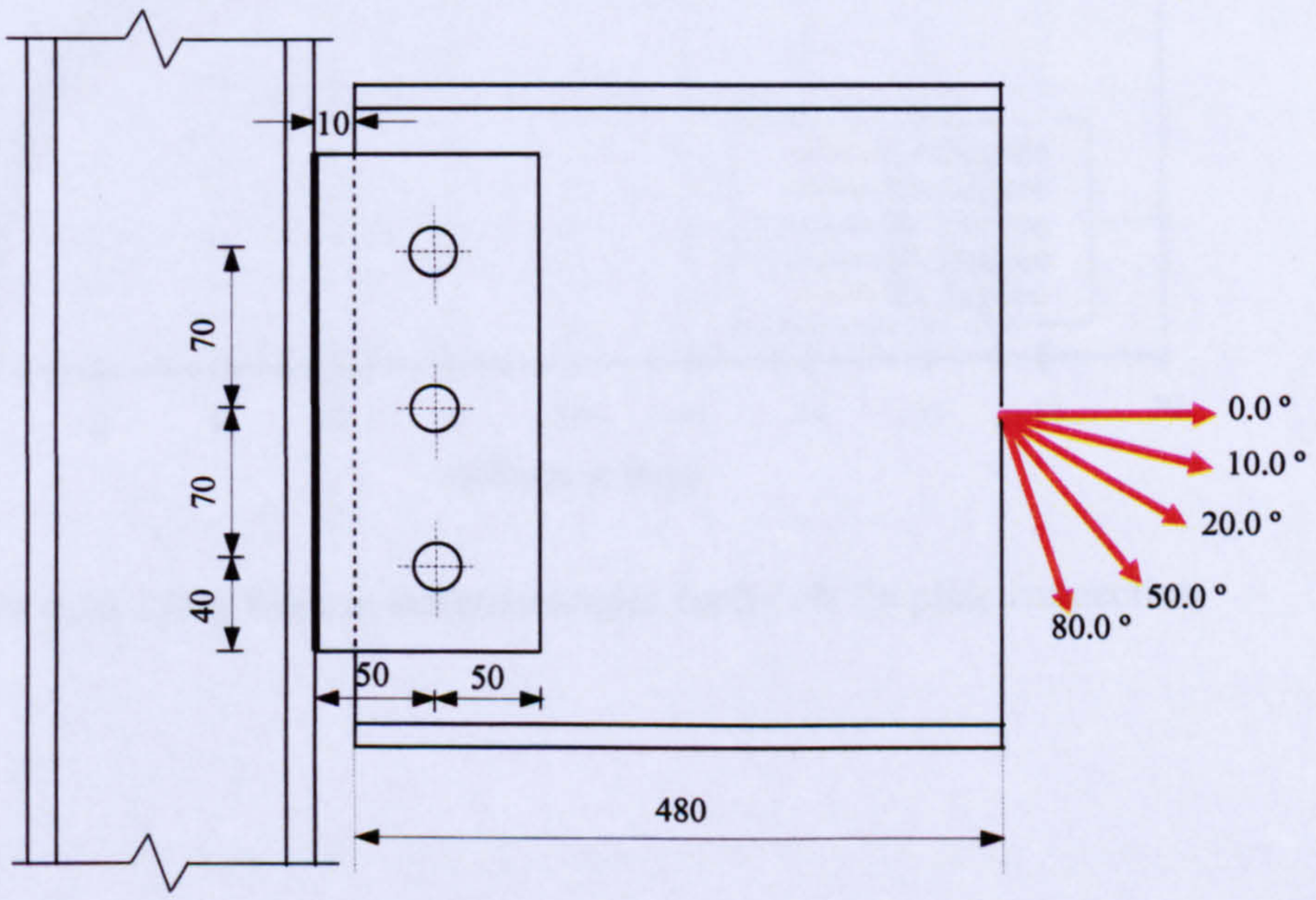

Figure 4.24 Tying force applied in different angles on a fin plate connection

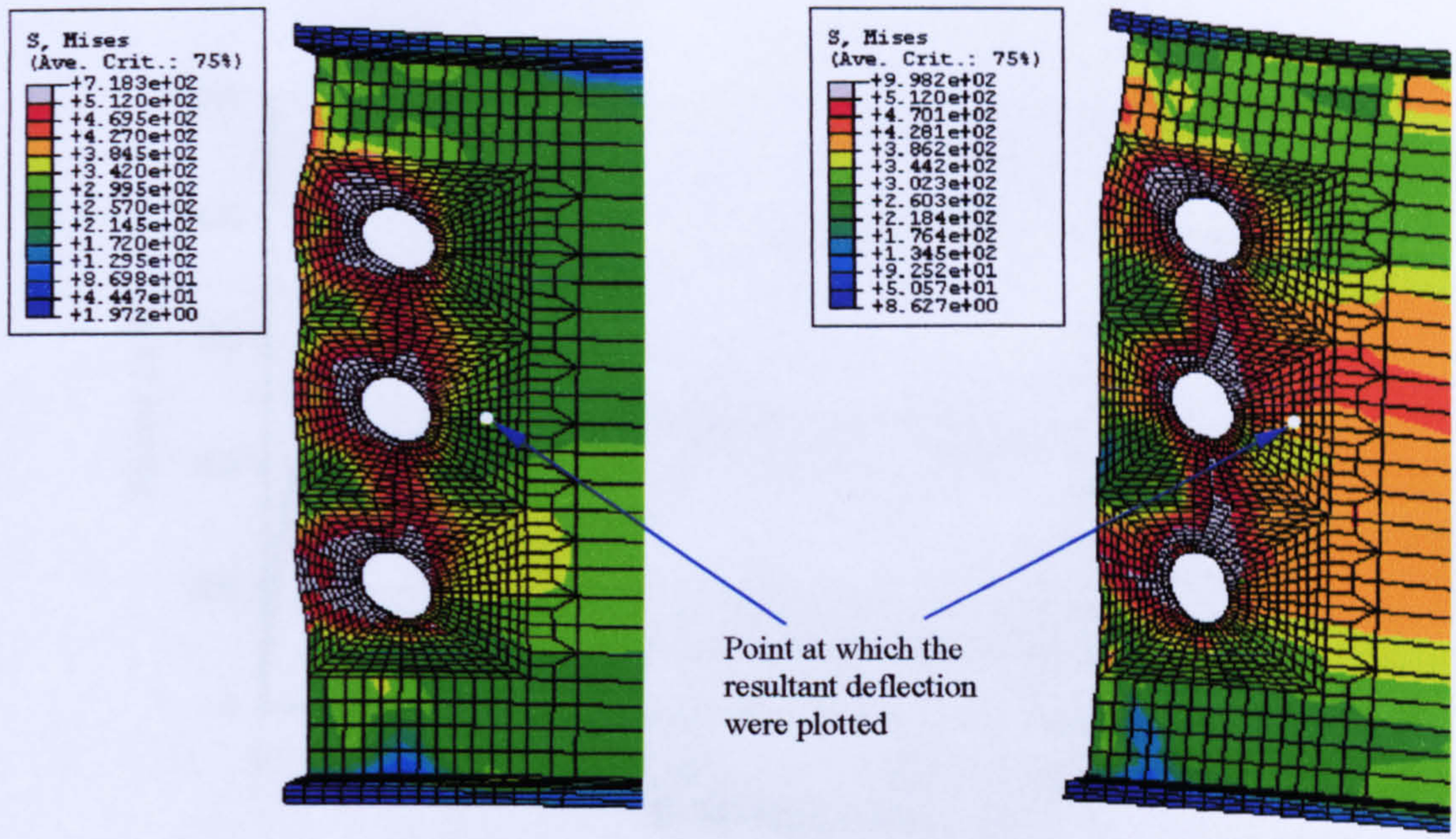

a) 50 Degree **b**) 80 Degree

Figure 4.25 Von Mises stresses contours for 3-bolt joint under tying force applied at **a**) 50° and **b**) 80°

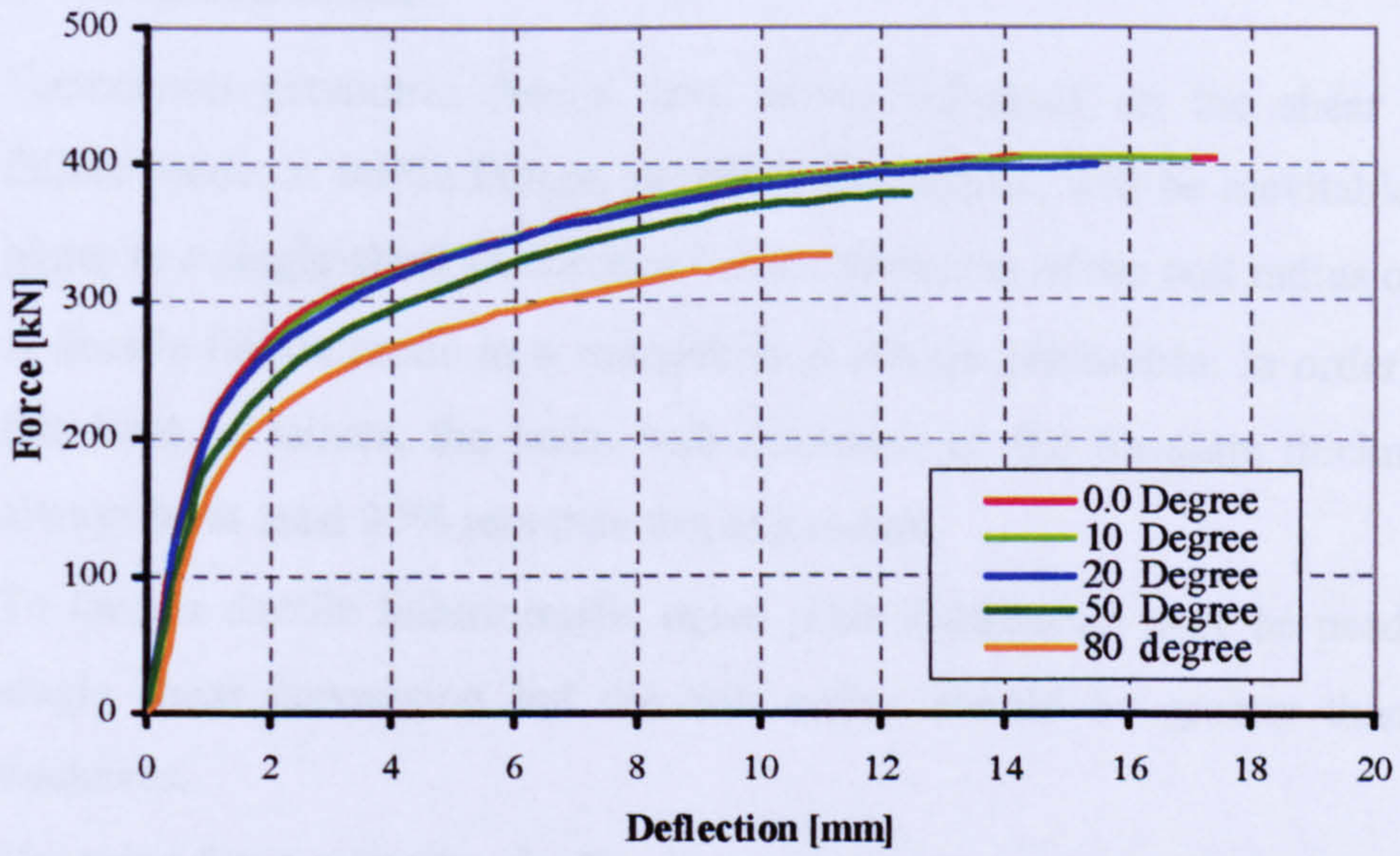

Figure 4.26 Tying force at different angles for 3-bolt fin plate connection

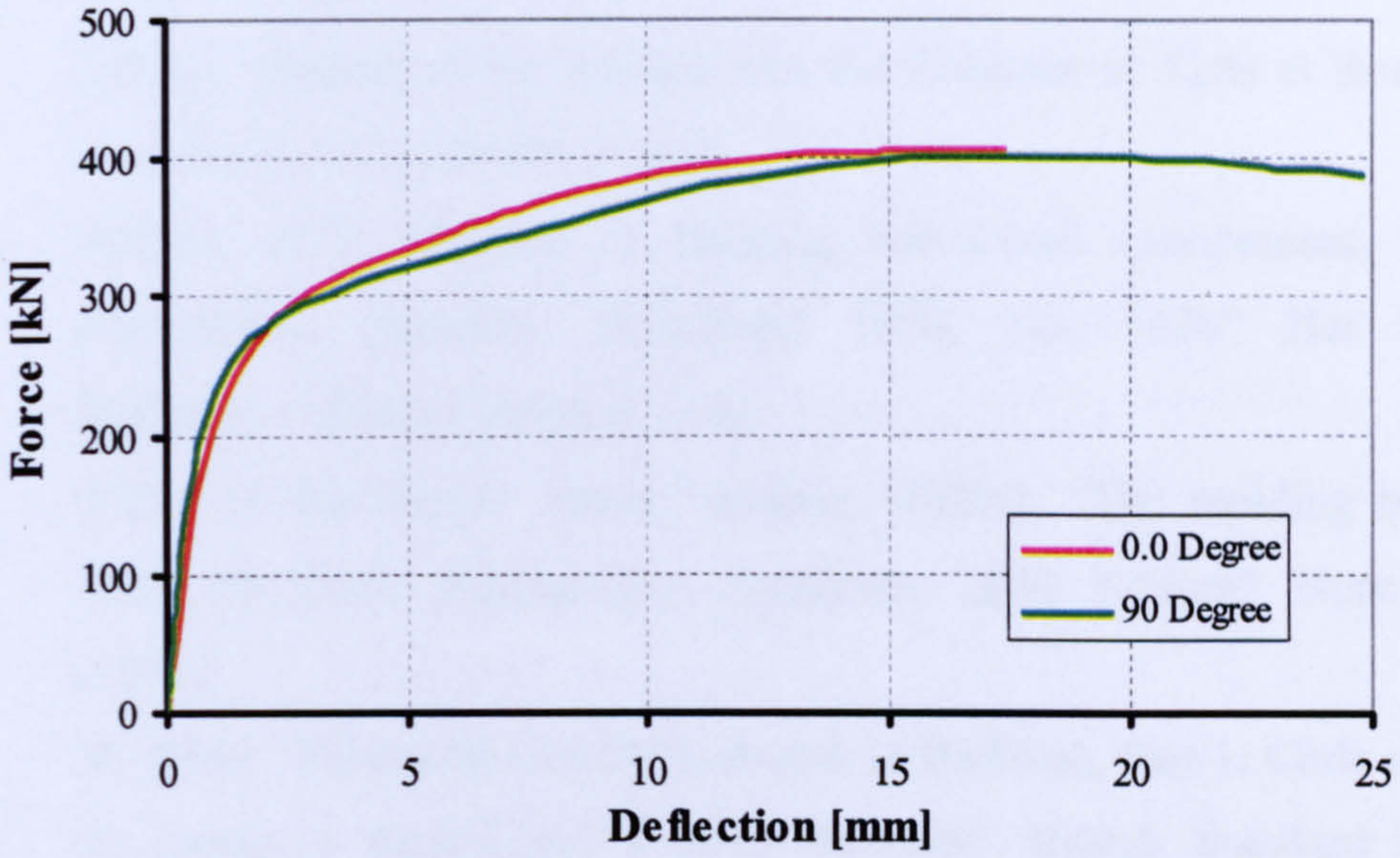

Figure 4.27 Tying force and vertical shear force capacity comparison for 3-bolt fin plate connection

4.8. Conclusions

- Connection geometric details have strong influence on the shear connection failure mode. A brittle failure, i.e. bolt shear failure, will be inevitable once both plates in a single-shear connection have a thickness of the bolt radius or greater.
- A ductile failure mode in a connection is always preferable. In order to achieve this kind of failure, the beam web thickness or the fin-plate thickness should always be at least 20% less than the bolt radius.
- To have a ductile failure mode, equal plate thicknesses may be used to form a single shear connection but the bolt radius should be greater than the plate thickness.
- The tying force capacity of a fin plate connection is equal to a single shear single-bolt lap joint's capacity multiplied by the number of bolt rows in the connection.
- The horizontal tying force resistance of fin a plate connection is equal to its vertical shear capacity.
- The angle of the tying force has little influence on a fin plate connection's tying resistance.

4.9. References

[4.1] HMSO, "Report of the inquiry into the Collapse of Flats at Ronan Point, Canning Town", London, (1968).

[4.2] HMSO, 1976, Ministry of Housing and Local Government, "Building Regulations, Statutory Instrument 1976, No. 1676" Her Majesty's Stationary Office, London, (1976).

[4.3] Office of the Deputy Prime Minister, HMSO, "The building regulations 2000 Approved Document-A Structure: 2004 Edition" Norwich, UK, (2004).

[4.4] BS 5950: "Structural Use of Steelwork in Building, Part 1: Code of Practice for Design - Rolled and Welded Sections", British Standard Institution (BSI), London (2000).

[4.5] American Institute of Steel Construction, AISC, "Load and Resistance Factor Design Specification for Structural Steel Buildings (LRFD)", Chicago, (1999).

[4.6] European Committee for Standardization (CEN). "Eurocode 3: Design of Steel Structures, Part 1.8: Design of joints", EN 1993-1-8, British Standard Institution, London, (2005).

[4.7] BCSA, "The British Constructional Steelwork Association LTD., Joints in Steel Construction: Simple Connections," The Steel Construction Institute (2002).

[4.8] Kim, H. J., and Yura J. A., "The effect of ultimate-to-yield ratio on the bearing strength of bolted connections", *J. Construct. Steel Research* Vol. **49**, (1999) pp 255–269.

[4.9] Rex, C. O., and Easterling, S. W. "Behaviour and modeling of a bolt bearing on a single plate", *Journal of Structural Engineering*, ASCE, Vol. **129**, No. 6, (2003) pp 792-800.

Chapter 5

Evaluation and Examination of the Finite Element Model at Elevated Temperature

5.1. Introduction

Beam-to-column connections are required to resist any resultant forces at the end of the supported beams and transfer them into the columns. In a fire, large axial forces can often be generated in steel beams. Due to restraint to thermal expansion these forces are initially compressive. At later stages the forces become tensile as catenary action starts to develop. This action helps steel beams to survive by behaving like suspension cables, hanging from the adjacent supporting members as a result of their loss of strength and bending stiffness, as shown by Liu *et al.* [5.1]. Furthermore, during the cooling stage of the fire, the deformed beams contract considerably and experience additional tension forces as described by Bailey *et al.* [5.2]. Consequently, for a structure to survive in fire conditions, it is crucial for any connection to have sufficient strength, stiffness and ductility to accommodate the induced end beam actions. Recent research by Yin *et al.* [5.3] has shown that the level of axial force developed depends strongly on the stiffness of the joints and the surrounding structure. Evidently, overall analysis of steel structures and composite frame buildings in fire conditions needs reliable prediction methods that focus on joint stiffness as well as resistance, in order to provide realistic and safe connection design.

5.2. FE model Description at Elevated Temperature

The FE model created in the previous chapter to analyse the connection at ambient temperature was developed further to study the connection at elevated temperature. The element type was changed from C3D8I to the C3D8T, which is another brick element designed for coupled temperature-displacement analysis [5.4], and allows non-uniform temperature distributions to be considered. The material properties were modified to follow temperature-dependence according to Eurocode 3, Part 1.2 [5.5]. A non-uniform temperature-dependent thermal expansion coefficient [5.5] was adopted in the entire analysis. The high-temperature analysis was divided into a few time steps, in which the structural load was applied first, followed by non-uniform temperature increase in the beam and connection components in the following steps. Poisson's ratio of steel at elevated temperatures was taken to be the same as at ambient temperature, (ν_s = 0.3). The contact element arrangement stays the same as in the ambient-temperature analysis.

The shear behaviour of the fin plate connection FE model has proved satisfactory compared with test results at ambient temperature, presented in the previous chapter. However, it is obvious that the behaviour of the steel connection components (bolts, plate, weld, etc.) can not be isolated from the behaviour of the beam to which it is connected. In other words, the actions imposed on the connection components are always intimately linked with the beam behaviour. This interaction between the beam and its supporting connection has been well highlighted since the Broadgate Phase 8 fire occurred in 1990 [5.6, 5.7], and the Cardington full scale building fire tests [5.2, 5.8 - 5.10]. It is therefore important first to establish and evaluate the beam behaviour at high temperature in terms of deflection and catenary action before evaluating the connection model itself at high temperature. Then with a working the beam model, the only remaining uncertainty about the behaviour of the complete connection assembly at elevated temperature would be the connection itself. Therefore, the connection model evaluation firstly examines the two basic phenomena of beam behaviour at elevated temperature, which are the large deflection and catenary action. For this purpose, an isolated three-dimensional beam model was created with brick elements, and was evaluated by comparison with existing test data and other available analytical tools. During this stage of the research, there was a complete lack

of suitable fire test data for a steel fin plate connection, including its supported steel beam. This makes it difficult to evaluate the whole fin plate connection model at elevated temperature. Fortunately, at a later stage, the fin plate connection fire test conducted in 2005 by Professor Wald, of the Czech Technical University [5.11], created a new opportunity to validate the FEM behaviour of the whole connection assembly against real fire test.

5.3. Deflection Evaluation of The Beam FE Model

When a steel beam on simple end supports is uniformly heated to high temperatures it starts to suffer a large increase in deflection after 400°C [5.12] because the steel loses strength and stiffness as its temperature increases beyond this point. Therefore, it is essential to establish this phenomenon in the FE model. El-Rimawi *et al* [5.13 - 5.17] performed a numerical analysis using a secant stiffness approach to investigate different factors that affect the steel beam behaviour under fire conditions. Although the comparisons with results of tests conducted in the UK [5.12] showed good accuracy, it important to highlight the fact that the study did not consider the effect of axial restraints at the beam ends, so the beams were supported vertically on roller supports only.

For the purpose of this evaluation, some of El-Rimawi's analytical results and test data will be used to check the accuracy of the ABAQUS finite element model to simulate the beam's large-deflection behaviour under fire conditions. Three cases of a roller-ended beam and one case of a rotationally fixed-ended beam have been chosen for this evaluation. All these cases have the same beam cross section (UB254×146×43). The values of the Young's modulus and yield stress of steel at ambient temperature were assumed to be 205 kN/mm^2 and 275 N/mm^2 respectively. The mechanical properties of steel at elevated temperatures followed Eurocode 3 Part 1.2 [5.5]. The beams were assumed to support a concrete slab on their top flanges and to be subjected to three- side heating. The time-temperature relationships for the beam web and flanges are shown in **Figure 5.1.**

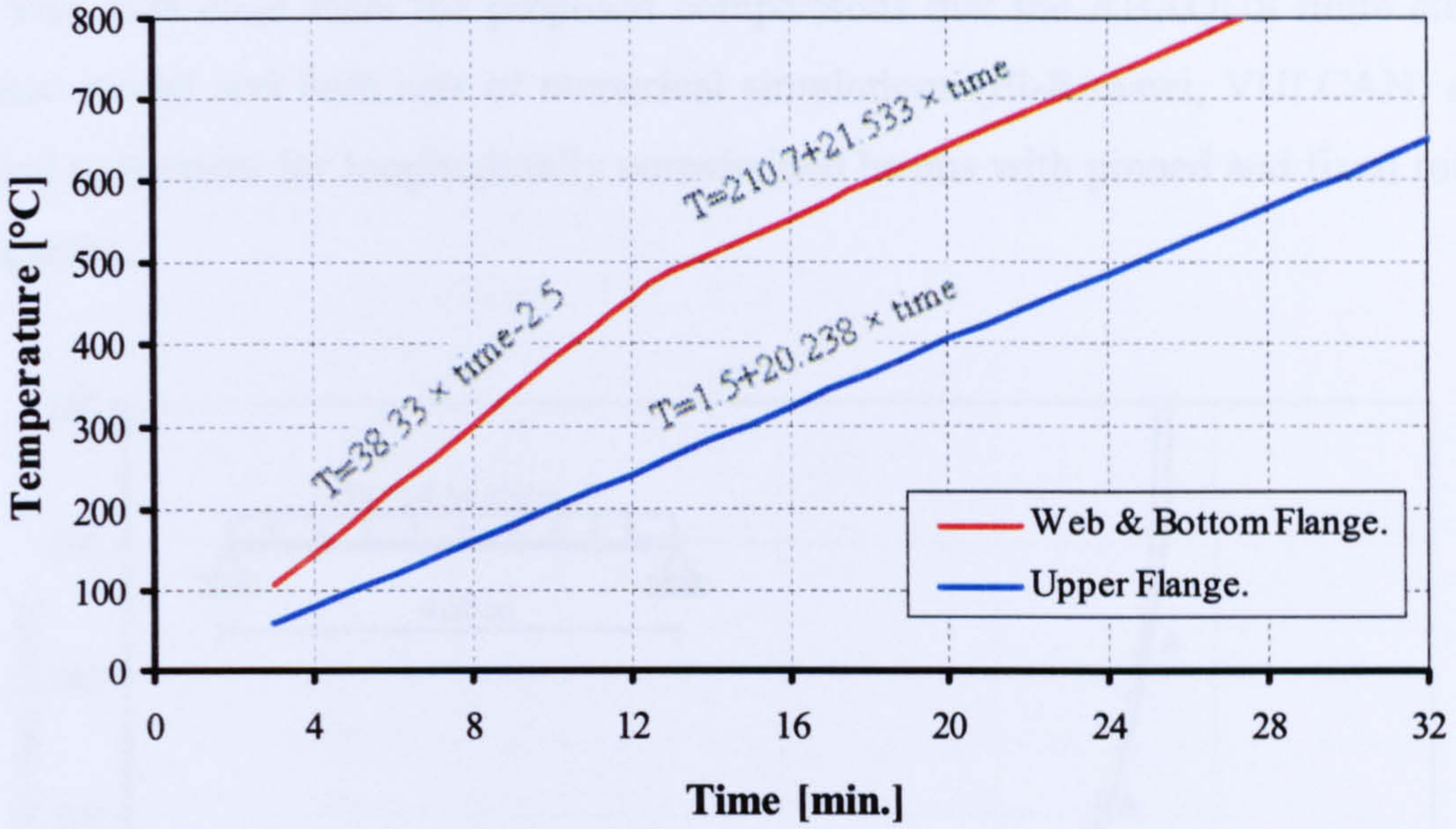

Figure 5.1 Time-Temperature relationships used in the El-Rimawi *et al* analysis [5.16]

The first two comparisons were for a beam with a 4.5m span (**Figure 5.2**), supported on rollers at both ends. Uniformly distributed loads of 16.34 kN/m or 31.92 kN/m were applied (**Figures 5.3 and 5.4**). Another comparison (**Figure 5.5**) was for a beam of 8m span and a uniform load of 11.46 kN/m was applied. The last comparison (**Figure 5.6**) was for a 8m beam span, with uniform load of 17.18 kN/m, but with both ends fully restrained rotationally and free to move longitudinally.

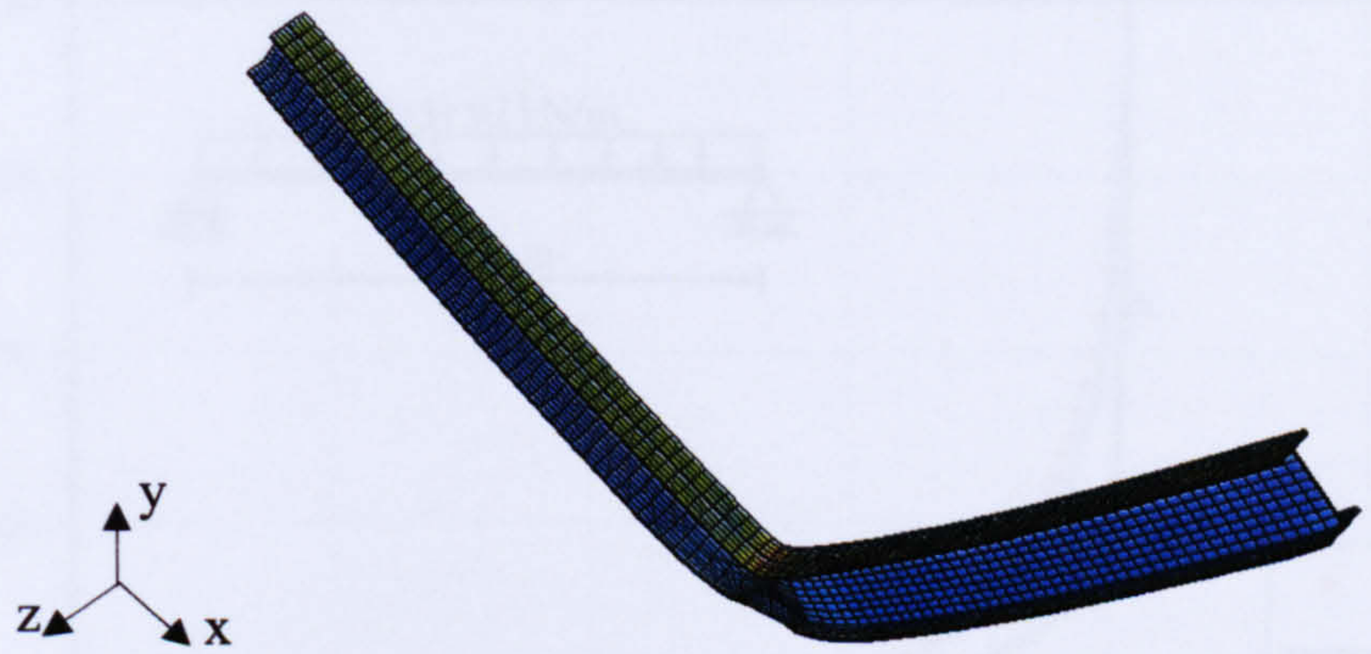

Figure 5.2 Final deflected shape of 4.5m span beam model at the end of the analysis

VULCAN is software developed at the University of Sheffield [5.18]. It has been developed through long term research [5.19 - 5.21] and evaluated against beams tested in fire conditions [5.1, 5.12]. Part of its capability is analysing a steel beam under elevated temperature for any chosen time-temperature history and any boundary conditions. The deflection of the ABAQUS brick element beam model was compared to

VULCAN, in combination with the results of the El-Rimawi analyses (**Figures 5.3s – 5.6**). It is clear from the proposed comparisons that the ABAQUS finite element beam model and both sets of numerical simulations (El-Rimawi, VULCAN) are in good agreement for longitudinally unrestrained beams with pinned and fixed rotation supports.

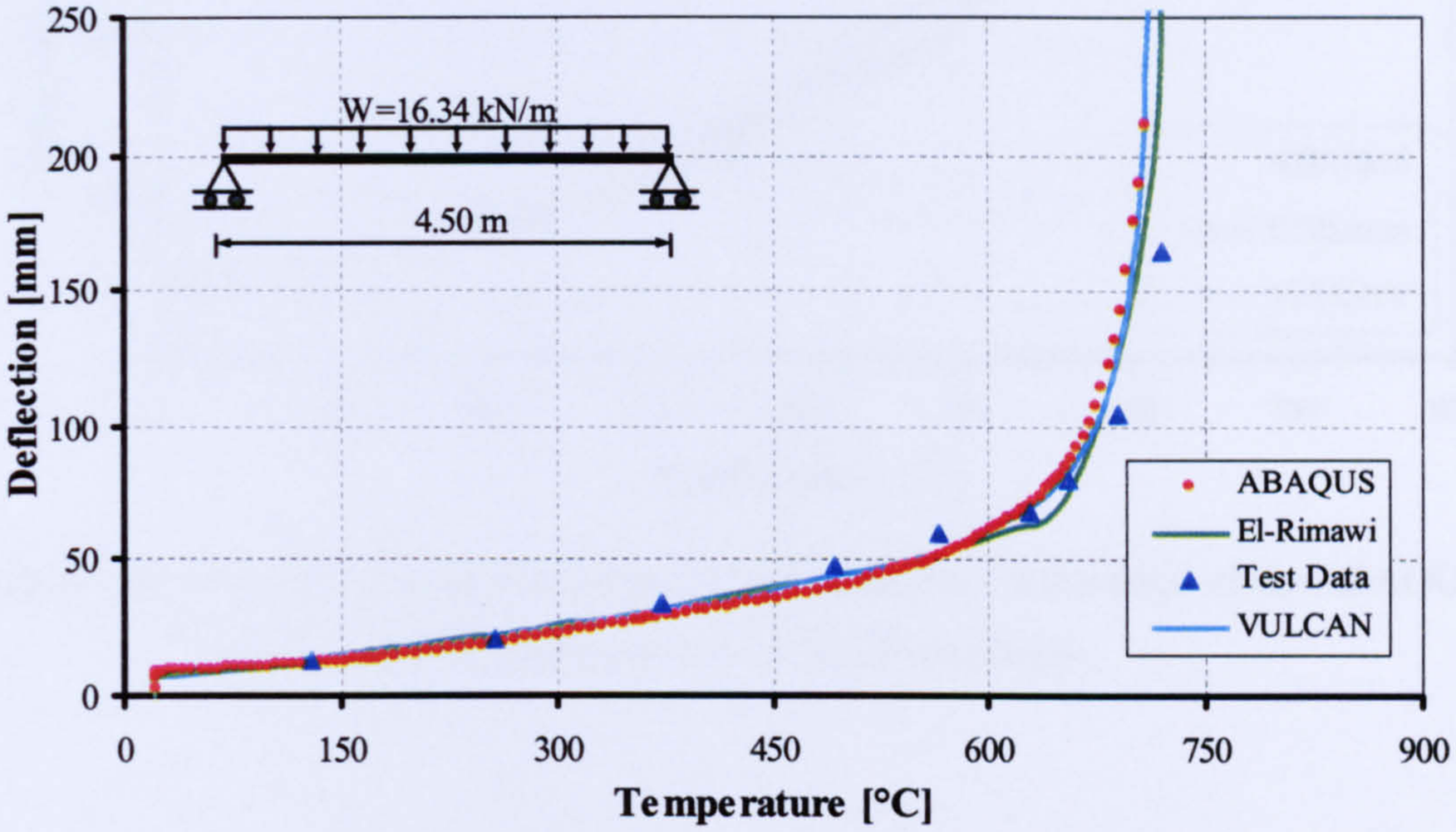

Figure 5.3 Comparison between Temperature-Deflection relationships of the ABAQUS simulation, El-Rimawi *et al*, VULCAN software and test data

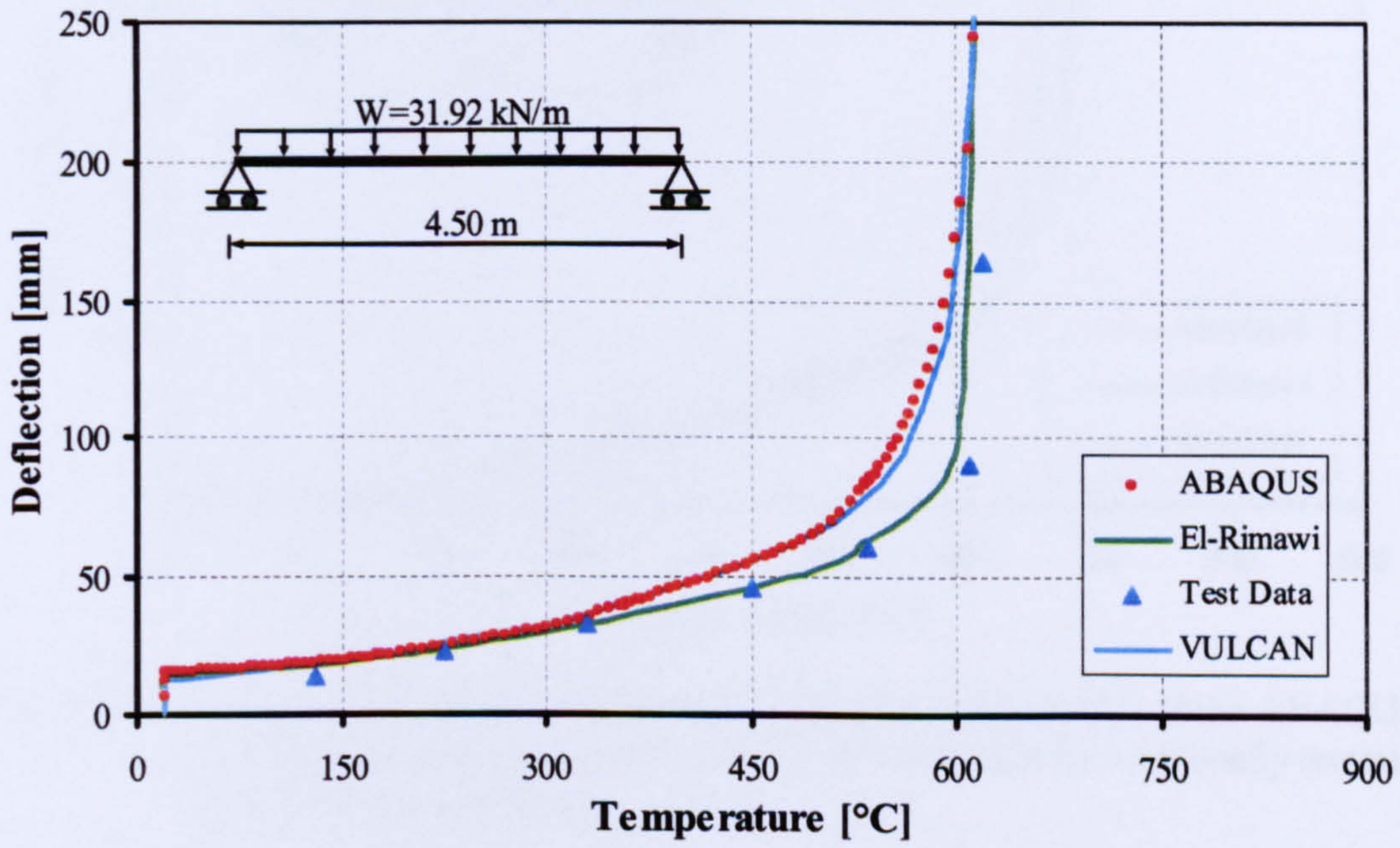

Figure 5.4 Comparison between Temperature-Deflection relationships of the ABAQUS simulation, El-Rimawi *et al*, VULCAN software and test data

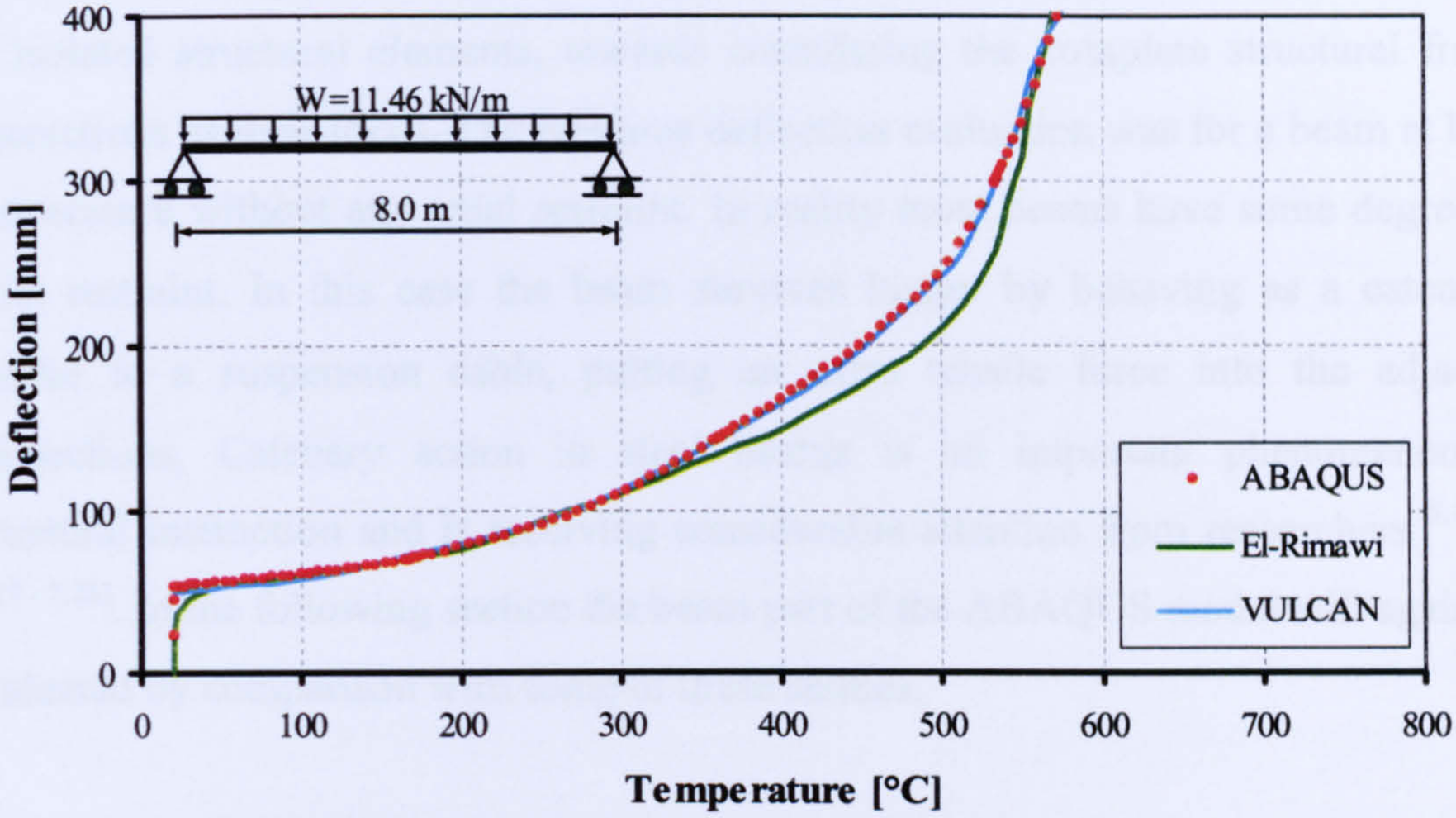

Figure 5.5 Comparison between Temperature-Deflection relationships of the ABAQUS simulation, El-Rimawi *et al* and VULCAN software

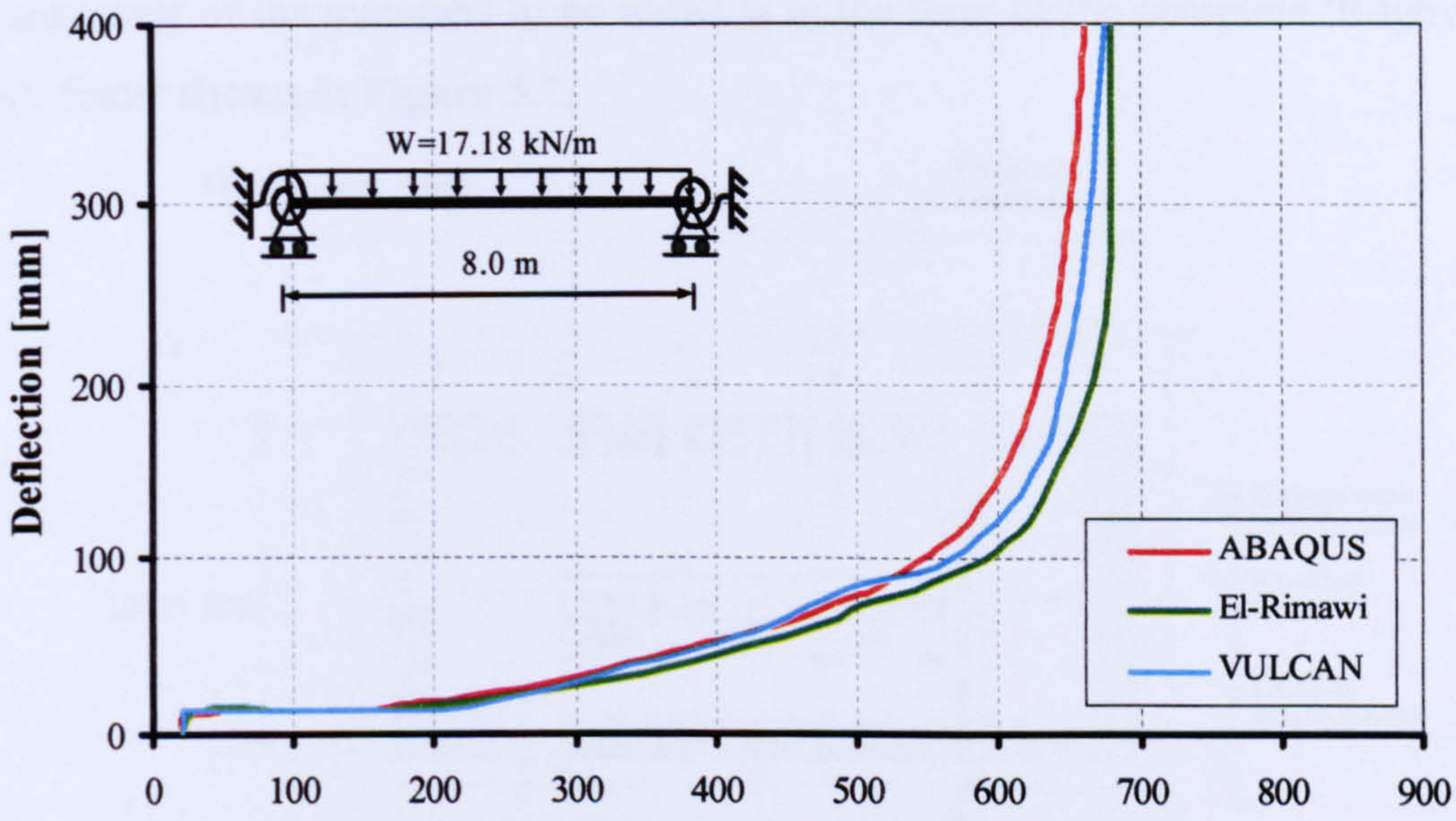

Figure 5.6 Comparison between Temperature-Deflection relationships of the ABAQUS simulation, El-Rimawi *et al* and VULCAN software for rotationally restrained beam on roller supports

5.4. Evaluation of The Beam for Catenary Action

Studies in the area of structural fire engineering have moved beyond the assessment of isolated structural elements, towards considering the complete structural frame interactions as their focus. The previous deflection evaluation was for a beam at high temperature without any axial restraint. In reality most beams have some degree of axial restraint. In this case the beam survives longer by behaving as a catenary, similar to a suspension cable, putting an extra tensile force into the adjacent connections. Catenary action in steel beams is an important phenomenon of structural interaction and is receiving considerable attention from researchers [5.1, 5.3, (5.22 - 5.26)]. In the following section the beam part of the ABAQUS model will again be evaluated by comparison with some of these studies.

5.4.1. Comparison with experimental and numerical analysis

Liu *et al* (2002) [5.1] conducted a series of fire tests on axially restrained steel beams at the Fire Research Laboratory of the University of Manchester. The main objective was to investigate large deflection behaviour of steel beams and the effect of different levels of axial restraint due to adjacent cooler parts of the structure. The arrangement of the members to be tested is in the form of the complete 'Rugby goal post' frame shown in **Figure 5.7**.

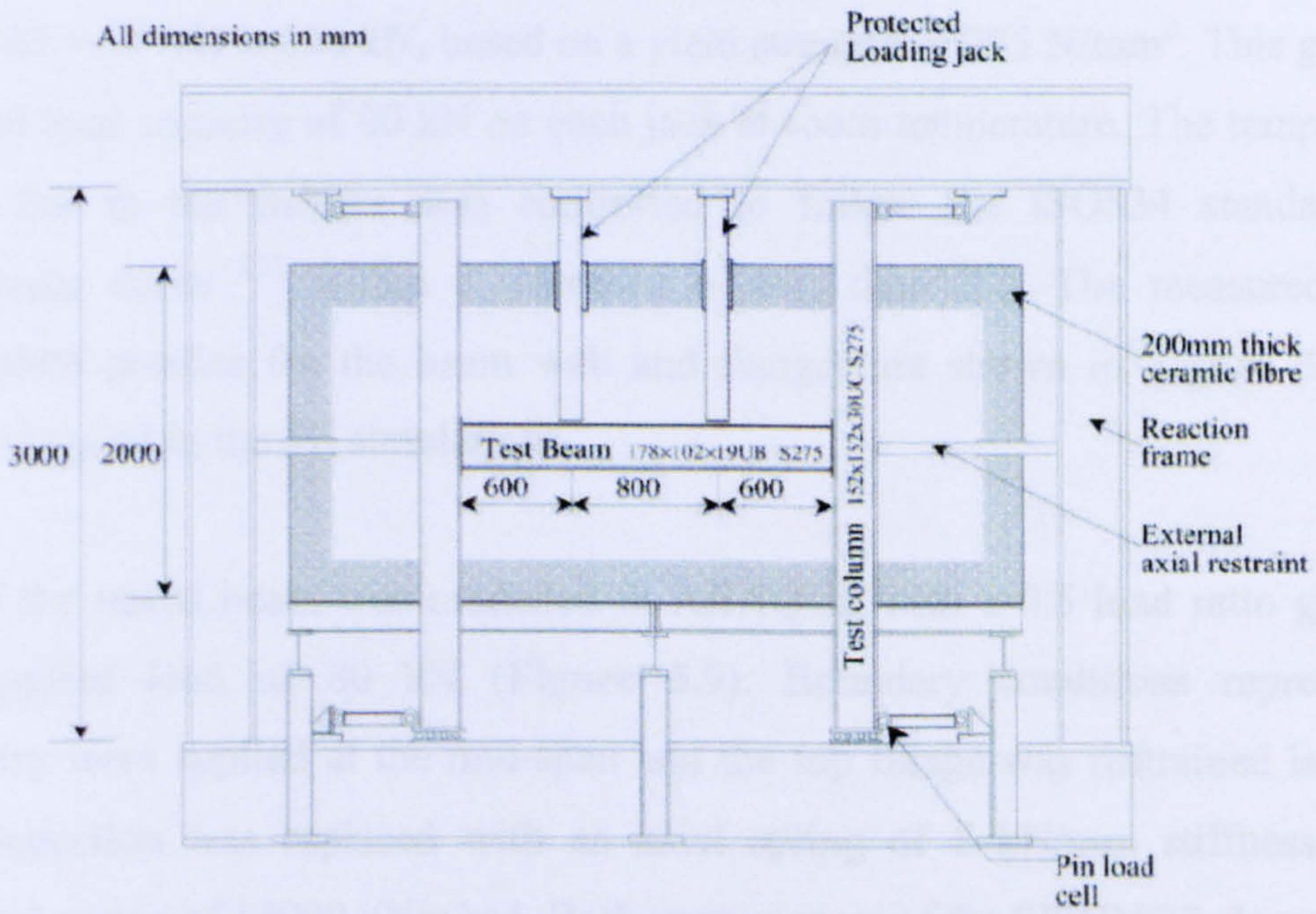

Figure 5.7 Test assembly (elevation) [5.1]

The tested beam was a mainly-unprotected 178 × 102 × 19UB (S275) section. The shielding effect due to the concrete slab was considered by wrapping the top flange with 15 mm thick ceramic fibre blanket. The supporting columns were of 152×152×30UC (S275) section. The columns were held in position at the top and bottom by four pin load-cells. The column posts, together with the connections, were fire-protected by the use of 50 mm thickness of ceramic fibre blanket. Two types of connections commonly used in practice, double web-cleats and flush end-plates, were chosen as the beam end joints. The present study only compares numerical simulation results against tests using flush end-plate connections. An end-plate of 10 mm thickness with M16 Grade 8.8 bolts was used in the test. The flush end-plate connections and the Rugby post were estimated to provide a rotational restraint stiffness of 14000 kNm/rad to the tested beam. An axial restraint stiffness of 8 kN/mm was provided by the goal post columns to the tested beam.

The loads were applied to the beam using two hydraulic jacks connected to the top member of the reaction frame surrounding the furnace to form a self-equilibrating system. The experimental study considered three different load levels, having load ratios of 0.3, 0.5 or 0.7. The load ratio is defined as the ratio of the applied maximum bending moment in a simply supported beam to the beam's plastic bending moment capacity at ambient temperature. The design shear capacity of the 178 × 102 × 19 UB is 156 kN, based on a yield strength of 275 N/mm^2. This gives an expected load capacity of 80 kN on each jack at room temperature. The temperature of the fire in the furnace was controlled to follow the ISO834 standard fire temperature curve [5.27] within a tolerance of less than 2%. The measured time-temperature profiles for the beam web and flanges are shown in **Figure 5.8,** and there were used in the FE simulations.

Half of the tested beam was modelled in ABAQUS with a 0.5 load ratio giving a total applied load of 80 kN **(Figure 5.9)**. Boundary conditions representing symmetry were applied at the mid-span and the top flange was restrained laterally. The connection was replaced with an axial spring of 8 kN/mm stiffness and a rotational spring of 14000 kNm/rad. Both springs were of the SPRING2 element type [5.4] in the ABAQUS element library.

Figure 5.10 compares the ABAQUS simulation and experimental results. The figure contains two comparisons, one for the bottom flange temperature-axial reaction relationship (**Figure 5.10-a**) and one for the temperature-mid-span vertical deflection relationship (**Figure 5.10-b**). The independent analysis results given by the VULCAN software are also included in the same figure for comparison.

It can be seen that the ABAQUS simulation results are in very good agreement with the test results and VULCAN software, with less than 3% difference. Referring to **Figure 5.10** again, it can be seen that in the fire tests no catenary action was observed. This is because the fire tests had to be terminated due to an acceleration in the beam vertical deflection rate which might have damaged the fire test furnace [5.1]. ABAQUS numerical simulations show an accurate prediction of the vertical deflections and the rapid change in beam end axial reaction forces from compression to tension just before termination of the test.

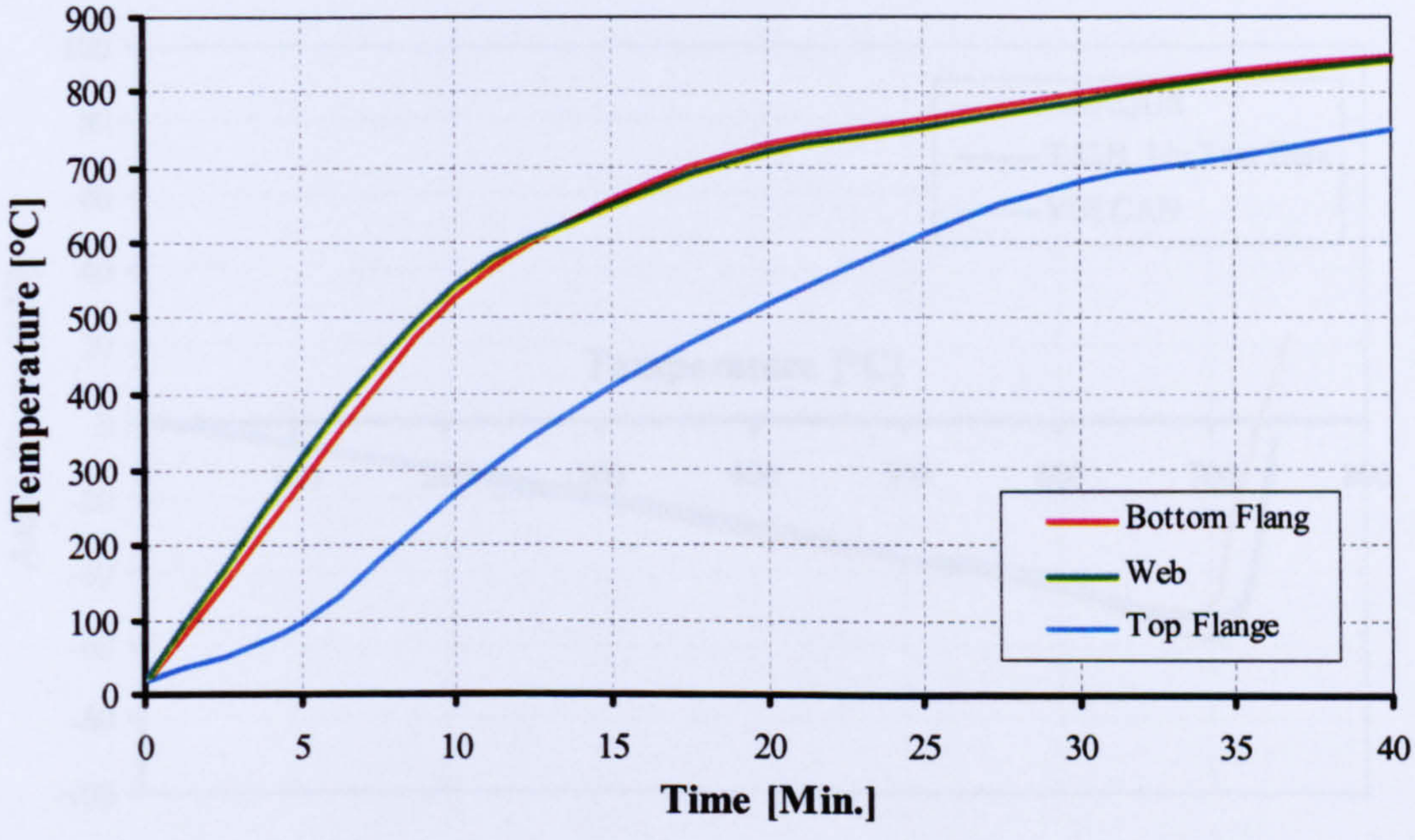

Figure 5.8 Measured Time-Temperature relationships in the tests of Liu *et al*

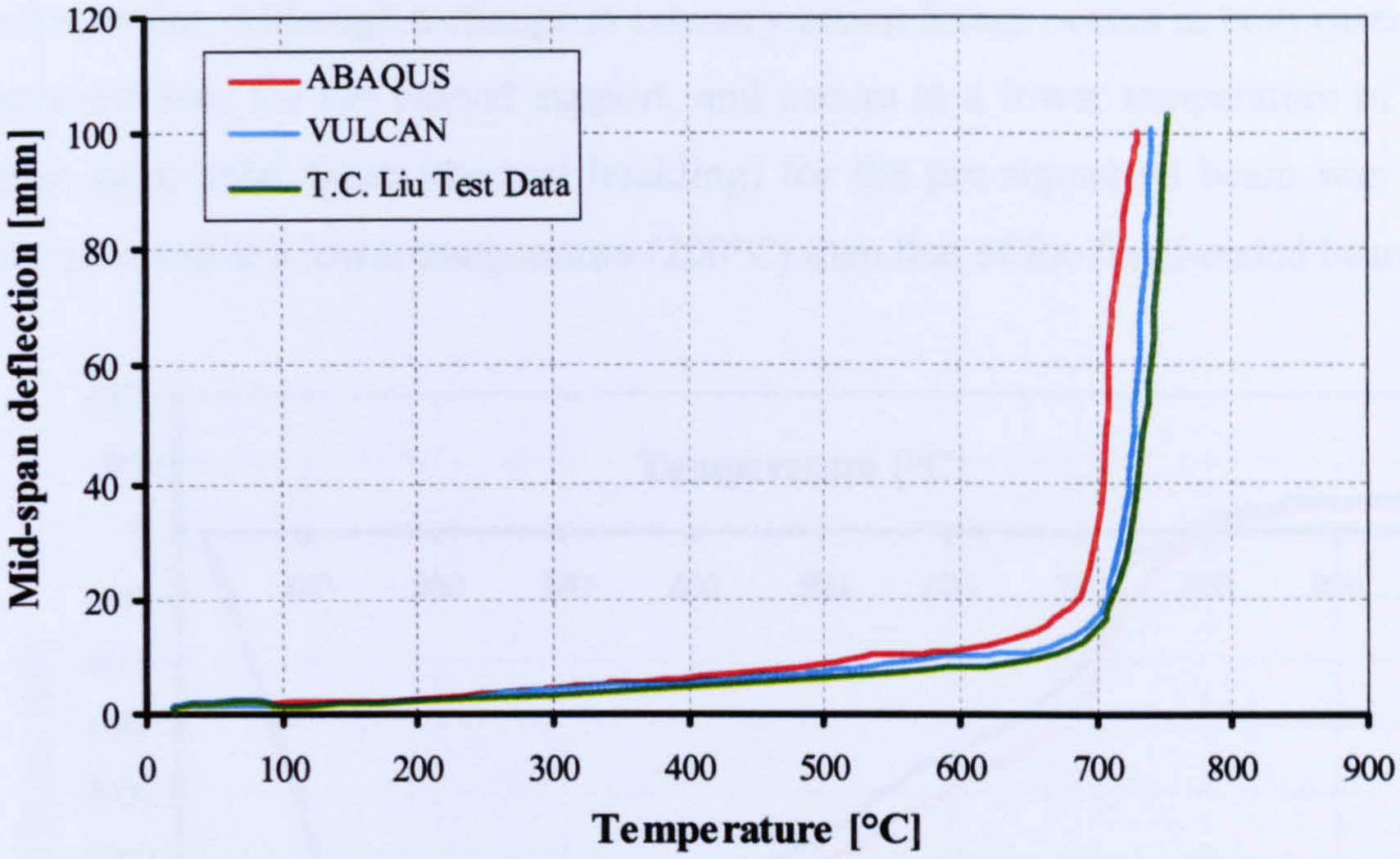

(b) Temperature-Deflection reaction relationship

Figure 5.10 Comparison between the result of ABAQUS simulation, Liu test data, and VULCAN results for beams with 8 kN/mm axial restraint

5.4.2. VULCAN numerical results

The two-dimensional beam element in the VULCAN [5.18] software was used to model and evaluate the three-dimensional ABAQUS beam model for catenary action behaviour. A 610x229x101 UB steel beam of 8m length was analysed under two ideal cases of end support conditions, pin support (pinned at both ends), and fixed support (fixed against all movement at both ends). The beam in both cases was subjected to 25 kN/m uniformly distributed load and non-uniform three-sided heating. The bottom flange and the beam web were subjected to a linear time-temperature increase at 10°C/min, whereas the top flange temperature was assumed to be 0.5 of this. At ambient temperature, the steel beam had yield strength of 430 N/mm^2, elastic (Young's) modulus of 210 kN/mm^2 and 0.3 Poisson's ratio.

Figure 5.11 shows comparisons of the temperature-axial force and temperature-deflection relationships between the ABAQUS and VULCAN analyses for the pin-supported beam, which has full axial restraint but is free to rotate at its ends. Similarly, **Figure 5.12** shows further comparisons with the results for the fixed-ended beam. These comparisons demonstrate clearly the good correlation between

the VULCAN beam model and the ABAQUS brick element model for both cases of end restraint. Although a change in catenary action forces occurs in both cases, this is more obvious for the pinned support, and occurs at a lower temperature of 800°C. Also, peak axial force (thermal buckling) for the pin-supported beam was sharper and occurred at a lower temperature (200°C) than that of the fixed-ended beam.

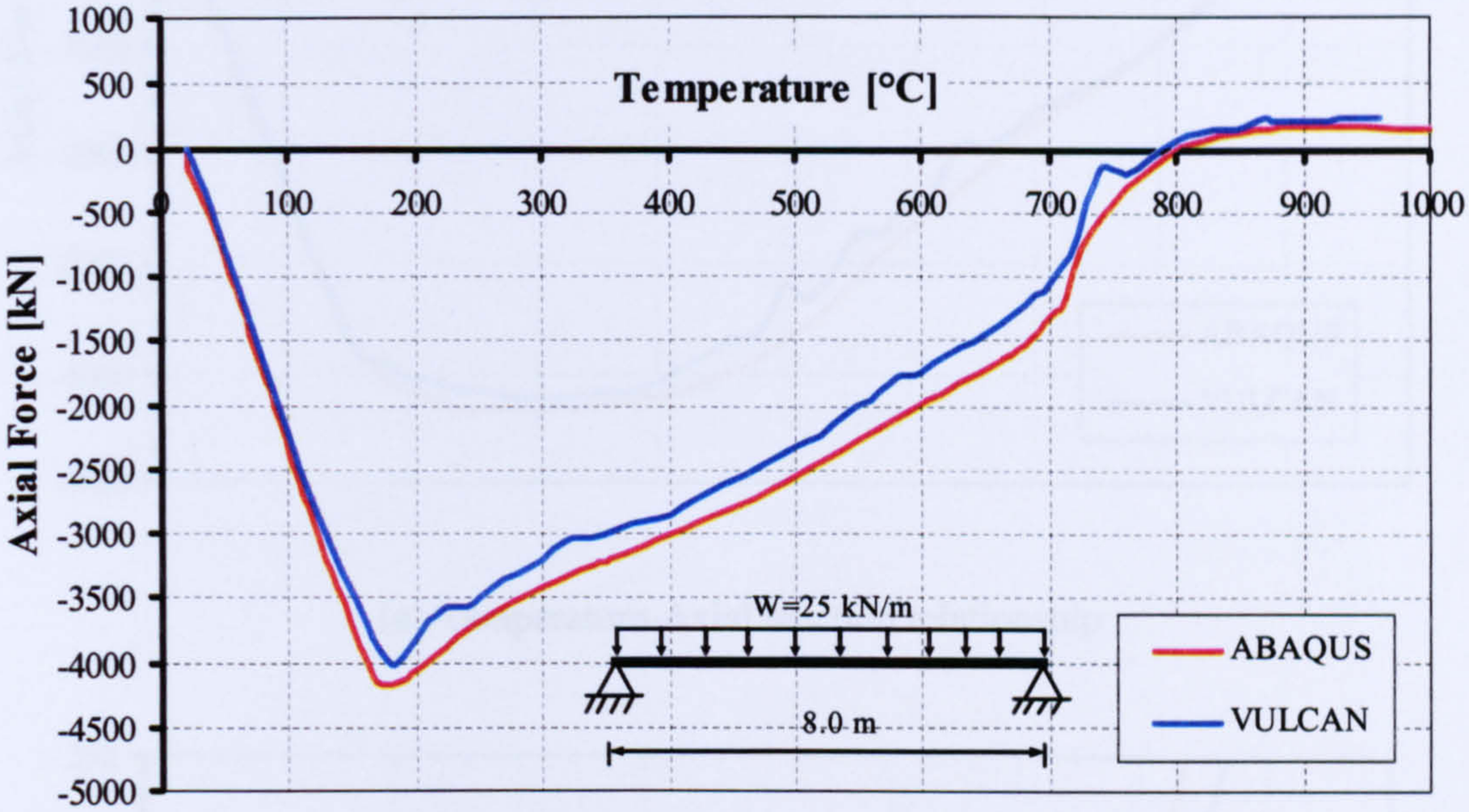

(a) Temperature-Axial reaction relationship

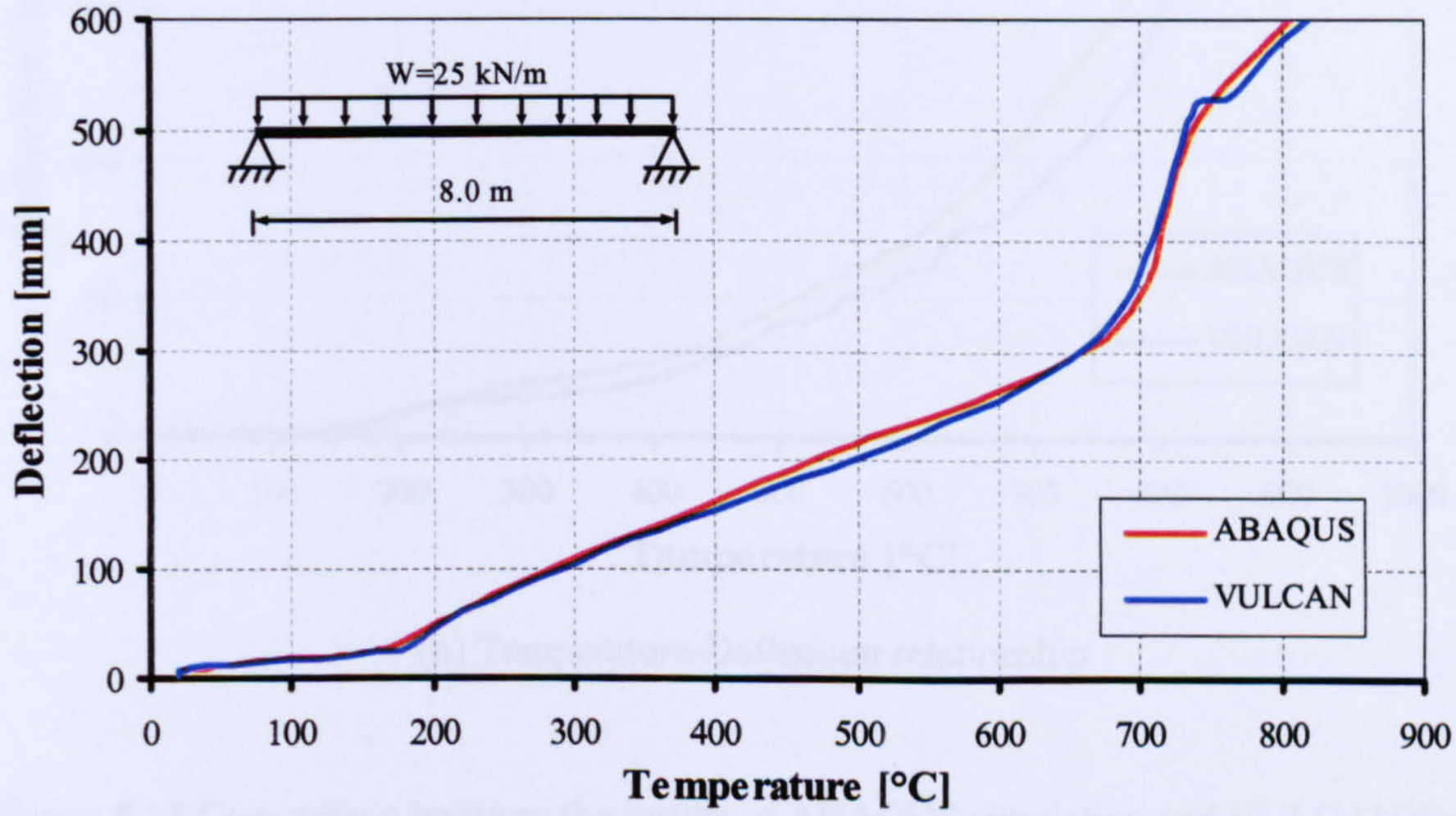

(b) Temperature-Deflection relationship

Figure 5.11 Comparison between the results of ABAQUS simulation and VULCAN for the pin-supported beam

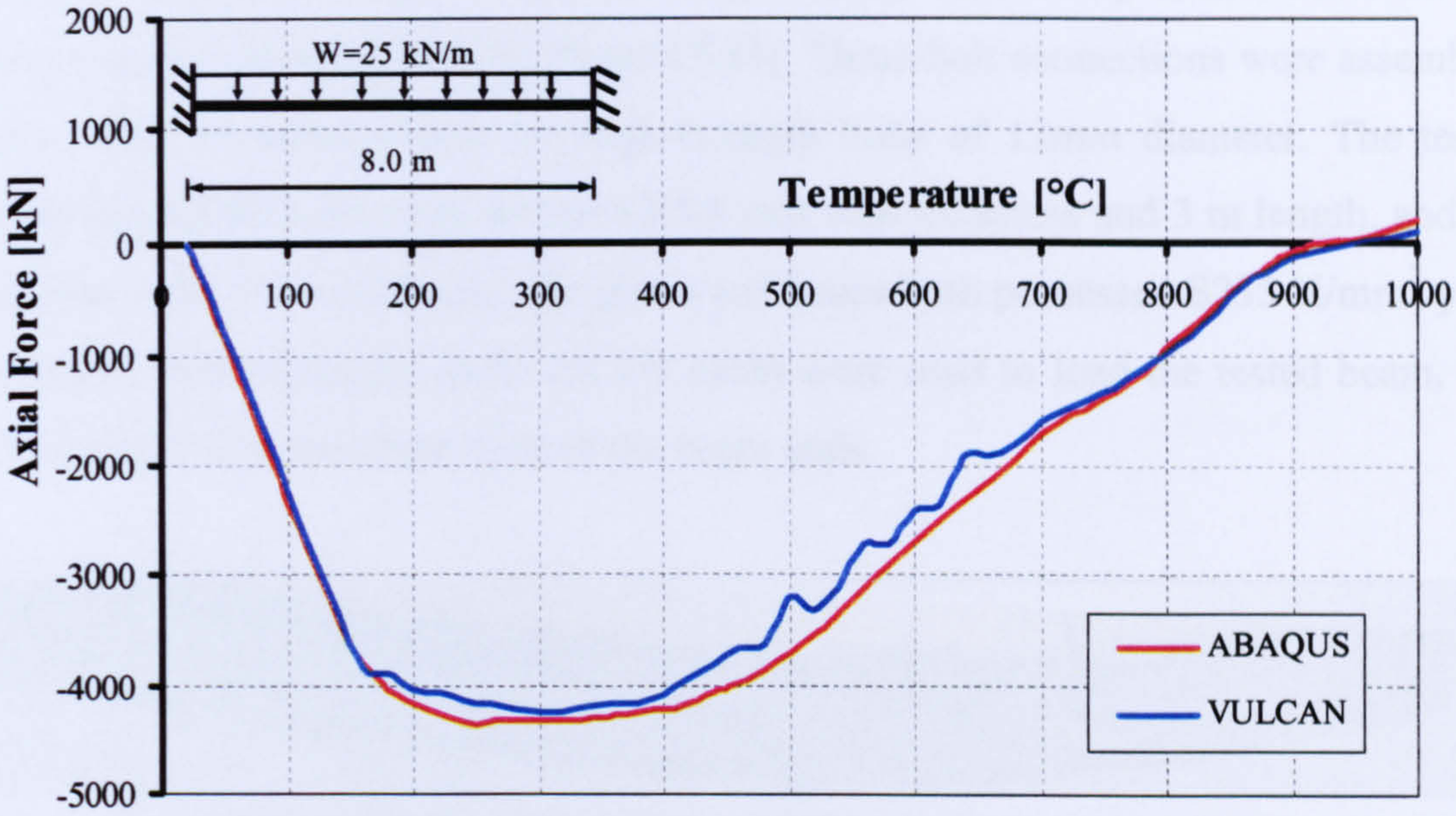

(a) Temperature-Axial reaction relationship

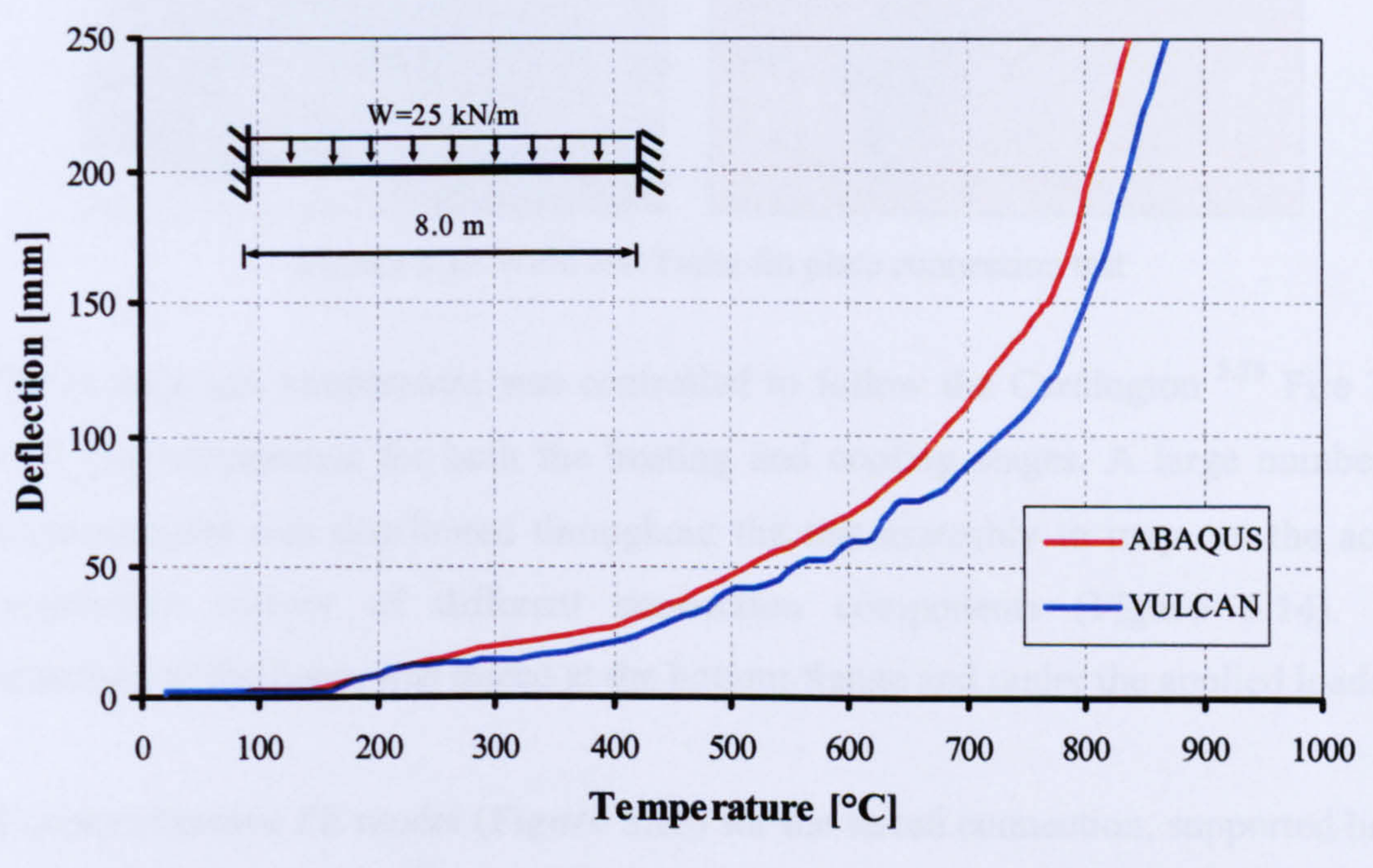

(b) Temperature-Deflection relationship

Figure 5.12 Comparison between the results of ABAQUS simulation and VULCAN for the fixed-ended beam

5.5. Evaluation of Fin Plate Connection to Real Fire Test

In 2005 Wald and Ticha [5.11] of the Czech Technical University conducted a fire test on a steel fin plate connection (**Figure 5.13**). Three-bolt connections were assembled using fully threaded Grade 8.8 high-strength bolts of 12mm diameter. The tested beam was an IPE160 cross section of 5.8 mm web thickness and 3 m length, and the fin plate was 6×60×125 mm. Fin plates and beam both possessed S235 N/mm^2 yield strength. Two hydraulic jacks (60 kN each) were used to load the tested beam, and were placed 250 mm from each of the beam ends.

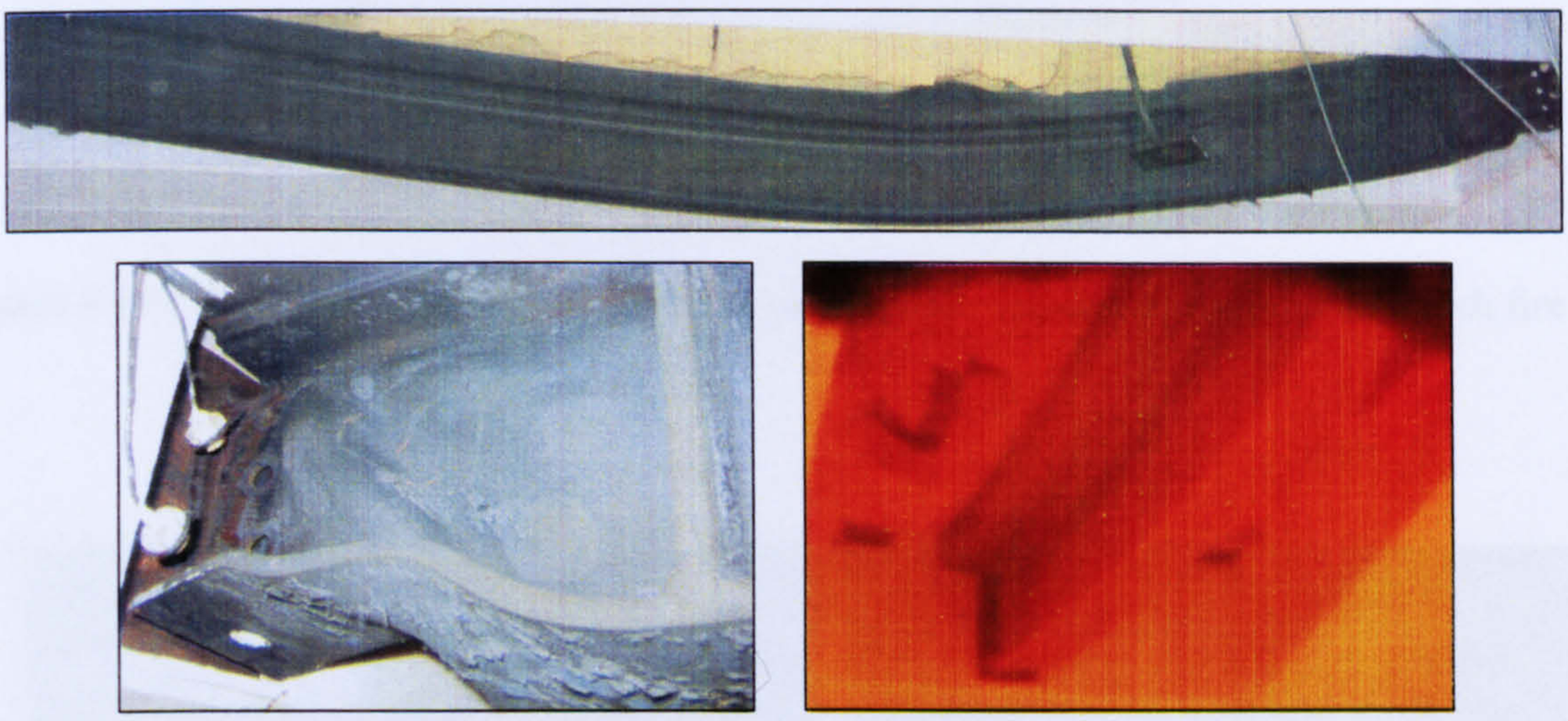

Figure 5.13 Wald and Ticha fin plate connection test

The furnace gas temperature was controlled to follow the Cardington [5.28] Fire Test No.7 gas temperature for both the heating and cooling stages. A large number of thermocouples was distributed throughout the test assembly to map out the actual temperature history of different connection components (**Figure 5.14**). The deflection of the beam was traced at the bottom flange and under the applied loads.

A comprehensive FE model (**Figure 5.15**) for the tested connection, supported beam and restraints was created to match as precisely as possible the test condition. Half of the tested beam was modelled with axis-of-symmetry boundary conditions on its free edge. Lateral restraints were applied at selected nodes on the top flange. The actual test temperature histories of the different connection components were applied in the FE model through time stepping after the load had been applied in the first time step.

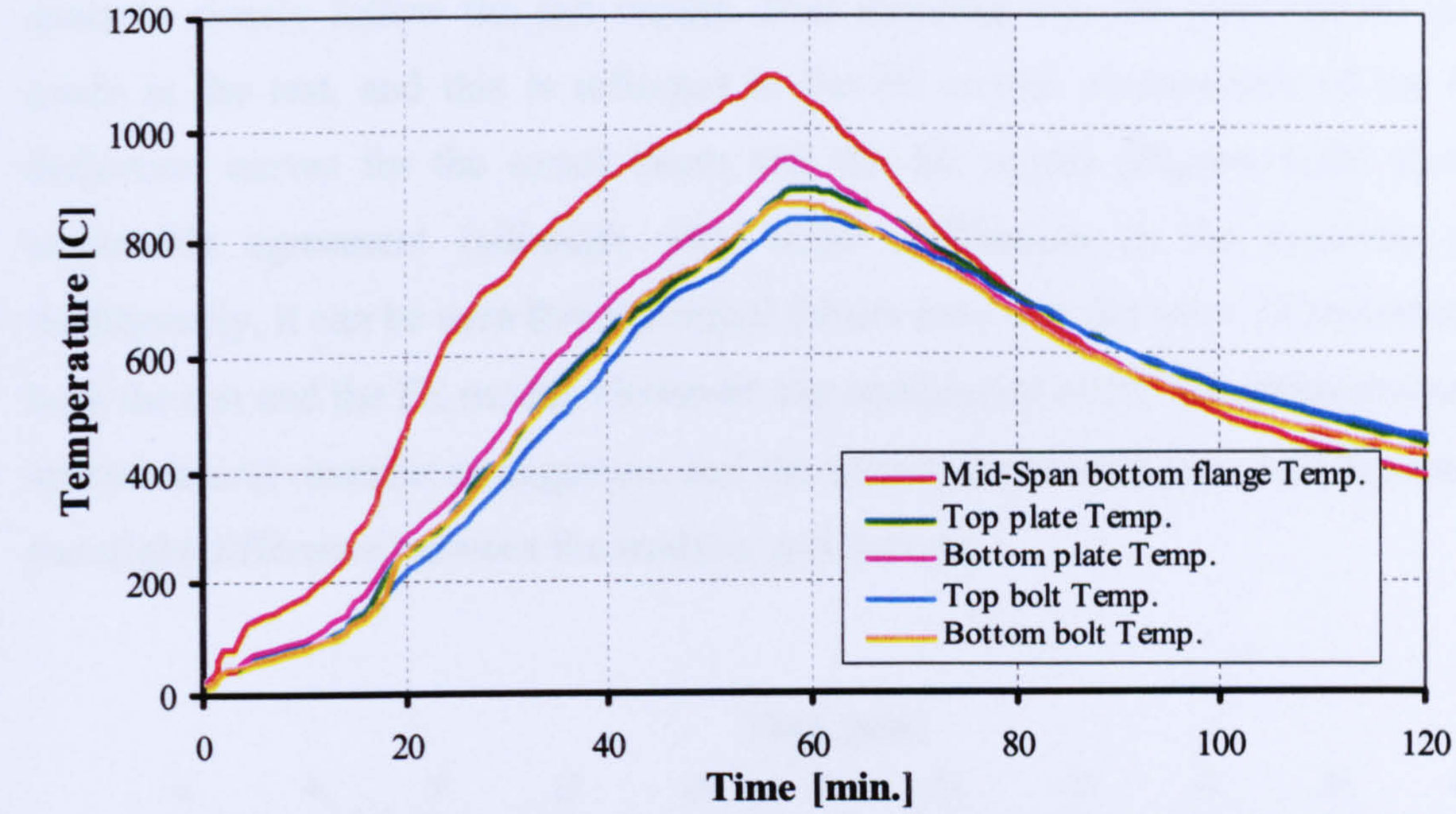

Figure 5.14 Time-temperature curves of the fin plate connection components in the Czech fire test.

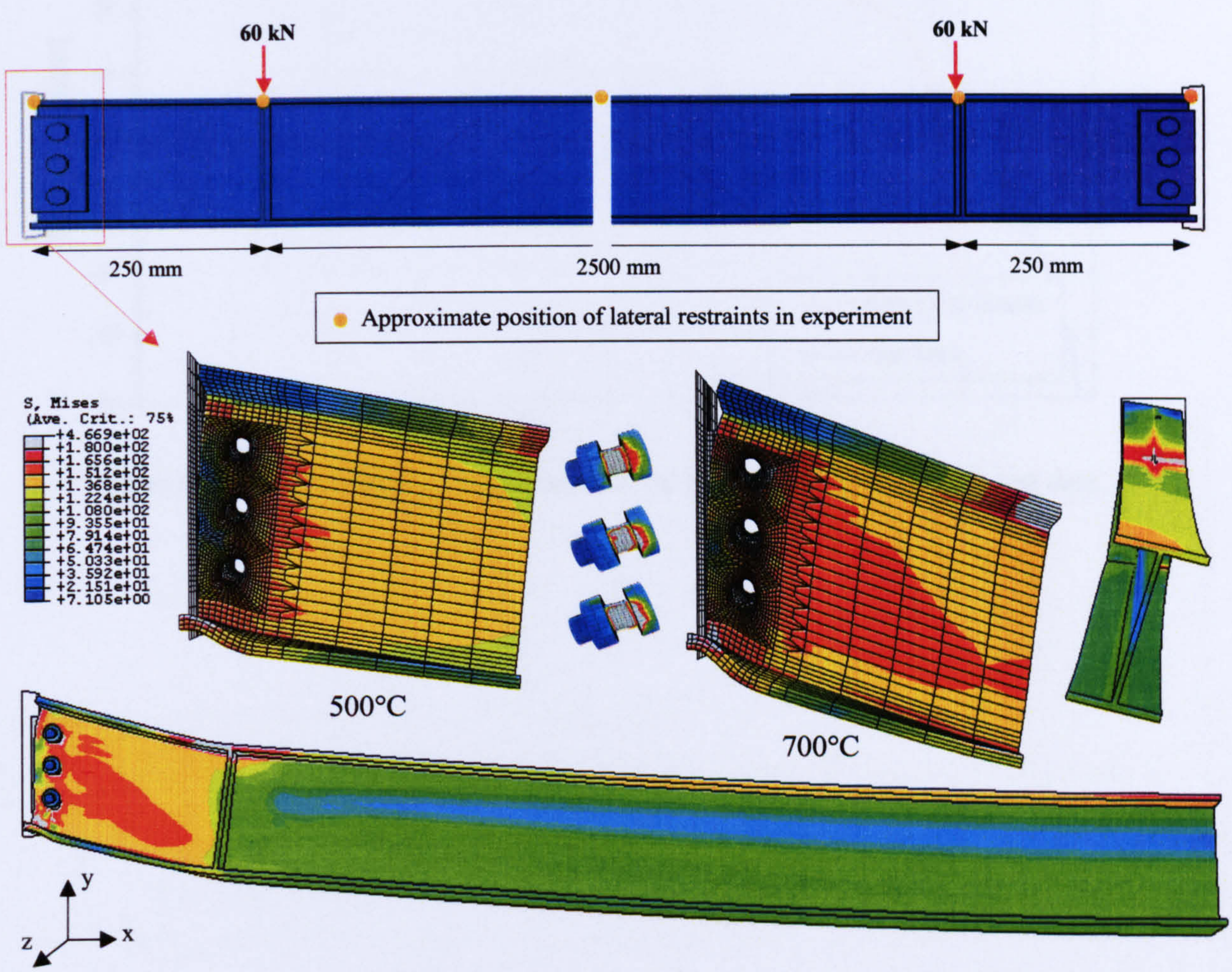

Figure 5.15 FE model of the tested fin plate connection and the connected beam

It can be observed that the resulting deflected shape and the failure mode in the FE analysis closely follow the test results. Bolt shearing was the predominant failure mode in the test, and this is reflected in the FE model. Comparison of the time-deflection curves for the tested beam and the FE model (**Figure 5.16**) shows a reasonable agreement (although with slight differences in the runaway part). Additionally, it can be seen that the initial failure time was the same (32 minutes) for both the test and the FE model. However, the complexity of the test arrangement (the special lateral restraint arrangement and the composite action) may well account for the slight difference between the analysis and the test.

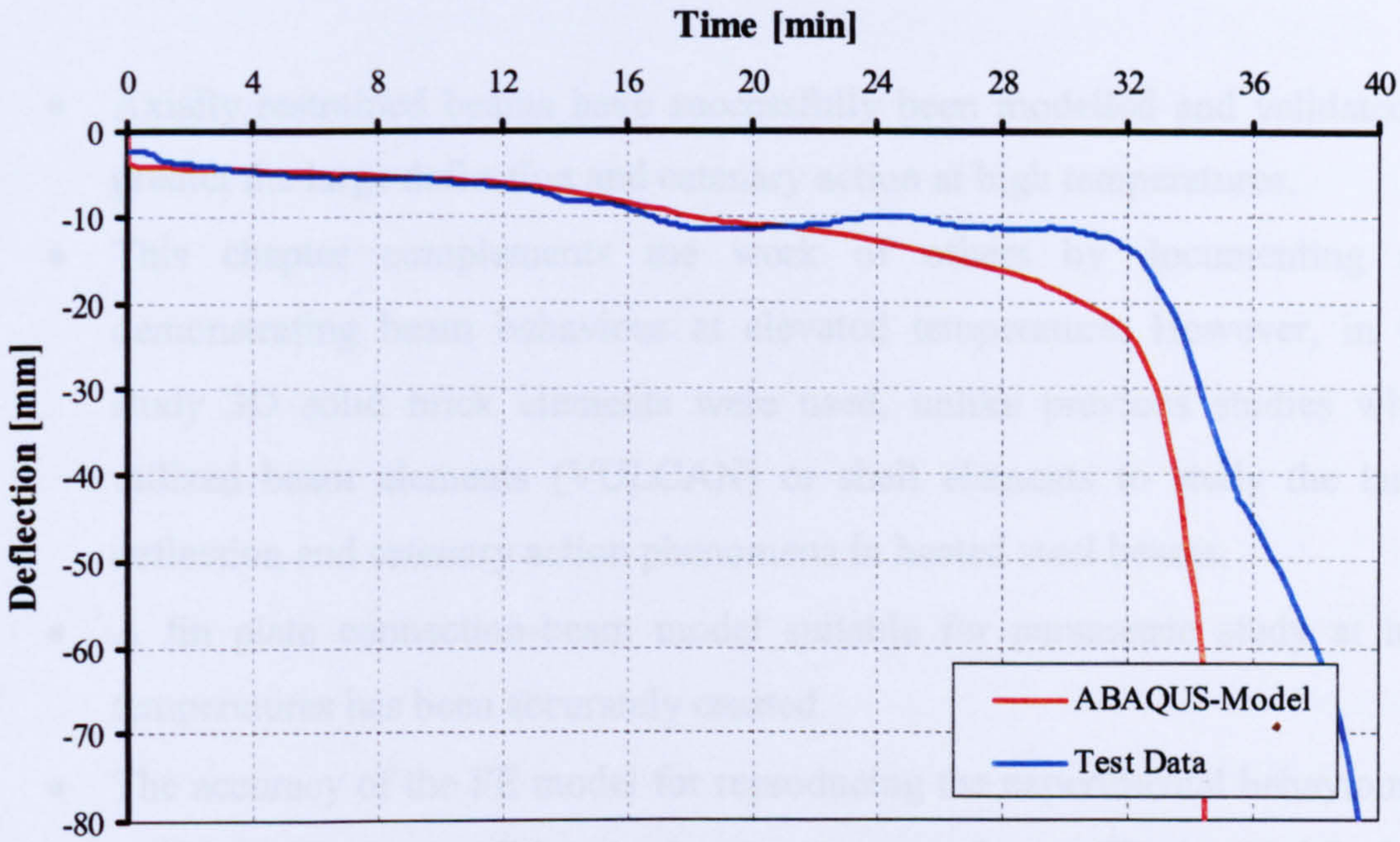

Figure 5.17 Time-Deflection comparisons of the FE simulation and Czech test data

5.6. Conclusions

The ABAQUS/Standard 3D finite element model created for ambient-temperature analysis was amended for elevated-temperature analysis by using a coupled temperature-displacement element type. The models incorporate non-uniform temperature distribution history for each connection component, in addition to material and geometric non-linearity and contact interaction. This chapter has presented the results of an evaluation study of the steel beam FE modelling to analyse the large-deflection behaviour and catenary action of steel beams at elevated temperatures, with or without axial restraint, and has demonstrated the accuracy of the connection-beam FE model. The following main conclusions may be drawn:

- Axially restrained beams have successfully been modelled and validated to predict the large deflection and catenary action at high temperatures.
- This chapter complements the work of others by documenting and demonstrating beam behaviour at elevated temperature. However, in this study 3D solid brick elements were used, unlike previous studies which utilized beam elements (VULCAN) or shell elements to study the large-deflection and catenary action phenomena in heated steel beams.
- A fin plate connection-beam model suitable for parametric study at high temperatures has been accurately created.
- The accuracy of the FE model for reproducing the experimental behaviour of steel joints in fire conditions makes it a strong and cost-effective tool for both analytical and parametric studies, which may lead to improvements in joint configuration and joint performance.
- Chapter 4 made a distinction between plate bearing and bolt shearing failure modes' and emphasised that a bolt inevitably shears when the fin plate thickness, web thickness and bolt radius are the same. This is basically the observed behaviour of the fin plate connection in the Czech fire test, when a combination of plate thickness of 6 mm and beam web thickness of 5.8 mm were used together with 12 mm diameter bolts. The complete shearing of the bolts in the fire test reveals how fragile bolts can be at elevated temperatures.

5.7. References

[5.1] Liu, T. C. H., Fahad, M. K. and Davies, J. M. "Experimental investigation of behaviour of axially restrained steel beams in fire", *Journal of Constructional Steel Research*, Vol. **58**, (2002) pp 1211-1230.

[5.2] Bailey, C. G., Lennon, T., and Moore, D. B. "The behaviour of full-scale steel-framed buildings subjected to compartment fire", *The Structural Engineer*, Vol. **77**, No. 8, (1999) pp15-21.

[5.3] Yin, Y.Z. and Wang, Y.C. "A numerical study of large deflection behaviour of restrained steel beams at elevated temperatures", *J. Construct. Steel Research*, Vol. **60**, (2004) pp 1029–1047.

[5.4] ABAQUS (2004), *Standard User's Manual, Version 6.5*, Hibbitt, Karlsson & Sorensen Inc.

[5.5] European Committee for Standardization (CEN), "Eurocode 3: Design of Steel Structures, Part 1.2: General rules - Structural fire design", EN 1993-1-2, British Standard Institution, London, (2005).

[5.6] Robinson, J. "Fire - A Technical Challenge and a Market Opportunity", *J. Construct. Steel Research*, Vol. **46**, Pager No. 179, (1998).

[5.7] Johnson, P. F. "International Developments in Fire Engineering of Steel Structures", *J. Construct. Steel Research*, Vol. **46**, Pager No. 415, (1998).

[5.8] Newman, G. M., Robinson, J. T., and Bailey, C. G. "Fire Safety Design: A New Approach to Multi-storey Steel Framed Buildings", SCI Publication 288, The Steel Construction Institute, (2000).

[5.9] Martin, D. M., and Moore, D. B. "Introduction and Background to the Research Programme and Major Fire Tests at BRE Cardington", *Proceedings of the National Steel Construction Conference*, London, (1997).

[5.10] Buchanan, A., Moss, P., Seputro, J., and Welsh R. "Effect of Support Conditions on the Fire Behaviour of Steel Beams", *Engineering Structures*, under review, (2002).

[5.11] Wald, F., Strejcek, M., Ticha, A., "On bolted connection with intumescent coatings", *Proceedings of the fourth International Workshop Structural in Fire*, Aveiro, Portugal, (2006). pp 371-22.

[5.12] BRITISH STEEL CORPORATION, Compendium of UK Standard Fire Test Data on Unprotected Structural Steel. Contract Report for Department of Environment, Ref. No. RS/RSC/S10328/1/87/B, Marc, (1987).

[5.13] Burgess, I. W., El Rimawi, J., and Plank, R. J., "A Secant Stiffness Approach to the Fire Analysis of Steel Beams", *J. Construct. Steel Research*, Vol. **11**, (1988) pp 105-120.

[5.14] Burgess, I. W., El Rimawi, J., and Plank, R. J., "Analysis of Beams with Non-uniform Temperature Profile", *J. Construct. Steel Research*, Vol. **16**, (1990) pp 169-192.

[5.15] Burgess, I. W., El Rimawi, J., and Plank, R. J., "Studies of the Behaviour of Steel Beams in Fire", *J. Construct. Steel Research*, Vol. **19**, (1991) pp 285-312.

[5.16] El-Rimawi, J. A., Burgess, I. W., and Plank, R. J., "The Influence of Connection Stiffness on the Behaviour of Steel Beams in Fire", *J. Construct. Steel Research*, Vol. **43**, (1997) pp1-15.

[5.17] El-Rimawi, J. A., "The Behaviour of Flexural Members under Fire Conditions", PhD. thesis of the University of Sheffield, Sheffield, 1989.

[5.18] http://www.vulcan-solutions.com/index.

[5.19] Saab, H.A., "Nonlinear finite element analysis of steel frames in fire", PhD. thesis of the University of Sheffield, Sheffield, 1990.

[5.20] Najjar, S.R., "'Three-dimensional analysis of steel frames and subframes in fire", PhD. thesis of the University of Sheffield, Sheffield, 1994.

[5.21] Bailey, C.G., "Simulation of the structural behaviour of steel framed buildings in fire", PhD. thesis of the University of Sheffield, Sheffield, 1995.

[5.22] Allam, A. M., Burgess, I. W. and Plank, R. J., "Simple Investigations of Tensile Membrane Action in Composite Slabs Fire", Paper 03.02, *Proceedings of the International Conference on Steel Structures of the 2000s*, Istanbul, Turkey, (2000) pp327-332.

[5.23] Allam, A. M., Burgess, I. W. and Plank, R. J., "Performance-Based Simplified Model for a Steel Beam at Large Deflection in Fire", *Proceedings 4th International Conference on Performance-Based Codes and Fire Safety Design Methods*, Melbourne, Australia, (2002).

[5.24] Allam, A. M., Green, M. G., Burgess, I. W., and Plank, R. J., "Fire Engineering Design of Steel-Framed Structures - Integration of Design and Research", Second World Conference on Constructional Steel Design, San Sebastian, *J. Construct. Steel Research*, Vol. **46**, Pager No. 170, (1998).

[5.25] Yin, Y.Z. and Wang, Y.C., "Analysis of Catenary action in steel beams using a simplified hand calculation method, Part 1: theory and validation for uniform temperature distribution", *J. Construct. Steel Research*, Vol. **61**, (2005) pp 183–211.

[5.26] Yin, Y.Z. and Wang, Y.C., "Analysis of Catenary action in steel beams using a simplified hand calculation method, Part 2: validation for non-uniform temperature distribution", *J. Construct. Steel Research*, Vol. **61**, (2005) pp 213–234.

[5.27] British Standards Institute. BS 476: "Fire Tests on Building Materials and Structures, Part 21: Methods for Determination of the Fire Resistance of Load-Bearing Elements of Construction", (1987).

[5.28] Wald, F., Simoes da Silva, L., Moore, D., and Santiago, A. Lennon T, Chaldna M, Santiago M, et al., "Experimental behaviour of a steel joints under natural fire", *Fire Safety Journal*, Vol. **41**, (2006) pp 509-22.

Chapter 6

Component Method Model

6.1. Introduction

Inclusion of the real behaviour of connections in structural design leads to reduction in both beam moments and beam deflections' and may result in an overall improvement in design efficiency. In order to integrate the semi-rigid connection approach in the design of a steel structure, it is necessary to identify the joint characteristics, (stiffness, resistance, shear capacity, ductility). These joint characteristics can be established by experimental testing or mathematical modelling according to the geometrical and mechanical properties of the joint. Full-scale experimental testing is naturally the most reliable method to describe the rotational behaviour of structural joints. However, it is time consuming, expensive, and can not be considered as a design tool. Also, joint testing data are limited, and in general restricted to certain connection details; therefore the results cannot be extended to different joint configurations. Nevertheless, tests provide accurate information on the connection response which is crucial to validate any proposed mathematical models for the prediction of the moment-rotation and/or load-deflection connection response under any corresponding actions. Many mathematical modelling approaches [6.1] can be applied to represent the connection behaviour; some of these methods are as follows:

i) Curve fitting to test results.
ii) Simplified analytical models.
iii) Numerical models.
iv) Component models.

Because of the nonlinear interaction of joint loads and the large number of possible variables in the detailed design of a bolted joint, the component method is believed to be the most effective solution to predict the complex bolted joint behaviour with sufficient accuracy. The Component Method was initially developed by

Tschemmernegg *et al.* [6.2, 6.3] and later introduced into Eurocode 3 Part 1.8 [6.4]. Primarily, the method was developed to predict the moment-rotation behaviour of semi-rigid moment connections, but gradually it has been extended to express the joint overall response (rotational, shear and axial stiffness) and also the capacity of joints. The original feature of this method was based on investigating each connection component (tension, compression, and shear) independently to determine its characteristics (stiffness, strength) by means of nonlinear or bilinear load-deflection curves. Then, modelling a joint as an assembly of these components in an appropriate mechanical spring model with rigid links, the connection overall behaviour at ambient and elevated temperatures can be expressed. In structural fire analysis, each component will have its own temperature-dependent load-displacement curve, and the whole joint will therefore interact realistically with the surrounding structure.

In the last decade the component method approach has gradually gained great popularity simply because of the advantages it offers over the other analytical methods. For instance, it may apply to any joint type, different connection configurations and loading conditions provided that the description of the load-deflection curve of each component is properly characterized. Basically, the method consists of three basic steps [6.5]:

i) Identification of the active components for a given joint.
ii) Characterization of the load-deflection response of each individual component.
iii) Assembly of the joint mechanical model, which is made up of extensional springs and rigid links **(Figure 6.1-b)**. This spring assembly is used to describe the full joint behaviour.

The method is illustrated in **Figure 6.1** for the particular case of a bolted fin plate connection with three bolt lines. The active joint components for this configuration, according to Eurocode 3 [6.4], are: fin plate in bearing, beam web in bearing, bolts in single shear, beam web-to-fin plate in friction, and weld in tension. Also, if a large rotation occurs then the column flange in compression is another component to be considered.

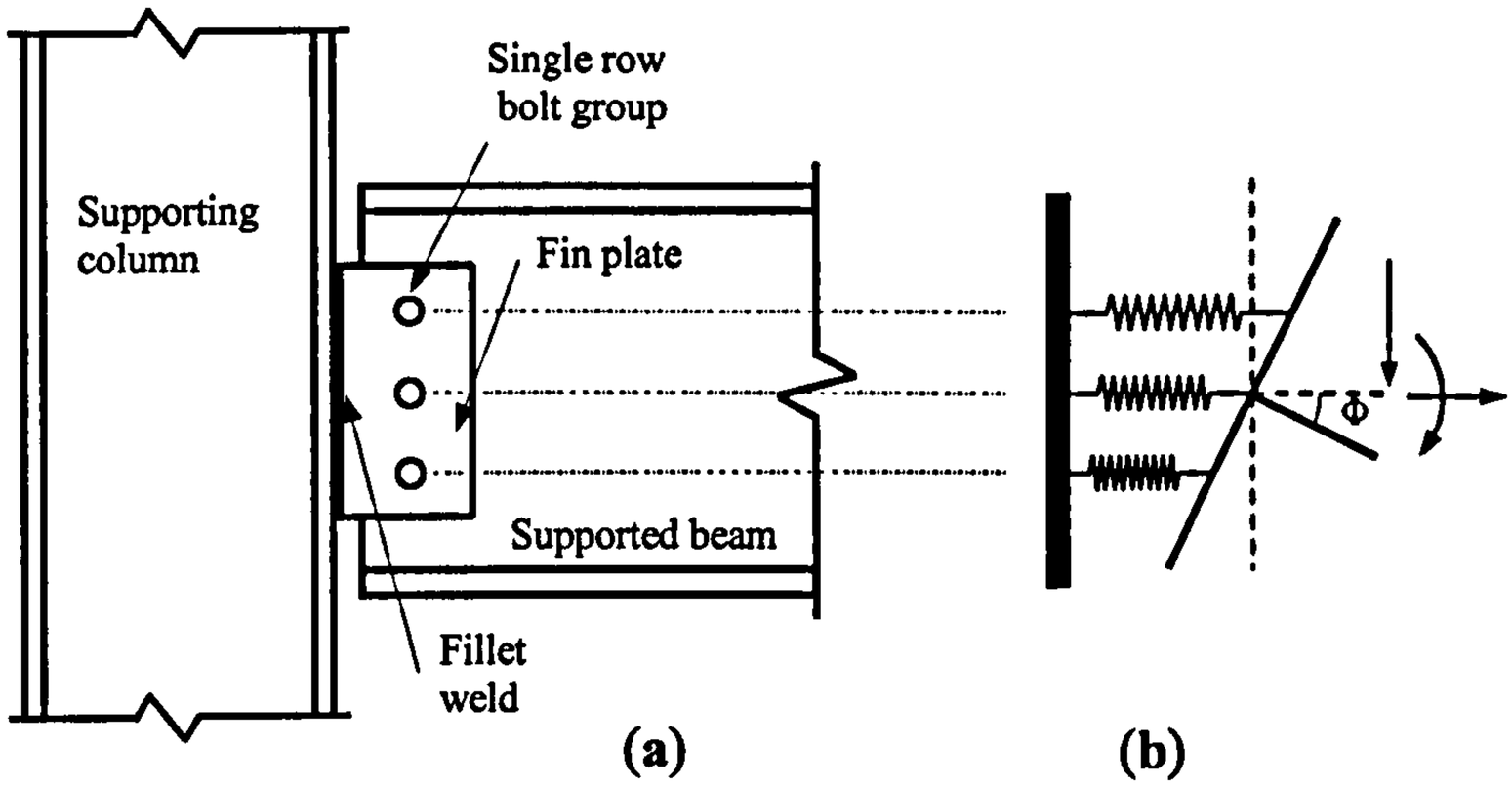

Figure 6.1 Fin plate connection equivalent component model

6.2. Plate Bearing Component

A research programme conducted by Rex [6.6] conducted detailed investigations on the plate bearing component. In this research, 48 tests were conducted on a single bolt bearing onto a single plate **(Figure 6.2)**. A number of parameters were varied in the experimental programme, such as end distance, plate width, plate thickness, and bolt size. The main difference between the test set up and the complete joint configuration is that the nut was not fully tightened because of the 51 mm gap between the cover plates **(Figure 6.2)**.

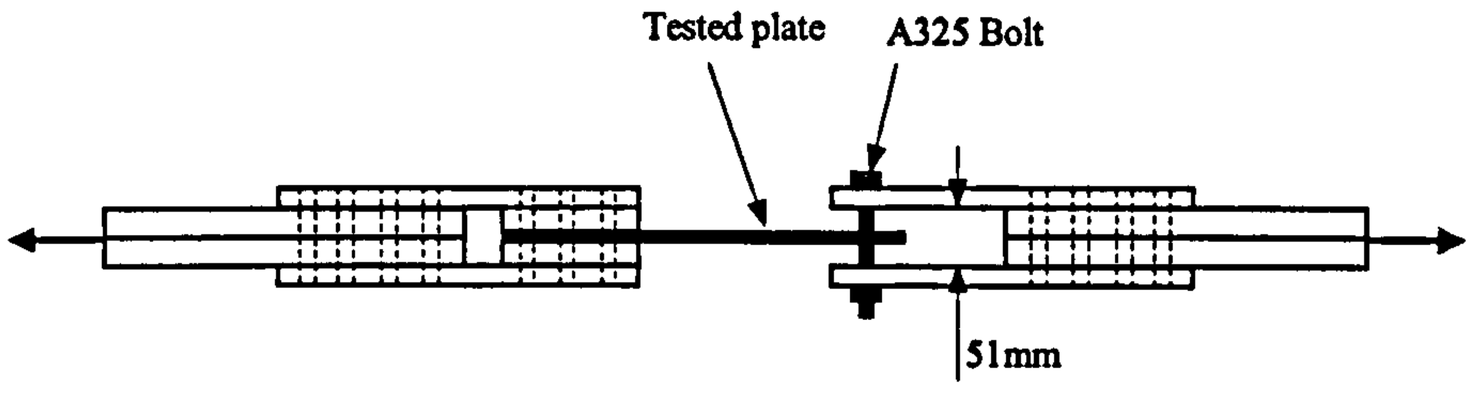

Figure 6.2 Rex test set up

Rex then used the Richard non-linear equation [6.7] to approximate the load-deflection behaviour for a single plate bearing against a single bolt.

$$\frac{F}{F_{b,Rd}} = \frac{1.74\ \bar{\Delta}}{\left(1 + \bar{\Delta}^{0.5}\right)^2} - 0.009\ \bar{\Delta} \qquad (6.1)$$

Where F is plate load [N]; $F_{b,\,Rd}$ is nominal plate strength [N]; $\bar{\Delta}$ is normalized deformation ($\bar{\Delta} = \Delta\,\beta\,K_i / F_b$) ; Δ is hole elongation [mm]; β is steel correction factor (β = 30% / %Elongation) (for typical steels taken as one); and K_i is initial stiffness [N/mm] **(Equ. 6.2)**.

Initial stiffness $$K_i = \frac{1}{\frac{1}{K_{br}} + \frac{1}{K_b} + \frac{1}{K_V}} \qquad \textbf{(6.2)}$$

Bearing stiffness $$K_{br} = 120\,t_p\,f_y\,(d_b/25.4)^{0.8} \qquad \textbf{(6.3)}$$

Bending stiffness $$K_b = 32\,E\,t_p\,(e_2/d_b - 0.5)^3 \qquad \textbf{(6.4)}$$

Shearing stiffness $$K_V = 6.67\,G\,t_p\,(e_2/d_b - 0.5) \qquad \textbf{(6.5)}$$

With regard to the plate strength $F_{b,\,Rd}$ two expressions are included in the American LRFD [6.8, 6.9] code, and another one in the Eurocode 3 [6.4], as follows:

LRFD 1993 [6.8] bearing strength $$F_{b,\,Rd} = \frac{e_2}{d_b} \times f_u \times d_b \times t \qquad \textbf{(6.6)}$$

LRFD 1999 [6.9] bearing strength $$F_{b,\,Rd} = 1.2 \times \frac{e_2 - 0.5d_b}{d_b} \times f_u \times d_b \times t \qquad \textbf{(6.7)}$$

Eurocode 3 [6.4] bearing strength $$F_{b,\,Rd} = \frac{2.5}{3} \times \frac{e_2}{d_h} \times f_u \times d_b \times t \qquad \textbf{(6.8)}$$

It has been proven by Rex [6.6] that the plate bearing strength provided in the LRFD 1993 **(Equ. 6.6)** seems to provide the best correlation to the test result with only 10% difference. However, the plate bearing strength presented in the LRFD 1999 **(Equ. 6.7)** shows 30% difference against the test data, and to the Eurocode 3 [6.4] equation **(Equ. 6.8)** shows 11% difference. Also Eurocode 3 [6.4] has proposed an expression for calculating bearing stiffness **(Equ. 6.9)**.

Bearing stiffness $$K_i = 24\,k_b\,k_t\,d_b\,F_u \qquad \textbf{(6.9)}$$

Where as $$k_b = e_2/(4\,d_b) + 0.5 \leq 1.25 \qquad \textbf{(6.10)}$$

$$k_t = 1.5\,t_p/d_{m16} \leq 2.5 \qquad \textbf{(6.11)}$$

d_{m16}: nominal diameter of a M16 bolt (16 mm)

In the current research project, the plate bearing component has been investigated via the plate bearing FE model (**Figure 3.7-a**) which was validated in the previous chapter (**3.6.1**). The main difference between this model and the previous research is that the nut was considered to be fully tightened onto the plate, so that the bolt head and nut are in complete contact with the plate's two outer surfaces. Five plate parameters were varied in order to explore their influence on the load-deflection characteristics. These are, end distance, plate thickness, plate width, the angle of bearing and plate temperature.

6.2.1. End distance

In order to investigate the end distance effect on the plate bearing behaviour seven FE models were created. Each model represents a S275 steel plate, with different end distances ranging from $2d_b$ to $7.5d_b$ (**Figures 6.3, 6.4**). The plate width was sufficiently large that net section failure would not occur. A constant plate thickness of 10 mm was assigned, also a constant bolt type; of M20 high strength Grade 8.8 installed in a 22 mm hole. The plate was clamped along one edge while the other edge, close to the bolt hole, was free. In addition, the bolt was given displacement boundary conditions in order to apply bearing stress to the hole surface towards the free edge.

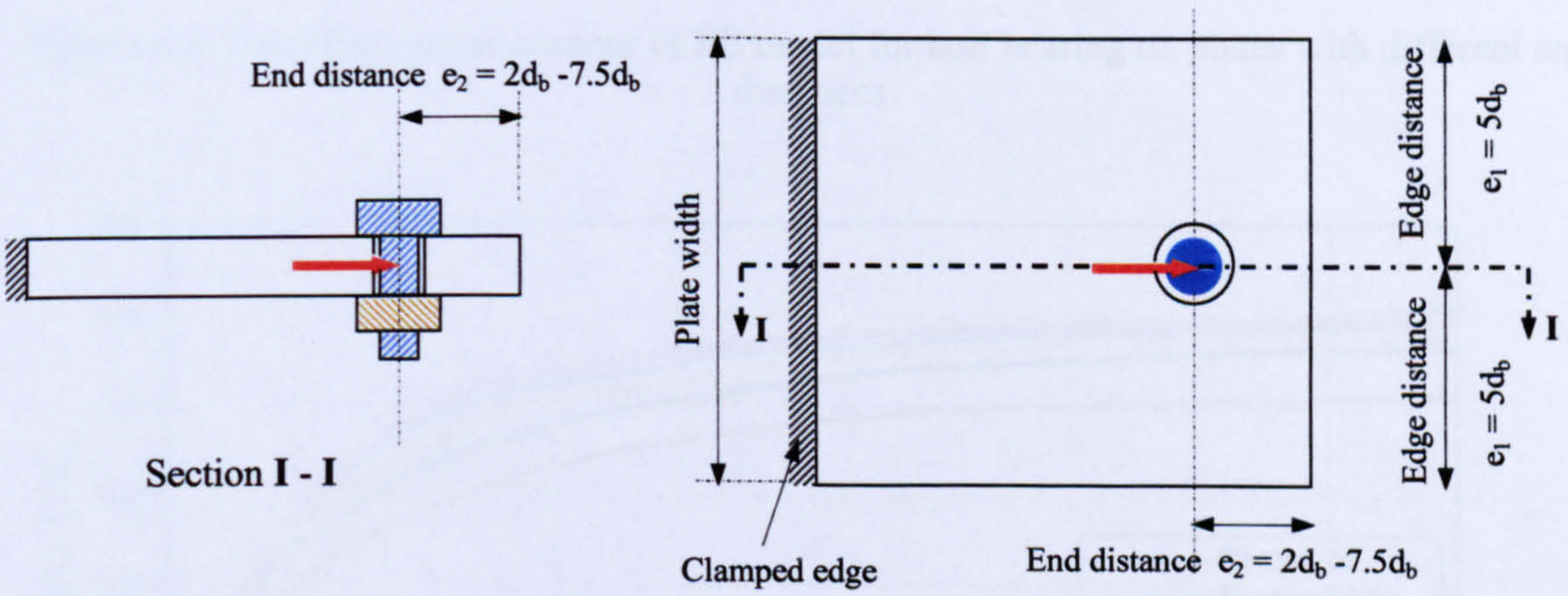

Figure 6.3 Geometrical detail of the plate studied under bolt bearing

The load against bolt movement for each case investigated was plotted on the same graph, shown as **Figure 6.5**. From of these relationships it can be observed that the ultimate bearing strength was improved gradually as the end distance increased from $2d_b$ to $3d_b$. From this value ($3d_b$), increasing the end distance shows no real influence on the ultimate bearing strength.

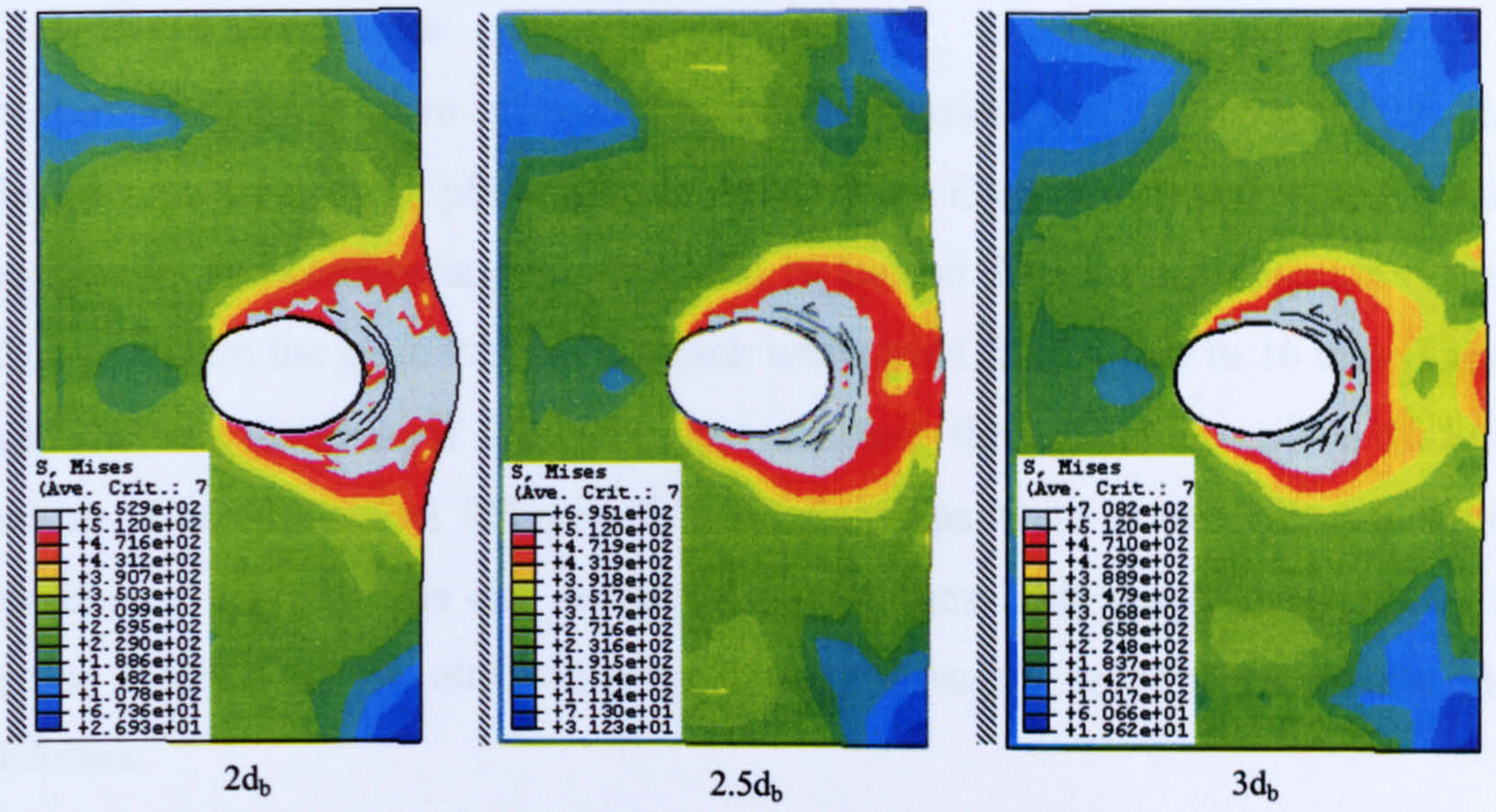

Figure 6.4 Von Mises stress contour of FE model for bolt bearing on plates with different end distances

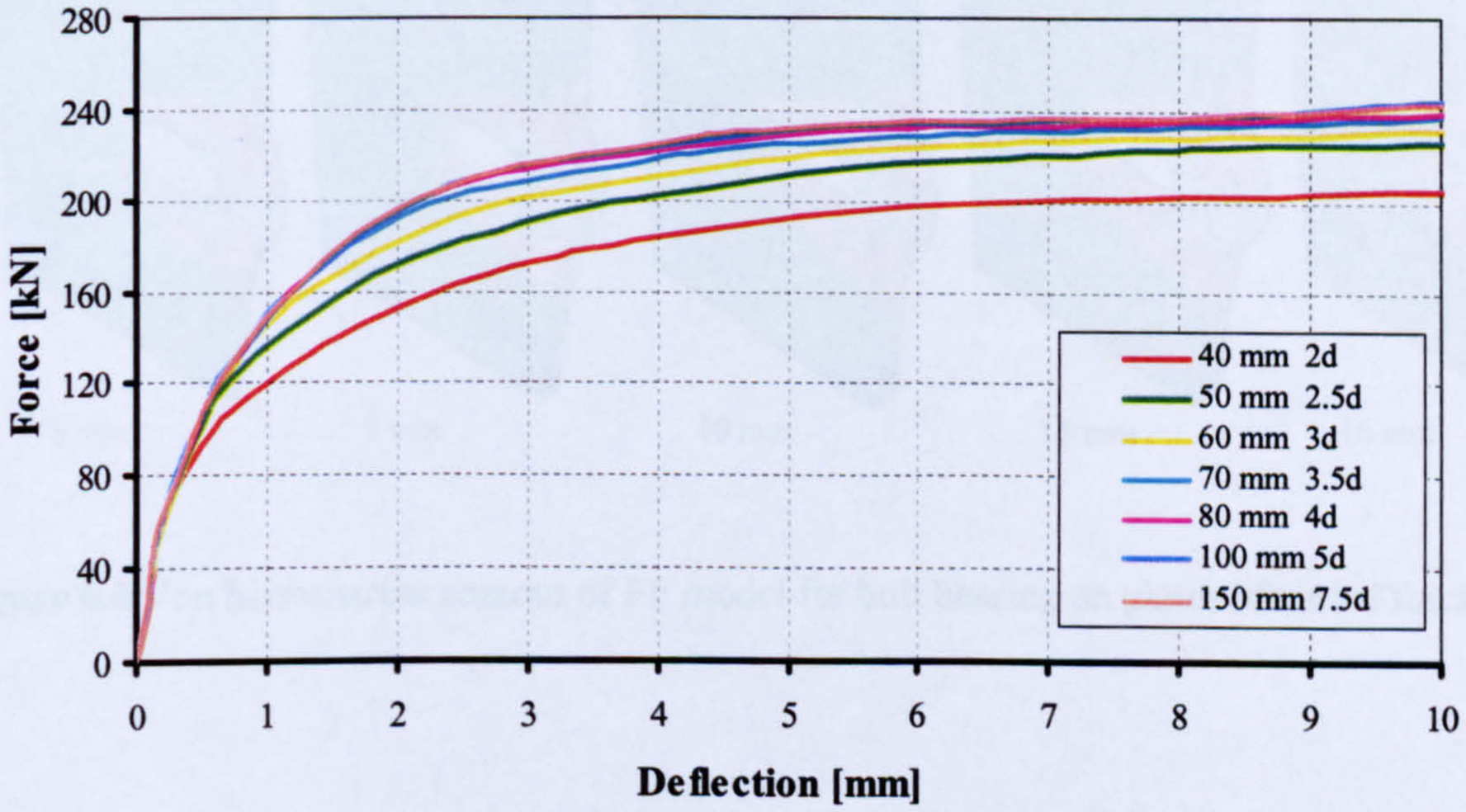

Figure 6.5 Force-deflection for plate bearing FE model with different end distances

6.2.2. Plate thickness

Thirteen FE models were processed in order to assess the influence of the plate thickness parameter on plate bearing behaviour. Each FE model has a similar arrangement and configuration to that used in the end distance investigation (**Figure 6.3**), apart from the plate thickness, which was varied from 4 mm to 16 mm (**Figure 6.6**). An end distance of $2d_b$ was kept constant throughout the plate thickness analysis. Load-deflection (**Figure 6.7**) relationships were drawn using a similar procedure to the previous end distance investigations. This graph demonstrates the regular increase in the ultimate plate bearing strength, proportional to the plate thickness.

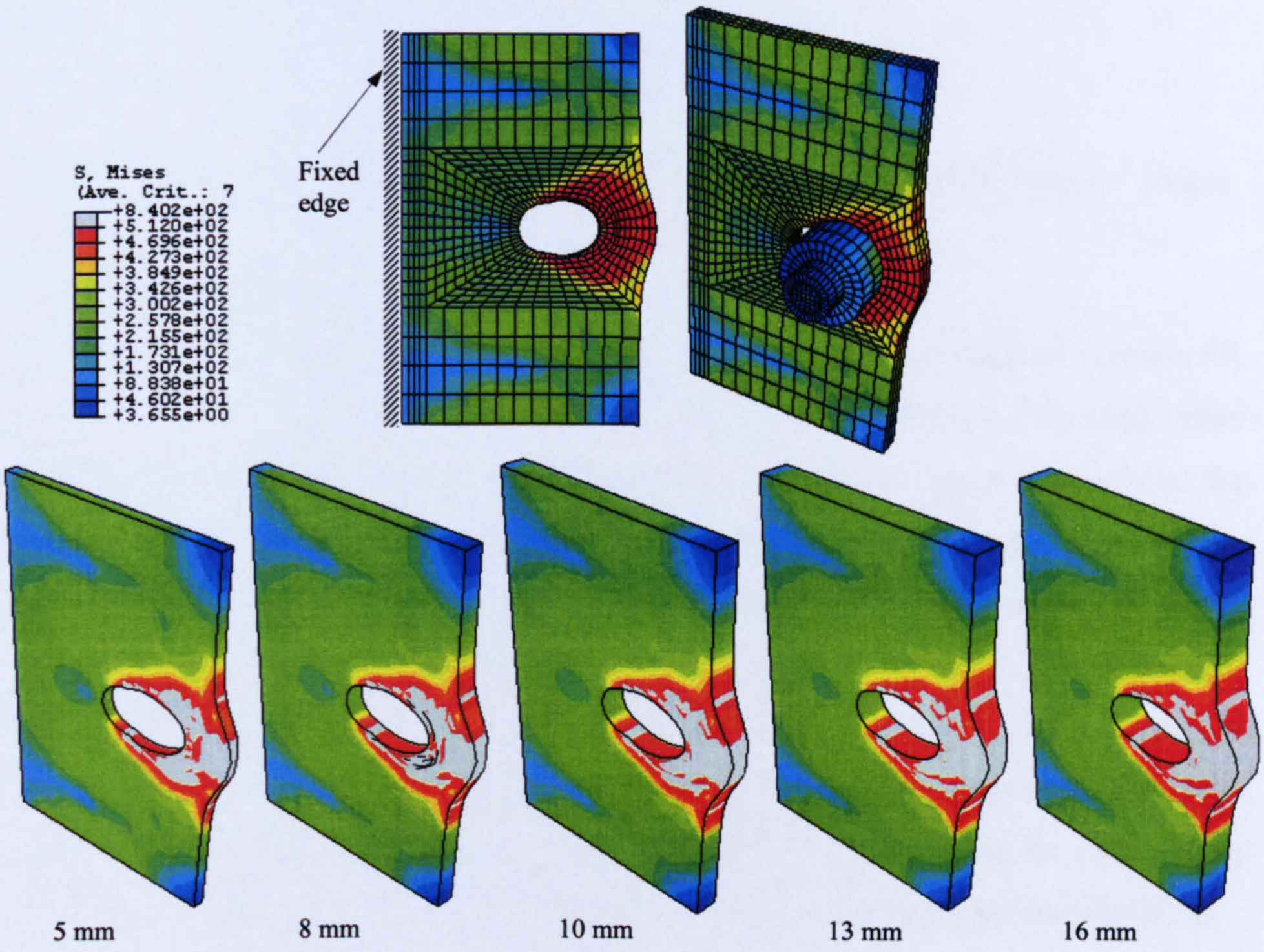

Figure 6.6 Von Mises stress contour of FE model for bolt bearing on plates of varied thickness

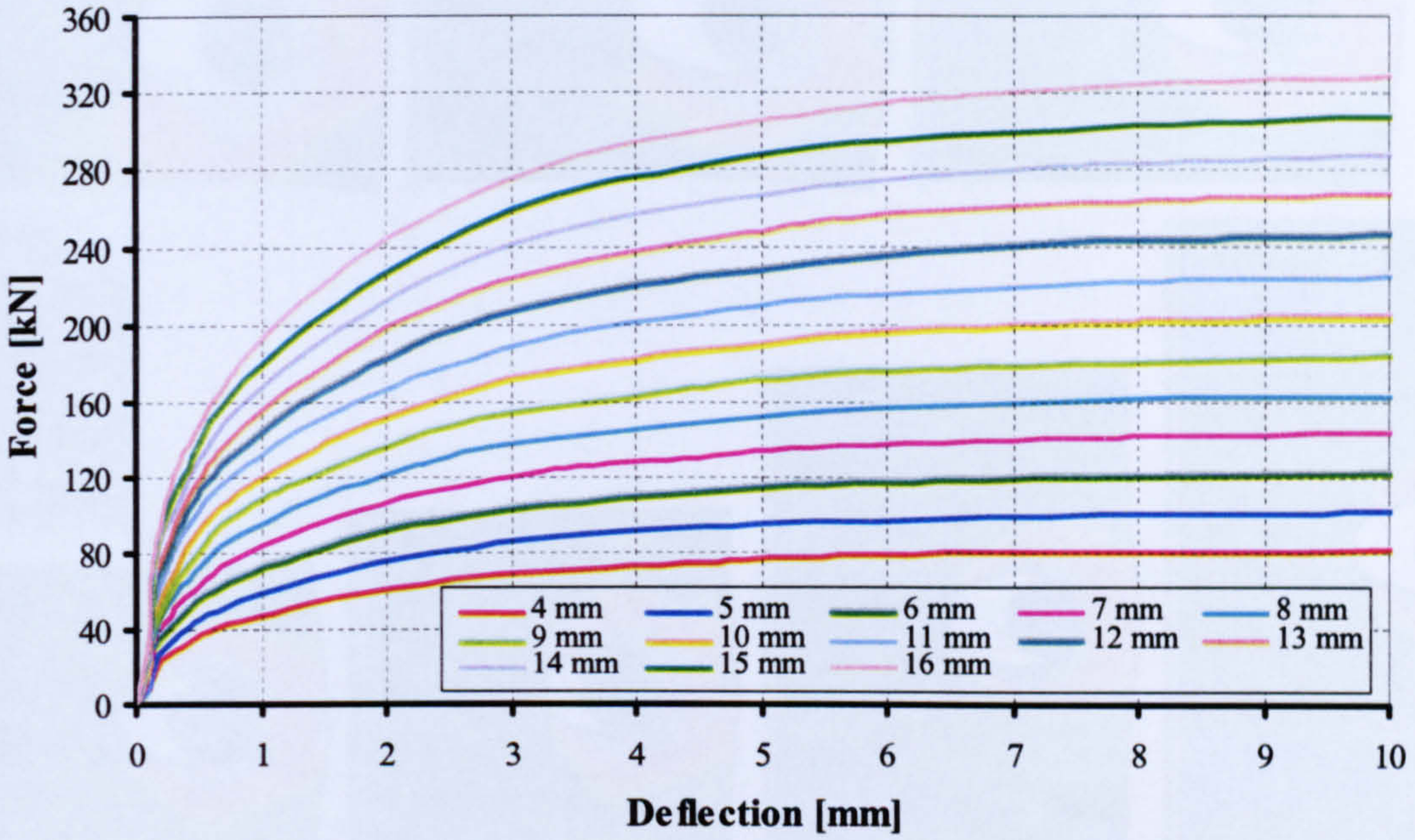

Figure 6.7 Force-deflection of bolt bearing on plates of thicknesses in the range 4 – 16 mm

6.2.3. Plate width

The effect of plate width on the plate bearing behaviour was investigated via nine FE models (**Figure 6.8**). Bolt type (M20, 8.8 bolt), plate thickness (10 mm), plate material (S275) and end distance ($2d_b$) were kept constant in these models so that the only variable in this group of models was the plate width. The edge distance in these models ranged from $1.5d_b$ – $4.5d_b$. The compressive load-deflection behaviour is presented in graph **Figure 6.9** for each FE model. Based on this graph, plate width has no significant influence on the initial stiffness of plate bearing load-deflection behaviour, but it does have a slight influence (5%) on the ultimate strength plate bearing. This finding is consistent with those of Rex [6.6]. Therefore, the plate width effect may be ignored in describing the plate bearing load-deflection characteristics.

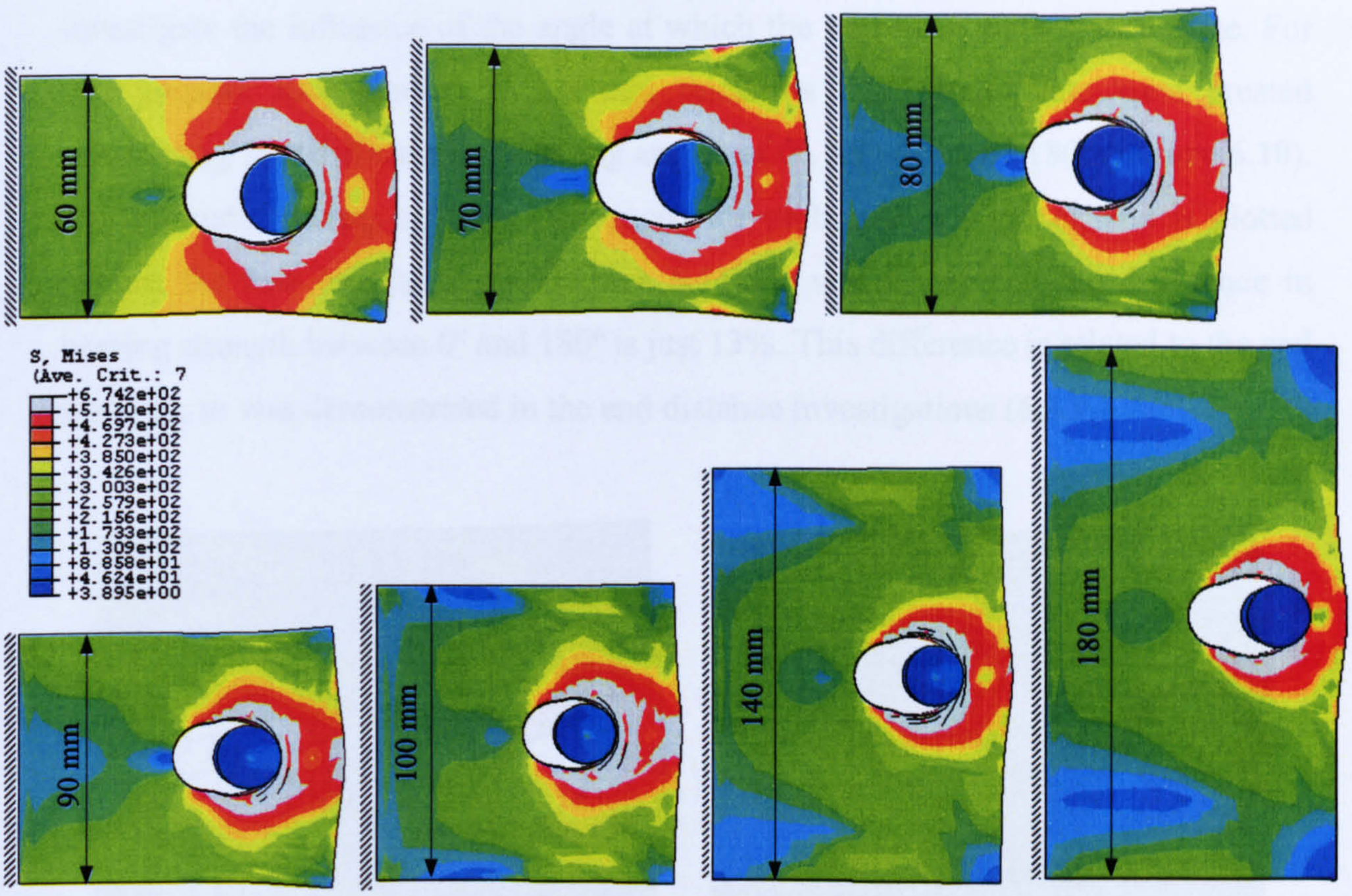

Figure 6.8 Von Mises stress contour of FE model for bolt bearing on plates of different widths

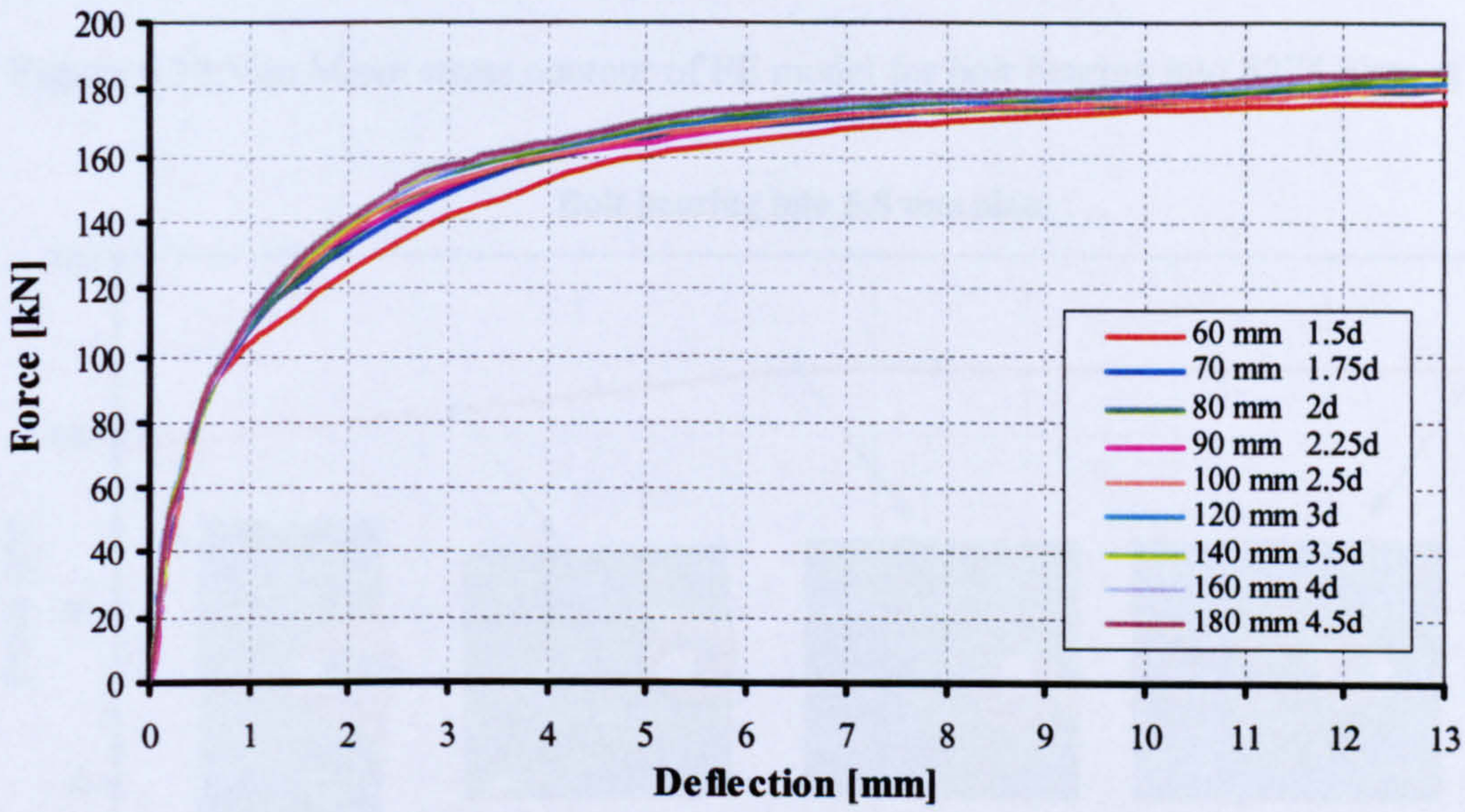

Figure 6.9 Force-deflection of bolt bearing on plates with widths in the range 60 – 180 mm

6.2.4. The angle of bolt bearing

In a fin plate connection, the direction of the bolt bearing force relative to the axis of the plate may vary depending on whether the connection is subjected to vertical shear, moment, direct tension or a combination of these. It was therefore essential to

investigate the influence of the angle at which the bolt bears onto a steel plate. For this purpose four models of 5.8 mm thickness S275 steel plate were created considering four different bolt bearing angles of 0°, 45°, 90°, and 180° (**Figure 6.10**). The ultimate bearing capacity was traced for each analysed model, and is plotted against the bolt bearing angle (**Figure 6.11**). It was found that the difference in bearing strength between 0° and 180° is just 13%. This difference is related to the end distance, as was demonstrated in the end distance investigations (**6.3.1.**).

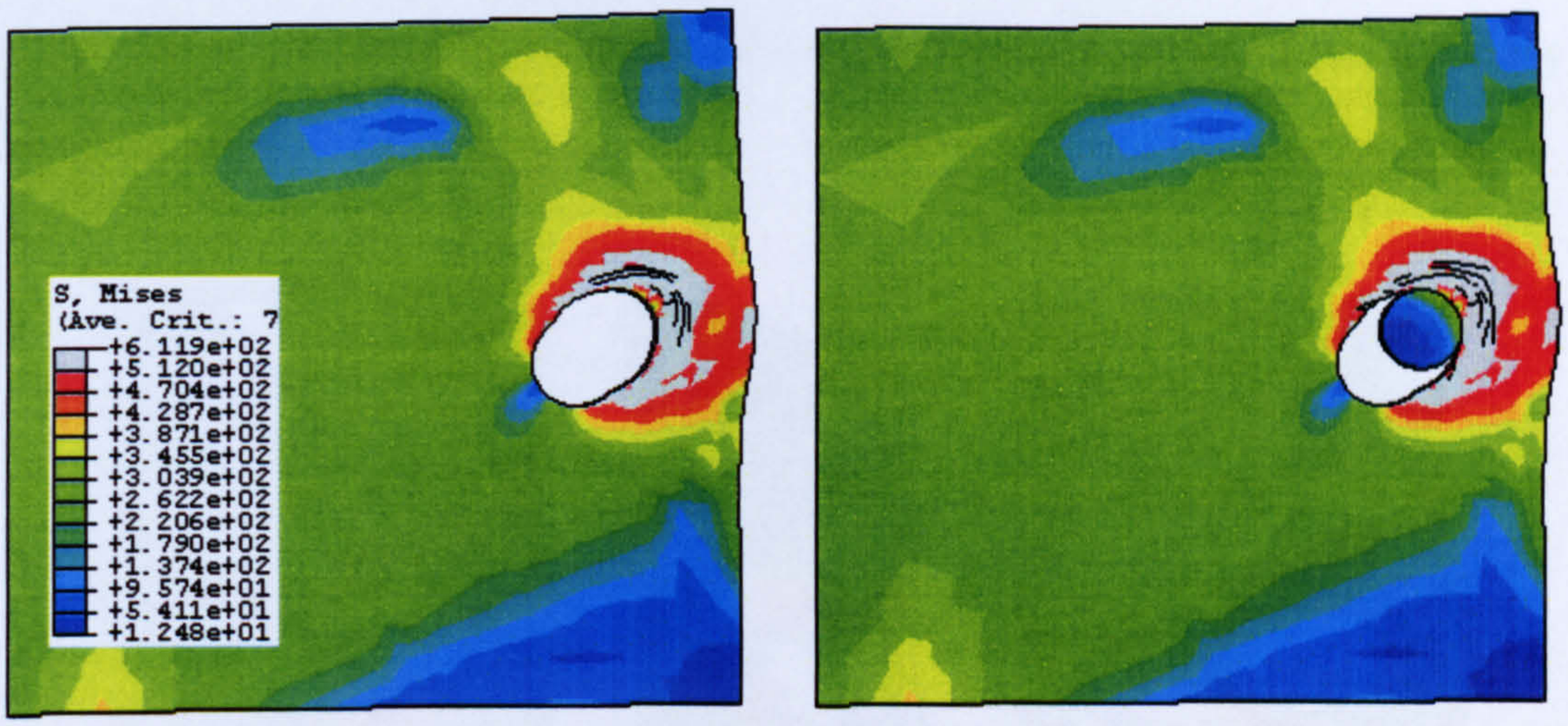

Figure 6.10 Von Mises stress contour of FE model for bolt bearing into S275 plate at 45°

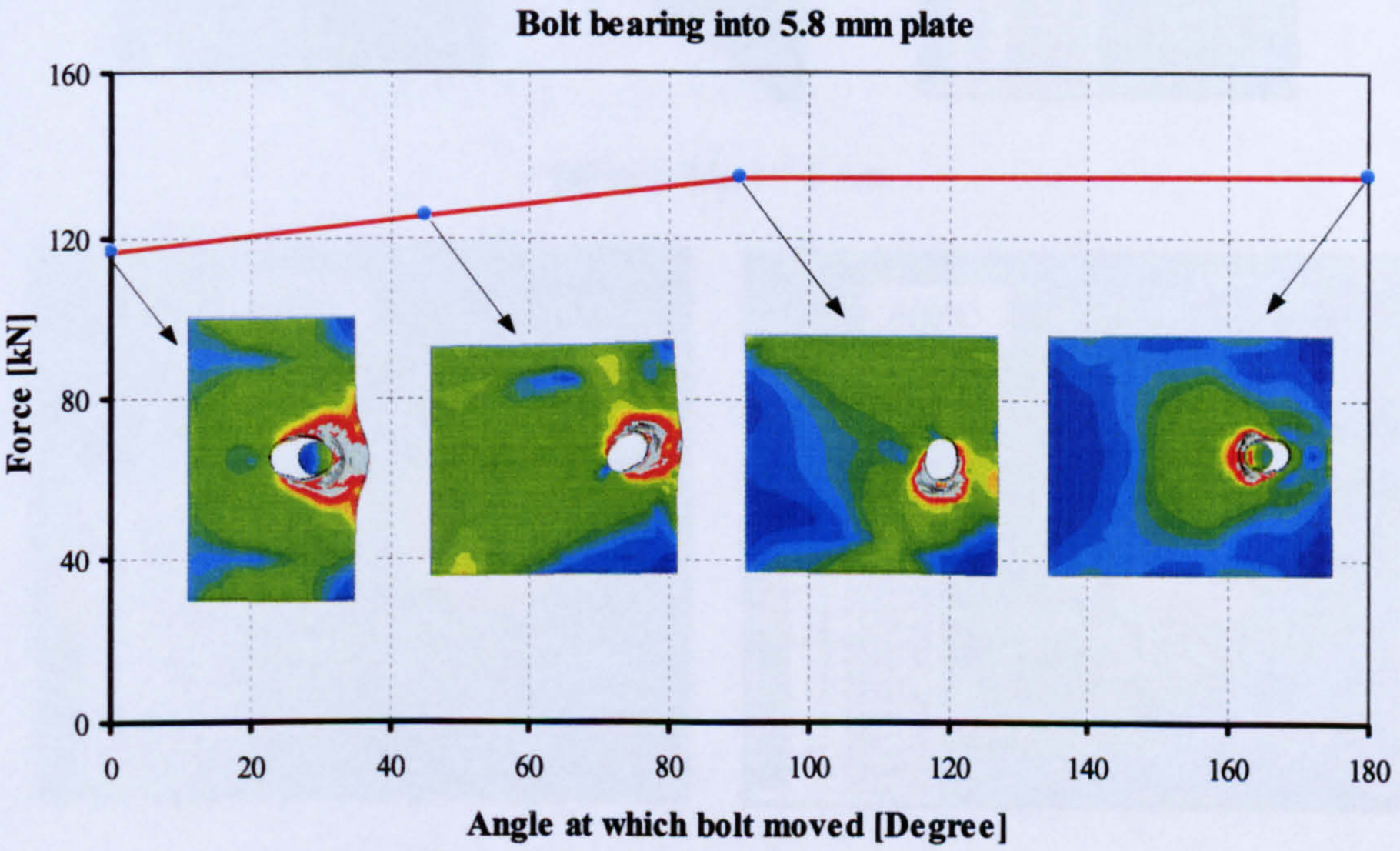

Figure 6.11 Ultimate bearing strength against bolt bearing angle

6.2.5. Plate temperature

In order to investigate the effect of temperature on the plate bearing behaviour, the FE plate bearing model (**Figure 6.12-a**) was analysed under steady state temperatures ranging from 400ºC to 800ºC. Plate thickness and end distance were kept constant at 6 mm and $2d_b$ respectively. Other cases were analysed under end distances greater than $3d_b$ (**Figure 6.12-b**) in which a constant plate thickness of 10 mm, steel material of S275 and various temperatures (400ºC to 800ºC) were implemented. A Grade 8.8 M20 bolt has been used throughout the temperature investigations. The resulting load-deflection plots are shown for each case study in **Figures 6.13**, and **6.14**.

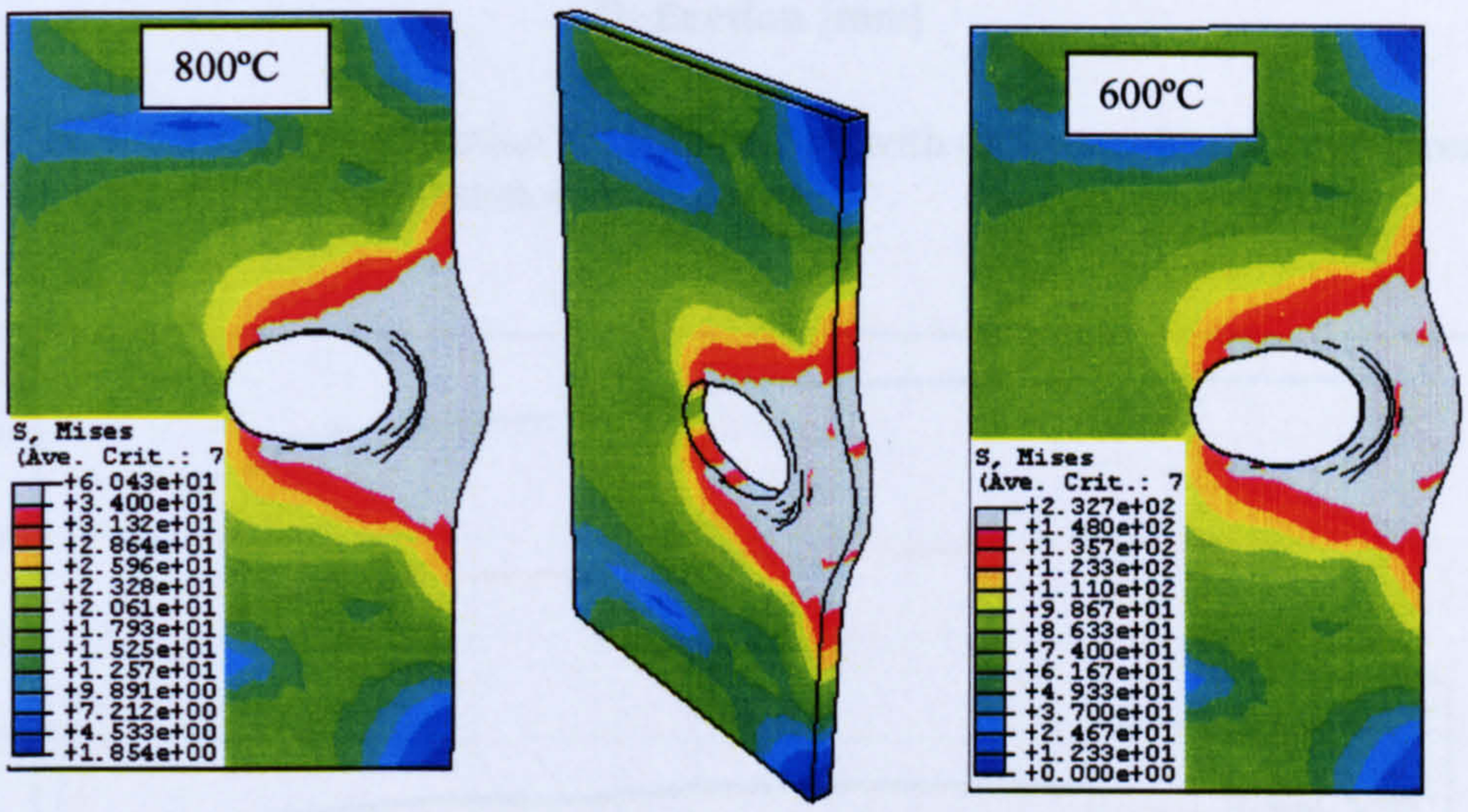

(a) $e_2 = 2d_b$, t = 6 mm

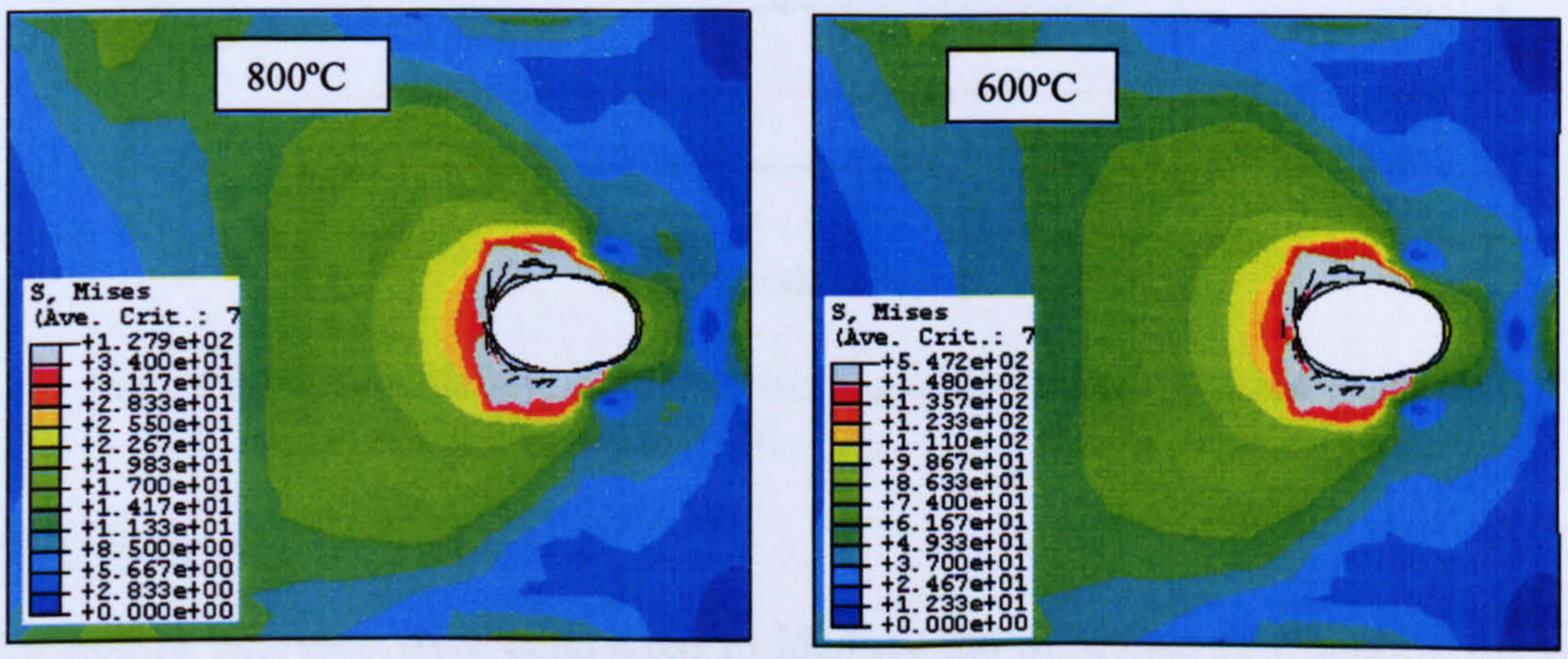

(b) $e_2 \geq 3d_b$, t = 10 mm

Figure 6.12 Von Mises stress contour of FE model for bolt bearing at different temperatures

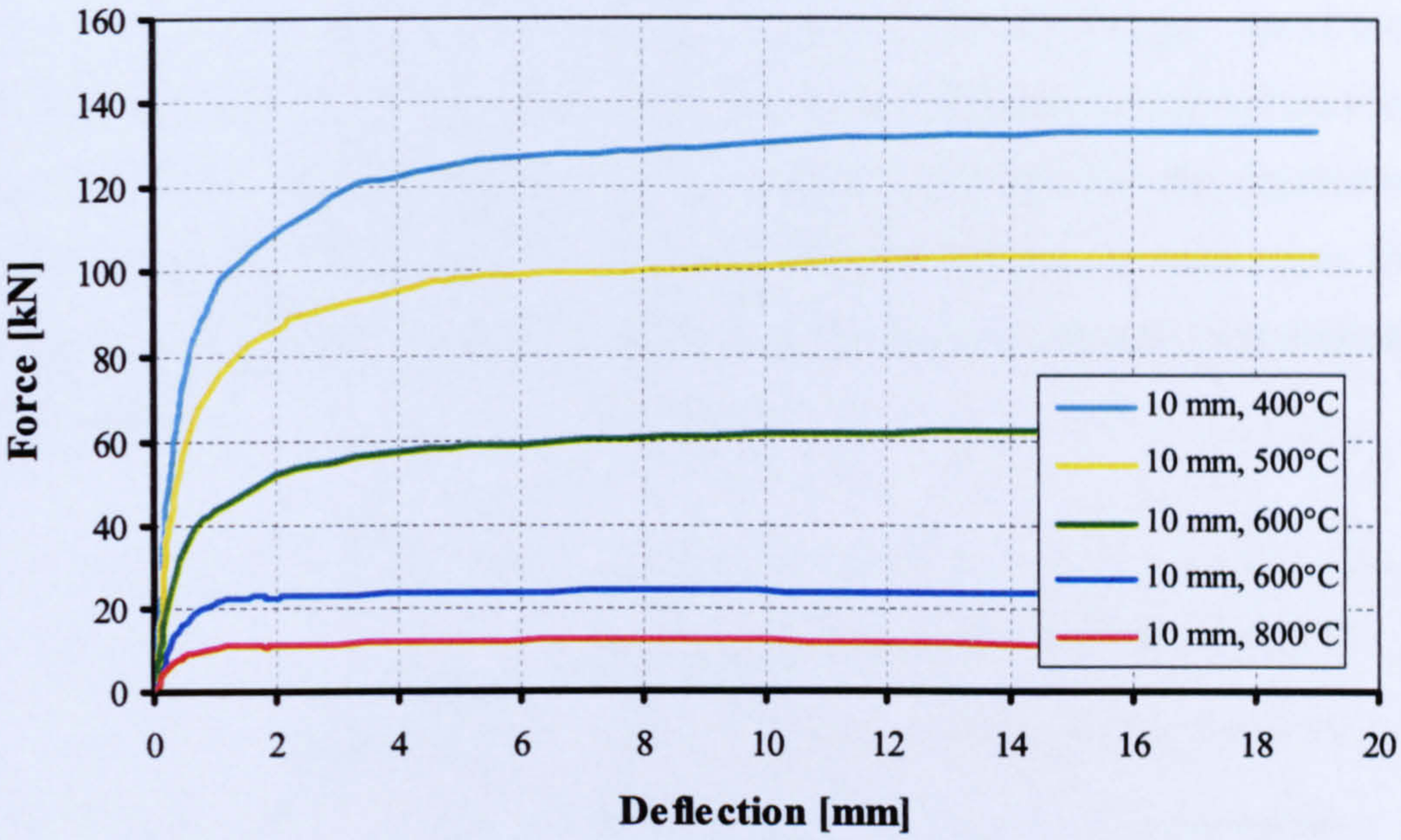

Figure 6.13 Force-deflection for bolt bearing with different plate temperatures for end distance $e_2 \leq 2d_b$

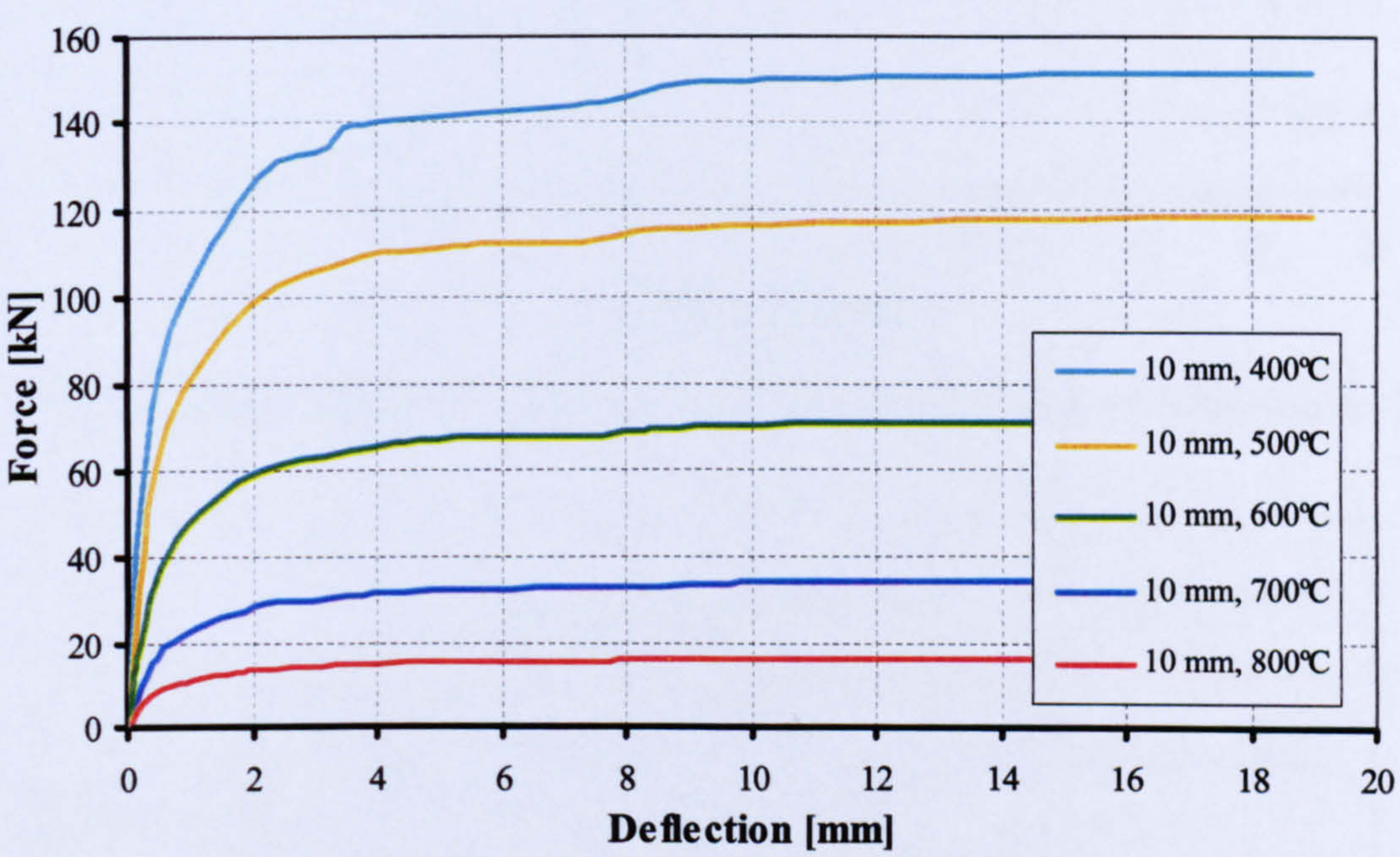

Figure 6.14 Force-deflection for bolt bearing with different plate temperatures for end distance $e_2 \geq 3d_b$

6.2.6. Bolt size

Independent analyses were conducted to identify the influence of changing the bolt size on the plate bearing component. Three FE models were created for single bolt bearing in a single S275 steel plate with constant thickness of 6 mm. Various Grade 8.8 bolt sizes were considered (M16, M20, and M24) according to BS3692 [6.10]

specifications. The end distances were also varied according to the bolt diameter. Two cases of end distance were considered, one at $2d_b$ and a larger one of more than $3d_b$. **Figure 6.15** shows the load-deflection curve for plate bearing for each bolt size bearing on the $2d_b$ end distance, whereas **Figure 6.16** presents the responses of the same bolt sizes bearing on the larger end distance ($\geq 3d_b$). In both cases the load-deflection curves show a regular increase in the bearing strength proportional to the bolt diameter.

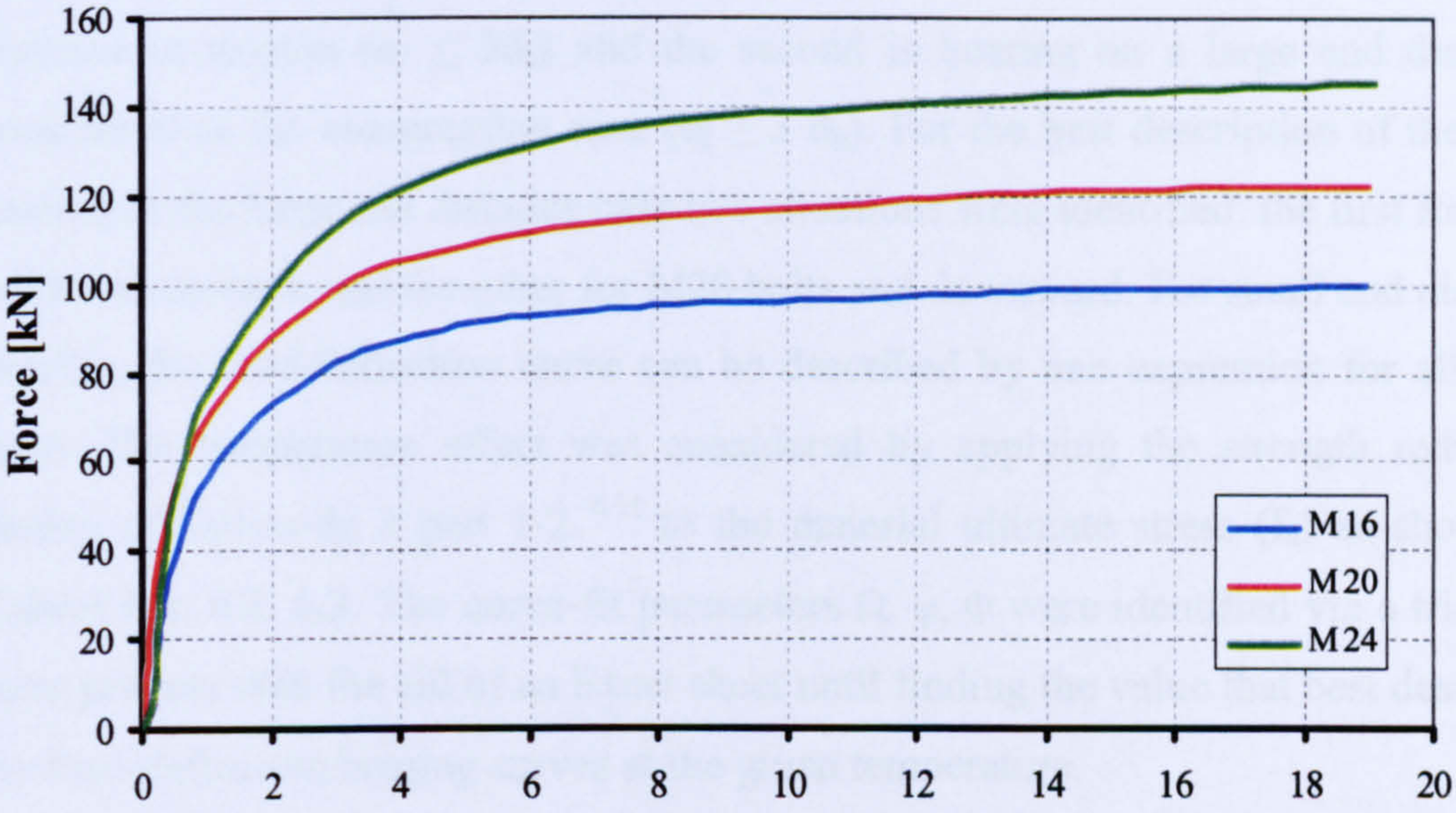

Figure 6.15 Load-deflection of various bolt sizes bearing on 5.8 mm plate with $e_2 = 2d_b$

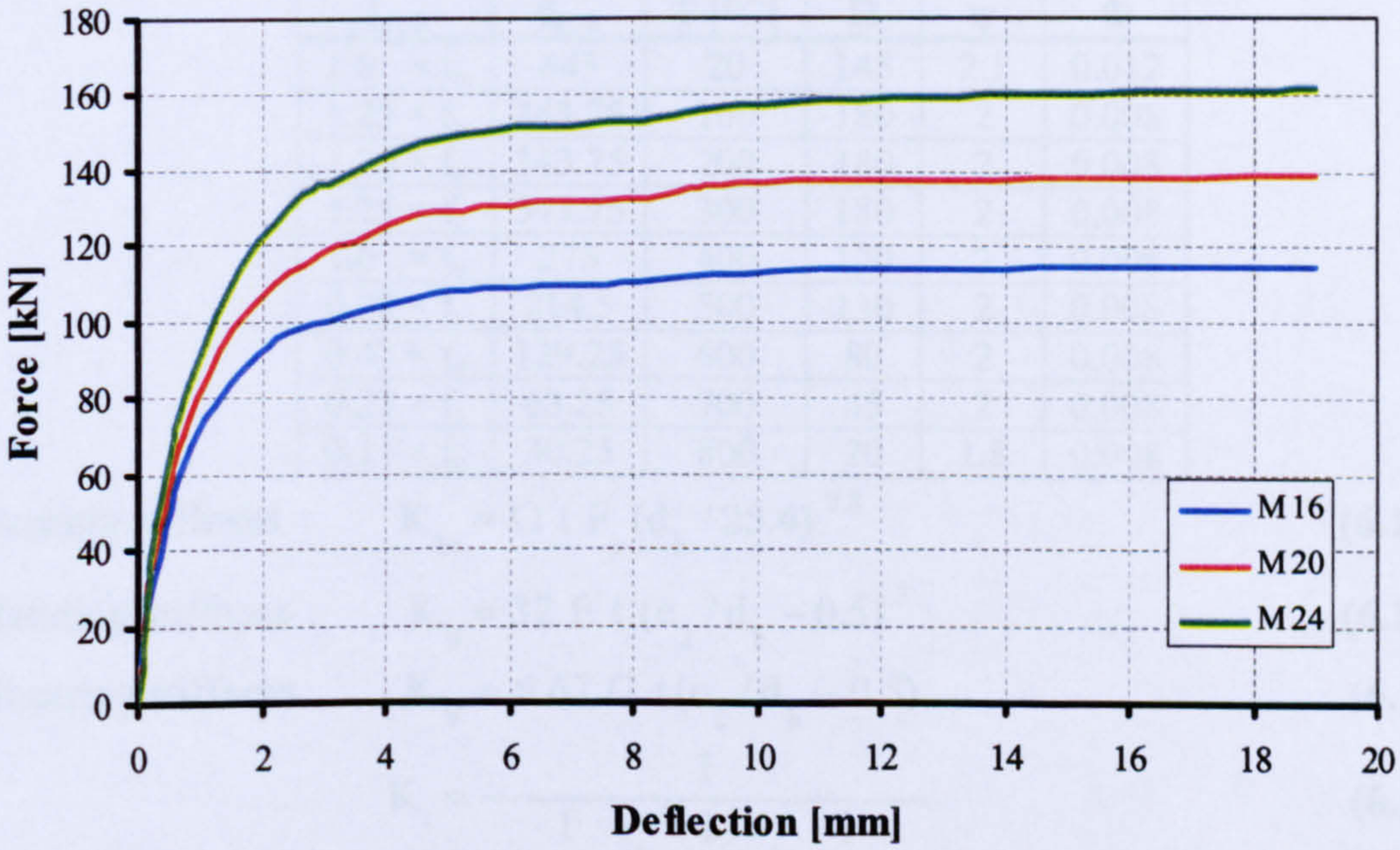

Figure 6.16 Load-deflection of various bolt sizes bearing on 5.8 mm plate with $e_2 \geq 3d_b$

6.3. Description of Plate Bearing Component

Through the previous intensive FE parametric study, various factors that influence the plate bearing behaviour were well investigated. The resulting graphs were used to produce general expressions to describe the load-deflection behaviour of plates in bearing. Eventually, after several attempts at curve fitting using different non-leaner equations, it was found that the Richard equation [6.7] **(Equ. 6.1)** was the most effective curve-fit to the plate bearing load-deflection behaviour. The process distinguishes between two cases of bearing. The first is bearing on a small end distance in tension ($e_2 \leq 2d_b$) and the second is bearing on a large end distance, considered as the compression case ($e_2 \geq 3\ d_b$). For the best description of the plate bearing in the large end distance case two situations were identified: the first for M24 bolts and upward, and the other for M20 bolts and downward. For small end distance bearing, the load-deflection curve can be described by one expression for all bolts sizes. The temperature effect was considered by applying the strength reduction factors of Eurocode 3 part 1-2 [6.11] to the material ultimate stress (f_u) as shown in **Tables 6.1, 6.2, 6.3**. The curve-fit parameters Ω, ψ, Φ were identified via a trial and error process with the aid of an Excel sheet until finding the value that best described the load-deflection bearing curves at the given temperature.

- **Bearing in small end distance case ($e_2 \leq 2d_b$) for all sizes of bolt (Tension)**

Table 6.1 Curve fitting parameters corresponding to the analysed temperature ($e_2 \leq 2d_b$), all bolt sizes.

$f_{u,\theta}$	$f_{u,\theta}$	T [°C]	Ω	ψ	Φ
$1.0 \times f_u$	445	20	145	2.1	0.012
$1.25 \times f_y$	343.75	100	180	2	0.008
$1.25 \times f_y$	343.75	200	180	2	0.008
$1.25 \times f_y$	343.75	300	180	2	0.008
$1.0 \times f_y$	275	400	170	2	0.008
$0.78 \times f_y$	214.5	500	130	2	0.008
$0.47 \times f_y$	129.25	600	80	2	0.008
$0.23 \times f_y$	63.25	700	45	2	0.008
$0.11 \times f_y$	30.25	800	20	1.8	0.008

Bearing stiffness $$K_{br} = \Omega\ t\ F_y (d_b / 25.4)^{0.8} \quad \textbf{(6.12)}$$

Bending stiffness $$K_b = 32\ E\ t\ (e_2 / d_b - 0.5)^3 \quad \textbf{(6.13)}$$

Shearing stiffness $$K_V = 6.67\ G\ t (e_2 / d_b - 0.5) \quad \textbf{(6.14)}$$

$$K_i = \frac{1}{\frac{1}{K_{br}} + \frac{1}{K_b} + \frac{1}{K_V}} \quad \textbf{(6.15)}$$

$$\frac{F}{F_{b,rd}} = \frac{\psi\ \overline{\Delta}}{\left(1 + \overline{\Delta}^{0.5}\right)^2} - \Phi\ \overline{\Delta} \qquad (6.16)$$

$$\overline{\Delta} = \Delta\ \beta\ K_i / F_{b,rd} \qquad (6.17)$$

$$F_{b,Rd} = \frac{e_2}{d_b} \times f_u \times d_b \times t \qquad (6.6)$$

- **Bearing in large end distance case ($e_2 \geq 3\ d_b$) for M24 bolt (compression)**

In this case e_2 is set at $3 \times d_b$ for calculating $F_{b,Rd}$ only.

$$F_{b,Rd} = 0.92 \times \frac{e_2}{d_b} \times f_u \times d_b \times t \qquad (6.18)$$

Table 6.2 Bearing curve fit parameters corresponding to analysed temperature ($e_2 \geq 2d_b$), M24 bolt.

$f_{u,\theta}$	$f_{u,\theta}$	T [°C]	Ω	ψ	Φ
$1.0 \times f_u$	445	20	250	1.7	0.011
$1.25 \times f_y$	343.75	100	250	1.7	0.011
$1.25 \times f_y$	343.75	200	250	1.7	0.011
$1.25 \times f_y$	343.75	300	250	1.7	0.011
$1.0 \times f_y$	275	400	200	1.7	0.009
$0.78 \times f_y$	214.5	500	170	1.7	0.007
$0.47 \times f_y$	129.25	600	110	1.7	0.0055
$0.23 \times f_y$	63.25	700	40	1.7	0.0055
$0.11 \times f_y$	30.25	800	20	1.7	0.001

- **Bearing in large end distance case ($e_2 \geq 3\ d_b$) for M20 bolt and downward (compression)**

In this case e_2 is also set at $3 \times d_b$ for calculating $F_{b,Rd}$ only.

$$F_{b,Rd} = 0.92 \times \frac{e_2}{d_b} \times f_u \times d_b \times t \qquad (6.19)$$

Table 6.3 Bearing curve fit parameters corresponding to analysed temperature ($e2 \geq 3db$), M20 bolt and downward.

$f_{u,\theta}$	$f_{u,\theta}$	T [°C]	Ω	ψ	Φ
$1.0 \times f_u$	445	20	250	1.7	0.008
$1.25 \times f_y$	343.75	100	220	1.7	0.008
$1.25 \times f_y$	343.75	200	220	1.7	0.008
$1.25 \times f_y$	343.75	300	220	1.7	0.008
$1.0 \times f_y$	275	400	200	1.7	0.008
$0.78 \times f_y$	214.5	500	170	1.7	0.008
$0.47 \times f_y$	129.25	600	110	1.7	0.008
$0.23 \times f_y$	63.25	700	40	1.7	0.007
$0.11 \times f_y$	30.25	800	20	1.7	0.007

An application of the proposed procedure is shown in **Figure 6.17** which shows the full description of the plate bearing component at small and large end distance (towards and away from the free edge respectively) for a S275 steel plate which has 5.8 mm thickness. It is clear that the proposed curve fitting procedure has been investigated carefully in such a way that provides a good correlation with the FE modelling outcome.

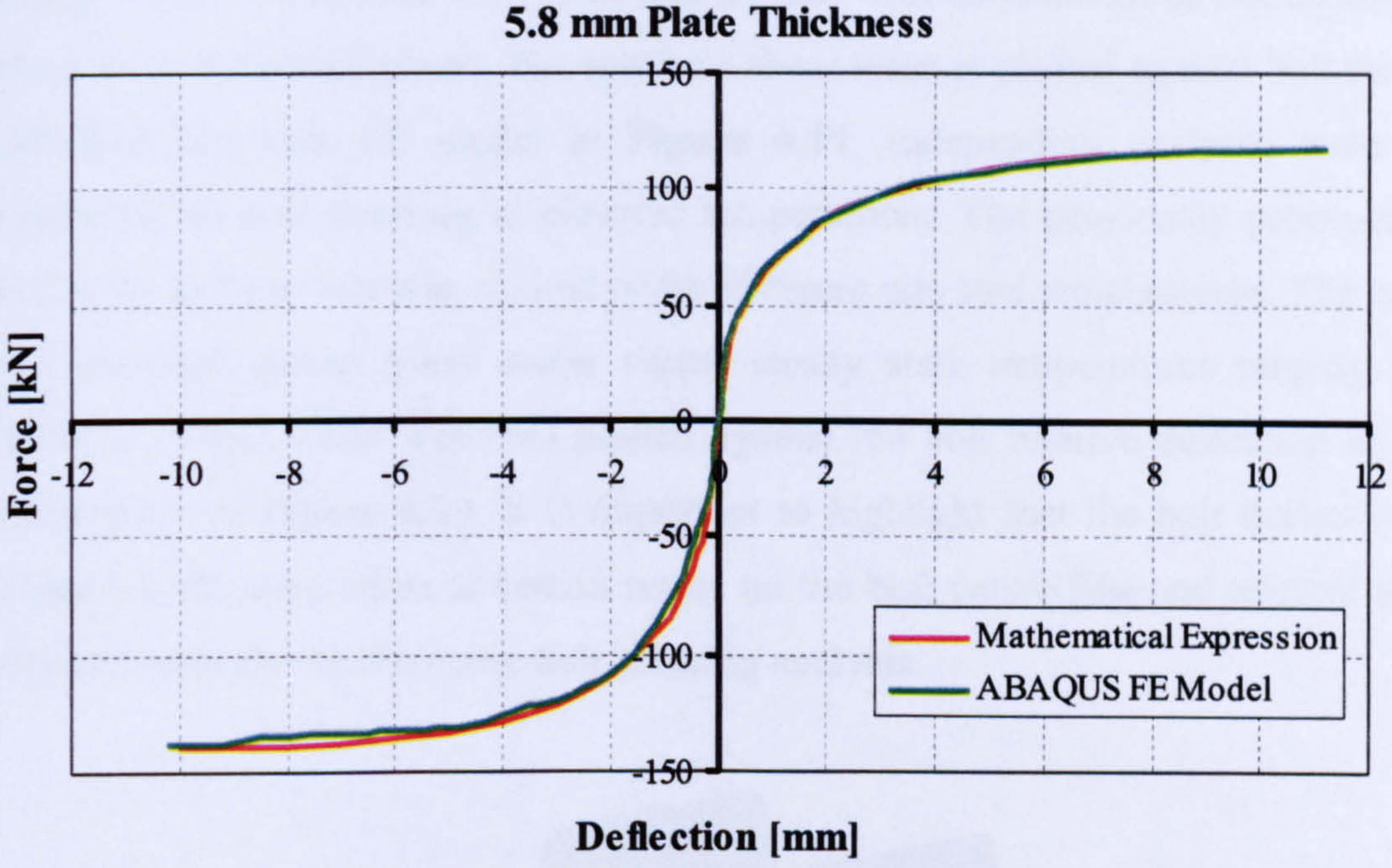

Figure 6.17 Force-deflection comparison between the proposed expression and ABAQUS FEM

6.4. Bolt in Single Shear Component

Very little literature exists that investigates bolts in single shear at elevated temperature or even at ambient temperature, although Eurocode 3 part-1.8 [6.4] presents an equation for bolt shear strength (**Equ. 6.20**) and another equation (the basis of which is unclear) for the initial stiffness of bolt shearing at ambient temperature (**Equ. 6.21**). This stiffness was actually proposed in the context of connection rotational stiffness. Therefore the term (z) represents the lever arm between bolts in tension and the others in compression within a moment connection.

$$F_{v,rd} = 0.6 \times f_{ub} \times A \qquad \textbf{(6.20)}$$

$$S_{ij} = \frac{E z^2}{K_{11}} \qquad \textbf{(6.21)}$$

$$K_{11} = \frac{16\, d_b^2\, f_u\, n_b}{E\, M_{16}} \qquad \textbf{(6.22)}$$

In this research program the bolt shearing component was investigated at both ambient and elevated temperatures. In order to conduct the investigation, FE models of lap joints were created for two S275 steel plates, each one having a thickness of $0.5d_b$ (**Figure 6.18**). One of these plates was clamped at its end and the other plate was forced to move axially by applying displacement boundary conditions to its far edge. At ambient temperature, the analyses were conducted for Grade 8.8 high strength bolts of diameter 12, 16, 20 and 24 mm with corresponding end distance of $2d_b$ in both connected plates. The resultant shear force is plotted against bolt relative deflection for each FE model in **Figure 6.19**. Independent analyses were also conducted on bolt shearing at elevated temperatures. The previously proposed FE model for an M20 bolt was studied under different elevated temperatures. The model was analysed eleven times under varied steady state temperatures ranging from 100°C to 900°C. Load was then plotted against the bolt relative deflection at each temperature in **Figure 6.20**. It is important to highlight that the bolt deflections Δ (**Figure 6.18**) were taken at certain nodes on the bolt centre line and relative to the opposite node during the entire bolt shearing analysis.

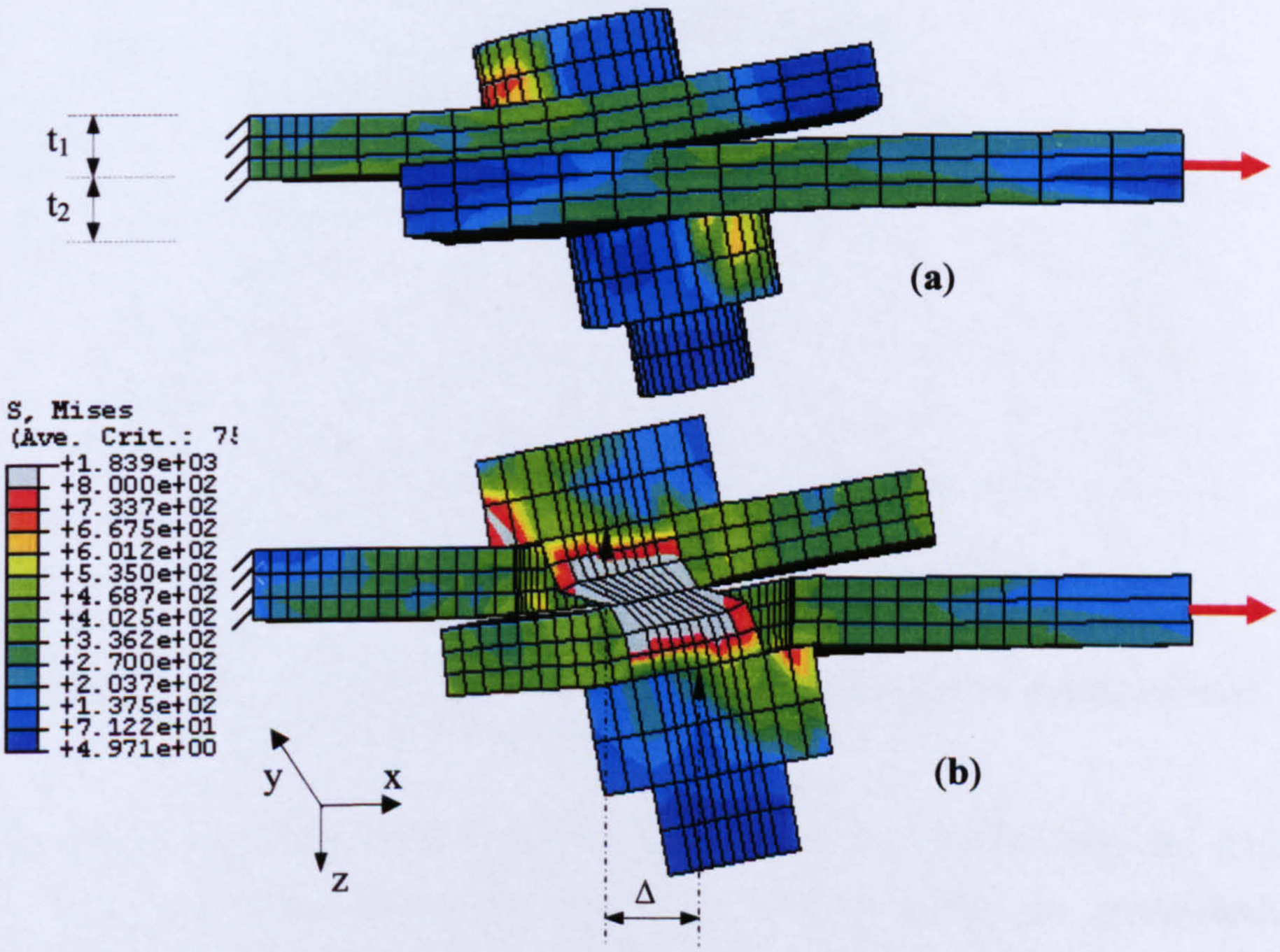

Figure 6.18 FE model of lap joint of two 10 mm thickness plates and M20 8.8 bolt at 20°C

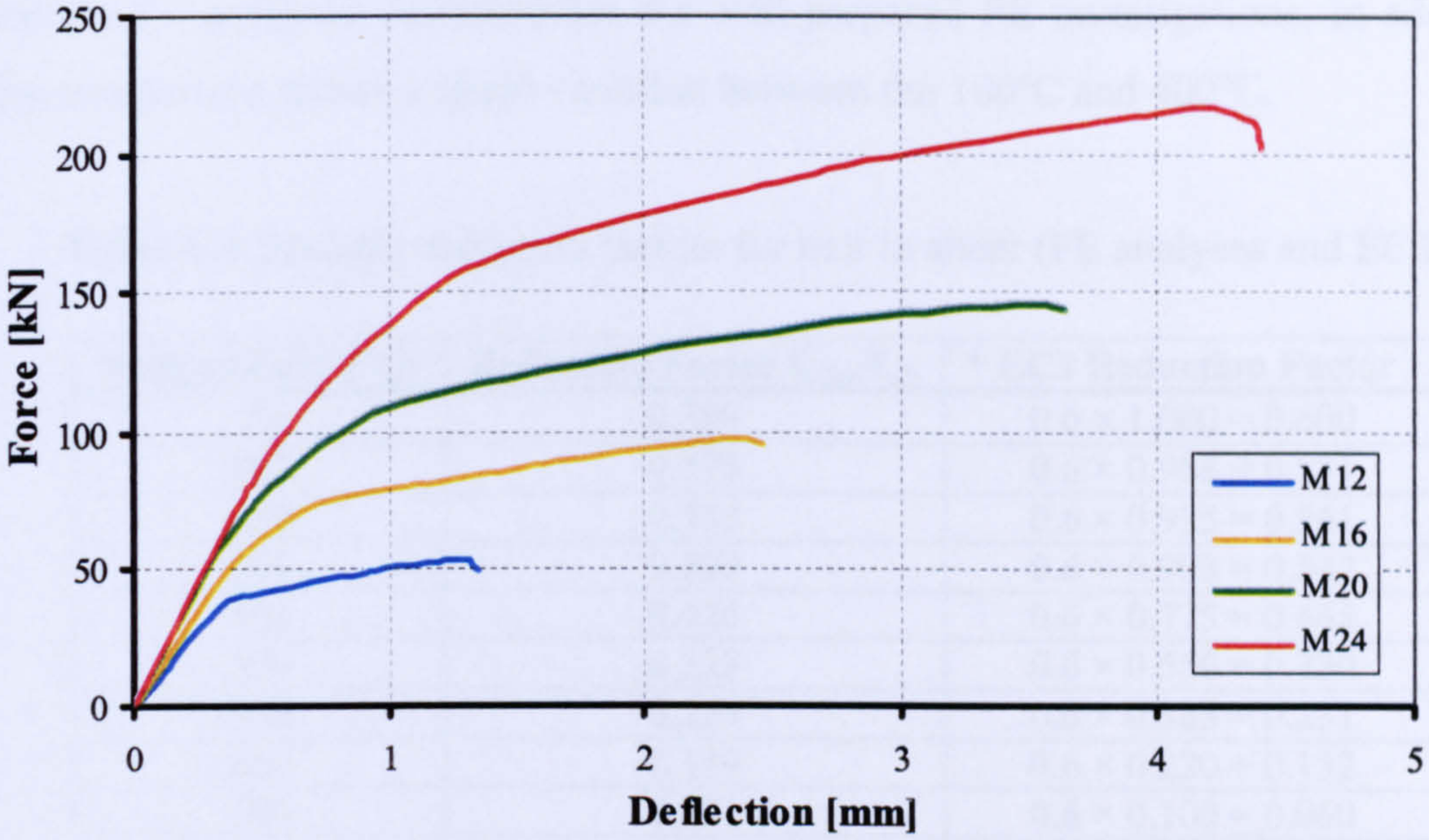

Figure 6.19 Bolt shearing characteristic at 20°C (M12, M16, M20, M24)

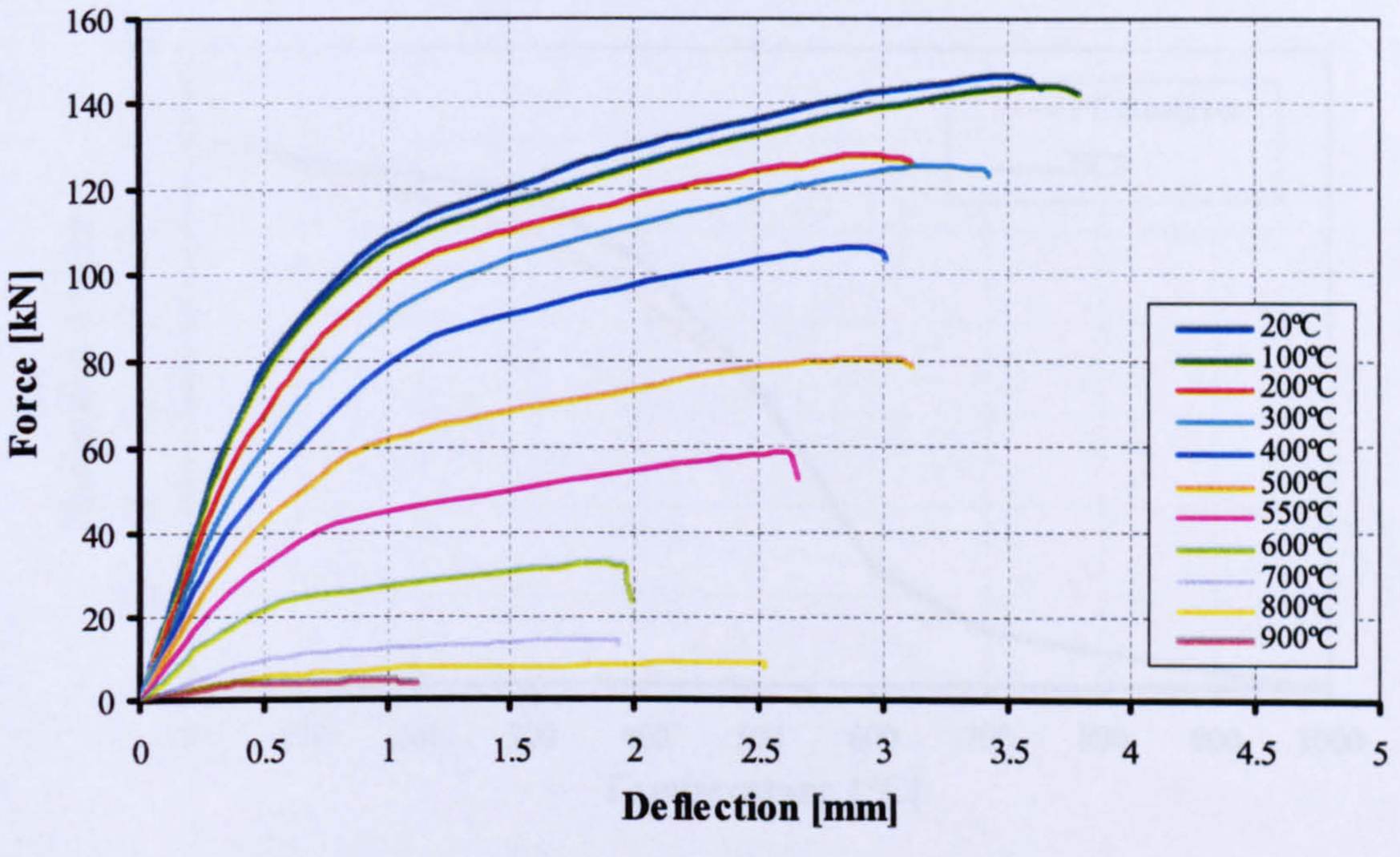

Figure 6.20 Load-deflection plot for (M20) 8.8 bolt shearing under various elevated temperatures from FE analyses

From **Figure 6.20** ultimate strength reduction factors were derived from the current FE analyses in **Table 6.4** and graphically plotted against the corresponding temperature in **Figure 6.21**. In addition, bolt shearing strength reduction factors proposed Eurocode 3 Part-1.2 [6.11] were also plotted on the same graph for

comparison. Consequently, the good correlation between the Eurocode 3 part-1.2 [6.11] and the FE analyses, demonstrates the well prepared FE investigations. In addition this comparison shows a slight variation between the 100ºC and 400ºC.

Table 6.4 Strength reduction factors for bolt in shear (FE analyses and EC3)

Temperature [°C]	Reduction Factor $f_{u.b,\theta}/f_{u,b}$	* EC3 Reduction Factor
20	0.580	0.6 × 1.000 = 0.600
100	0.575	0.6 × 0.968 = 0.581
200	0.538	0.6 × 0.935 = 0.561
300	0.500	0.6 × 0.903 = 0.542
400	0.426	0.6 × 0.775 = 0.465
500	0.323	0.6 × 0.550 = 0.330
550	0.234	0.6 × 0.385 = 0.231
600	0.139	0.6 × 0.220 = 0.132
700	0.061	0.6 × 0.100 = 0.060
800	0.041	0.6 × 0.067 = 0.040
900	0.019	0.6 × 0.033 = 0.019

* 0.6 is the conversion factor for bolt shear

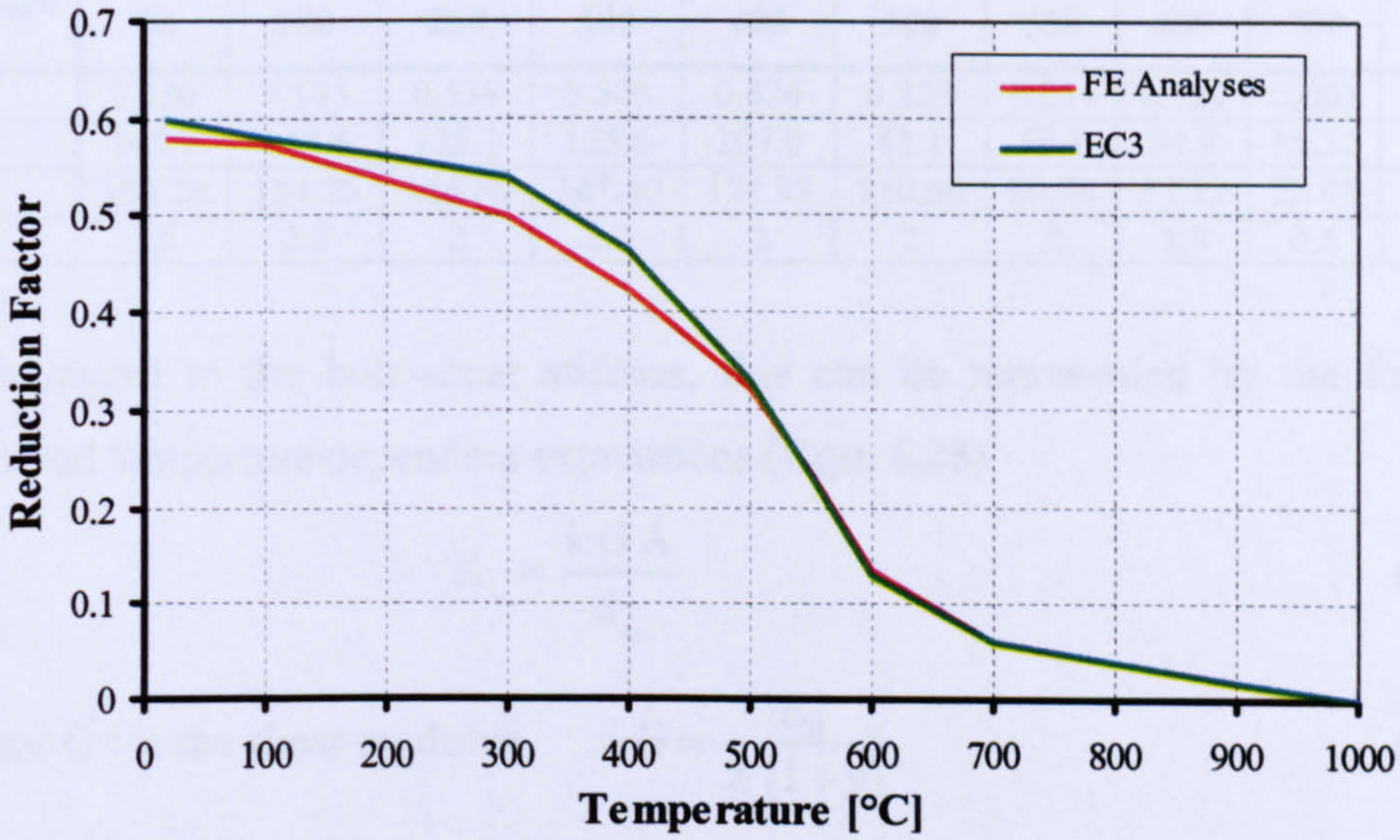

Figure 6.21 Comparison of EC3 bolt shearing strength reduction factors with those resulting from the FE analyses

In order to represent the bolt shear load-deflection data at elevated temperature in a form suitable for incorporation in component modelling, the load–deflection–temperature data obtained from the FE modelling were fitted using a modified Ramberg–Osgood expression [6.12, 6.13] of the following form:

$$\Delta = \frac{F}{k_{v,b}} + \Omega \left(\frac{F}{F_{v,Rd}} \right)^{n} \qquad (6.23)$$

Where

Δ : relative bolt deflection [mm];

F : the corresponding level of shear force [N];

$K_{v,b}$: temperature dependent bolt shearing stiffness [N/mm];

$F_{v,Rd}$: temperature dependent bolt shearing strength **(Equ. 6.24)** [N];

$$F_{v,Rd} = R_{f,v,b} \times f_{u,b} \times A \qquad (6.24)$$

$R_{f,v,b}$: strength reduction factor for bolt in shear;

n : parameter defining the curve sharpness, (n = 6);

Ω : temperature dependent parameter for curve fitting.

These parameters are defined in **Table 6.5** below

Table 6.5 Bolt shearing curve fit parameters corresponding to analysed temperature

Temperature [°C]	20	100	200	300	400	500	550	600	700	800	900
$R_{f,v,b}$	0.580	0.575	0.538	0.500	0.426	0.323	0.234	0.139	0.061	0.041	0.019
$F_{v,Rd}$	145.7	144.4	128.1	125.6	107.0	81.1	58.8	34.9	15.32	10.3	4.77
$k_{v,b}$	184.26	184.26	165.80	147.40	128.98	110.56	83.84	57.12	23.95	16.58	12.43
Ω	2.5	2.8	2	2.2	2	2	2	1.3	0.6	0.7	0.02

With regard to the bolt shear stifness, this can be represented by the following proposed temperture dependent expressions **(Equ. 6.25)**.

$$K_v = \frac{kGA}{d_b} \qquad (6.25)$$

Where G : is the shear modulus $\quad G = \frac{E_\theta}{2(1+\nu)} \qquad (6.26)$

E_θ : is the temperature dependent Elastic modulus.

k is a shear correction factor introduced to account for the error in the shear strain energy caused by assuming a constant shear strain through the bolt section, as opposed to the classical parabolic distribution. The shear correction factor depends upon the cross-sectional shape and material properties [6.14, 6.15]. It was found that a value of k = 0.15 would be suitable for the bolt shearing analyses.

6.5. Friction Component

A friction component was investigated by analysing two FE model lap joints, one with a friction coefficient of 0.25 between the surfaces, and the other model with almost zero friction coefficient value. The force-deflection graphs for the zero-friction case was subtracted from the other to produce the final graph in **Figure 6.22**. This graph represents the friction behaviour history throughout the analysis of the lap joint FE model. To generalize this graph as a mathematical expression, firstly it has been simplified into two straight lines **Figure 6.22, 6.23**. Then the main five parameters describing the force-deflection relationship were derived as an appropriate expression.

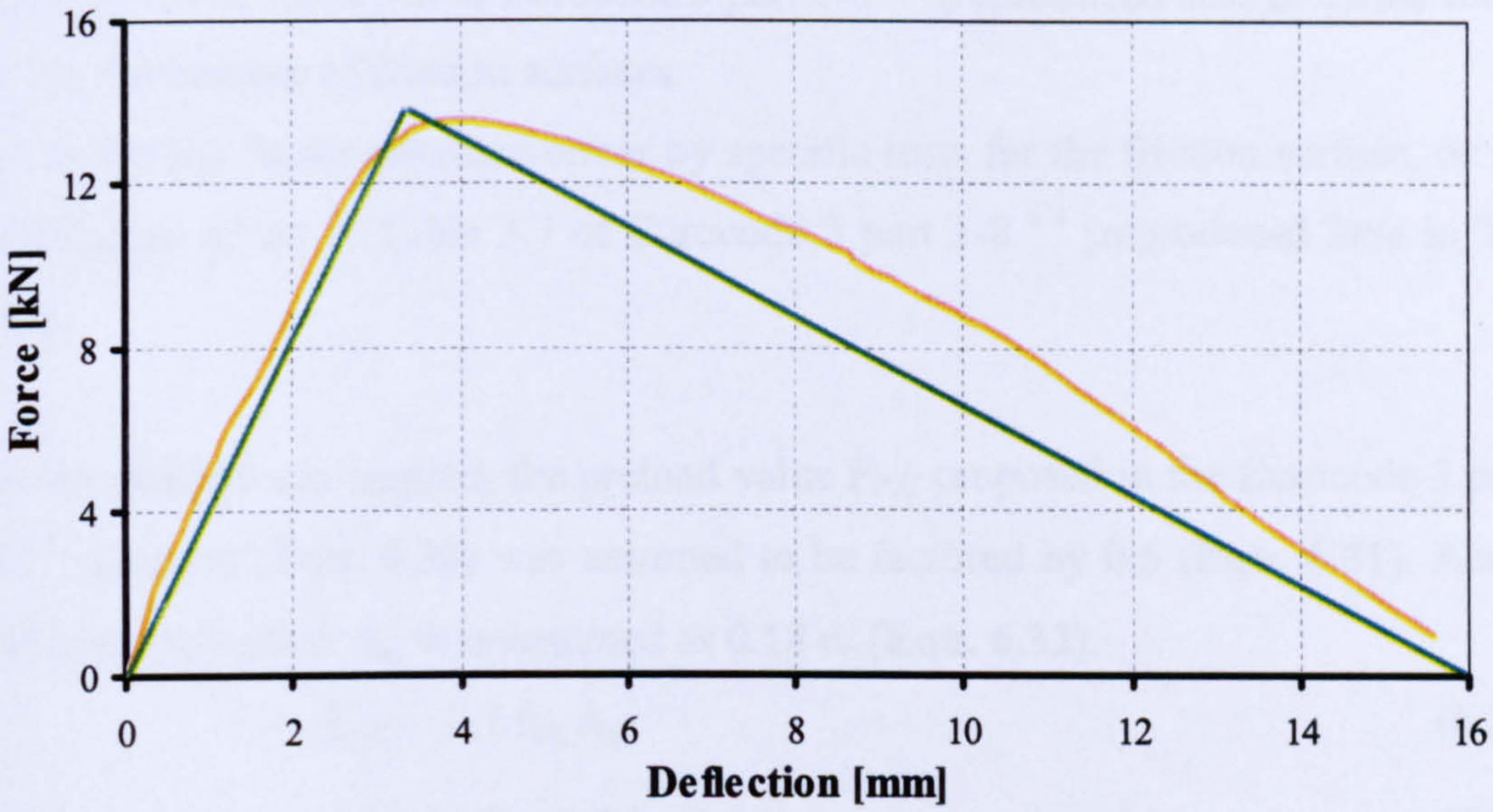

Figure 6.22 Friction load-deflection and the relevant simplified linear graph

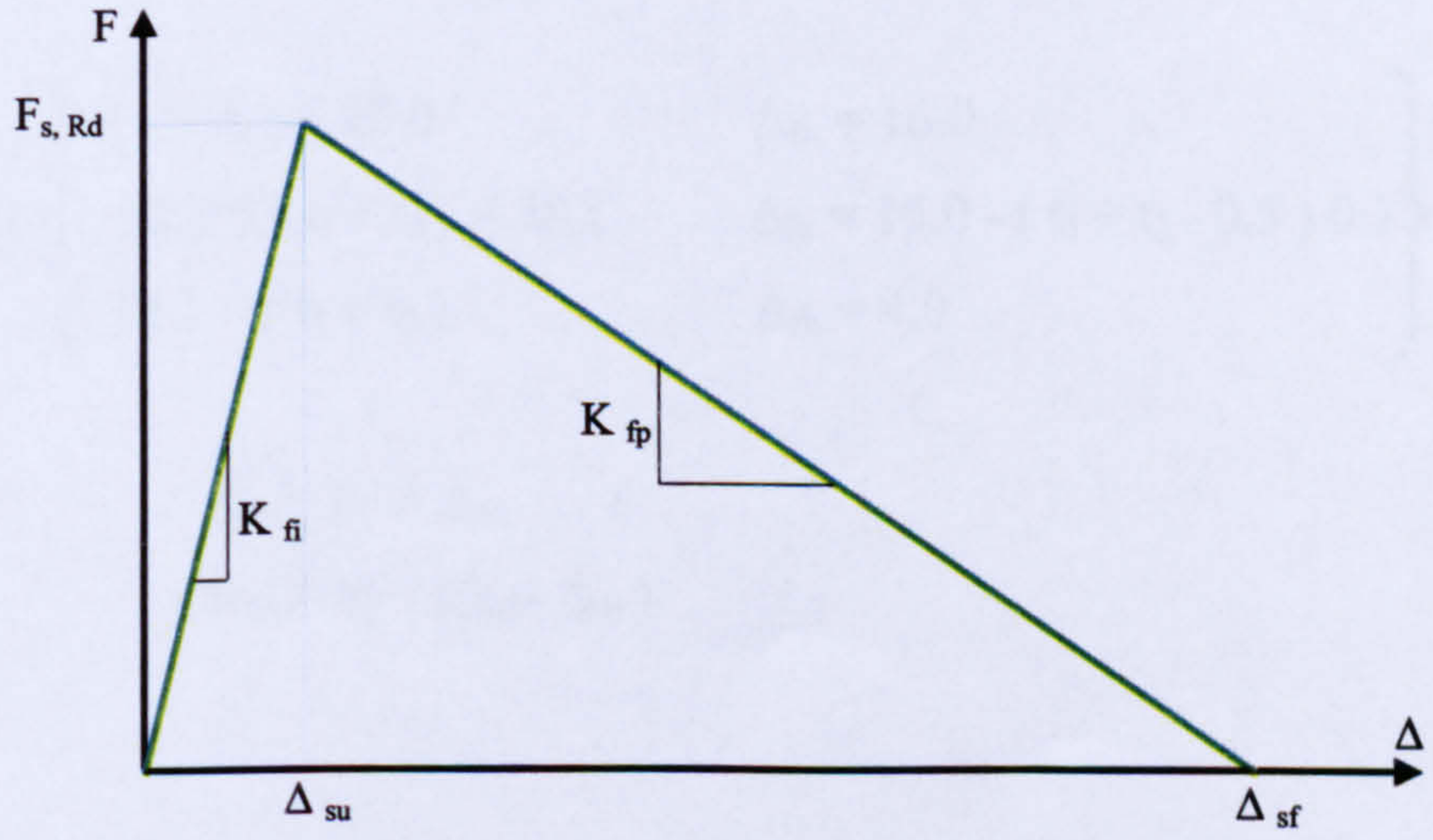

Figure 6.23 Simplified friction load-deflection description and the corresponding parameters

To find the slip resistance $F_{s,Rd}$ of a class 8.8 or 10.9 bolt the following suggested equation **(Equ. 6.27)** may be used:

$$F_{s,Rd} = 0.28 \times \mu \times f_{u,b} \times A_s \qquad \textbf{(6.27)}$$

A_s : The stressed area of the bolt (for instance, M20 bolt A_s=245 mm^2).

The Eurocode 3 [6.4] equation **(Equ. 6.28)** may also be used

$$F_{s,Rd} = \frac{k_s\ n\ \mu}{\gamma_{M3}} F_{p,C} \qquad \textbf{(6.28)}$$

where:

k_s : is given in Table 3.6 of Eurocode 3 part 1-8 [6.4] (reproduced here in **Table 6.6)**

n : is the number of friction surfaces

μ : is the slip factor obtained either by specific tests for the friction surface, or when relevant as given in Table 3.7 of Eurocode 3 part 1-8 [6.4] (reproduced here in **Table 6.7**).

As no preload was applied, the preload value $F_{P,C}$ proposed in the Eurocode 3 part 1-8 [6.4] equation **(Equ. 6.30)** was assumed to be factored by 0.5 **(Equ. 6.31)**. Also the ultimate deflection Δ_{su} was assumed as 0.18 d_b **(Equ. 6.32)**.

$$F_{p,C} = 0{,}7\ f_{ub}\ A_s \qquad \textbf{(6.29)}$$

$$F_{p,C} = 0.5 \times 0{,}7\ f_{ub}\ A_s \qquad \textbf{(6.30)}$$

$$\Delta_{su} = 0.18\ d_b \quad [mm] \qquad \textbf{(6.31)}$$

$$\Delta_{sf} = \begin{cases} (t_1 + t_2) < 20.0 & \Delta_{fu} = 16.0 \\ 20.0 \le (t_1 + t_2) \le 38.1 & \Delta_{fu} = 16.0 - (t_1 + t_2 - 0.5)\ 0.3 \\ 38.1 < (t_1 + t_2) & \Delta_{fu} = 4.0 \end{cases} \qquad \textbf{(6.32)}$$

$$K_{fi} = F_f\ /\ \Delta_{su} \qquad \textbf{(6.33)}$$

$$K_{fp} = F_f\ /\ (\Delta_{sf} - \Delta_{su}) \qquad \textbf{(6.34)}$$

Table 6.6: Values of k_s

Description	k_s
Bolts in normal holes.	1,0
Bolts in either oversized holes or short slotted holes with the axis of the slot perpendicular to the direction of load transfer.	0,85
Bolts in long slotted holes with the axis of the slot perpendicular to the direction of load transfer.	0,7
Bolts in short slotted holes with the axis of the slot parallel to the direction of load transfer.	0,76
Bolts in long slotted holes with the axis of the slot parallel to the direction of load transfer.	0,63

Table 6.7: Slip factor, μ, for pre-loaded bolts

Class of friction surfaces	Slip factor μ
A	0,5
B	0,4
C	0,3
D	0,2

6.6. Lap Joint Simplified Component Model

Having described in detail each component characteristic in the previous studies, it is possible for the component mechanical model of any shear joint to be constructed. Simply, following the load transformation route through a single bolt lap joint under tensile load, a component mechanical model can be drawn in the form shown in **Figure 6.24**. The two main components, plate bearing and bolt shearing, are represented by three springs joined in series, and a friction component is combined in parallel to the other components. For instance, the characteristics of these components for a lap joint, comprising of two S275 steel plates 6 mm and 10 mm in thickness and fastened by an M20 high strength bolt, can be generated from the previous parametric expressions and shown in **Figure 6.25, 6.26, 6.27.** The behaviour of the FE model and that of the component model can be compared through their load-deflection response **(Figure 6.28)**. The good correlation between the two models can be seen from this comparison. In addition, the component model has described the failure of the joint by plate bearing, in contrast to the FE model. The failure criteria were not assigned in the FE model, in order to overcome convergence problems, but in the component model the failure criteria were described for each component. For the bearing component, failure was defined when a bolt hole deflected by half of the bolt diameter ($0.5d_b$). Bolt shear failure at various elevated temperatures has been shown for M20 high strength 8.8 bolts in **Figure**

6.20. The bolt shear component for other bolt sizes at elevated temperatures can be derived relative to the ambient failure temperature shown in **Figure 6.19**.

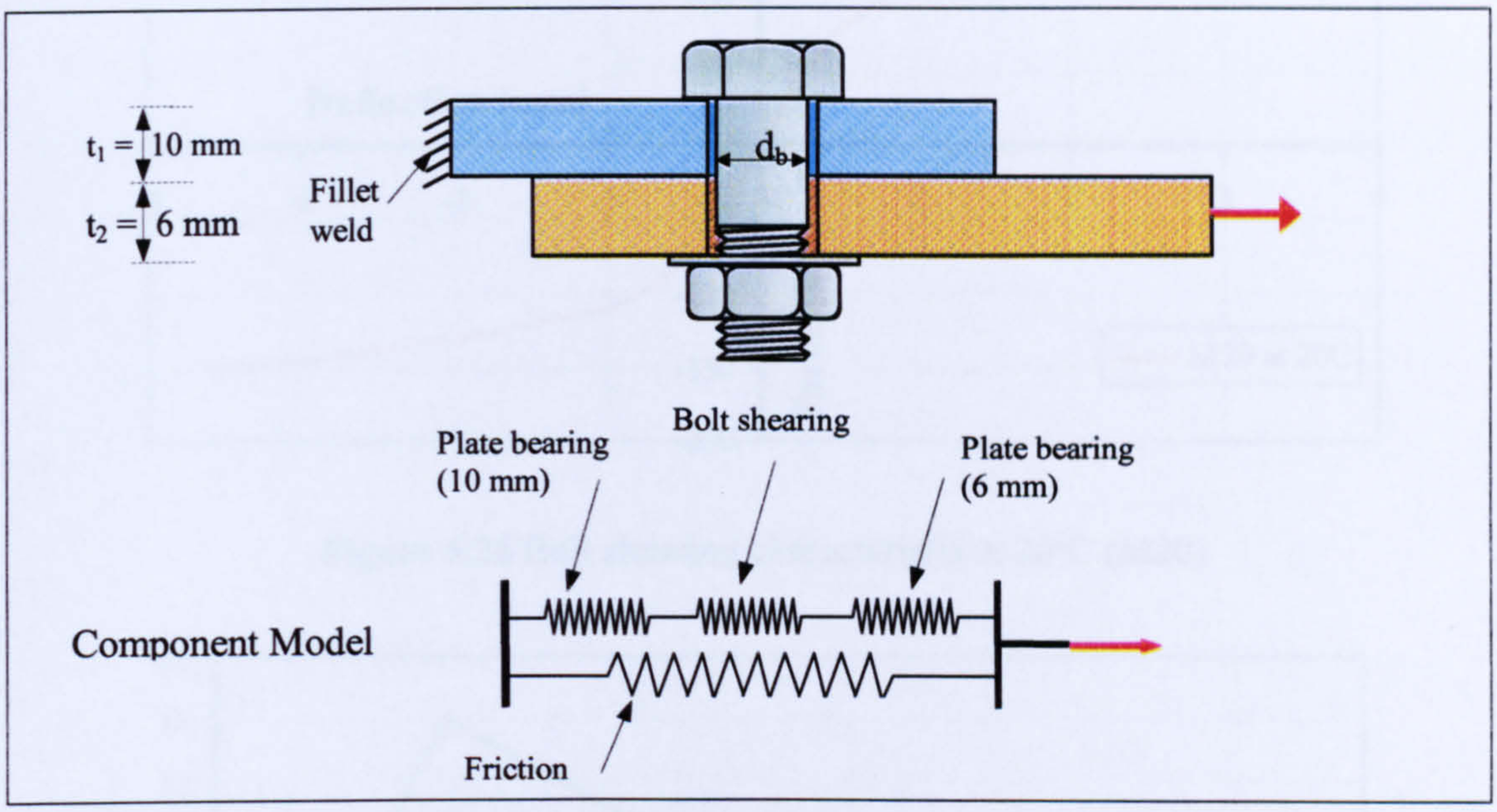

Figure 6.24 Lap joint component model

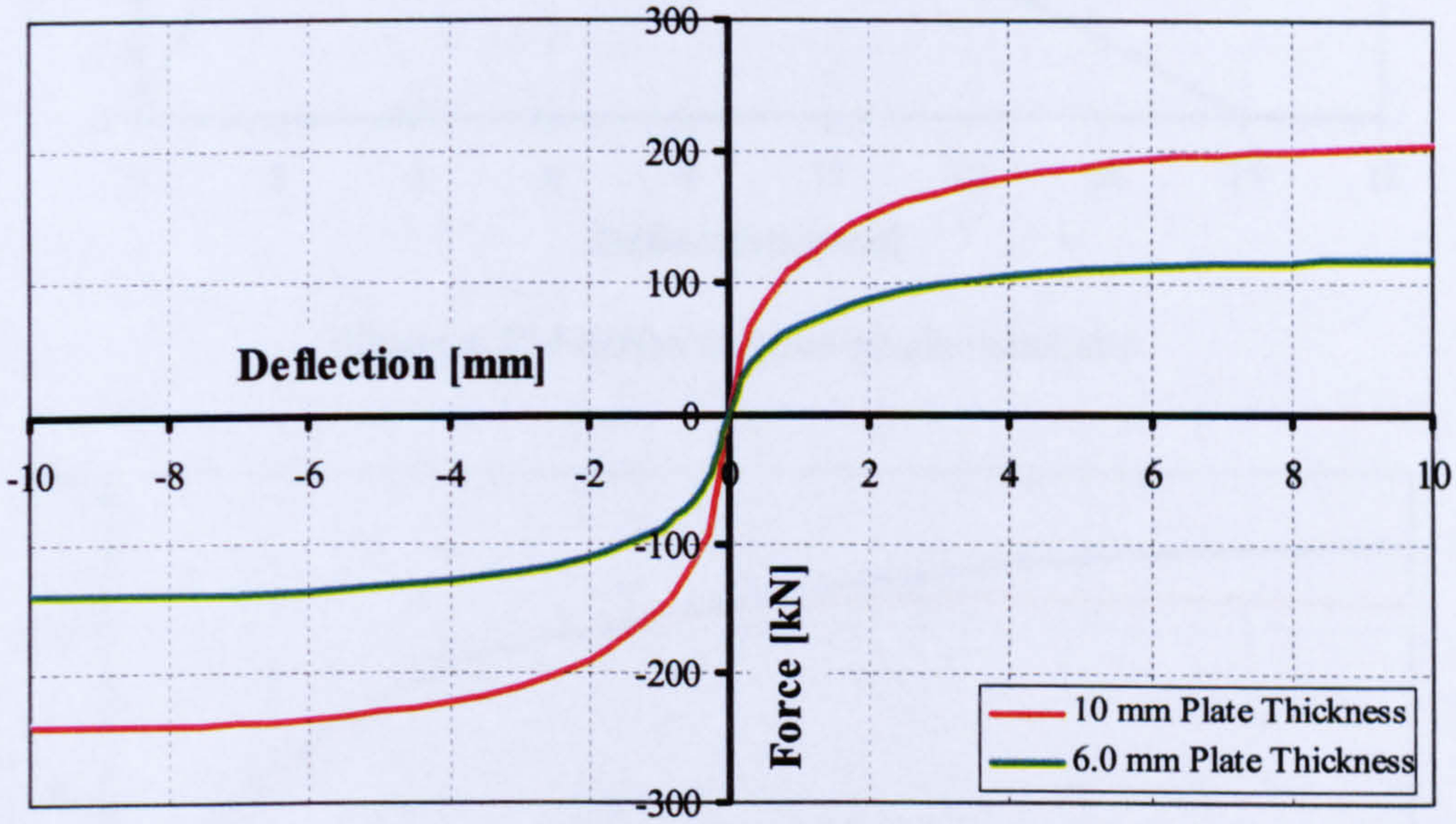

Figure 6.25 Plate bearing characteristic at 20°C (10 mm, and 6 mm thickness)

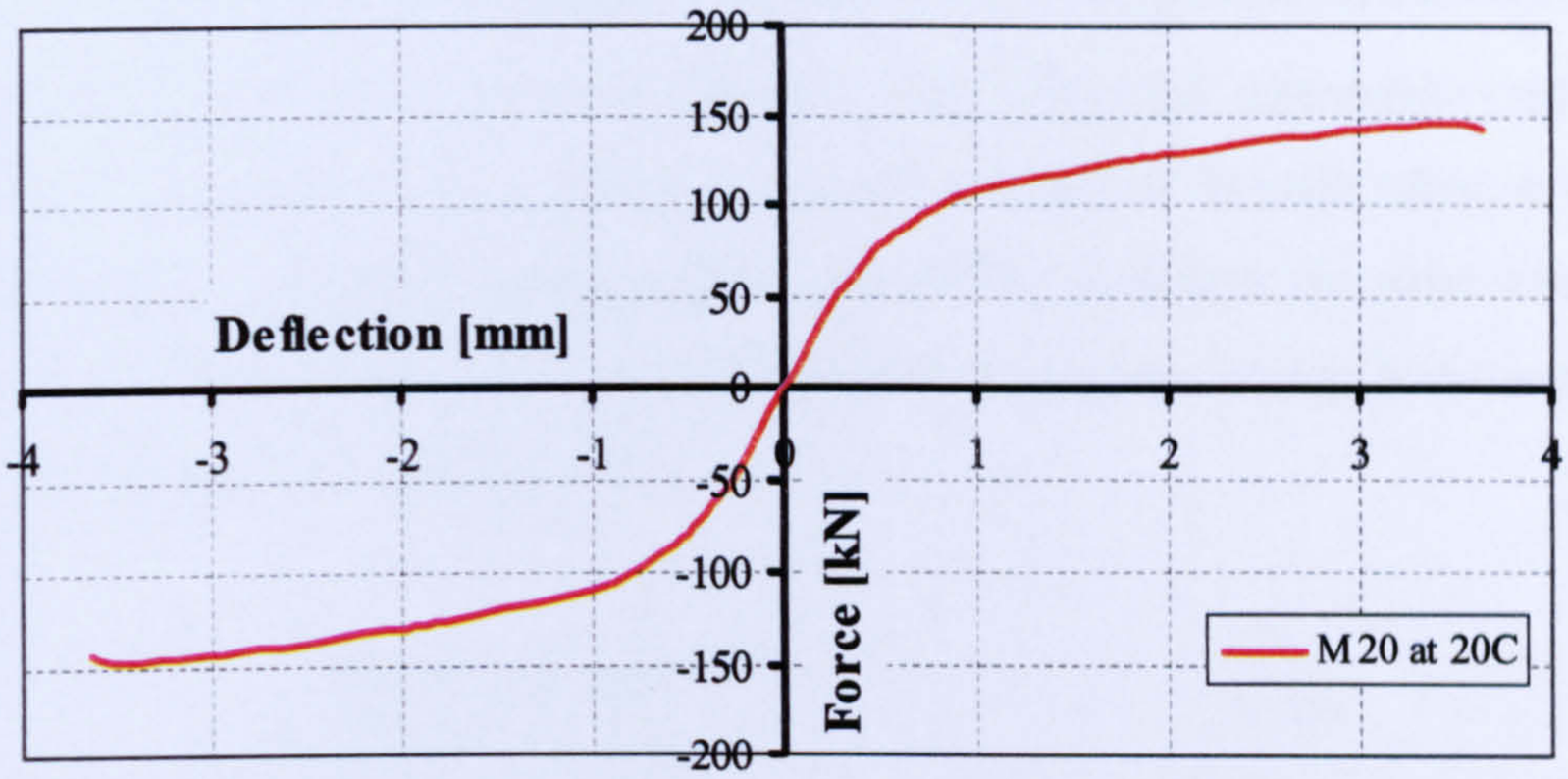

Figure 6.26 Bolt shearing characteristic at 20°C (M20)

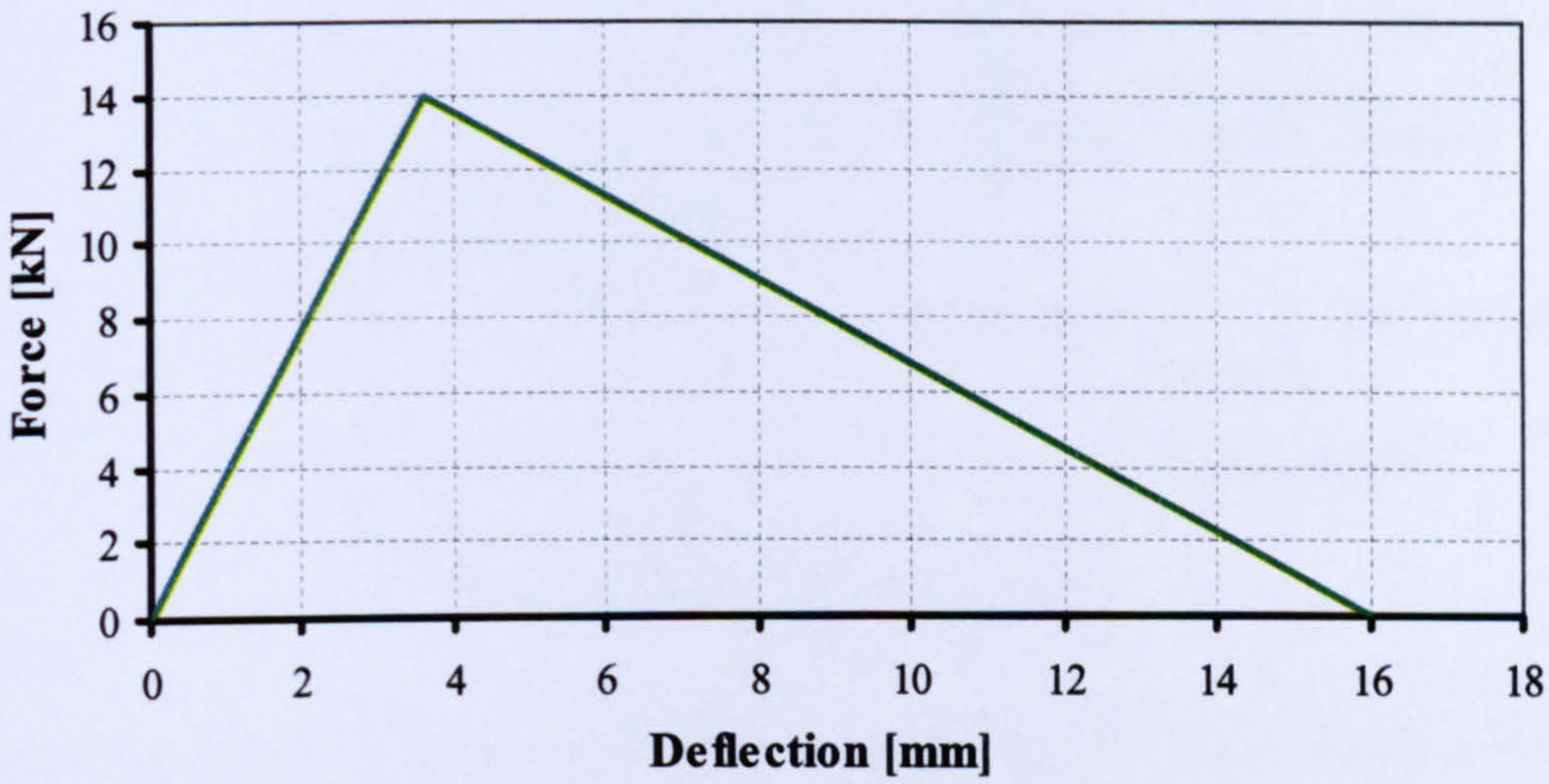

Figure 6.27 Friction component characteristic

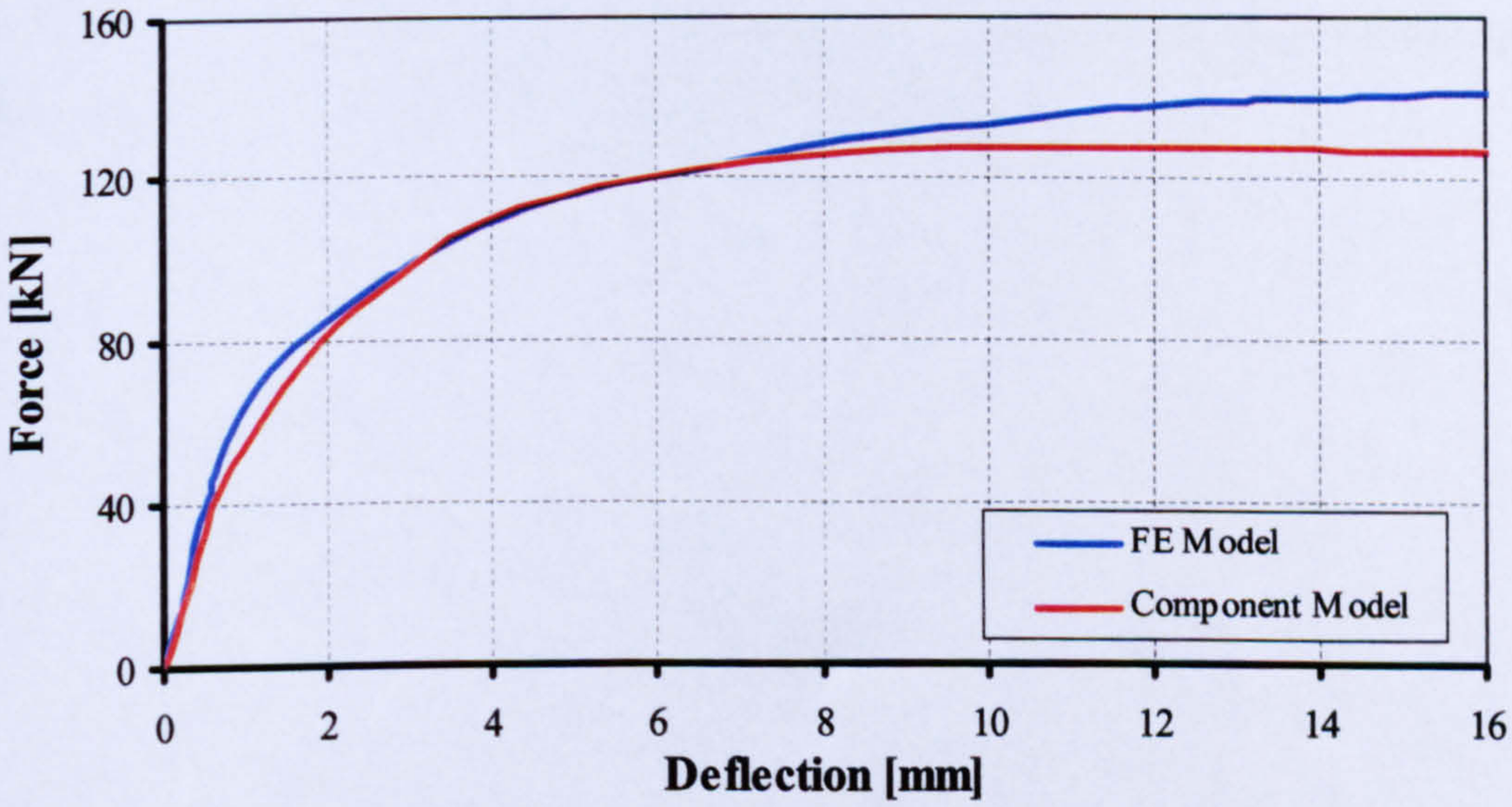

Figure 6.28 Lap joint load-deflection response comparison of component model and the FE model

6.7. Simplified Component Model of Fin plate Connection

It has been demonstrated earlier in Chapter 4 that a fin plate connection under tying force can be represented via a series of lap joints attached to each other in parallel. Similarly, the component mechanical model of the complete fin plate connection presented in **Figure 6.29** has been constructed as a series of lap joint component models as shown in **Figure 6.24**.

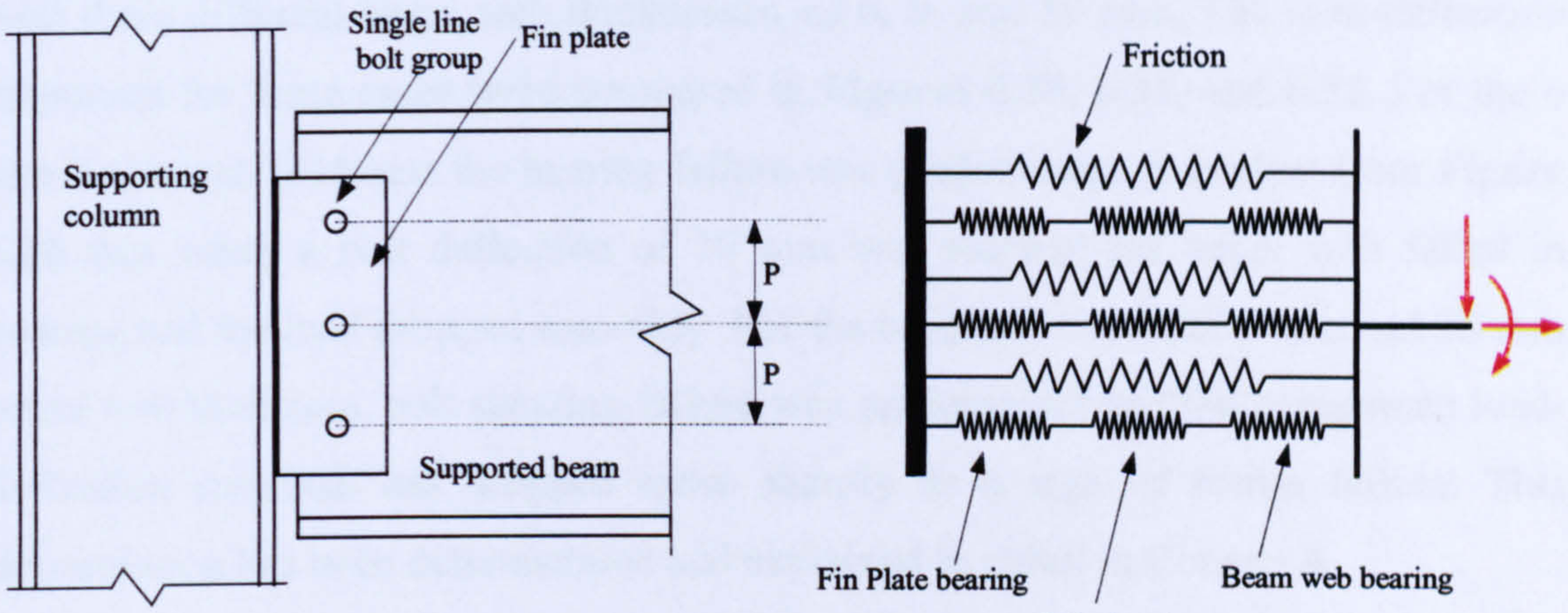

(a) Fin plate connection **(b)** Component Model

Figure 6.29 Fin plate component model

This model has two basic assumptions. Firstly, that the weld forms a strong link between the column flange and the fin plate and will not tear under any fire conditions. This is a reasonable assumption as demonstrated by tests at Cardington and in the Czech Republic. Secondly, beam end rotation is not large enough such for the beam bottom flange to contact the column flange.

6.8. Evaluation of The Tying Force

Earlier, in Chapter 4, six fin plate FE models were proposed along with their tying force-horizontal deflection graphs. These models have been used in this chapter to evaluate the developed component model for tying force capacity. For the two-bolt fin plate connection, investigations were widened to highlight the effect of beam web thickness on the connection failure type. Therefore, the FE model and the corresponding component model for a two bolt connection were analysed three times with three different beam web thicknesses, of 6, 9, and 10 mm. The load-deflection responses for these cases were compared in **Figures 6.30, 6.31,** and **6.32**. For the 6 mm beam web thickness the bearing failure was predominant. It is clear from **Figure 6.30** that when a bolt deflection of 10 mm was reached the beam web failed in bearing and the load dropped smoothly. For the other two cases, of 9 mm and 10 mm beam web thickness, bolt shearing failure was predominant and the component load-deflection response has dropped more sharply as a sign of brittle failure. This phenomenon has been demonstrated and explained in detail in Chapter 4.

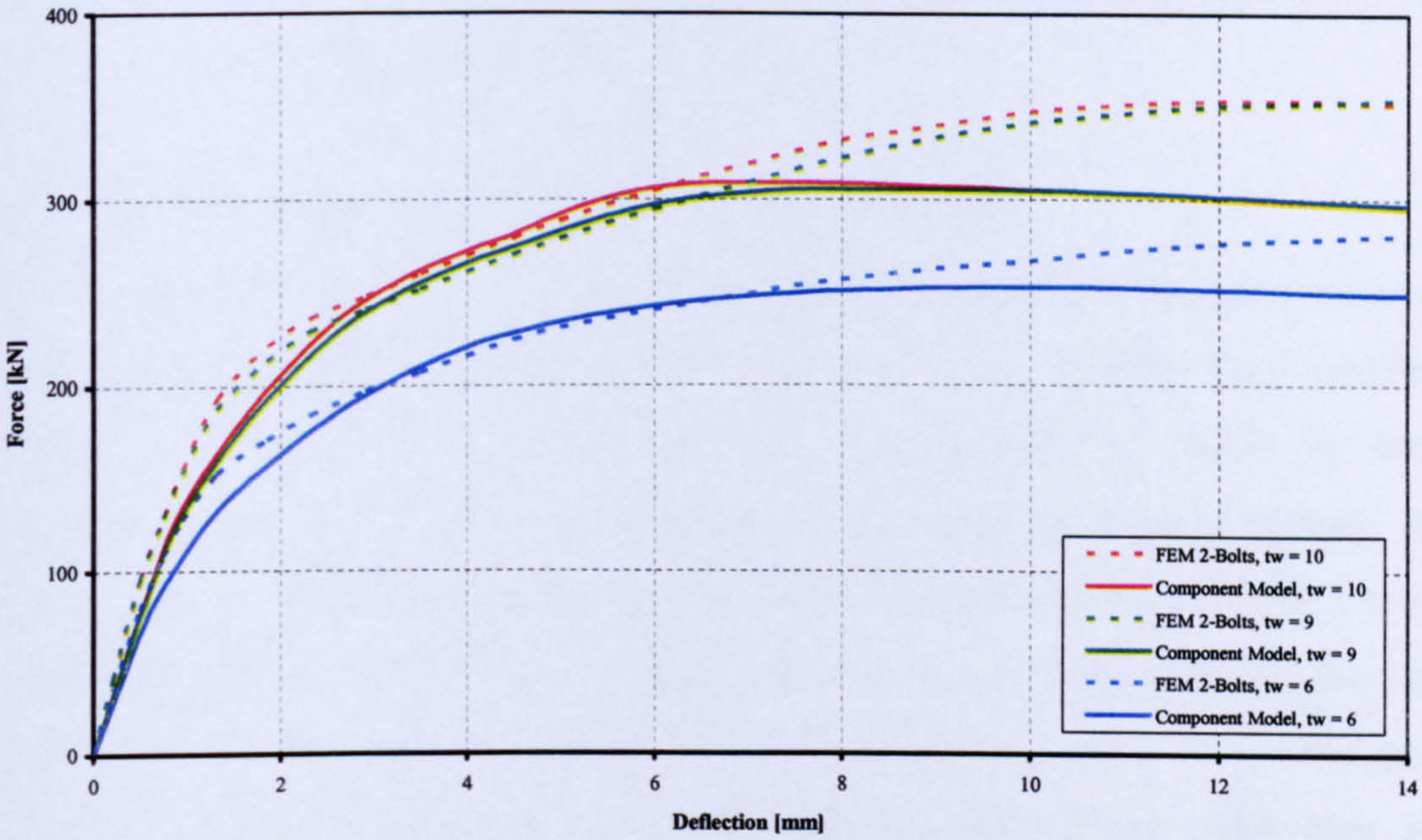

Figure 6.30 Tying force-deflection comparison for 2-bolt FEM and corresponding component model for different beam web thicknesses

Another ductile failure was indicated in the three-bolt connection model with 5.8 mm beam web thickness (**Figure 6.33**). The tying force response of other fin plate connection models with various bolt numbers (4-bolt, 5-bolt, 7-bolt and 8-bolt), is

shown in graph **Figure 6.31,** in which bolt shearing failure was dominant throughout these models.

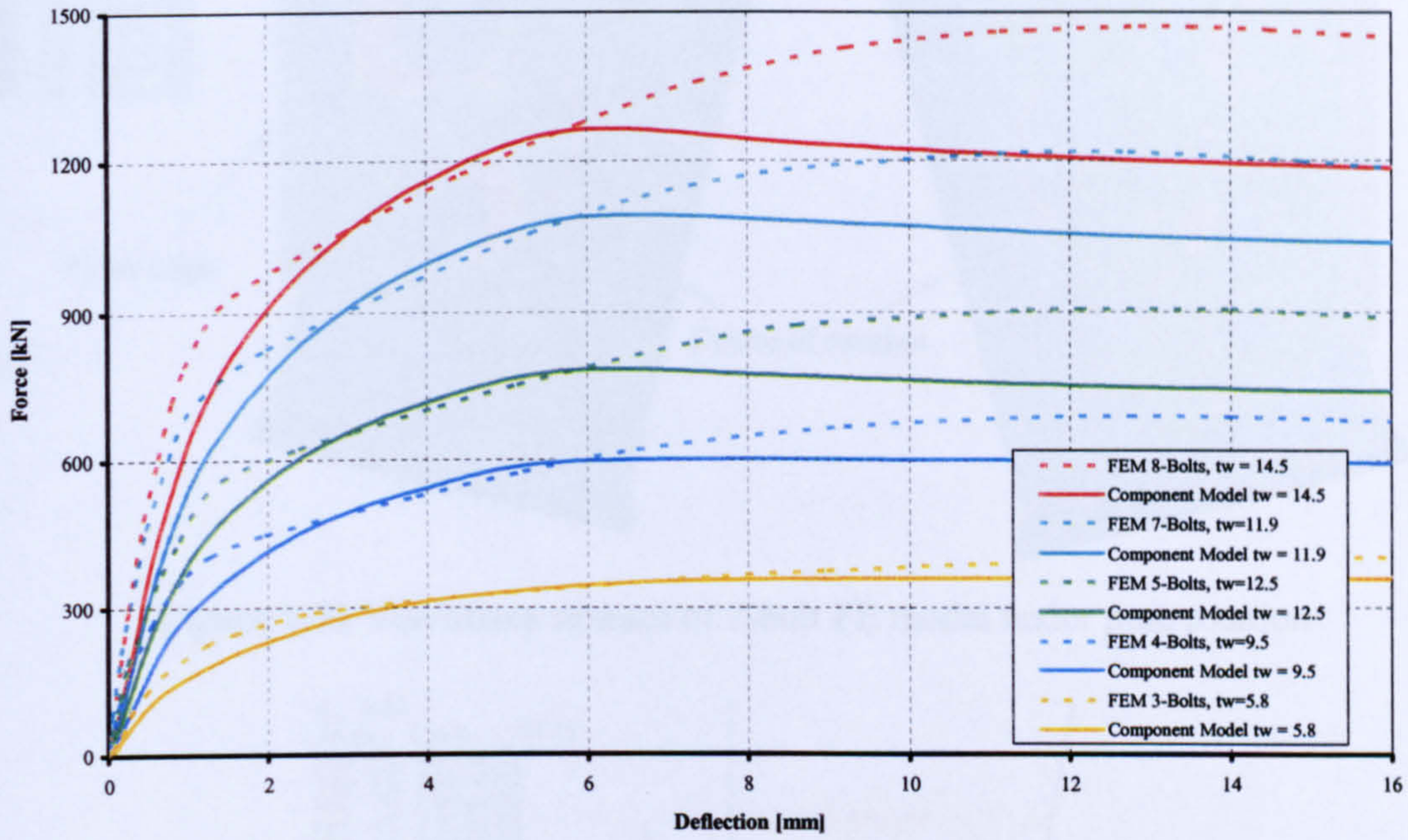

Figure 6.31 Tying force-deflection comparison for FE models with different bolt numbers and the corresponding component models

6.9. Evaluation of The Bending Moment

The rotational response of the proposed component model for fin plate connections was examined through intensive FE analyses. Six FE models were created and analysed under pure rotation. Then moment-rotation response graphs for each FE model were compared with the corresponding component model response. An FE model for a two-bolt fin plate connection under pure rotation was analysed as shown in **Figure 6.32**. The centre of rotation was chosen at a node between the top and bottom bolts and between the fin plate and the beam web. The corresponding component models presented in **Figure 6.33** consist of two rigid bars with a reference node each (a, b). Node (**a**) was clamped with respect to all degrees of freedom, while node (**b**) was restrained in z and y directions but permitted to rotate about the z-axis. Two series of spring groups, each one representing a lap joint component model, link rigid bars separated by the pitch distance (P). The comparison of moment-rotation curves for both models (**Figure 6.34**) demonstrates the good agreement in response for the two models.

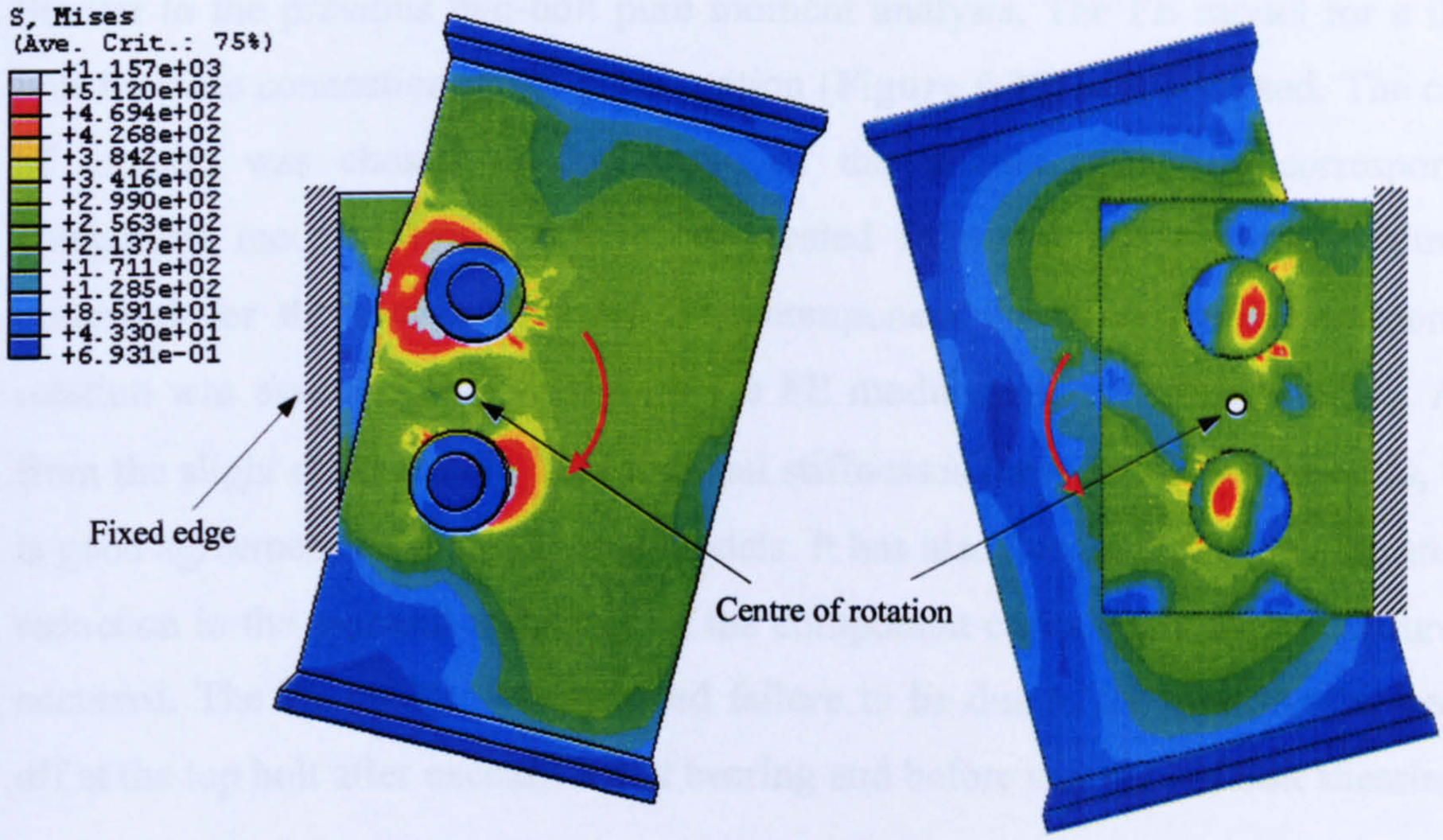

Figure 6.32 Von Mises stresses of 2-bolt FE model under pure rotation

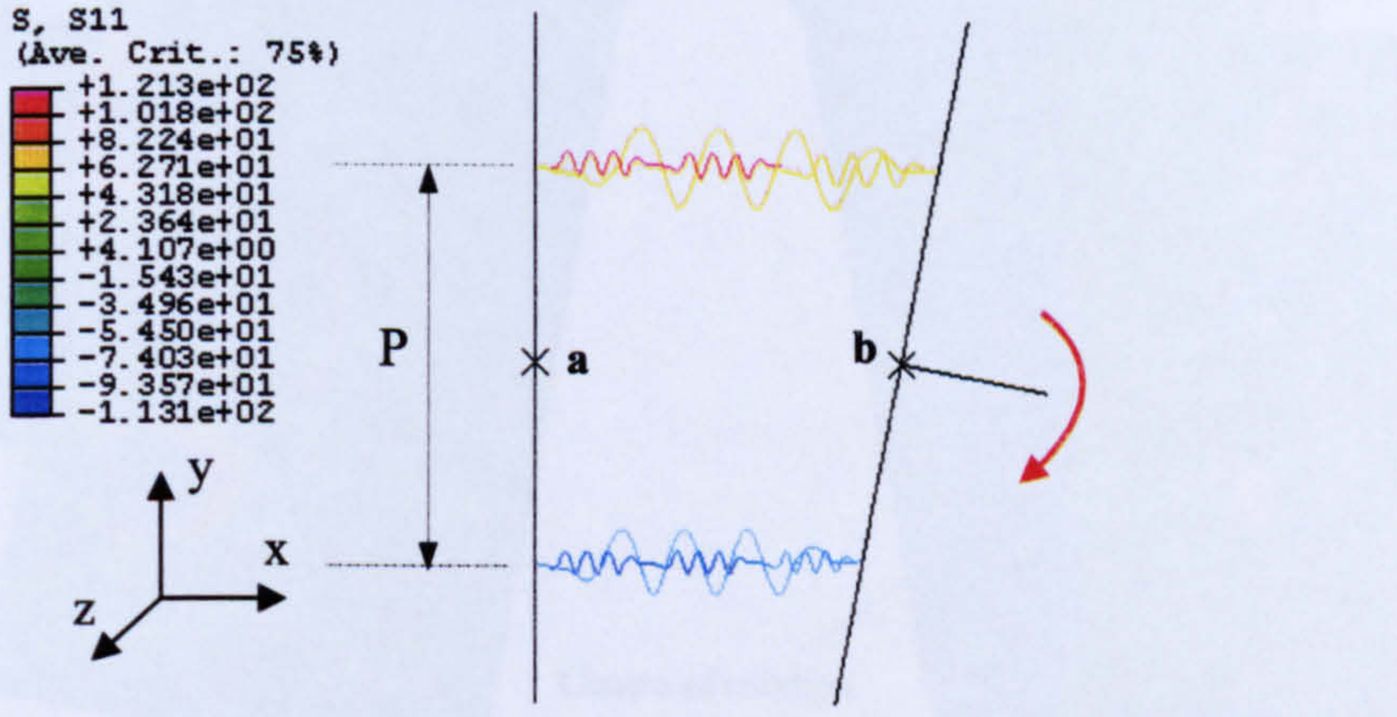

Figure 6.33 2-bolt component model under pure rotation

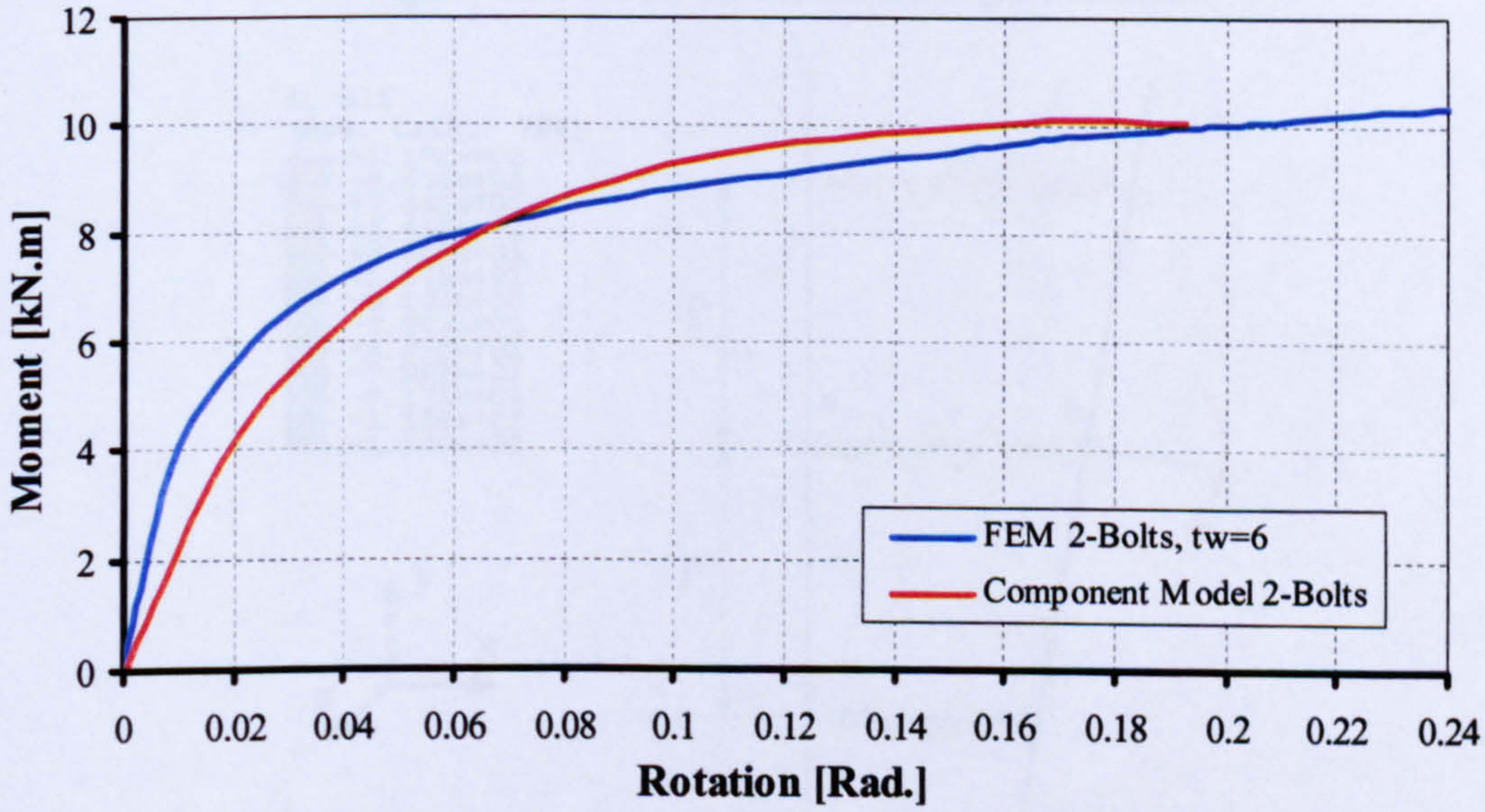

Figure 6.34 Moment-rotation comparison for the 2-bolt FEM and equivalent component model

Similar to the previous two-bolt pure moment analysis, The FE model for a three-bolt fin plate connection under pure rotation (**Figure 6.35**) was analysed. The centre of rotation was chosen as the centre of the middle bolt. The corresponding component model (**Figure 6.36**) was created following the same procedure as described for the two-bolt model. The component model response for moment-rotation was assessed compared with the FE model response (**Figure 6.37**). Apart from the slight difference in the rotational stiffnesses between the two models, there is good agreement between the two models. It has also been indicated by the smooth reduction in the moment resistance of the component curve that a ductile failure has occurred. The FE model demonstrated failure to be due to the end distance tearing off at the top bolt after excessive bolt bearing and before any sign of bolt shearing.

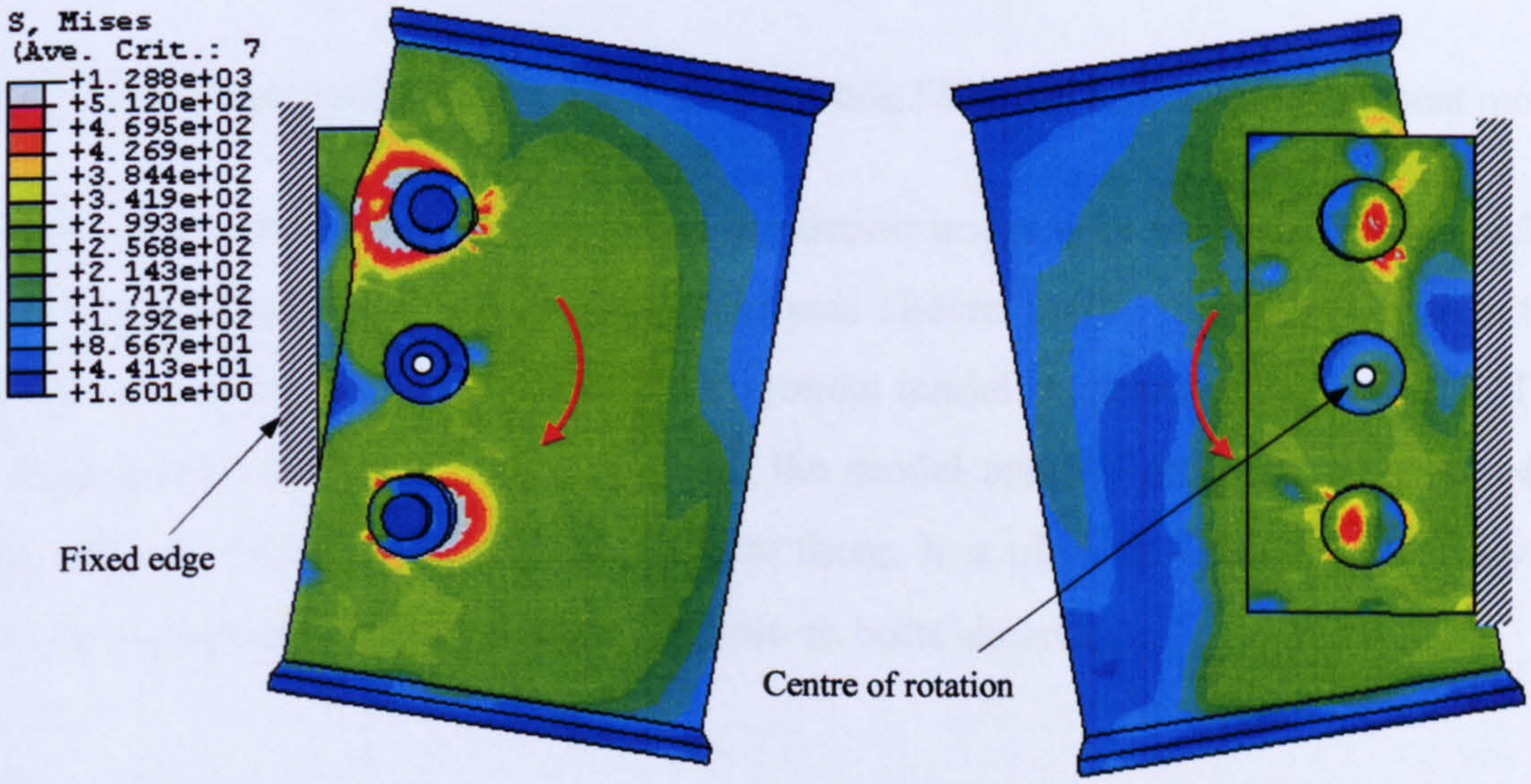

Figure 6.35 3-bolt FE model under pure rotation

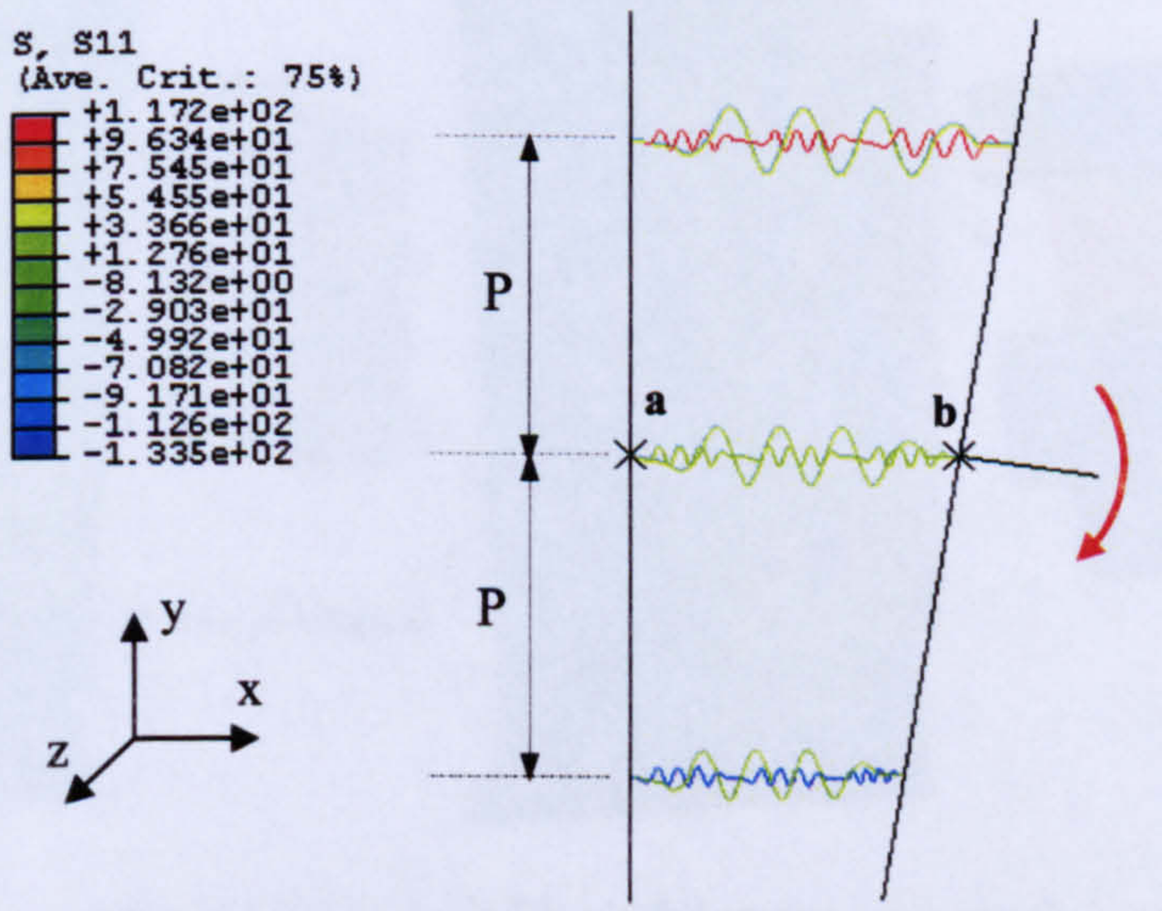

Figure 6.36 3-bolt component model under pure rotation

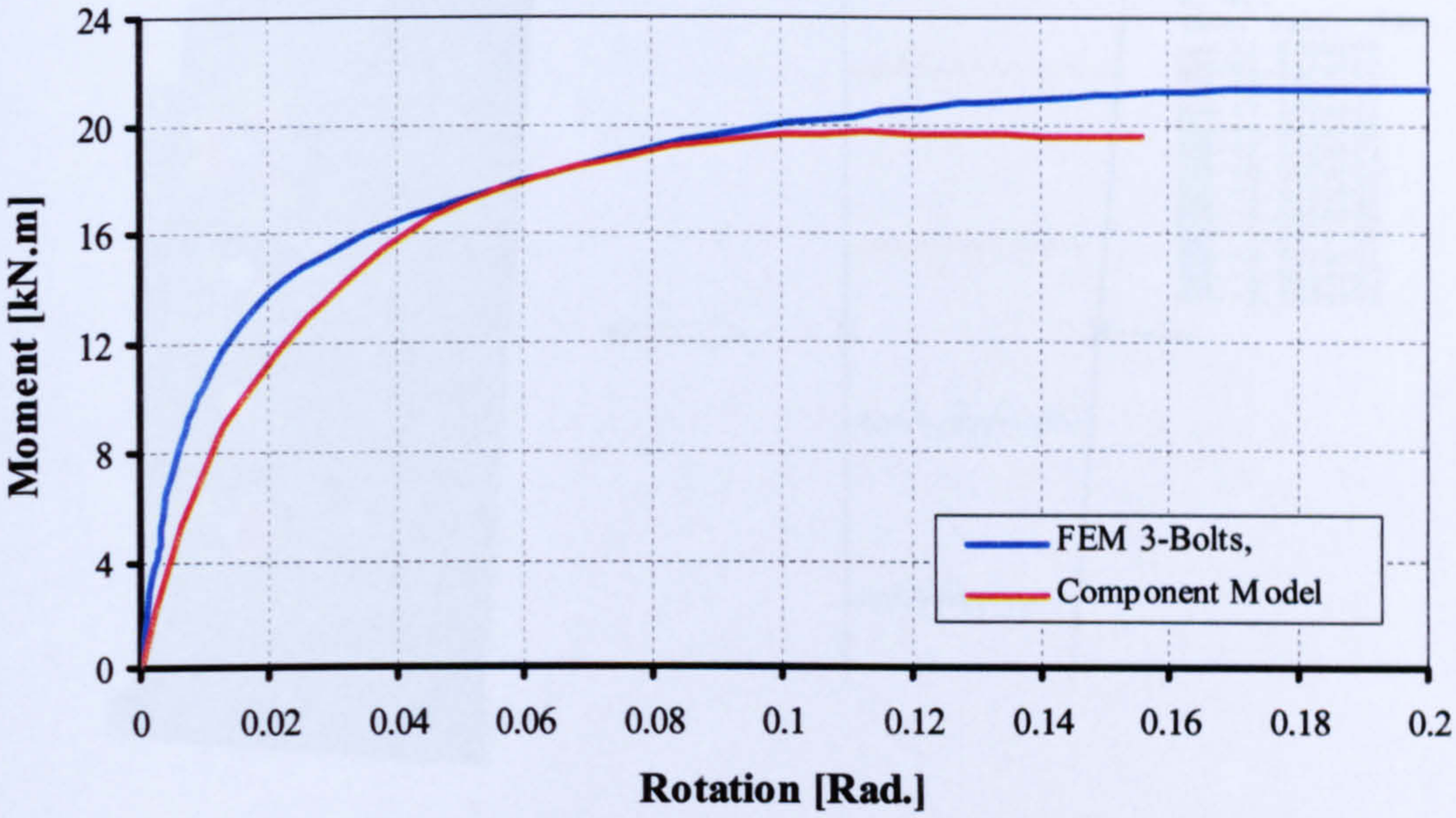

Figure 6.37 Moment-rotation comparison for the 3-bolt FEM and equivalent component model

An FE model of a four- bolt fin plate connection under pure rotation (**Figure 6.38**) was also analysed. The centre of rotation was chosen as the midpoint between the middle two bolts. The corresponding component model is shown in **Figure 6.39**. The comparison of moment-rotation for both the model and FE analysis (**Figure 6.40**) demonstrates the good agreement between them. It is obvious from the FE analysis that the connection fails by the top and bottom bolts shearing.

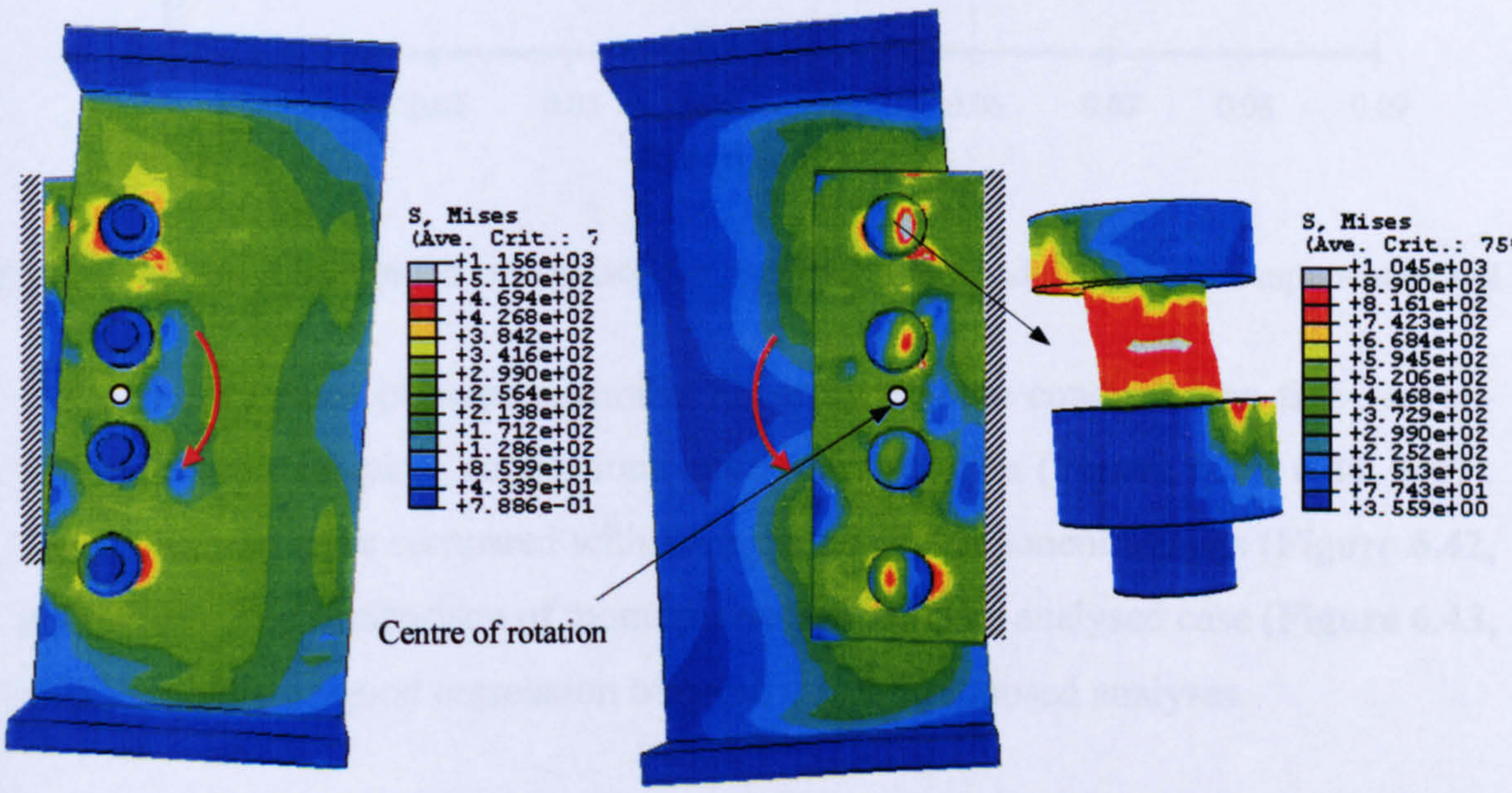

Figure 6.38 4-bolt FE model under pure rotation

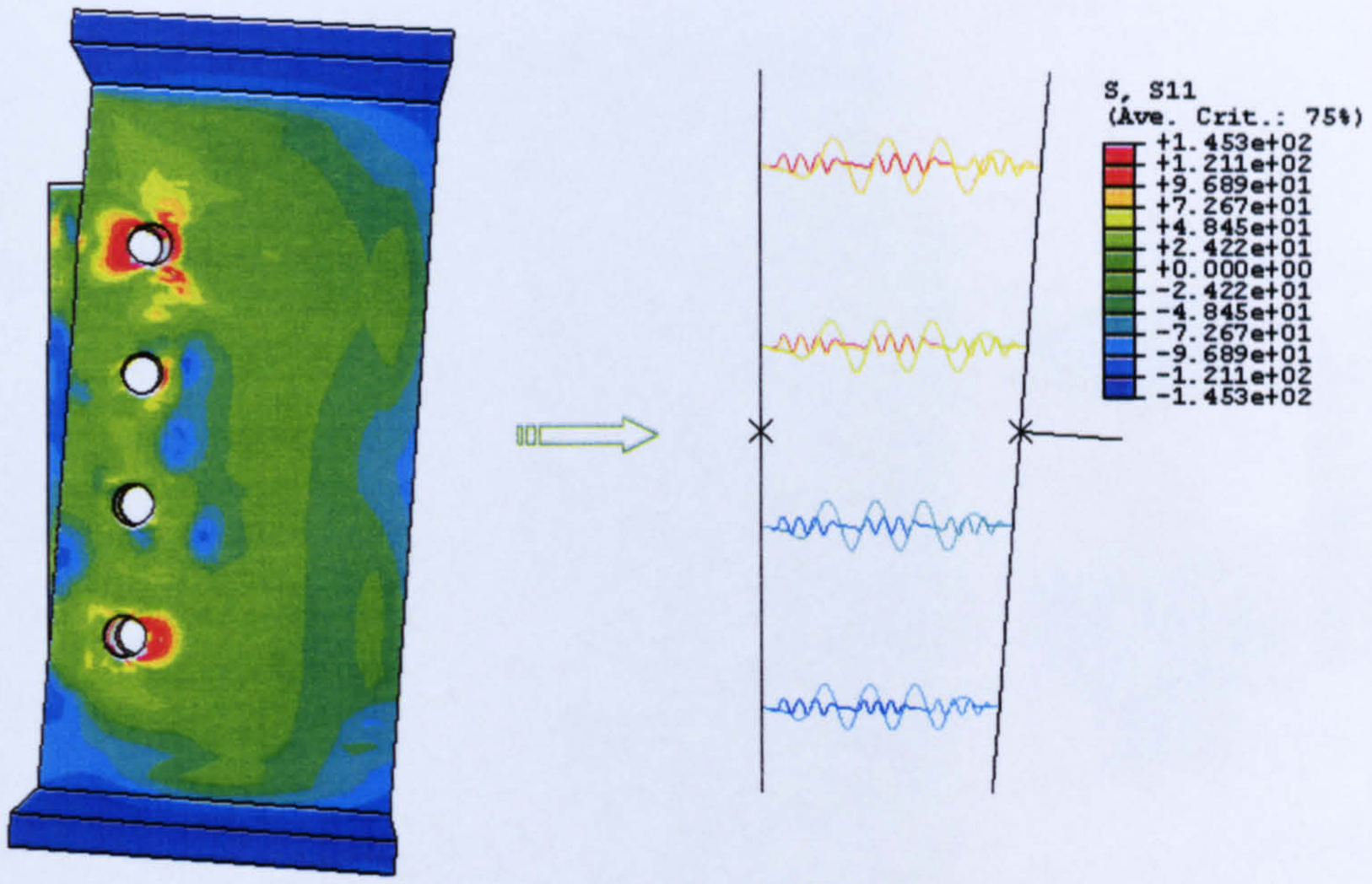

Figure 6.39 4-bolt FE model and the corresponding component model under pure rotation

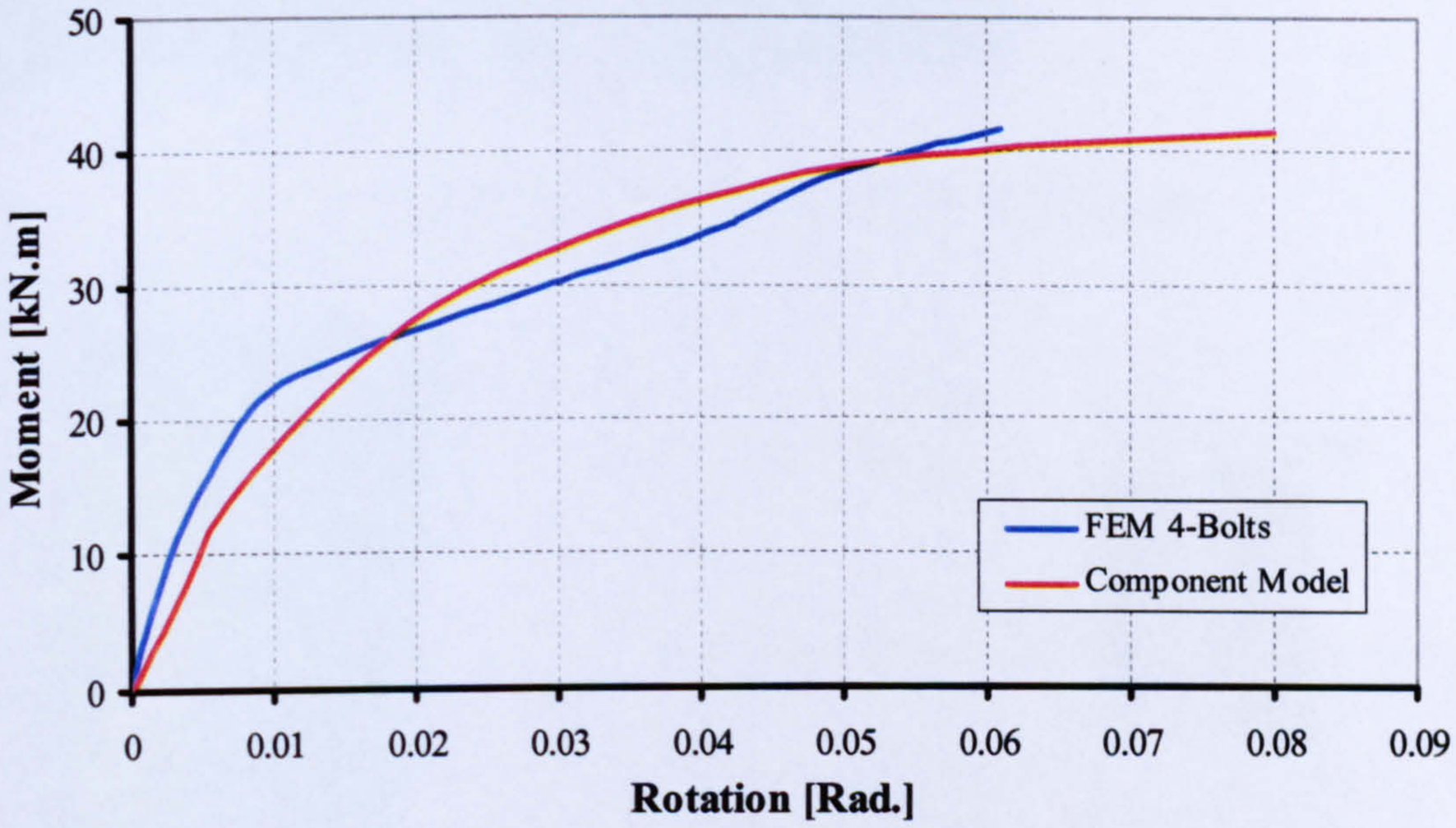

Figure 6.40 Moment-rotation comparison for the 4-bolt FEM and equivalent component model

Following the same principles, similar FE analyses were conducted on five-, seven- and eight- bolt fin plate connections under pure rotation (**Figure 6.41, 6.44, 6.47**). These analyses were compared with corresponding component models (**Figure 6.42, 6.45, 6.48**). The comparison of moment-rotation for each analysed case (**Figure 6.43, 6.46, 6.49**) shows good correlation between the two proposed analyses.

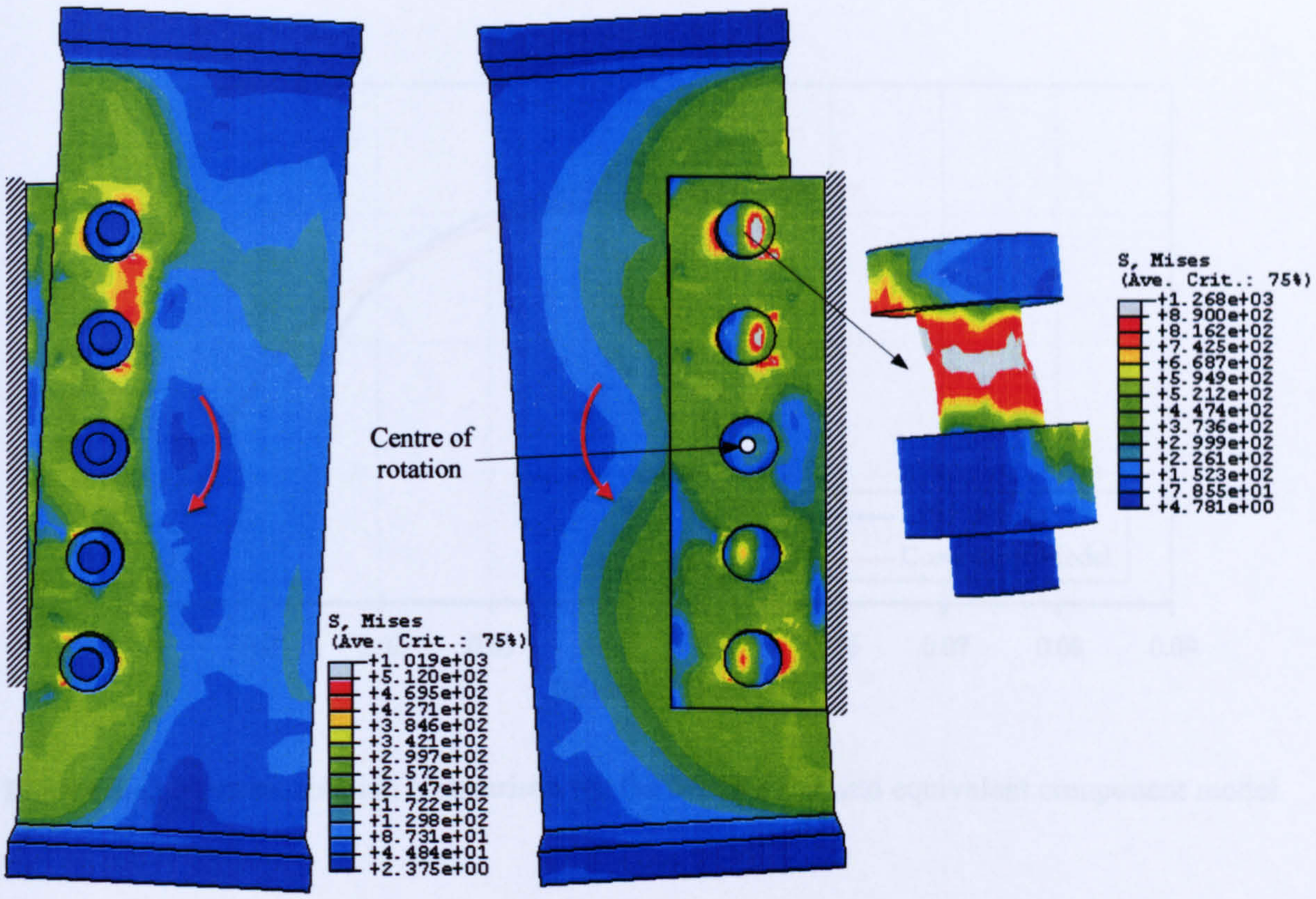

Figure 6.41 5-bolt FE model under pure rotation

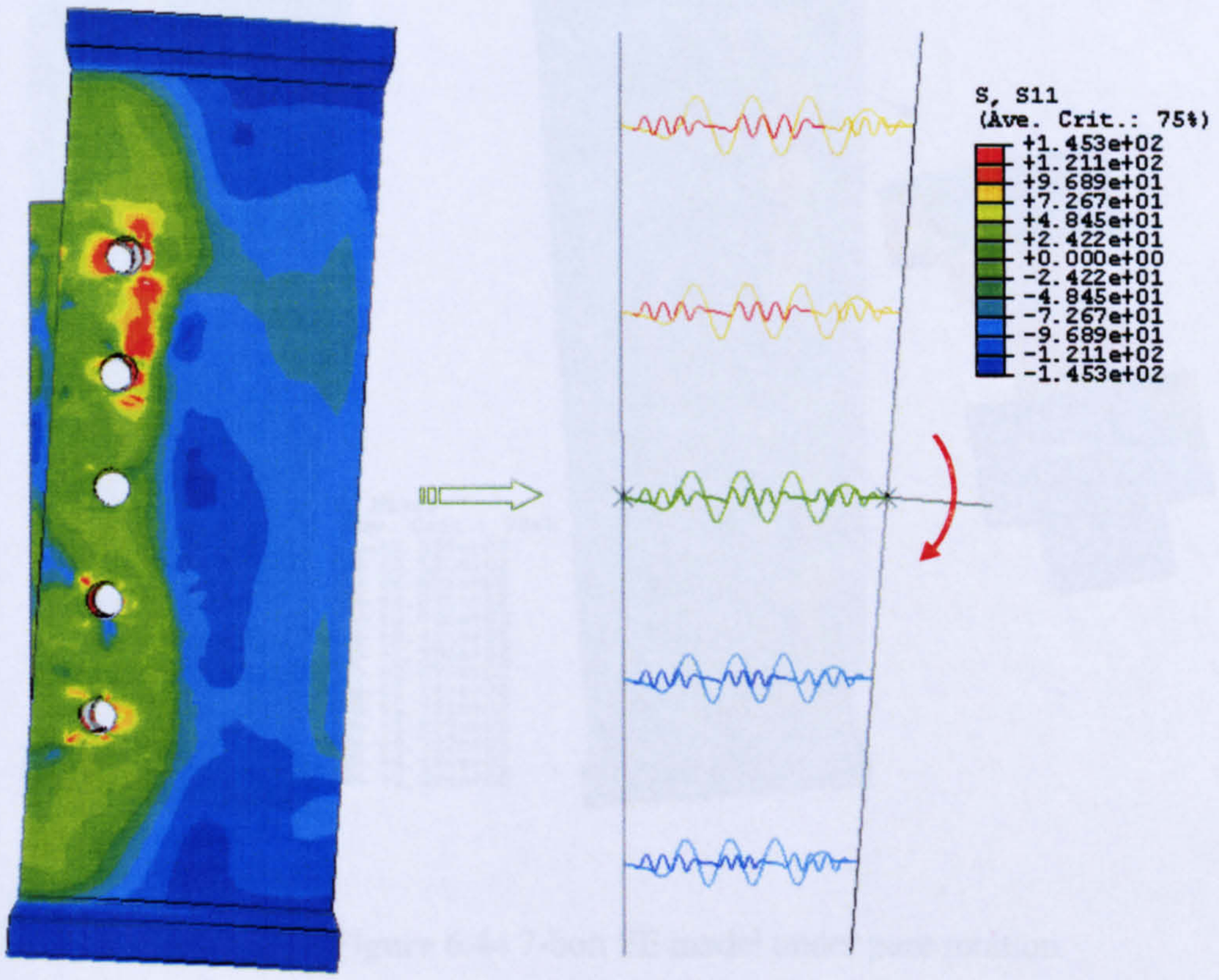

Figure 6.42 5-bolt FE model and the corresponding component model under pure rotation

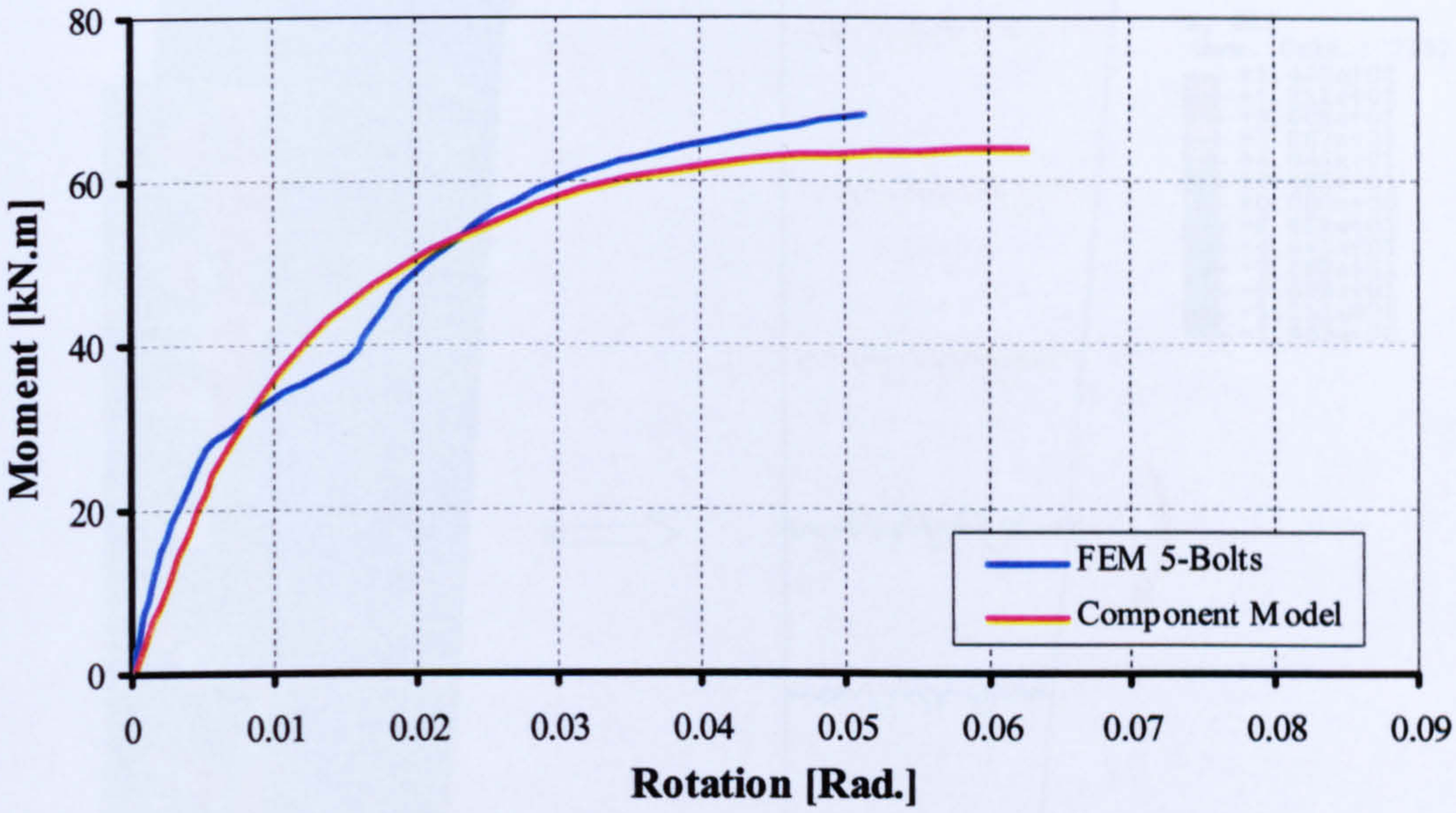

Figure 6.43 Moment-rotation comparison for the 5-bolt FEM and equivalent component model

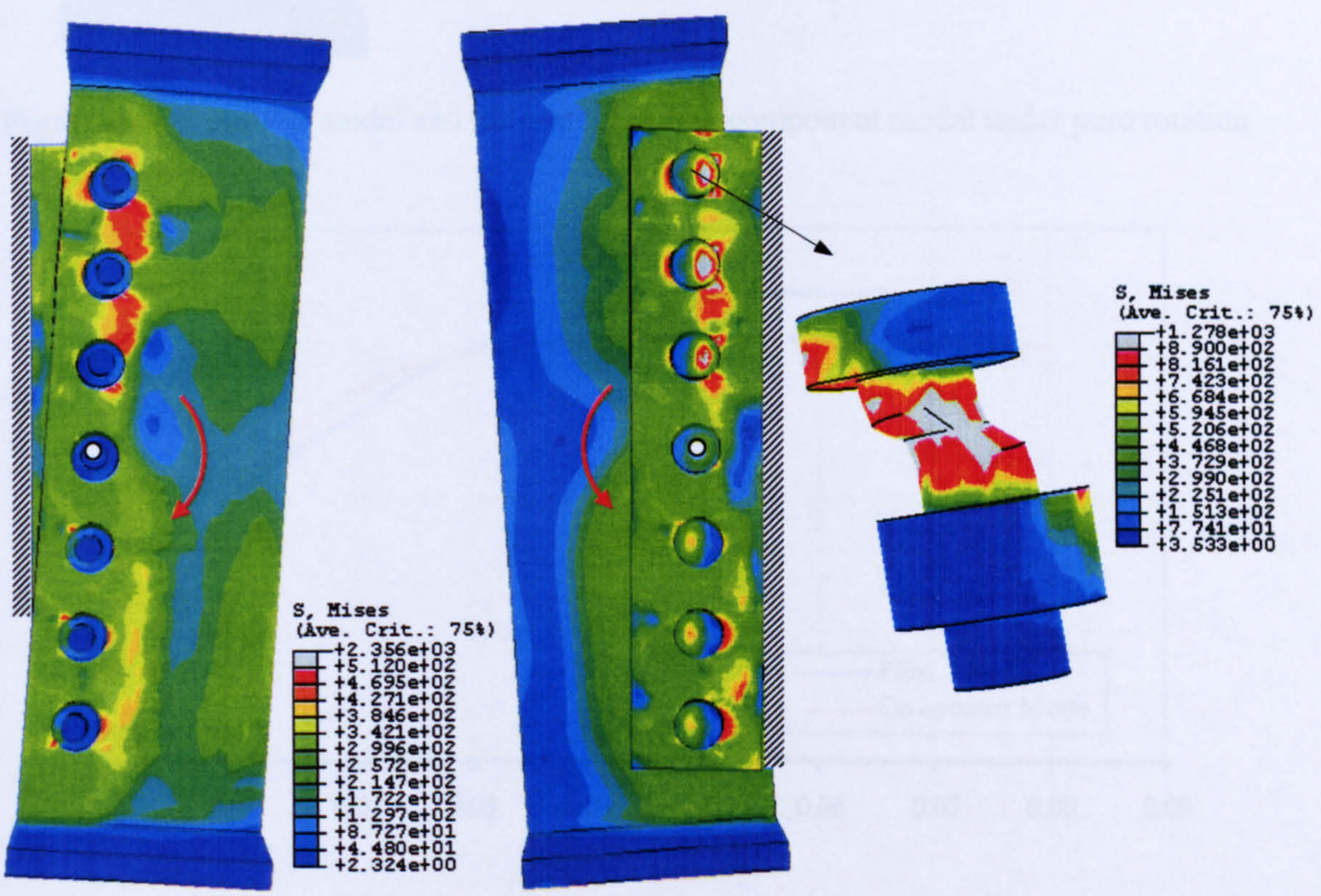

Figure 6.44 7-bolt FE model under pure rotation

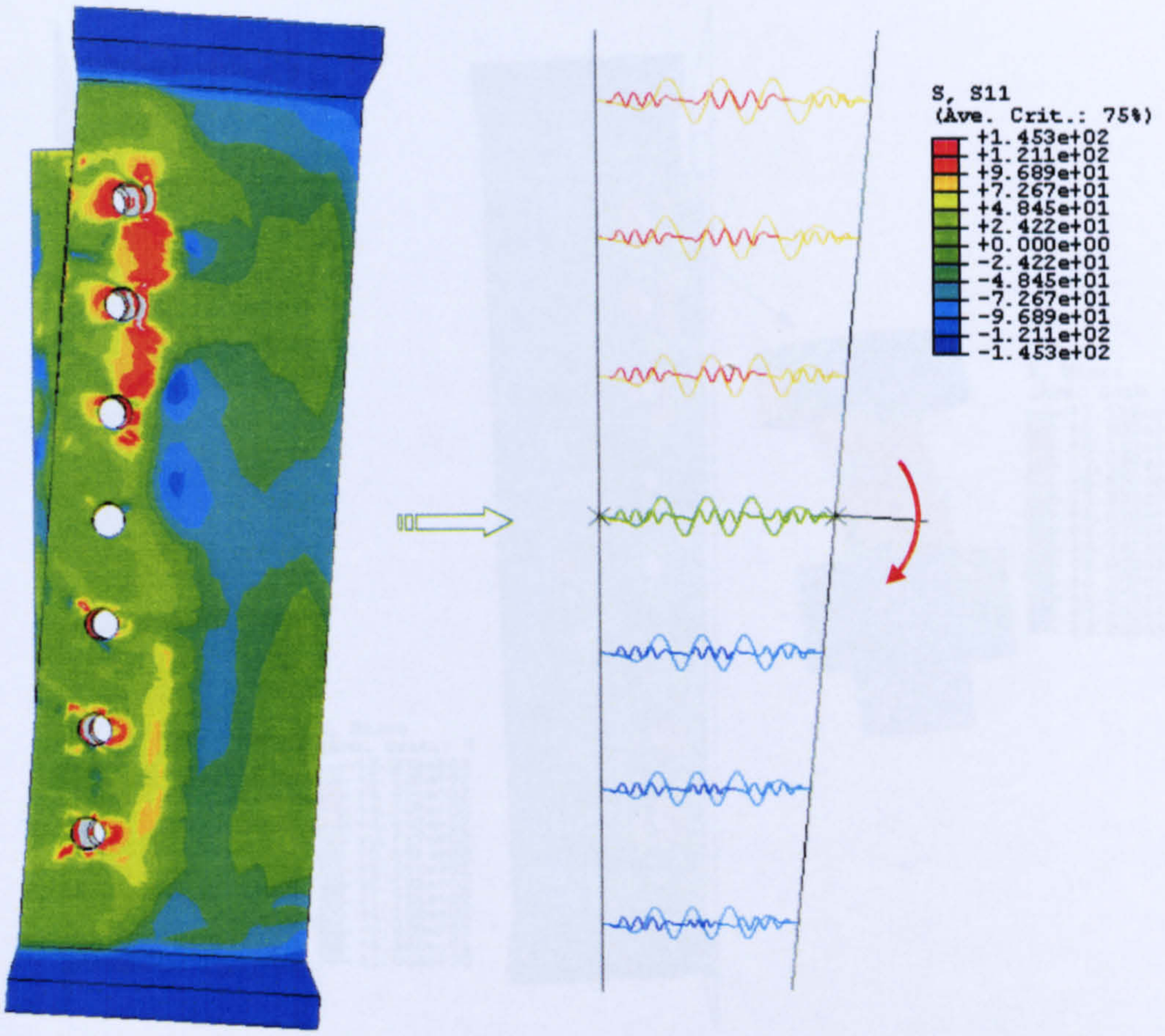

Figure 6.45 7-bolt FE model and the corresponding component model under pure rotation

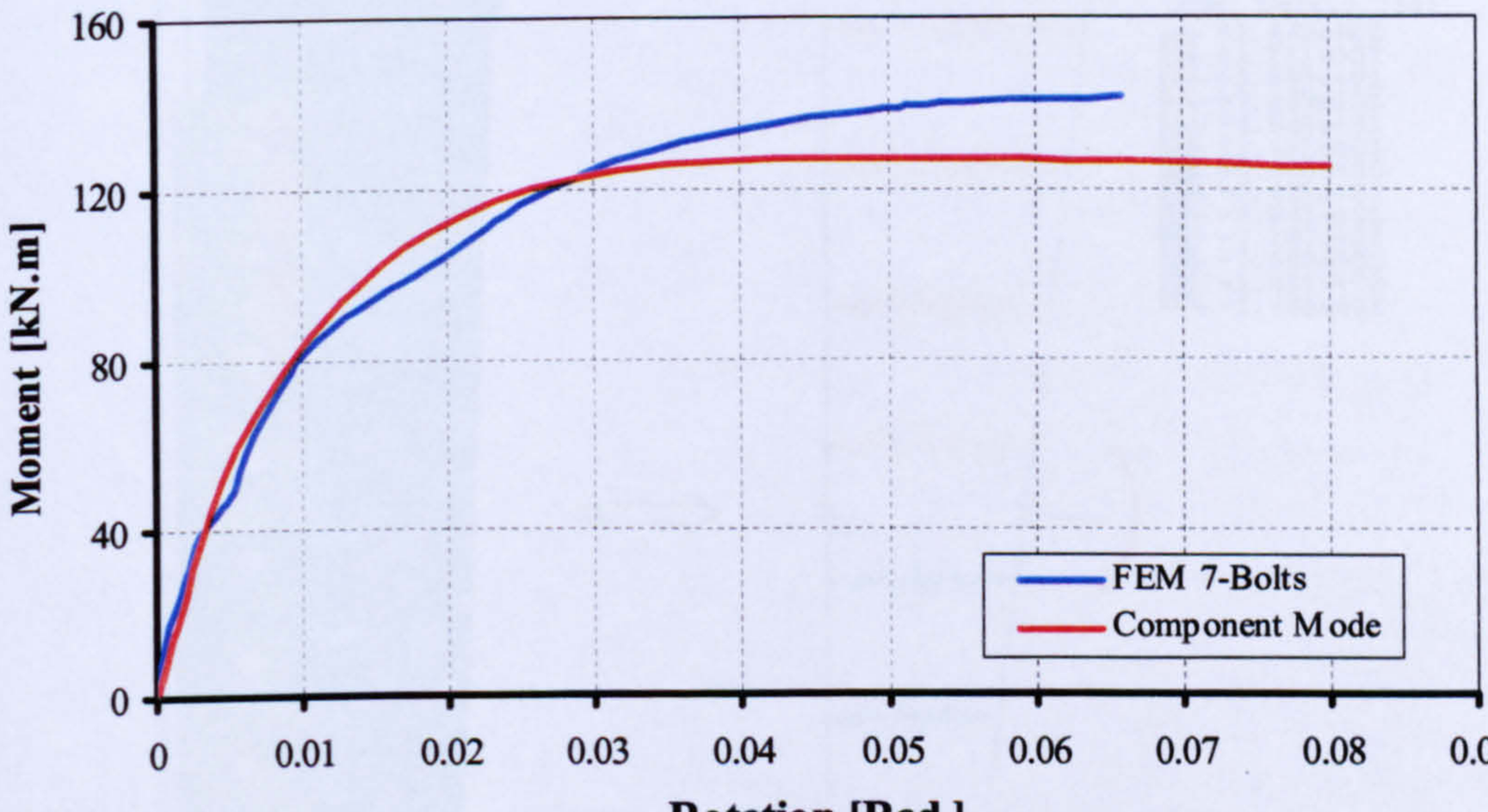

Figure 6.46 Moment-rotation comparison for the 7-bolt FEM and equivalent component model

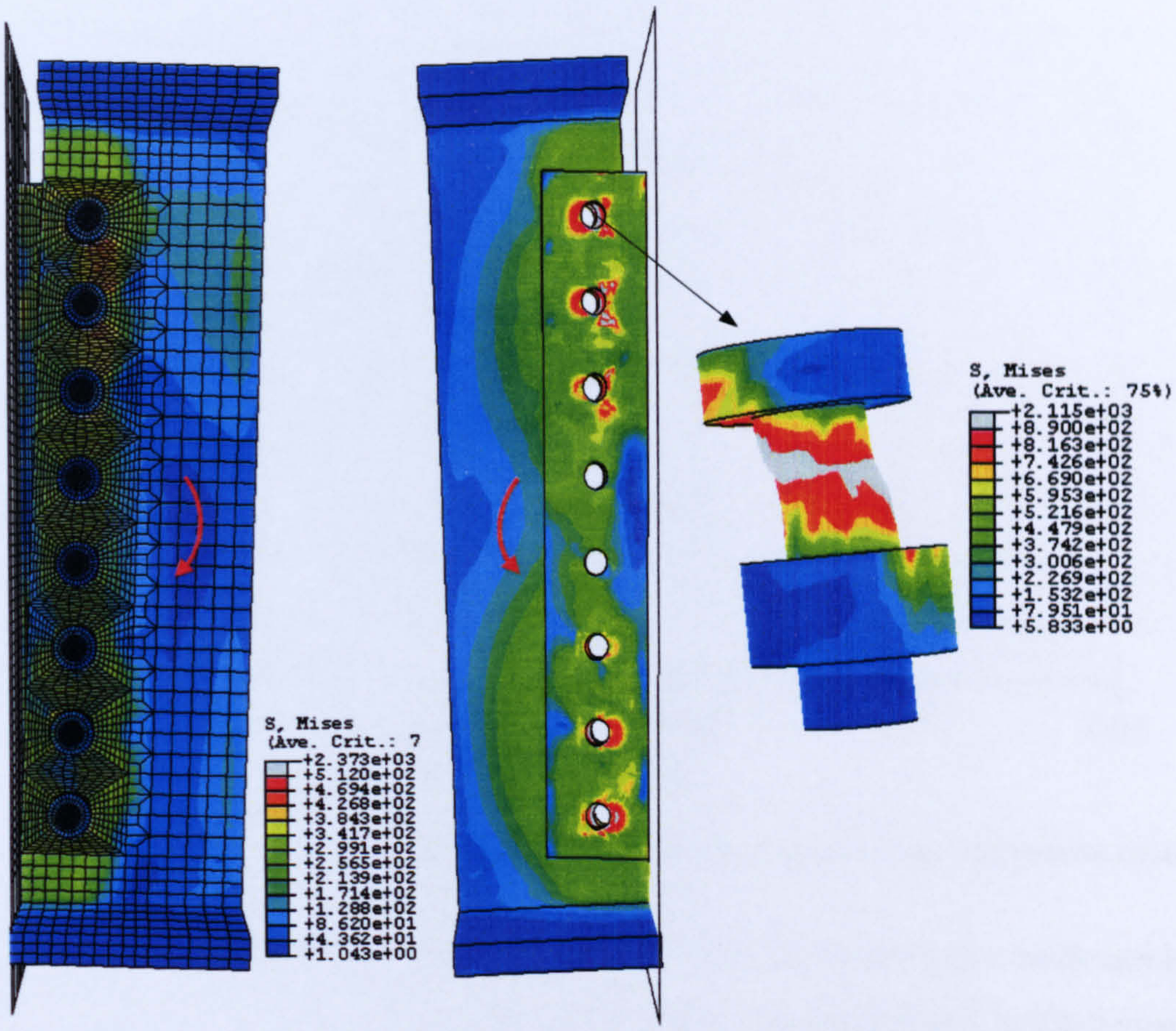

Figure 6.47 8-bolt FE model under pure rotation

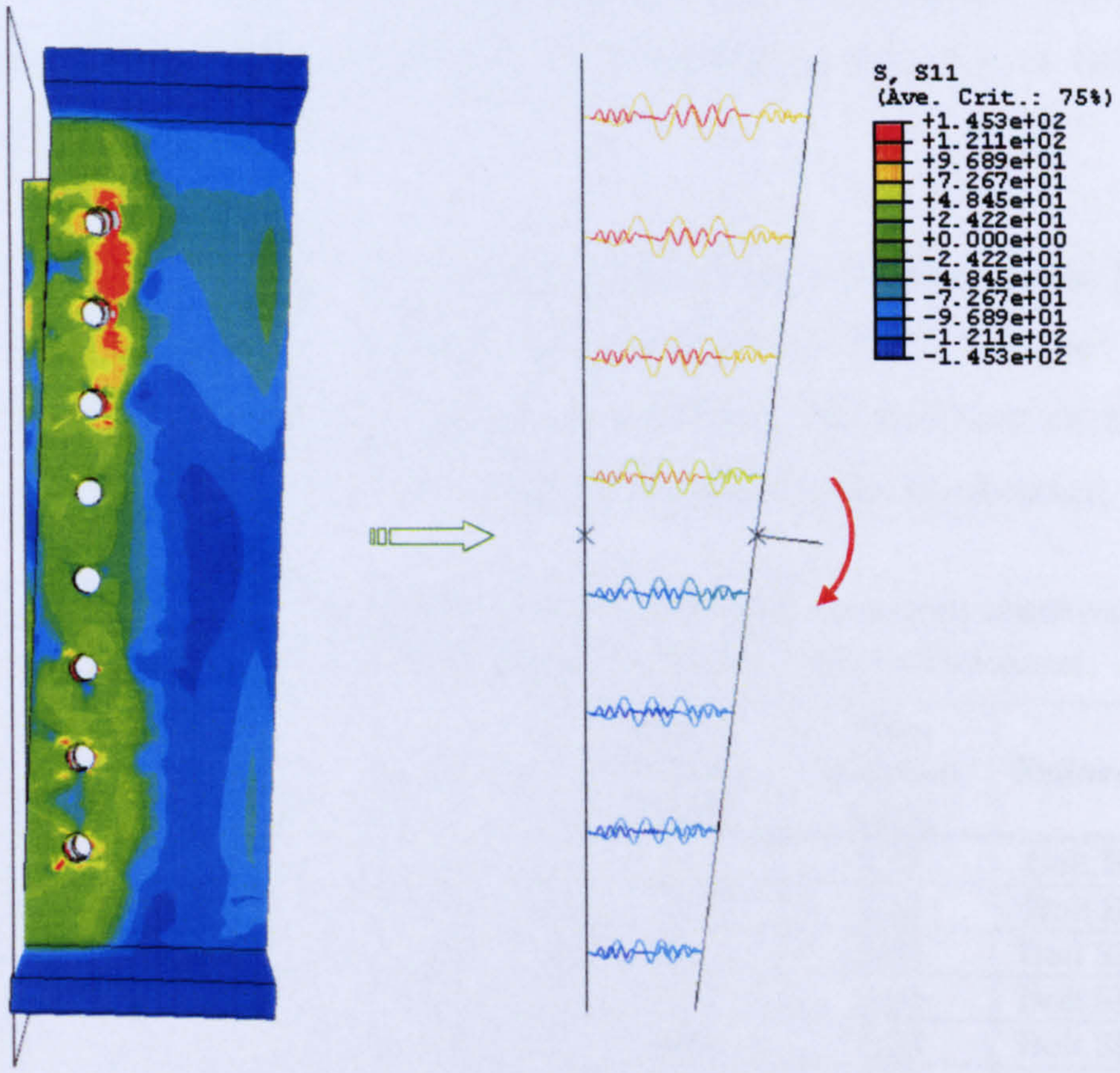

Figure 6.48 8-bolt FE model and the corresponding component model under pure rotation

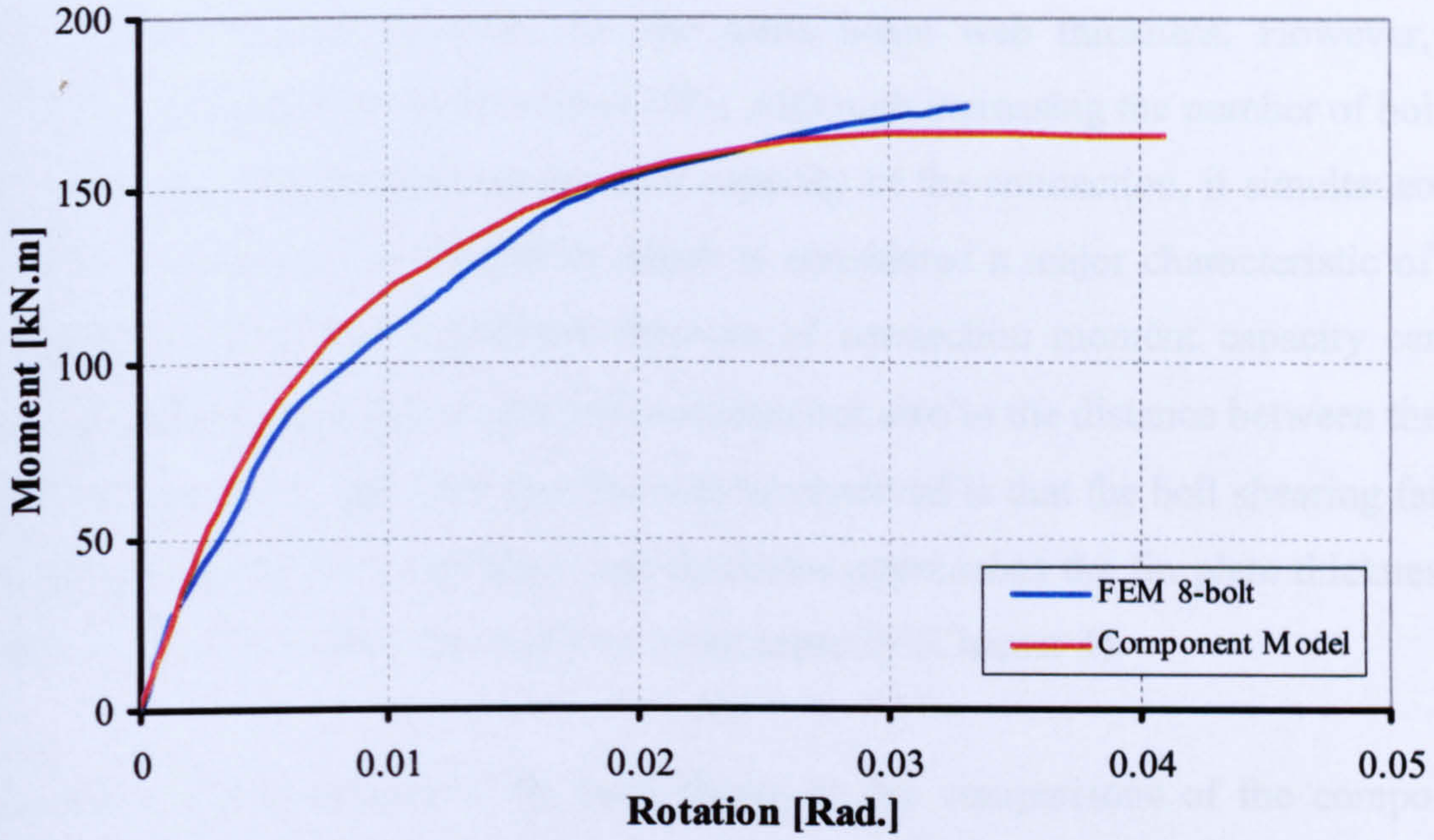

Figure 6.49 Moment-rotation comparison for the 8-bolt FEM and equivalent component model

An obvious bolt shearing failure of the top two bolts and the bottom two bolts can be observed in the component models of the 7-bolt and 8-bolt connections as the springs representing these bolts are the most distorted ones in the model. Therefore the component model has the advantage of demonstrating the type of failure more clearly than the FE analysis.

A summary of the parametric study of fin plates under pure rotation can be seen in **Table 6.8**. A consistent increase of maximum moment can be observed, corresponding to the number of bolts and the beam web thickness; in addition, a consistent decrease of the maximum angle of rotation can also be observed.

Table 6.8: Summary of FEM parametric study of fin plate connection under pure rotation in accordance with bolt number, fin plate and beam web thickness

No. of Bolt	t_w [mm]	t_p [mm]	Max. Moment [kN.m]	Max. Rotation [rad.]	Failure Type
2	5.8	10	10	0.18	Bolt Bearing
3	5.8	10	20	0.12	Bolt Bearing
4	9.5	10	42	0.08	Bolt Shearing
5	12.7	10	62	0.06	Bolt Shearing
7	11.9	10	128	0.04	Bolt Shearing
8	14.5	10	160	0.03	Bolt Shearing

It can also be seen that adding one bolt to a 2-bolt fin plate connection double the connection moment capacity, for the same beam web thickness. However, the rotation capacity reduced by almost 30%. Although increasing the number of bolts in a connection can increase the moment capacity of the connection, it simultaneously reduces the connection flexibility which is considered a major characteristic of this connection type. The significant increase of connection moment capacity can be strongly related, not only to the bolt numbers but also to the distance between the top and bottom bolts. The other fact that can be observed is that the bolt shearing failure mode dominates once the beam web thickness approaches the fin plate thickness or exceeds it. This reflects the study on tying capacity (Chapter 4).

Although good agreement has been shown in the comparisons of the component models against FEM for fin plates under pure rotation, some discrepancies have also been shown. These differences can be related to several causes. The first is that the FEM uses an over-sized bolt hole, whereas this can not be represented in the component model. The other valid point to be highlighted from the moment-rotation study is that the FEM represents the column flange by modelling a stiff plate connected to the fin plate. An extra action on the top bolts can be created if the bottom flange contacts the column flange. This situation has not been represented in the component model.

6.10. Evaluation of Shearing Resistance

The component model evaluation of the vertical shear response of the fin plate connection was achieved through comparison of a 3-bolt fin plate connection FE model (**Figure 6.50**) with the corresponding component model (**Figure 6.51**). In the FE model, a UB305×165×40 beam section was used, along with a 10 mm fin plate thickness, both the beam and the plate being of S275 steel. Three Grade 8.8 high strength M20 bolts were used to assemble the connection model. A vertical displacement boundary condition was applied on the bottom flange nodes. The vertical reaction is traced against the beam vertical movement in **Figure 6.52** for both the FE model and the component model. This plot shows good correlation between the FE model and the component model.

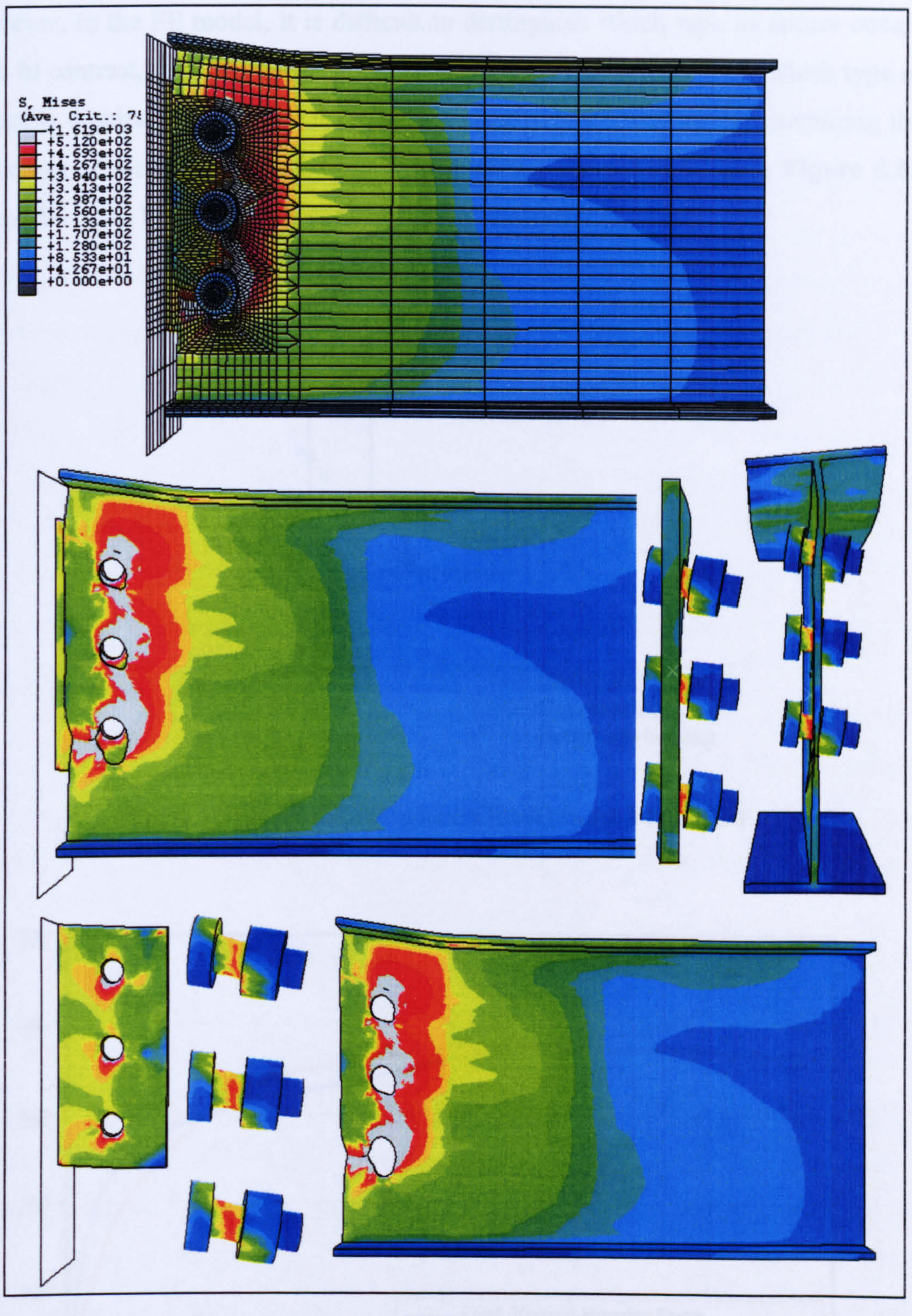

Figure 6.50 Von Mises stresses for vertically loaded FE model of Fin plate connection

From the component model load deflection response (**Figure 6.52**), one can identify the type of failure which is likely to be dominant, that is plate bearing as shown in **Figure 6.50**. Notice that the component model graph has a large deflection and an extended plateau after 10mm deflection. If a bolt shearing failure occurred, the graph would drop suddenly and at a smaller deflection (see for example **Figure 7.23**).

However, in the FE model, it is difficult to distinguish which type of failure occurs first. In contrast, the component model is able to describe more clearly which type of failure is dominating, whether it is bolt shearing or plate bearing, by examining the distortion of the component springs in the model, for example as in **Figure 6.51** where the beam bearing component spring has distorted the most.

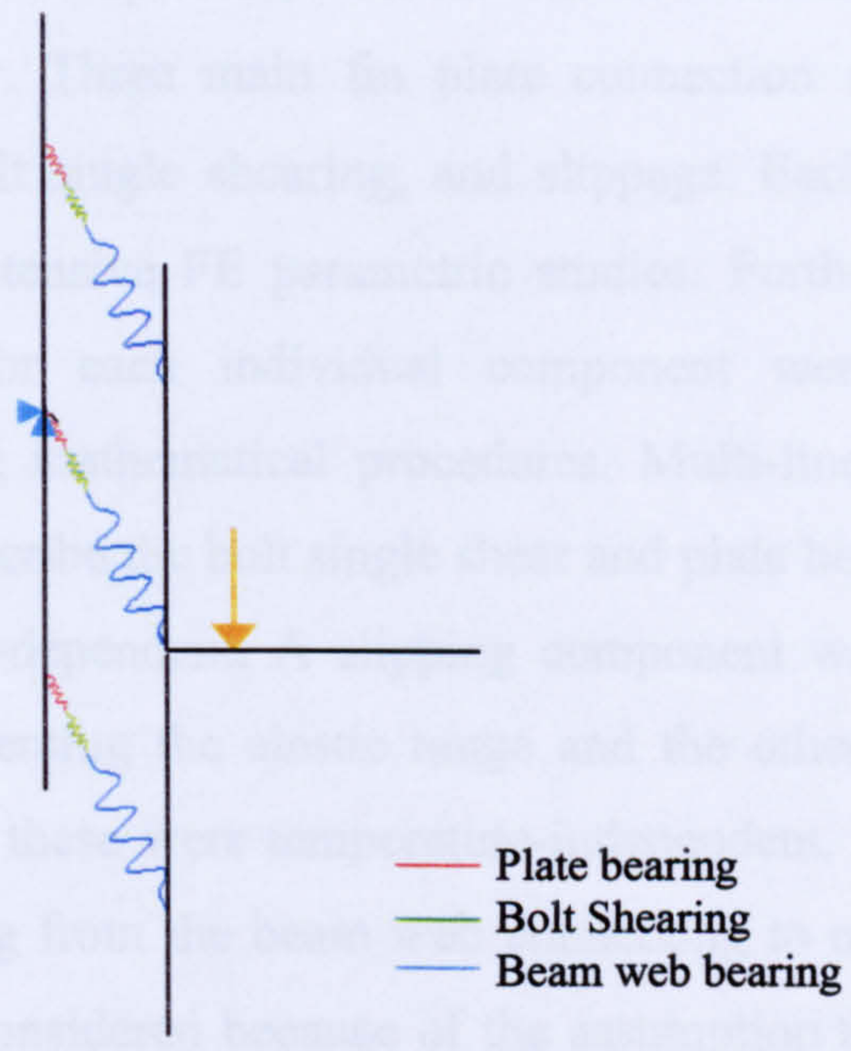

Figure 6.51 Equivalent component model to the 3-bolt FEM

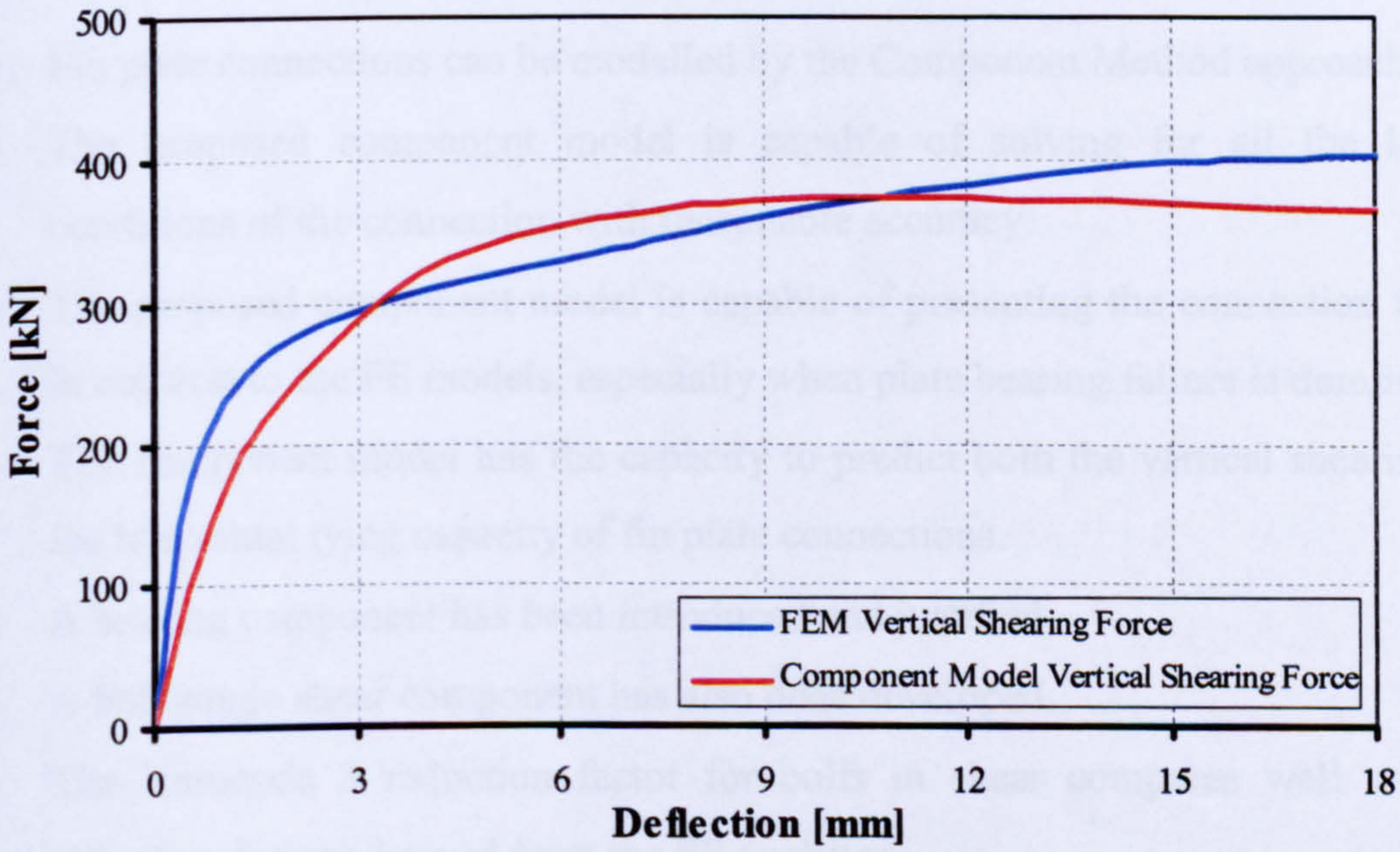

Figure 6.52 Shearing force-deflection comparison for 3-bolt FEM and equivalent component model

6.11. Conclusions

In this chapter an effective computational connection spring model has been proposed for use in global structural analysis of steel frames at ambient and elevated temperature. The fin plate shear connection was successfully modeled via a component method approach to represent, with reasonable accuracy, the actual non-linear connection behaviour. Three main fin plate connection components were identified; plate bearing, bolt single shearing, and slippage. Each component was investigated in detail via intensive FE parametric studies. Furthermore, the load-deflection characteristics for each individual component were described and generalized via curve-fitting mathematical procedures. Multi-linear, elastic-plastic expressions were used to describe the bolt single shear and plate bearing components and these were temperature-dependent. A slipping component was represented by two linear parts, one representing the elastic range and the other representing the slippage behaviour. Both of these were temperature-independent. The eccentricities of the internal forces coming from the beam web connecting to one side of the fin plate at the joint were not considered because of the assumption that the composite action will minimize their effects. In addition, several important results have been found in the course of the component simulation performed on this connection type:

- Fin plate connections can be modelled by the Component Method approach.
- The proposed component model is capable of solving for all the loading conditions of the connection with reasonable accuracy.
- The proposed component model is capable of presenting the connection failure, in contrast to the FE models, especially when plate bearing failure is dominant.
- The component model has the capacity to predict both the vertical shearing and the horizontal tying capacity of fin plate connections.
- A bearing component has been introduced and justified.
- A bolt single shear component has also been developed.
- The Eurocode 3 reduction factor for bolts in shear compares well with the reduction factors derived from the FE analyses.
- The Eurocode 3 equation for calculating the bolt stiffness in single shear does not appear to have appropriate justification.
- A friction component has been developed and its effect evaluated.

6.12. References

[6.1] Nethercot, D. A., and Zandonini R., "Methods of prediction of joint behaviour: beam-to-column connections", Chapter 2 in Structural connections, stability and strength (Ed.: R. Narayanan). Elsevier Applied Science, London, UK, (1989) pp 23-62.

[6.2] Tschemmernegg, F., Tautschnig, A., Klein, H., Braun, Ch. and Humer, Ch., "Zur Nachgiebigkeit von Rahmenknoten (Semi-rigid joints of frame structures)", Stahlbau **56**, (1987) pp 299-306.

[6.3] Tschemmernegg F., "The Design of Structural Steel Frames under Consideration of the Nonlinear Behaviour of Joints" *J. Construct. Steel Research*, Vol. **11**, (1988) pp 73-103.

[6.4] European Committee for Standardization (CEN). "Eurocode 3: Design of Steel Structures, Part 1.8: Design of joints", EN 1993-1-8, British Standard Institution, London, (2005).

[6.5] Jaspart, J. P., "General report: session in connections" *J. Construct. Steel Research*, Vol. **55**, (2000) pp 69-89.

[6.6] Rex, C. O., and Easterling, S. W., "Behaviour and modeling of a bolt bearing on a single plate", *Journal of Structural Engineering,* ASCE, Vol. **129**, No. 6, (2003) pp 792-800.

[6.7] Richard, R. M., and Elsalti, M. K., "PRCONN, Moment-Rotation Curves for Partially Restrained Connections", Users manual for program developed at The University of Arizona, Department of Civil Engineering and Engineering Mechanics, Tucson, Ariz, (1991).

[6.8] LRFD. Load and resistance factor design: manual of steel construction. 3rd ed. American Institute of Steel Construction; 1993.

[6.9] LRFD. Load and resistance factor design: manual of steel construction. 3rd ed. American Institute of Steel Construction; 1999.

[6.10] BS3692: "ISO metric precision hexagon bolts, screws and nuts specification" (2001).

[6.11] European Committee for Standardization (CEN), "Eurocode 3: Design of Steel Structures, Part 1.2: General rules - Structural fire design", EN 1993-1-2, British Standard Institution, London, (2005).

[6.12] Ramberg W., and Osgood WR., "Description of stress–strain curves by 3 parameters", Technical Report 902, National Advisory Committee for Aeronautics, (1943).

[6.13] Jones, S. W, Kirby, P. A., and Nethercot, D. A., "The analysis of frames with semi-rigid connections a state-of-the-art report", *J. Construct. Steel Research,* Vol. 2, (1983) pp 2–13.

[6.14] Hayes, M. D. "Structural analysis of a pultruded composite beam: shear stiffness determination and strength and fatigue life predictions", PhD. Thesis in Engineering Mechanics, Faculty of the Virginia Polytechnic Institute and State University, 2003.

[6.15] Madabhusi-Raman, P., and Davalos, J. F., "Static shear correction factor for laminated rectangular beams", *Composites Part B: Engineering*, 27 (3-4): (1996) pp 285-293.

Chapter 7

Applications of the Component Model at Elevated Temperature

7.1. Introduction

The previous chapter has explained in detail the development of a component model for fin plate connections. In addition, successful evaluations of the component model against FEM analyses have been made at ambient temperature. Consistent with the research objective of investigating this connection under the effect of fire, this chapter validates the proposed component model at elevated temperature. For this purpose the FEM model was analysed under different actions (shear, tying force, moment) and varied elevated temperatures, and then compared with the corresponding component model. The component model was also compared with a fin plate connection fire test conducted in the Czech Republic to evaluate the component model under combined actions at elevated temperature.

7.2. Shear Force in the Component Model

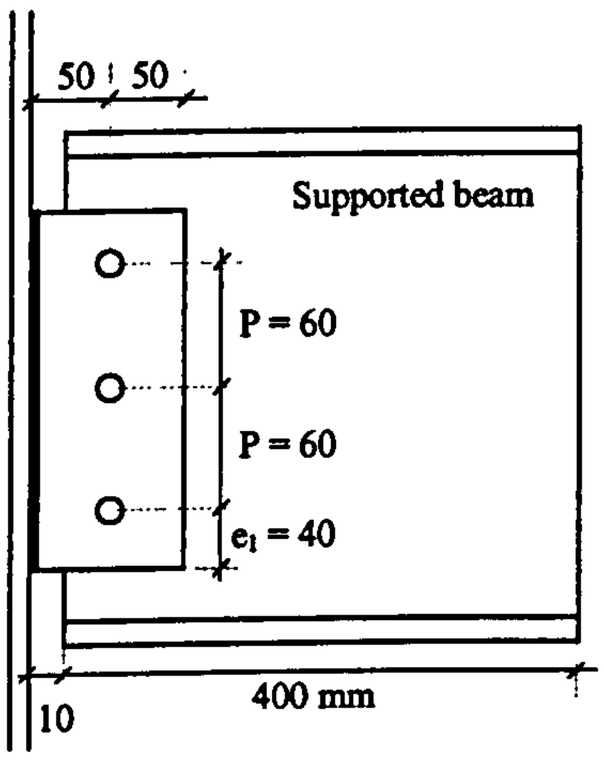

Figure 7.1 FEM geometric detail

In this application a FE model of a fin plate connection was assembled for a S275 steel UB305×165×40 beam section connected to a S275 steel fin plate of 10 mm thickness and three M20, Grade 8.8 bolts. The connection geometric details (bolt pitch, end distance and the edge distance) were as shown in **Figure 7.1**. The FE connection model (**Figure 7.2**) was subjected to vertical force by applying a totally vertical movement to the beam part of the connection. The entire connection model was analysed considering two different steady-state temperatures, 550°C and 750°C.

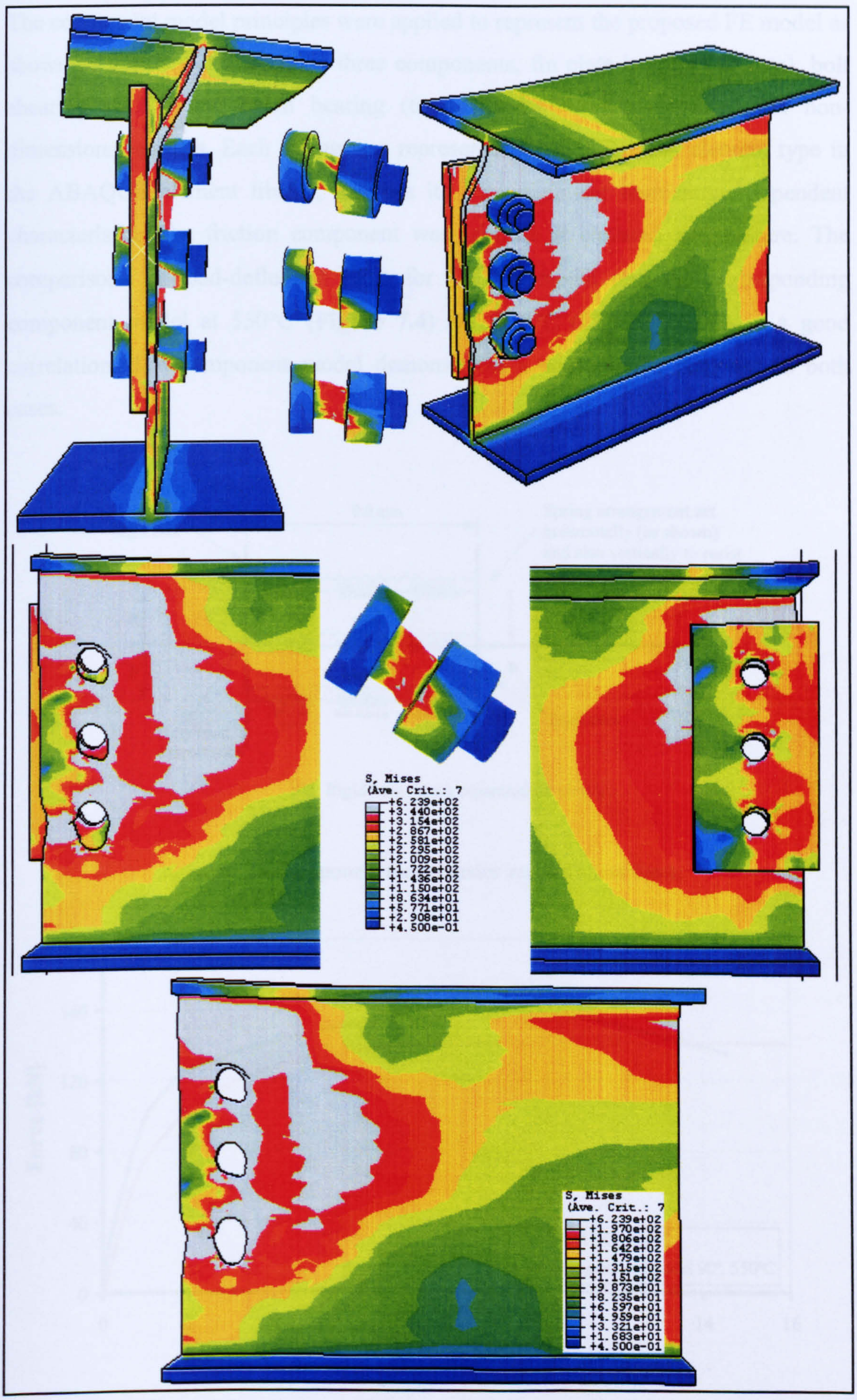

Figure 7.2 FE model under vertical shear force at 550°C.

The component model principles were applied to represent the proposed FE model as shown in **Figure 7.3**. The main three components, fin plate bearing (10 mm), bolt shearing (M20), and beam bearing (6 mm web), were represented via non-dimensional springs. Each spring was represented by a SPRINGA element type in the ABAQUS element library, and has its own nonlinear temperature-dependent characteristic. The friction component was ignored at elevated temperature. The comparisons of load-deflection plots for the FE model and the corresponding component model at 550°C (**Figure 7.4**) and 750°C (**Figure 7.5**) show a good correlation. The component model demonstrates a conservative response in both cases.

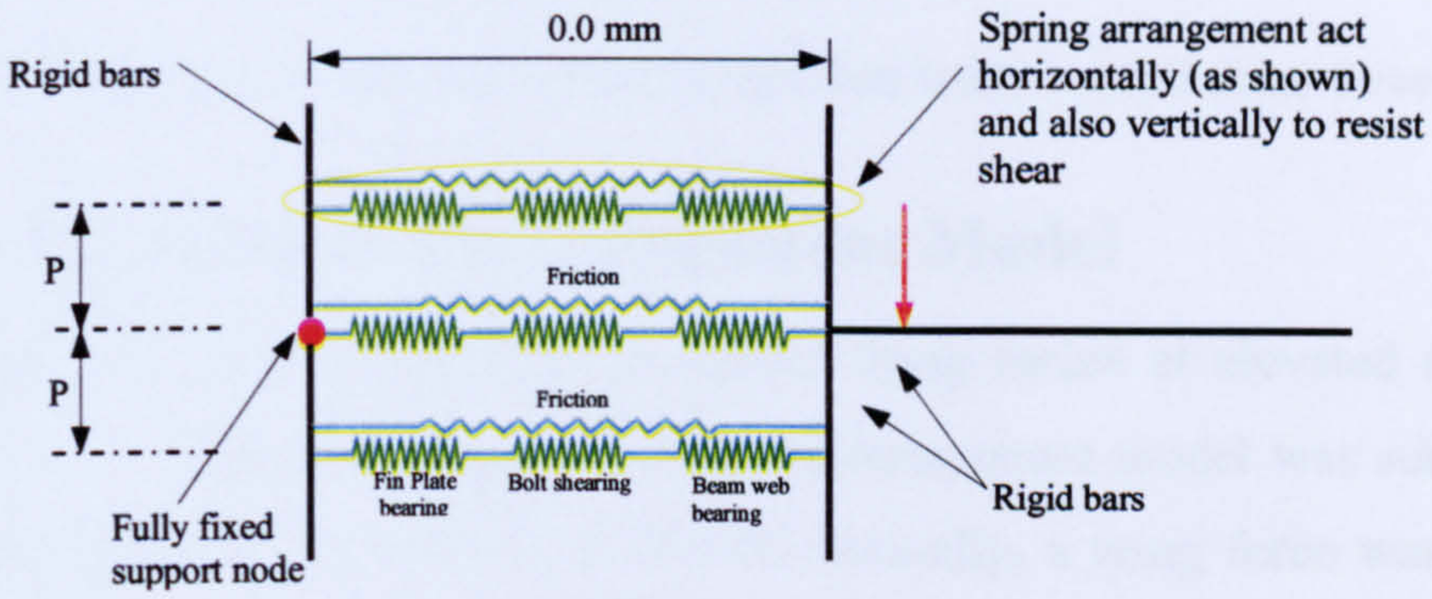

NB. Rigid bars shown separated for clarity

Figure 7.3 Component model under vertical shear force.

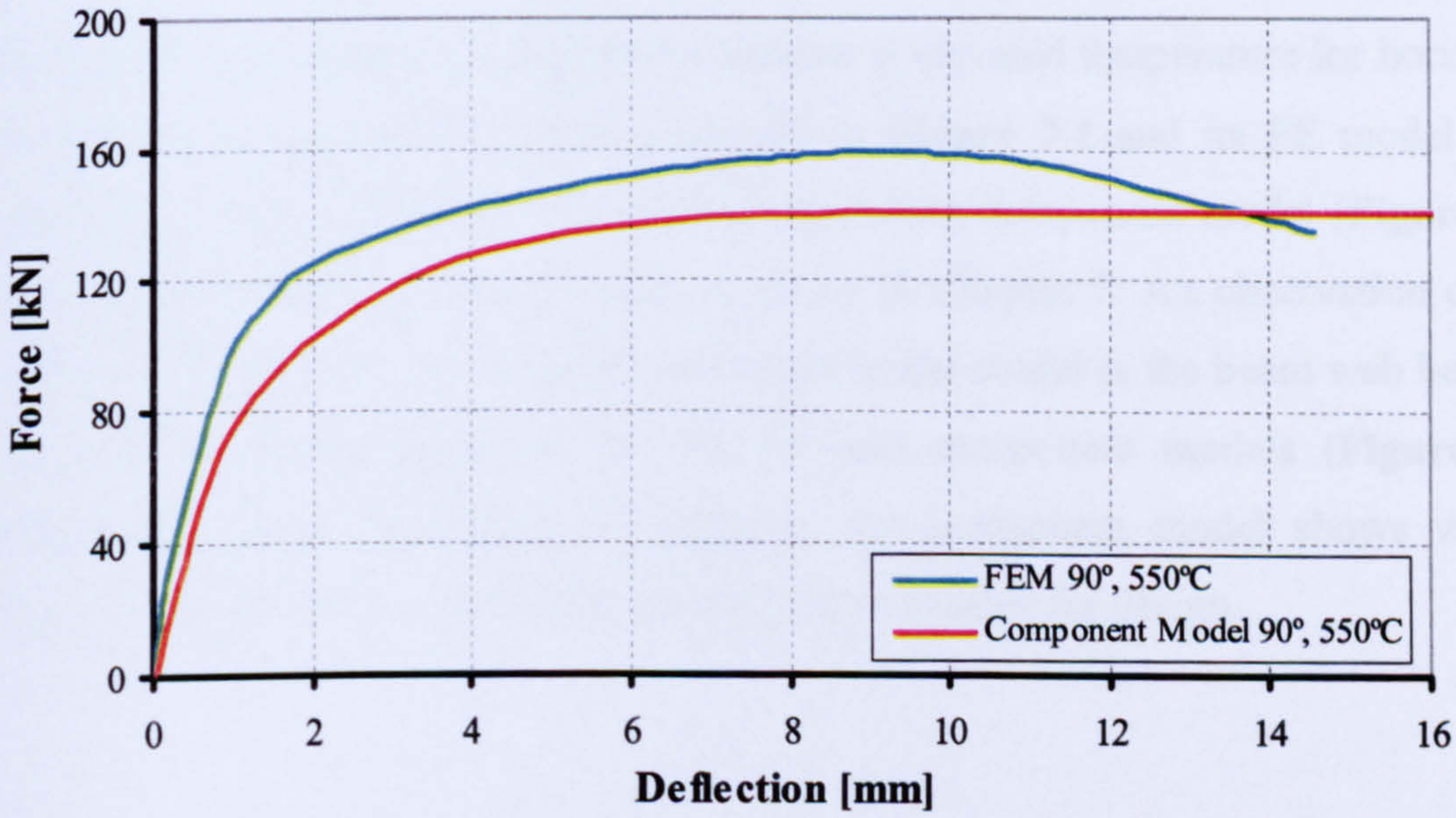

Figure 7.4 FEM and Component model comparison under vertical shear force at 550°C.

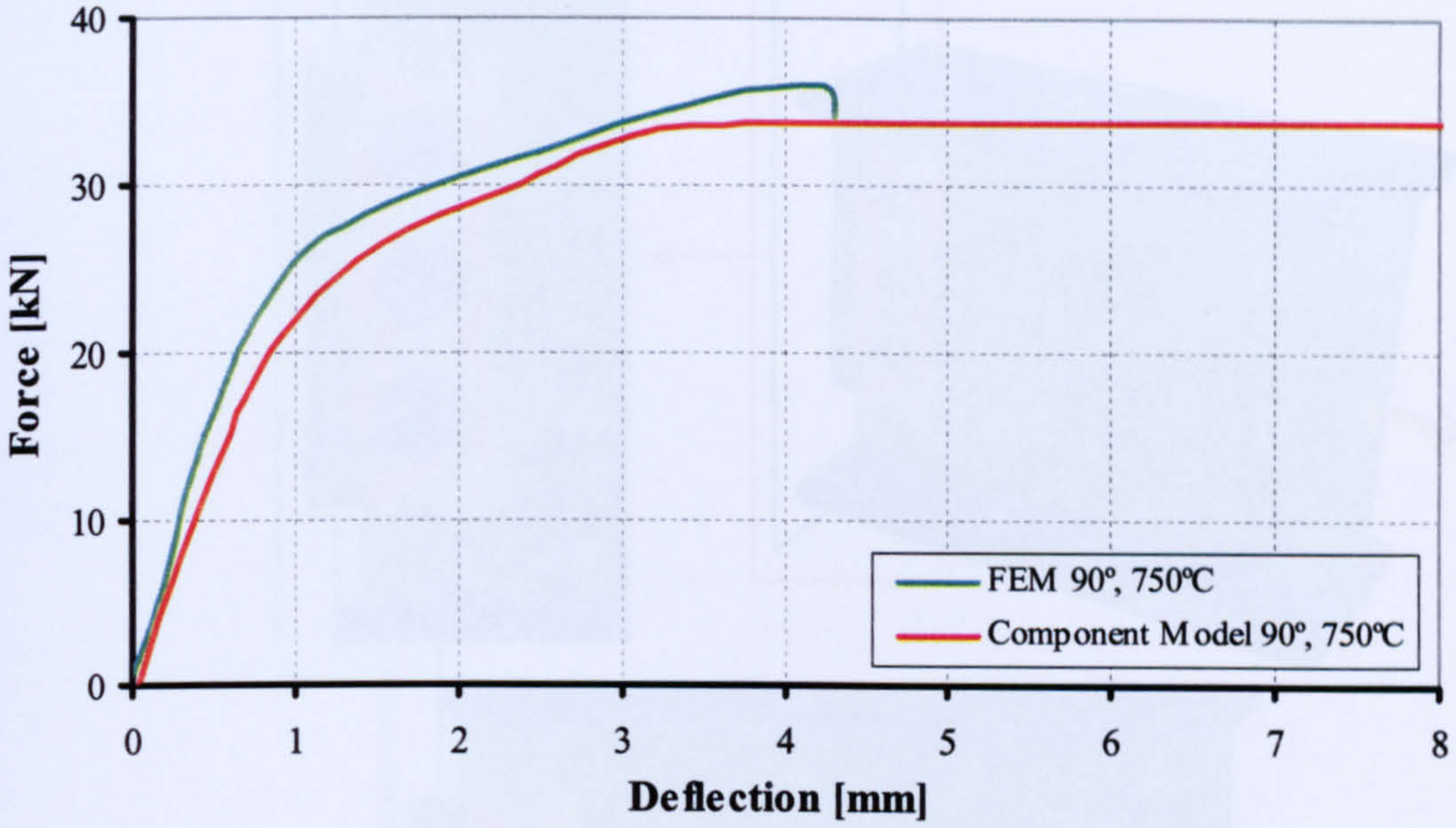

Figure 7.5 FEM and Component model comparison under vertical shear force at 750°C.

7.3. Tying Force in the Component Model

The component model's capability to predict tying forces at elevated temperature was assessed through three stages. Firstly, the component model was subjected to a completely horizontal tying force at 550°C. Secondly, a tying force was applied at 35° inclination at 450°C, 550°C, 650°C and 750°C. Thirdly, a tying force applied at 45° inclination was applied successively at temperatures of 450°C, 550°C, 650°C and 750°C.

In order to investigate the component response at elevated temperature for horizontal tying force the connection detail proposed in **Figure 7.1** and its FE model were analysed at 550°C (**Figure 7.6**). The corresponding component model (**Figure 7.7**) was applied following the principles proposed in Chapter 7. An observation of this model confirmed that the weakest component in the model is the beam web bearing. The load-deflection responses for the FE and component models (**Figure 7.8**) demonstrate good correlation. In addition, the component model shows weaker response than the FE model which makes it conservative for design.

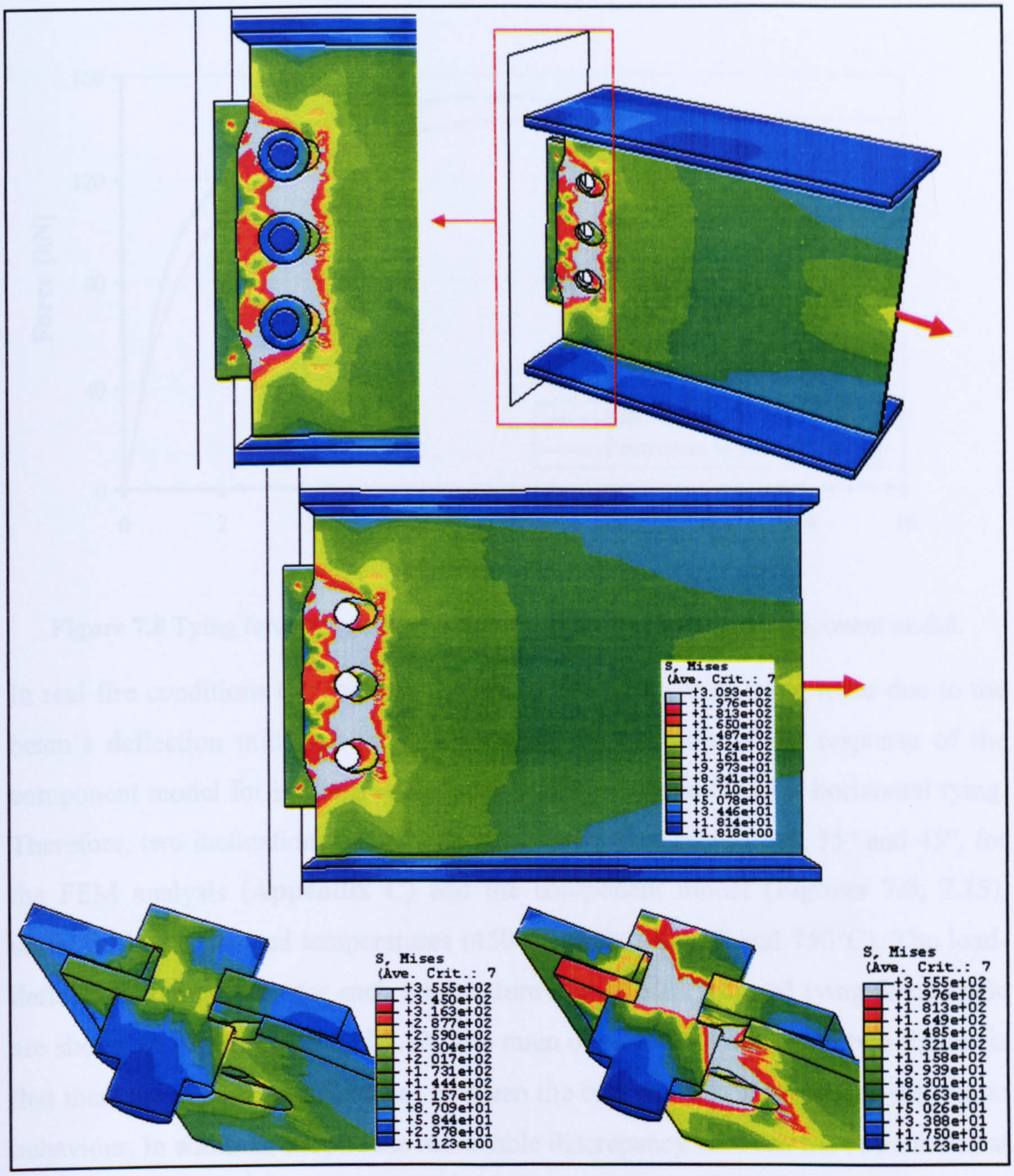

Figure 7.6 FE model under totally horizontal tying force at 550°C.

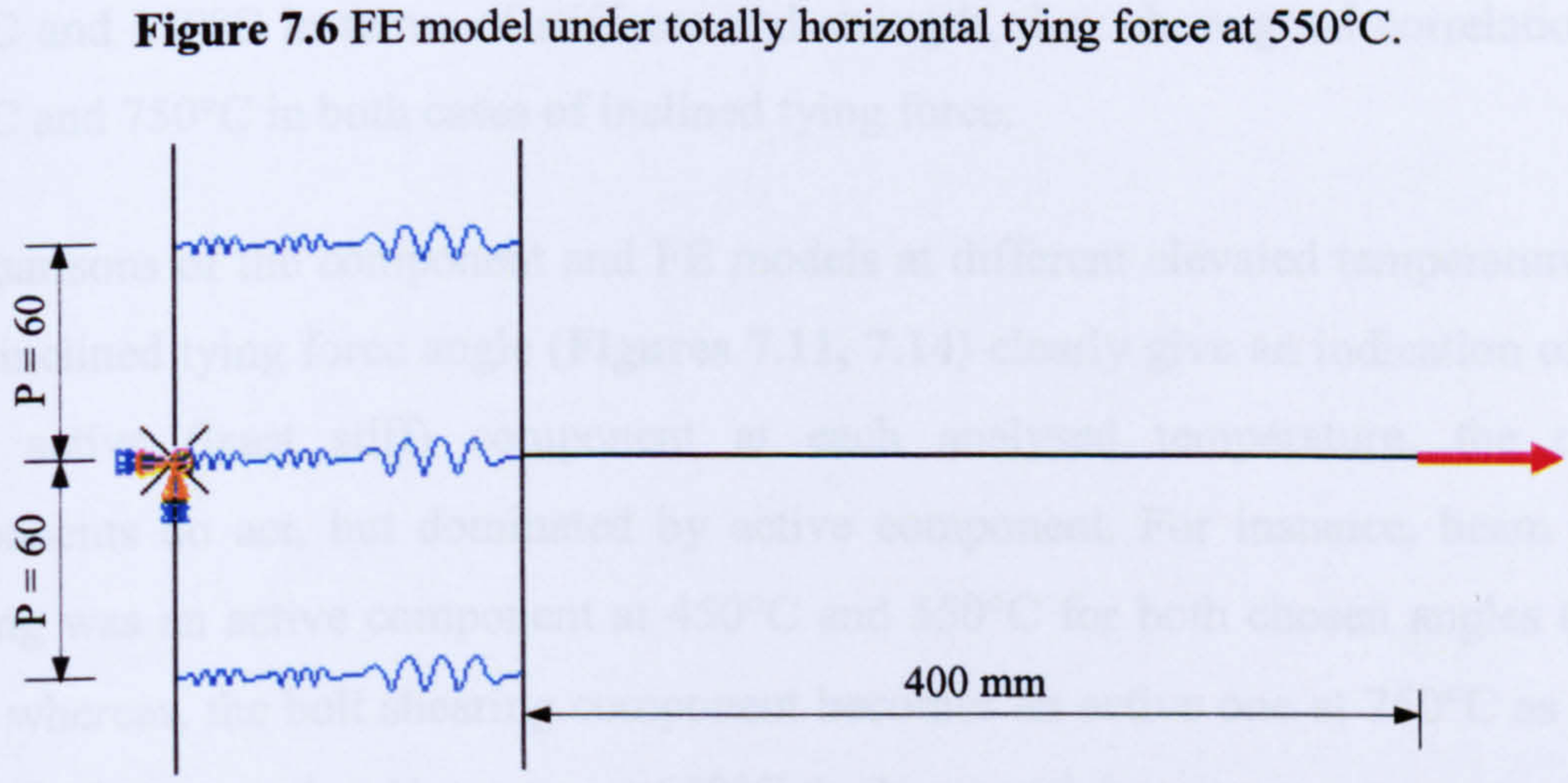

Figure 7.7 Component model under totally horizontal tying force at 550°C.

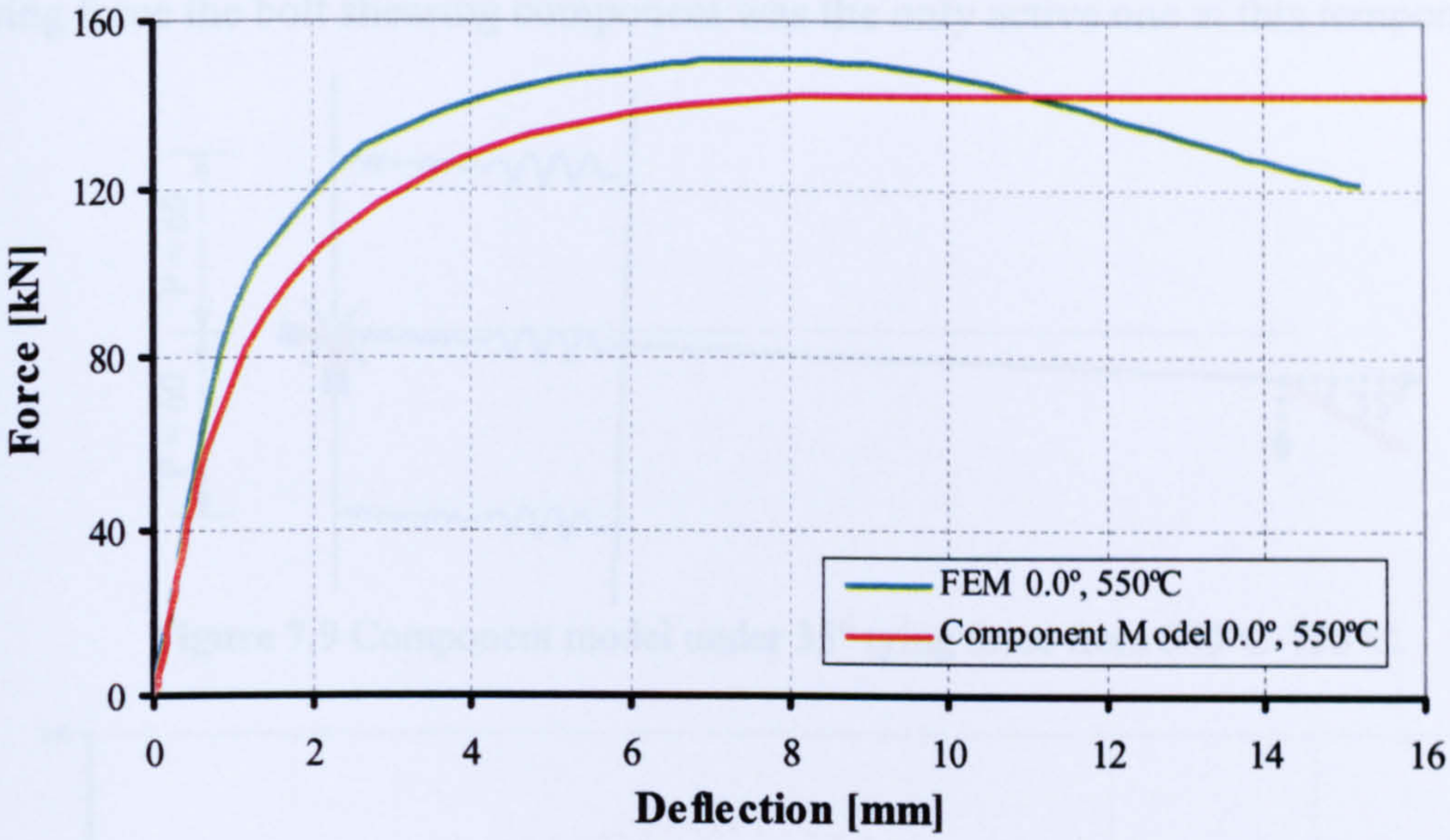

Figure 7.8 Tying force comparison at 550°C for the FEM and the Component model.

In real fire conditions the connection experiences an inclined tying force due to the beam's deflection mid-span large. Therefore, examination of the response of the component model for inclined tying force is more realistic than for horizontal tying. Therefore, two inclinations of inclined tying force were considered, 35° and 45°, for the FEM analysis (**Appendix C**) and the component model (**Figures 7.9, 7.15**), under different elevated temperatures (450°C, 550°C, 650°C and 750°C). The load-deflection comparisons for each temperature and at each inclined tying force angle are shown in **Figures 7.10** and **7.13**. The main observation from these two figures is that there are not many differences between the two cases in term of load-deflection behaviour. In addition, despite the reasonable discrepancy between the two models at 450°C and 550°C in terms of stiffness and strength, they show good correlation at 650°C and 750°C in both cases of inclined tying force.

Comparisons of the component and FE models at different elevated temperatures at each inclined tying force angle (**Figures 7.11, 7.14**) clearly give an indication of the most active (least stiff) component at each analysed temperature, the other components do act, but dominated by active component. For instance, beam web bearing was an active component at 450°C and 550°C for both chosen angles (35°, 45°), whereas, the bolt shearing component becomes an active one at 750°C as well for both chosen angles. However, at 650°C the beam web bearing component was an

active component, along with bolt shearing, for the 35° tying force, whereas for 45° tying force the bolt shearing component was the only active one at this temperature.

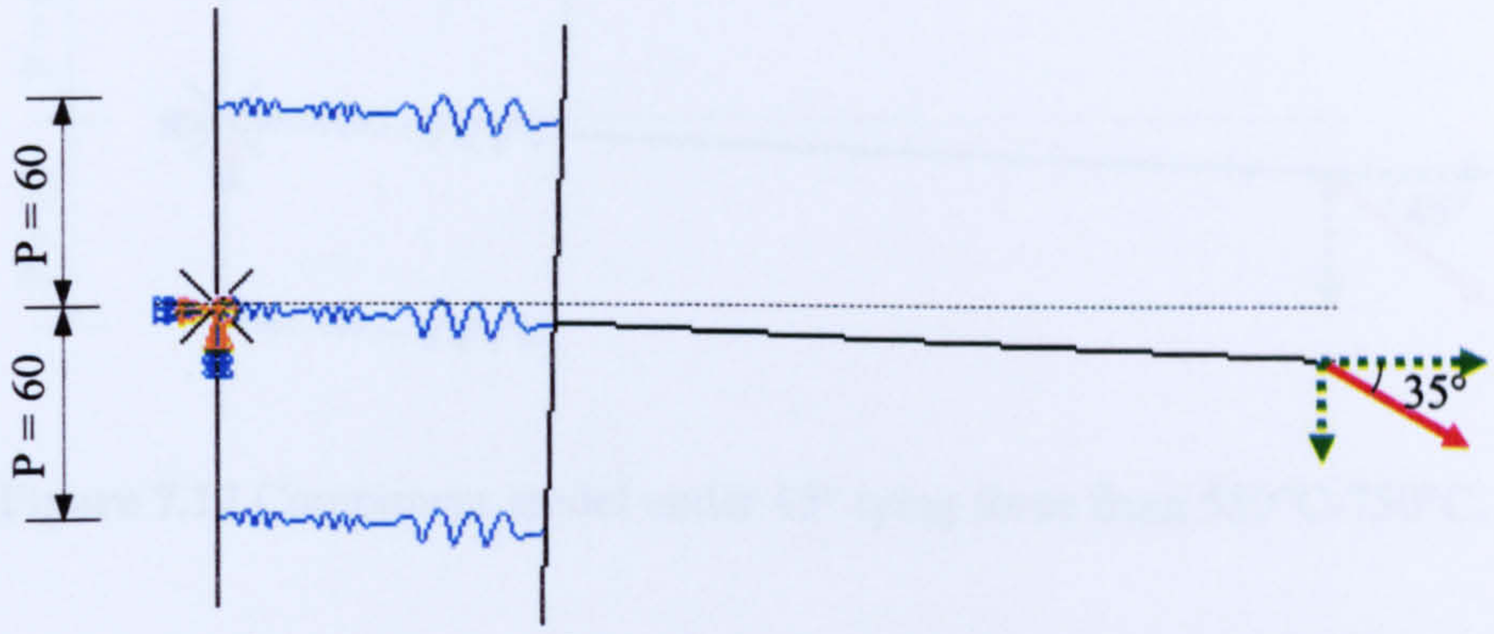

Figure 7.9 Component model under 35° tying force from 550°C-750°C.

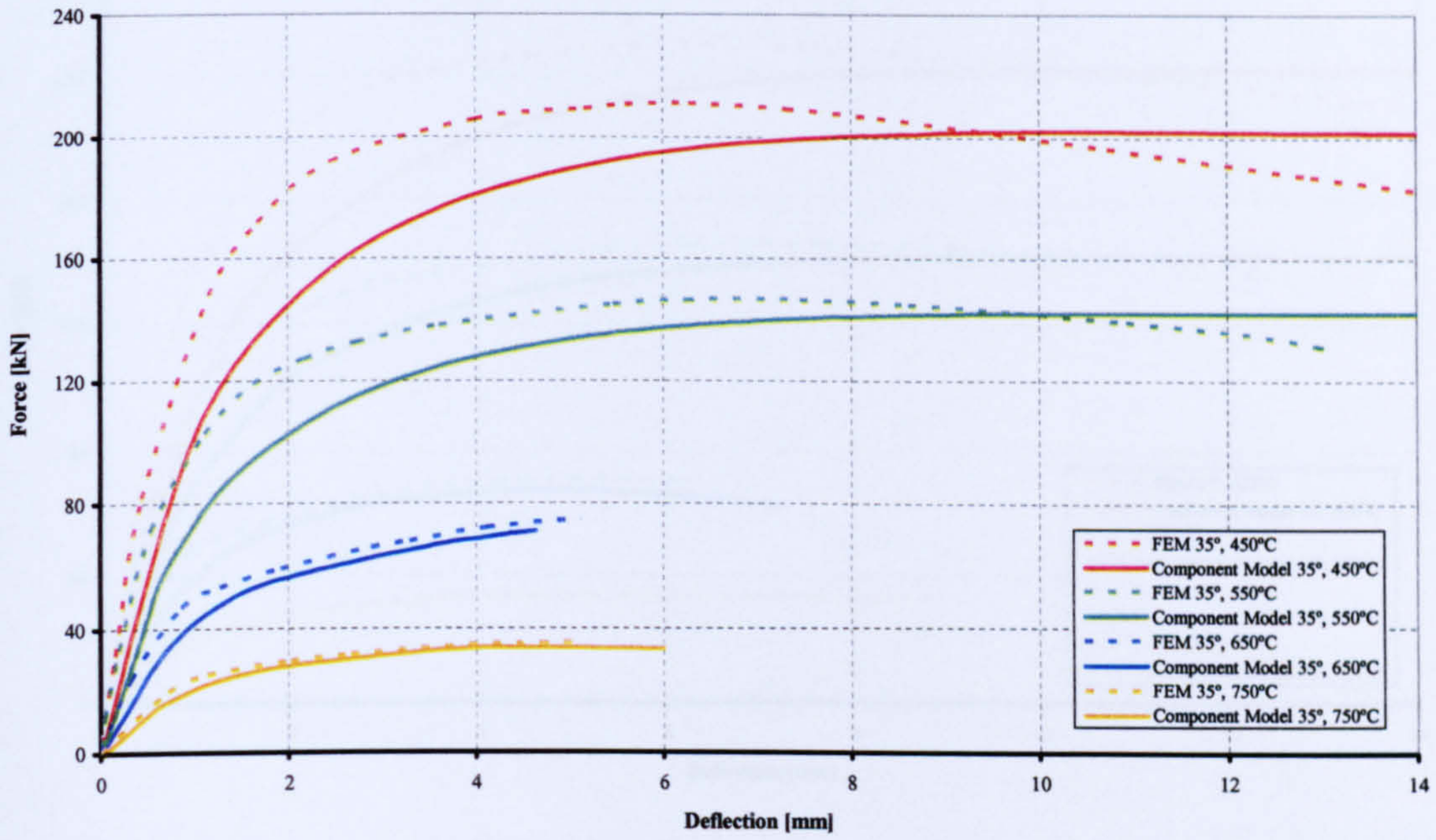

Figure 7.10 Comparison of FEM and the Component model under 35° tying force from 450°C-750°C.

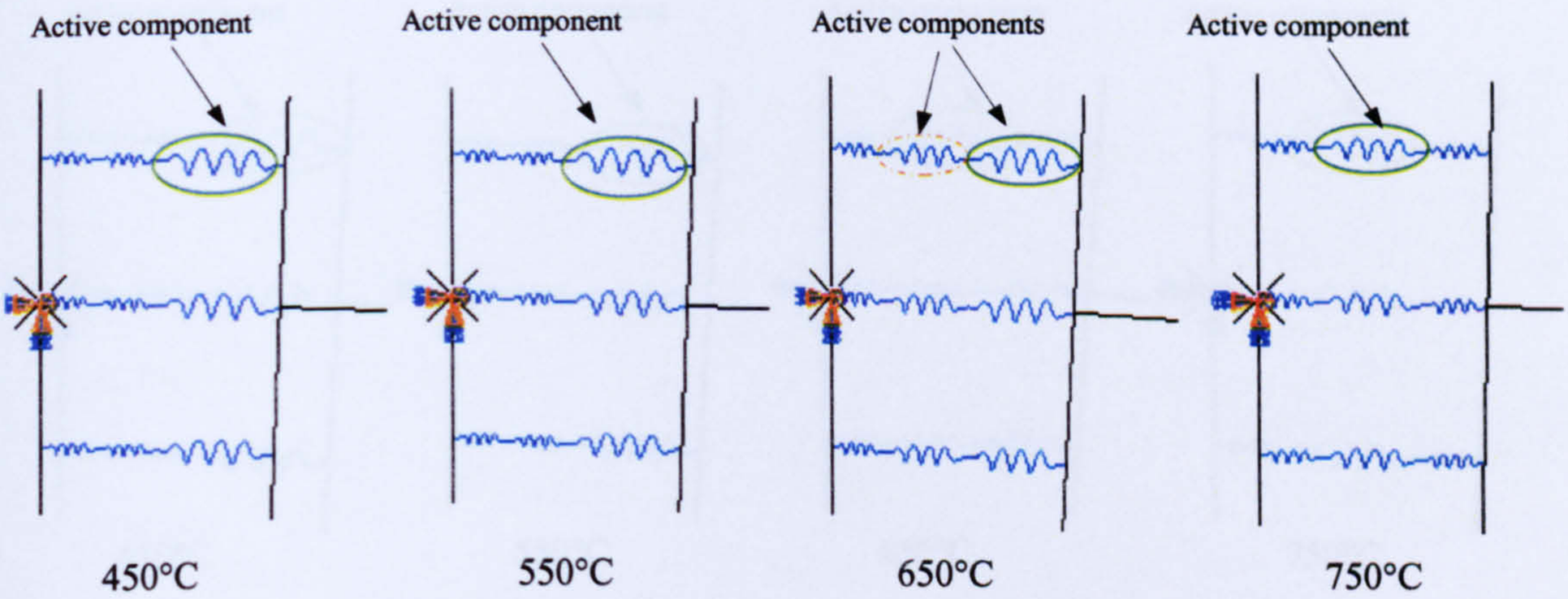

Figure 7.11 Component models' responses to 35° tying force at different elevated temperatures.

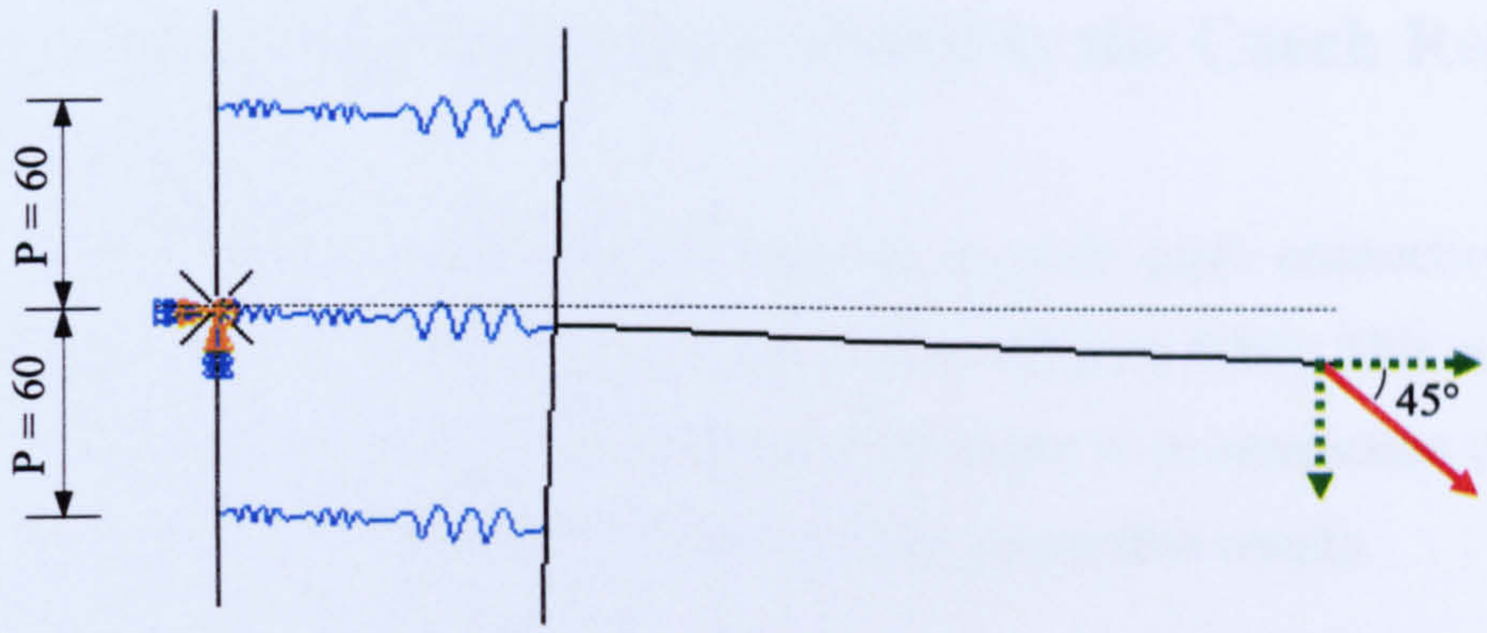

Figure 7.12 Component model under 45° tying force from 550°C-750°C.

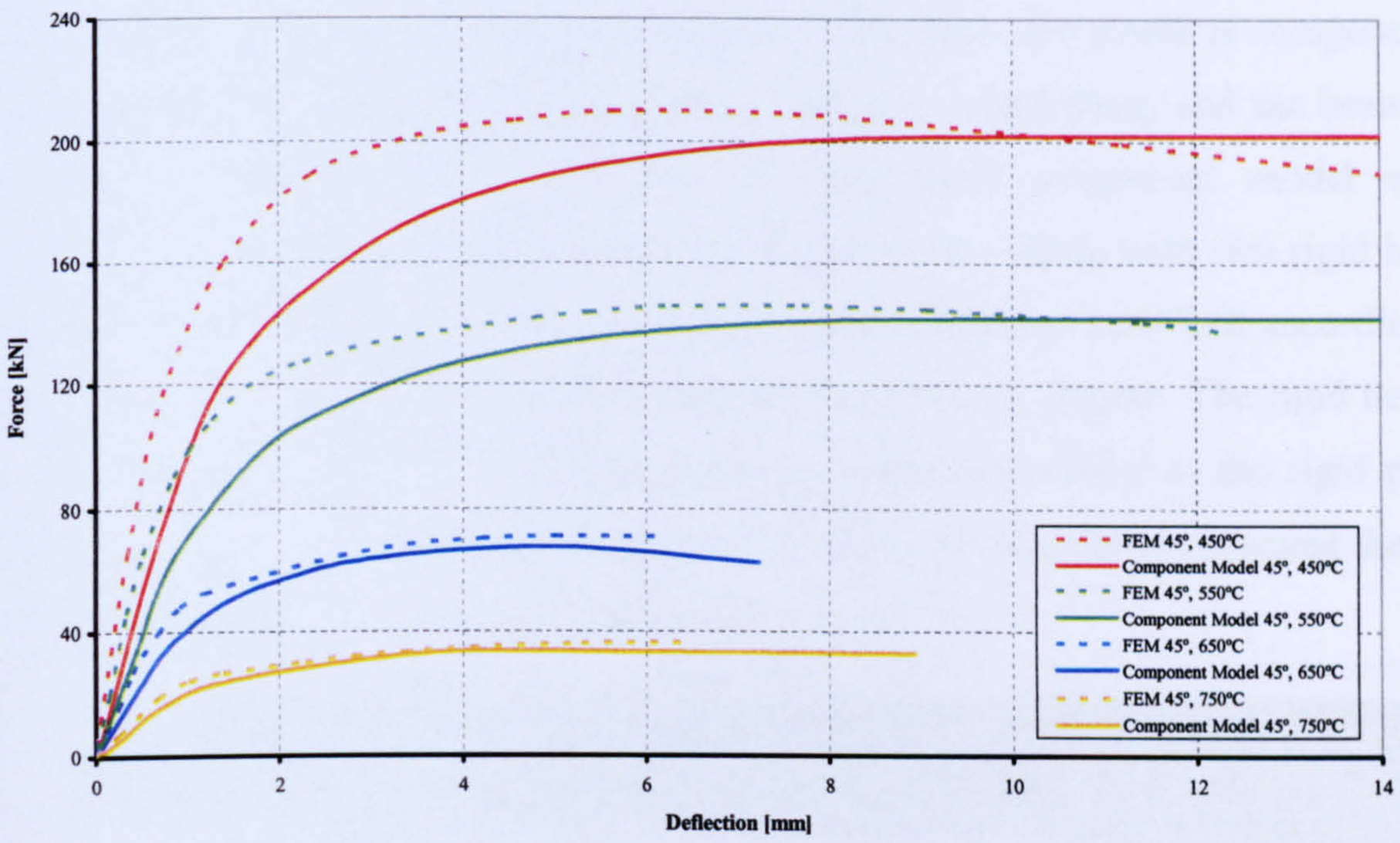

Figure 7.13 Comparison of FEM and the Component model under 45° tying force from 450°C-750°C.

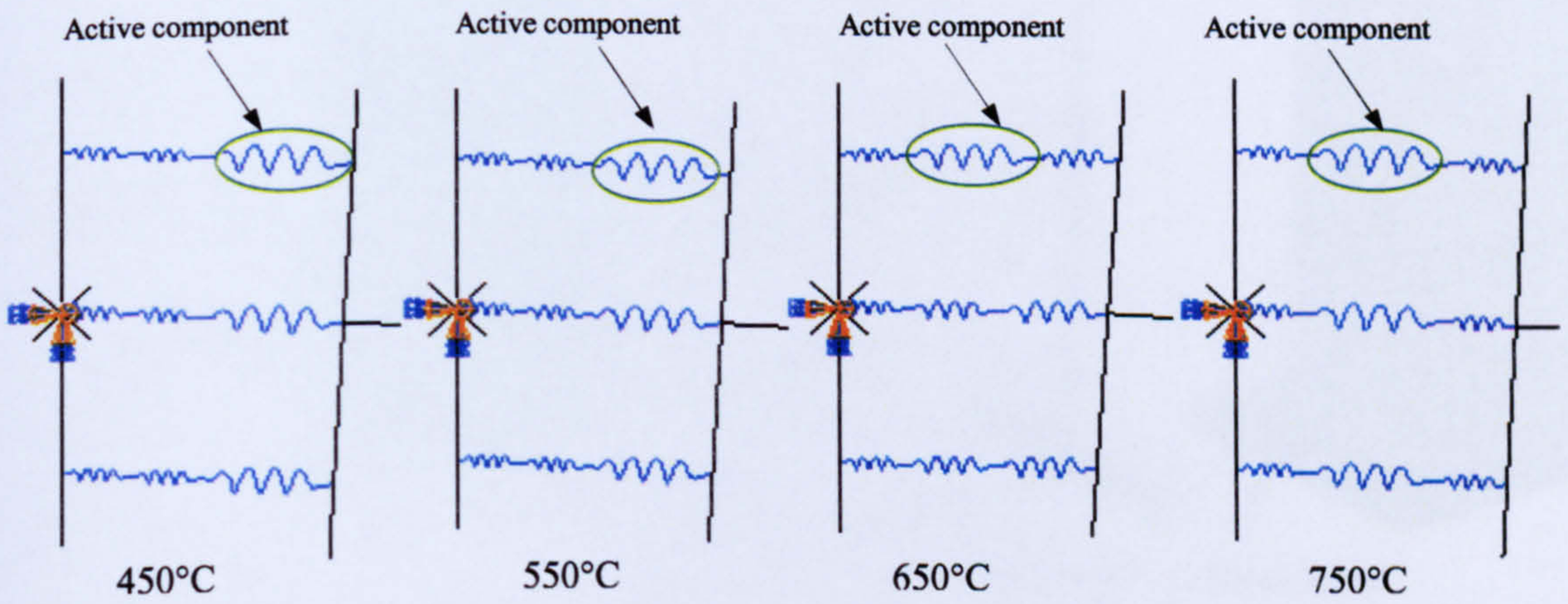

Figure 7.14 Component models' responses to 45° tying force at different elevated temperatures.

7.4. Applying the Component Model to the Czech Republic Fire Test

The FE analysis of the Czech Republic fire test on a fin plate connection (**Figure 5.15**) has shown good correlation with test results (**Figure 5.16**). This model took almost 18 hours to run given the data shown in Chapter 5. A connection component model could take considerably less time to produce acceptable results.

The FE analysis of the Czech Republic fin plate connection fire test was adjusted to evaluate the component model at elevated temperature by replacing the connection parts with the fin plate components (**Figure 7.15**). This new model is composed of four parts; the component spring model, a rigid tie, a rigid plate, and the beam FE model. The spring model represents the connection component model using SPRINGA elements from the ABAQUS element library along with two rigid beam elements. Each spring characteristic is illustrated in **Figures 7.16-7.18** according to the component model procedure described in the previous chapter. The rigid tie is a non-dimensional means of linking the spring component model to the rigid plate. This rigid plate was connected to the beam's edge nodes in order to represent the real beam edge behaviour and avoid local stress concentration.

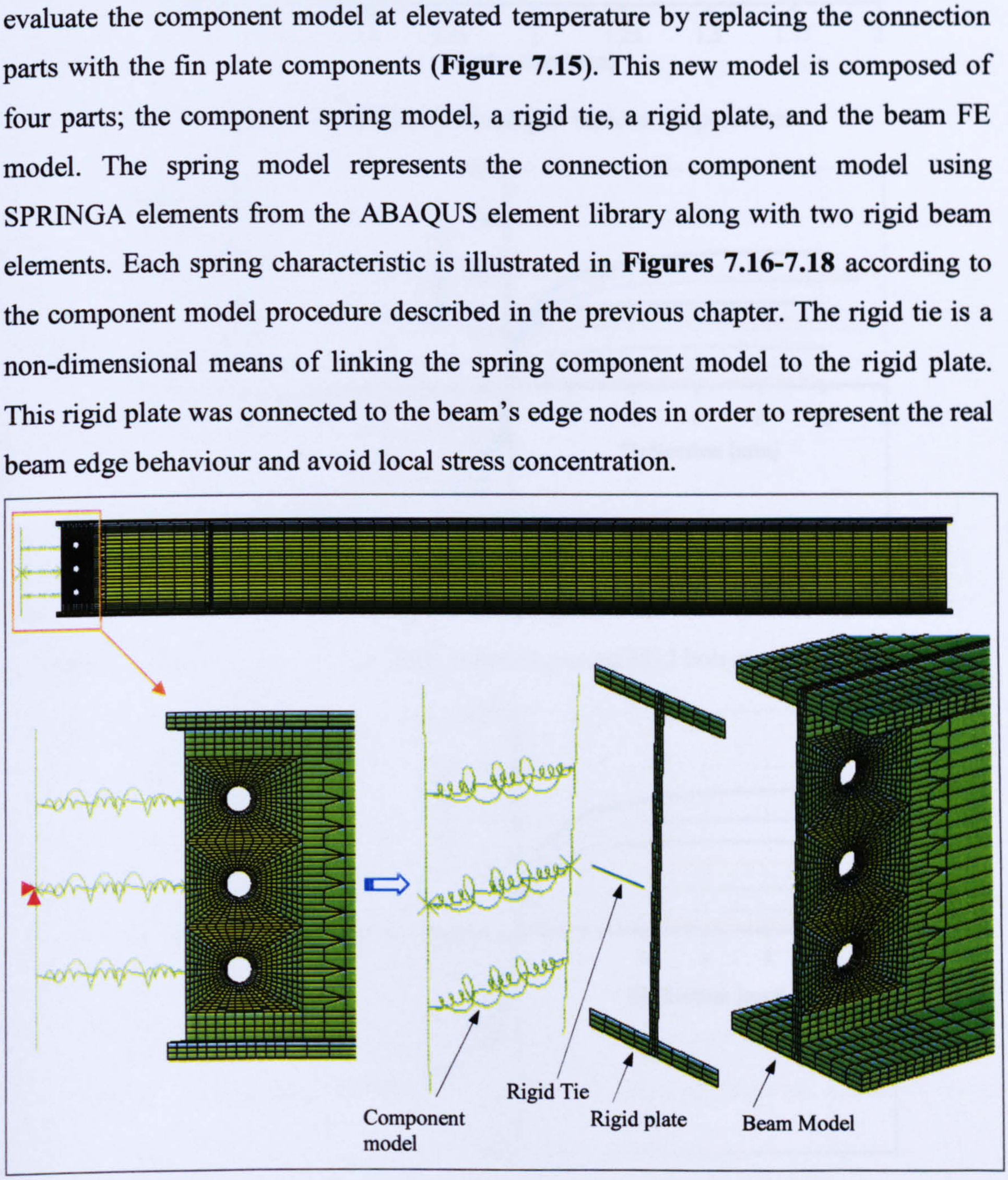

Figure 7.15 Component model of the fin plate connection along with beam FE model.

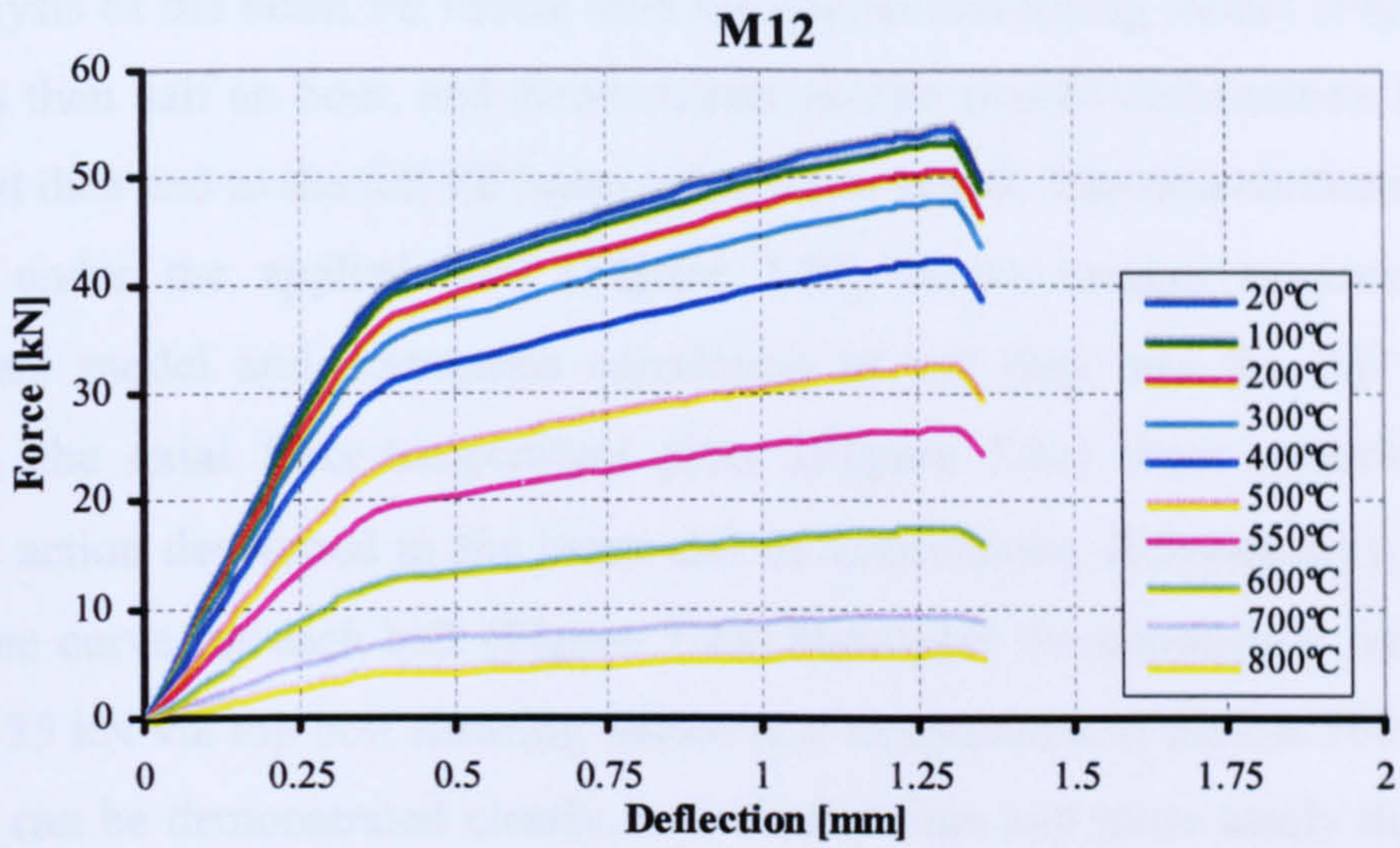

Figure 7.16 M12 bolt shearing at various temperatures.

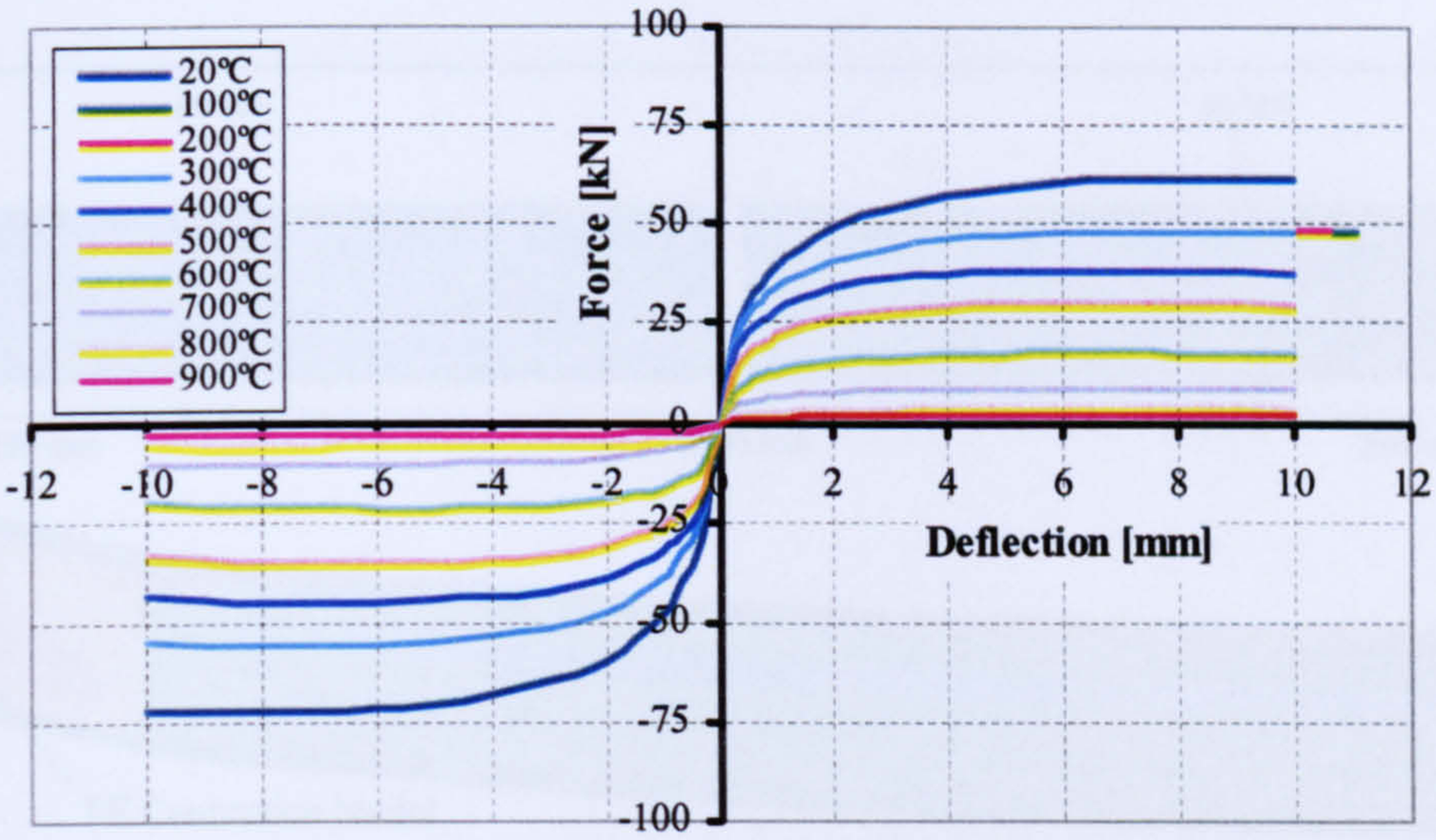

Figure 7.17 Beam web, 5.8 mm thick, in bearing using M12 bolt at various temperatures.

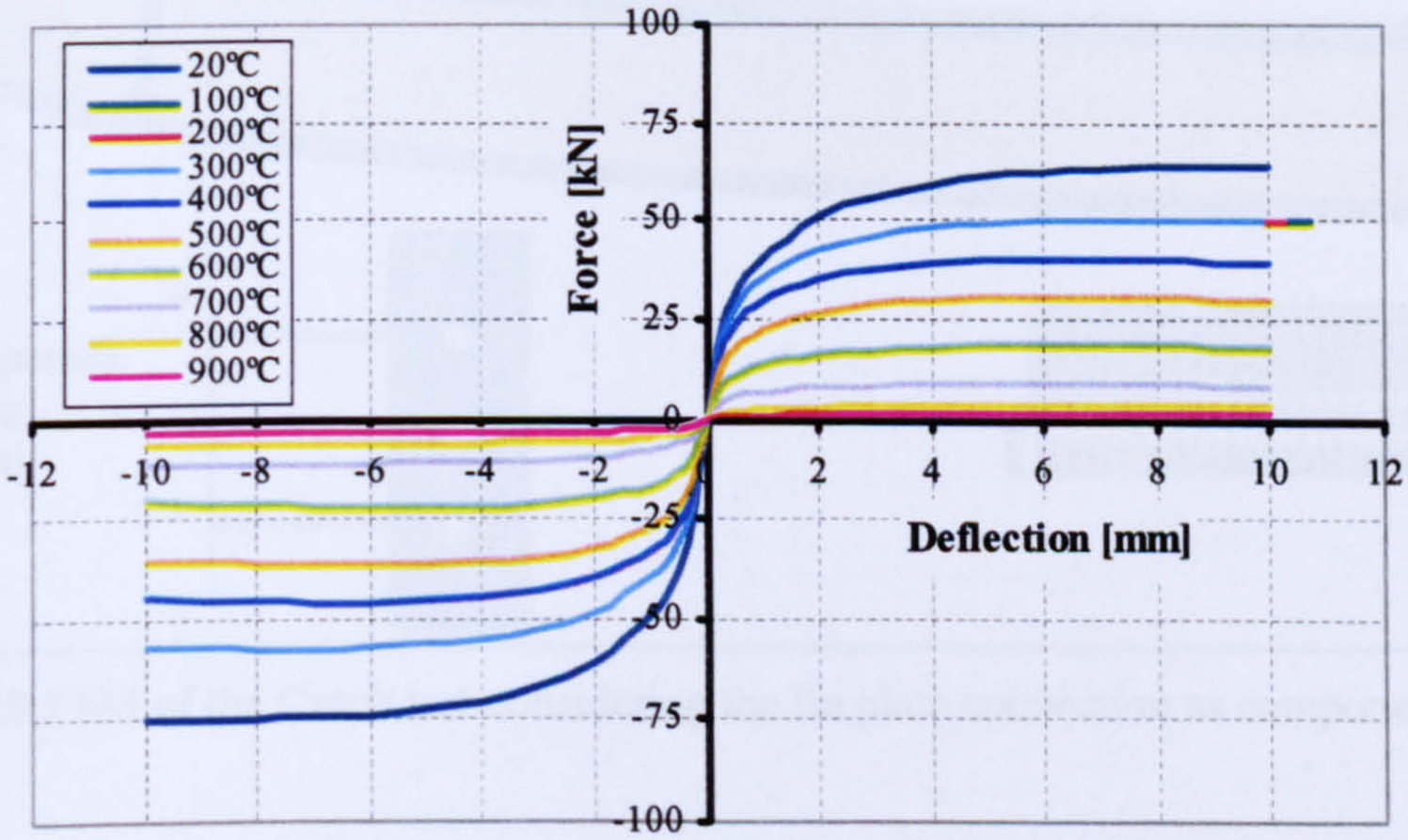

Figure 7.18 Fin plate, 6 mm thick, in bearing using M12 bolt at various temperatures.

The analysis of the beam FE model with the connection spring model (**Figure 7.19**) took less than half an hour, and demonstrates similar overall deformation behaviour to the test data and to the full FE beam-connection model. The time-deflection plot at a point under the applied load (**Figure 7.20**) shows weaker response by the component model and reasonable correlation to test data and the full FEM. In addition, the axial force-temperature plots (**Figure 7.21**) draw attention to the catenary action developed in the beam and its connections. Subsequently, the axial force-time curve for each bolt (**Figure 7.22**) highlights the connection failure tying force of 35 kN via top bolt shearing failure at a temperature of almost 500°C. These findings can be demonstrated clearly, in a shorter time and more easily than the FE analysis, illustrating the advantages of developing the connection component model.

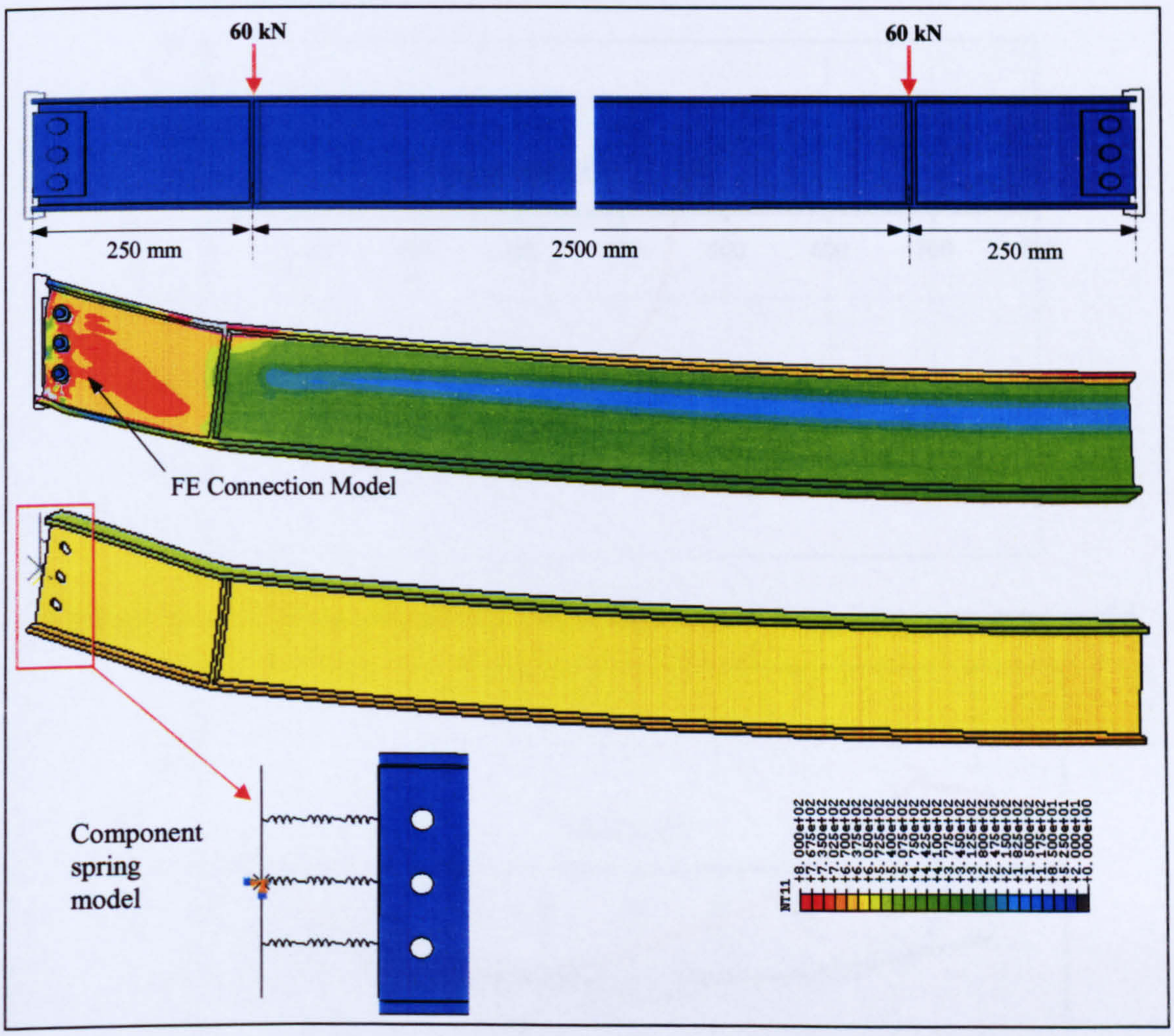

Figure 7.19 FEM of the Czech test considering the fin plate connection as component model.

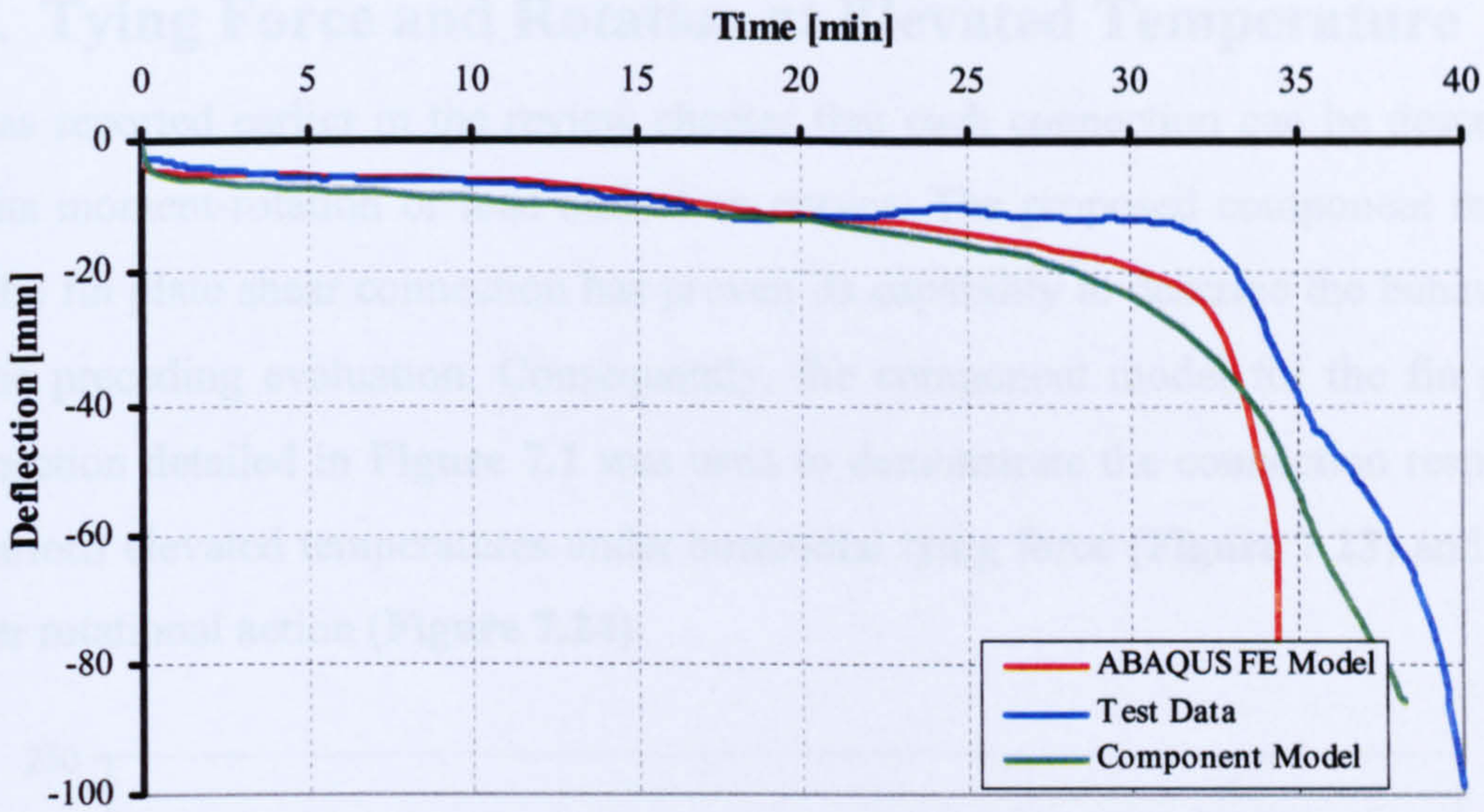

Figure 7.20 Time-Deflections of the Czech test, corresponding beam-connection FEM and other beam FEM with joint component model.

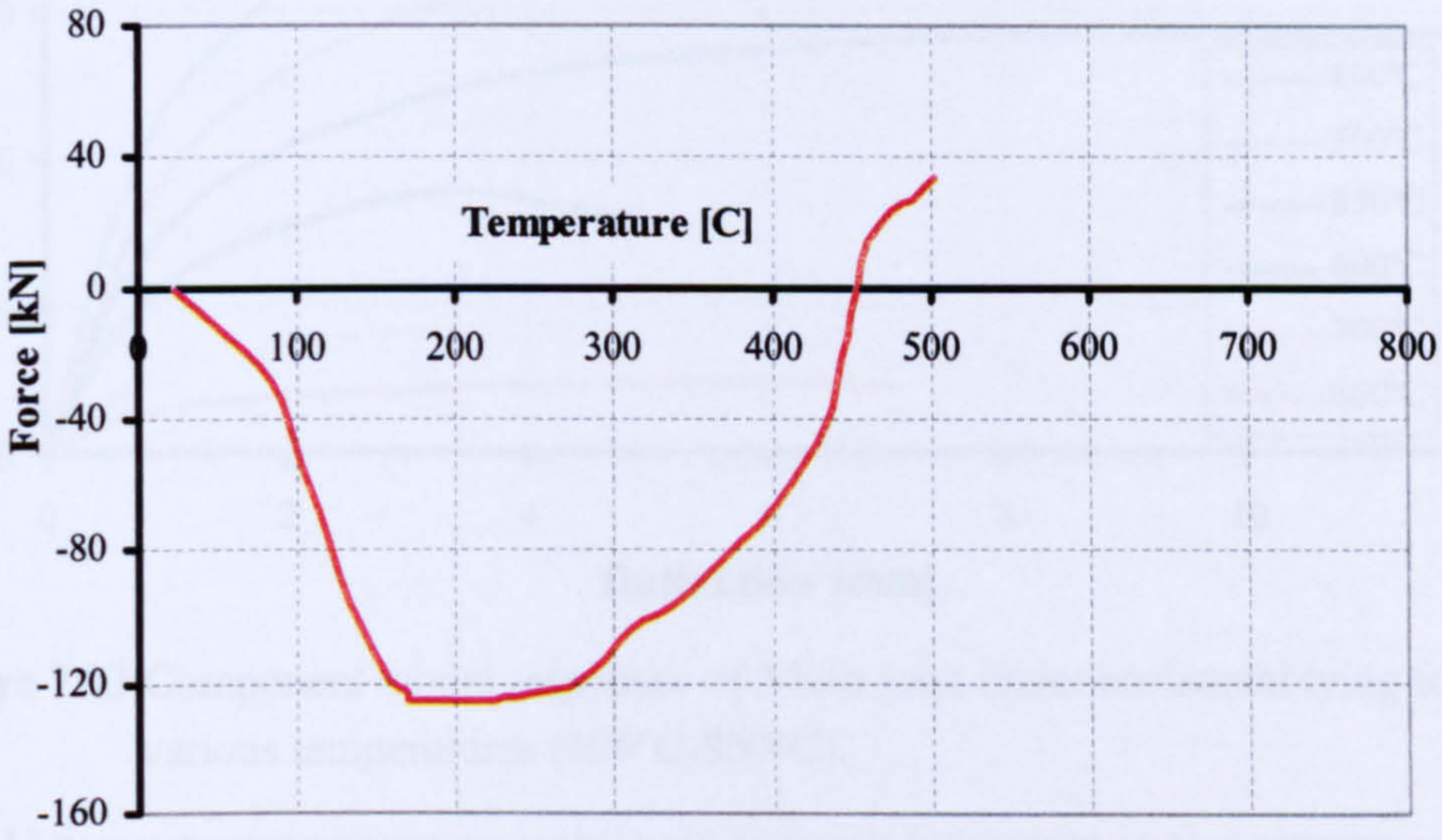

Figure 7.21 Axial force-temperature of the Czech fire test using joint component model.

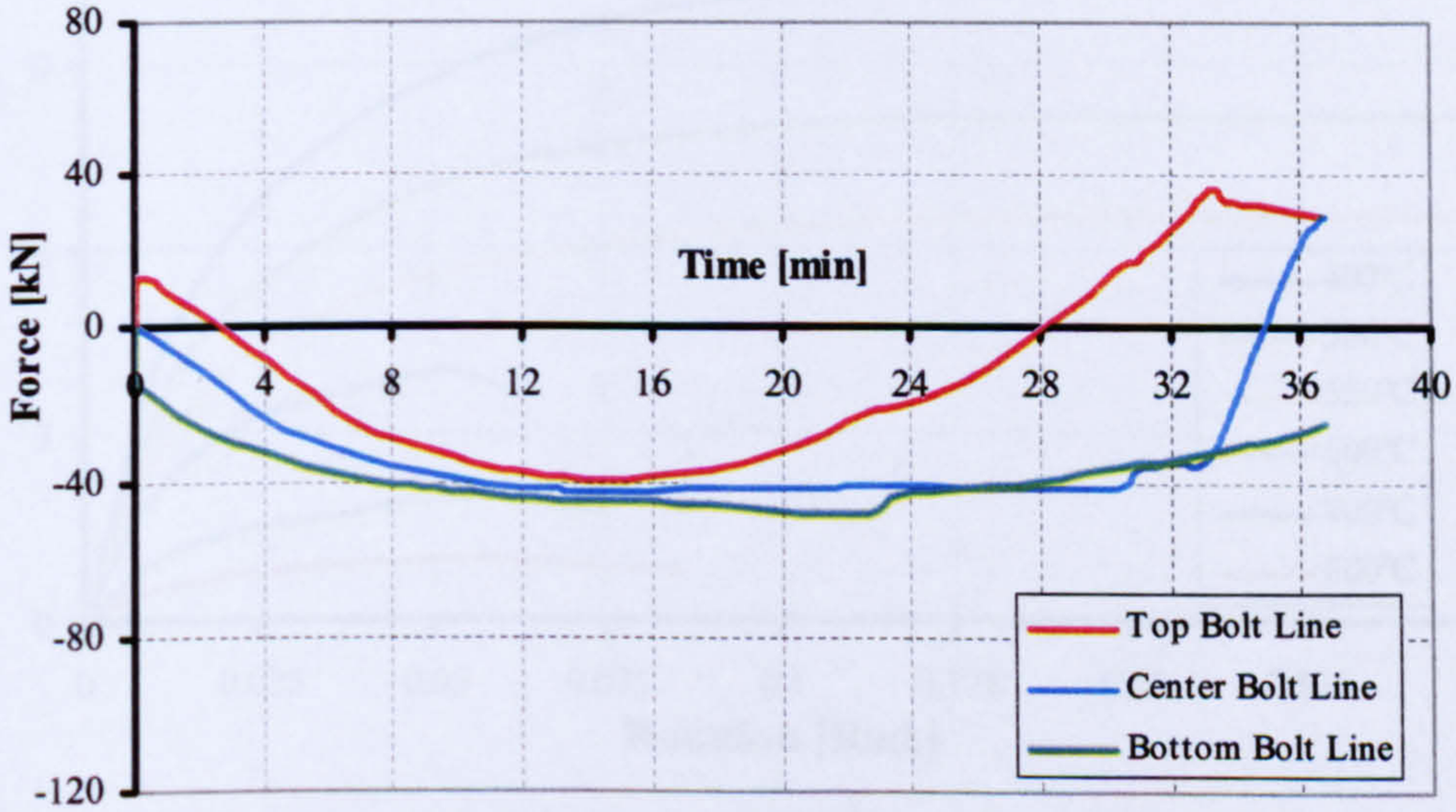

Figure 7.22 Axial force-time of each bolt in the Czech fire test using joint component model.

7.5. Tying Force and Rotation at Elevated Temperature

It was reported earlier in the review chapter that each connection can be described via its moment-rotation or load-deflection curves. The proposed component model for the fin plate shear connection has proven its capability to describe the behaviour in the preceding evaluation. Consequently, the component model for the fin plate connection detailed in **Figure 7.1** was used to demonstrate the connection response at various elevated temperatures under horizontal tying force (**Figure 7.23**) and also under rotational action (**Figure 7.24**).

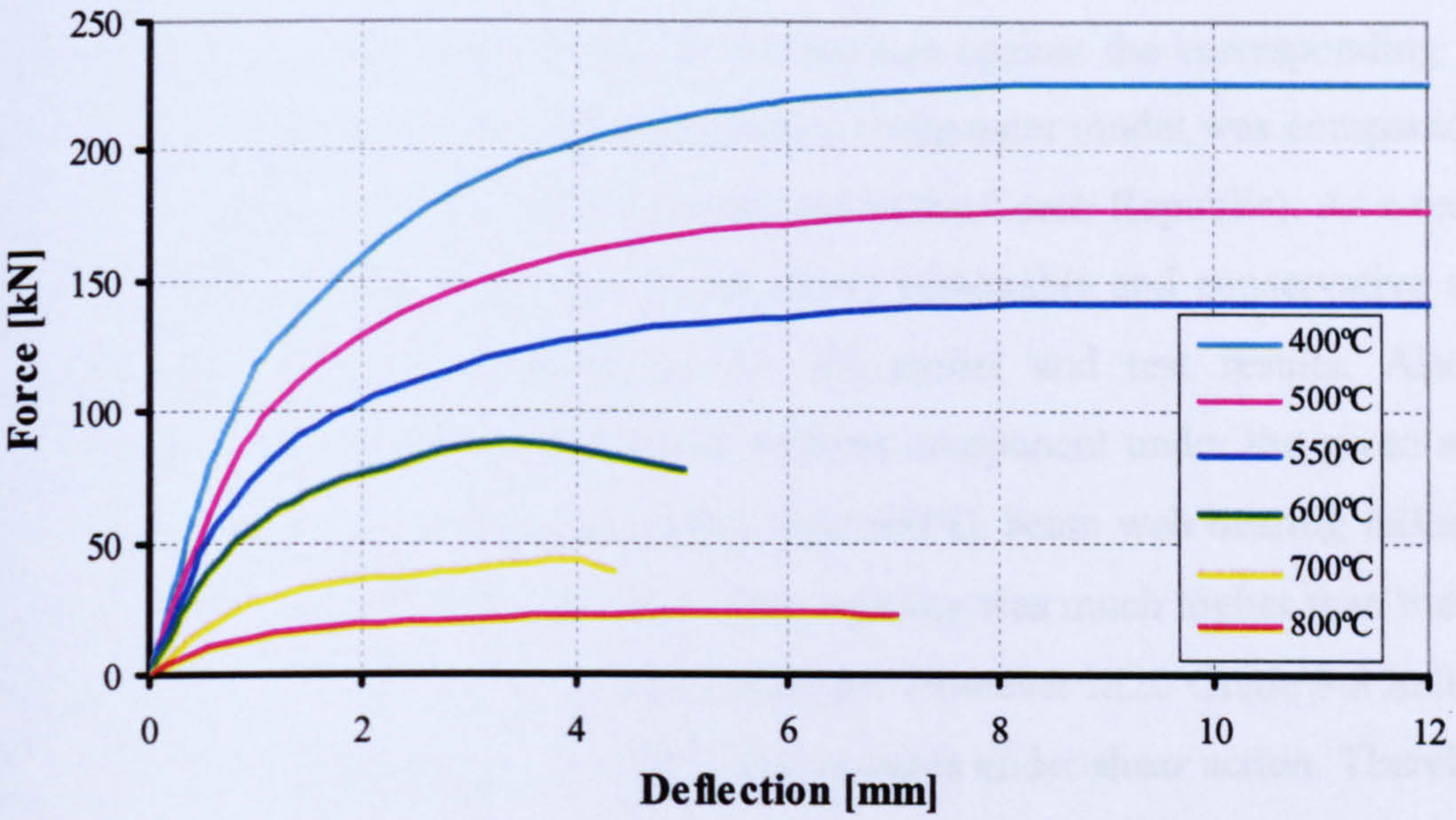

Figure 7.23 Component model responses of 3-bolt joint under horizontal tying force at various temperatures (400°C-800°C).

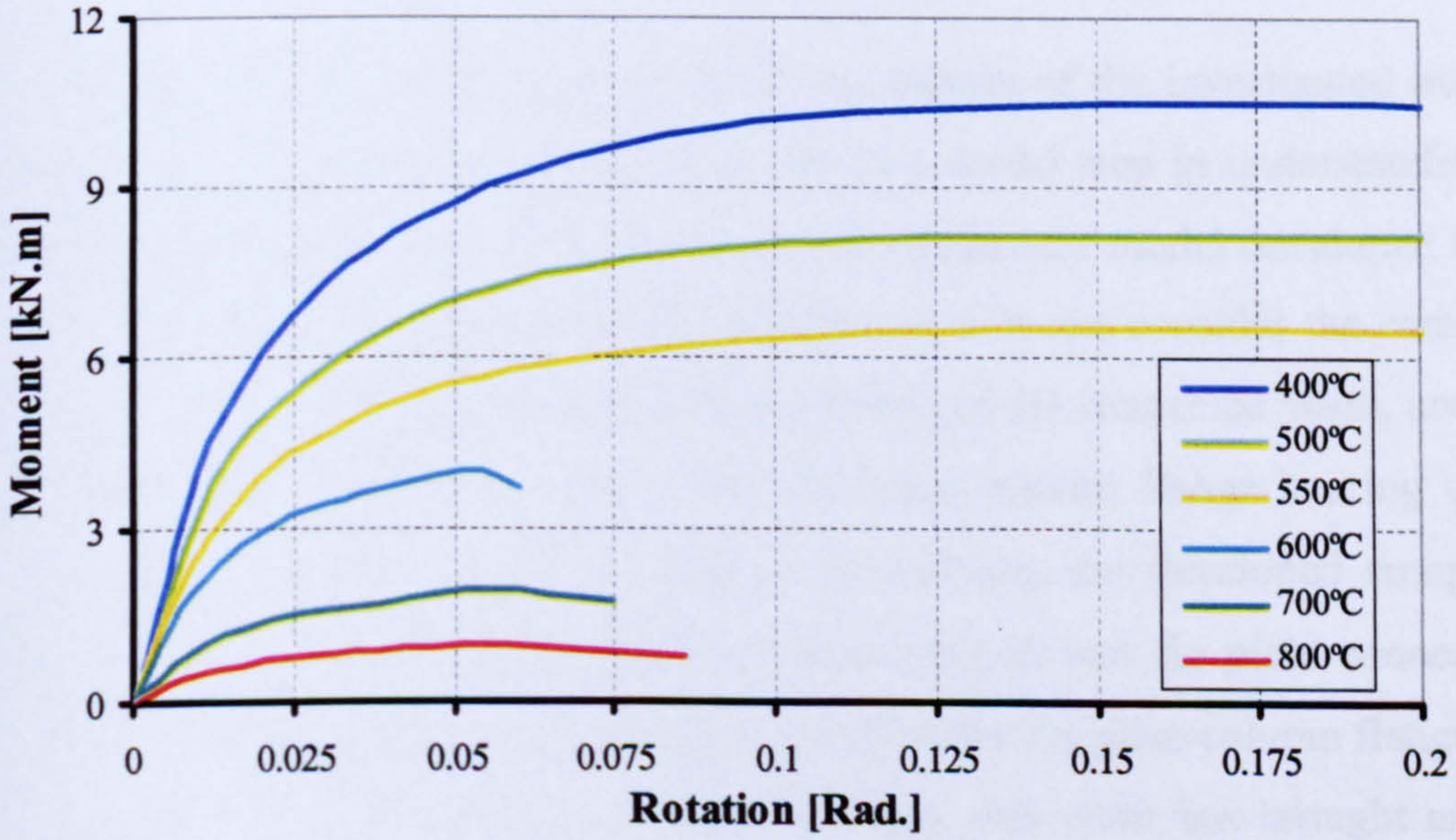

Figure 7.24 Component model responses of 3-bolt joint under moment at various temperatures (400°C-800°C).

These data for the component model were generated in a very short time, yet still show a reasonable description of the connection behaviour and the predicted failure mode. For instance, up to a temperature of 550°C plate bearing failure can be identified from limiting loads in both the load-deflection and moment-rotation plots. **(Figures 7.23, 7.24)**. In addition, the bolt shearing failure mode was obvious in both curves **(Figures 7.23, 7.24)** at temperatures of 600°C and upwards.

7.6. Conclusions

The proposed fin plate connection component model was examined under different conditions at elevated temperature via comparison against the corresponding FEM. In addition, the proposed fin plate connection component model was compared with the only available fin plate fire test (conducted in the Czech Republic). As a result of these evaluations, the component model shows reasonable and conservative design strength and stiffness compared to the FE model and test results. Also, the component model clearly identifies the weakest component under the given actions and temperatures. At temperatures lower than 600°C, beam web bearing failure was predominant, and M20 Grade 8.8 bolt shear capacity was much higher than the block shear capacity of the beam or fin plate material. However M20 Grade 8.8 bolts start to deteriorate at temperatures of 600°C and upwards under shear action. Therefore, it is essential to protect the connection's bolts in order to delay and avoid sudden failure by bolt shearing and gain a more ductile connection response.

It is obvious that no research can cover all the aspects of the investigated problem completely. The development reported herein is a useful step in understanding the robustness of connections in fire. However, the component model developed in this research still has some limitations. For instance, it does not consider the composite action of a concrete slab connected to the top flange of the connected beam, and does not consider the compression component of beam bottom flange bearing on the column flange after an excessive rotation. In addition, the developed component model does not contain all the possible components in real fin plate connections; there are other components still to consider, such as the fin plate-column flange weld component. In common with much other research, this work has brought answers

and solutions for its objectives, as was intended, but has also created opportunities for further research work.

Chapter 8

Conclusions, Recommendations and Further Work

8.1. Summary of Work Completed

Though many research investigations have been conducted on steel connections in fire conditions, relatively little research have focused on steel fin plate beam-to-column shear connections, when compared with the volume of work addressing moment connections such as extended and flush end-plate connections. This was an obvious key finding of the proposed literature review. In addition, this review identified and highlighted gaps in the previous research on fin plate beam-to-column connections. These include the need for a better understanding of plate bearing and bolt shearing in the shear connection, and for exploring the tying force tolerance of fin plate connections at ambient and elevated temperatures. Furthermore, a great concern has been raised in recent years about understanding the role of connections in overall frame response, and possibly their beneficial effects in a fire. In order to provide a better understanding of the gaps identified in the behaviour of fin plate connections, four main research approaches have been used, namely experimental testing, FE modelling, curve fitting and simplified modelling.

Advanced three-dimensional finite element models have simulated the bolt shearing and bearing behaviour in simple shear connections. The models incorporate non-linear material properties, geometric non-linearity and contact interaction by means of the ABAQUS/Standard code. Although contact elements were difficult to implement in modelling shear connections, contact interaction between the connection components was introduced and achieved successfully. Published experimental data were used to evaluate the proposed FE model at ambient and elevated temperatures. The model provided qualitative and quantitative understanding about shear connection behaviour, and may also be used as a

benchmark for FE modelling of similar steel shear connections. The proposed models were then used to perform an intensive parametric study in order to describe the plate bearing and bolt shearing components via curve fitting expressions. Next, a simplified spring component model for fin plate connections was assembled and evaluated. This spring model may be used to incorporate actual joint behaviour in the analysis of structures, either at ambient or at elevated temperature.

In general, the key objectives of this research have been achieved, and may be summarised under the following broad key points: understanding of the plate bearing phenomena and bolt shearing behaviour; investigating the fin plate connection tying capacity; development of a fin plate connection component model which greatly minimises the connection analysis time at both ambient and elevated temperatures.

8.2. Plate Bearing, Bolt Shearing, and Tying Resistance

It has been proven through the FE analysis that plate bearing strength is directly proportional to the plate thickness. In addition, plate bearing strength is proportional to the plate end-distance up to a value of $3d_b$. Nevertheless, end-distance above this value ($3d_b$) makes almost no improvement to the bearing strength. However, the difference between the recommended Code of Practice [8.1, 8.2] end-distance $2d_b$ and the $3d_b$ in terms of the bearing strength is just 6%. In other words, the direction at which a bolt bears into a plate (**Figure 8.1**) has relatively little influence on the bearing strength provided the bolt is located at a minimum end-distance of $2d_b$.

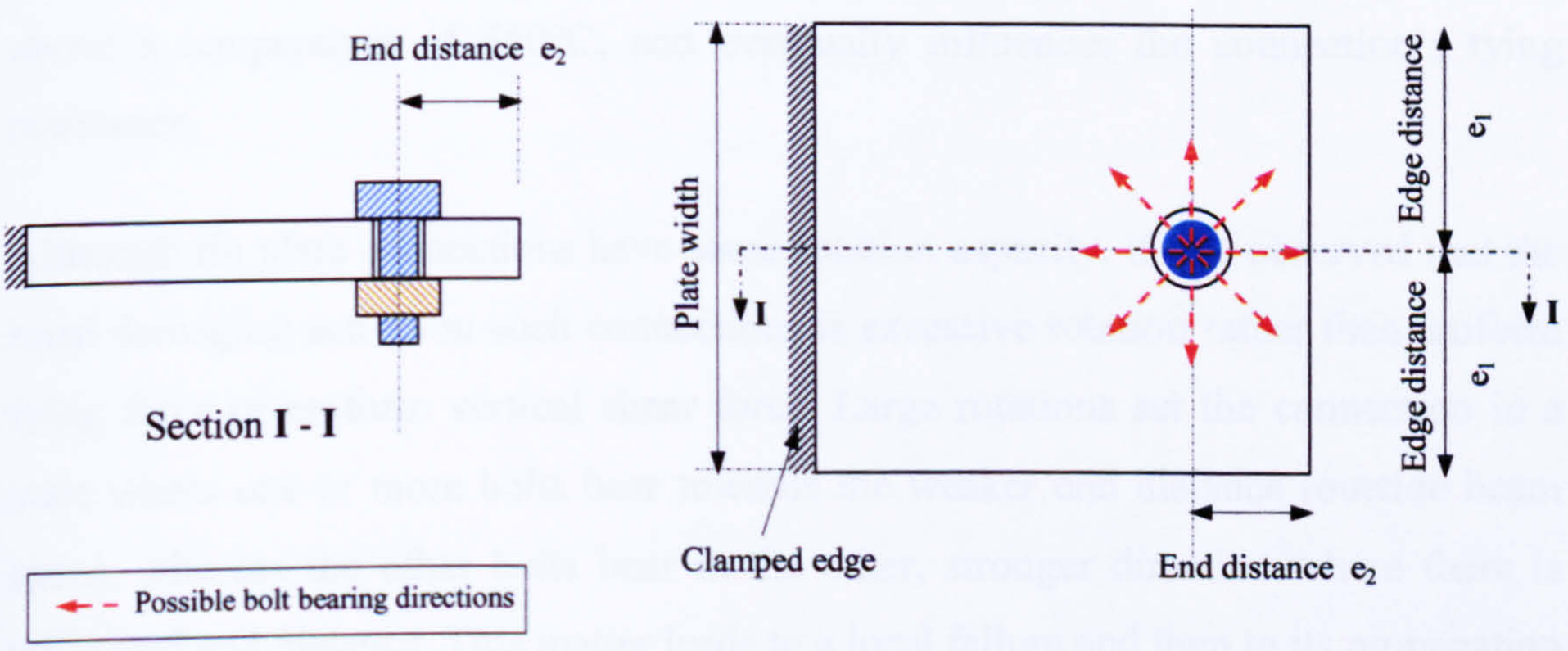

Figure 8.1 Geometrical detail of bolt bearing into plate hole

However, plate edge distances below $2d_b$ may lead the plate to net section failure, whereas a plate edge distance bigger than $2d_b$ has no influence on the bearing strength. At elevated temperature, bearing strength degradation with temperature was an obvious fact, and was seem to be proportional to the material strength reduction factors with temperature. A ductile bearing failure mode of fin plate connections can be achieved if the beam web thickness is at most 20% less than the bolt radius.

A high strength bolt is a vulnerable part of any shear connection under extreme actions such as a severe fire. Shear connection failure modes are strongly influenced by the geometric detail of the connection itself. It was found that an unfavourable "brittle" bolt shearing failure mode will occur if both plates (web and fin plate) in single-shear connections have a thickness equal to, or greater than, the bolt radius. Even though shear connections may be assembled via two plates with equal plate thickness to form a single shear connection, the bolt radius should be chosen bigger than either plate's thickness.

Tying force capacity of fin plate connections may be predicted as a single lap joint's tensile capacity multiplied by the number of bolt rows involved in the fin plate connection. Furthermore, fin plate connections have horizontal tying force resistance almost equal to their uniform vertical shear capacity. On the other hand, the angle of the applied tying force at ambient temperature has little influence on the connection's tying resistance. However, at elevated temperature, the inclination of the tying force is a great influence on the type of failure that may occur (bolt shear or plate bearing) above a temperature of 550°C, and eventually influences the connection's tying resistance.

Although fin plate connections have some rotation capacity, it was observed that the most damaging action on such connections is excessive rotation rather than uniform tying force or uniform vertical shear force. Large rotations set the connection in a state where one or more bolts bear towards the weaker end distance (outside beam span), whereas the other bolts bear in the other, stronger direction where there is unlimited end distance. This matter leads to a local failure and then to its propagation by an "unzipping" type of failure of the entire connection in the bolted area.

8.3. Component Model

The proposed component model has demonstrated that shear connections such as fin plate connections can be modelled by the component method approach. The component model has been shown to be capable of describing the connection response (moment-rotation and force-deflection) with reasonable accuracy. In addition, the model highlights clearly the first connection component to fail under the applied actions. Also, the computation time required by the component model, in contrast to a pure FE analysis, makes it an advantageous design tool.

The plate bearing component has been investigated and justified in great detail at both ambient and elevated temperature, and has been described using an empirical expression. A bolt single-shear component has also been developed, justified and described at various elevated temperatures. Consequently, it was found that the Eurocode 3 Part 1.8 [8.2] equation for calculating the bolt stiffness in single shear does not appear to have appropriate justification. However, the Eurocode 3 [8.2] reduction factors for bolts in shear compare well with the reduction factors derived from the FE analyses. Additionally, the friction component has been developed and its effect evaluated.

The component model analysis shows that fin plate connections can achieve sufficient rotation capacity provided that the beam web is a "weak link" relative to the bolts. In addition, the component model analysis has shown that, at a temperature lower than 600°C, the shear capacity of M20 Grade 8.8 bolts was higher than the block shear capacity of the beam or fin plate material. However, the bolts' shear capacity started to decline at temperatures of 600°C and upwards under shear action. Therefore, it is essential for a shear connection's bolts to be protected, with the purpose of delaying any sudden bolt shear failure and achieving more ductility for the connection.

The component model's applications illustrate its ability to predict the vertical shearing capacity, the horizontal tying force and the rotation capacity of fin plate connections at both ambient and elevated temperatures. Accordingly, the component method presented in this thesis can be utilised in global 3-D frame analysis.

8.4. Recommendations

Based on the reported study, a few important recommendations can be drawn with regard to the use of steel fin plate connections in building structures with regard to fire resistance.

A necessary property of fin plate connections is ductility, but bolt shear limits the ductile performance of the whole joint, and therefore it should be avoided. The current study has shown that, in order to maintain the ductility required, especially in fire conditions, beam web thickness should be at most 20% less than the bolt radius, or the bolt radius should be at least one and half times the beam web or fin plate thickness, whichever is thicker.

Steel fin plate connections are shown to be adequate for tying purposes, and it is proven that they have a tying resistance equal to the vertical shear resistance, which is consistent with the new tying requirements [8.3]. If fin plate connections are used to connect the internal beams to supporting columns, these connections will suffer a combination of severe actions in the case of a serious fire. The remaining dead load, as well as the fire loads, leads to excessively large deflection and eventually, to high tying and rotational actions in the connection parts. Therefore, when a fin plate connection is used as a beam-to-column connection it is recommended that fire protection material should be applied to the bolts in order to delay the critical bolt shear failure.

8.5. Further Work (Extension of the current study)

Some relevant issues have been uncovered during this research that could form key directions for further research to improve the current component model for fin plate connections. These issues are listed below, and are proposed for future research:

- The lower beam flange in contact with the column flange is an important component in end-plate and extended end-plate connections. This is because the beam flange at both ends is always in initial contact with the supporting column's flange. This behaviour does not apply to fin plate connections (**Figure 8.2**). In a fin plate the beam flange is not initially in contact with the column. However, as

the beam rotates the beam flange may come into contact with the column at a rotation dependent on the connection geometry. Once contact has been established, the beam flange component is mobilised. Therefore, an extension of the current study would investigate the component of the beam flange pushed into the column flange (**Figure 8.2**) and how this could be added to the component model (**Figure 8.3**).

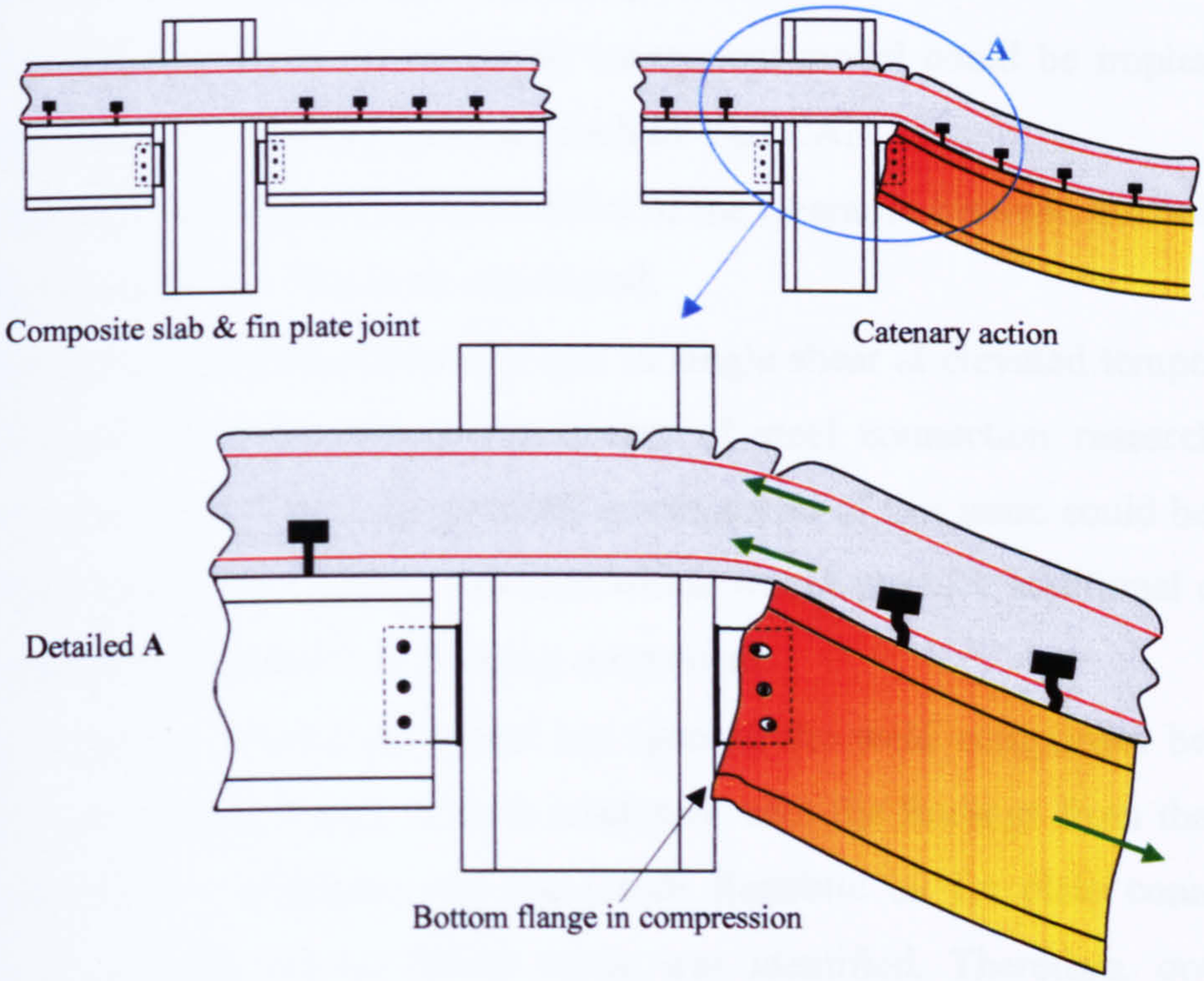

Figure 8.2 Steel fin plate joint and composite slab response to beam catenary action in fire

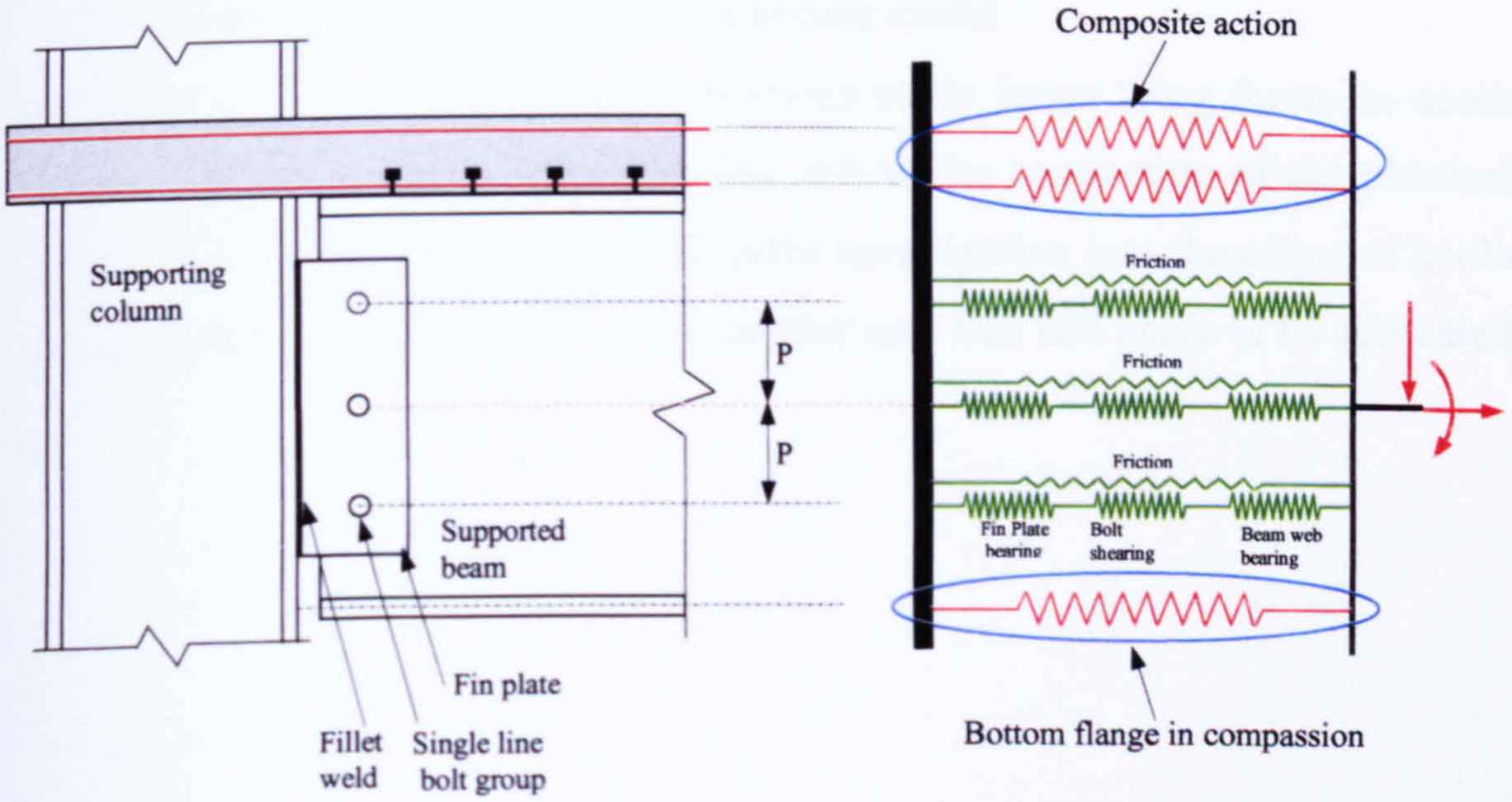

Figure 8.3 Fin plate joint component model considering composite action and the component of the bottom flange in compression

- Composite action between the beam and the slab can be of great benefit to the behaviour of fin plate connections **(Figure 8.2)**. This action may delay the activation of bottom flange to the column flange compression component. Once this happens it increases the lever arm of the tying force applied to the connection upper bolt, eventually unzipping the connection zone. Hence, another area further work would be to investigate how composite action can be considered in a fin plate connection component model **(Figure 8.3)**.
- Investigation of how the proposed component model could be implemented in global structural analysis software such as VULCAN.
- Study could be conducted on the effect of the clearance between the bolt and bolt hole, and how this should be considered.
- Experimental investigations of a bolt in single shear at elevated temperature are an almost missing topic in the library of steel connection research for fire conditions. Therefore, experimental investigation of this issue could be a further study related to the current research which would produce additional evaluation data for the proposed bolt shearing component.
- The proposed component model has ignored the weld component between fin plate and column flange. This is consistent with the findings from the fire tests conducted at Cardington and the Czech Republic on fin plate connections, I which no weld tearing failure mode was identified. Therefore, investigating whether weld needs to be considered as a separate component is important to complete the fin plate connection component model.
- It is widely believed that steel connections suffer larger tying forces in cooling than during the heating stage of a fire, due to the contraction of the plastically deformed connected beam. More detailed investigation into the effect of cooling on fin plate connection behaviour is another area that still needs to be addressed.

8.6. References

[8.1] BCSA, "The British Constructional Steelwork Association LTD., Joints in Steel Construction: Simple Connections", The Steel Construction Institute (2002).

[8.2] BS 5950: "Structural Use of Steelwork in Building, Part 1: Code of Practice for Design - Rolled and Welded Sections", British Standard Institution (BSI), London (2000).

[8.3] European Committee for Standardization (CEN). "Eurocode 3: Design of Steel Structures, Part 1.8: Design of joints", EN 1993-1-8, British Standard Institution, London, (2005).

Appendix A

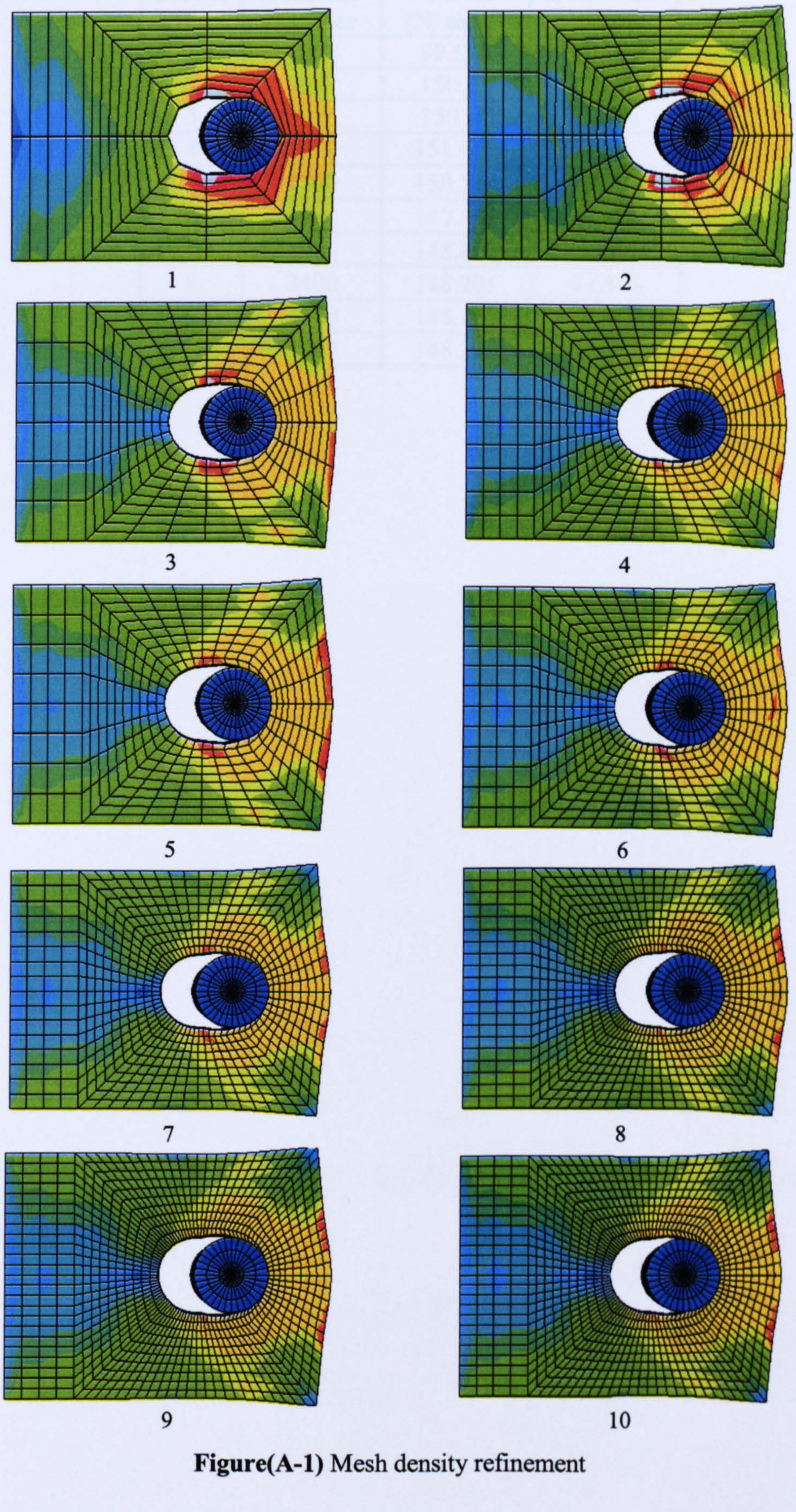

Figure(A-1) Mesh density refinement

Table 3.2 Convergence test

Model No.	Element Number	Stress [N/ mm^2]	Deflection [mm]
1	240	99.574	2.2828
2	480	150.21	2.9397
3	720	150.87	3.6043
4	960	151.089	4.07
5	1200	150.514	4.32
6	1440	147.858	4.457
7	1920	148.478	4.604
8	2400	148.201	4.6548
9	2880	148.185	4.662
10	3840	148.282	4.689

Appendix B

FE Modelling of Fin Plate Connections under Tying Force at Ambient Temperature

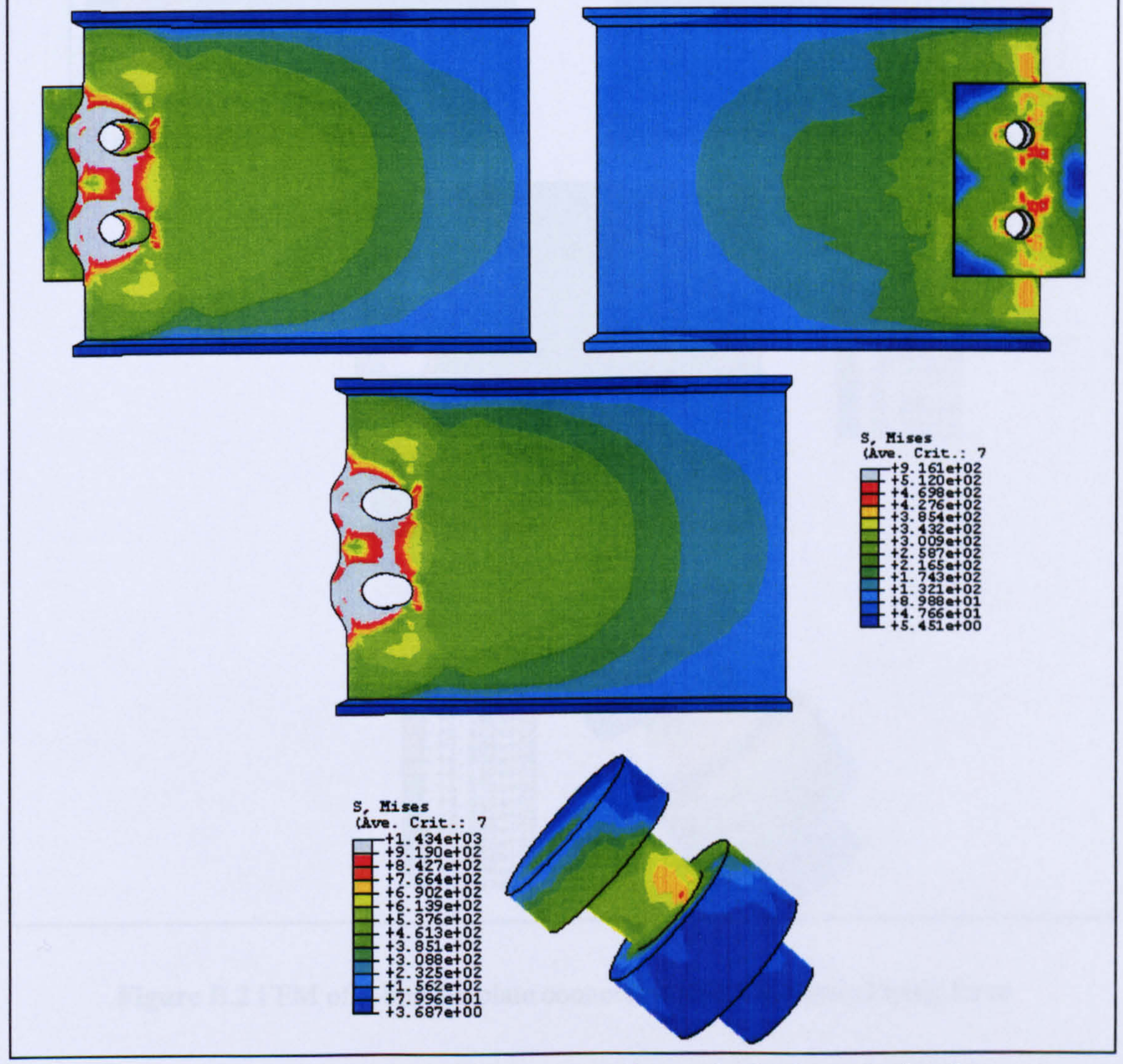

Figure B.1 FEM of 2-bolt fin plate connection under horizontal tying force

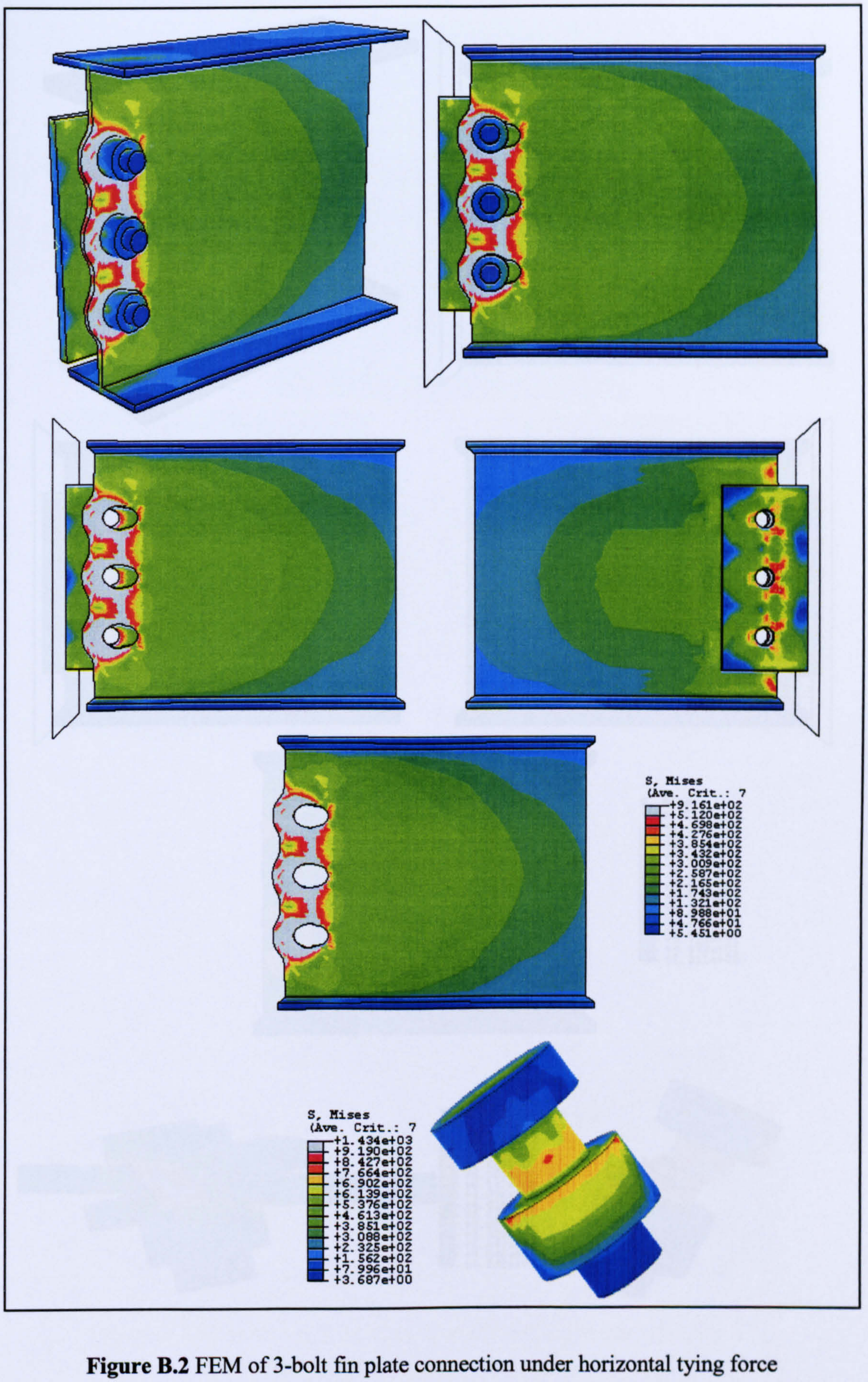

Figure B.2 FEM of 3-bolt fin plate connection under horizontal tying force

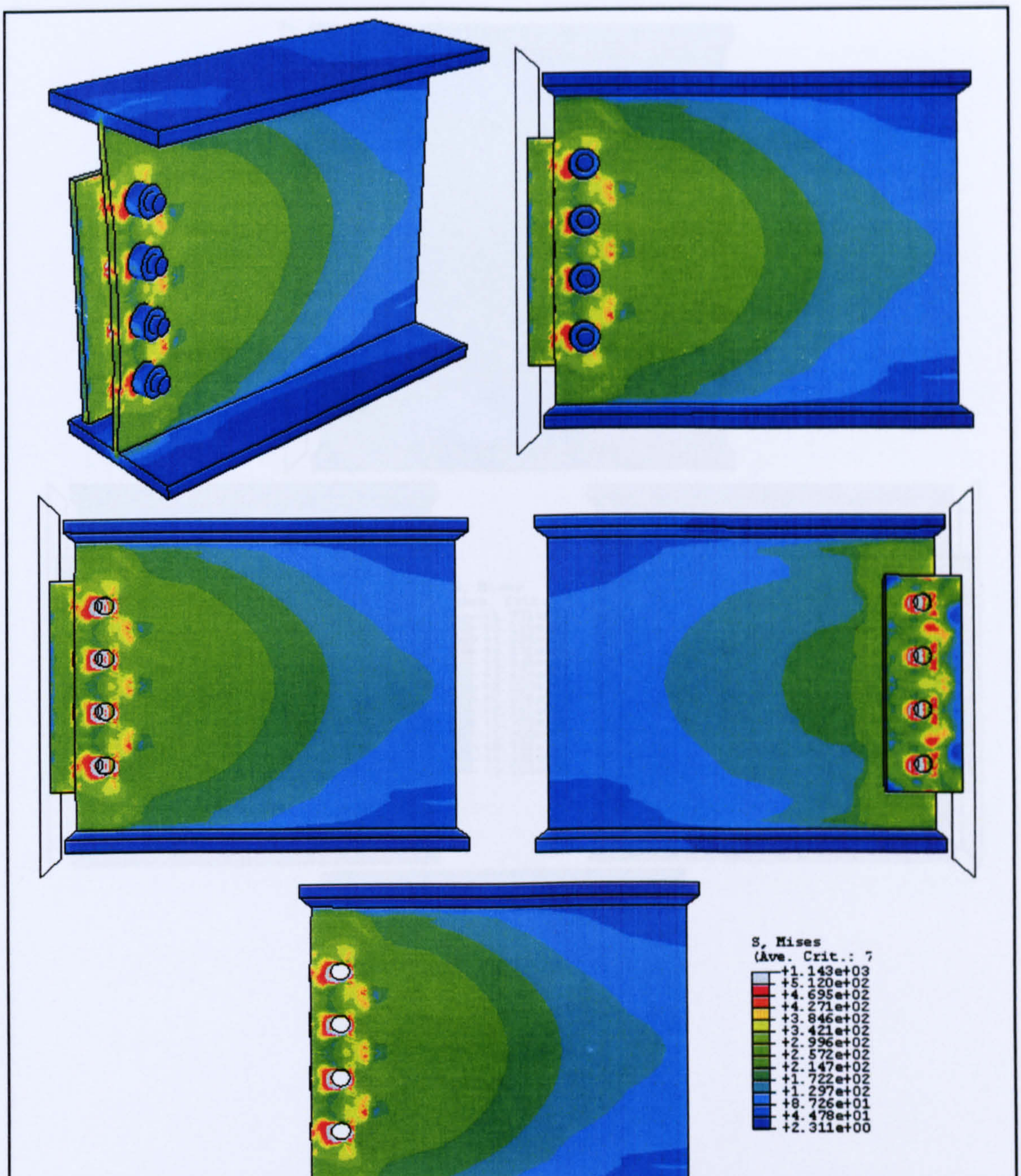

Figure B.3 FEM of 4-bolt fin plate connection under horizontal tying force

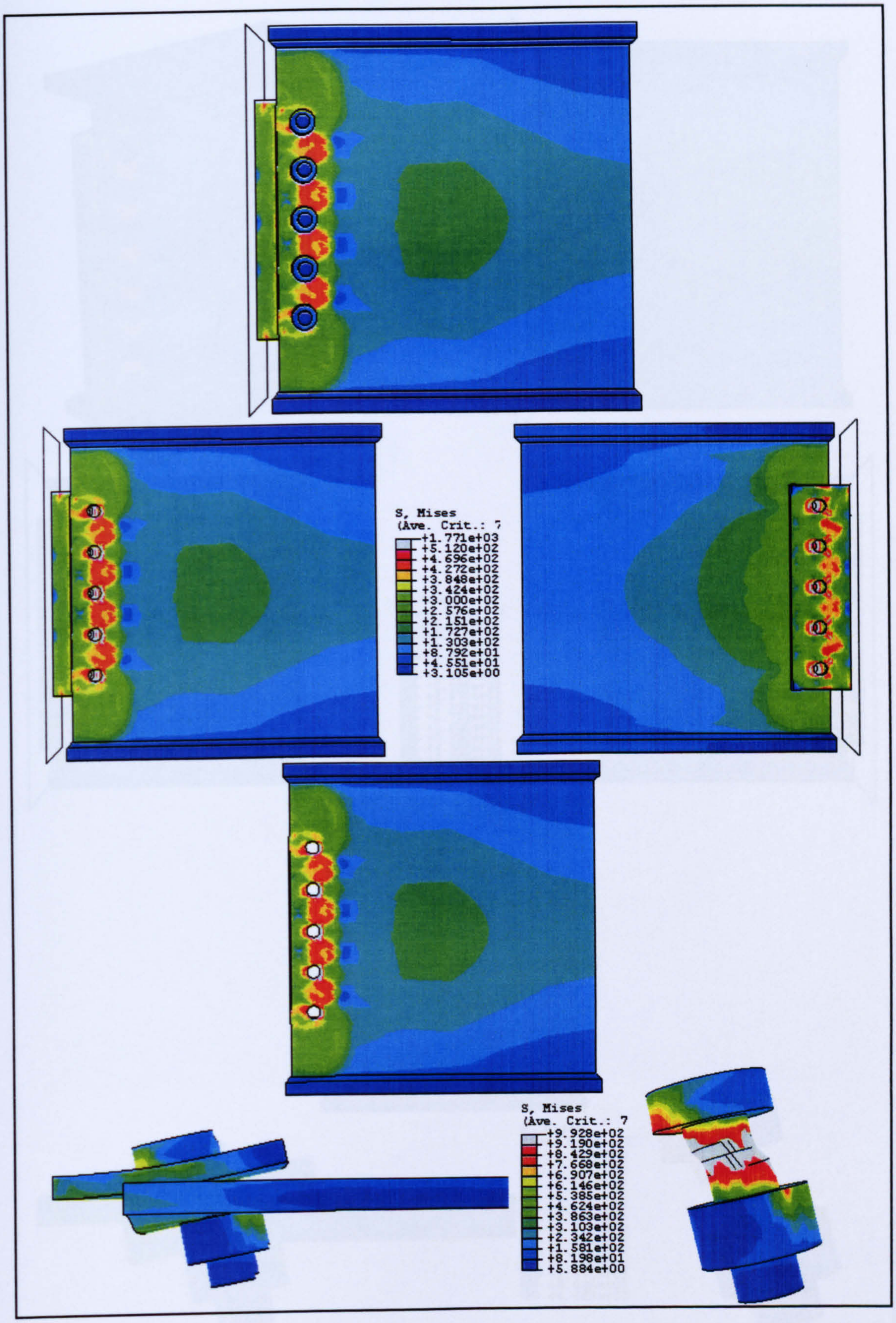

Figure B.4 FEM of 5-bolt fin plate connection under horizontal tying force

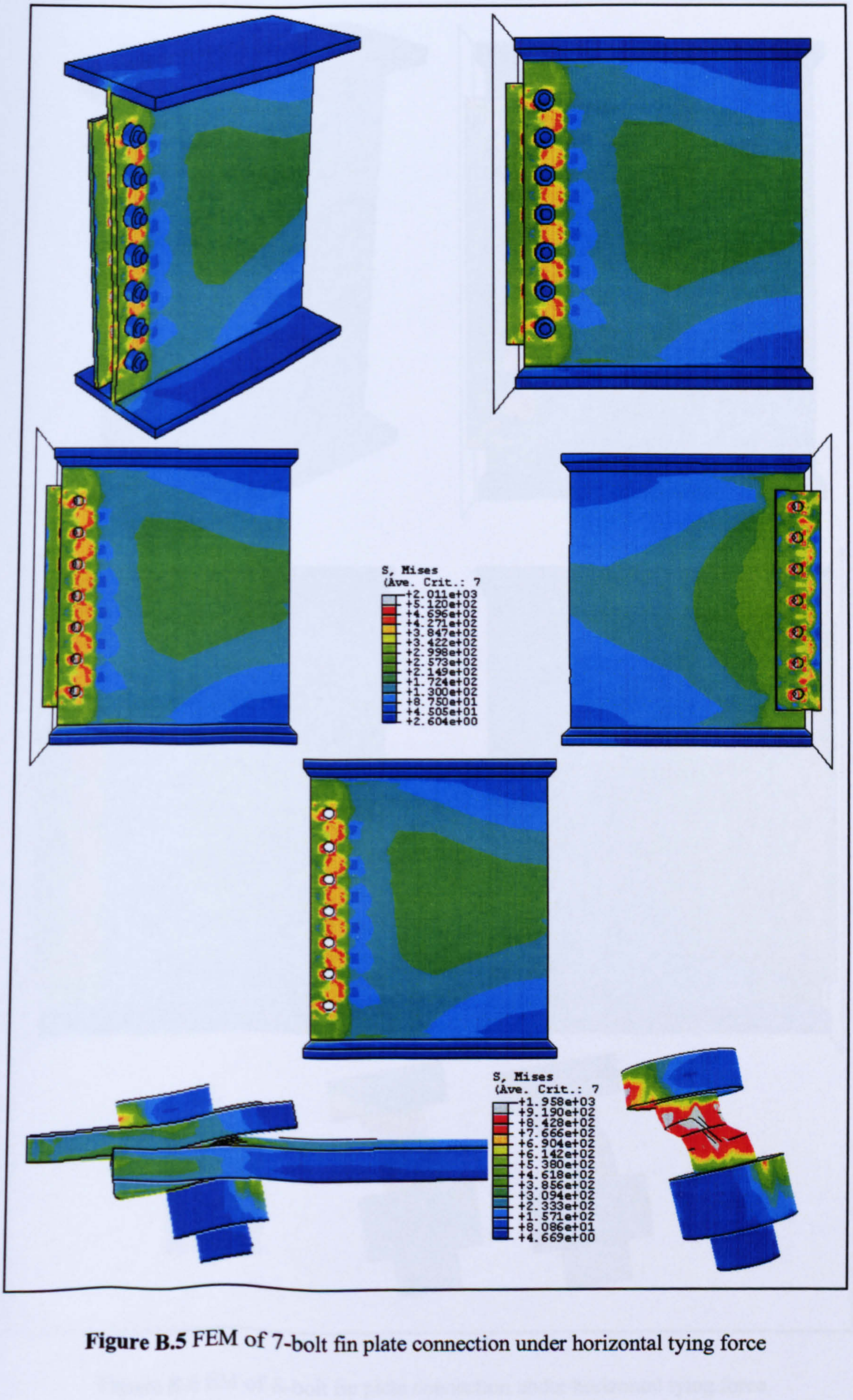

Figure B.5 FEM of 7-bolt fin plate connection under horizontal tying force

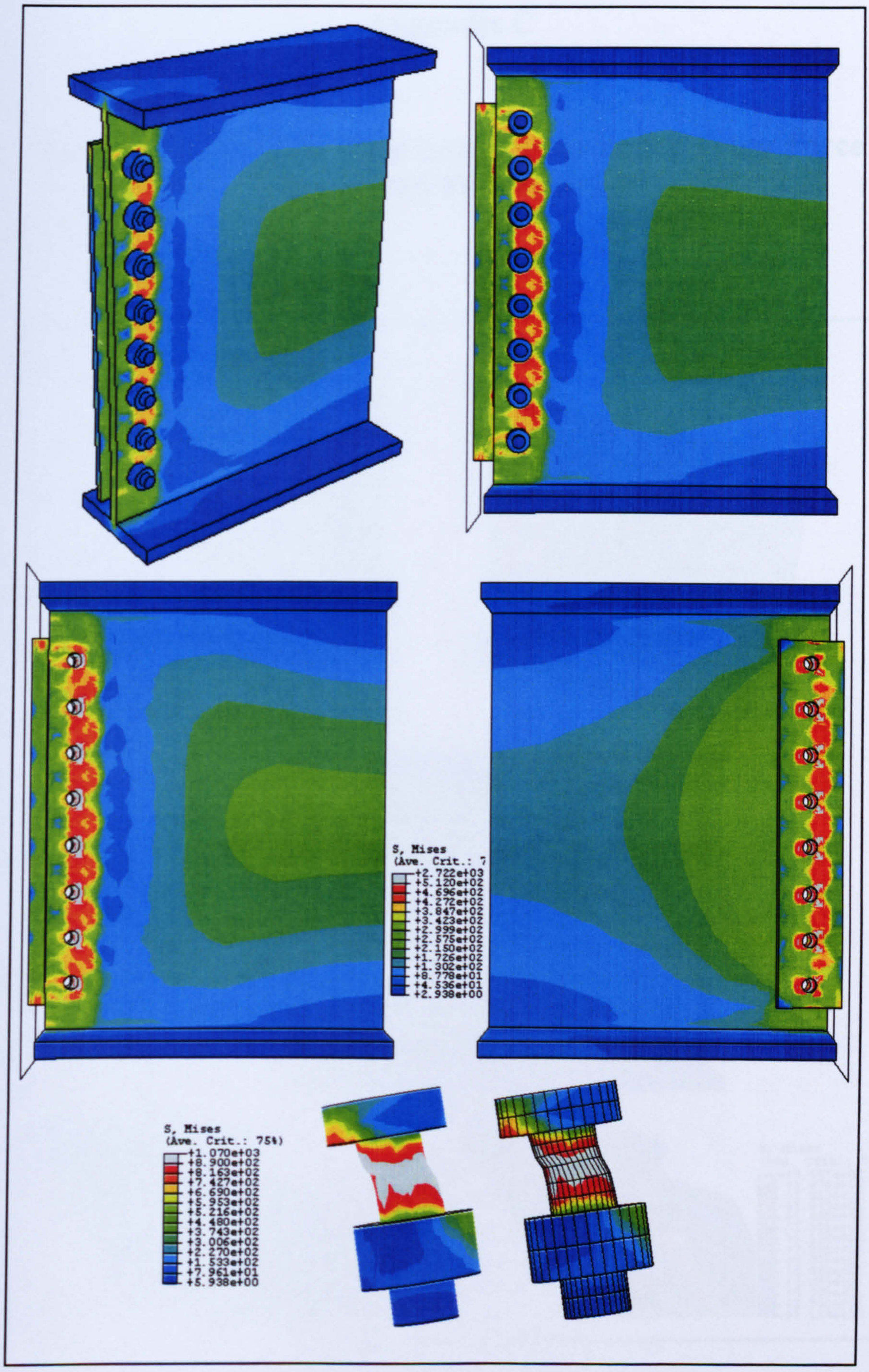

Figure B.6 EM of 8-bolt fin plate connection under horizontal tying force

Appendix C

FE Modelling of Fin Plate Connections under Tying Force at elevated Temperature

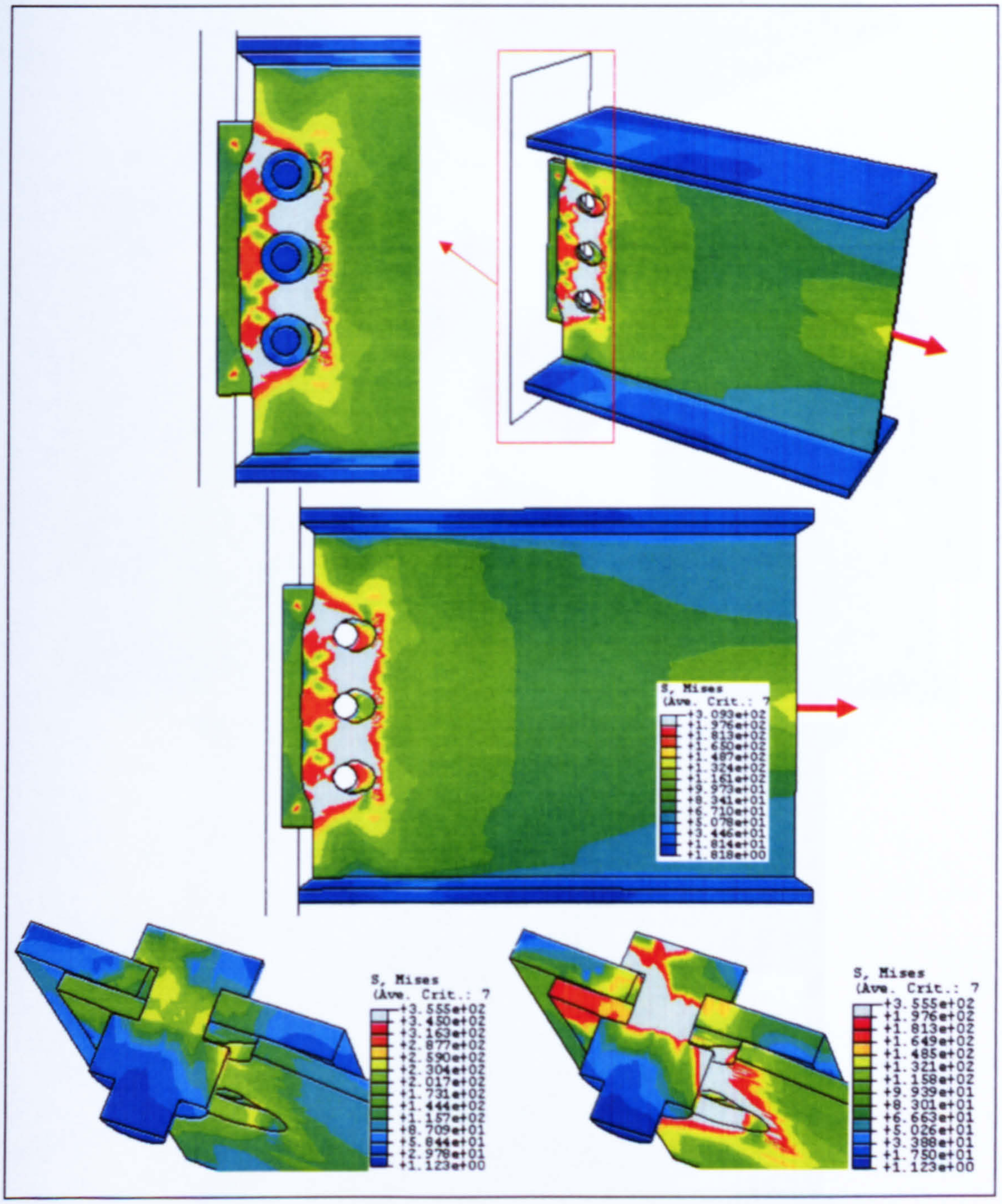

Figure C.1 FEM with load applied horizontally at 550°C

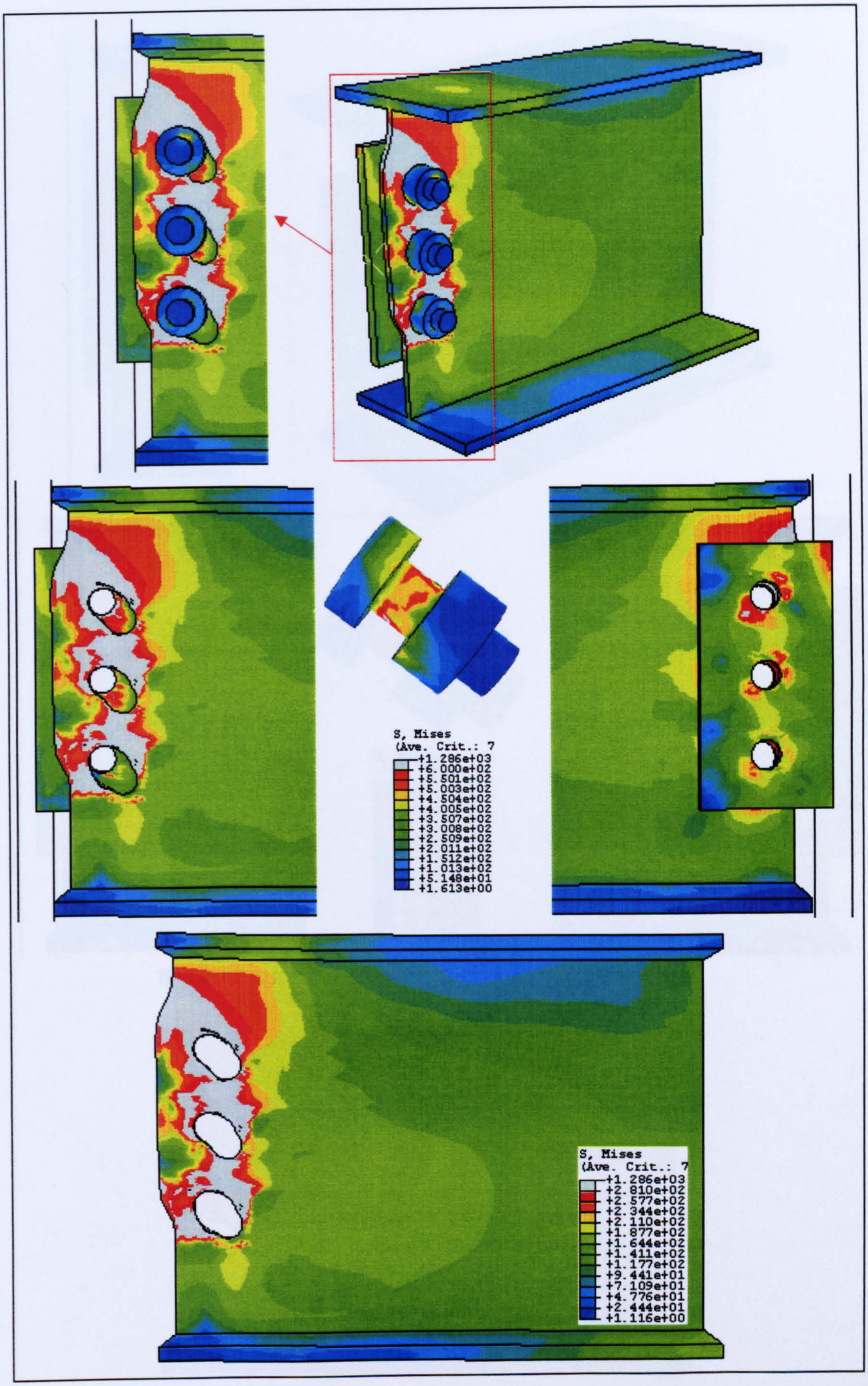

Figure C.2 FEM with load applied at 45° inclination at 450°C

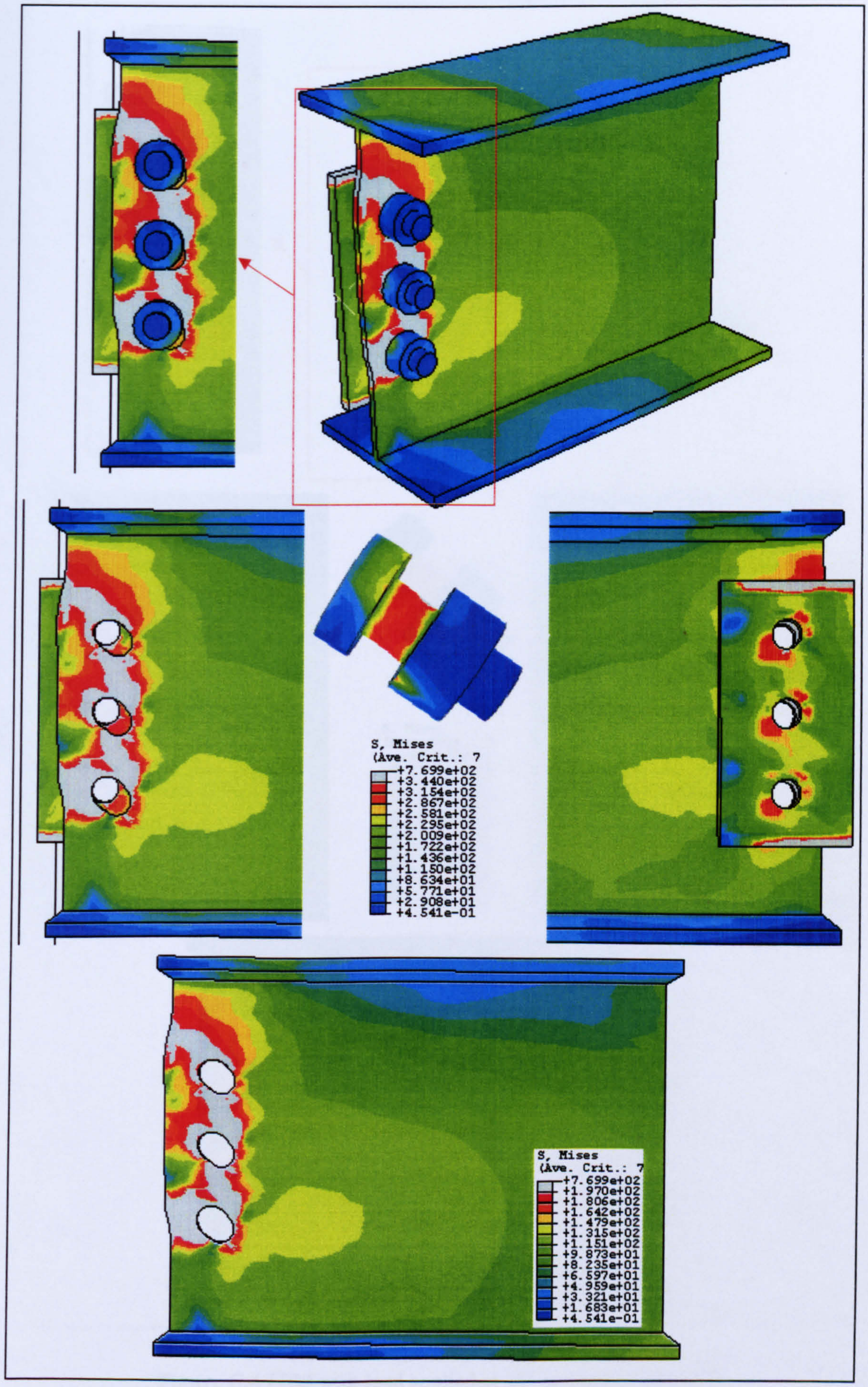

Figure C.3 FEM with load applied at 45° inclination at 550°C

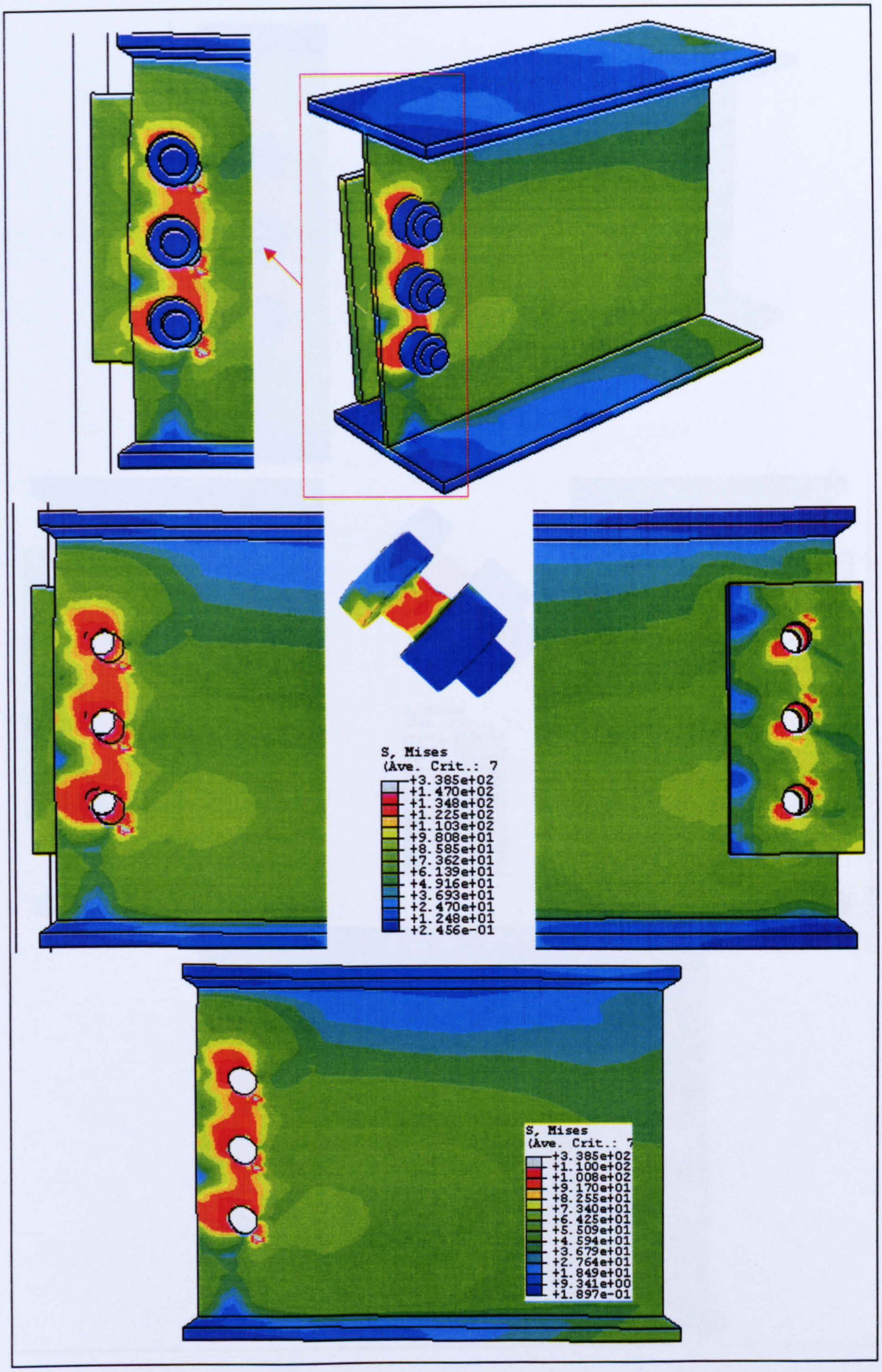

Figure C.4 FEM with load applied at 45° inclination at 650°C

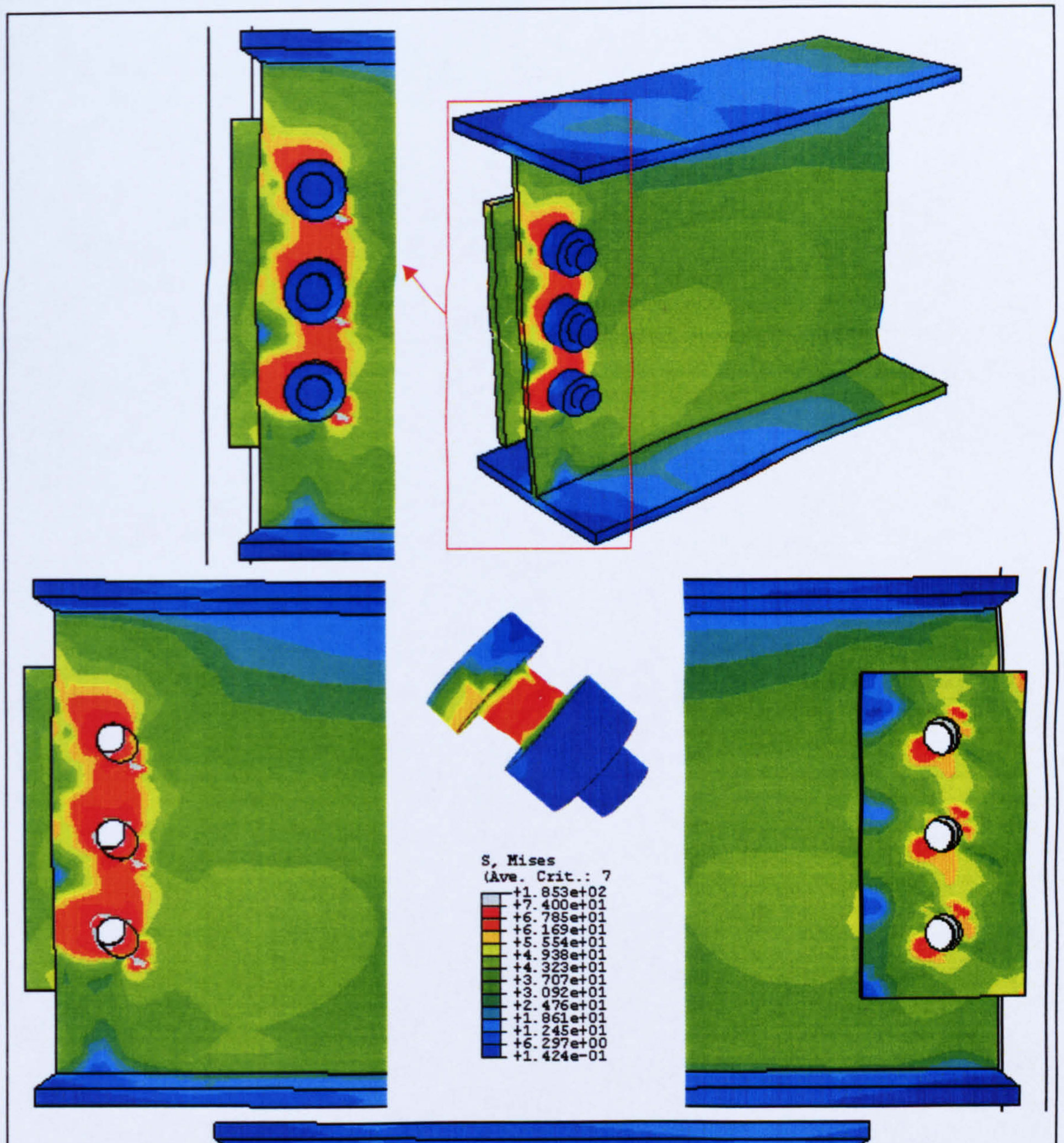

Figure C.5 FEM with load applied at 45° inclination at 750°C